DISSERTATION

SYNTHESIS OF NITROGEN-CONTAINING MOLECULES BY ZINC-CATALYZED [4+2] CYCLOADDITION AND PHOTOREDOX-CATALYZED C-H FUNCTIONALIZATION

Submitted by

John Chun Kit Chu

Department of Chemistry

In partial fulfillment of the requirements

For the Degree of Doctor of Philosophy

Colorado State University

Fort Collins, Colorado

Spring 2017

Doctoral Committee

Advisor: Tomislav Rovis

Alan Kennan
Amy Prieto
Shane Kanatous

ABSTRACT

SYNTHESIS OF NITROGEN-CONTAINING MOLECULES BY

ZINC-CATALYZED [4+2] CYCLOADDITION AND C-H FUNCTIONALIZATION

This work first describes an enantioselective Zn-catalyzed [4+2] cycloaddition of 1-azadienes and nitro-alkenes for the synthesis of medicinally valuable piperidines. The detrimental coordination of 1-azadienes to the Zn catalysts undermines the stereochemical control of the reaction. Fortunately, a novel bisoxazoline ligand limits this undesired coordination and delivers high stereoselectivity. Mechanistic studies suggest the reaction proceeds via a stepwise mechanism in which aza-Michael addition is followed by cyclization. This proposed mechanism also explains the successful cycloaddition between two electron-deficient reaction partners.

Secondly, amide-directed carbon-carbon bond formation at unactivated sp^3 C-H bonds has been achieved using photoredox catalysis. The reaction features a hydrogen atom abstraction from the C-H bond to a nitrogen radical generated from the amidyl N-H bond, leading to the formation of a carbon-centered radical. Trapping of the resulting alkyl radical with an electrophilic alkene gives the desired C-C bond formation. Experimental evidence supports the generation of the nitrogen radical through a stepwise deprotonation/oxidation event in a closed catalytic cycle. The potential to incorporate other functionalities in the C-H bonds, as well as γ functionalization of carbonyl compounds, is disclosed.

ACKNOWLEDGEMENTS

Tom, it's my honor to work under your supervision. I know I have been difficult to deal with because of my strong personality but thank you for bearing with me and allowing me to do chemistry in the way that I wished. No other professor would have given me the freedom that I enjoyed in the Rovis Group.

All Rovis group members, past and current, you are fantastic colleagues. In particular, Dr. White Tiger, Darren Flangian, Dr. A., Phil Zero, Spring Chicken, Dr. Mum, Mr. Dan Dan Dan, Nick Buddy and Kyle, thank you for all your help and friendship. Chuan, your presence in the lab gave me joy. Thanks are also extended to Fedor because you fed me with food. Tiff, sincere discussions with you about chemistry were always inspiring. Guidance from Derek and Dr. Tim Tim is acknowledged. Last but not least, thank you all for accommodating my moderate craziness in the lab.

Appreciation is extended to the McNally group. Andy, thank you for accommodating me in your lab in the last 6 months of my graduate studies and all your help with postdoctoral applications. All members in the group, talking with you gave me enjoyment and fueled me with energy for writing my dissertation, proposals and research summary. In particular, thanks to Luke, who proof-read the acknowledgements section of my dissertation.

I must show my gratitude to all my family members, all my uncles, aunts, older brother, cousins (Sandy, Angel, Bonnie, Candy, Kitty, Meimei, Tony, Gary, Jason, Craig, Amy, Hysan and

Anson) and especially my parents and grandma. All your support and care in my life has made me determined to pursue science despite opposition from many.

Mr. Lee Ying Choi, Ms. Chan Ching Yan, Mr. Ma Chun Man and Mr. Lau Kei Wai, former or current teachers from South Tuen Mun Government Secondary School, all of your teachings were enlightening and have sowed the passion of science within me. Prof. Pauline Chiu, my undergraduate mentor at the University of Hong Kong, the education and care from you has paved my success in graduate school and beyond.

My friends, Yim Chicken, Pang Pang, Fat Ben, Menu Lai, Fanny Yau, Ivy Ho, Vanessa Wong, Emily Wong, Tim Lo, Samson Yuen and Alice Chan, all of you are amazing companions.

This final paragraph is dedicated to my DEAREST LORD JESUS CHRIST because you are the LIVING GOD that I was able to experience in my graduate studies. The Church, as your Body, has always been a support to me and all the saints are important for my going on. Special thanks to Brothers Jonathan Karr and Eric Swanson, who shared all the joy and worries during my graduate studies.

TABLE OF CONTENTS

CHAPTER ONE: ASYMMETRIC SYNTHESIS OF PIPERIDINES BY ZINC-CATALYZED [4+2] CYCLOADDITION of 1-AZADIENES and NITRO-ALKENES

1.1 Introduction

1.1.1 Nitrogen-Heterocycles in Pharmaceuticals

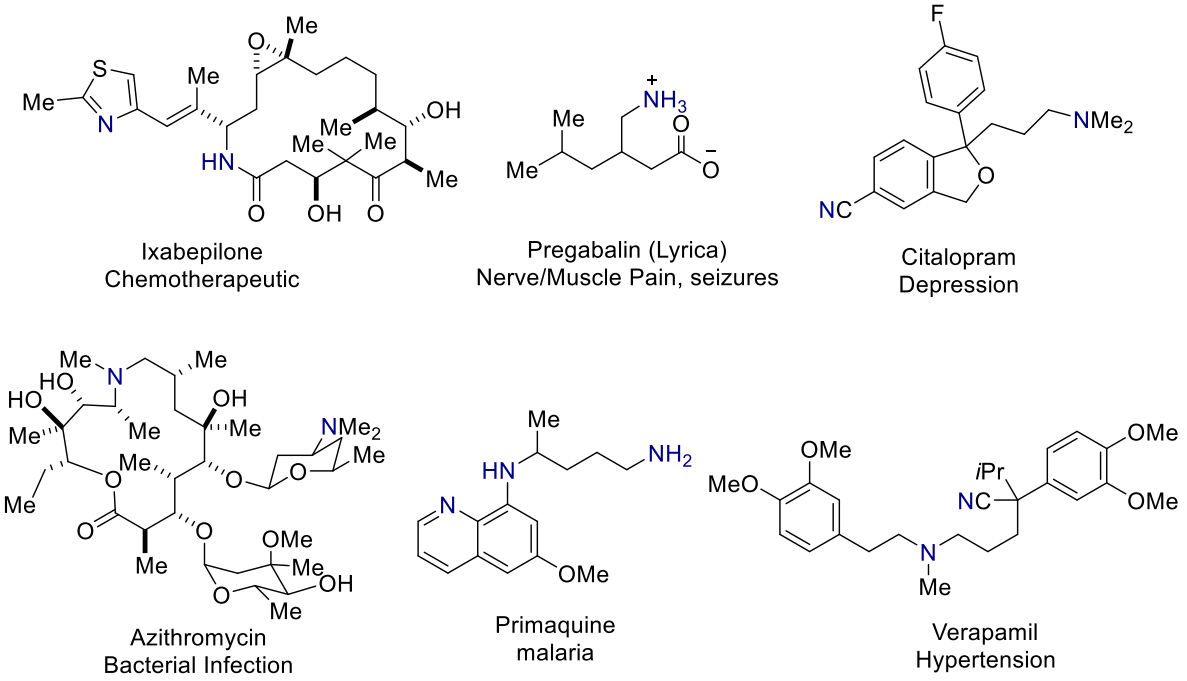

Figure 1.1.1: Examples of Nitrogen-Containing Drug Molecules

The overwhelming presence of nitrogen in pharmaceuticals underscores the need for efficient synthesis of nitrogen-containing molecules. Among all small-molecule drugs approved by the Food and Drug Administration through 2012, 84% contain at least one nitrogen atom (Figure 1.1.1).[1] There are two main impacts nitrogen atoms have on the pharmaceutical properties of a molecule. First, the presence of a nitrogen atom provides many potential pathways for the molecule to interact with a biological target. An N-H bond and a lone pair of

nitrogen can serve as a hydrogen bond donor or acceptor respectively. An ionic interaction with anions is possible upon acquiring a position charged through protonation or alkylation of the nitrogen. Secondly, the nitrogen can adjust the bioavailability of the molecule due to the nitrogen's capacity to form hydrogen bonding and the potential to acquire a charge, as well as the increased polarity of the molecule.

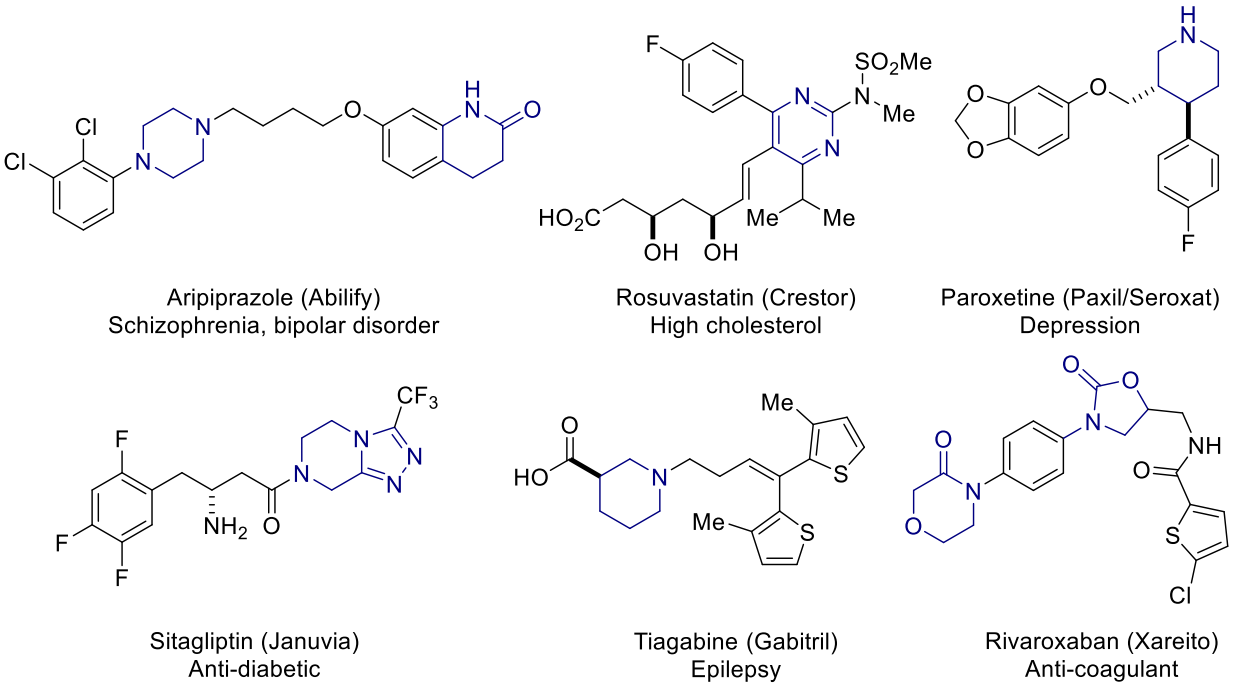

Figure 1.1.2: Examples of Nitrogen-Heterocycle-Containing Drug Molecules

In pharmaceuticals, 59% of small-molecule-drugs contain at least one nitrogen-heterocycle (Figure 1.1.2).[1] The rationale behind the abundance of nitrogen heterocycles is that the nitrogen atom is configurationally locked in the ring. As a consequence, the entropy cost associated with the binding is smaller compared to their acyclic counterparts. Efficient syntheses of nitrogen heterocycles can streamline studies of medicinal chemistry on structural-activity relationship and the optimization of drug candidates, accelerating the drug discovery process.

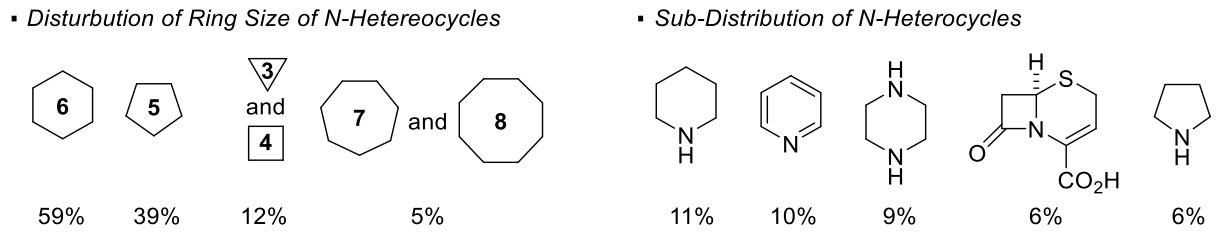

Figure 1.1.3: Distribution of Nitrogen-heterocycles in Drug Molecules

The Njardarson group has summarized the distribution of different nitrogen-heterocycles among small-molecule drugs approved by the FDA (Figure 1.1.3).[1] Five- and six-membered are the most common nitrogen-heterocycles found. A deeper analysis further reveals that piperidines and pyridines are the most common motif.

1.1.2 Aza-[4+2] Cycloaddition and Its Challenges

Figure 1.1.4: Diels-Alder Cycloaddition and Aza-[4+2] Cycloaddition

The Diels-Alder reaction of dienes and dienophiles is arguably the most common strategy for the assembly of cyclohexane rings.[2] Similarly, 6-membered nitrogen-heterocycles, piperidine derivatives, can also be accessed via aza-[4+2] cycloaddition (Figure 1.1.4).[3] However, several aspects of aza-[4+2] cycloaddition have hindered its development. First, the presence of a basic nitrogen atom in the starting materials and the products can coordinate to a transition-metal complex or a Lewis acid strongly or irreversibly, preventing the transition metal complex or the Lewis acid from promoting the reaction. This undesired coordination becomes a serious issue especially in the context of catalysis since the transition metal complex or the Lewis acid is only

present in a catalytic amount. In addition, the starting materials and products are either imines or enamines which are prone to decomposition under the reaction conditions or during purification.

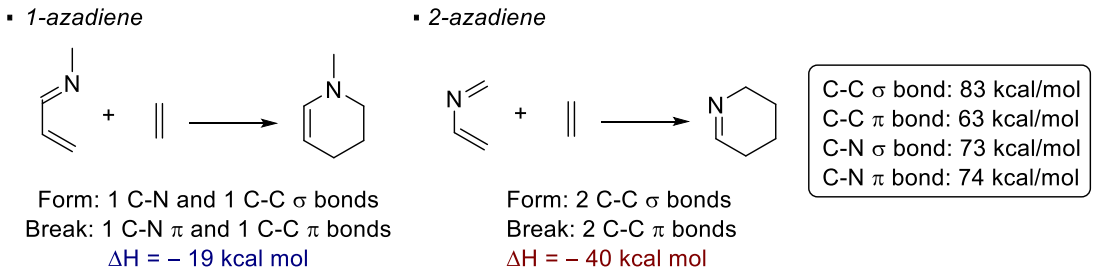

Figure 1.1.5: Consideration of Bond Energy in aza-[4+2] Cycloaddition

Simple imines, 1-azadienes and 2-azadienes are three different classes of competent partners for aza-[4+2] cycloaddition.[4] The reaction of simple imines in catalytic enantioselective [4+2] cycloaddition is largely limited to the use of highly electron-rich dienes such as Danishefsky's dienes as the reaction partners. This has been reviewed by Jorgensen and will not be discussed here.[5] The use of 2-azadienes is more investigated than 1-azadienes, as exemplified by the Povarov reaction, a formal cycloaddition between aniline-derived imines and electron-rich alkenes for the construction of tetrahydroquinolines.[6] Although 1-azadienes can be readily accessed through amines and enals/enones, their use in aza-[4+2] cycloaddition represents a challenge,[7] which is unsurprising when the bond strengths of the forming and breaking bonds are considered (Figure 1.1.5). In the event of an aza-[4+2] cycloaddition with 2-azadienes, two C-C σ bonds (83 kcal/mol) are formed at the expense of two C-C π bonds (63 kcal/mol). The estimated enthalpy change is calculated to be −40 kcal/mol. On the other hand, for the use of 1-azadienes, one C-N σ bond (73 kcal/mol) and one C-C σ bond (83 kcal/mol) are formed while one C-N π bond

(74 kcal/mol) and one C-C π bond (63 kcal/mol) are broken. The net enthalpy is estimated to be -19 kcal/mol, approximately 20 kcal/mol less in thermodynamic driving force than in the case of 2-azadienes, because of the weaker forming C-N σ bond and the stronger breaking C-N π bond.

Similar to the all-carbon [4+2] cycloaddition, aza-[4+2] cycloadditions can potentially proceed through concerted and stepwise mechanisms. Frontier molecular orbital theory can be applied for the analysis of a concerted cycloaddition (Figure 1.1.6).[8] For 1-azadienes, the presence of the electronegative nitrogen decreases the electron density of the dienes and thus lowers the energy of its highest-occupied-molecular-orbital (HOMO). Compared to the all-carbon analogue of a concerted [4+2] cycloaddition, the lower energy level of the HOMO of the dienes disfavors the interaction with the lowest-unoccupied-molecular-orbital (LUMO) of the dienophiles. This unfavorable HOMO-LUMO interaction renders a concerted normal-electron-demand Diels-Alder reaction kinetically slow. In contrast, a concerted inverse-electron-demand Diels-Alder cycloaddition is more feasible because the lower energy level of the LUMO of the dienes will lead to a favorable interaction with the HOMO of the dienophiles, especially when the dienophiles are made electron rich by conjugation with a heteroatom. In addition, because of the electron-withdrawing nature of the nitrogen, the dienes are polarizable. This would render the transition-state of the [4+2] cycloaddition asynchronous in the case of a concerted mechanism. A stepwise mechanism is the extreme case of a highly asynchronous transition state where the extent of bond-forming at the two ends of the dienes differs infinitely. The mechanism of a particular aza-[4+2] cycloaddition is likely contingent on the electronics of the dienes and the alkenes, and therefore should be determined on a case-by-case basis. Although efforts have been devoted to develop new aza-[4+2] cycloadditions to streamline the synthesis of piperidines, the

mechanistic aspects are often neglected. Mechanisms are proposed without any experimental evidence, and in most cases, no mechanism is proposed.

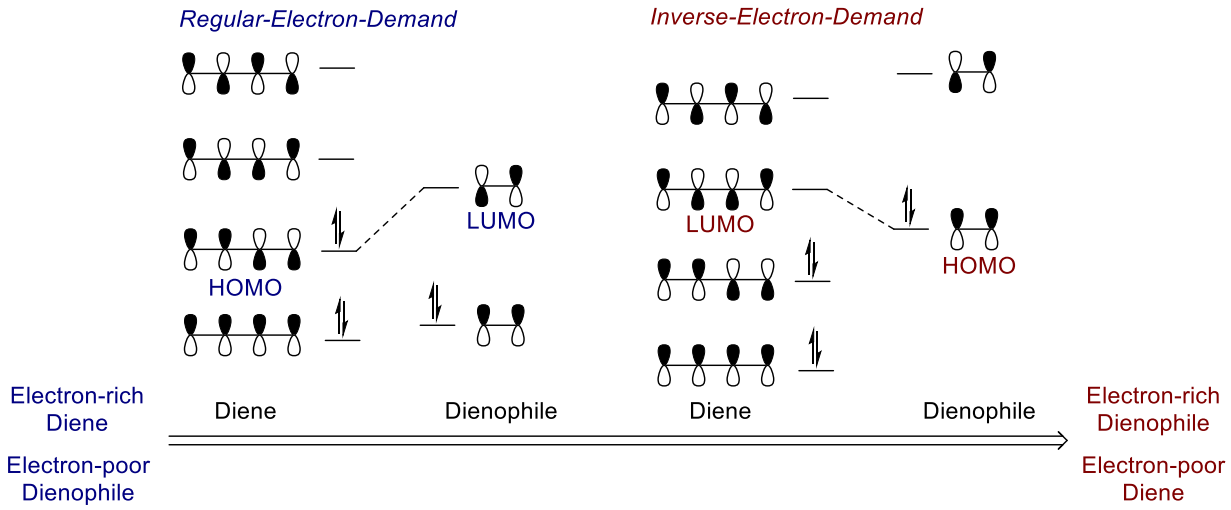

Figure 1.1.6: Frontier Molecular Orbital Analysis of [4+2] Cycloaddition

1.1.3 Asymmetric Aza-[4+2] Cycloaddition with 1-Azadienes

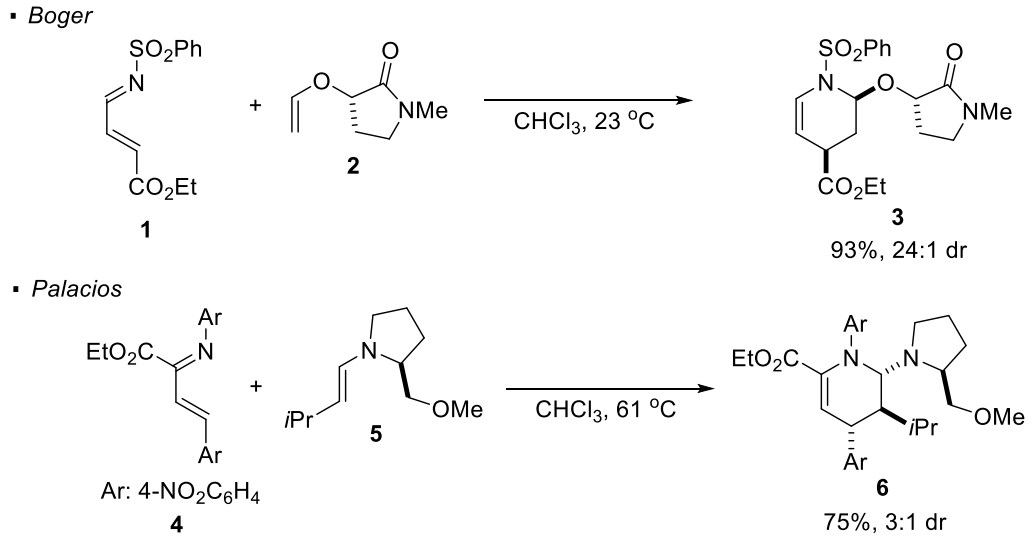

Scheme 1.1.1: Use of Chiral Auxiliary in [4+2] Cycloaddition with Electron Rich Alkenes

Examples of asymmetric aza-[4+2] cycloaddition with 1-azadienes and electron-rich alkenes are limited. Boger developed a highly diastereoselective aza-[4+2] cycloaddition with *N*-sulfonyl-1-azadienes **1** and homochiral enols **2** (Scheme 1.1.1).[9] A single example of a moderately selective [4+2] cycloaddition of *N*-aryl-1-azadiene **4** with enantiomerically-enriched enamine **5** is reported by Palacios.[10] In addition to the use of chiral auxiliaries, a few methods based on asymmetric catalysis can be found (Scheme 1.1.2). A chiral phosphoric acid catalyzed asymmetric cycloaddition of *N*-aryl-1-azadienes **7** and enecarbamates **8** was disclosed by Masson and co-workers.[11] Arrayas and Carretero reported a Ni-catalyzed enantioselective inverse-electron-demand Diels Alder reaction with *N*-sulfonyl-1-azadienes **11** and enol ethers **12**.[12] The Wang group applied a thiourea/primary amine bifunctional catalyst **18** for the [4+2] cycloaddition of sodium enolates **15** and 1-azadienes **16**.[13] The thiourea is believed to activate the 1-azadienes through hydrogen bonding while the condensation of the primary amine on the carbonyl group in the sodium enolates to form an iminium is proposed to be important for achieving high enantioselectivity.

In addition, various groups have demonstrated the *in-situ* generation of an electron rich alkene with a chiral catalyst and the subsequent stereoselective [4+2] cycloaddition with electron poor *N*-sulfonyl 1-azadienes (Scheme 1.1.3). The Bode,[14] Rovis[15] and Ye[16] groups generated the electron-rich alkenes, azolium enolates, from aldehydes or ketenes with nucleophilic heterocycle carbene catalysts **21**, **26** and **30**. As demonstrated by Smith group, the same kind of electron-rich alkene intermediates can also be generated from activated carboxylic acids and isothiourea catalyst **37**.[17] The Chen group condensed proline-derived secondary amine catalyst **36** onto a carbonyl group to give an electron rich enamine that allows the aza-[4+2] cycloaddition.[18]

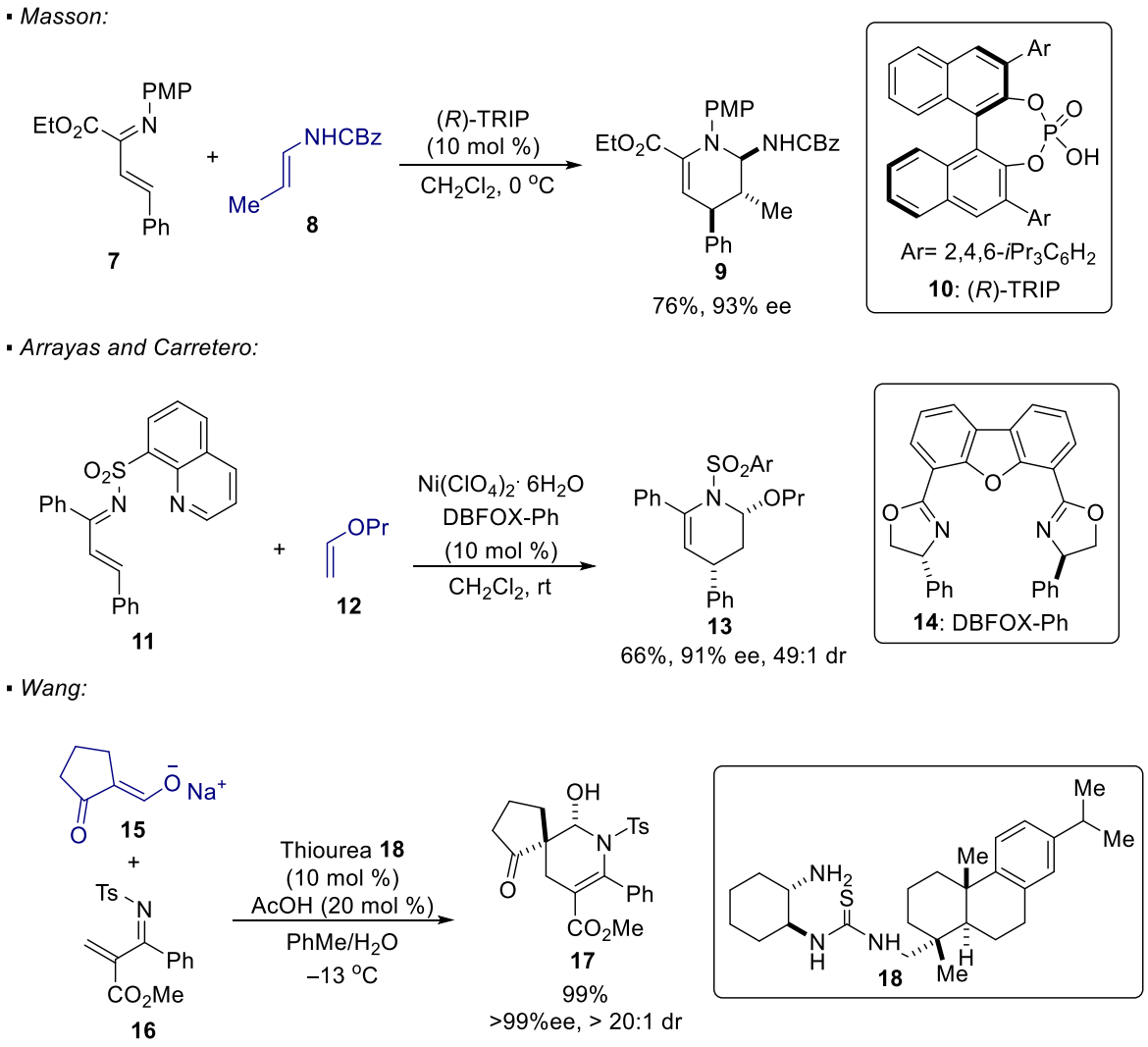

Scheme 1.1.2: Catalytic Enantioselective aza-[4+2] Cycloaddition with Electron-rich Alkenes

Considering the electron-deficiency of the 1-azadienes, the use of an electron-poor alkene is considered to be more challenging with a concerted pericyclic mechanism. Indeed, there is only one report on catalytic enantioselective [4+2] cycloaddition of 1-azadienes with electron poor alkenes (Scheme 1.1.4). In this example, the electronic requirement for a concerted mechanism is obviated by a stepwise aza-Rauhut-Currier pathway. Other asymmetric cycloadditions of 1-azadienes with electron poor alkenes rely on the application of chiral auxiliaries. Ghosez demonstrated the diastereoselective aza-cycloaddition of 1-azadiene **42** and

maleic anhydride **43**.[19] There is also a single example of successful aza-cycloaddition of 1-azadienes with chiral tungsten alkynylcarbene **47**, as demonstrated by the Barluenga group.[20]

1.1.4 [4+2] Cycloaddition of 1-Azadienes and Nitro-alkenes

A former co-worker in the Rovis group, Dr. Derek Dalton, discovered that 3-nitropiperidines can be assembled by the aza-[4+2] cycloaddition of 1-azadienes and nitro-alkenes (Scheme 1.1.5).[21] The cycloadducts can be derivatized to 3-aminopiperidines, a medicinally valuable motif (Figure 1.1.7). Examples of drug molecules containing this motif include Tofacitinib,[22] Alogliptin,[23] Palonosetron,[24] Lenalidomide[25] and Maropitant.[26]

The aza-[4+2] reaction developed by Dr. Dalton requires an earth-abundant Zn catalyst and different substitution patterns on both reaction partners are tolerated (Scheme 1.1.5). Nitro-alkenes with small or relatively bulky substituents (**49**, **50**, **51** and **53**) on the β-carbon are competent reaction partners. Other functionalities, such as protected alcohol (**52**), also do not affect the outcome of the reaction. For the 4-substituents on 1-azadienes, electron-rich, electron-neutral and electron-poor aromatic rings (**49**, **54** and **55**) are tolerated. Good yield of the cycloadducts can also be obtained with hetereoaryl furan (**56**) or even alkyl group (**57**).

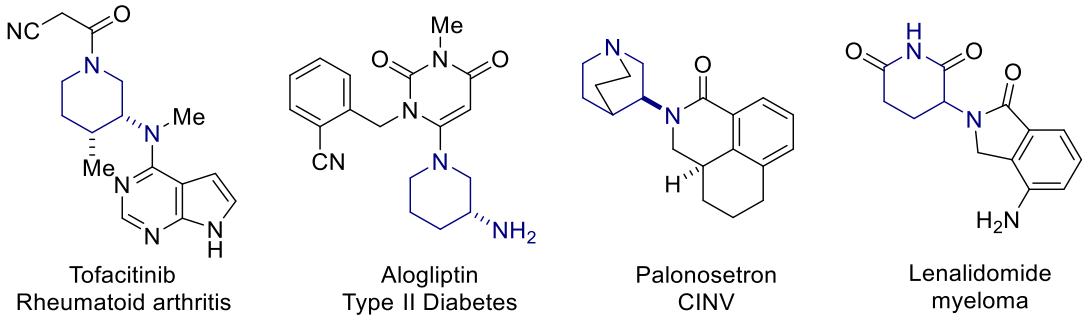

Figure 1.1.7: Examples of Drug Molecules Containing 3-aminopiperidines

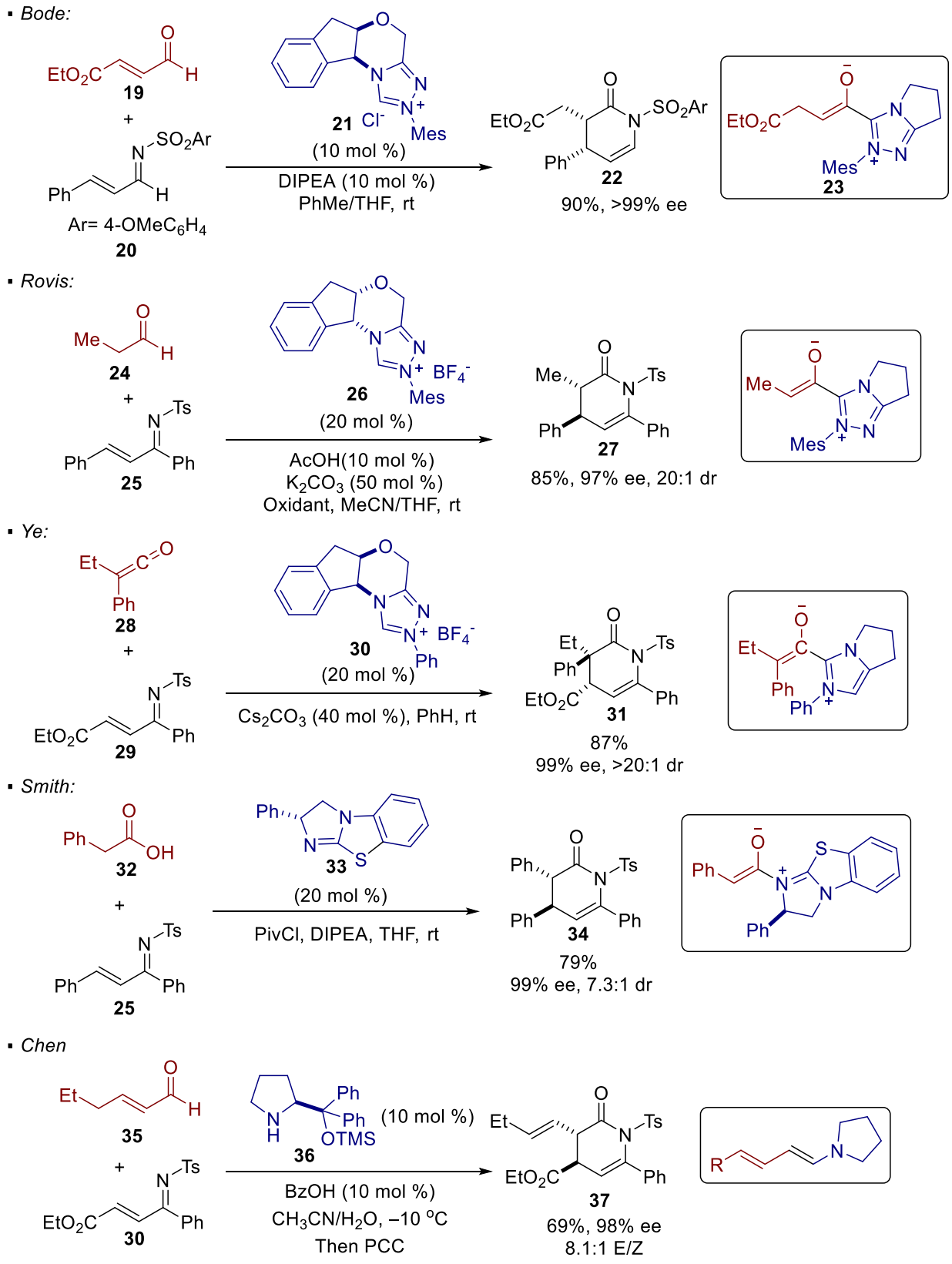

Scheme 1.1.3: *In-situ* Generation of Electron-rich Alkenes for aza-[4+2] Cycloaddition

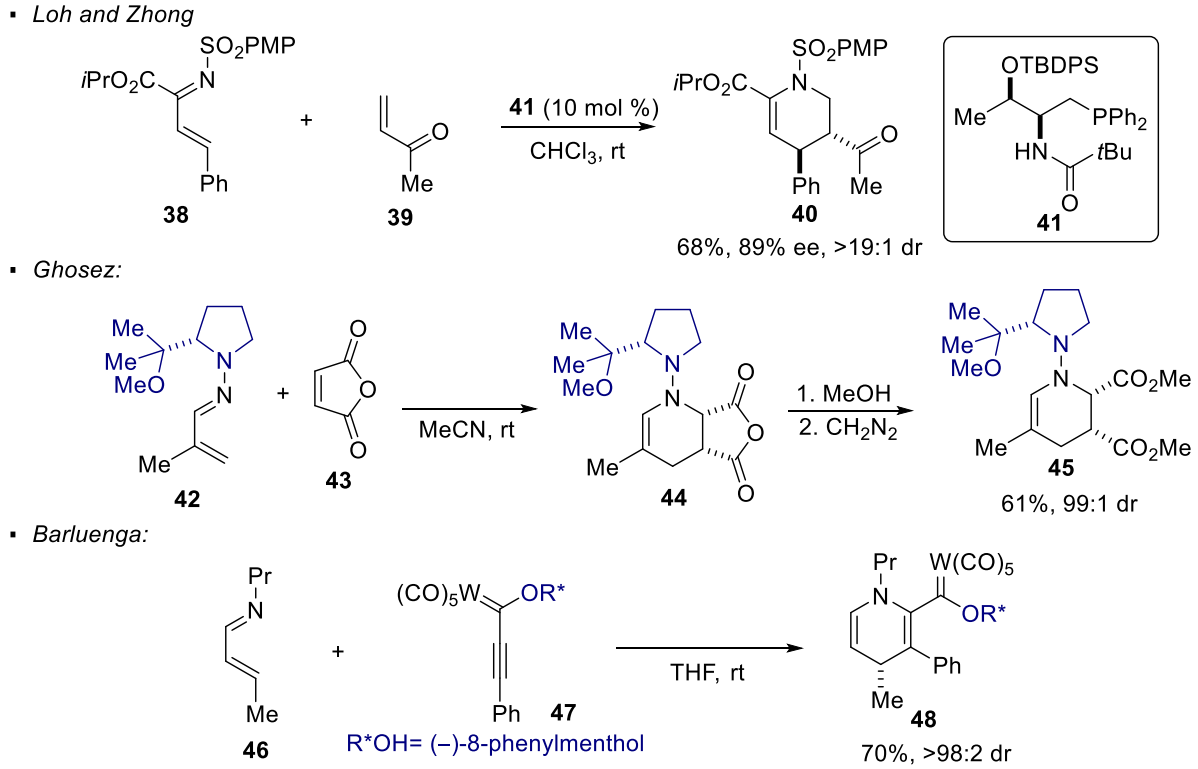

Scheme 1.1.4: Asymmetric aza-[4+2] Cycloaddition of 1-azadienes with Electron-poor Alkenes

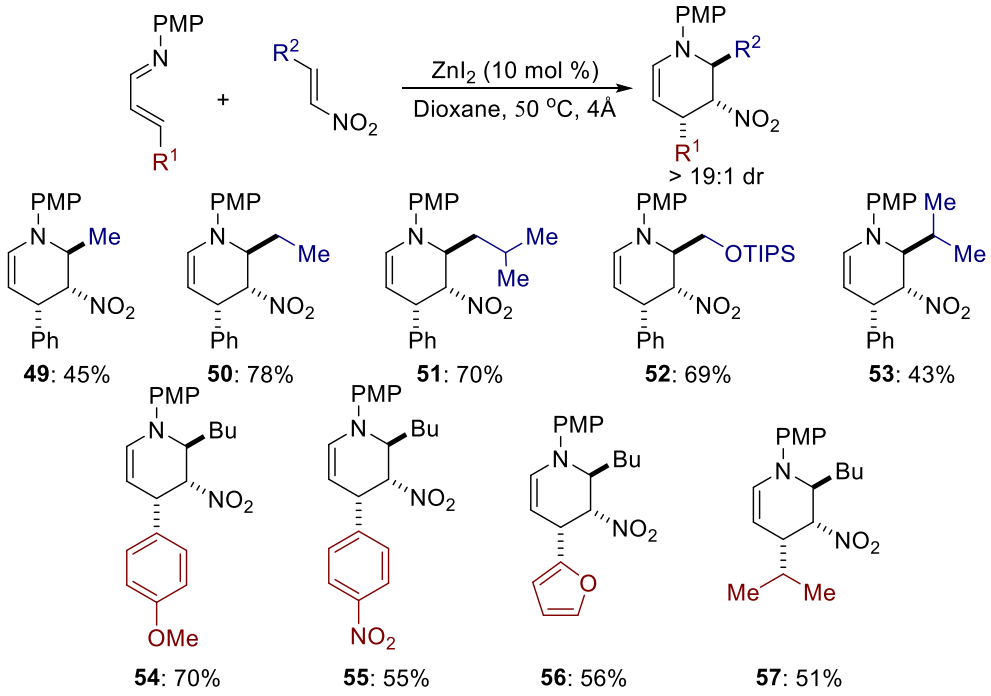

Scheme 1.1.5: Selected Scope for aza-[4+2] Cycloaddition of 1-azadienes and Nitro-alkenes

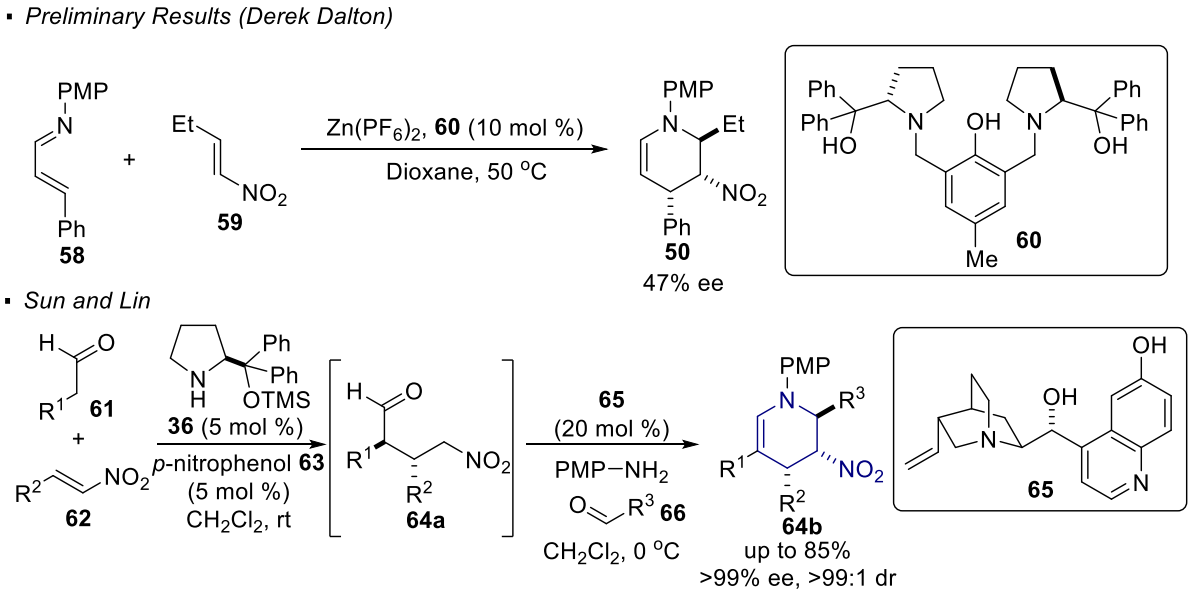

Scheme 1.1.6: Catalytic Enantioselective Synthesis of 3-nitropiperidines

After extensive optimization with high throughout experimentation, the highest ee obtained for the [4+2] cycloaddition was 47% with Prophenol **60** (Scheme 1.1.6).[27] During the course of this work, Sun and Lin reported catalytic enantioselective synthesis of 3-nitropiperidines **64b** with different substitution.[28]

1.2 Results

1.2.1 Initial Screening of Ligands

Considering the medicinal relevance of 3-aminopiperidines, an asymmetric variant of the aza-[4+2] cycloaddition of 1-azadienes and nitro-alkenes is highly desired. Building off the work from Dr. Dalton, the objective of our work was to develop a catalytic enantioselective aza-[4+2] cycloaddition of 1-azadienes and nitro-alkenes. Initial efforts focused on the application of bisoxazoline ligands, the most common class of ligands for asymmetric Zn-catalyzed transformations (Scheme 1.2.1). Since the product from the aza-[4+2] cycloaddition contains an

enamine that is prone to hydrolysis during purification, a reductive workup protocol with $ZnCl_2$, $NaCNBH_3$ in MeOH was adopted to reduce the cycloadduct to stable piperidine **68**. The result shows the commercial bisoxazolines **L1**, **L2**, **L3** and **L4** give apparently no stereochemical control for the [4+2] cycloaddition. Therefore, we explored other bisoxazoline ligands.[29]The biphenyl-derived bisoxazoline **L5** gives modest enantioselectivity. The axially chiral bisoxazoline **L6** gives a moderate enantiomeric excess of 34%. Efforts to improve the selectivity by the installation of chiral elements at the oxazolines are not fruitful. In the mismatched case in ligand **L7**, almost all stereochemical control is lost. When both chiral elements from the binapthyl and the oxazolines in **L8** favor the formation of the same stereoisomer, only a moderate ee (52%) is obtained.

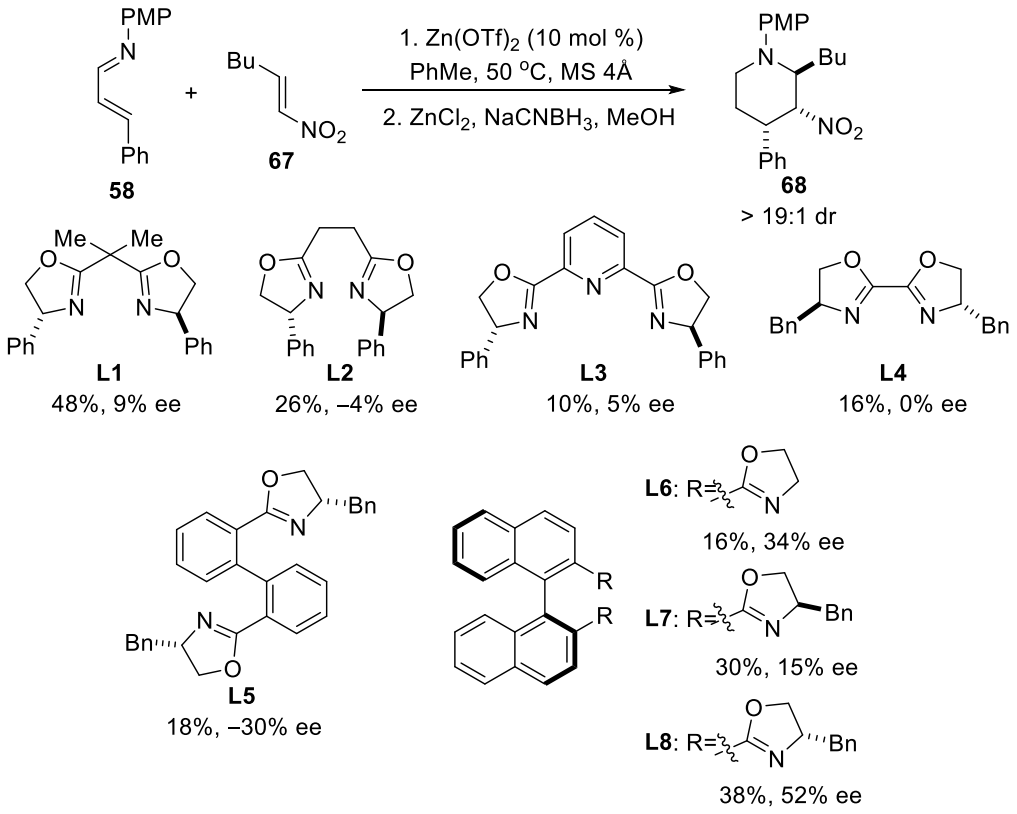

Scheme 1.2.1: Initial Screening of Bisoxazoline Ligands

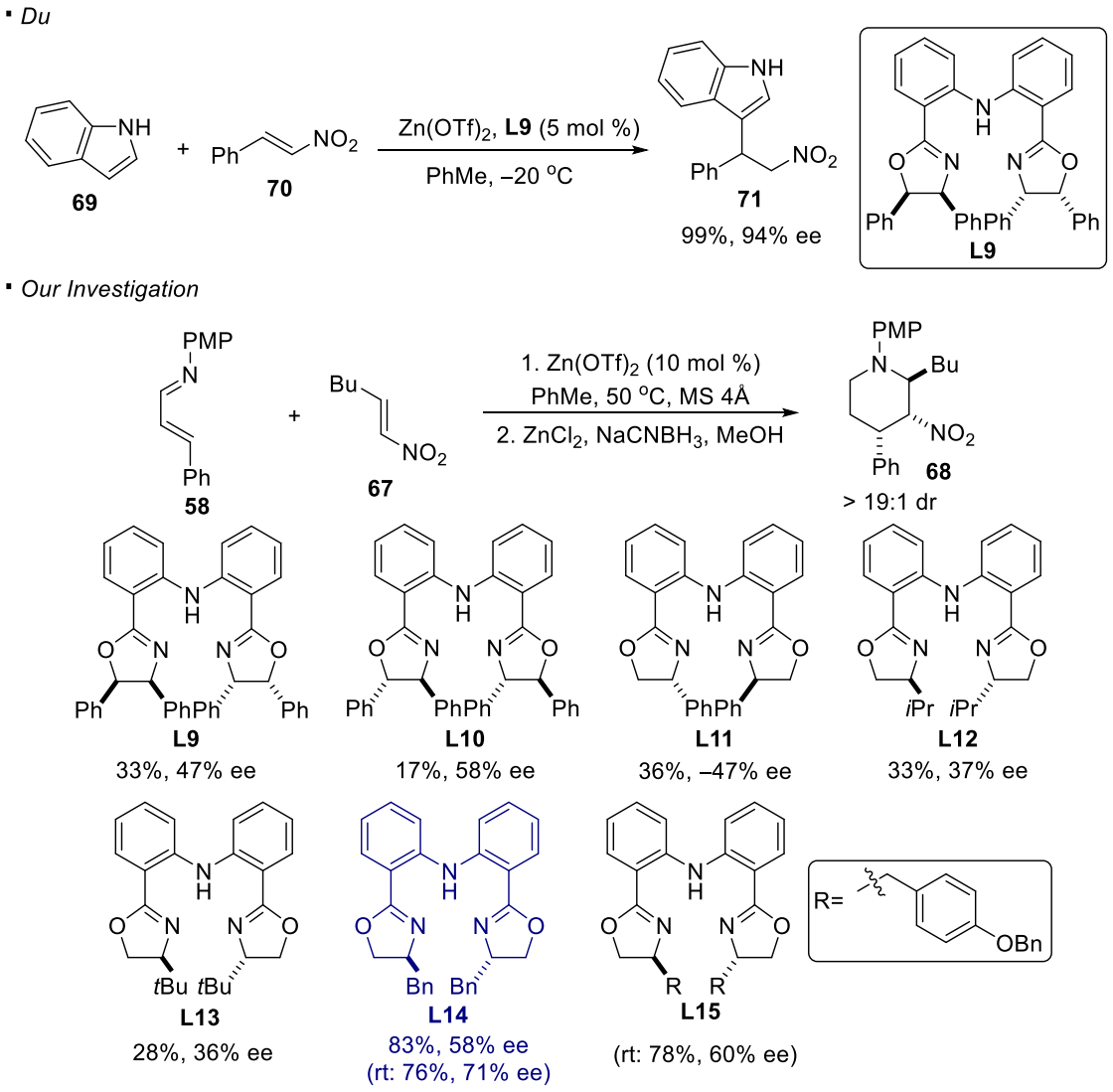

Scheme 1.2.2: Screening of BOPA Ligands Derived from Different Amino-alcohols

Inspired by Du's work on Zn-catalyzed enantioselective Michael addition with nitro-alkenes and indoles,[30] we investigated the use of BOPA (bis(oxazolinylphenyl)amide) ligands. Ligand **L9** gives an enantioselectivity (47% ee) similar to that obtained with **L8**. Considering its ease of modification, we focused on the use of BOPA ligands for subsequent studies. Screening with BOPA ligands derived from commercial chiral amino alcohols or those derived from amino acids was undertaken (Scheme 1.2.2). Changing the *syn*-relation of the two phenyl groups in **L9**

to *anti* in **L10** leads to a slight increase in enantioselectivity. **L11**, which bears one phenyl group at each oxazoline, gives the same enantio-control as **L9**. Different substituents at the oxazolines have a significant impact on the outcome of the reaction. With bisoxazolines **L12** and **L13**, derived from valine or *tert*-leucine respectively, a decrease in stereoselectivity was found. The use of phenylalanine-derived ligand **L14** gives essentially the same selectivity as ligand **L10** with a much higher conversion. This higher catalytic efficiency allows the reaction to be conducted at rt and leads to an improvement in enantiomeric excess (71%). However, attempts to further lower the temperature result in poor conversion (<5%). **L15**, despite having extended benzyloxy groups at the *para* positions compared to ligand **L14**, does not lead to any improvement of stereochemical control. With ligand **L14**, extensive optimization with Zn(II) sources, solvents, concentration, metal/ligand ratio were undertaken, but no improvement in stereoselectivity was achieved.

1.2.2 Structural and Selectivity Relationship of BOPA Ligand

Seeking new directions to improve the catalyst, we turned our attention toward understanding how the ligand's structure impacts enantioselectivity. To this end, we synthesized the sulfur- and oxygen-analogues of BOPA ligands **L16** and **L17**. A significant reduction in enantioselectivity with the sulfur analogue **L16** is observed while the oxygen analogue **L17** gives the opposite enantiomer in moderate selectivity (Scheme 1.2.3). Considering the similar bond length and bond angle an oxygen atom and a nitrogen atom can adopt, we attributed the different behavior with ligands **L14** and **L17** to the presence of the N-H bond in ligand **L14**. This is confirmed with ligand **L18**, which gives no apparent stereochemical control for the [4+2] cycloaddition. Although the significance of the N-H bond in the BOPA ligands remained unclear,

this observation is consistent with previously published Zn-catalyzed enantioselective Michael additions with this class of ligands.[31]

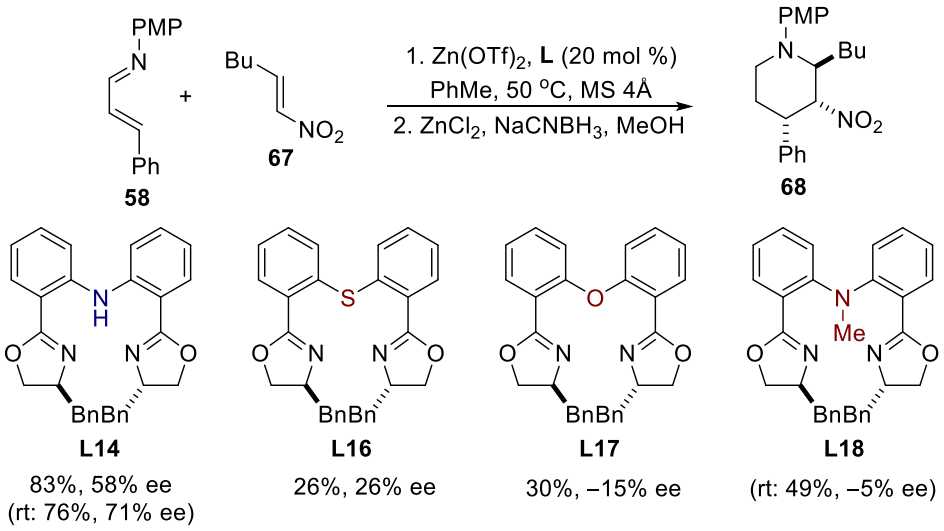

Scheme 1.2.3: Significance of N-H Bond in BOPA Ligands

In addition to the N-H bond, the role of the bisoxazolines were also studied. Ligand **L19**, bearing one oxazoline unit and a methyl ester was synthesized. This ligand lacking the C2 symmetry in the BOPA ligand resulted in product formation with reversal of enantioselectivity and little stereochemical control (Scheme 1.2.4). The result suggests that both oxazolines are necessary for the enantioselectivity observed with ligand **L14**.

1.2.3 Electronic Effects of BOPA Ligands

After demonstrating the importance of both the N-H bond and the presence of both oxazoline units on the ligand, we became curious how the electronics of the BOPA ligands could affect enantioselectivity. Little effort has been devoted to study the electronic effects of BOPA ligands on metal-catalyzed reactions. The Du group reported the synthesis of BOPA ligands **L20** and **L21** and their use in a Zn-catalyzed Michael addition reaction of indole **69** to nitro-styrene

70.[32] Their results show that the electronics of the BOPA ligands have essentially no impact on both the stereochemical outcome and the catalytic efficiency of the reaction (Scheme 1.2.5).

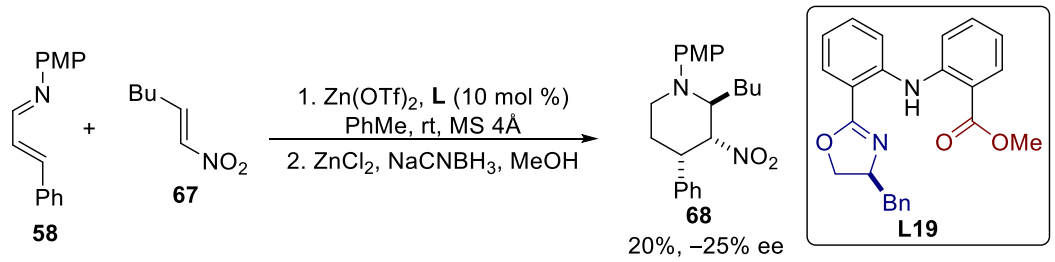

Scheme 1.2.4: Significance of Bisoxazolines in BOPA Ligands

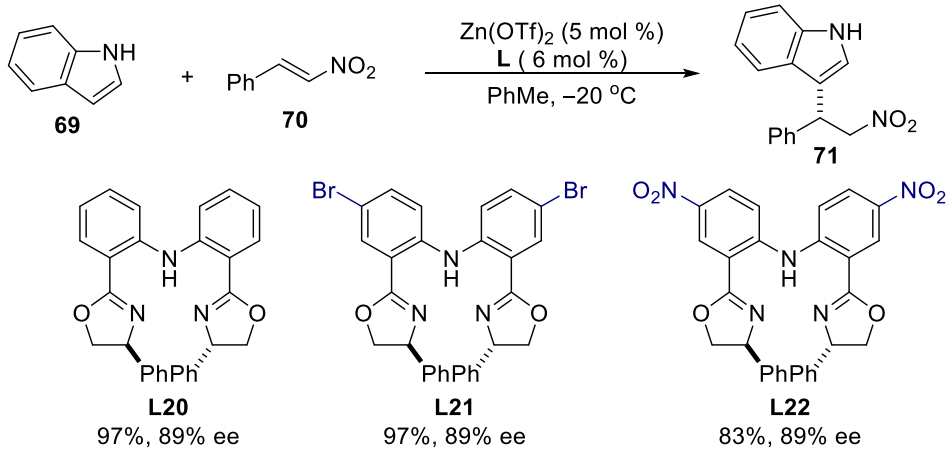

Scheme 1.2.5: Lack of Electronic Effect of Ligands for Zn-catalyzed Michael Addition

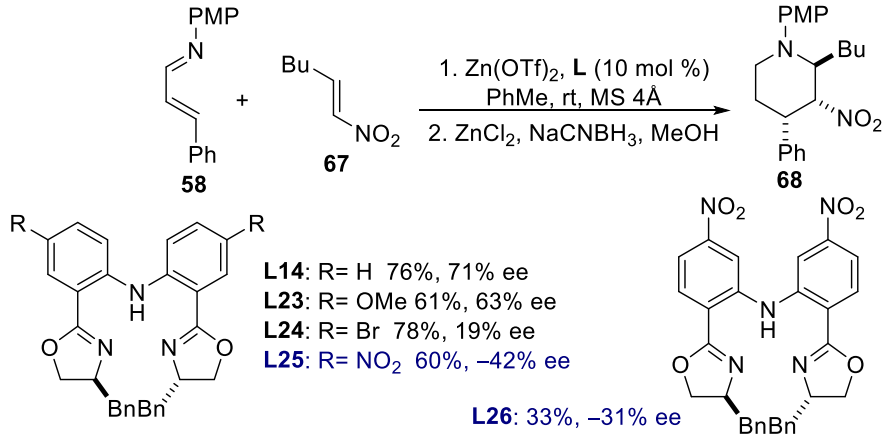

Scheme 1.2.6: Intriguing Electronic Effect of Ligands on Enantioselectivity

In contrast to Du's work, our reaction is highly sensitive to the electronic properties of the BOPA ligands (Scheme 1.2.6). The enantioselectivity decreases when the electron density of the BOPA ligands decreases. With novel ligand **L23**, a slight drop of enantioselectivity was observed. The use of more electron-deficient ligand **L24** results in a larger decrease in selectivity. Intriguingly, with the BOPA ligand **L25**, the opposite enantiomer is formed in moderate enantiomeric excess. The reversal of enantioselectivity is also observed with novel ligand **L26**. Since the *m*-nitro and *p*-nitro benzoic acid have almost the same pka,[33] the electronics of the bisoxazoline units in ligands **L25** and **L26** should be similar. On the other hand, due to delocalization of the lone pair of nitrogen to the nitro group in **L26**, the N-H bond in ligand **L25** should be significantly less acidic.[34] Therefore, the similar stereochemical control observed with **L25** and **L26** suggests that the reversal of enantioselectivity observed is due to the change in the electronics of the bisoxazoline units, rather than the acidity of the N-H bond.

We applied σ values, which were first used to describe the electronic effects of different substituents on the aromatic rings on the acidity of benzoic acids, to quantify the electronic effect of the bisoxazoline units on the enantioselectivity.[35] A Hammett plot indicates that such relationship is linear (Figure 1.2.1). The y-axis is $\log(k_1/k_2)$, where k_1 and k_2 are the rates of the formation of the two enantiomers, and k_1/k_2 is thus the enantiomeric ratio of the reaction.

Although the origin of the electronic effects was unclear at this point, we reasoned that 4-methoxy groups would increase the electron-density of the bisoxazoline and **L27** would confer excellent enantioselectivity, as guided by the Hammett plot. Disappointingly, novel ligand **L27** gives an even lower enantio-control than the electron-neutral BOPA ligand **L14** (Scheme 1.2.7). The puzzling behavior of this ligand could be explained by the previously reported crystal

structure of a Zn complex bearing a thio-linker analogue of BOPA (Figure 1.2.2).[36] The crystal structure showed that the phenyl rings and the oxazolines are nearly perpendicular to each other. Therefore, there is a minimal overlap between the p-orbitals of the oxygen in OMe groups and the π orbitals of the oxazolines. Thus, the delocalization of the lone pair of oxygen to the oxazolines is minimized. The σ electron-withdrawing nature of the oxygen becomes dominant and renders the 4-OMe groups in ligand **L27** electron-withdrawing. A similar scenario is observed in *m*-OMe benzoic acid where the *m*-OMe group behaves as a mild electron-withdrawing group and increases the acidity of the benzoic acid.[33] We are aware that the aromatic backbone and the bisoxazoline unit are only slightly out of plane in the crystal structure of a Ca-BOPA complex.[37] However, in this case, the N-H bond is deprotonated by a strong base and the resulting negative charge on nitrogen might require the backbone and the bisoxazoline to be in plane for stabilization by delocalization.

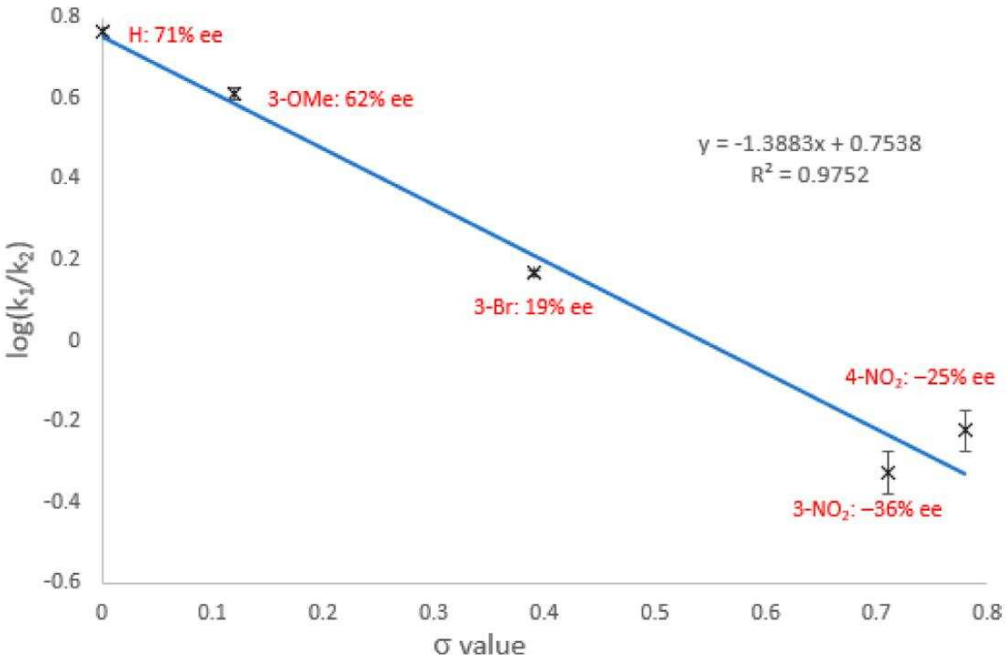

Figure 1.2.1: Hammett Plot for Linear Relationship for Electronic Effect

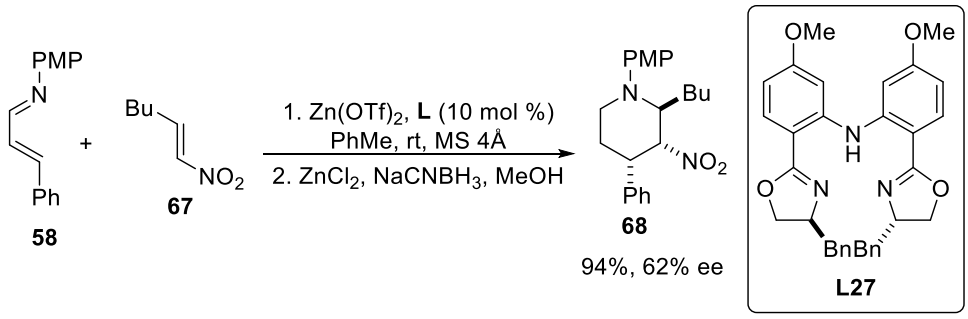

Scheme 1.2.7: [4+2] Cycloaddition with BOPA Ligand Bearing p-OMe Groups

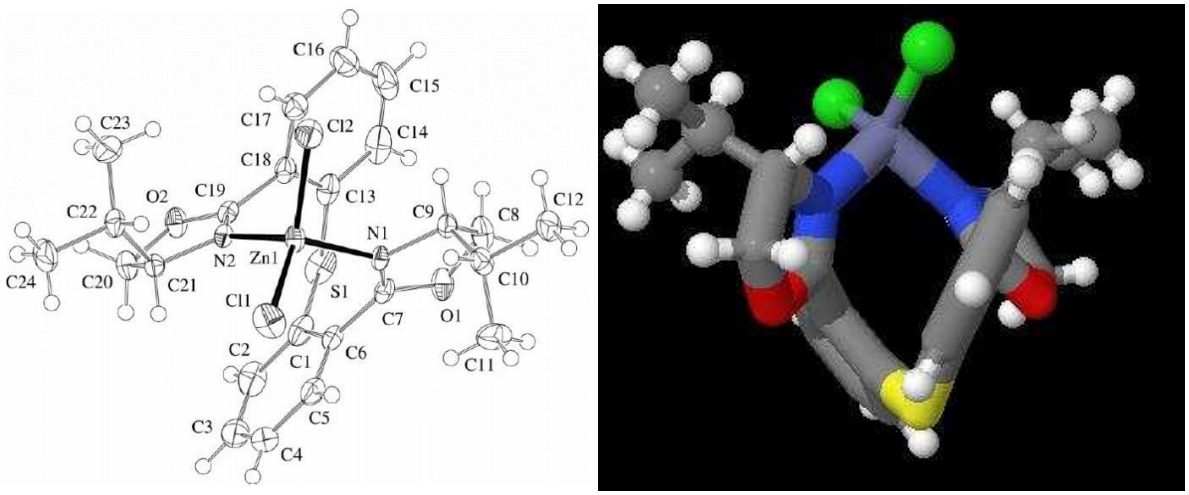

Figure 1.2.2: Crystal Structure of a thio-analogue of BOPA Ligand

An alternative strategy to harness the observed electronic effect was to render the bisoxazolines highly electron deficient to favor the formation of the opposite enantiomer. To this end, *ortho*-nitro bisoxazolines **L28** was synthesized (Scheme 1.2.8). Disappointingly, the use of ligand **L28** provides no stereochemical control. We reasoned that the oxazolines might not be electron-rich enough to coordinate to Zn and thus fluorinated BOPA ligand **L29** was synthesized. Surprisingly, this ligand gave the same level of enantiomeric induction as the parent unsubstituted ligand. More synthesis and screening of more ligands revealed that the electronic effect disappeared in the presence of *ortho* substituents to the oxazolines. F-, Cl-, OMe- and Me-

bearing BOPA ligands (**L29**, **L30**, **L31** and **L32**) give no apparent difference in the enantiomeric excess of the product.

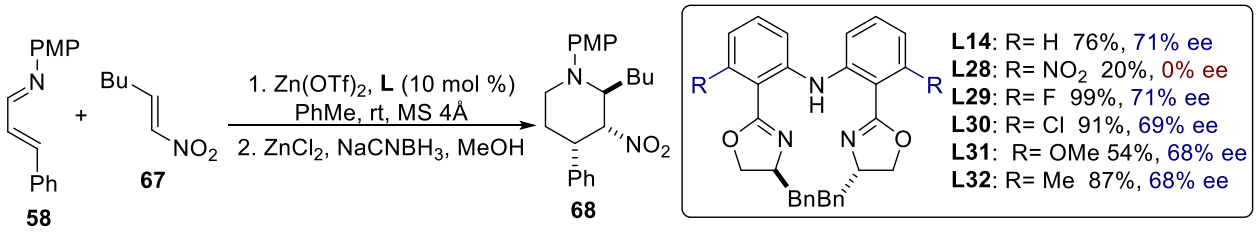

Scheme 1.2.8: Disappearing Electronic Effects of *ortho*-substituted Bisoxazoline

1.2.4 Mechanism, Origin of Electronic Effect and Implications

▪ *Concerted Aza-Diels Alder Cycloaddition*

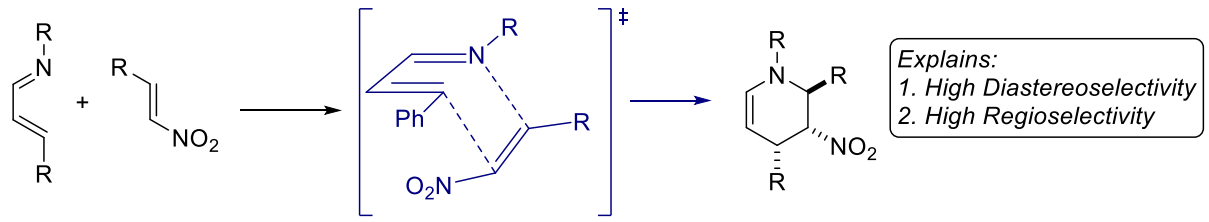

▪ *Stepwise Aza-Michael Addition/Cyclization*

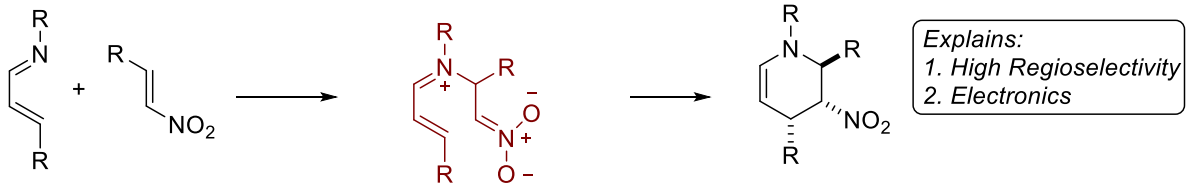

Figure 1.2.3: Concerted and Stepwise Mechanisms for aza-[4+2] Cycloaddition

We strived to gain insight into the mechanism in order to understand the origin of the electronic effects. The cycloaddition can potentially proceed through a concerted (aza-Diels Alder cycloaddition) or a stepwise (aza-Michael addition followed by cyclization) mechanism (Figure 1.2.3). It is tempting to believe a concerted mechanism is operative because the high diastereoselectivity can be easily explained by an endo-transition state, as in many cases of the

all-carbon [4+2] Diels-Alder reaction. In addition, the nitrogen atom has the highest coefficient in the HOMO of the 1-azadienes and the β carbon has the highest coefficient in the LUMO of the nitro-alkene. The favorable interaction between the nitrogen of the 1-azadiene and the β-carbon of the nitro-alkene can explain the high regioselectivity of the cycloaddition if a concerted normal-electron-demand aza-Diels Alder cycloaddition is invoked. On the other hand, considering the high electron-deficiency of both reaction partners, the overlap between the HOMO of the 1-azadiene and the LUMO of the nitro-alkene would not be effective. This prompted us to design control experiments to differentiate the two mechanisms.

First, the feasibility of a concerted mechanism was probed. 1,4-diphenyldiene and nitro-alkene were subject to the reaction conditions, compared to 1-azadiene, the more electron rich nature of **72** should favor the [4+2] cycloaddition if a concerted mechanism is operative. However, no cyclohexene **73** is formed under the reaction conditions (Scheme 1.2.9). In addition, the role of the Zn catalyst is difficult to explain in the concerted mechanism. The Lewis acidity of the Zn catalyst would increase the electron-deficiency of the 1-azadiene and/or the nitro-alkene and should disfavor the required HOMO/LUMO interaction for a concerted cycloaddition.

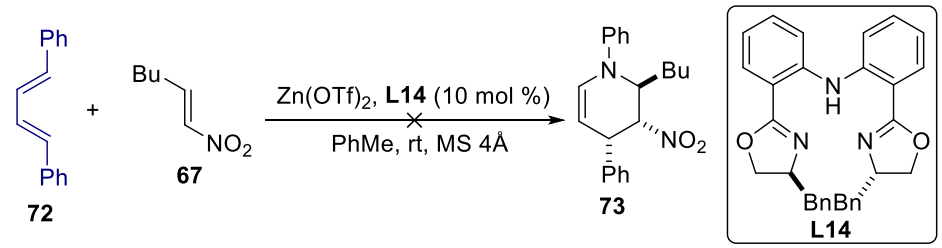

Scheme 1.2.9: No Cycloaddition with 1,4-diphenylbutadiene

We then investigated the viability of a stepwise mechanism. Jorgensen previously reported a thiourea- catalyzed aza-Michael addition reaction of imine **74** with nitro-alkene **75**

(Scheme 1.2.10).[38] Thiourea catalyst **76** was proposed to activate nitro-alkene **75** through hydrogen bonding and increases its electrophilicity to allow for the nucleophilic attack of the imine **74**. When the same conditions were applied to 1-azadiene **58**, instead of imine **74**, the aza-[4+2] cycloadduct **68** was formed, indicating the feasibility of the stepwise aza-Michael addition/cyclization pathway. Similarly, when imine **75** was treated with nitro-alkene **75** in the presence of Zn(II)-catalyst, the formation of aza-Michael adduct **77** implicates a stepwise aza-Michael addition/cyclization pathway in our aza-[4+2] chemistry.

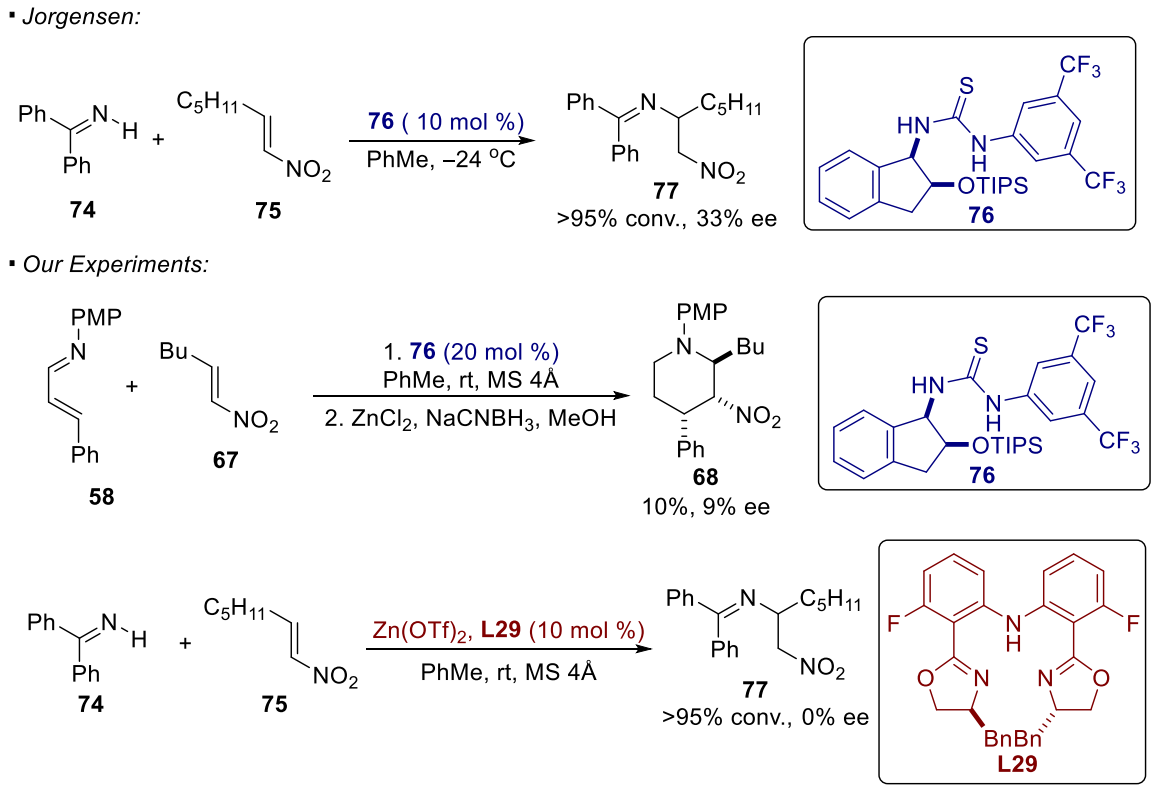

Scheme 1.2.10: Feasibility of Stepwise aza-Michael/Cyclization Pathway

Thirdly, secondary kinetic isotope studies[39] were undertaken (Scheme 1.2.11). An inverse secondary kinetic isotope effect was observed with nitro-alkene **67** but not 1-azadiene **78**. This result is consistent with a change of hybridization state of sp^2 to sp^3 of the β carbon of the nitro-

alkene but not the 1-azadiene. This implicates a stepwise mechanism with the aza-Michael addition as the turnover-limiting and the enantio-determining step. Overall, all our experimental results support a stepwise mechanism.

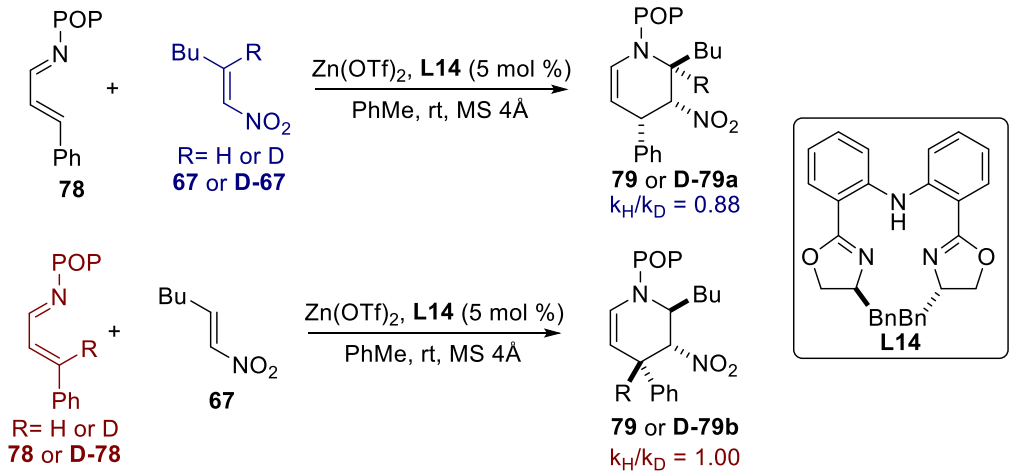

Scheme 1.2.11: Secondary Kinetic Isotope Studies

▪ *RajanBaBu*

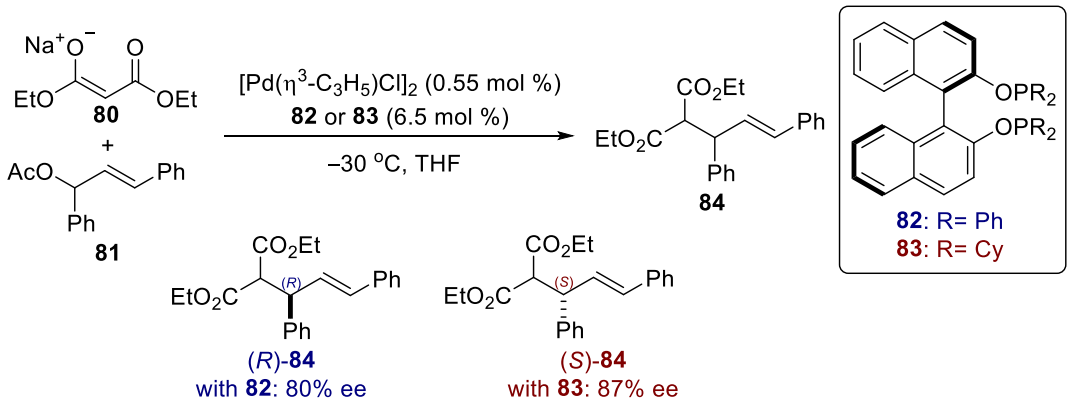

Scheme 1.2.12: Reversal of Enantioselectivity due to Structural Change of Catalysts

With a better understanding of the mechanism of the reaction, we were poised to probe the origin of the electronic effects of the BOPA ligands in the aza-[4+2] cycloaddition. Hayashi has recently reviewed the reversal of enantioselectivity with catalysts of the same chiral sources.[40]

The phenomenon of the reversal of enantioselectivity are mostly explained by three factors, a structural change of the catalysts, the presence/absence of hydrogen bonding and a change in the mechanism. These were the three hypotheses that we initially formulated to explain the electronic effect.

Concerning the structural change of catalysts, RajanBaBu reported that in the event of Pd-catalyzed allylation of diethyl malonate **80**, different absolute stereochemistry of product **84** can be obtained with the same chiral source when the R group on the axially-chiral phosphine ligands changes from phenyl to cyclohexyl ring (Scheme 1.2.12).[41] Supported by the drastically different NMR spectra of the two Pd catalysts formed by the two ligands **82** and **83**, it is proposed that the structural differences of the Pd catalysts upon switching ligands leads to the formation of different enantiomers in the reaction. We speculated that different coordination environments of Zn with BOPA ligands of different electronics would contribute to the observed trend in enantioselectivity in our aza-[4+2] cycloaddition. However, no electronic effect of the ligand was observed with the previously- reported Zn-catalyzed Michael addition of indoles to nitro-alkenes using the same class of ligands (Scheme 1.2.5).[32] Not only was there no reversal of enantioselectivity, the application of BOPA ligands of different electronics gave essentially the same level of enantiomeric excess of the Michael adduct and an insignificant change in catalytic efficiency. This observation suggests a structural change of the Zn complex as the origin of the electronic effect is not likely.

To explain the reversal of enantioselectivity obtained with bisoxazolines **86** and **87**/**88** for the same transformations, Ait-Haddou and Balavoine propose the presence of a hydrogen bond between the hydroxyl group in **86** and the nucleophile, the sodium salt of dimethyl malonate

(Scheme 1.2.13).[42] While a structural difference between Pd complexes ligated by **86** and **88** is disproved by X-ray crystallography, the proposal for the hydrogen bonding is supported by the lack of the reversal of enantioselectivity with dimethyl malonate-derived silyl enol ether, which does not possess a negative charge on oxygen for hydrogen bonding interaction, as the nucleophile.

- *Ait-Haddou and Balavoine*

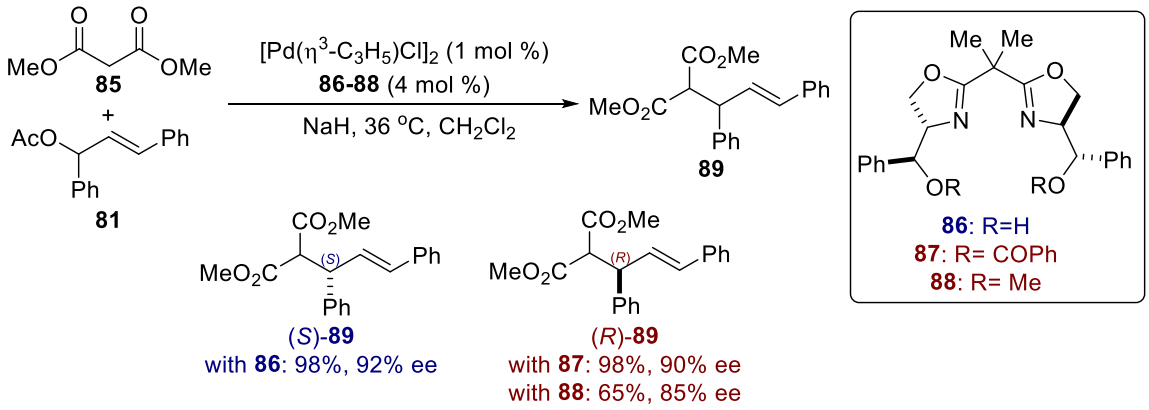

Scheme 1.2.13: Reversal of Enantioselectivity due to Hydrogen-bonding

Since the N-H bond is significant in achieving the observed enantioselectivity in our aza-[4+2] cycloaddition, the change in the strength of a putative hydrogen bond appeared to us a plausible origin of the electronic effects of the BOPA ligands. In this case, drastically different stereoselectivity would be expected for **L25/L26** or **L23/L27** because there is a significant difference in the acidity of the N-H bond. The essentially equal enantioselectivity obtained with these two sets of ligands strongly implies that the change in hydrogen-bonding strength or the acidity of the N-H bonds is not the origin of the electronic effect (Scheme 1.2.14).

Sawamura and Ito put forward two competitive pathways to explain the different absolute stereochemistry of the hydrogenation product **93** catalyzed by Rh(I) ligated by different

TRAP ligands **91** and **92** at different pressure of hydrogen gas (Scheme 1.2.15). Casey reported a stereo-divergent formation of **96** from Pt-catalyzed hydroformylation of styrene **94** at different temperatures. It is proposed that the enantio-determining step changes from platinum hydride addition at high temperature to partially reversible alkyl migration to CO and hydrogenolysis at low temperature.

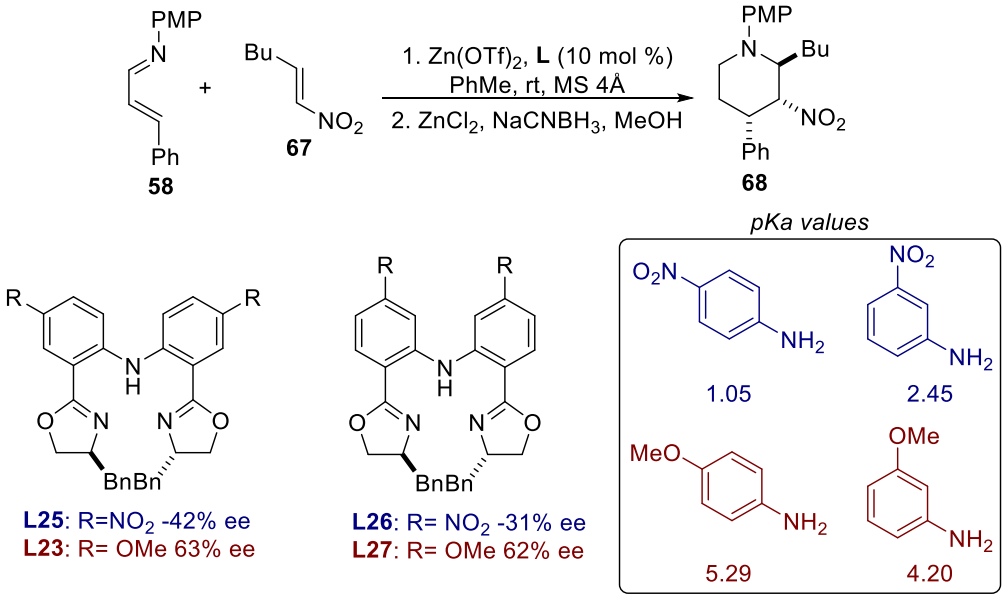

Scheme 1.2.14: Counter-evidence for Hydrogen Bond as Origin of Electronic Effects

We were curious whether a change in the reaction mechanism attributed to the observed electronic effect of the BOPA ligands on stereoselectivity in the aza-[4+2] Cycloaddition. When the BOPA ligand becomes less electron rich, the increased Lewis acidity of the Zn complex would accelerate the aza-Michael step. On the other hand, the Zn nitronate intermediate is more stabilized and the cyclization step would become slower. This change in the relative rate of the two steps could potentially lead to a switch in the enantio-determining step from the aza-Michael addition step to the cyclization step. In this case, if the chiral element of the Zn complex favored

the formation of different enantiomers in the Michael and cyclization step, a reversal of enantioselectivity could be obtained. To test this hypothesis, secondary kinetic isotope effects with ligands of different electronics were investigated (Scheme 1.2.16). The same inverse secondary kinetic isotope effect from **L14**, **L29** and **L26** contradicts the hypothesis and suggests that the aza-Michael addition step remains the turnover-limiting step and enantio-determining step with all ligands.

- *Sawamura and Ito: Two Competitive Pathways*

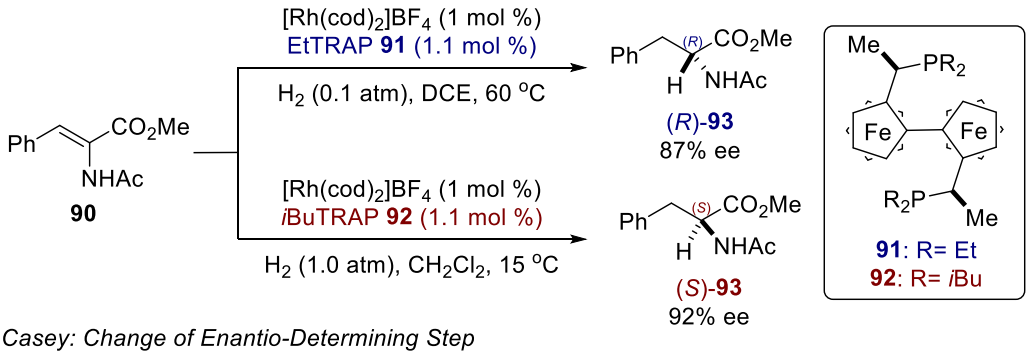

- *Casey: Change of Enantio-Determining Step*

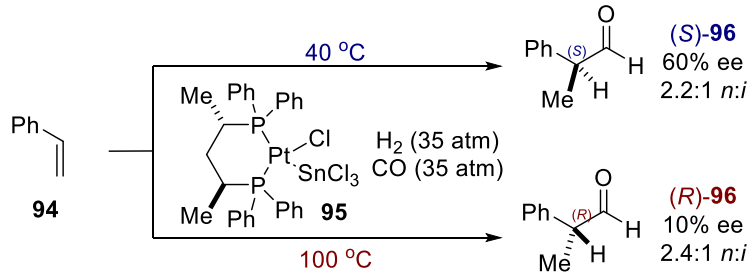

Scheme 1.2.15: Reversal of Enantioselectivity due to Change of Reaction Mechanism

Further evidence that supports the aza-Michael addition is the enantio-determining step with ligands of different electronics is established with the use of α-methyl nitro-ethylene **97** (Scheme 1.2.17). With **97**, no stereogenic center is formed in the first aza-Michael addition step. Therefore, opposite enantiomers would still be expected with ligands **L14** and **L26** if the secondary cyclization step was enantio-determining for these ligands. In the cycloaddition of **97**

and **78**, the same enantiomer is obtained with both ligands **L14** and **L26**. This observation is consistent with the establishment of the absolute stereochemistry in the first aza-Michael addition step with both ligands in the case of nitro-alkene **67**.

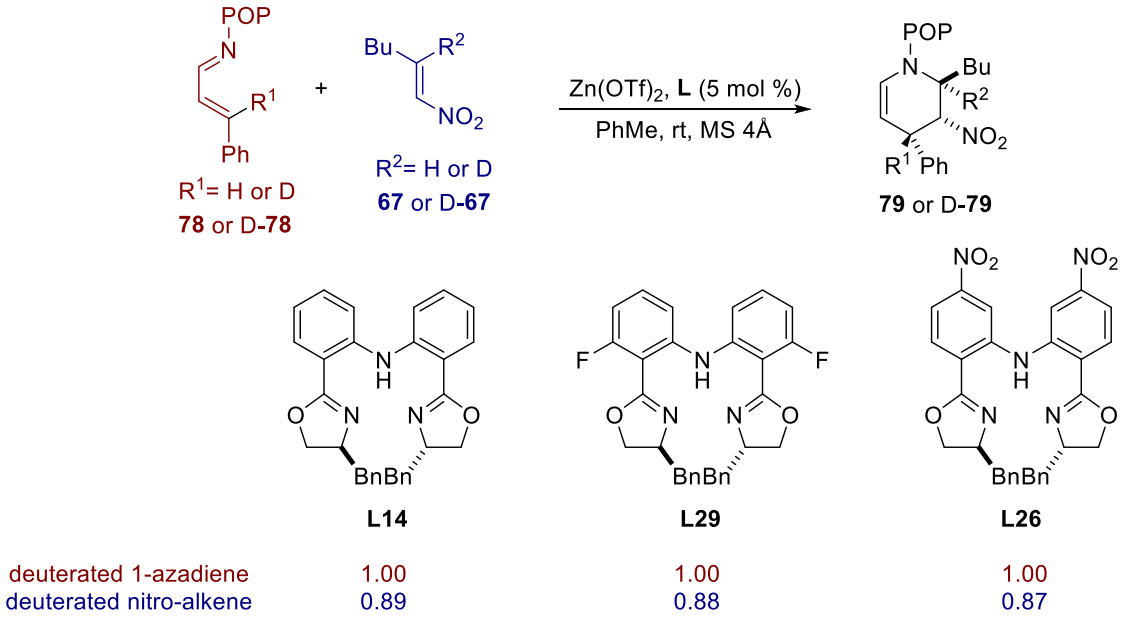

Scheme 1.2.16: Secondary Kinetic Isotope Effects with Different Ligands

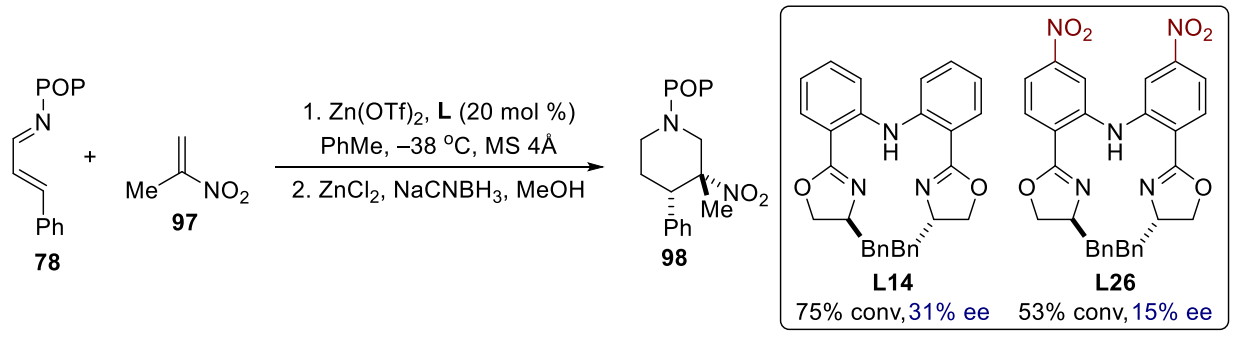

Scheme 1.2.17: Formation of Same Enantiomer with α-methyl Nitro-ethylene

While studying the impact of the substituents of nitrogen in 1-azadienes, we observed a trend that could shed light on the origin of the electronic effect. The enantioselectivity of the reaction increases with the electron density of the 1-azadienes but the exceptionally rich 1-

azadiene **101** gives the same selectivity as **58** (Scheme 1.2.18). To explain this observation, we hypothesized that 1-azadiene **101** can deleteriously coordinate to the Zn catalyst, forming a distorted Zn complex that gives rise to the formation of the opposite enantiomer (Figure 1.2.3). Such distorted Zn complex was only formed when the 1-azadiene is highly electron-rich.

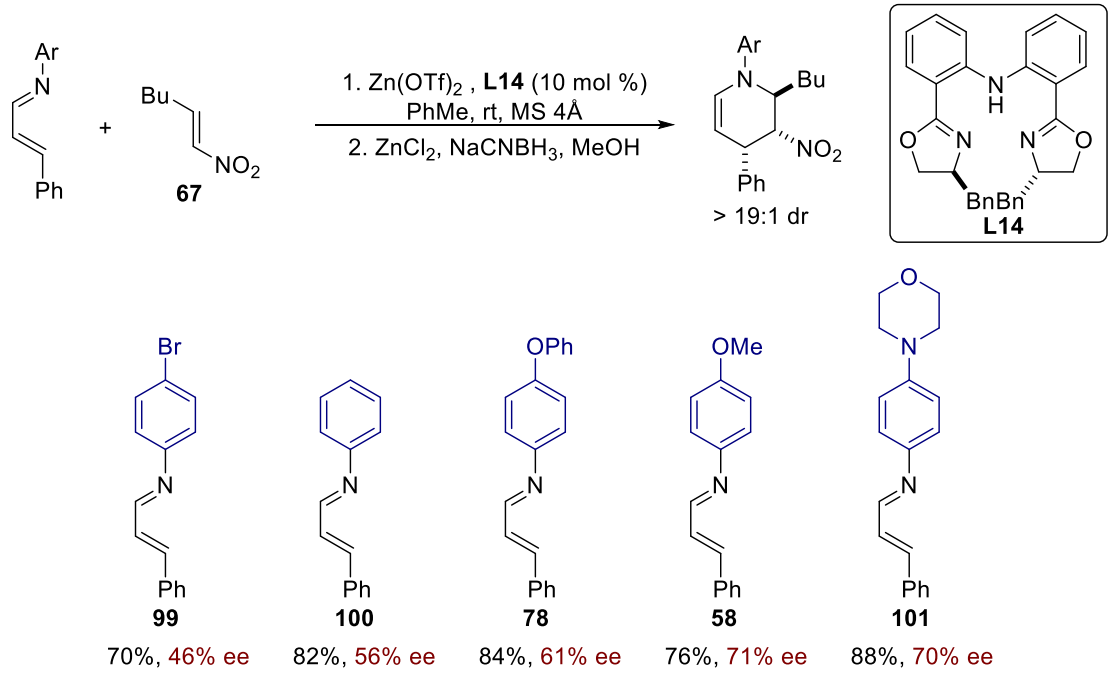

Scheme 1.2.18: Electronic Effect of 1-azadienes on Enantioselectivity

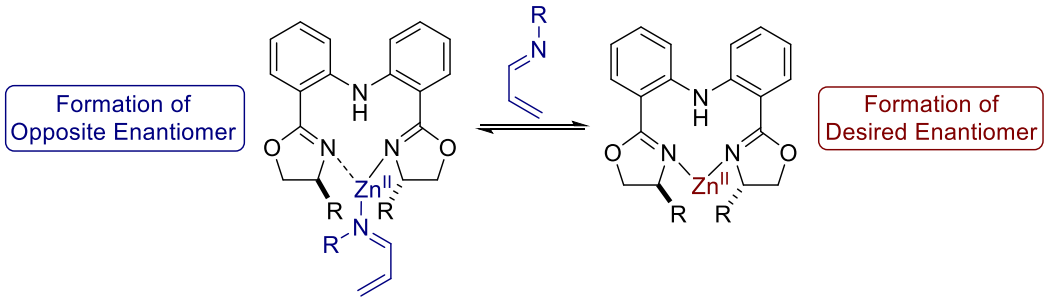

Figure 1.2.3: Origin of Electronic Effect

To test this hypothesis, electron-rich imine **102** was added for the [4+2] cycloaddition of **58** and **67** with ligand **L14** (Scheme 1.2.19). The observed drop in enantioselectivity is consistent

with the formation of a Zn complex that gives a lower level of enantio-control through the coordination of iminyl nitrogen in **102** to Zn.

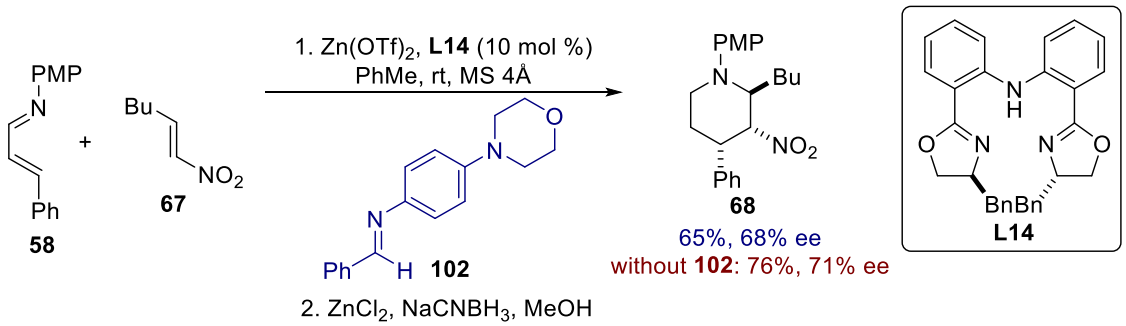

Scheme 1.2.19: Drop in Enantioselectivity in the Presence of Imine Additive

To explain the electronic effect of the ligands, we hypothesized that Zn catalysts with less electron rich bisoxazolines are more susceptible to the coordination of the 1-azadienes and would thus exhibit a larger drop in enantioselectivity or a reversal of enantioselectivity.

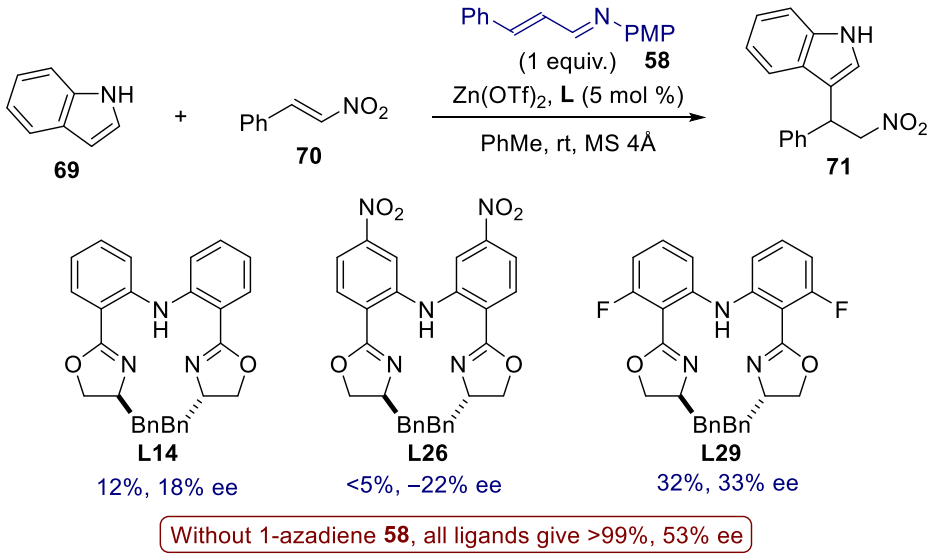

Scheme 1.2.20: Evidence for Undesired Coordination of 1-azadiene as Origin of Electronic Effect

We verified the hypothesis with an established Michael addition of indole **69** and nitro-styrene **70** catalyzed by Zn(BOPA) catalysts.[32] In the absence of 1-azadiene, the same enantiomer

of **71** is obtained with the same yield and same level of stereochemical control, regardless of the electronic properties of the BOPA ligands on Zn (Scheme 1.2.20). On the other hand, the same electronic effect on enantioselectivity of the BOPA ligands as in our [4+2] cycloaddition was observed in the presence of 1-azadiene **58**. The opposite enantiomer is formed with highly electron deficient bisoxazoline **L26** and the electronic effect is minimized with bisoxazolines bearing *ortho*-substituent **L29**. Therefore, we believe the undesired coordination of 1-azadiene to the Zn catalysts is the origin of the electronic effect on the stereochemical outcome of the [4+2] cycloaddition. This coordination is disfavored when the bisoxazolines bear *ortho*-substitution because of sterics, explaining the disappearing electronic effects with this class of BOPA ligand.

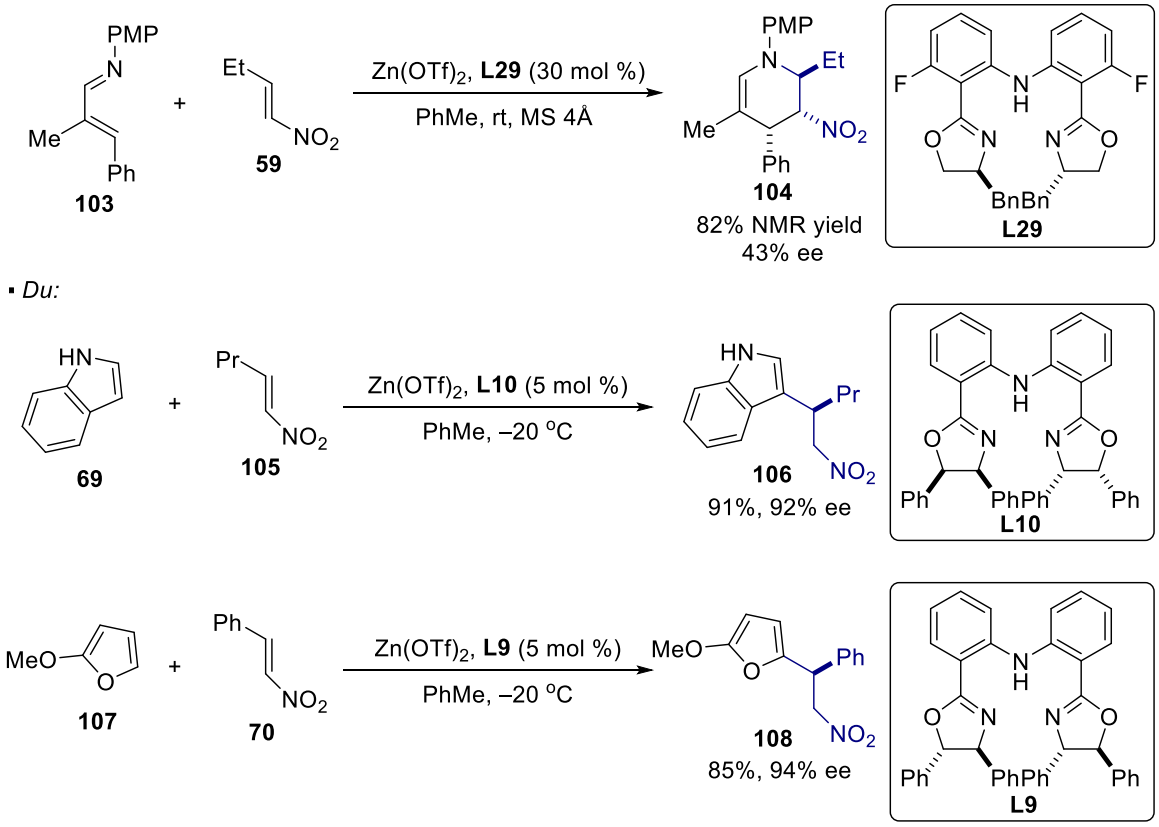

Scheme 1.2.21: Consistency of Absolute Stereochemistry

The absolute stereochemistry of the aza-[4+2] cycloaddition was also established for the comparison of that obtained with the aza-Michael addition catalyzed by Zn-BOPA complexes (Scheme 1.2.21). 3-methyl-substituted 1-azadiene **103** was subject to the reaction conditions to give enantiomerically-enriched cycloadduct **104**, which was previously synthesized and characterized.[28] Through the measurement of the optical activity, the absolute stereochemistry of **104** was determined (Scheme 1.2.21). This stereochemical outcome is consistent with that obtained from enantioselective Michael additions of other nucleophiles to nitro-alkenes catalyzed by Zn-BOPA complexes with **L10** and **L9**, which have the same configuration at the bisoxazolines.[30,43]

In addition to the enantioselectivity, we observed that the yield of the model aza-Michael addition reaction is also impacted by the electronics of the BOPA ligands (Scheme 1.2.20). A lower conversion to **71** is obtained with more electron deficient BOPA ligand **L26** while this decrease in conversion is recovered when using ortho-substituted bisoxazoline ligand **L29** that minimize undesired coordination of 1-azadiene to the Zn catalysts. Therefore, the deleterious coordination of 1-azadiene does not only impact the stereochemical outcome, but also the catalytic efficiency. This implication regarding the catalytic efficiency should be put into serious consideration at lower reaction temperature because the coordination of the 1-azadiene has a lower entropy cost. While the use of **L14** in our [4+2] cycloaddition leads to poor conversion (<5%) at 0^{o}C, we proposed that this poor conversion at low temperature can be overcome by the higher catalytic efficiency with the *ortho*-substituted BOPA ligands and the low reaction temperature would serve as a solution to achieving high enantioselectivity.

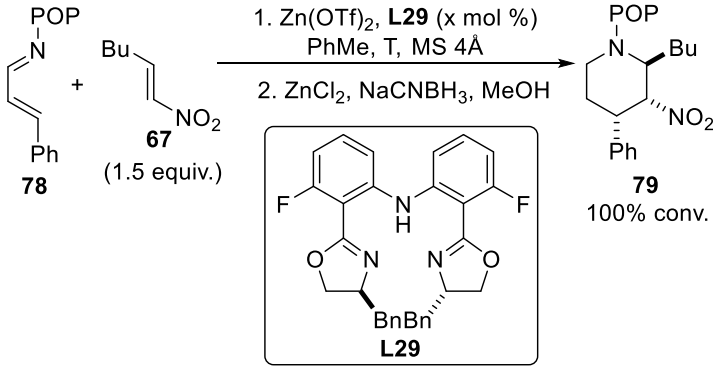

x	T (°C)	conc (M)	t (d)	ee (%)
10	rt	0.09	<1	61
10	3	0.09	<1	73
10	–18	0.09	2	78
10	–38	0.09	5	89
20	–38	0.09	3	89
20	–38	0.18	1.5	89
20	**–38**	**0.18**	**1**	**89[a]**

a: 3 equiv. nitro-alkene, 82% isolated yield

Scheme 1.2.22: Optimization with *ortho*-substituted BOPA ligand

Due to solubility issues, *N*-(4-phenoxyphenyl)-1-azadiene **78** was used to investigate the temperature effect (Scheme 1.2.22). We were delighted to find that the [4+2] cycloaddition with **L29** proceeds smoothly at 3 °C with a slight increase in enantioselectivity, consistent with our proposal. The reaction temperature can be further adjusted to −18 °C with increased reaction time. In this case, the ee increases slightly to 78%. In order to improve the stereoselectivity, we further lowered the temperature to −38 °C and high enantiomeric excess (89%) was obtained, albeit with a longer reaction time (4 days). We were able to shorten the reaction time to 1 day by increasing the catalytic loading, the amount of nitro-alkene and the concentration. The desired 3-nitro piperidine product was isolated in 82% yield and 89% ee with 20 mol % Zn catalyst at 0.18 M.

1.2.5 Reaction Scope under Optimized Conditions

With the optimized conditions, the scope of the reaction was investigated (Scheme 1.2.23). Due to differences in solubility, the reaction time did not reflect the intrinsic reactivity of the 1-azadiene and different concentrations were applied. Regardless of the electronic nature of

the aromatic ring on nitrogen in the 1-azadiene, excellent yields of the cycloadducts (**79**, **68** and **109**) can be obtained. Compared to **79**, the enantioselectivity of **109** drops as the aromatic ring becomes less electron rich. The more electron rich 4-methoxyphenyl cycloadduct **68** also gives a lower ee than **79**. Given that an opposite trend is obtained at rt, this observation is consistent with a lower entropy cost for the undesired coordination of the 1-azadiene to the Zn catalyst at lower temperatures.

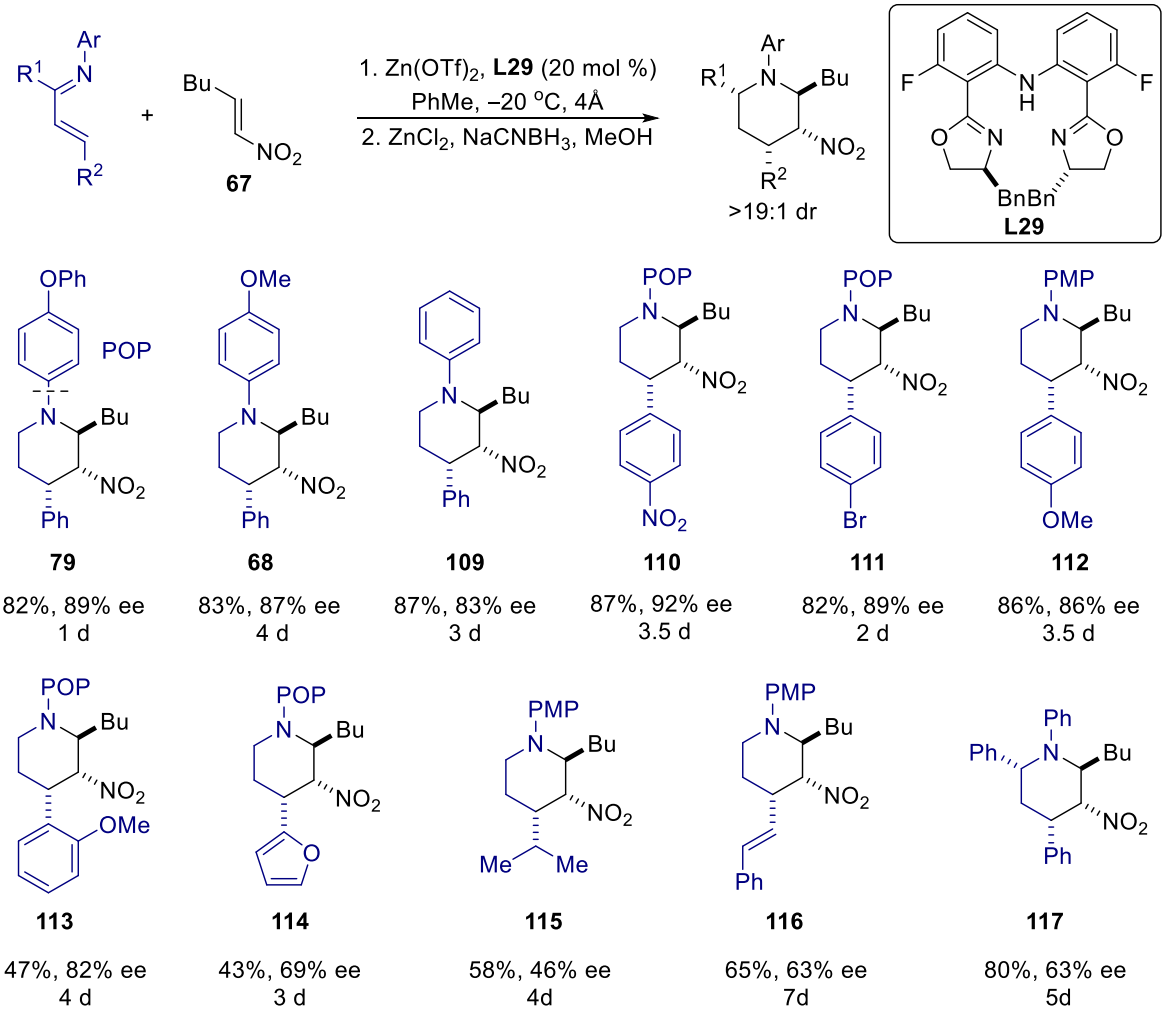

Scheme 1.2.23: The Scope of 1-Azadienes

To study the effect of the 4-substituents of 1-azadiene, different protecting groups on nitrogen are used and the one with a higher solubility is always used (Scheme 1.2.23). The yield does not vary with the electron density of the 4-substituent in the 1-azadiene. Cycloadducts **110**, **111** and **112** are all obtained in excellent yield. On the other hand, the enantioselectivity decreases when the substituents become more electron rich. This trend is again consistent with the proposed undesired coordination of 1-azadienes to Zn. The *ortho* substitution has a large impact on the yield and the cycloadduct **113** is obtained in moderate yield with a slight decrease of enantioselectivity. The reaction with the furan-substituted 1-azadiene is sluggish and affords **114** in moderate yield and ee. With a 1-azadiene derived from an aliphatic enal, the yield and the enantioselectivity of **115** are modest. The reaction of more conjugated azatriene does not go to completion, even in the presence of a large excess of the nitro-alkene and a higher catalyst loading and the cycloadduct **116** is obtained in moderate enantioselectivity. Excellent yield of cycloadduct **117** can be obtained from chalcone-derived 1-azadiene with a moderate level of stereochemical control.

For the scope of the nitro-alkenes, as the nitro-alkenes become more sterically bulky, the reaction gives the cycloadducts (**79** vs **118** and **119**) in lower enantioselectivity and requires a longer reaction time and/or a higher catalyst loading (Scheme 1.2.24). With even more bulky isopropyl nitro-alkene, an even bigger drop in enantiomeric excess in cycloadduct **120** is observed. Protected alcohol in the nitro-alkene is tolerated. This opens the possibility of further manipulation of piperidine **121** after the aza-[4+2] cycloaddition. The cycloaddition with nitro-ethylene proceeds to give the product **122**. However, its instability hinders the determination of enantioselectivity. α-methyl nitro-ethylene is not a competent reaction partner and its use gives

123 in both moderate yield and ee. The use of nitro-styrene or more conjugated nitro-alkenes results in no conversion and the formation of **124** and **125** is not observed.

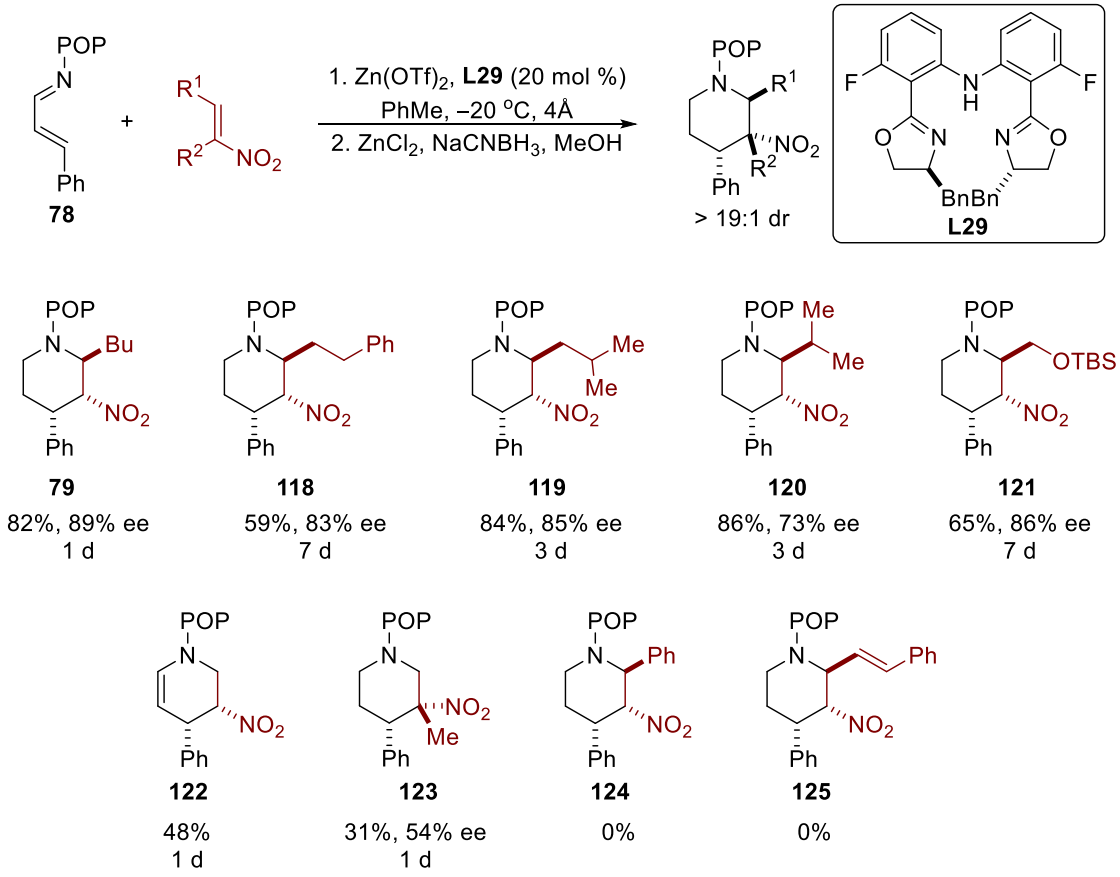

Scheme 1.2.24: The Scope of Nitro-alkene

1.2.6 Derivatization of Cycloadducts

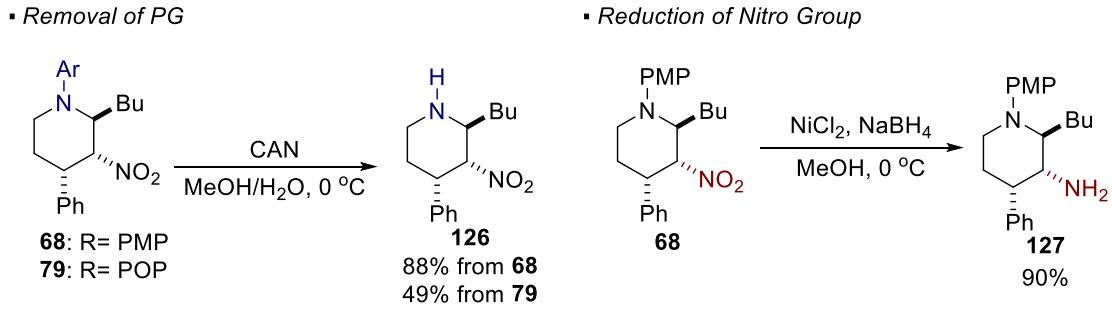

Scheme 1.2.25: Derivatization of Aza-[4+2] Cycloadducts

The protecting groups, 4-$OMeC_6H_4$ and 4-$PhOC_6H_4$ groups, on the nitrogen in cycloadducts **68** and **79** can be removed easily with cerium ammonium nitrate (CAN) to give free secondary amine **126** in satisfactory yield (Scheme 1.2.25). The resulting free N-H bond allows further manipulation for accessing structurally-diverse piperidines. Because 3-aminopepridine represents an important motif in medicinal chemistry, we investigated the reduction of the nitro-group of **68** to primary amine **127**. We found that reduction can be achieved by a $NiCl_2/NaBH_4$ system, which is believed to generate nickel boride *in-situ*.[44]

1.3 Summary

The Zn-catalyzed asymmetric synthesis of piperidines was described, and represents a rare example of a catalytic enantioselective [4+2] cycloaddition reaction with 1-azadienes and electron-poor alkenes. Key to the success of this reaction is the use of a novel F-BOPA ligand, which disfavors the undesired coordination of 1-azadiene to the Zn catalyst. Experimental results support a stepwise aza-Michael/cyclization mechanism that explains the obviation of the electronic requirement of the two reaction partners inherent to a concerted mechanism. The product 3-nitropiperidines can be reduced to afford 3-aminopiperidine, an important structural motif in medicinal chemistry.

REFERENCES

1. Vitaku, E.; Smith, D. T.; Njardarson, J. T. *J. Med. Chem.* **2014**, *57*, 10257-10274.

2. (a) Funel, J.-A.; Abele, S. *Angew. Chem. Int. Ed.* **2013**, *52*, 3822-3863; (b) Nicolaou, K. C.; Snyder, S. A.; Montagnon, T.; Vassilikogiannakis, G. *Angew. Chem. Ind. Ed.* **2002**, *41*, 1668-1698.

3. (a) Masson, G.; Lalli, C.; Benohoud, M.; Dagousset, G. *Chem. Soc. Rev.* **2013**, *42*, 902-923; (b) Boger, D. L. *Chem. Rev.* **1986**, *86*, 781-793.

4. Boger, D. L. *Tetrahedron* **1983**, *39*, 2869-2939.

5. Jorgensen, K. A. *Angew. Chem. Int. Ed.* **2000**, *39*, 3558-3558.

6. (a) Kouznetsov, V. V. *Tetrahedron* **2009**, *65*, 2721-2750; (b) Fochi, M.; Caruana, L.; Bernardi, L. *Synthesis* **2014**, 135-157.

7. (a) Behforouz, M.; Ahmadian, M. *Tetrahedron* **2000**, *56*, 5259-5288; (b) Daniels, P. H.; Wong, J. L.; Atwood, J. L.; Canada, L. G.; Rogers, R. D. *J. Org. Chem.* **1980**, *45*, 435-440.

8. Houk, K. N. *Acc. Chem. Res.* **1975**, *8*, 361-369.

9. Clark, R. C.; Pfeiffer, S. S.; Boger, D. L. *J. Am. Chem. Soc.* **2006**, *128*, 2587-2593.

10. Vicario, J.; Aparicio, D.; Palacios, F. *Tetrahedron Lett.* **2011**, *52*, 4109-4111.

11. He, L.; Laurent, G.; Retailleau, P.; Follesa, B.; Brayer, J.-L.; Masson, G. *Angew. Chem. Int. Ed.* **2013**, *52*, 11088-11091.

12. Esquivisa, J.; Arrayas, R. G.; Carretero, J. C. *J. Am. Chem. Soc.* **2007**, *129*, 1480-1481.

13. Jiang, X.; Shi, X.; Wang, S.; Sun, T.; Cao, Y.; Wang, R. *Angew. Chem. Int. Ed.* **2012**, *51*, 2084-2087.

14. He, M.; Struble, J. R.; Bode, J. W. *J. Am. Chem. Soc.* **2006**, *128*, 8418-8420.

15. Zhao, X.; Ruhl, K. E.; Rovis, T. *Angew. Chem. Int. Ed.* **2012**, *51*, 12330-12333.

16. Jian, T.-Y.; Shao, P.-L.; Ye, S. *Chem. Commun.* **2011**, *47*, 2381-2383.

17. Simal, C.; Lebl, T.; Slawin, A. M. Z.; Smith, A. D. *Angew. Chem. Int. Ed.* **2012**, *51*, 3653-3657.

18. Han, B.; He, Z.-Q.; Li, J.-L.; Li, R.; Jiang, K.; Liu, T.-Y.; Chen, Y.-C. *Angew. Chem. Int. Ed.* **2009**, *48*, 5474-5477.

19. Beaudegnies, R.; Ghosez, L. *Tetrahedron: Asymmetry* **1994**, *5*, 557-560.

20. Barluenga, J.; de la Rua, R. B.; de Saa, D.; Ballesteros, A; Tomas, M. *Angew. Chem. Int. Ed.* **2005**, *44*, 4981-4983.

21. Dalton, D. M. Mechanistic Investigations and Ligand Development for Rhodium Catalyzed [2+2+2] and Zinc catalyzed [4+2] Cycloaddition. Ph.D. Thesis, Colorado State University, Fort Collins, CO 2013.

22. Clark, J. D.; Flanagan, M. E.; Telliez, J.-B. *J. Med. Chem.* **2014**, *57*, 5023-5038.

23. Baetta, R.; Corsini, A. *Drugs* **2011**, *71*, 1441-1467.

24. Keating, G. M. *Drugs* **2015**, *75*, 2131-2141.

25. Palumbo, A.; Facon, T.; Sonneveld, P.; Blade, J.; Offidani, M.; Gay, F.; Moreau, P.; Waage, A.; Spencer, A.; Ludwig, H.; Boccadoro, M.; Harousseau, J.-L. *Blood* **2008**, *111*, 3968-3977.

26. Trepanier, L. *J. Feline Med. Surg.* **2010**, *12*, 225-230.

27. Trost, B. M.; Bartlett, M. J. *Acc. Chem. Res.* **2015**, *48*, 688-701.

28. Lin, H.; Tan, Y.; Liu, W.-J.; Zhang, Z.-C.; Sun, X.-W.; Lin, G.-Q. *Chem. Commun.* **2013**, *49*, 4024-4026.

29. Zhang, W.; Xie, F.; Matsuo, S.; Imahori, Y.; Kida, T.; Nakatsuji, Y; Ikeda, I. *Tetrahedron: Asymmetry* **2006**, *17*, 767-777.

30. Lu, S.-F.; Du, D.-M.; Xu, J. *Org. Lett.* **2006**, *8*, 2115-2118.

31. Liu, H.; Lu, S.-F.; Xu, J.; Du, D.-M. *Chem. Asian J.* **2008**, *3*, 1111-1121.

32. Liu, H.; Li, W.; Du, D.-M. *Sci. China Ser. B-Chem.* **2009**, *52*, 1321-1330.

33. Gross, K. C.; Seybold, P. G. *Int. J. Quantum. Chem.* **2000**, *80*, 1107-1115.

34. Hollingsworth, C. A.; Seybold, P. G.; Hadad, C. M. *Int. J. Quantum. Chem.* **2002**, *90*, 1396-1403.

35. Hansch, C.; Leo, A.; Taft, R. W. *Chem. Rev.* **1991**, *91*, 165-195.

36. Kooijman, H.; Spek, A. L.; Zondervan, C.; Feringa, B. L. *Acta Crystallogr., Sect. E: Struct. Rep. Online* **2002**, *58 (8)*, m429-431.

37. Nixon, T. D.; Ward, B. D. *Chem. Commun.* **2012**, *48*, 11790-11792.

38. Lykke, L.; Monge, D.; Nielsen, M.; Jorgensen, K. A. *Chem. Eur. J.* **2010**, *16*, 13330-13334.

39. (a) Van Sickle, D. E.; Rodin, J. O. *J. Am. Chem. Soc.* **1964**, *86*, 3091-3094; (b) Taagepera, M.; Thornton, E. R. *J. Am. Chem. Soc.* **1972**, *94*, 1168-1177; (c) Gajewski, J. J.; Peterson, K. B.; Kagel, J. R.; Huang, Y. C. J. *J. Am. Chem. Soc.* **1989**, *111*, 9078-9081.

40. Tanaka, T.; Hayashi, M. *Synthesis* **2008**, 3361-3376.

41. Clyne, D.S.; Mermet-Bouvier, Y. C.; Nomura, N.; RajanBabu, T. V. *J. Org. Chem.* **1999**, *64*, 7601-7611.

42. (a) Hoarau, O.; Ait-Haddou, H.; Daran, J.-C.; Cramailere, D.; Balavoine, G. G. A. *Organometallics* **1999**, *18*, 4718-4723; (b) Ait-Haddou, H.; Hoarau, O.; Cramailere, D.; Pezet, F.; Daran, J.-C.; Balavoine, G. G. A. *Chem. Eur. J.* **2004**, *10*, 699-707.

43. Liu, H.; Xu, J.; Du, D.-M. *Org. Lett.* **2007**, *9*, 4725-4728.

44. Nose, A.; Kudo, T. *Chem. Pharm. Bull.* **1981**, *29*, 1159-1161.

CHAPTER TWO: BACKGROUND ON DIRECTED FUNCTIONALIZATION OF SP^3 C-H BONDS

2.1 General Aspects of C-H Functionalization

C-H functionalization is a powerful tool to derivatize organic molecules.[1] Unlike most established transformations, no pre-existing functional group is required at the reactive site. The potential for new and diverse bond disconnections arising from the ability to discretely functionalize a specific C-H bond represents a valuable opportunity. Theoretically, such a strategy can be applied to the derivatization of any molecule to access a large array of derivatives, and is particularly appealing in late stage modification.[2]

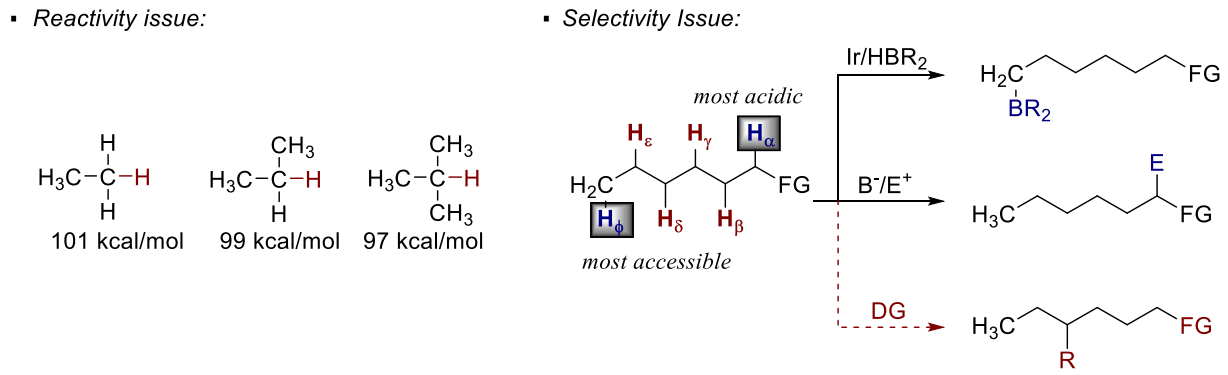

Figure 2.1.1: Challenges of C-H functionalization

The major challenges associated with C-H functionalization are related to the reactivity and ubiquity of C-H bonds (Figure 2.1.1). There is a high activation barrier due to the high bond strength of C-H bonds. This reactivity issue can be addressed through the use of a directing group to provide a lower-energy pathway for the cleavage of the C-H bonds or the generation of a high-energy reactive species such as highly unstable radicals, carbenes and nitrenes. The application

of a directing group is the major way to address the selectivity issue, with few exceptions where the bias for a particular C-H bond derives from its electronic and steric properties. For instance, the most acidic C-H bonds α to electron-withdrawing group can be deprotonated by a strong base, and terminal C-H bonds are the most sterically accessible and can be functionalized with emerging transition metal catalysis.[3]

This chapter focuses on the directed functionalization of unactivated sp^3 C-H bonds, where unactivated sp^3 C-H bonds are defined as those are not allylic/benzylic/α to heteroatoms and do not include cyclopropyl or cyclobutyl C-H bonds. The three major strategies for the functionalization of these C-H bonds are transition-metal-catalyzed C-H activation, hydrogen atom transfer (HAT) to reactive radicals and the chemistry of metal carbenoids/nitrenoids. The transformations that can be accomplished with each strategy will be emphasized to show its strengths and limitations.

2.2 Transition-Metal Catalyzed C-H Activation

2.2.1 Introduction

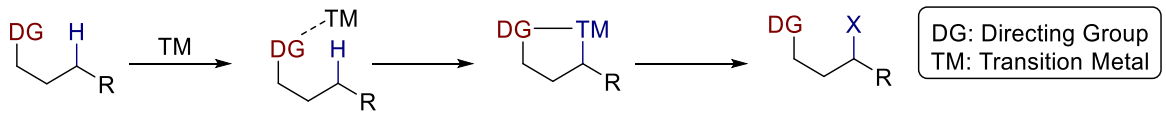

Figure 2.2.1: Transition-Metal Catalyzed C-H Activation

Transition-metal catalyzed C-H activation has received tremendous attention in the past decade (Figure 2.2.1).[4] The directing group brings the transition metal into close proximity to a particular C-H bond and facilitates its cleavage. Activation of a sp^3 C-H bond might seem less

challenging due to the fact that sp^3 C-H bonds (97-105 kcal/mol) are weaker than sp^2 C-H bonds (113 kcal/mol) (Figure 2.2.2).[5] However, transition-metal catalyzed activation of sp^2 C-H bond is far more explored and well developed. This surprising fact could be explained by the consideration of the relative bond strength of metal-carbon bonds. As demonstrated by the Ir(III) and Rh(III) complexes in Figure 2.2.2, metal-sp^3 carbon bonds are significantly weaker than metal-sp^2 carbon bonds.[6] Therefore, the formation of an alkyl metal species is much more difficult than that of an aryl metal species. Furthermore, the ubiquity of sp^3 C-H bonds in most organic frameworks poses a greater challenge for regioselectivity. Early development of transition-metal catalyzed directed activation of inert sp^3 C-H bonds was inspired by established works on either sp^2 C-H bonds or undirected systems. The following is a brief review on the seminal reports and representative examples, and is not an exhaustive list of published works in this area.

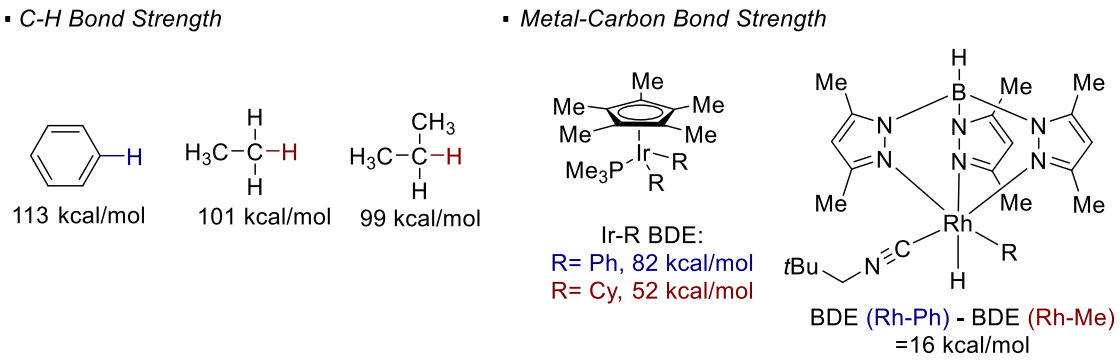

Figure 2.2.2: Consideration of Bond Energies for Transition-Metal Catalyzed C-H Activation

2.2.2 Catalysis with Noble Metals (Pt, Pd, Ir, Rh and Ru)

Based on Shilov's system[7] and its catalytic variant[8] for the hydroxylation of hydrocarbons with $PtCl_4^{2-}$, Sames demonstrated that aliphatic amines and carboxylic acids can act as a directing group to install a hydroxyl group at either the δ or γ positions although both the yield and the selectivity of the

reactions is moderate (Scheme 2.2.1).[9] Proline does not show any reactivity under the reaction conditions, supporting the role of carboxylic acid as a directing group in the latter case. A potential mechanism includes electrophilic C-H activation with Pt(II), subsequent oxidation of Pt(II) to Pt(IV) and final reductive elimination to furnish the C-O bond.

- *Shilov (Undirected)*

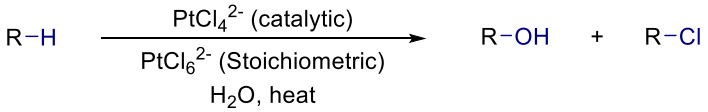

- *Sames (Directed)*

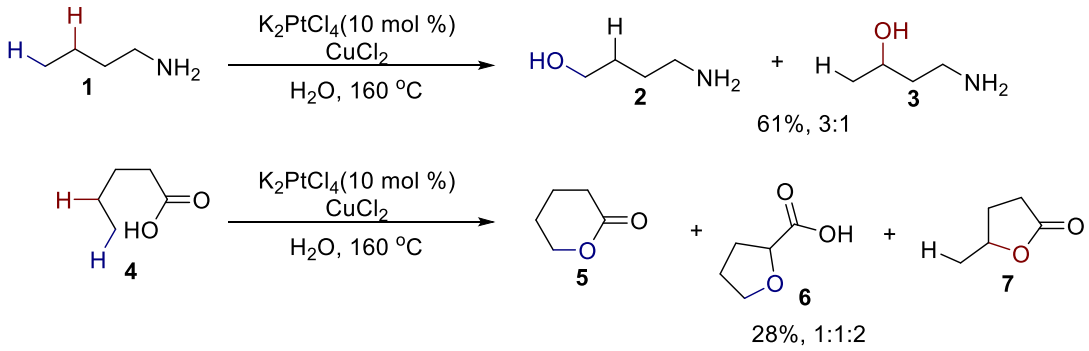

Scheme 2.2.1: Pt-Catalyzed sp^3 C-H Activation

Despite Sames' contribution, it was not until the reports from the Sanford and Yu groups on Pd catalysis that transition-metal catalyzed sp^3 C-H activation garnered tremendous attention. Based on their previous work on nitrogen-directed acetoxylation of sp^2 C-H bonds and benzylic sp^3 C-H bonds with catalytic $Pd(OAc)_2$ and oxidant $PhI(OAc)_2$, the Sanford group developed an oxime-directed acetoxylation of primary C-H bonds (Scheme 2.2.2).[10] The reaction features the formation of a Pd(II) alkyl species and the subsequent oxidation of Pd(II) to Pd(IV) by $PhI(OAc)_2$ to drive reductive elimination to form a C-O bond. Soon after this report, Yu demonstrated the iodination of primary C-H bonds in **14** with oxazolines as the directing group.[11] Similar to Sanford's report, a Pd(II)/Pd(IV) catalytic cycle is proposed.

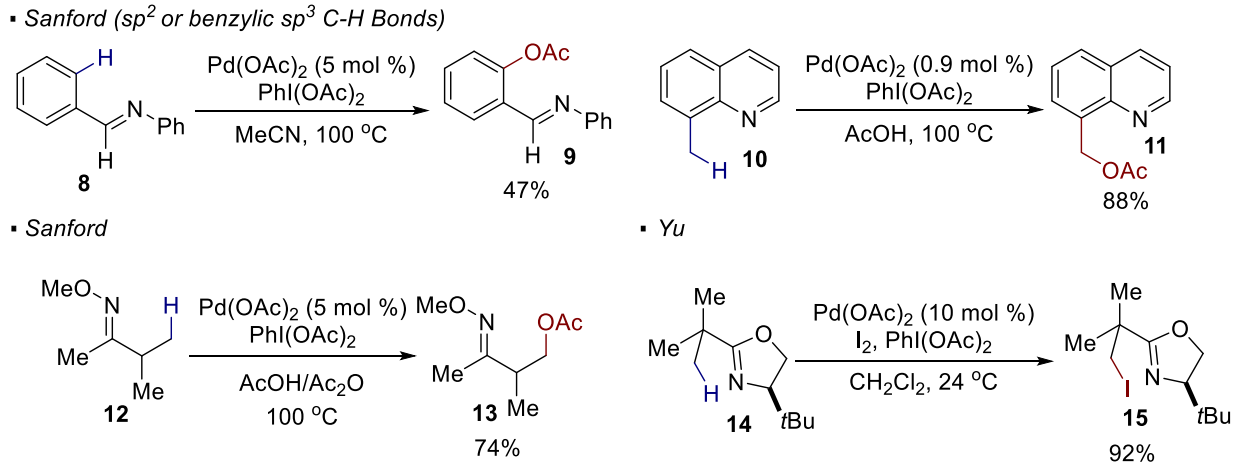

Scheme 2.2.2: Initial Reports on Pd-Catalyzed Activation of sp^3 C-H Bonds

Since the initial reports, various groups have developed different transformations featuring the activation of inert sp^3 C-H bonds with Pd catalysis (Scheme 2.2.3). Yu reports the incorporation of different functionalities such as aryl, alkyne, fluorine and carbonyl groups at the β C-H bond of carbonyl groups. The success of these transformations is the use of a highly electron-deficient amide as a directing group.[12] Trifluoromethanesulfonyl group can also be used as a directing group to activate the C-H bond γ to the nitrogen. The resulting palladacycle can undergo a heck reaction and cyclization to yield pyrrolidines such as **21**.[13] Another remarkable example is the contributions from the Dong group that allows β oxygenation of alcohol and amine derivatives such as **23**.[14] A Pd(II)/Pd(IV) is believed to be operative to drive the reductive elimination of the C-O bond. Sanford developed a protocol for C-H arylation of medicinally valuable alicyclic amines such as **25**.[15] This represents the first report on transition-metal catalyzed transannular C-H activation. The Gaunt group also reported a synthesis of strained nitrogen-heterocycles like **29** featuring a 4-membered cyclopalladation of sp^3 C-H bond in which unprotected secondary amines serve as a directing group.[16] The palladacycle intermediate can

undergo carbonylation and reductive elimination to form β-lactams. Although the rationale for the change in regioselectivity is unclear, 5-membered palladacycles can be formed from a sp^3 C-H bond γ to sterically hindered amino-alcohols **30**.[17]

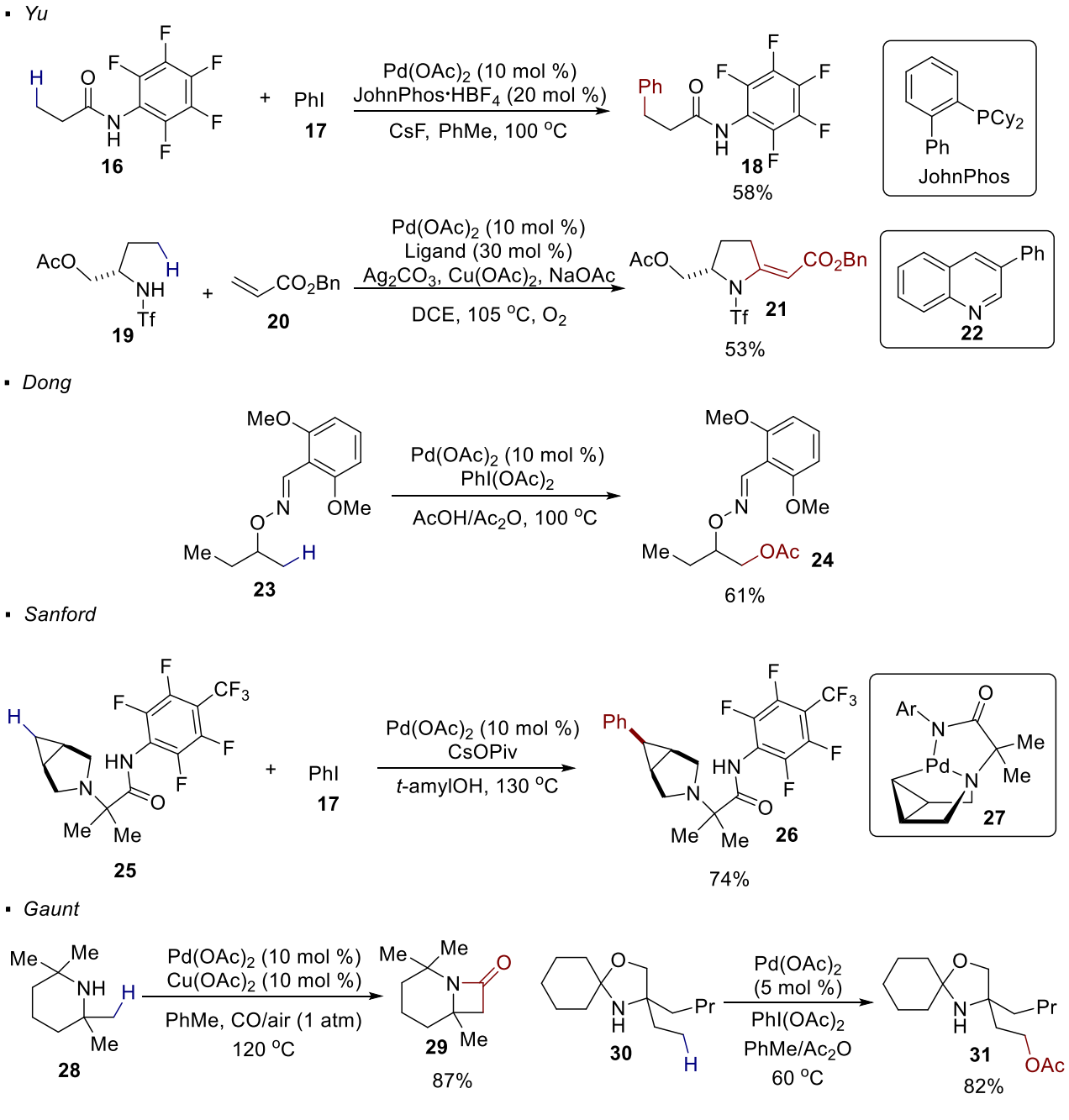

Scheme 2.2.3: Pd-Catalyzed sp^3 C-H Activation

Asymmetric Pd-catalysis allows the establishment of the absolute stereochemistry during the C-H functionalization step (Scheme 2.2.4). Yu reported that with the use of amino acid derivatives as chiral ligands, desymmetrization of prochiral methyl groups in **32** can be achieved in moderate enantioselectivity.[18] Yu also developed a protocol for highly enantioselective arylation of β methylene C-H bonds of carbonyl compounds.[19]

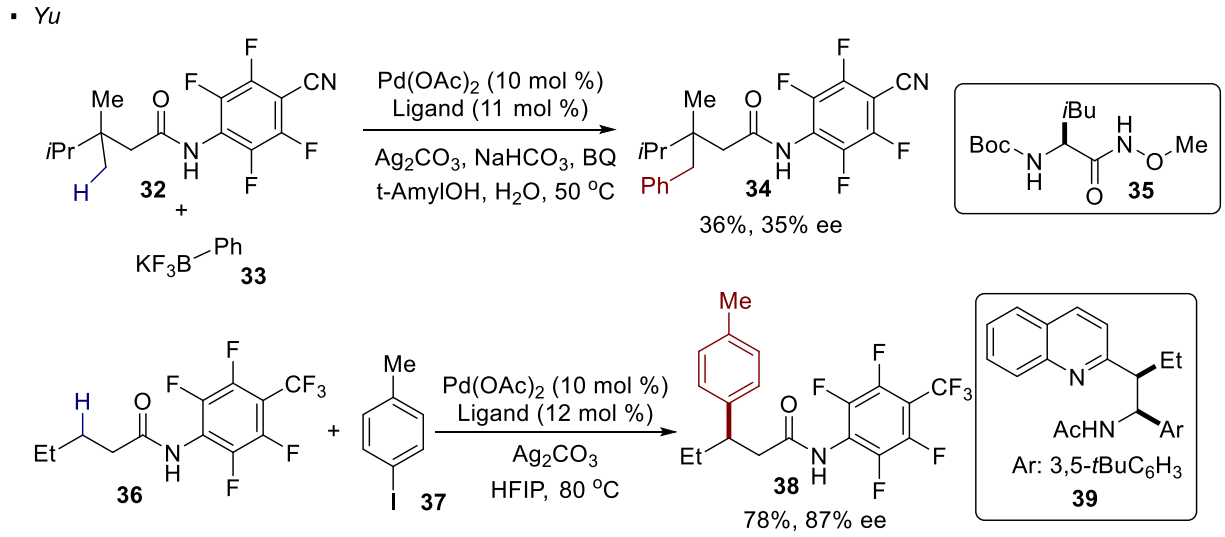

Scheme 2.2.4: Asymmetric Pd-Catalyzed sp^3 C-H Activation

In addition to Pd, other noble transition metals have also shown to be competent catalysts for sp^3 C-H activation (Scheme 2.2.5). Hartwig reported a low-valent Ir-catalyzed alcohol directed silylation of primary C-H bonds in a 3-step sequence.[20] With Ir(III) catalysis, Chang successfully developed a protocol for β-amination of oximes **42**.[21] Pyridine-directed amination and arylation of primary C-H bonds in **45** and **48** can be accomplished with cationic Rh(III) pre-catalysts, as demonstrated by You[22] and Glorius.[23] A-Ru-catalyzed synthesis of succinimides **52** featuring β-carbonylation of amides is reported by Chatani.[24]

2.2.3 Catalysis with Earth-Abundant Metals (Ni, Fe, Co and Cu)

- *Hartwig*

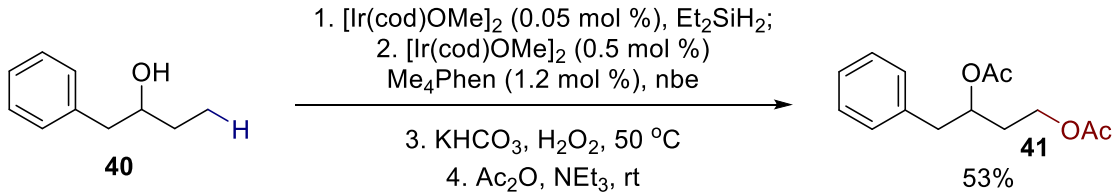

- *Chang*

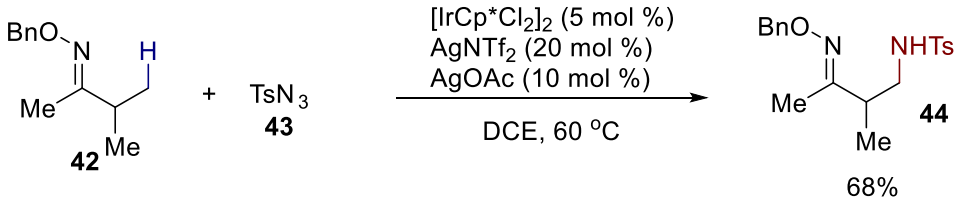

- *You*

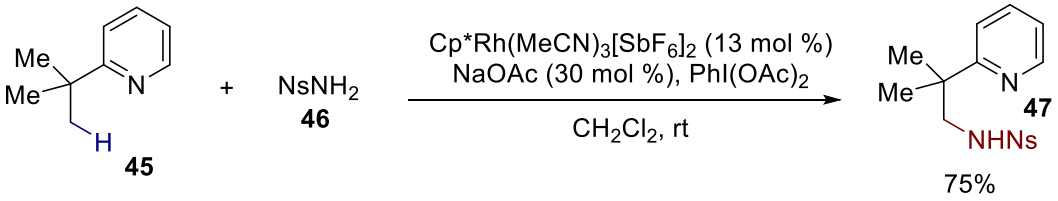

- *Glorius*

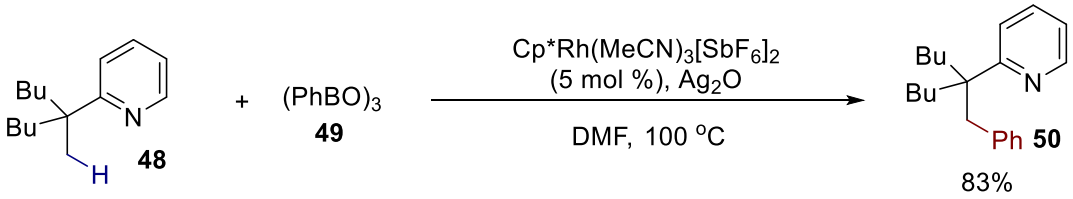

- *Chatani*

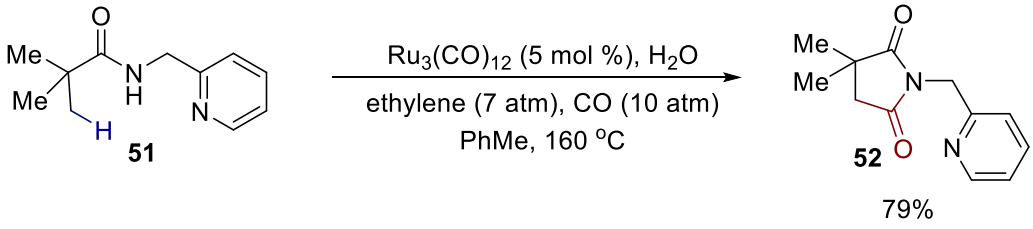

Scheme 2.2.5: Catalytic sp^3 C-H Activation with Other Noble-Metals

Efforts have been devoted to replace these precious metals by less expensive first row earth abundant metals such as nickel, cobalt and iron (Scheme 2.2.6). Unsurprisingly, nickel,

which is in the same group as Pd, is the initial focus. Hiyama first employed a low valent Ni(0) pre-catalyst and an $AlCl_3$ co-catalyst for the dehydrogenative [4+2] cycloaddition of formamide **53** and alkyne **54** for the synthesis of piperidine **55**.[25] The research with Ni(II) pre-catalysts has been inspired by a bidentate 8-aminoquinoline directing group introduced to Pd-catalyzed sp^3 C-H activation by Daugulis.[26] For instance, Chatani[27] and Ge[28] reported Ni-catalyzed β-arylation and alkylation of carbonyl compounds respectively with this directing group.

- *Hiyama*

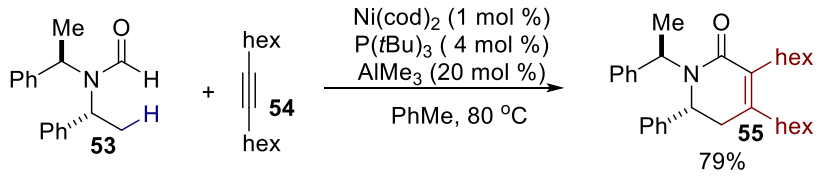

- *Chatani*

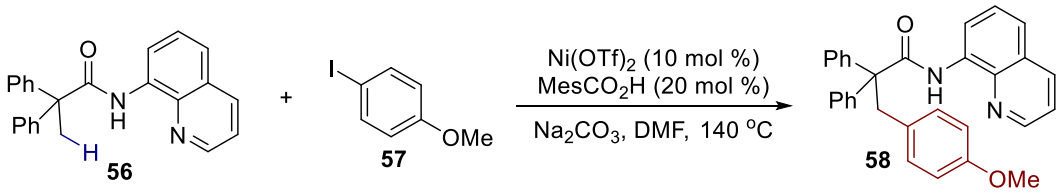

- *Ge*

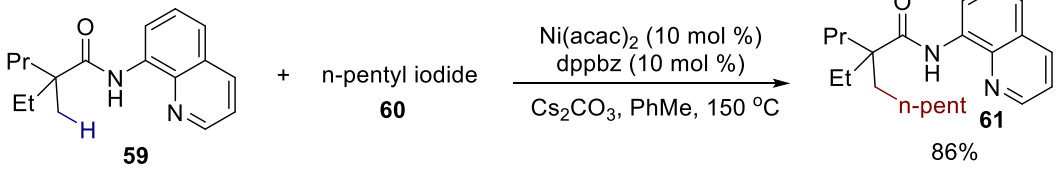

Scheme 2.2.6: Ni-Catalyzed sp^3 C-H Activation

For other first row-metals, 8-aminoquinoline is uniformly applied as the directing group (Scheme 2.2.7). With iron catalysis, Nakamura achieved β arylation of carbonyl groups with Grignard and diaryl zinc reagents.[29] As demonstrated by Zhang, cobalt is also a competent catalyst for β-functionalization of carbonyl groups. Concomitant alkynylation and cyclization is accomplished to assemble pyrrolidine derivatives **67**. More recently, β-lactams **68** can be

synthesized through the cobalt-catalyzed activation of the β C-H bonds of carbonyl groups, a contribution from Ge.[30] CuCl is also a competent catalyst for the same transformation.[31]

- *Nakamura*

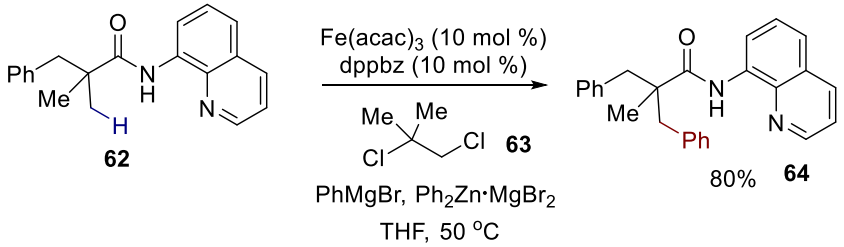

- *Zhang*

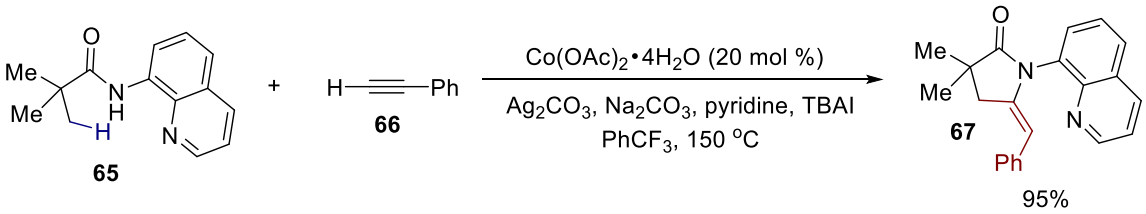

- *Ge*

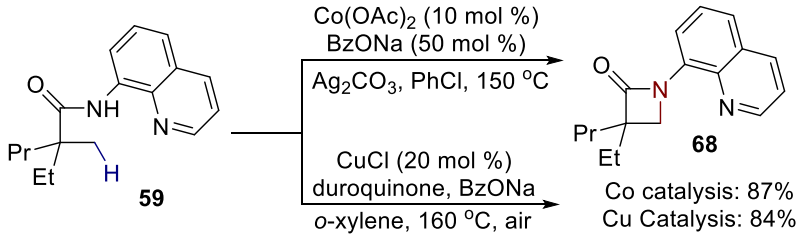

Scheme 2.2.7: Fe-, Co- and Cu-Catalyzed C-H Activation

The implication drawn from these representative examples is that the C-H activation reactions with first row transition metals require harsh conditions. The scope of the transformation is limited and only β functionalization of carbonyl compounds can be achieved.

2.2.4 Applications in Natural Product Synthesis

Even before Sames, Sanford and Yu's initial reports on catalysis, the power of sp^3 C-H activation with a stoichiometric amount of transition metals, such as Pd,[32] Pt,[33] and Cu[34] was recognized for the context of natural product synthesis. Only Pd can be used in catalytic amounts.

▪ *Baudoin*

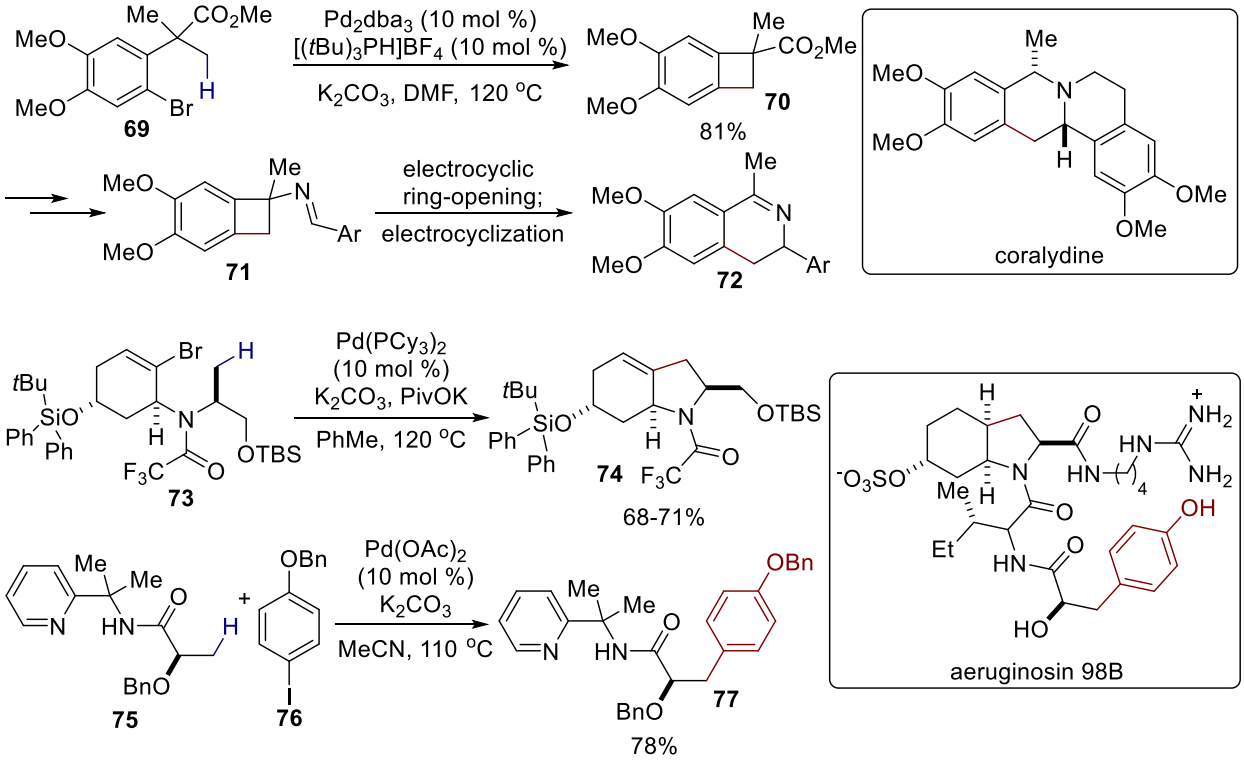

▪ *Chen*

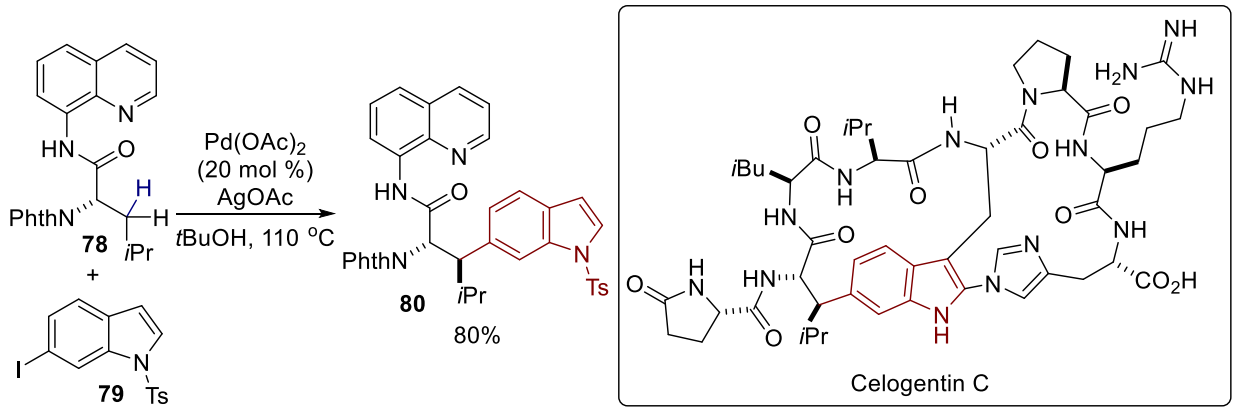

▪ *Sorensen*

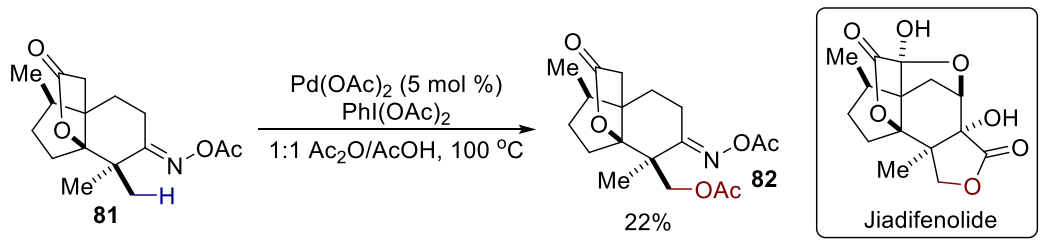

Scheme 2.2.8: Applications of Transition-Metal Catalyzed C-H Activation

Baudoin applied an aryl bromide as a directing group in **69** to activate the homobenzylic sp^3 C-H bond for the synthesis of cyclobutane **70** (Scheme 2.2.8).[35] The cyclobutane can be fragmented with a tandem Curtius rearrangement, electrocyclic ring opening and 6π electrocyclization reaction generate the isoqunoline framework of coralydine. Additionally, two sp^3 C-H activation strategic steps are applied for the synthesis of aeruginosin B. The first step features the formation of a vinyl Pd intermediate from vinyl bromide **73** that activates a C-H bond β to nitrogen for the assembly of the bicyclic framework of **74**. Another Pd-catalyzed reaction for β-arylation delivers α-hydroxy-β-aryl amide **77** that is present in the natural product. Chen also demonstrates the power of β-functionalization of carbonyl groups in natural product synthesis. For instance, a Pd-catalyzed β arylation of amide **78** is utilized for the installation of the indole in the synthesis of Celogentin C.[36] A late-stage oxime-directed acetoxylation is used to install an alcohol functionality to yield **82** for the synthesis of the lactone in Jiadifenolide by Sorensen.[37]

2.2.5 Strengths and Limitations

Currently, transition-metal catalyzed sp^3 C-H activation is the most powerful tool to functionalize primary C-H bonds. Various C-X bond formation is possible when switching the coupling partner. On the other hand, the shortcomings lie in the functionalization of unactivated methylene and tertiary C-H bonds. Despite the weaker bond strength of methylene and tertiary C-H bonds, the corresponding transition metal species are less stable than their primary counterparts. This is supported by the observations made on these alkyl Pd species which are equilibrating by β-H elimination and re-insertion (Figure 2.2.3). Primary Pd alkyl is the thermodynamic sink and tertiary Pd alkyl is the least stable.[38] This relative stability is parallel to

the ease of the activation of these C-H bonds with transition metal, as exemplified by Hartwig's Ir-catalyzed silylation of C-H bonds in which the primary C-H bonds are approximately 80 times more reactive than the secondary C-H bonds (Scheme 2.2.9). Therefore, the activation of secondary C-H bonds requires harsh conditions, as in the recent contributions from Yu[19] and Sanford.[15] The activation of tertiary C-H bonds with remains a formidable difficulty.

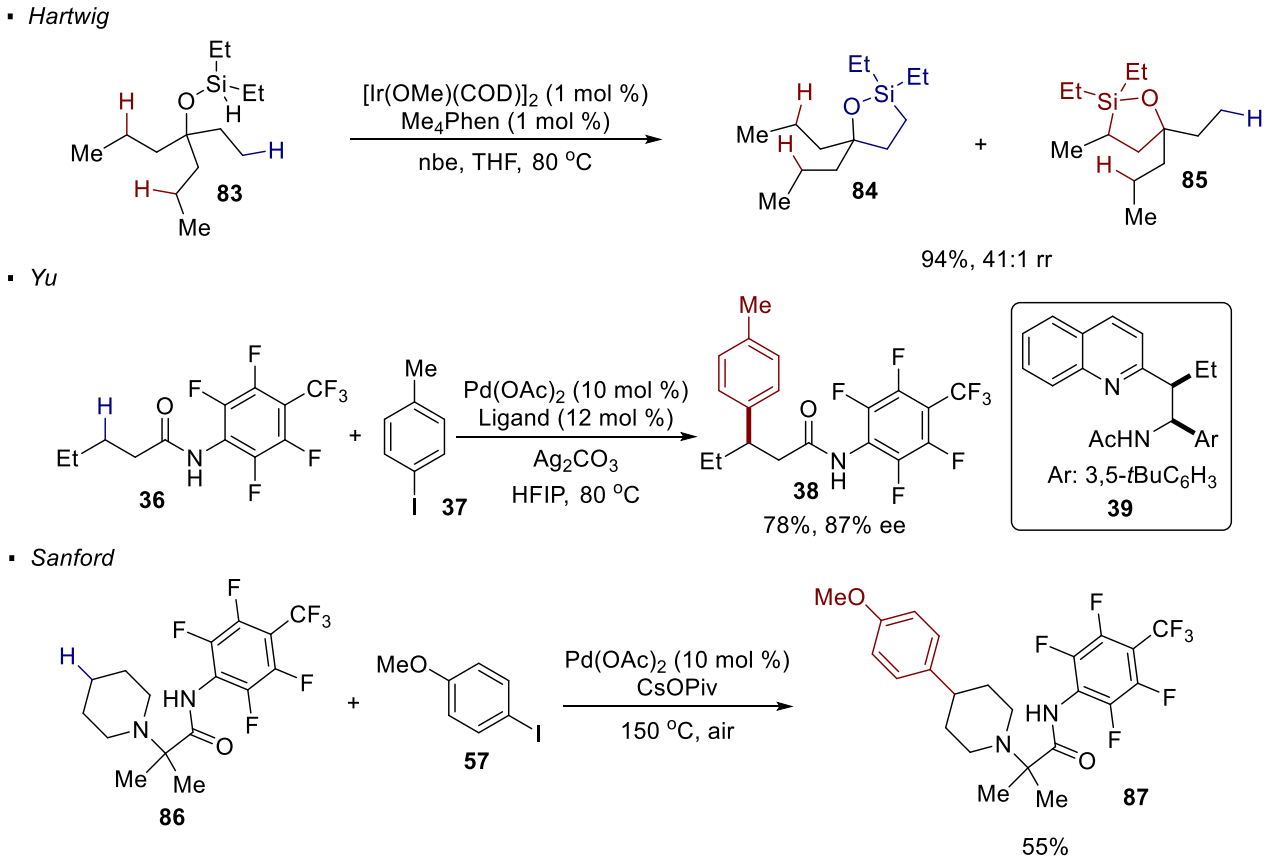

Scheme 2.2.9: Limitations for Activation of Methylene C-H bonds

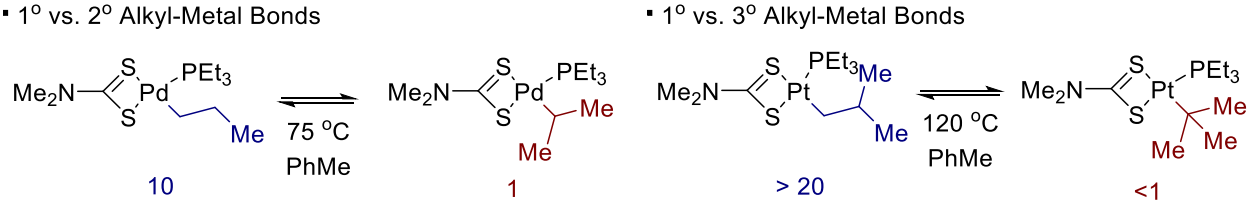

Figure 2.2.3: Relative Energies of Different Alkyl Metal Species

2.3 Hydrogen Atom Transfer to Reactive Radicals

2.3.1 Introduction

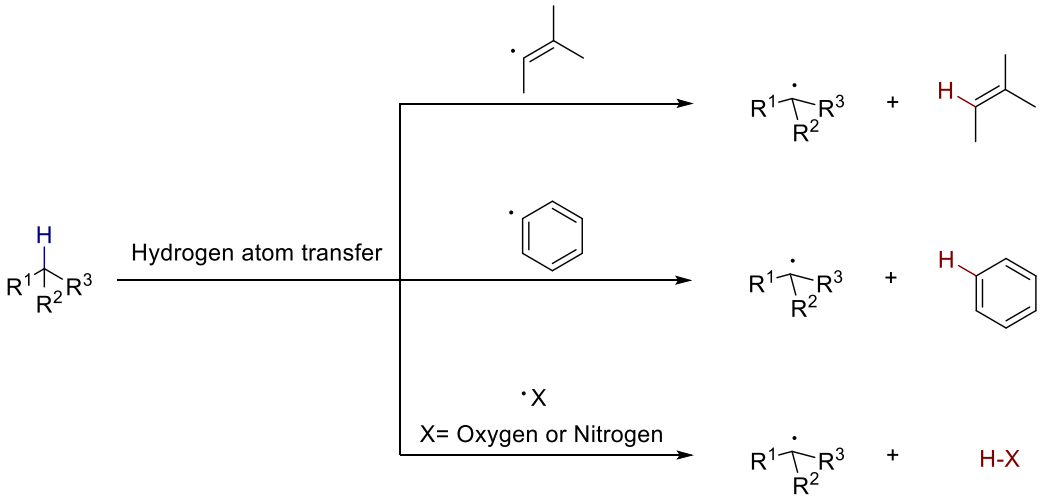

Figure 2.3.1: Cleavage of C-H Bonds with Unstable Radicals

- *Vandewalle*

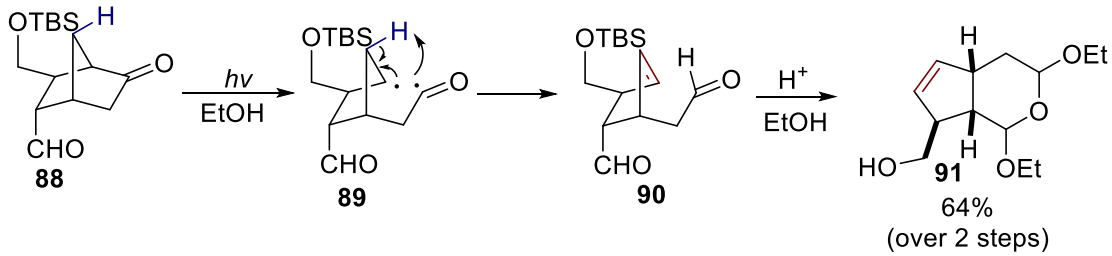

Scheme 2.3.1: 1,4 HAT to Cleave Unactivated C-H Bonds

In addition to transition-metal-catalyzed C-H activation, a C-H bond can also be cleaved by hydrogen atom transfer to a highly unstable radical species (vinyl, aryl, oxygen and nitrogen radicals) (Figure 2.3.1).[39] The driving force for this process is the stronger bond strength of the formed X-H bond than that of the broken C-H bond. The resulting alkyl radical can be intercepted with a radical coupling partner to furnish a new bond. An intermolecular hydrogen atom transfer

event is less favorable than an intramolecular one due to higher entropy cost. Therefore, there are only a few examples of synthetically useful transformations with intermolecular hydrogen abstract from inert C-H bonds. Our discussion focuses on intramolecular HAT, where the initial radical can be viewed as a directing group.

2.3.2 Selectivity of Intramolecular Hydrogen Atom Transfer

For intramolecular hydrogen atom transfer (HAT) events, the site-selectivity is mainly determined by the geometry of the substrate. 1,4 HAT is uncommon and is mostly for the cleavage of activated C-H bonds (e.g. allylic, benzylic, or α to an electron-withdrawing group or donating groups). An exception is a Norrish-type-I reaction of **88** reported by Vandewalle (Scheme 2.3.1).[40] A hydrogen atom from an unactivated sp^3 C-H bond is transferred to a carbonyl radical. On the other hand, the C-H being cleaved in this case is weakened by the presence of the radical α to it. Strictly speaking, it cannot be regarded as an unactivated sp^3 C-H bond. Despite observations in spectroscopic studies,[41] the use of 1,4 HAT to functionalize unactivated sp^3 C-H bonds remains to be developed.

1,5 HAT is the most common observed pathway due to a relatively low energy 6-membered chair-like transition state (Scheme 2.3.2).[42] As a representative example with alkoxy-radicals, 1,5 HAT is favored over 1,6 HAT. Mihailovic observed that in acyclic substrates such as **92**, the ratio of 1,5 to 1,6 HAT is about 11:1 to 12:1.[43] This ratio can be adjusted with the geometry of the substrate. As demonstrated by Wille, the vinyl radical generated by the addition of nitrate radical to cyclooctyne **95** gives rise to [5.2.0]-bicyclo and [4.4.0]-bicyclodecane **98** and **100** respectively, which reflects a 3:1 ratio of 1,5 HAT to 1,6 HAT.[44]

There are limited examples of synthetically useful reactions with 1,6 HAT. Baran reports the synthesis of 1,3 diols featuring 1,6 HAT (Scheme 2.3.3).[45] The three sp^2 hybridized atoms in **101** are believed to change the relative energy of the transition states for 1,5 and 1,6 HAT. A control experiment reveals that the selectivity for 1,6 HAT over 1,5 HAT is also explained by the weaker bond strength of tertiary C-H bonds and secondary C-H bonds since **105** and **106** are obtained in equal amount with **104**. When there are no δ C-H bonds available for 1,5 HAT, exclusive 1,6 HAT can operate. Penenory demonstrates that the aryl group in **107** can be transferred to the methyl group through 1,6 HAT (Scheme 2.3.3).[46]

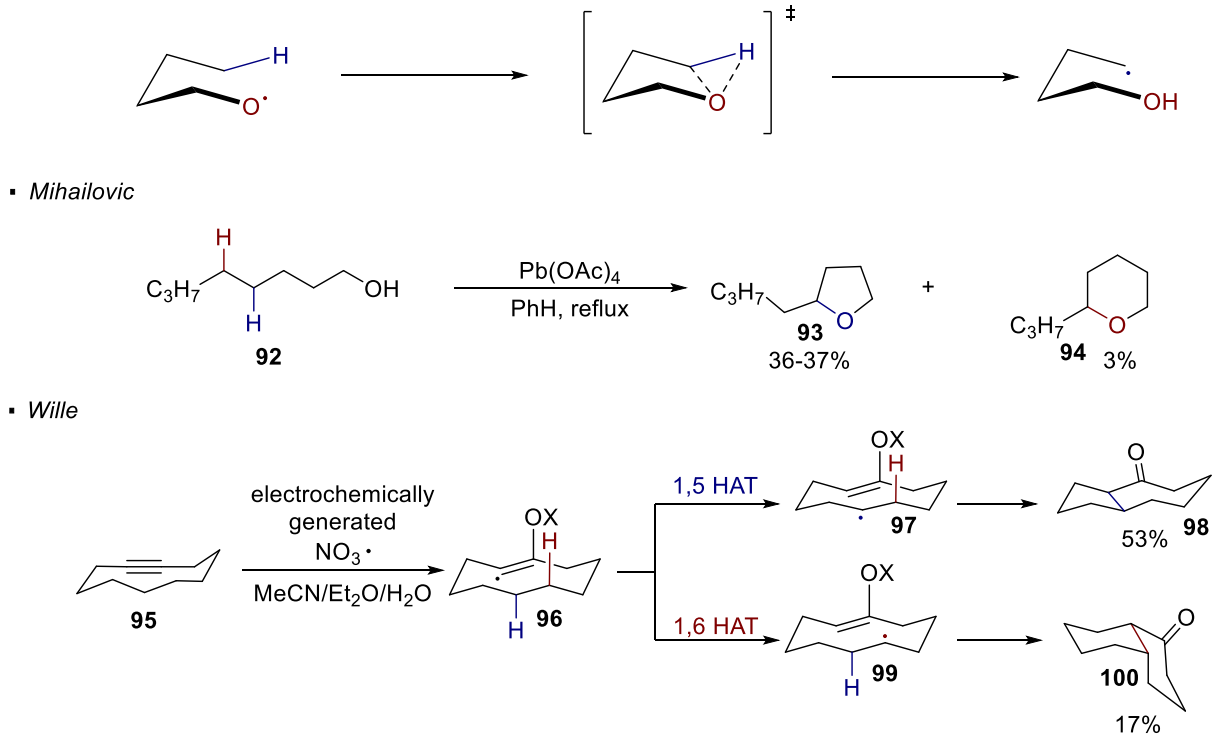

Scheme 2.3.2: Predominance of 1,5 HAT over 1,6

For long-range 1,n HAT (n >6), the transition state would be a medium-size ring and the enthalpy/entropy penalty associated with the HAT would be high.[47] Therefore, for successful applications of long-range HAT, conformational constraint on the substrates is required to

minimize the cost of enthalpy/entropy needed to reach the transition state. Related to the functionalization of unactivated sp^3 C-H bonds is an example from Nishio, who demonstrated the synthesis of a polycyclic nitrogen heterocycle **113** through 1,8 HAT with a Norrish-type II reaction of **112** (Scheme 2.3.4).[48] In this case, there is a strong conformational bias to drive the HAT. Overall, long-range HAT has not found general applications to functionalize unactivated sp^3 C-H bonds.

- *Baran*

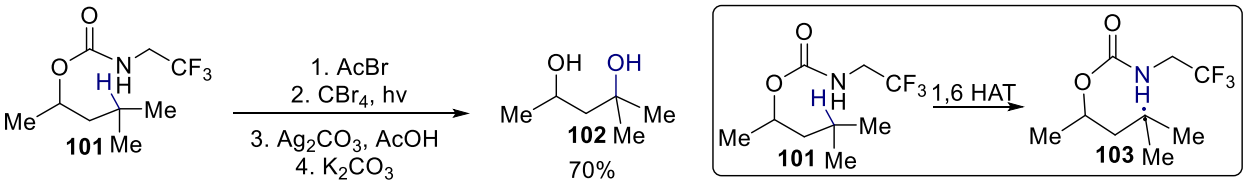

- *Penenory*

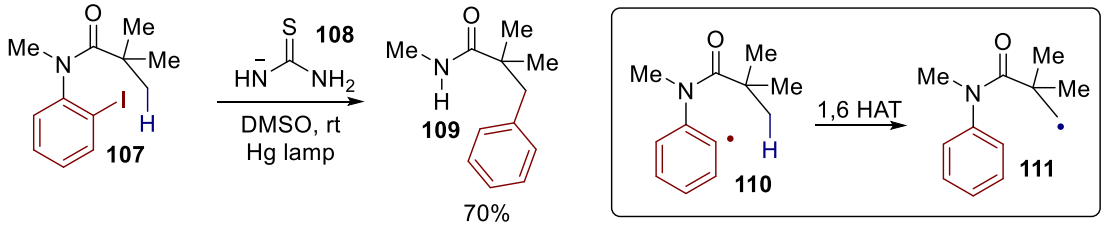

Scheme 2.3.3: Dependence of Selectivity of 1,5 vs. 1,6 HAT on Geometry

- *Nishio*

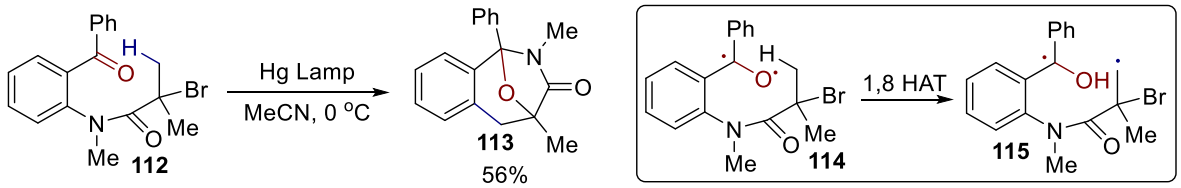

Scheme 2.3.4: Long-Range Hydrogen Atom Transfer

2.3.3 Use of Nitrogen Radicals

2.3.3.1 Generation and Transformations

The first class of radicals capable of engaging in 1,5 HAT are nitrogen radicals. An N-H bond of a neutral organic amine has a bond energy of approximately 93-95 kcal/mol, comparable to unactivated sp^3 C-H bonds.[49] There lacks an appreciable driving force for 1,5 HAT with the use of nitrogen radicals. Therefore, a nitrogen radical is made more electron deficient by protonation. This increased electron deficiency of the nitrogen radicals strengthens the potential N-H bond and provides a thermodynamic driving force for abstraction of a hydrogen atom from an inert C-H bond.

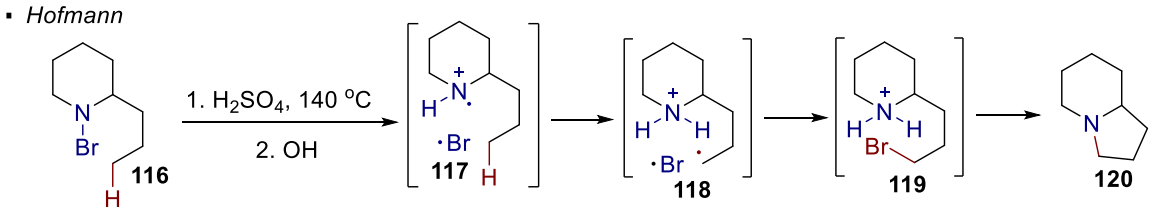

Scheme 2.3.5: Nitrogen Radicals for Intramolecular HAT

The first successful reaction for harnessing a nitrogen radical for functionalizing sp^3 C-H bonds is the Hoffman-Loffler-Freytag reaction (HLF reaction), a serendipitous discovery made by Hoffman (Scheme 2.3.5).[50] In the HLF reaction of **116**, a nitrogen radical is generated through the light- or heat-induced homolytic cleavage of a nitrogen-halogen bond. The protonated nitrogen radical **117** abstract a hydrogen atom of a C-H bond that is δ to the nitrogen. The resulting alkyl radical **118** can then combine with the halogen radical formed from the first step. This results in the formation of a carbon-halogen bond. A subsequent workup with base effects a S_N2 cyclization event to yield pyrrolidine **120**.

With the Suarez modification, the electron-deficiency of the nitrogen radical is increased by installing an electron-withdrawing group, such as a sulfonyl or carbonyl group, on the nitrogen which allows the reaction to be carried out under neutral conditions (Scheme 2.3.6).[51] The *in situ*-formed nitrogen-halogen bond from a strong oxidant and a halogen can be cleaved homolytically to generate a nitrogen radical that can effect the HLF reaction.

- *Suarez*

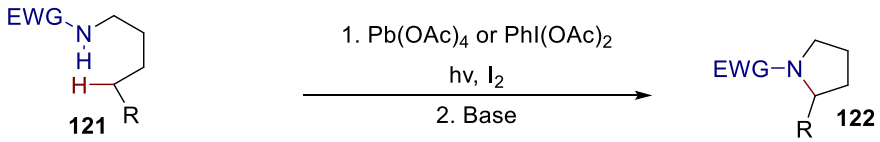

EWG: NO_2, CN, $PO(OR)_2$, Cbz, Boc

Scheme 2.3.6: Suarez Modification for HLF Reactions

There are other reports on the use of an N-H bond as a nitrogen radical precursor. The success of the majority of these protocols is the *in-situ* generation of a nitrogen-halogen bond. Muniz, Gonzalez and Herrera developed an iodine-catalyzed/mediated HLF reaction of sulfonamides **123** or **126** in the presence of a stoichiometric amount of hypervalent iodine reagent (Scheme 2.3.7). The key to the success is the *in situ* generation of a nitrogen-iodine bond for the generation of the nitrogen radical, as in the Suarez modifications. As a consequence, the scope for the use of a nitrogen radical has not received a significant attention and is mainly restricted to the formation of a carbon-halogen bond at the γ position and the synthesis of pyrrolidines via subsequently S_N2 reaction. A noteworthy exception is a report from Yu, who shows that the formation of pyrrolidine **130** is accompanied by the iodination of a ε C-H bond (Scheme 2.3.7).[52] To account for the reactivity at the ε C-H bond, the authors propose a hydrogen atom abstraction from the C-H bond in **131** from an azide radical generated *in situ* although the

more reasonable explanation by an E_2 mechanism to eliminate an amidyl anion remains a possibility.

- *Muniz*

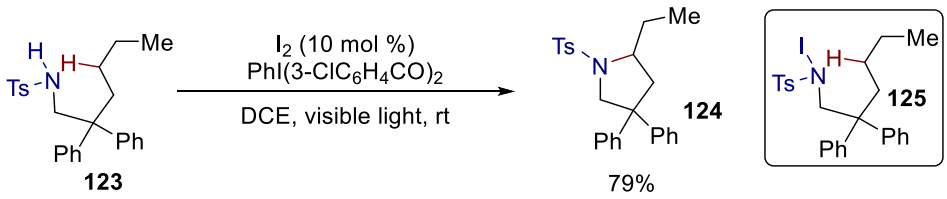

- *Gonzalez, Herrera*

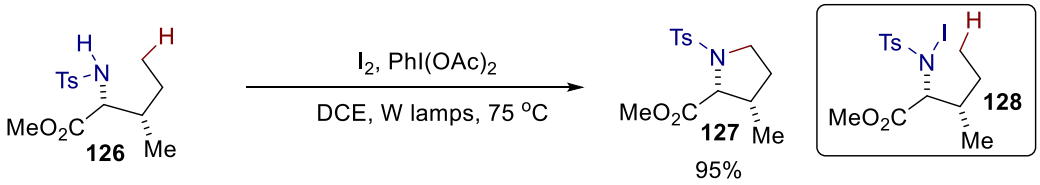

- *Yu*

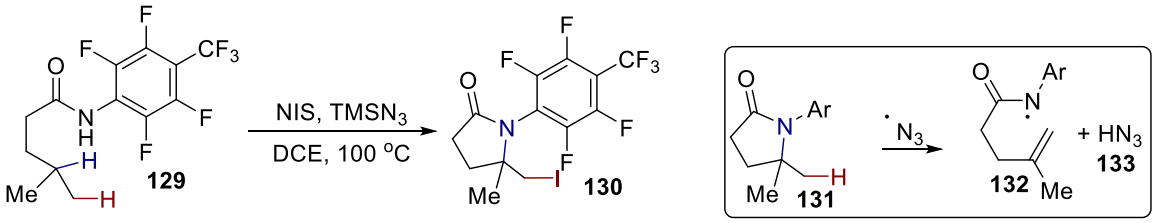

Scheme 2.3.7: *In-situ* Generation of Nitrogen-Halogen Bonds

In addition, an N-H bond can be oxidized with a strong oxidant to provide a nitrogen radical, obviating the need of a nitrogen-halogen bond. Nikishin reports the HLF reaction of sulfonamide **134** in the presence of a strong oxidant, $K_2S_2O_8$ (Scheme 2.3.8).[53] A nitrogen radical is a potential intermediate and can abstract a hydrogen atom from the δ C-H bond. The resulting alkyl radical is oxidized to form a carbocation to allow cyclization to occur. Another HLF reaction that potentially proceeds with the same mechanism is the silver-catalyzed intramolecular C-H amination of trifluoromethanesulfonamide **137** reported by Shi (Scheme 2.3.8).[54] The authors propose the formation of an Ag-alkyl intermediate through sulfonamide-directed concerted

metalation/deprotonation at the metal center. On the other hand, a nitrogen radical intermediate is proposed by the authors to account for another transformation under essentially the same reaction conditions.[55] As demonstrated by Chiba, the N-H bond in amidine **140** can also be oxidized in the presence of a copper catalyst and molecular oxygen, resulting in the formation of an alkyl radical at the δ C-H bond after 1,5 HAT.[56] The alkyl radical can be trapped by oxygen and thus oxygenation of the C-H bond is realized.

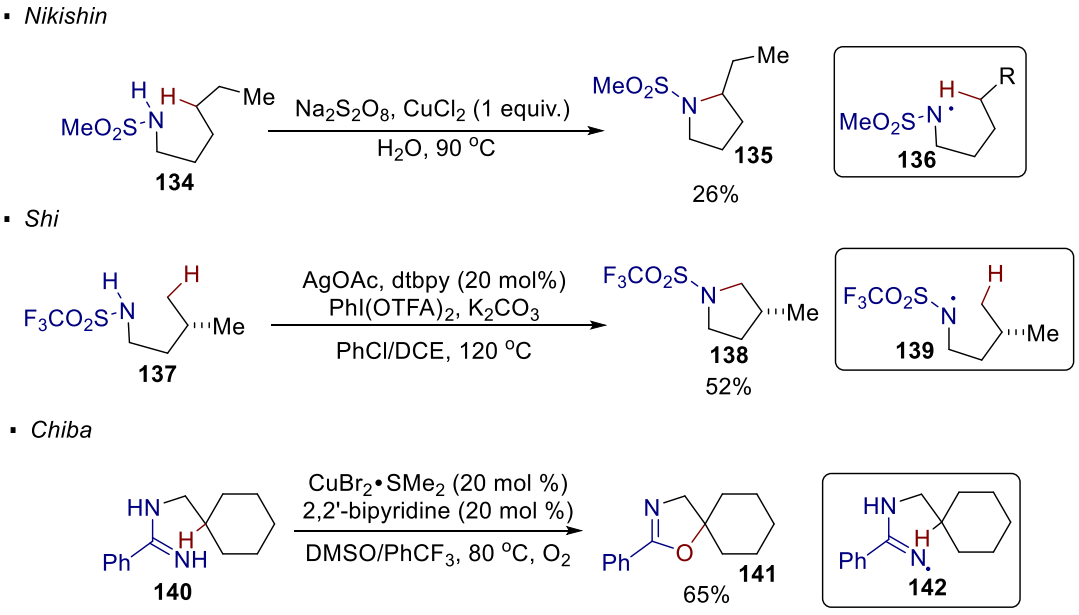

Scheme 2.3.8: Generation of Nitrogen Radicals by Oxidation

With a relatively weak N-H bond, the homolytic cleavage of the N-H bond is another way to generate a nitrogen radical. Chiba shows that the hydrogen atom in the N-H bond in **143** can be transferred to TEMPO (Scheme 2.3.9).[57] Since the nitrogen radical is stabilized by the iminyl nitrogen, an equilibrium exists between the nitrogen radical and the alkyl radical by 1,5 HAT, favoring the nitrogen radical. Despite its low concentration, the alkyl radical can be trapped by TEMPO. Substitution of TEMPO with the N-H bond results in the formation of pyrazole **144**.

▪ *Chiba*

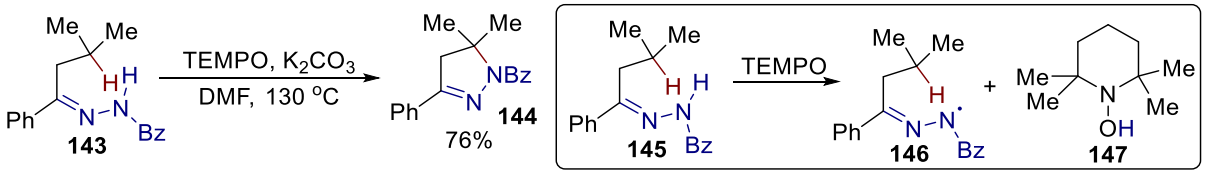

Scheme 2.3.9: Homolytic Cleavage of N-H Bonds for Nitrogen Radical Generation

▪ *Kim*

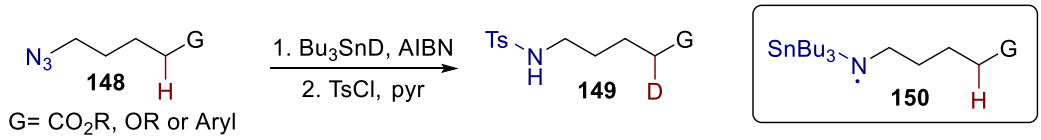

▪ *Chiba*

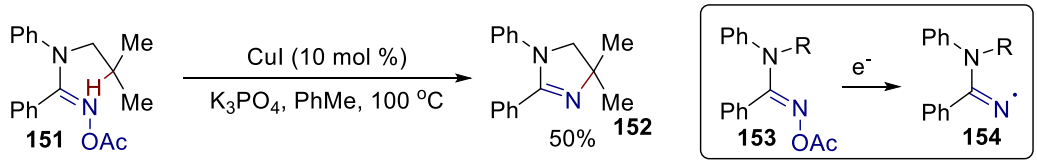

▪ *Bower*

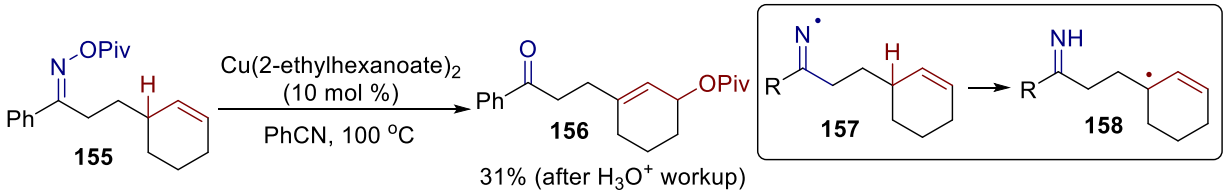

▪ *Yu*

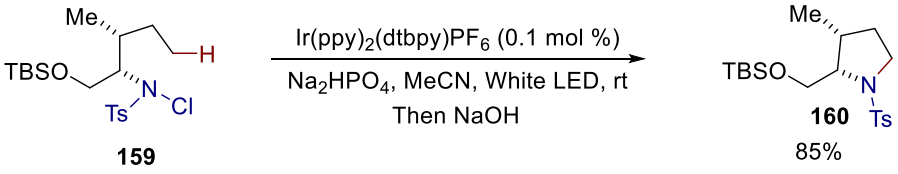

Scheme 2.3.10: Generation of Nitrogen Radicals by Reducing Agents

The reduction of nitrogen functionality at high oxidation level is an alternative way to generate nitrogen radicals. Kim reported the generation of *N*-tributyltin substituted aminyl radicals from organic azides **148** and Bu_3SnH or Bu_3SnD (Scheme 2.3.10).[58] Such tin-substituted nitrogen radicals can abstract a hydrogen atom from activated C-H bonds but not inert sp^3 C-H

bonds. Generation of nitrogen radicals by the decomposition of organic azides with other reducing agents suffer the same limitation.[59] Amidoxime **151** can be reduced by a copper catalyst to afford an amidinyl radical that is capable of abstracting a hydrogen atom from tertiary C-H bonds.[60] Subsequently oxidation of the radical to a carbocation allows cyclization to yield dihydroimidazole **152**. Similarly, Bower demonstrated that iminyl radical can be generated through a single-electron reduction of a N-O bond in oxime-ester **155**. The resulting neutral iminyl radical is responsible for the cleavage of the activated tertiary allylic C-H bond.[61] With photoredox catalysis, the N-Cl bond in **159** can be reduced to form a nitrogen radical that abstracts a hydrogen atom from the δ C-H bond.[62] The resulting alkyl radical is oxidized by the photocatalyst to complete the catalytic cycle. Cyclization to form HLF product **160** follows.

2.3.3.2 Applications and Limitations

Nitrogen radicals have been used to generate pyrrolidines or to realize C-H halogenation in the context of natural product synthesis. Corey reported the use of a HLF reaction of **161** to furnish the pyrrolidine ring in the synthesis of dihydroconessine (Scheme 2.3.11).[63] Williams accessed pyrrolidine **164**, which can be functionalized to VM55599, by a HLF reaction.[64] For the synthesis of (–)-isoatisine, a Suarez-modified HLF reaction featuring a 1,6 HAT is employed by Baran to incorporate a iodine functionality in the C-H bond of a methyl group in **166**.[65] In this case, the diaxial relationship of the nitrogen and the methyl groups in the cyclohexane puts them in proximity, leading to a favorable 1,6 HAT event. Building off his previous work on hydroxyl-directed C-H bromination, Baran utilized a Suarez-modified HLF reaction of **167** to install the 1,3 diol motif in the syntheses of eudesmane terpenes, a class of natural products that comprise dihydroxyeudesmane, pygmol, eudesmantetraol, and 11-epieudesmantetraol.[66]

▪ *Corey*

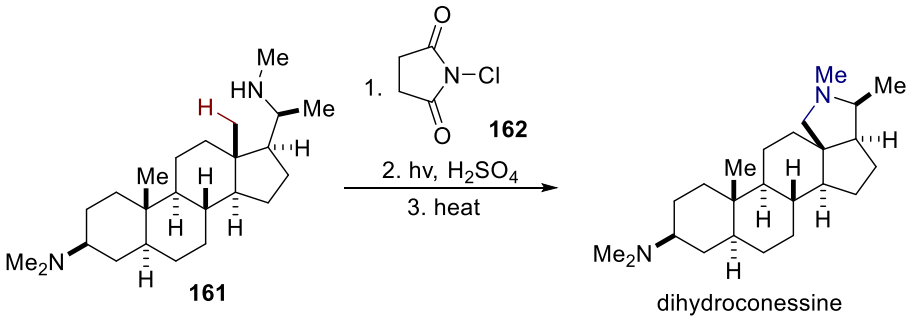

▪ *Williams*

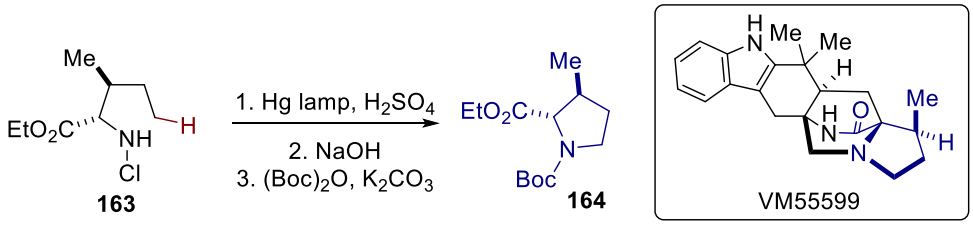

▪ *Baran*

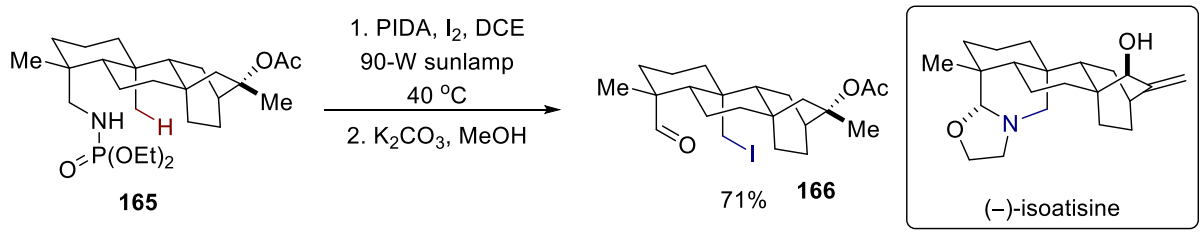

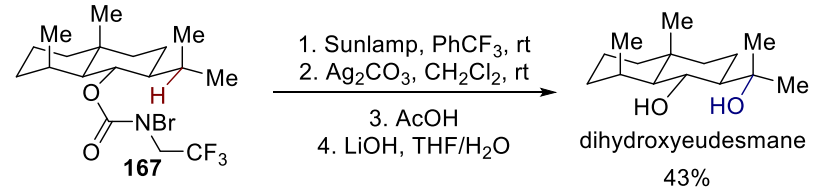

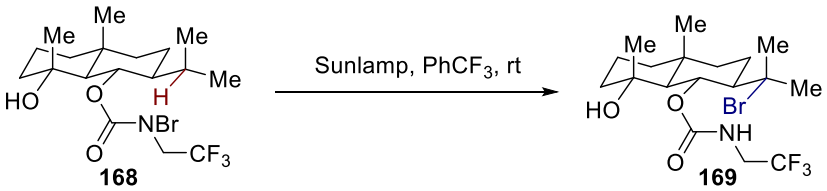

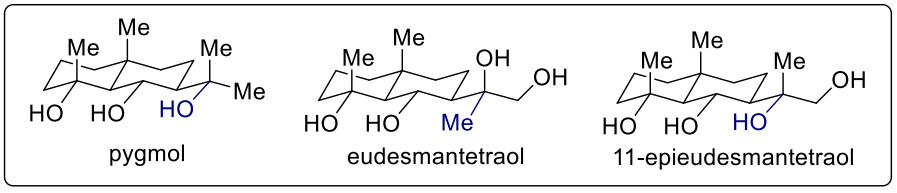

Scheme 2.3.11: Applications of Nitrogen Radicals for Intramolecular HAT

The limitation of the use of nitrogen radicals in C-H functionalization stems from the use of a nitrogen-halogen bond as the nitrogen-radical precursor. The concomitant formation of the halogen radical through homolysis leads to the inevitable formation of a carbon-halogen bond. This greatly limits the versatility of the alkyl radical formed by 1,5 HAT. As discussed earlier, efforts have been devoted to utilize a nitrogen-hydrogen bond as a nitrogen radical precursor. While this strategy addresses the synthetic efforts required to access the HLF substrates, the incorporation of non-halogen functionalities still represents a challenge. The only example in this regard is the C-H oxygenation reaction developed by Chiba.[56]

2.3.4 Oxygen Radical

2.3.4.1 Generation and Transformations

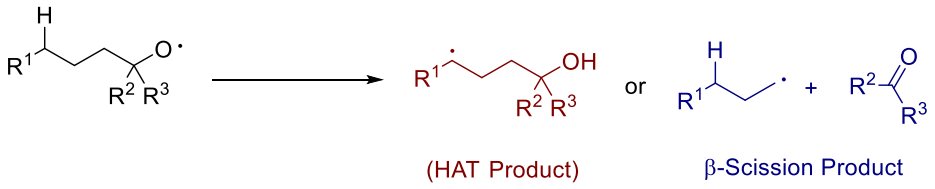

Scheme 2.3.12: Reactions of Oxygen Radicals

Oxygen radicals are more electrophilic than neutral nitrogen radicals due to the higher electronegativity of oxygen. Therefore, oxygen radicals are more reactive than neutral nitrogen radicals and the high O-H bond energy (105 kcal/mol)**Error! Bookmark not defined.** provides enough driving force for the abstraction of a hydrogen atom from inert C-H bonds without the need of the protonation of the oxygen atom. On the other hand, because of the strong bond strength of C=O bonds, an oxygen radical can lead to the cleavage of the C_α-C_β bond with the

simultaneous formation of a carbonyl group and a more stable alkyl radical. This β scission process is sometimes a competitive pathway with 1,5 HAT (Scheme 2.3.12).

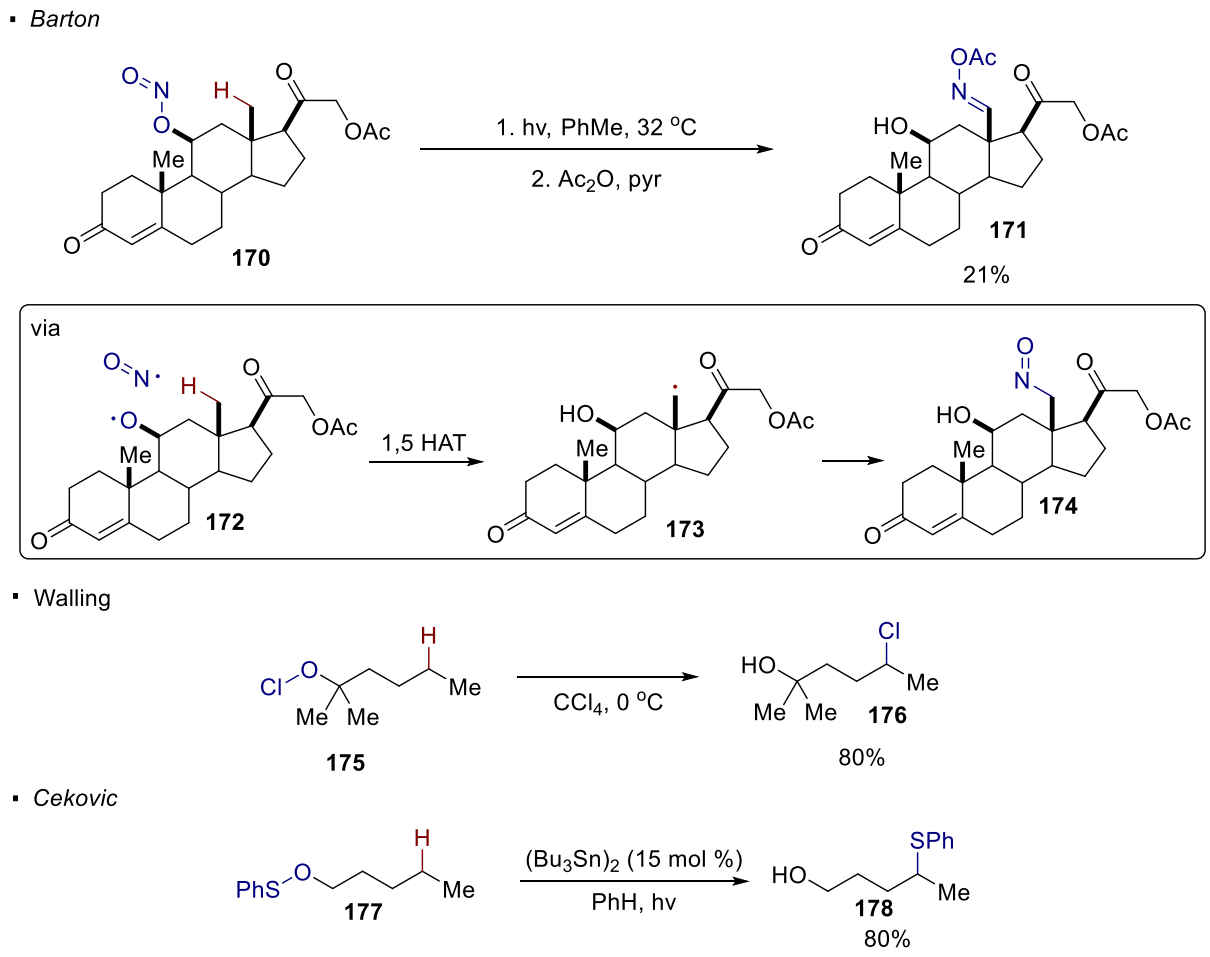

Scheme 2.3.13: C-X Bond Formation at C-H Bonds with O-X Bond as Radical Precursors

One of the most common precursors to oxygen radicals is an oxygen-heteroatom bond. The functionalities that can be incorporated depends on the identity of the heteroatom in the oxygen-heteroatom bond. For instance, in the well-known Barton reaction, an alcohol functionality is first converted to nitrile ester **170** (Scheme 2.3.13).[67] The N-O is then cleaved in the presence of a light source to yield an oxygen radical **172**. A hydrogen atom from the δ C-H bond is transferred to the oxygen radical and therefore the radical is transposed to the carbon.

The alkyl radical **173** combines with the nitrosyl radical to give the oxime product **171** after tautomerization. With the O-Cl bond[68] and O-S bond[69] in **175** and **177**, a C-Cl bond and a C-S bond can be formed respectively.

In some cases, the functionality incorporated into the C-H bonds depend on the conditions applied, instead of the identity of the oxygen radical precursor. As demonstrated by Cekovic, when the reaction with **179** proceeds in the presence of Bu_3SnH, the alkyl radical can be trapped with an electrophilic alkene, resulting in the alkylation of the inert C-H bonds (Scheme 2.3.14).70 He also shows that when a peroxy group in **182** is used to generate an oxygen radical in the presence of $FeSO_4$ and a Cu(II) salt, various C-X bond can be formed at the inert C-H bonds, depending on the identity of the counter ion of the Cu(II) salts.[71]

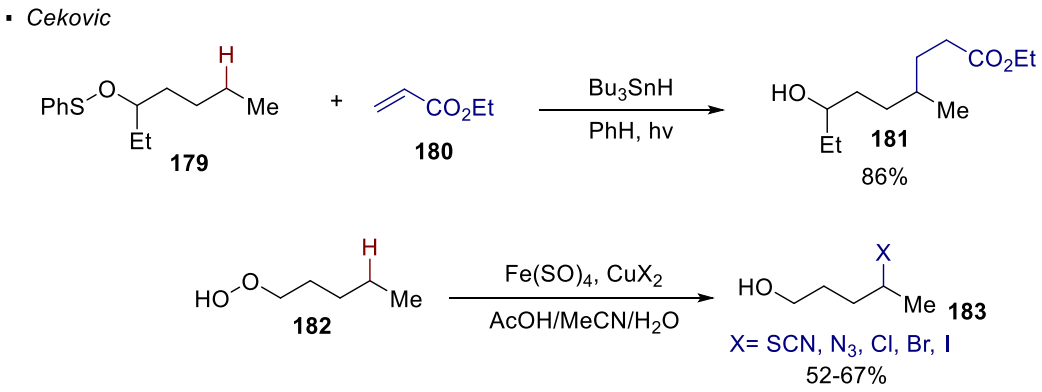

Scheme 2.3.14: Trapping of Alkyl Radicals with Other Reagents

An oxygen-centered radical can also be formed from free alcohol with a strong oxidant. $Pb(OAc)_4$ is one of the most commonly employed reagents (Scheme 2.3.15).[42] It is proposed that Pb alkoxide intermediate **185** formed by ligand exchange between the alcohol and one of the acetates can undergo homolysis to give oxygen-centered radical **186** and Pb(III) species **187**. The alkyl radical **188** formed from 1,5 HAT can be intercepted by the Pb(III) species. The

intramolecular nucleophilic attack by the oxygen at the carbon-lead bond furnishes furan **189**. Other oxidizing agents, such as $PhI(OAc)_2$, HgO or Ag_2O, can be used in conjunction with elemental halogens to generate an oxygen-halogen bond *in-situ*.[42] The weak oxygen-halogen bond is unstable and will break homolytically to give an oxygen radical and a halogen radical. The alkyl radical formed from HAT can capture the halogen radical and a subsequent S_N2 reaction yield a furan ring, as exemplified by Suarez's conditions with alcohol **190**. It should be noted that with free alcohols as the oxygen radical precursor, the reactions invariably give furans as the final product, except in cases where a high pressure of CO is applied and a lactone can be obtained, a discovery made by Ryu.[72]

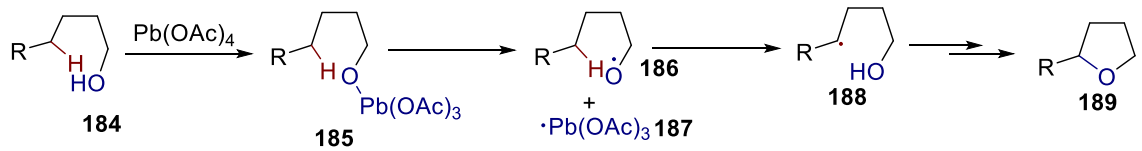

▪ *Suarez*

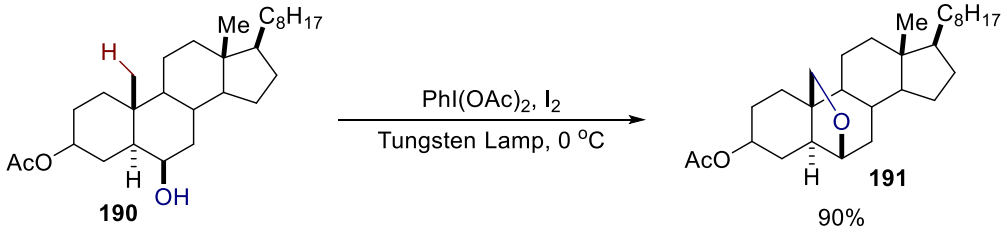

▪ *Ryu*

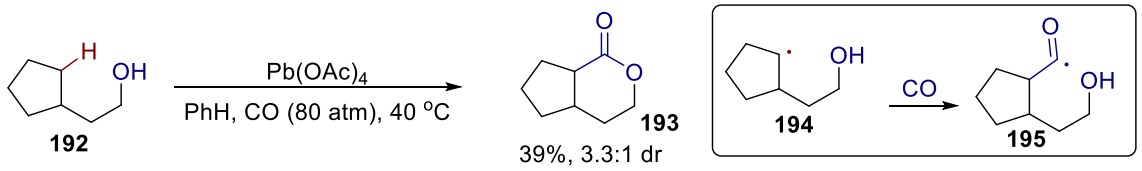

Scheme 2.3.15: Furan or Lactone Formation with Free Alcohols as Oxygen Radical Precursors

An alternative way to generate an oxygen radical is the illumination of UV light on a carbonyl group (Scheme 2.3.16). An electron is excited from the *n* orbital of the C-O bond to the

π*antibonding orbital of the same bond resulting in the formation of a diradical species, where the radicals reside on both the carbonyl oxygen and carbon. The oxygen-centered radical can then undergo 1,5 hydrogen atom transfer and dislocate the radical to the carbon atom δ to the oxygen. In the Norrish-Yang cyclization of **196**, the newly formed carbon radical can combine to the carbonyl carbon radical to form alkoxy-cyclobutane **199**.[73]

- *Yang*

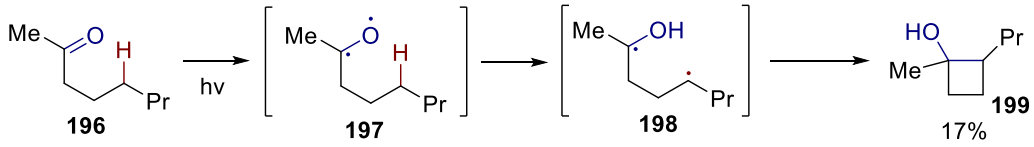

Scheme 2.3.16: Norrish-Yang Cyclization

- *Breslow*

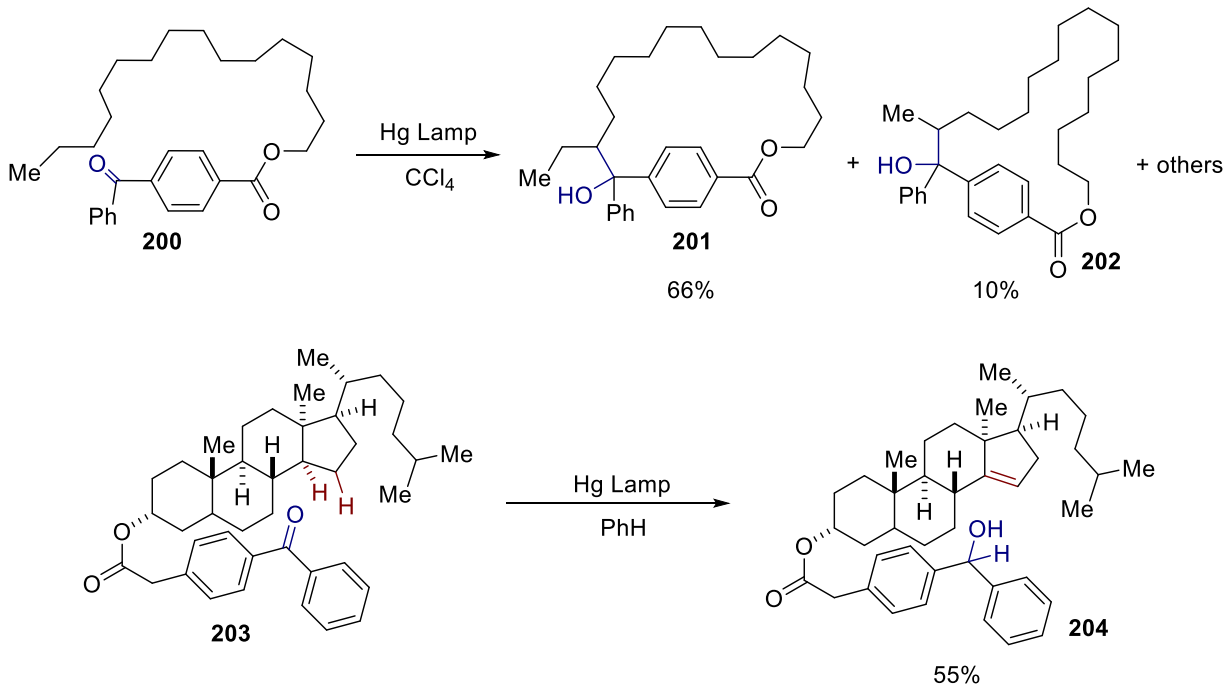

Scheme 2.3.17: Remote C-H Functionalization with Oxygen Radicals from Carbonyl Groups

Breslow demonstrated that this way of generating oxygen radicals can be harnessed for remote functionalization of unactivated C-H bonds (Scheme 2.3.17). For **200**, the long hydrogencarbon chain tethered to a benzoquinone through an ester linkage can be selectively oxidized for carbon-carbon bond formation at the terminal methylene groups.[74] This strategy has been extended to selective oxidation for complex steroid molecules such as **203**.[75]

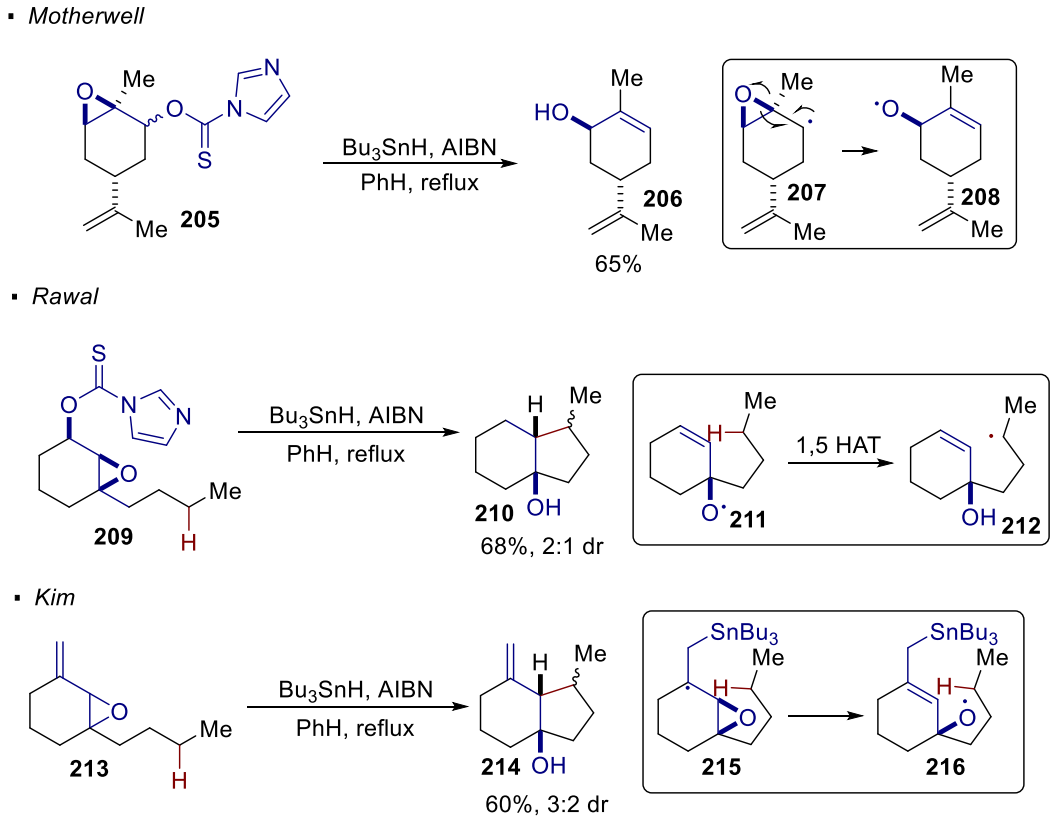

Scheme 2.3.18: Generation of Oxygen Radicals by Cleavage of Epoxides

The homolytic cleavage of a C-O bond of epoxides represents another way to generate an oxygen-centered radical. As demonstrated by Barton and Motherwell, the formation of a carbon radical α to the epoxide from **205** would lead to the homolytic cleavage of the C-O bond to form oxygen-centered radical **208** due to the ring strain of the epoxide (Scheme 2.3.18).[76] Rawal[77] and Kim[78] took the advantage of this way to generate an oxygen radical for inert sp^3 C-H bond

functionalization. The alkyl radical formed by 1,5 HAT can cyclize onto the alkene to from a cyclopentane (Scheme 2.3.18). Cyclopentanes **210** and **214** are synthesized in this way.

Recently, Chiba shows that a hydrogen atom in oxime **217** can be transferred to TEMPO to give oxygen radical **219** (Scheme 2.3.19).[57] The alkyl radical generated by 1,5 HAT can be trapped by TEMPO. After elimination and cyclization, isoxazole **218** is formed as the final product. The overall transformation is the oxidation of the C-H bond.

- *Chiba*

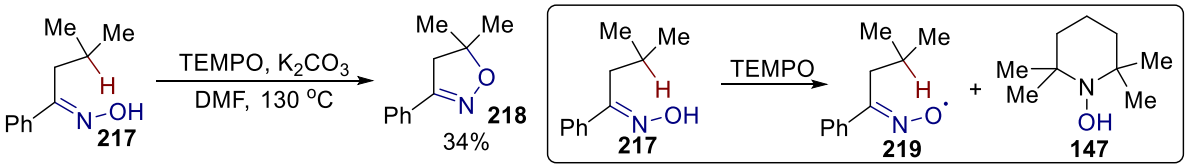

Scheme 2.3.19: Transfer of Hydrogen from Oxime to TEMPO for Oxygen Radical Generation

2.3.4.2 Applications and Limitations

Oxygen radicals are also often used in natural product syntheses (Scheme 2.3.20). Burke reported the oxidation of **220** to furan **221**, which is later oxidized to a γ-lactone for the synthesis of Nagilactone F.[79] In the total synthesis of punctatin A by Paquette, cyclobutane **222** is assembled by a Norrish-Yang cyclization of ketone **223**.[80] Baran uses an alcohol as a directing group in **224** to install functionalities in a remote methyl group, allowing the formation of cycloheptane in cortistatin A. Again by Baran, a Norrish-Yang cyclization of **226** is applied as the key step in the synthesis of ouabagenin to access cyclobutane **227**, which fragments to yield a primary alcohol.[81] The use of oxygen radicals for C-H functionalization shows a higher versatility than nitrogen radicals. If the OH bond is pre-activated to be a C-X bond, difficult functionalities can be incorporated. However, this pre-activation step is non-trivial and shows poor functional

group compatibility due to the strongly oxidizing conditions. In addition, the O-X bond is highly unstable and difficult to handle. This limits the utility of oxygen radicals. As demonstrated by the representative examples in natural product synthesis, an oxygen radical is mainly used for the formation of carbon-halogen bonds and Norrish-Yang cyclization. In these cases, a free O-H bond and a carbonyl group can be used to generate the oxygen radicals respectively.

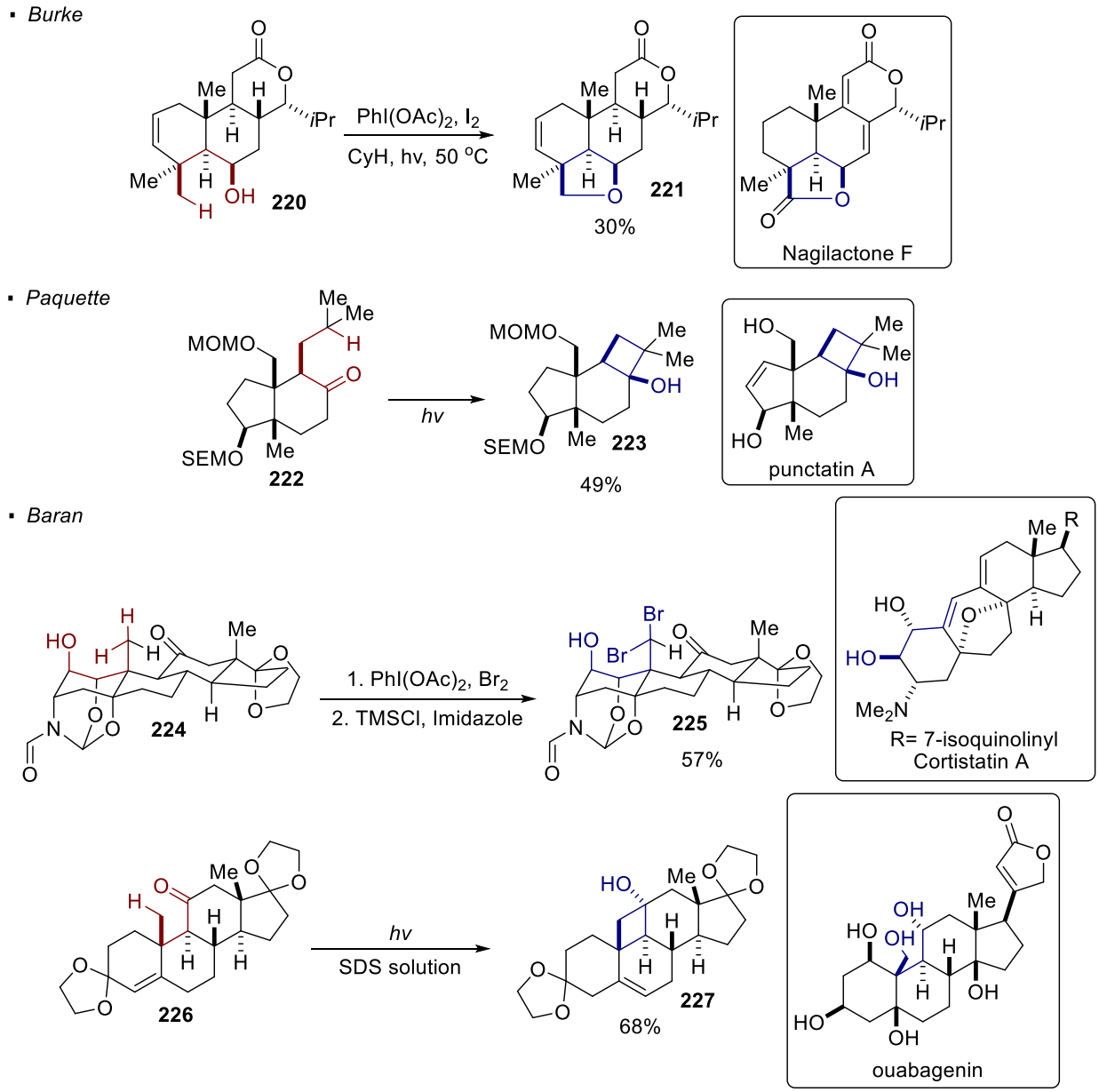

Scheme 2.3.20: Applications of Oxygen Radicals for Intramolecular HAT

2.3.5 Vinyl and Aryl Radicals

2.3.5.1 Generation and Transformations

The last class of high-energy radicals that can abstract a hydrogen atom form sp^3 C-H bonds are vinyl or aryl radicals. The higher bond strength of sp^2 C-H bonds (113 kcal/mol) than sp^3 C-H bonds (<100 kcal/mol) renders the HAT feasible.

- *Parsons*

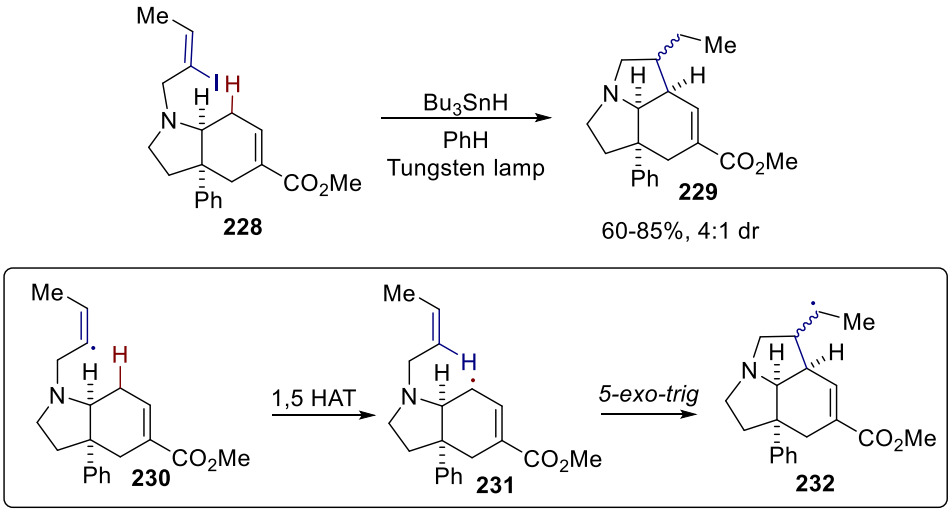

- *Curran*

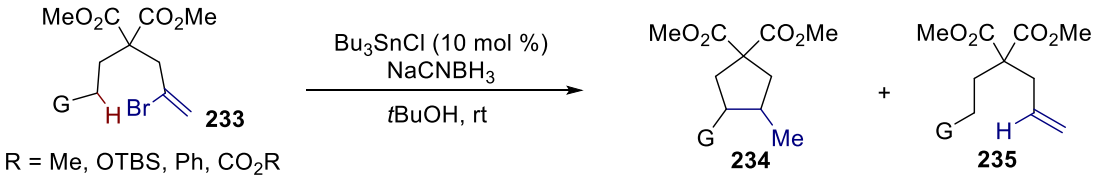

Scheme 2.3.21: Generation of Vinyl and Aryl Radicals by Reduction of Carbon-Halide Bonds

Generally, a vinyl or aryl radical is generated from the respective vinyl aryl halide in the presence of Bu_3SnH or other hydride sources and a radical initiator under thermal or photochemical conditions (Scheme 2.3.21). The reaction between the radical formed the initiator and the Sn hydride generates a Sn radical that can abstract the halogen atom from a carbon-

halogen bond to give the vinyl or aryl radical. If the vinyl halide is used, the alkyl radical formed by intramolecular HAT would be in the perfect position to cyclize on the vinyl group to from cyclopentanes, as demonstrated in the seminar report on the synthesis of **229** from **228** by Parsons.[82] Curran was the first to use this way of generating vinyl radicals for functionalizing unactivated sp^3 C-H bonds.[83] In these examples, a catalytic amount of Bu_3SnH is generated from Bu_3SnCl and $NaCNBH_3$.[84] This method of generating Sn-H is important to keep the concentration of Sn-H low and to minimize the reduction of the vinyl radical, a competitive pathway with 1,5 HAT.

- *Stork*

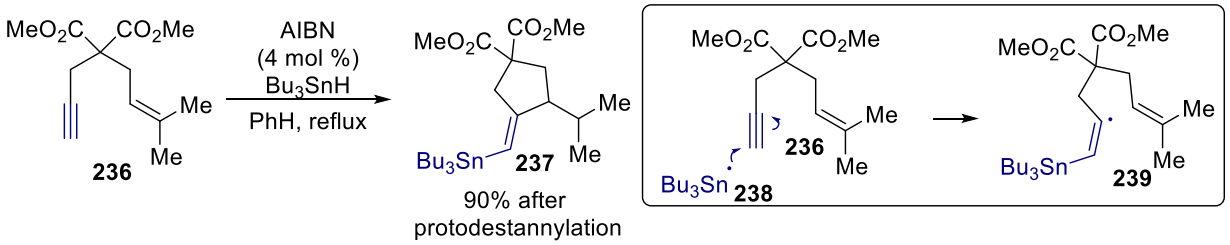

- *Malacria*

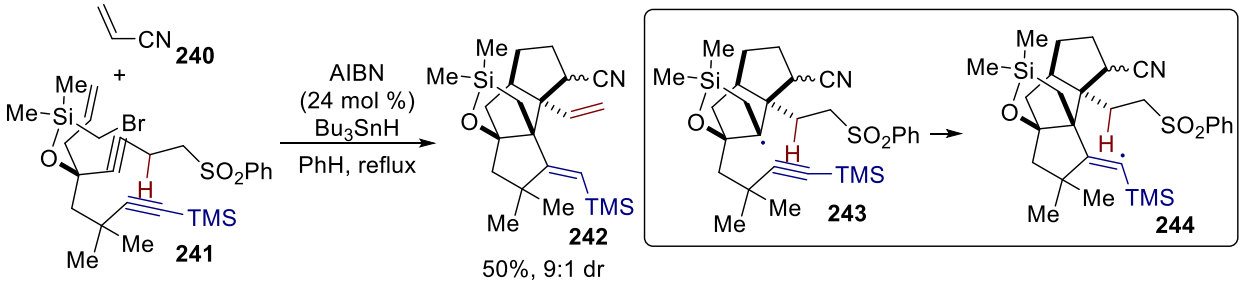

Scheme 2.3.22: Generation of Vinyl Radicals by Radical Addition to Alkynes

A vinyl radical can also be formed from radical addition to alkynes. Stork reported the addition of Sn(IV) radical **238** to alkyne **236** to form vinyl radical **239** (Scheme 2.3.22).[85] Malacria showed that linear triquinane **242** can be synthesized from acyclic **241** with a radical

cyclization/1,5 HAT/elimination cascade in which the alkyl radical in **243** adds to the alkyne to generate vinyl radical **244**.[86]

Furthermore, as demonstrated by Weinreb, aryl radicals can be generated from primary anilines with $NaNO_3$ under acidic conditions (Scheme 2.3.23).[87] The NH_2 group in **245** is converted into diazonium **247** whose decomposition is mediated by a copper salt to form aryl radical **248**. After 1,5 HAT and oxidation, α-oxygenated product **246** is formed. This method to generate aryl radicals for 1,5 HAT has been used to oxidize C-H bonds α to nitrogen, but not unactivated sp^3 C-H bonds.

- *Weinreb*

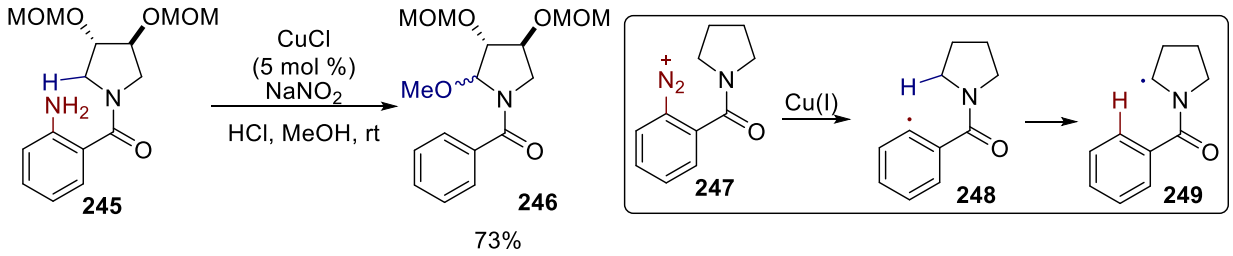

Scheme 2.3.23: Generation of Aryl Radicals with Diazonium Salts

2.3.5.2 Applications and Limitations

1,5 hydrogen atom transfer by vinyl or aryl radicals has been used for the functionalization of sp^3 C-H bonds in natural product synthesis. However, in all cases, the sp^3 C-H bonds are activated by a functional group such as a nitrogen atom. For instance, for the assembly of the [3.2.1] bicycloheptane framework of epibatidine, an aminyl radical is formed by the cleavage of a C-H bond α to nitrogen with an aryl radical (Scheme 2.3.24). [88] In the synthesis of phyllanthine and norsecurinine, Weinreb generates an aryl radical through copper-mediated decomposition

of an aryl diazonium species.[89] A 1,5 HAT event gives the aminyl radical that is subsequently oxidized for the formation of a C-Cl or C-O bond.

- *Ikeda*

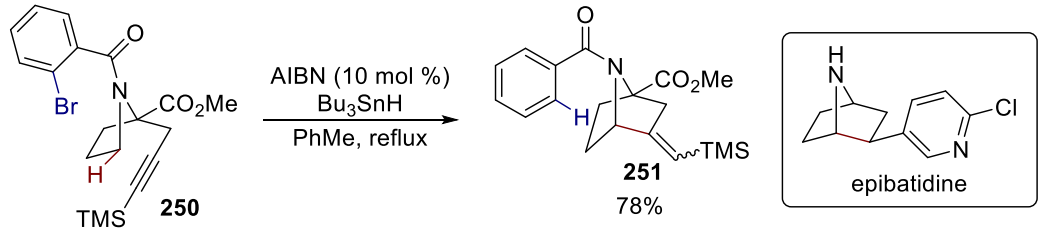

- *Weinreb*

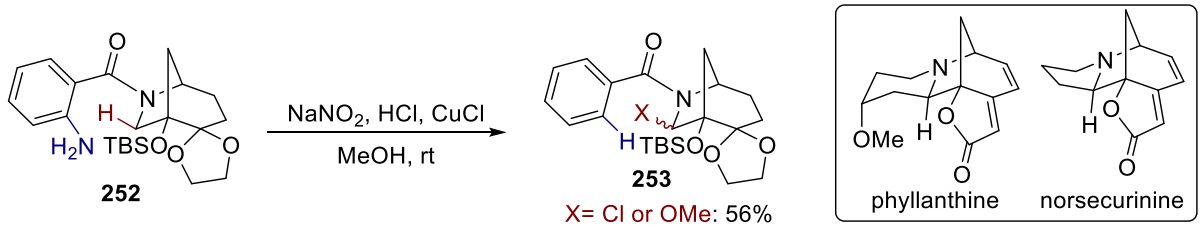

Scheme 2.3.24: Use of Aryl Radicals for Functionalization of C-H Bonds

Regarding the application of vinyl radicals to functionalize C-H bonds, Beaudry reported the formation of indole **255** through a radical translocation strategy that features a hydrogen atom transfer from a C-H α to nitrogen to an aryl radical in the synthesis of goniomitine (Scheme 2.3.25).[90]

- *Beaudry*

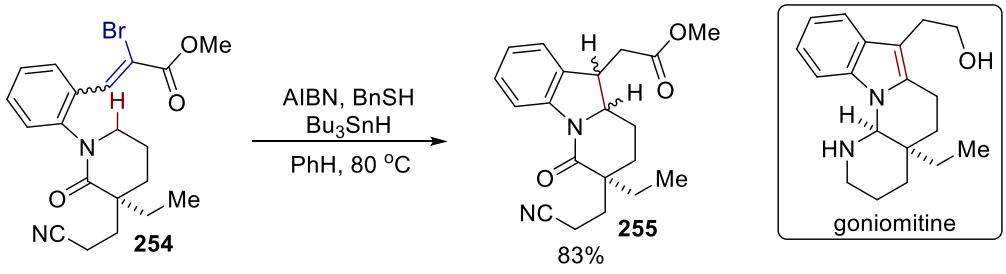

Scheme 2.3.25: Use of Vinyl Radicals for Functionalization of C-H Bonds

▪ *Curran*

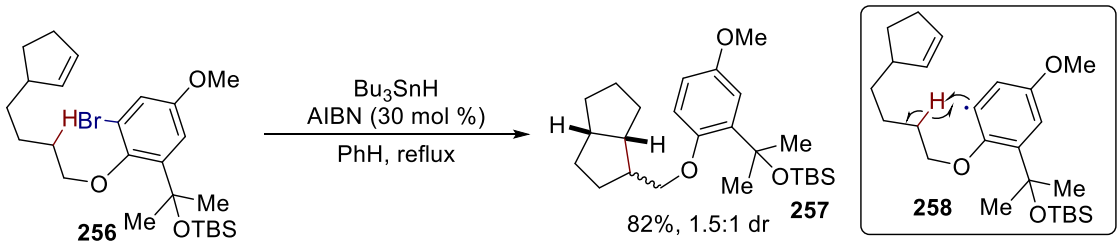

▪ *Malacria*

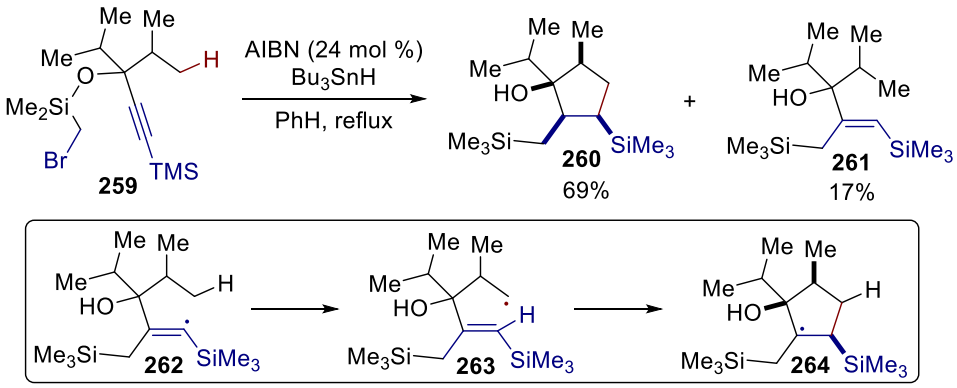

Scheme 2.3.26: Intramolecular Trapping of Alkyl Radicals with Tethered Alkenes

The functionalities that can be incorporated into an unactivated sp^3 C-H with the use of aryl or vinyl radicals are very limited. The hydride sources required to generate the vinyl/aryl radical can act as a hydrogen atom donor to the aryl radical before 1,5 HAT can take place or to the alkyl radical formed from 1,5 HAT. The overall transformation would be the net reduction of the vinyl or aryl halide while the alkyl C-H bond appears intact. Therefore, most of the successful reactions with this strategy have a tethered alkene or alkyne as the intramolecular radical trap to out-compete the side reaction between the alkyl radical and the hydride source. For instance, in Curran's protocol to functionalize the β C-H bond of alcohols, the alkyl radical is trapped by a tethered alkene to give cyclopentane **257** (Scheme 2.3.26).[91] The diastereoselective synthesis of cyclopentane **260** developed by Malacria also includes the addition of an alkyl radical formed from 1,5 HAT to a tethered alkene.[92] Alternatively, the nucleophilicity of the alkyl group is

enhanced by a heteroatom. Along with the use of a large excess of an electrophilic alkene (15 equiv.), the rate for the trapping of the radical with an untethered alkene increases drastically, leading to a synthetically useful reaction.[93] However, the C-H bonds applicable in this scenario are only limited to those α to oxygen or nitrogen and cannot be classified as inert C-H bonds. With the surge of photoredox catalysis, there appear novel ways to reduce an aryl halide to aryl radical with a photocatalyst but the use of the aryl intermediate for the functionalization of unactivated C-H bonds through intramolecular HAT remains to be explored.[94]

2.4 Chemistry of Metal Carbenoids/Nitrenoids

2.4.1 Reactivity

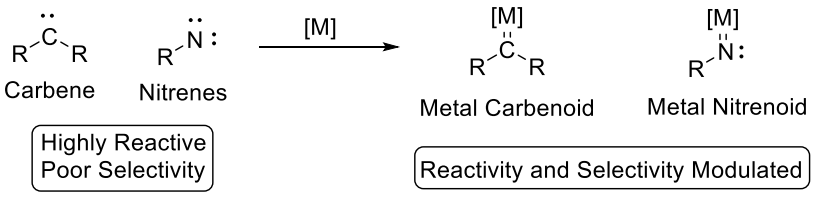

Figure 2.4.1: Trivalent Carbon and Nitrogen

Carbenes and Nitrenes are carbon and nitrogen with six electrons in the outermost shell. Because of the lack of an octet configuration, these species are highly unstable and can break even strong C-H bonds (Figure 2.4.1). On the other hand, the high reactivity also leads to selectivity issues and so in successful applications of carbenes and nitrenes in C-H functionalization, their reactivity is always modulated by stabilization by a transition metal catalyst, such as rhodium, copper or silver. With the resulting metal carbenoids and nitrenoids, the selectivity of a reaction can be tuned by the identity of the metals or the ligands on the metals.

The transition metal catalyst can also increase the ease of the formation of these species and allow reactions to be carried out under reasonably mild conditions.

There are two major classes of reactions that a metal carbenoid can undergo: cyclopropanation, and X-H insertion (X= C, O, N and Si) (Figure 2.4.2). Related to our discussion about sp^3 C-H functionalization is the C-H insertion reaction. The metal carbenoid, usually formed from the decomposition of α-diazo compounds in the presence of a metal, can insert into a C-H bond to form a C-C bond.

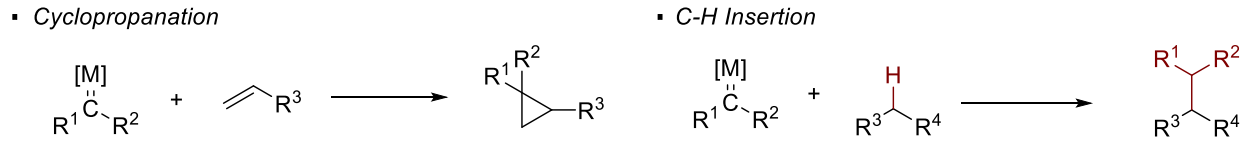

Figure 2.4.2: Reactivity of Metal Carbenoids

2.4.2 Intramolecular C-H insertion

Initial investigation of metal-mediated C-H insertion focused on the use of copper.[95] Teyssie first demonstrated the use of Rh carbenoids from diazo compounds with Rh(II) complexes for intermolecular O-H[96] and C-H insertions[97] (Scheme 2.4.1). Concurrently, Wenkert found that Rh(II) complexes are also competent catalysts for intramolecular allylic C-H insertion of **268**.[98] In the latter case, the excess of the substrates that bear the C-H bonds is not required and thus the reaction is synthetically useful. The focus here is the intramolecular C-H insertion in which the α-diazo compound can be viewed as a directing group. Soon after Wenkert's report, Taber demonstrated that unactivated sp^3 C-H bonds in **270** can also undergo insertion for the synthesis of cyclopentanone **271**.[99] In the current state-of-the-art for intramolecular C-H insertion reactions, Rh(II) complexes are the most common class of catalysts for C-H insertion.

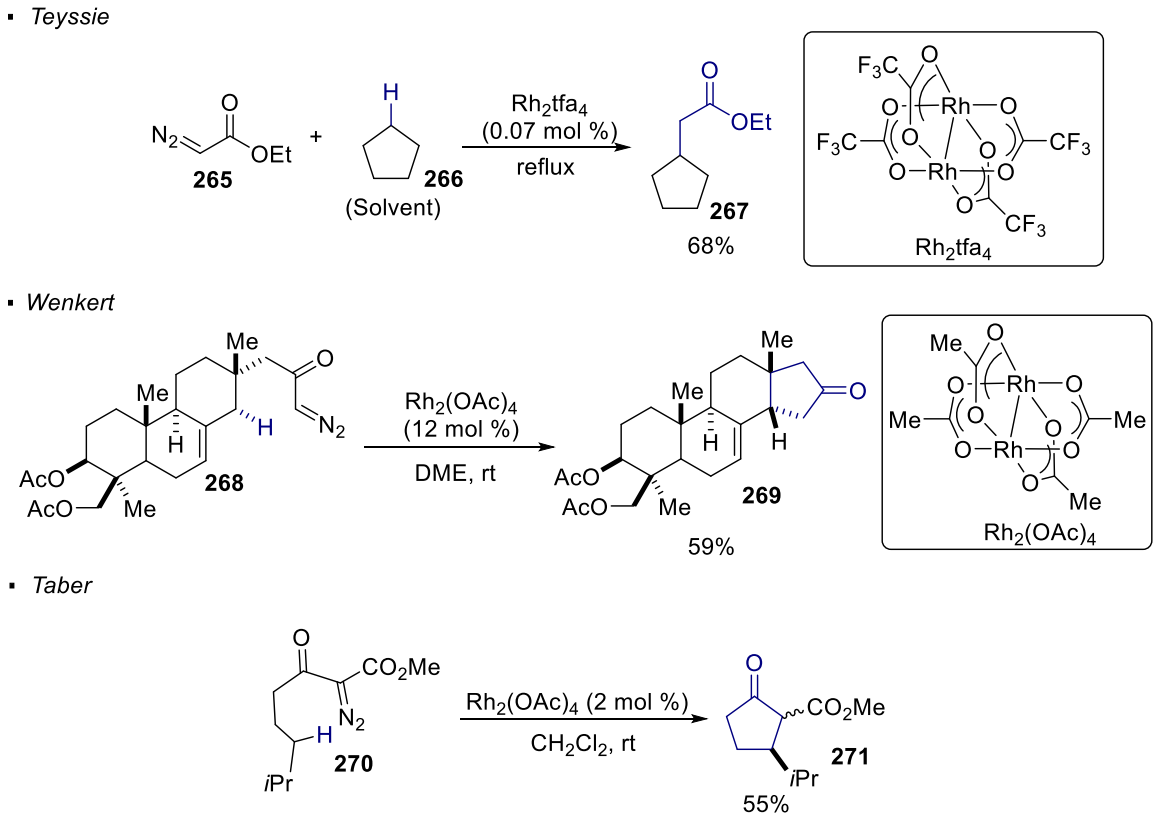

Scheme 2.4.1: Initial Reports on Rh(II)-Catalyzed C-H Insertion

The first highly enantioselective intramolecular C-H insertion, albeit applicable only for C-H bonds α to oxygen, was reported by Doyle (Scheme 2.4.2).[100] Enantiomerically enriched γ lactone **273** can be assembled from acyclic substrate **272** through Rh(II)-catalyzed C-H insertion. The key to the success is the use of novel chiral Rh(II) carboxamide catalysts. The extension to asymmetric insertion into unactivated C-H bonds, also a contribution from Doyle, can be achieved with Rh(II) complexes derived from chiral oxazolidinones.[101] Desymmetrization of prochiral alkyl groups in **276** can result in the generation of disubstituted γ lactone **277**.[102]

An intramolecular C-H insertion is a directed sp^3 C-H functionalization reaction, in which the geometry of the transition state plays the paramount role and favors the formation of cyclopentanes over cyclohexanes in acyclic substrates. Generally, Rh(II) catalyzed C-H insertion is

believed to be a single-step reaction with a concerted, yet asynchronous, transition state.[103] As a positive charge is being developed in the transition state, more electron rich C-H bonds are more reactive towards C-H insertion chemistry (Scheme 2.4.3).

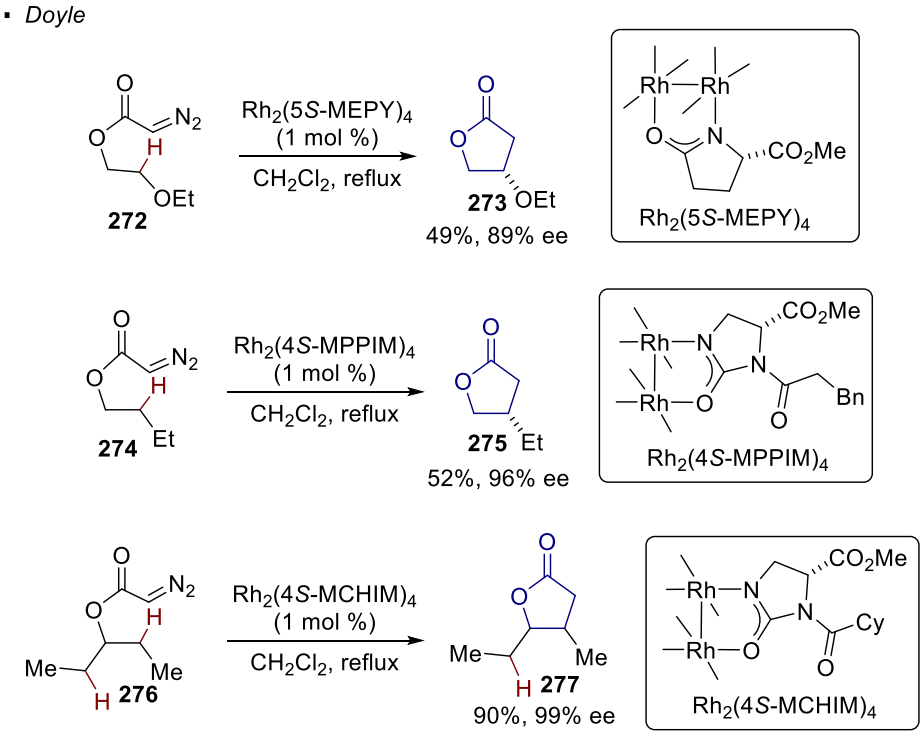

Scheme 2.4.2: Asymmetric Intramolecular C-H Insertion

2.4.3 Intramolecular C-H Amination

Similar to metal carbenoids, reactions that are feasible with metal nitrenoids include aziridination and amination of sp^3 C-H bonds. In regard to amination, Breslow first reported the tosylamidation of cyclohexane **282** with Mn or Fe catalysts ligated with tetraphenylporphyrin and (tosyliminoiodo)benzene **281** (Scheme 2.4.4).[104] Che demonstrated that the iminoiodobenzene reagents can be prepared *in-situ* with iodosobenzene and sulfonamides/ amides.[105]

▪ *Taber*

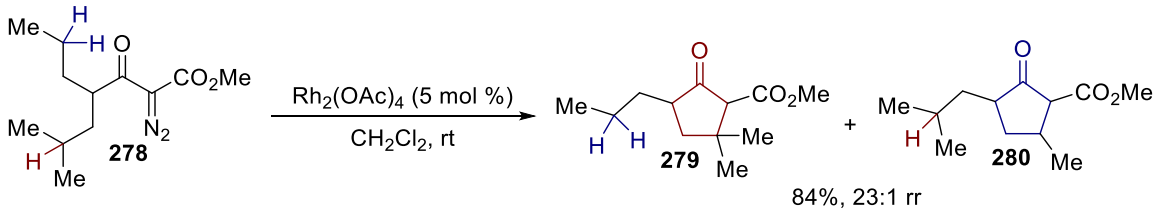

Scheme 2.4.3: Higher Reactivity with More Electron Rich C-H Bonds

▪ *Breslow*

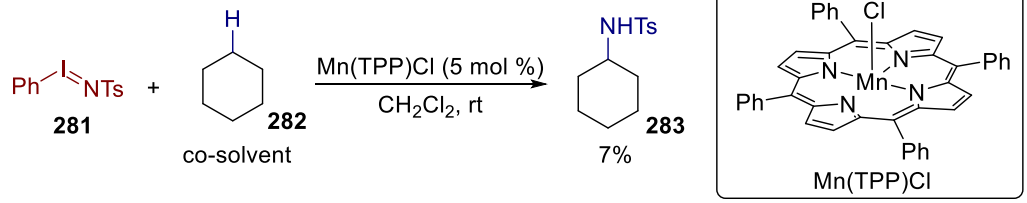

▪ *Che*

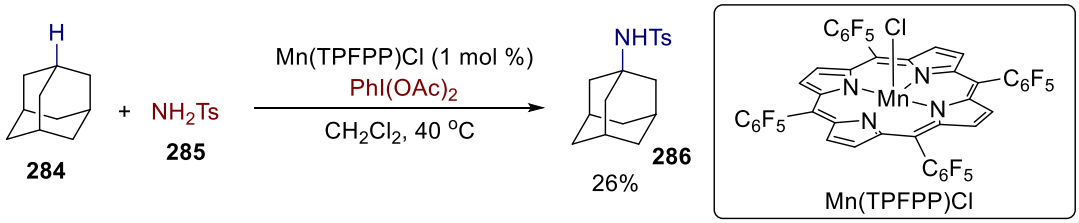

Scheme 2.4.4: Seminal Reports on Amination of Unactivated C-H Bonds

The first intramolecular amination reaction with metal nitrenoid where the amine derivatives can be viewed as a directing group, is reported by Du Bois with Rh(II) catalysis (Scheme 2.4.5).[106] The use of carbamate leads to selective formation of 5-membered pyrrolidines while 6-membered piperidines are the predominant product with sulfonamides and phosphoramidates. An alternative way to generate a metal nitrenoid is by the decomposition of organic azides. Betley reports that pyrrolidine **293** can be synthesized by the catalytic decomposition of organic azide **291** with a novel iron complex.[107]

Since then, intramolecular catalytic enantioselective C-H amination has been developed although high stereoselectivity can only be obtained with activated C-H bonds (Scheme 2.4.6).[108]

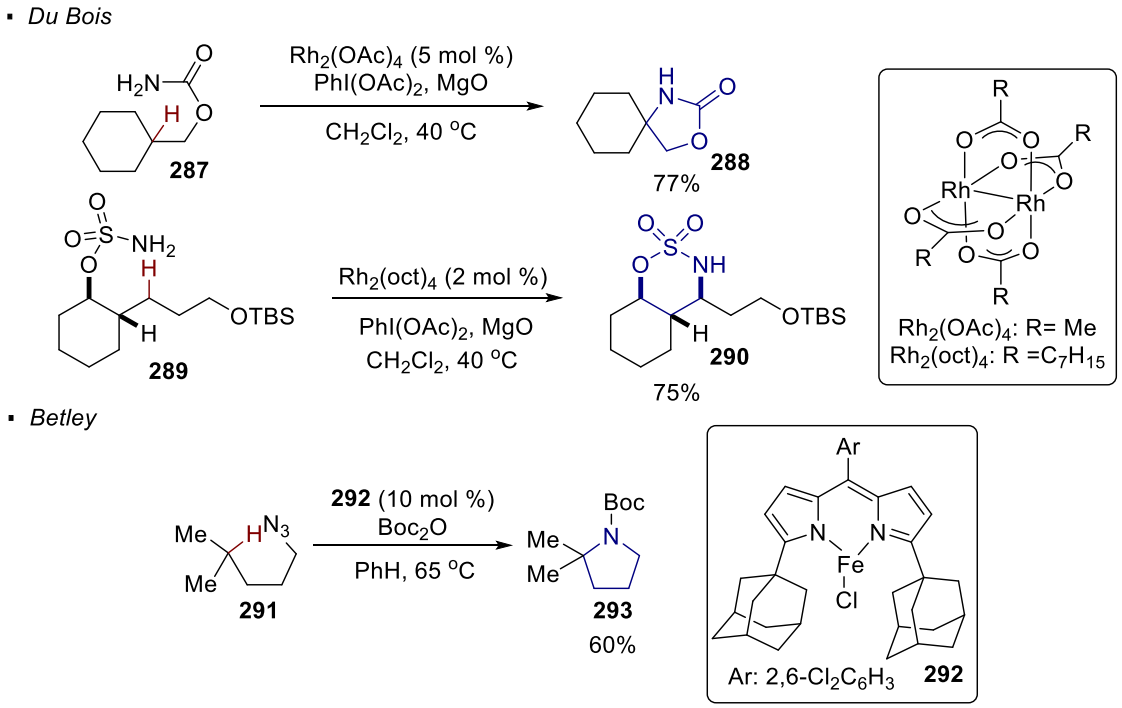

Scheme 2.4.5: Intramolecular C-H Amination for Synthesis of Nitrogen Heterocycles

The mechanism of C-H amination with metal nitrenoids is contingent on the identity of the metal catalysts. For Rh(II) catalyzed intramolecular C-H amination, experimental evidence and theoretical studies support a concerted asynchronous mechanism.[109] On the other hand, a carbon radical formed from the abstraction of a hydrogen atom from the C-H bond by the metal nitrenoid is proposed for Ru, Mn or Fe catalysts ligated by porphyrins (Figure 2.4.3).[110] The latter mechanism resembles a rebound mechanism that is believed to be responsible for the hydroxylation of C-H bonds by the cytochrome P450 class of enzymes.[111] Sometimes, the mechanism is less clear. Both mechanisms are believed to be feasible for Betley's case.

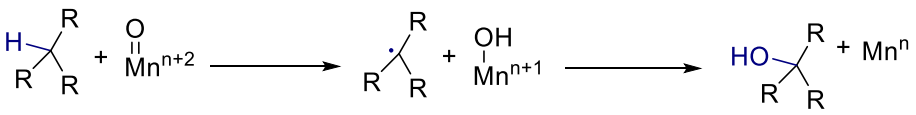

Figure 2.4.3: Rebound Mechanism for Hydroxylation

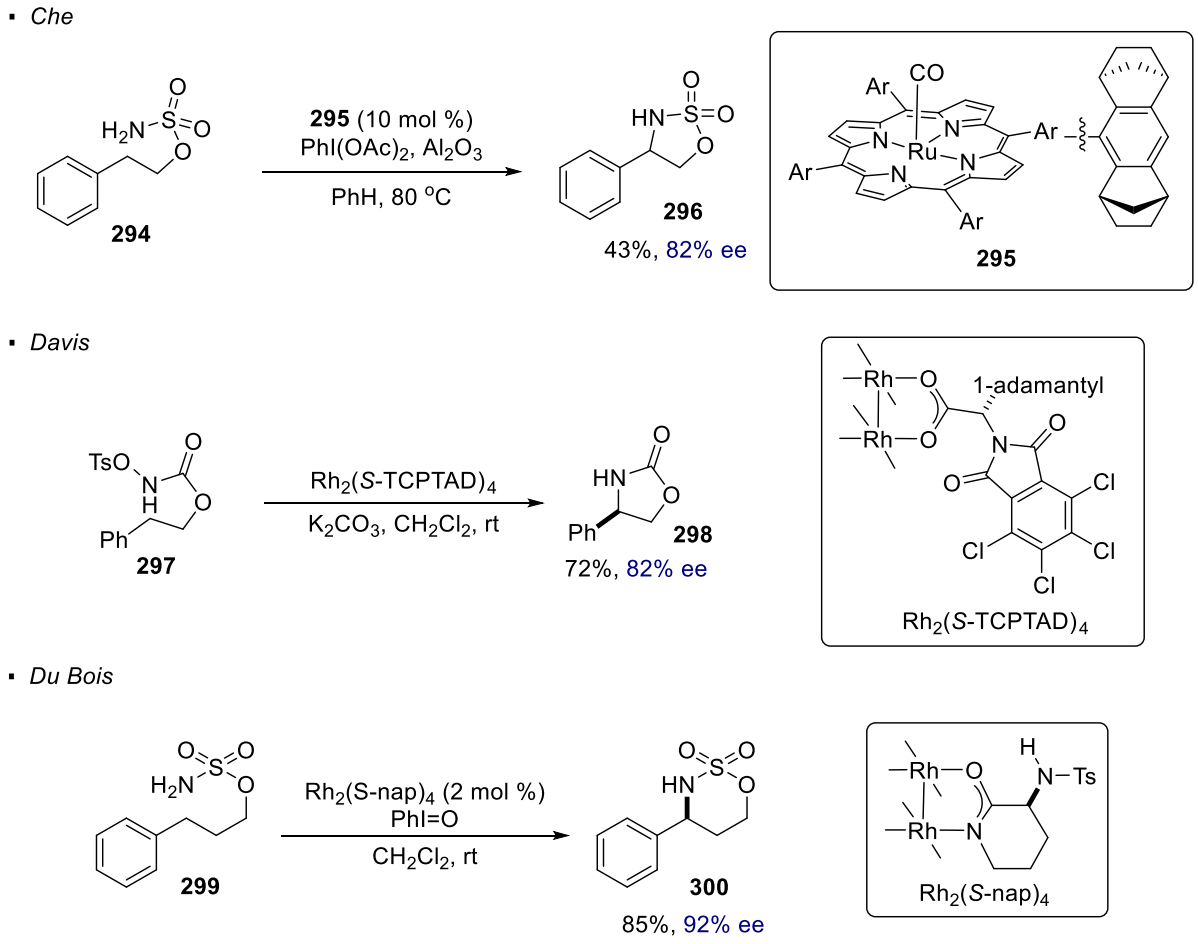

Scheme 2.4.6: Asymmetric Intramolecular C-H Amination

Brewlow demonstrated that selective oxidation of unactivated C-H bonds of steroid molecules can be accomplished by installation of sulfonic acid-containing-directing groups which have a strong affinity to the cyclodextrin on the Mn catalyst (Scheme 2.4.7).[112] More recently, White reported a Fe-catalyzed directed hydroxylation of unactivated sp^3 C-H bonds that features this rebound mechanism allowed by a high valent Fe-oxo catalytic species.[113] For instance, lactone **305** can be synthesized from carboxylic acid **304**.

2.4.4 Applications and Limitations

The chemistry of metal carbenoids and nitrenoids has found countless applications, especially as a strategy for late-stage sp^3 C-H functionalization in natural product synthesis. Early examples include contributions from Cane[114] and Taber[115], who independently synthesized the methyl ester of pentalenolactone E with Rh-catalyzed C-H insertion (Scheme 2.4.8). Cane assembles the six-membered lactone with the Rh carbenoid while one of the cyclopentanes is synthesized with the C-H insertion step in Taber's synthesis. Additionally, Taber prepared heavily functionalized cyclopentane **311**, which is elaborated into alkaloid 251F.[116]

- *Breslow*

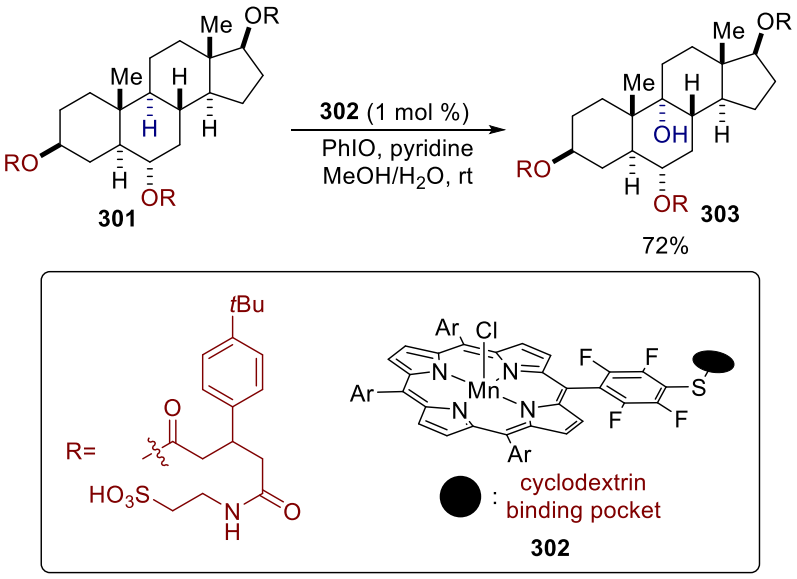

- *White*

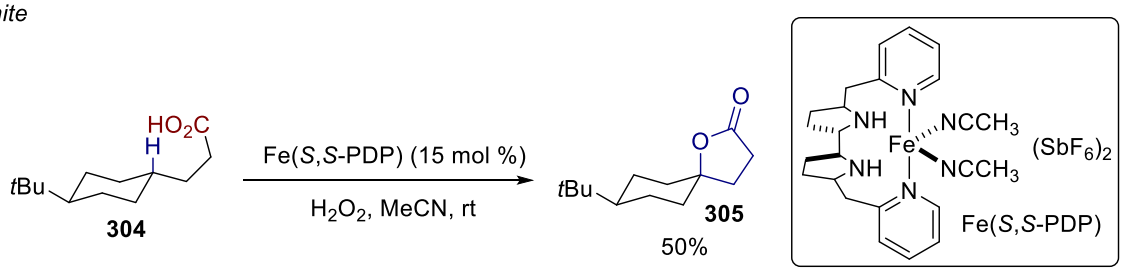

Scheme 2.4.7: Directed Hydroxylation with Rebound Mechanism

▪ *Cane*

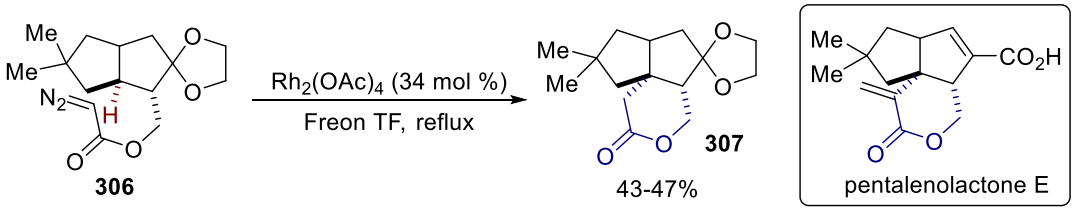

▪ *Taber*

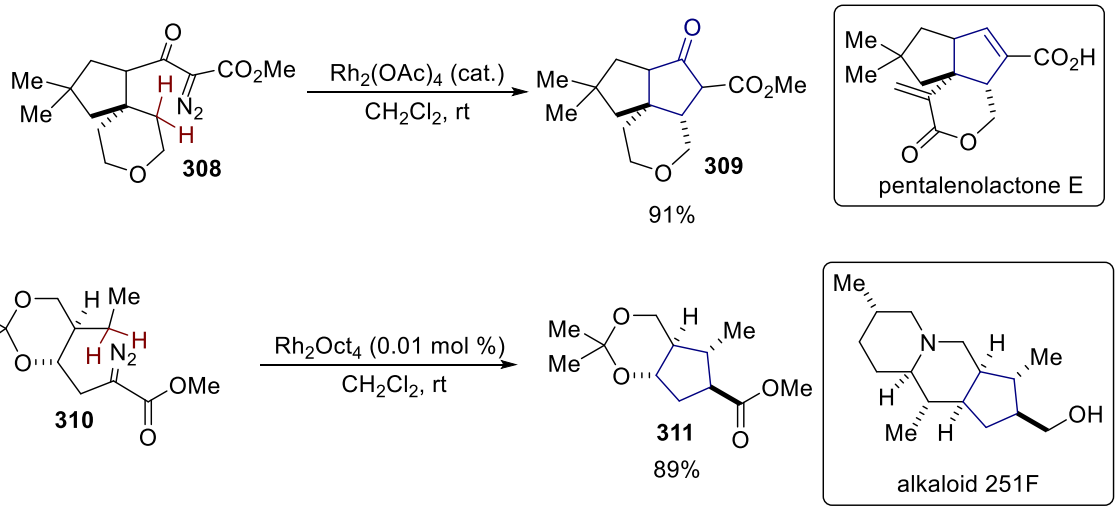

Scheme 2.4.8: Applications of C-H Insertion with Metal Carbenoids

Stereoselectivity of the C-H insertion is sometimes an important issue in natural product synthesis. In these cases, the chiral ligands on the metal carbenoids play an important role in governing the stereochemical outcome of the reaction. In the synthesis of (−)-astrogorgidiol by Taber, a diastereoselective C-H insertion reaction of **312** is used to construct cyclopentane **313** (Scheme 2.4.9).[117] While the use of non-chiral Rh catalysts gives almost no diastereoselectivity, the chiral catalyst derived from phenyl alanine favors the formation of the desired diastereomer. Doyle established the absolute stereochemistry of γ-lactone **315** through an enantioselective C-H insertion event for the synthesis of (+)-isolauricerisinol.[101]

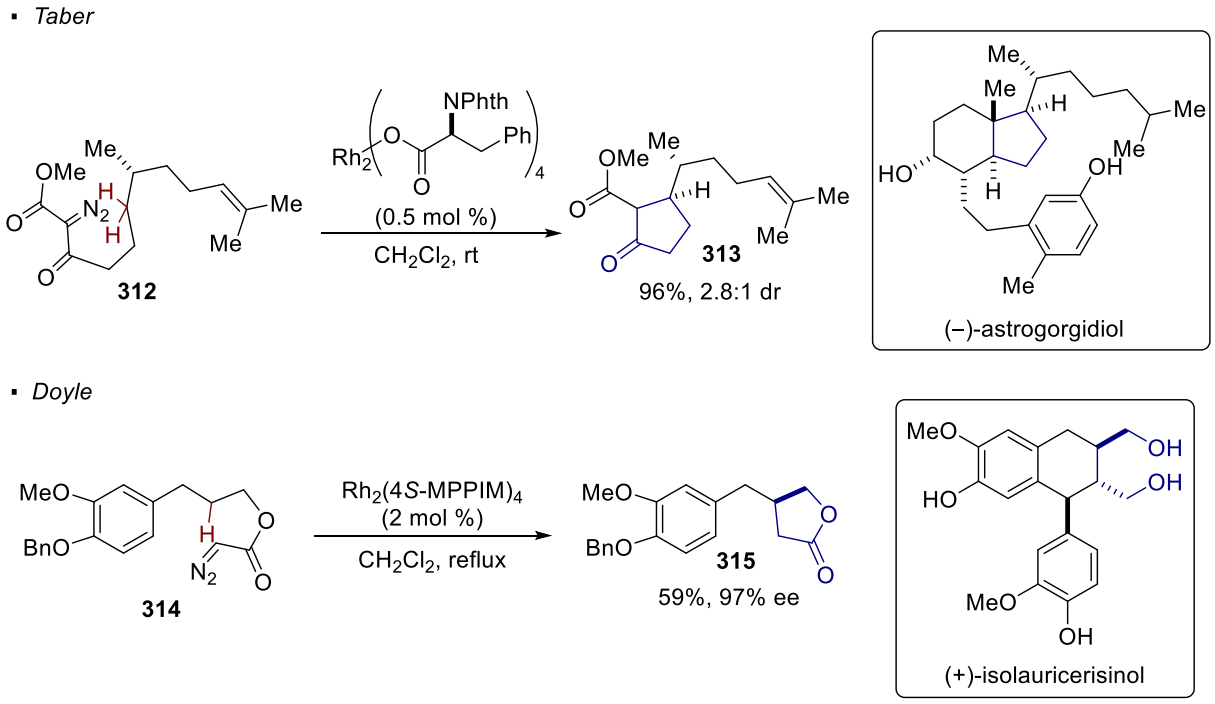

Scheme 2.4.9: Chiral Ligands for Stereoselective C-H insertion in Natural Product Synthesis

Regarding the use of metal nitrenoid in total synthesis, Du Bois reports a Rh(II)-catalyzed amination of a tertiary C-H bond as a key step in the synthesis of manzacidin A (Scheme 2.4.10).[118] For the synthesis of (–)-tetrodotoxin, he applied a Rh(II)-catalyzed C-H amination of a sterically hindered tertiary C-H bond in structurally complex polycyclic intermediate **318**.[119] Garg's synthesis of (–)-*N*-methylwelwitindolinone features the amination of the unactivated tertiary C-H bond of advanced intermediate **320** which bears multiple functionalities with a silver nitrenoid.[120] The two latter examples underscore the utility of the chemistry with metal carbenoid/nitrenoid in late-stage functionalization of complex molecules.

The power of C-H insertion and amination is demonstrated by the aforementioned examples in natural product synthesis. This kind of transformation is particularly useful for electron rich tertiary or secondary C-H bonds and is applicable even when the C-H bonds are in a

sterically encumbered environment. Despite its success, it does not provide a way to functionalize sp^3 C-H bonds beyond C-C bond formation and amination. In an intramolecular event where the carbenoids and nitrenoids act as a directing group to control the site-selectivity, a carbo- or heterocycle is inevitably formed. This lack of versatility falls short of the expectation to meet the need to derivatize an organic molecule with minimal structural distortion, especially in the context of medicinal chemistry and chemical biology.

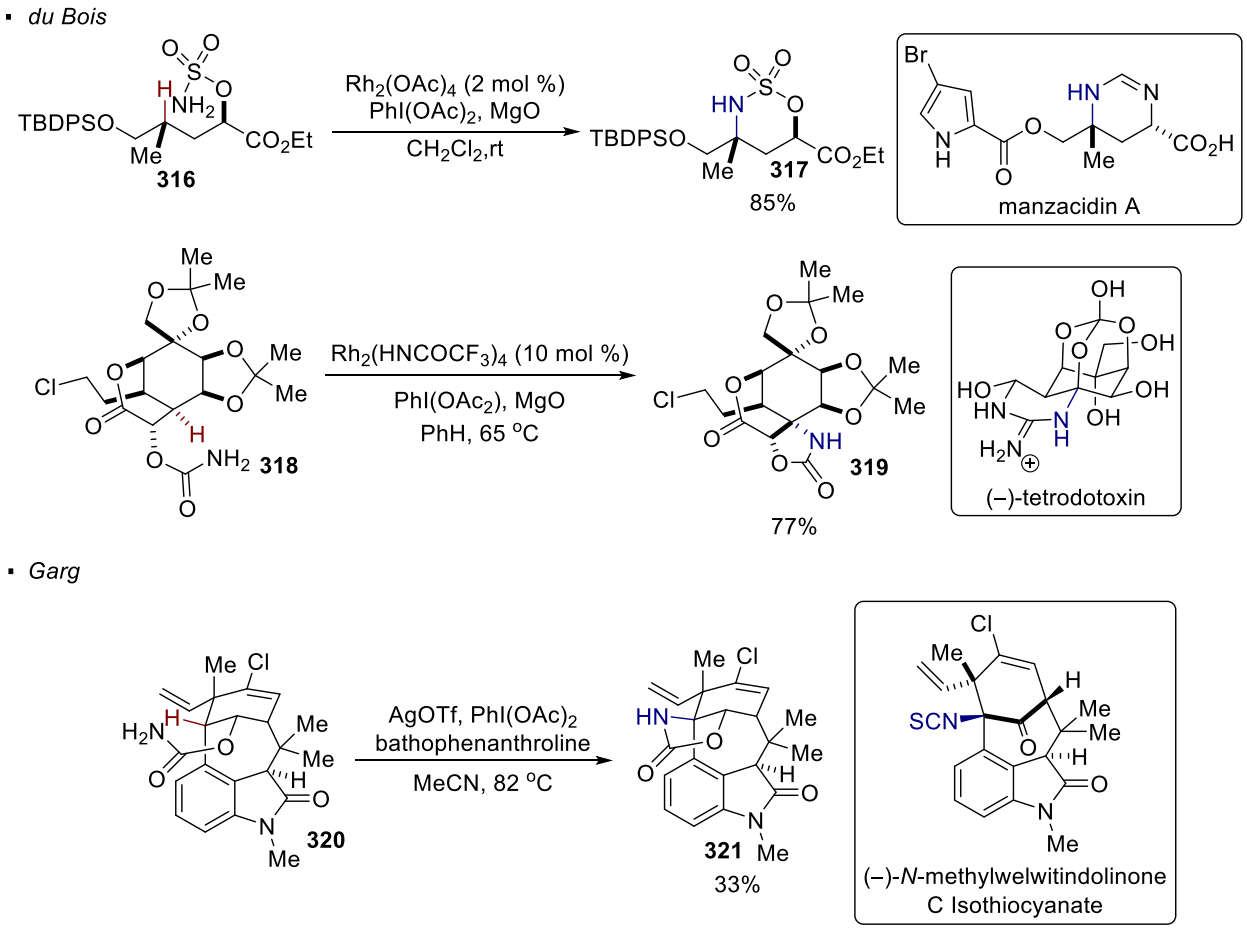

Scheme 2.4.10: Applications of C-H Amination with Metal Nitrenoids

2.5 Summary

The functionalization of unactivated sp^3 C-H bonds has served as the strategic steps in the synthesis of many natural products and biologically active molecules. In many cases, the directing group is the key for addressing reactivity and selectivity issues. The three main approaches for realizing C-H functionalization are transition-metal catalyzed C-H activation, hydrogen atom transfer, and C-H insertion/amination with metal carbenoids/nitrenoids. To further broaden the versatility of each of these already powerful approaches, future research should be directed to address the limitations associated with the scope of functionalities that can be encoded into the C-H bonds, the choice of directing groups, the position of the C-H bonds relative to the directing group and the types of C-H bonds that can be functionalized.

REFERENCES

1. (a) Chen, D. Y.-K.; Youn, S. W. *Chem. Eur. J.* **2012**, *18*, 9452-9474; (b) Yamaguchi, J.; Yamaguchi, A. D.; Itami, K. *Angew. Chem. Int. Ed.* **2012**, *51*, 8960-9009; (c) Gutekunst, W. R.; Baran, P. S. *Chem. Soc. Rev.* **2011**, *40*, 1976-1991; (d) Kakiuchi, F.; Chatani, N. *Adv. Synth. Catal.* **2003**, *345*, 1077-1101.

2. (a) Cernak, T.; Dykstra, K. D.; Tyagarajan, S.; Vachal, P.; Krska, S. W. *Chem. Soc. Rev.* **2016**, *45*, 546-576; (b) Wencel-Delord, J.; Glorius, F. *Nature Chem.* **2013**, *5*, 369-375.

3. Lawrence, J. D.; Takahashi, M.; Bae, C.; Hartwig, J. F. *J. Am. Chem. Soc.* **2004**, *126*, 15334-15335.

4. (a) Cho, S. H.; Kim, J. Y.; Kwak, J.; Chang, S. *Chem. Soc. Rev.* **2011**, *40*, 5068-5083; (b) McMurray, L.; O'Hara, F.; Gaunt, M. J. *Chem. Soc. Rev.* **2011**, *40*, 1885-1898.

5. Blanksby, S. J.; Ellison, G. B. *Acc. Chem. Res.* **2003**, *36*, 255-263.

6. (a) Stoutland, P. O.; Bergman, R. G.; Nolan, S. P.; Hoff, C. D. *Polyhedron* **1988**, *7*, 1429-1440; (b) Wick, D. D.; Jones, W. D. *Organometallics* **1999**, *18*, 495-505.

7. Shilov, A. E.; Shul'pin, G. B. *Russ. Chem. Rev.* **1987**, *56*, 442-464.

8. Lin, M.; Shen, C.; Garcia-Zayas, E. A.; Sen, A. *J. Am. Chem. Soc.* **2001**, *123*, 1000-1001.

9. Dangel, B. D.; Johnson, J. A.; Sames, D. *J. Am. Chem. Soc.* **2001**, *123*, 8149-8150.

10. Desai, L. V.; Hull, K. L.; Sanford, M. S. *J. Am. Chem. Soc.* **2004**, *126*, 9542-9543.

11. Giri, R.; Chen, X.; Yu, J.-Q. *Angew. Chem. Int. Ed.* **2005**, *44*, 2112-2115.

12. (a) Zhu, R.-Y.; Tanaka, K.; Li, G.-C.; He, J.; Fu, H.-Y.; Li, S.-H.; Yu, J.-Q. *J. Am. Chem. Soc.* **2015**, *137*, 7067-7070; (b) Chen, G.; Shigenari, T.; Jain, P.; Zhang, Z.; Jin, Z.; He, J.; Li, S.; Mapelli, C.; Miller, M. M.; Poss, M. A.; Scola, P. M.; Yeung, K.-S.; Yu, J.-Q. *J. Am. Chem. Soc.* **2015**, *137*, 3338-3351 (c) He, J.; Wasa, M.; Chan, K. S. L.; Yu, J.-Q. *J. Am. Chem. Soc.* **2013**, *135*, 3387-

3390; (d) Wasa, M.; Engle, K. M.; Yu, J.-Q. *J. Am. Chem. Soc.* **2010**, *132*, 3680-3681; (e) Yoo, E. J.; Wasa, M.; Yu, J.-Q. *J. Am. Chem. Soc.* **2010**, *132*, 17378-17380; (f) Giri, R.; Maugel, N.; Li, J.-J.; Wang, D.-H.; Breazzano, S. P.; Saunders, L. B.; Yu, J.-Q. *J. Am. Chem. Soc.* **2007**, *129*, 3510-3511.

13. Jiang, H.; He, J.; Liu, T.; Yu, J.-Q. *J. Am. Chem. Soc.* **2016**, *138*, 2055-2059.
14. (a) Ren, Z.; Mo, F.; Dong, G. *J. Am. Chem. Soc.* **2012**, *134*, 16991-16994; (b) Xu, Y.; Yan, G.; Ren, Z.; Dong, G. *Nature Chem.* **2015**, *7*, 829-834; (c) Thompson, S. J.; Thach, D. Q.; Dong, G. *J. Am. Chem. Soc.* **2015**, *137*, 11586-11589; (d) Huang, Z.; Wang, C.; Dong, G. *Angew. Chem. Int. Ed.* **2016**, *55*, 5299-5303.
15. Topczewski, J. J.; Cabrera, P. J.; Saper, N. I.; Sanford, M. S. *Nature* **2016**, *531*, 220-224.
16. (a) McNally, A.; Haffemayer, B.; Collins, B. S. L.; Gaunt, M. J. *Nature* **2014**, *510*, 129-133; (b) Smalley, A. P.; Gaunt, M. J. *J. Am. Chem. Soc.* **2015**, *137*, 10632-10641.
17. Calleja, J.; Pla, D.; Gorman, T. W.; Domingo, V.; Haffemayer, B.; Gaunt, M. J. *Nature Chem.* **2015**, *7*, 1009-1016.
18. Xiao, K.-J.; Lin, D. W.; Miura, M.; Zhu, R.-Y.; Gong, W.; Wasa, M.; Yu, J.-Q. *J. Am. Chem. Soc.* **2014**, *136*, 8138-8142.
19. (a) Chen, G.; Gong, W.; Zhuang, Z.; Andra, M. S.; Chen, Y.-Q.; Hong, X.; Yang, Y.-F.; Liu, T.; Houk, K. N.; Yu, J.-Q. *Science* **2016**, *353*, 1023-1027; (b) Wasa, M.; Chan, K. S. L.; Zhang, X.-G.; He, J.; Miura, M.; Yu, J.-Q. *J. Am. Chem. Soc.* **2012**, *134*, 18570-18572.
20. Simmons, E. M.; Hartwig, J. F. *Nature* **2012**, *483*, 70-73.
21. Kang, T.; Kim, Y.; Lee, D.; Wang, Z.; Chang, S. *J. Am. Chem. Soc.* **2014**, *136*, 4141-4144.
22. Huang, X.; Wang, Y.; Lan, J.; You, J. *Angew. Chem. Int. Ed.* **2015**, *54*, 9404-9408.

23. Wang, X.; Yu, D-.G.; Glorius, F. *Angew. Chem. Int. Ed.* **2015**, *54*, 10280-10283.

24. Hasegawa, N.; Charra, V.; Inoue, S; Fukumoto, Y.; Chatani, N. *J. Am. Chem. Soc.* **2011**, *133*, 8070-8073.

25. Nakao, Y.; Morita, E.; Idei, H.; Hiyama, T. *J. Am. Chem. Soc.* **2011**, *133*, 3264-3267.

26. Zaitsev, V. G.; Shabashov, D.; Daugulis, O. *J. Am. Chem. Soc.* **2005**¸ *127*, 13154-13155.

27. Aihara, Y.; Chatani, N. *J. Am. Chem. Soc.* **2014**, *136*, 898-901.

28. Wu, X.; Zhao, Y.; Ge, H. *J. Am. Chem. Soc.* **2014**, *136*, 1789-1792.

29. Shang, R.; Ilies, L.; Matsumoto, A.; Nakamura, E. *J. Am. Chem. Soc.* **2013**, *135*, 6030-6032.

30. Wu, X.; Yang, K.; Zhao, Y.; Sun, H.; Li, G.; Ge, H. *Nature Commun.* **2015**, *6*, 6462.

31. Wu, X.; Zhao, Y.; Zhang, G.; Ge, H. *Angew. Chem. Int. Ed.* **2014**, *53*, 3706-3710.

32. Dangel, B. D.; Godula, K.; Youn, S. W.; Sezen, B.; Sames, D. *J. Am. Chem. Soc.* **2002**, *124*, 11856-11857.

33. (a) Johnson, J. A.; Sames, D. *J. Am. Chem. Soc.* **2000**, *122*, 6321-6322; (b) Johnson, J. A.; Li, N.; Sames, D. *J. Am. Chem. Soc.* **2002**, *124*, 6900-6903.

34. (a) Fortner, K. C.; Kato, D.; Tanaka, Y.; Shair, M. D. *J. Am. Chem. Soc.* **2009**, *132*, 275-280; (b) Giannis, A.; Heretsch, P.; Sarli, V.; Stobel, A. *Angew. Chem. Int. Ed.* **2009**, *48*, 7911-7914; (c) See, Y. Y.; Herrmann, A. T.; Aihara, Y.; Baran, P. S. *J. Am. Chem. Soc.* **2015**, *137*, 13776-13779.

35. (a) Baudoin, O.; Herrbach, A.; Gueritte, F. *Angew. Chem. Int. Ed.* **2003**, *42*, 5736-5740; (b) Chaumontet, M.; Piccardi, R; Audic, N.; Nitce, J.; Peglion, J.-L.; Clot, E.; Baudoin, O. *J. Am. Chem. Soc* **2008**, *130*, 15157-15166; (c) Chaumontet, M.; Piccardi, R.; Baudoin, O *Angew. Chem. Int. Ed.* **2009**, *48*, 179-182.

36. Feng, Y.; Chen, G. *Angew. Chem. Int. Ed.* **2009**, *49*, 958-961.

37. Siler, D. A.; Mighion, J. D.; Sorensen, E. J. *Angew. Chem. Int. Ed.* **2014**, *53*, 5332-5335.

38. Reger, D. L.; Garza, D. G.; Baxter, J. C. *Organometallics* **1990**, *9*, 873-874.

39. Robertson, J.; Pillai, J.; Lush, R. K. *Chem. Soc. Rev.* **2001**, *30*, 94-103.

40. Van der Eycken, E.; Van der Eycken, J.; Vandewalle, M. *J. Chem. Soc. Chem. Commun.* **1985**, 1719-1720.

41. Rhodes, C. J.; Agirbas, H. *J. Chem. Soc. Perkin Trans. 2* **1992**, 397-402.

42. Cekovic, Z. *Tetrahedron* **2003**, *59*, 8073-8090

43. Micovic, V. M.; Mamuzic, R. I.; Jeremic, D.; Mihailovic, M. L. *Tetrahedron* **1964**, *20*, 2279-2287.

44. Wille, U.; Plath, C. *Liebigs Ann.* **1997**, 111-119.

45. Chen, K.; Richter, J. M.; Baran, P. S. *J. Am. Chem. Soc.* **2008**, *130*, 7247-7249.

46. Rey, V.; Pierini, A. B.; Penenory, A. B. *J. Org. Chem.* **2009**, *74*, 1223-1230.

47. Nechab, M.; Mondal, S.; Bertrand, M. P. *Chem. Eur. J.* **2014**, *20*, 16034-16059.

48. Nishio, T.; Koyama, H.; Sasaki, D.; Sakamoto, M. *Helv. Chim. Acta.* **2005**, *88*, 996-1003.

49. Lalevee, J.; Allonas, X.; Fourassier, J.-P. *J. Am. Chem. Soc.* **2002**, *124*, 9613-9621.

50. Hofmann, A. W. *Ber. Dtsch. Chem. Ges.* **1879**, *12*, 984-990.

51. (a) Hernandez, R.; Rivera, A.; Salazar, J. A.; Suarez, E. *J. Chem. Soc. Chem. Commun.* **1980**, 958-959; (b) Carrau, R.; Hernandez, R.; Suarez, E. *J. Chem. Soc. Perkin Trans. 1* **1987**, 937-943; (c) de Armas, P.; Francisco, C. G.; Hernandez, R.; Salazar, J. A.; Suarez, E. *J. Chem. Soc. Perkin Trans. 1* **1988**, 3255-3265; (d) Betancor, C.; Concepcion, J. I.; Hernandez, R.; Salazar, J. A.; Suarez, E. *J. Org. Chem.* **1983**, *48*, 4430-4432; (e) de Armas, P.; Carrau, R.; Concepcion, J. I.; Francisco, C. G.; Hernandez, R.; Suarez, E. *Tetrahedron Lett.* **1985**, *26*, 2493-2496.

52. Liu, T.; Mei, T.-S.; Yu, J.-Q. *J. Am. Chem. Soc.* **2015**, *137*, 5781-5874.

53. Nikishin, G. I.; Troyansky, E. I.; Laareva, M. I. *Tetrahedron* **1985**, *41*, 4279-4288.

54. Yang, M.; Su, B.; Wang, Y.; Chen, K.; Jiang, X.; Zhang, Y.-F.; Zhang, X.-S.; Chen, G.; Cheng, Y.; Cao, Z.; Guo, Q.-Y.; Wang, L.; Shi, Z.-J. *Nature Commun.* **2014**, *5*, 4707.

55. Zhou, T.; Luo, F.-X.; Yang, M.-Y.; Shi, Z.-J. *J. Am. Chem. Soc.* **2015**, *137*, 14586-14589.

56. (a) Wang, Y.-F.; Chen, H.; Zhu, X.; Chiba, S. *J. Am. Chem. Soc.* **2012**, *134*, 11980-11983; (b) Chen, H., Sanjaya, S.; Wang, Y.-F.; Chiba, S. *Org. Lett.* **2013**, *15*, 212-215.

57. Zhu, X.; Wang, Y.-F.; Ren, W.; Zhang, F.-L.; Chiba, S. *Org. Lett.* **2013**, *15*, 3214-3217.

58. Kim, S. Yeon, K. M.; Yoon, K. S. *Tetrahedron Lett.* **1997**, *38*, 3919-3922.

59. Minozzi, M.; Nanni, D.; Spagnolo, P. *Chem. Eur. J.* **2009**, *15*, 7830-7840.

60. Chen, H.; Chiba, S. *Org. Biomol. Chem.* **2014**, *12*, 42-46.

61. Faulkner, A.; Race, N. J.; Scott, J. S.; Bower, J. F. *Chem. Sci.* **2014**, *5*, 2416-2421.

62. Qin, Q.; Yu, S. *Org. Lett.* **2015**, *17*, 1894-1897.

63. Corey, E. J.; Hertler, W. R. *J. Am. Chem. Soc.* **1958**, *80*, 2903-2904. **,**

64. Sanz-Cervera, J. F.; Williams, R. M. *J. Am. Chem. Soc.* **2002**, *124*, 2556-2559.

65. Cherney, E. C.; Lopchuk, J. M.; Green, J. C.; Baran, P. S. *J. Am. Chem. Soc.* **2014**, *136*, 12592-12595.

66. Chen, K.; Baran, P. *Nature* **2009**, *459*, 824-828.

67. Barton, D. H. R.; Beaton, J. M. *J. Am. Chem. Soc.* **1960**, *82*, 2641.

68. Walling, C.; Padwa, A. *J. Am. Chem. Soc.* **1963**, *85*, 1597-1601.

69. Petrovic, G.; Saicic, R. N.; Cekovic, Z. *Tetrahedron Lett.* **1997**, *38*, 7107-7110.

70. Petrovic, G.; Cekovic, Z. *Tetrahedron* **1999**, *55*, 1377-1390.

71. Cekovic, Z.; Cvetkovic, M. *Tetrahedron Lett.* **1982**, *23*, 3791-3794.

72. Tsunoi, S.; Ryu, I.; Okuda, T.; Tanaka, M.; Komatsu, M.; Sonoda, N. *J. Am. Chem. Soc.* **1998**, *120*, 8692-8701.

73. Yang, N. C.; Yang, D.-D. H. *J. Am. Chem. Soc.* **1958**, *80*, 2913-2914.

74. Breslow, R.; Winnik, M. A. *J. Am. Chem. Soc.* **1969**, *91*, 3083-3084.

75. (a) Breslow, R.; Baldwin, S.; Flechtner, T.; Kalicky, P.; Liu, S.; Washburn, W. *J. Am. Chem. Soc.* **1973**, *95*, 3251-3262; (b) Brewslow, R.; Baldwin, S. *J. Am. Chem. Soc.* **1970**, *92*, 732-734; (c) Breslow, R.; Kalicky, P. *J. Am. Chem. Soc.* **1971**, *93*, 3540-3541.

76. Barton, D. H. R.; Motherwell, R. S. H.; Motherwell, W. B. *J. Chem. Soc. Perkin Trans. 1*, **1981**, 2363-2367.

77. Rawal, V. H.; Newton, R. C.; Krishnamurthy, V. *J. Org. Chem.* **1990**, *55*, 5181-5183.

78. Kim, S.; Lee, S.; Koh, J. S. *J. Am. Chem. Soc.* **1991**, *113*, 5106-5107.

79. Burke, S. D.; Kort, M. E.; Strickland, S. M. S.; Organ, H. M.; Silks, L. A. III *Tetrahedron Lett.* **1994**, *35*, 1503-1506.

80. Paquette, L. A.; Sugimura, T. *J. Am. Chem. Soc.* **1986**, *108*, 3841-3842.

81. Renata, H.; Zhou, Q.; Baran, P. S. *Science* **2013**, *339*, 59-63.

82. Lathbury, D. C.; Parsons, P. J.; Pinto, I. *J. Chem. Soc. Chem. Commun.* **1988**, 81-82.

83. Curran, D. P.; Shen, W. *J. Am. Chem. Soc.* **1993**, *115*, 6051-6059.

84. Stork, G.; Sher, P. M. *J. Am. Chem. Soc.* **1986**, *108*, 303-304.

85. Stork, G.; Mook, R., Jr. *J. Am. Chem. Soc.* **1987**, *109*, 2829-2831.

86. Devin, P.; Fensterbank, L.; Malacria, M. *J. Org. Chem.* **1998**, *63*, 6764-6765.

87. Han, G.; McIntosh, M. C.; Weinreb, S. M. *Tetrahedron Lett.* **1994**, *35*, 5813-5816.

88. Ikeda, M.; Kugo, Y.; Kondo, Y.; Yamazaki, T.; Sato, T. *J. Chem. Soc.* Perkin Trans. 1 **1997**, 3339-3344.

89. Han, G.; LaPorte, M. G.; Folmer, J. J.; Werner, K. M.; Weinreb, S. M. *Angew. Chem. Int. Ed.* **2000**, *39*, 237-240.

90. Vellucci, J. K.; Beaudry, C. M. *Org. Lett.* **2015**, *17*, 4558-4560.

91. Curran, D. P.; Xu, J. *J. Am. Chem. Soc.* **1996**, *118*, 3142-3147.

92. Bogen, S.; Gulea, M.; Fensterbank, L.; Malacria, M. *J. Org. Chem.* **1999**, *64*, 4920-4925.

93. Willams, L.; Booth, S. E.; Undheim, K. *Tetrahedron* **1994**, *50*, 13697-13708.

94. Nguyen, J. D.; D'Amato, E. M. D.; Narayanam, J. M. R.; Stephenson, C. R. J. *Nature Chem.* **2014**, *4*, 854-859.

95. Doyle, M. P.; Duffy, R.; Ratnikov, M.; Zhou, L. *Chem. Rev.* **2010**, *110*, 704-724.

96. Paulissen, R.; Reimlinger, H.; Hayez, E.; Hubert, A. J.; Teyssie, P. *Tetrahedron Lett.* **1973**, *14*, 2233-2236.

97. Demonceau, A.; Noels, A. F.; Hubert, A. J.; Teyssie, P. *J. Chem. Soc. Chem. Commun.* **1981**, 688-689.

98. Wenkert, E.; Davis, L. L.; Mylari, B. L.; Solomon, M. F.; da Silva, R. R.; Shulman, S.; Warnet, R. J. *J. Org. Chem.* **1982**, *47*, 3242-3247.

99. (a) Taber, D. F.; Petty, E. H. *J. Org. Chem.* **1982**, *47*, 4808-4809; (b) Taber, D. F.; Hennessy, M. J.; Louey, J. P. *J. Org. Chem.* **1992**, *57*, 436-441.

100. Doyle, M. P.; van Oeveren, A.; Westrum, L. J.; Protopopova, M. N.; Clayton, T. W. Jr. *J. Am. Chem. Soc.* **1991**, *113*, 8982-8984.

101. Bode, J. W.; Doyle, M. P.; Protopopova, M. N.; Zhou, Q.-L. *J. Org. Chem.* **1996**, *61*, 9146-9155.

102. Doyle, M. P.; Zhou, Q.-L.; Dyatkin, A. B.; Ruppar, D. A. *Tetrahedron Lett.* **1995**, *36*

103. Taber, D. F.; Ruckle, R. E., Jr. *J. Am. Chem. Soc.* **1986**, *108*, 7686-7693.

104. Breslow, R.; Gellman, S. H. *J. Chem. Soc. Chem. Commun.* **1982**, 1400-1401.

105. Yu, X.-Q.; Huang, J.-S.; Zhou, X.-G.; Che, C.-M. *Org.Lett.* **2000**, *2*, 2233-2236.

106. Du Bois, J., Espino, C. G. *Angew. Chem. Int. Ed.* **2001**, *40*, 598-600.

107. Hennessy, E. T.; Betley, T. A. *Science* **2013**, *340*, 591-595.

108. Zalatan, D. N.; Du Bois, J. *J. Am. Chem. Soc.* **2008**, *130*, 9220-9221.

109. Roizen, J.; Harvey, M. E.; Du Bois, J. *Acc. Chem. Res.* **2012**, *45*, 911-922.

110. Au, S.-M.; Huang, J.-S.; Yu, W.-Y.; Fung, W.-H., Che, C.-M. *J. Am. Chem. Soc.* **1999**, *121*, 9120-9132.

111. Isin, E. M.; Guengerich, P. *Biochim. Biophys. Acta.* **2007**, *1770*, 314-329.

112. Yang, J.; Gabriele, B.; Bevedere, S.; Huang, Y.; Breslow R. *J. Org. Chem.* **2002**, *67*, 5057-5067.

113. (a) Chen, M. S.; White, M. C. *Science* **2007**, *318*, 783-787; (b) Bigi, M. A.; Reed, S. A.; White, M. C. *Nature Chem.* **2011**, *3*, 216-222; (c) Bigi, M. A.; Reed, S. A.; White, M. C. *J. Am. Chem. Soc.* **2012**, *134*, 9721-9726.

114. Cane, D. E.; Thomas, P. J. *J. Am. Chem. Soc.* **1984**, *106*, 5295-5303.

115. Taber, D. F.; Schuchardt, J. L. *J. Am. Chem. Soc.* **1985**, *107*, 5289-5290.

116. Taber, D. F.; You, K. K. *J. Am. Chem. Soc.* **1995**, *117*, 5757-5762.

117. Taber, D. F.; Malcolm, S. C. *J. Org. Chem.* **2001**, *66*, 944-953.

118. Wehn, P. M.; Du Bois, J. *J. Am. Chem. Soc.* **2002**, *124*, 12950-12951.

119. Hinman, A.; Du Bois, J. *J. Am. Chem. Soc.* **2003**, *125*, 11510-11511.

120. Huters, A. D.; Quasdorf, K. W.; Styduhar, E. D.; Garg, N. K. *J. Am. Chem. Soc.* **2011**, *133*, 15797-15799.

CHAPTER THREE: AMIDE-DIRECTED PHOTOREDOX-CATALYZED C-C BOND FORMATION AT UNACTIVATED SP^3 C-H BONDS

3.1 Introduction

3.1.1 Research Design and Inspiration

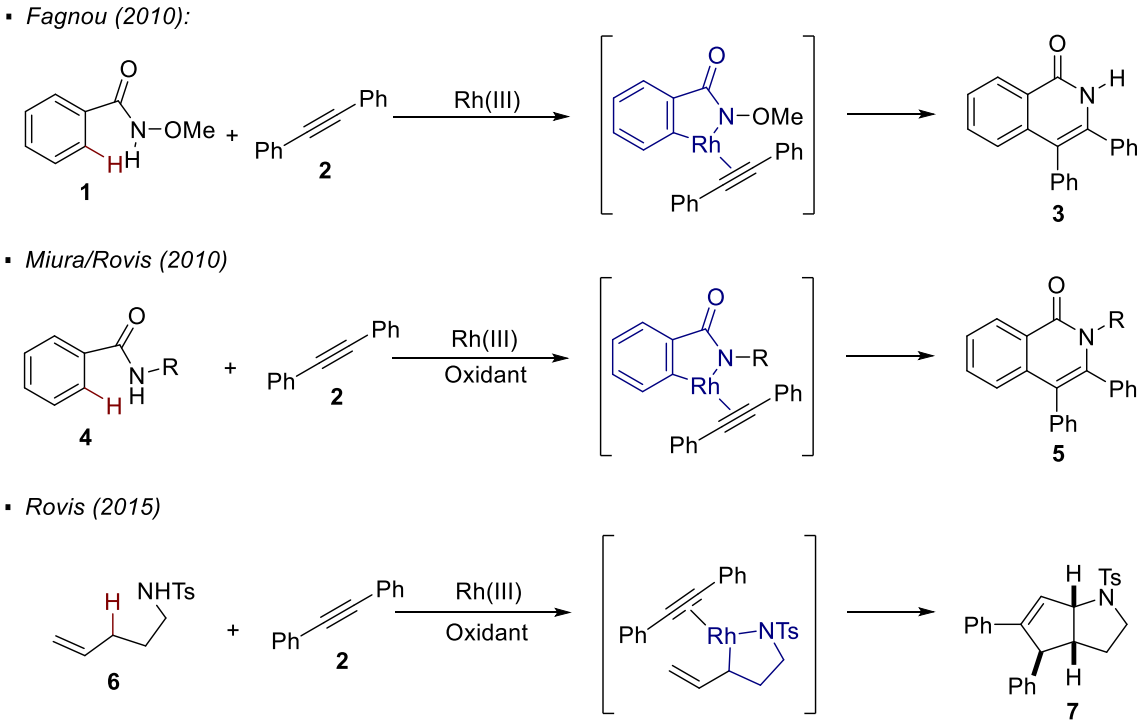

Scheme 3.1.1: Rh(III)-Catalyzed C-H Activation for Nitrogen-Heterocycles

As described in Chapter 1, the Rovis group has had a long-standing interest in the synthesis of nitrogen-heterocycles. In 2010, Fagnou,[1] Miura,[2] and Rovis[3] concurrently reported a Rh(III)-catalyzed 2-component synthesis of isoquinolines from benzamides and alkynes (Scheme 3.1.1). The key feature of this reaction is the use of an amide to direct the Rh(III) catalyst to cleave the *ortho* sp^2 C-H bond. This consequently generates a Rh-aryl intermediate that can insert into the alkyne. To enhance the power and versatility of Rh(III)-catalyzed C-H activation, we are

focusing our efforts towards the activation of sp^3 C-H bonds.[4] We developed a Rh(III)-catalyzed synthesis of azabicycles from the activation of allylic sp^3 C-H bonds. Since piperidines are the most prevalent nitrogen-heterocycles in small-molecule drugs,[5] our plan was to develop a Rh(III)-catalyzed synthesis of piperidines (**10**). This was envisioned via a formal [4+2] cycloaddition with aliphatic amines (**8**) and unsaturated systems, such as diphenylacetylene **9**. The key step would feature the activation of a sp^3 C-H bond to form a Rh(III)-alkyl intermediate (Scheme 3.1.2). Unfortunately, our efforts in this direction proved fruitless.

▪ *Proposed:*

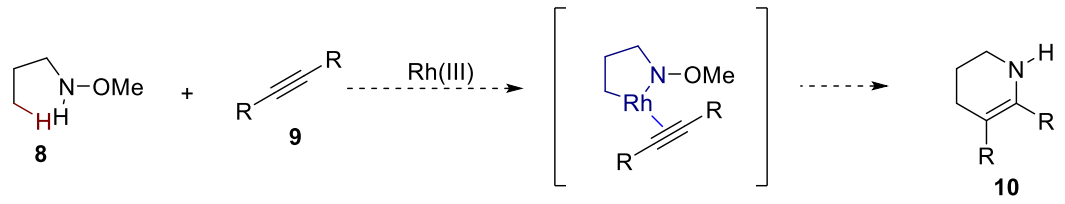

Scheme 3.1.2: Original Proposal on Rh(III)-Catalyzed sp^3 C-H Activation

▪ *Hofmann*

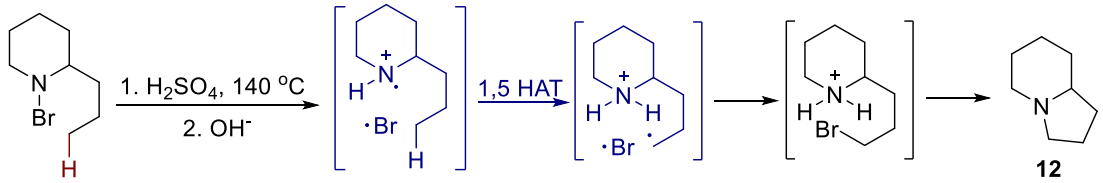

▪ *Suarez*

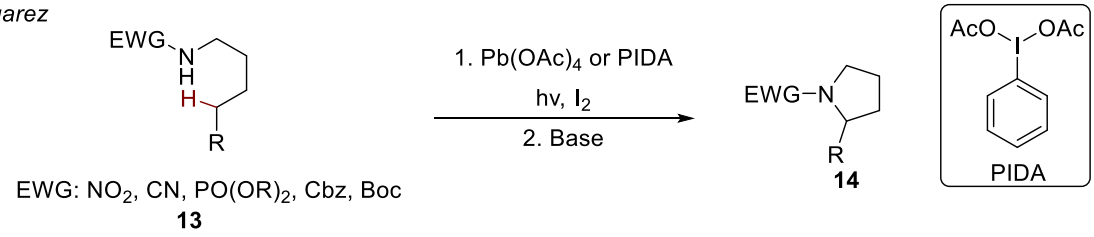

Scheme 3.1.3: Hofmann-Loffler-Freytag Reaction

While current research on functionalization of unactivated sp^3 C-H bonds is dominated by transition-metal catalysis, 1,5 hydrogen atom transfer (HAT)[6] appeared to us as an

alternative strategy to functionalize unactivated sp^3 C-H bonds (See chapter 2 for details of HAT). As shown in the Hofmann-Loffler-Freytag (HLF) reaction, a protonated nitrogen radical can abstract a hydrogen atom from an unactivated sp^3 C-H bond by 1,5 HAT (Scheme 3.1.3).[7] In the Suarez modification, the nitrogen radical is made electrophilic with an electron withdrawing group, rather than protonation.[8]

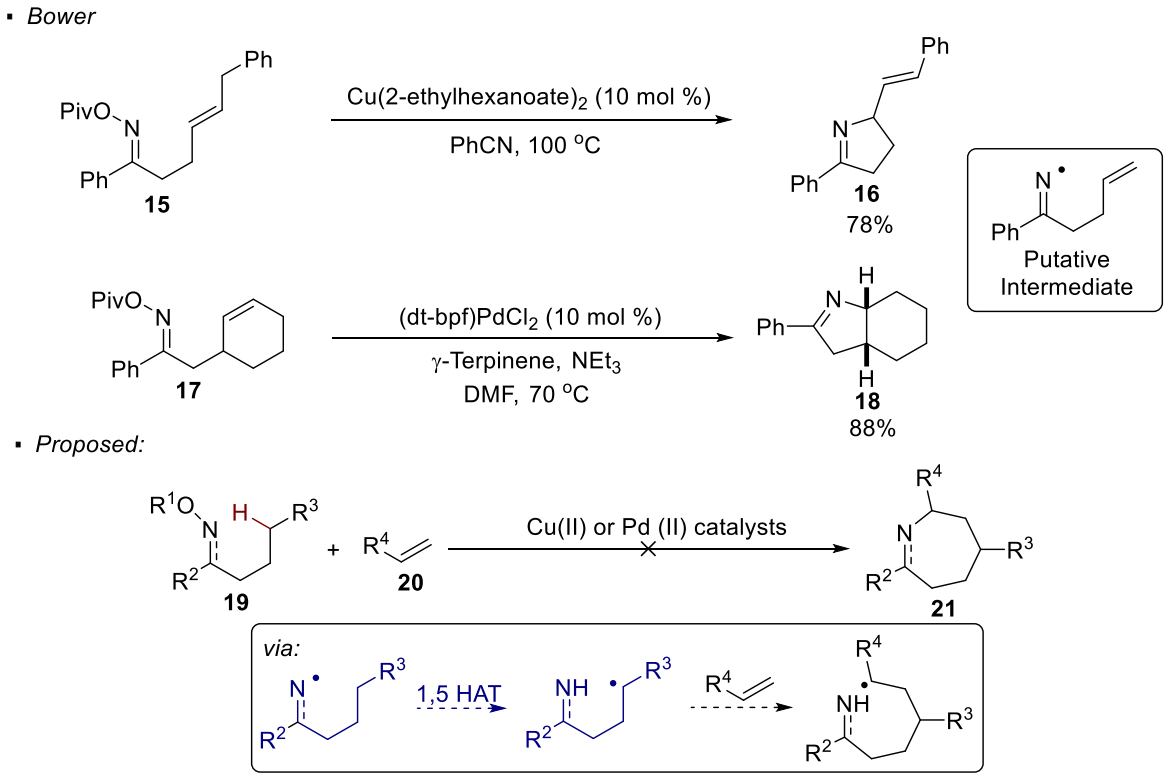

Scheme 3.1.4: Original Proposed Synthesis of Azepines with 1,5 HAT

Inspired by Bower's contributions of transition-metal catalyzed reductions of N-O bonds en route to nitrogen radicals,[9] we attempted to develop a transition-metal catalyzed synthesis of azepines (**21**) with oxime esters (**19**) and alkenes (**20**) (Scheme 3.1.4). In the proposed catalytic cycle, the low-valent metal catalyst (M^{n+}) reduces the nitrogen-oxygen bond generating a nitrogen radical. A subsequent 1,5 HAT leads to the formation of an alkyl radical, which can be

trapped by the alkene. The resulting radical can be oxidized by M^{n+1} affording a cation that will effect cyclization. Alternatively, the radical and M^{n+1} would react to form high valent M^{n+2} species. Final reductive elimination will furnish the C-N bond to yield the desired azepine upon regeneration of the catalyst M^{n+}.

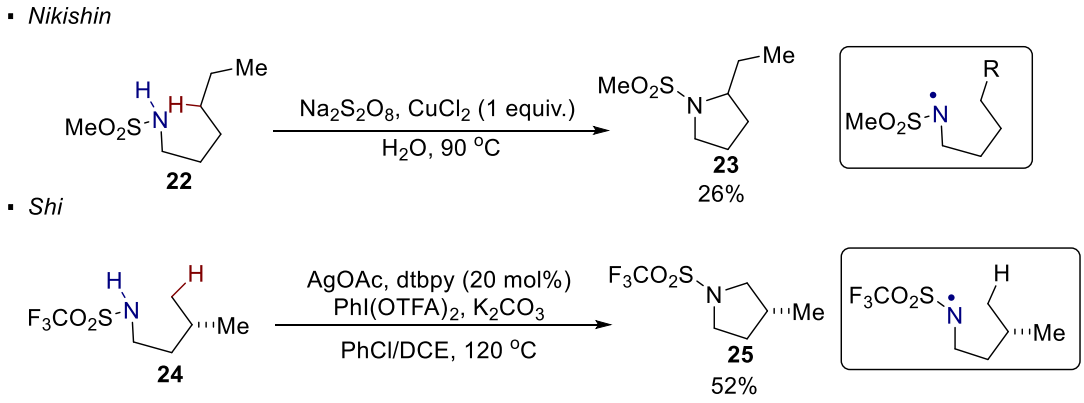

Scheme 3.1.5: Generation of Nitrogen Radicals from N-H Bonds

Despite failures to realize the proposed transformation, a report on a copper-mediated Hofmann-Loffler-Freytag reaction with **22** came to our attention (Scheme 3.1.5).[10] Remarkably, the precursor to the nitrogen radical is an N-H bond. We reasoned that the use of an N-H bond would substantially enhance the versatility of nitrogen radical chemistry. Currently, the most common way to generate a nitrogen radical is via homolytic cleavage of a nitrogen-halogen bond.[11] The halogen radical generated concomitantly combine with the alkyl radical from a 1,5 HAT to form a carbon-halogen bond. This subsequently hinders the interception of the alkyl radical with other radical couples. On the other hand, Nikishin reports that $CuCl_2$ and $K_2S_2O_8$ are also capable of reacting with the alkyl radical, leading to the formation of pyrrolidines. Similarly, the Shi group generates a nitrogen radical from an N-H bond in **24** with Ag(I) and a hypervalent iodine reagent (Scheme 3.1.5).[12] The use of stoichiometric amounts of strong oxidants to

generate the nitrogen radical eludes the trapping of the alkyl radical by radical couples. Our idea was to generate a nitrogen radical with an N-H bond in the absence of a transition metal or oxidants that can interfere with the alkyl radical. This would allow the trapping of the alkyl radical with various radical partners, resulting in the formation of various C-X bonds.

- *MacMillan*

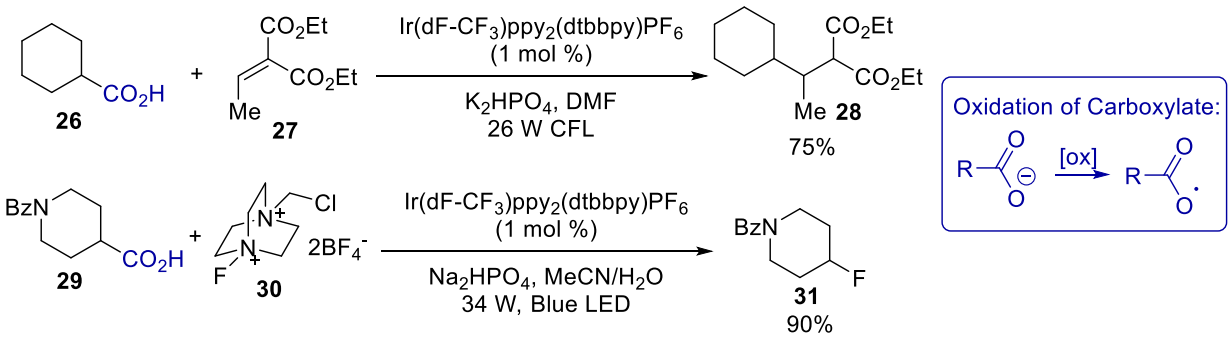

Scheme 3.1.6: Generation of Oxygen Radicals from Carboxylates

Recent reports from MacMillan and colleagues inspired us to incorporate photoredox catalysis in our research.[13] As illustrated in Scheme 3.1.6, the photoredox-catalyzed decarboxylative coupling of carboxylic acid **26** and electrophilic alkene **27** is proposed through the oxidation of the carboxylate by the excited photocatalyst. This generates an oxygen radical intermediate, which undergoes decarboxylation. The resulting alkyl radical is trapped by the electron-poor alkene forming a C-C bond. This reaction can be extended to decarboxylative fluorination, in which Selectfluor (**30**) is used as the radical partner with the alkyl radical (Scheme 3.1.6). These two reports from MacMillan demonstrate the feasibility of generating oxygen radicals from negatively-charged oxygen with photoredox catalysis.

3.2 Results

3.2.1 Reaction Discovery

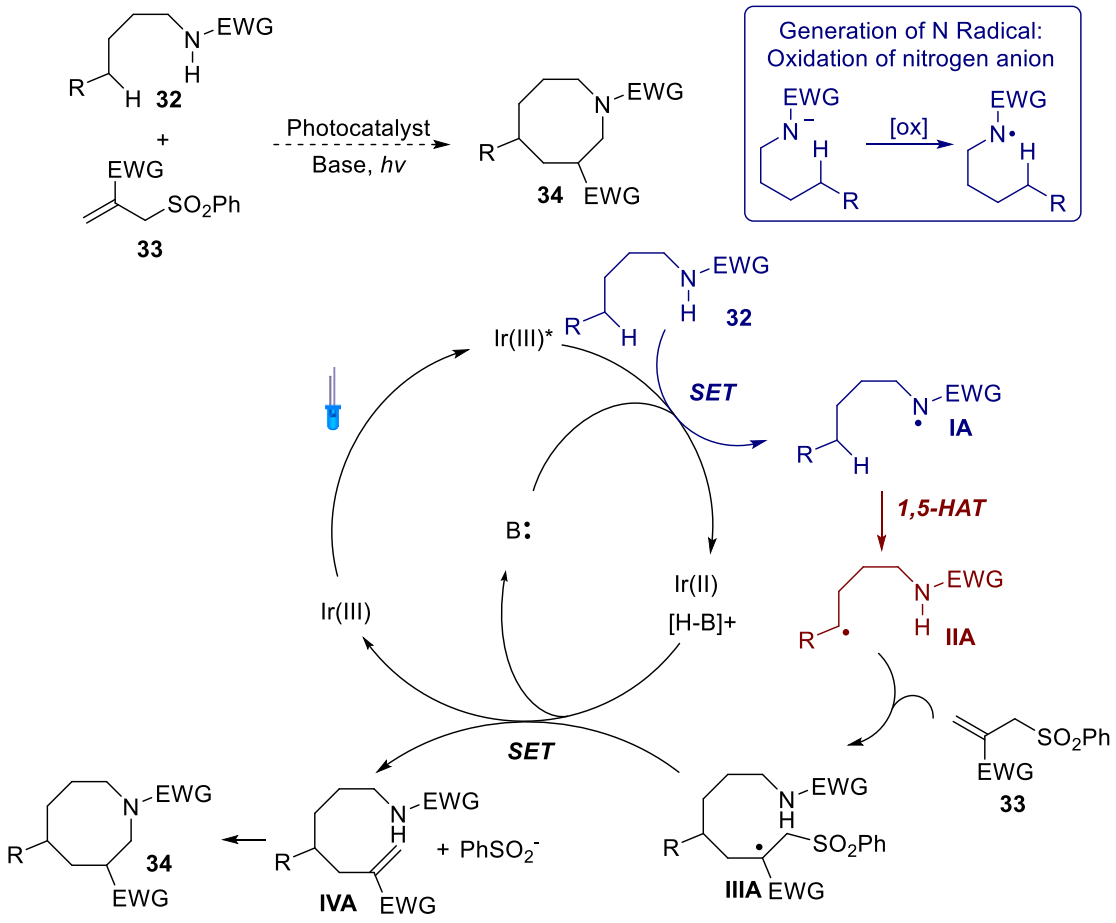

Scheme 3.2.1: Proposed Synthesis of Azocanes Featuring sp^3 C-H Functionalization

With the concept of generating a nitrogen radical from an N-H bond with photocatalysis, we proposed that a nitrogen radical can be generated from photoredox catalysis for the synthesis of 8-membered nitrogen heterocycles (**34**) (Scheme 3.2.1). An electron withdrawing group is installed on the nitrogen in **32** to facilitate deprotonation. This provides a driving force for 1,5 HAT as described in the Suarez modification. In the envisioned catalytic cycle, the excited photocatalyst oxidizes a negatively charged nitrogen. The nitrogen radical **IA** undergoes 1,5 HAT to propagate the radical to the δ carbon. The resulting alkyl radical **IIA** would be trapped by

electrophilic alkene **33**. Elimination of the sulfinate radical, which can be reduced by the photocatalyst to complete the catalytic cycle from **IIIA**, would install an electrophilic alkene at the amide (**IVA**). A subsequent intramolecular aza-Michael addition would realize cyclization, yielding the desired product **34**.

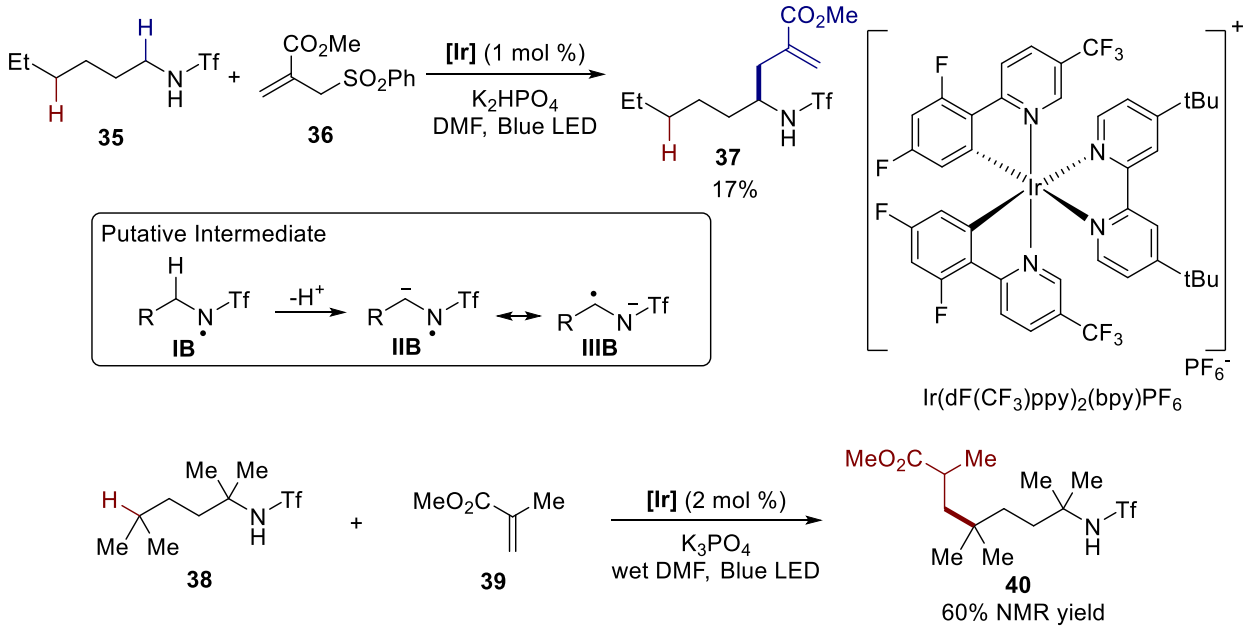

Scheme 3.2.2: Initial Results with Tf-Bearing Nitrogen

We began our investigation with the use of a Tf group on nitrogen. The pKa of the N-H is 6, close to that of carboxylic acids in MacMillan's report. Interestingly, when employing Ir(dF-(CF_3)ppy$)_2$(bpy)PF_6 as the photocatalyst under basic conditions, the alkylation of **35** with alkene **36** does not take place at the δ position, but the α position to give **37** (Scheme 3.2.2). We propose that deprotonation at the α position after generation of the nitrogen radical (**IB**) results in the formation of a radical anion. This radical anion is represented by a hybrid of resonance structures (**IIB** and **IIIB**). The trapping of this intermediate with **36** would explain the formation of **37**. To shut down this undesired pathway, sulfonamide **38** with full substitution at the α position was

investigated. Despite the failure to trap the putative alkyl radical with the electrophilic alkene (**36**), alkylation with methyl methacrylate (**39**) at the δ position was achieved in moderate yield. No conversion is observed when the reaction is conducted in the absence of the base K_2HPO_4, the photocatalyst or the Blue LED light source.

Although this transformation deviates from our original goal of accessing nitrogen-heterocycles, amide-directing C-C bond formations represent a powerful tool for the functionalization of nitrogen-containing molecules. It is noteworthy that 84% of all FDA-approved small molecule drugs in 2012 contain at least one nitrogen atom (Figure 3.2.1).[5] Considering their prevalence in pharmaceuticals, it is vital for synthetic chemists to develop efficient protocols for the functionalization of nitrogen-containing molecules to facilitate optimization of drug candidates.

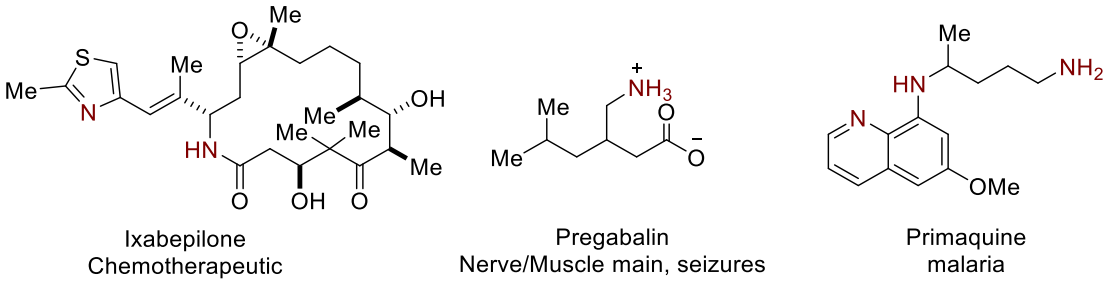

Figure 3.2.1: Examples of Nitrogen-Containing Small-Molecule Drugs

Currently, there are only limited reports of nitrogen-directed functionalization of inert sp^3 C-H bonds from Gaunt,[14] Daugulis,[15] Chen[16] and Yu.[17] These Pd-catalyzed C-H activation reactions functionalize the γ and β C-H bonds relative to the nitrogen (Scheme 3.2.3). Our approach functionalizes the δ position and is complementary to the Pd-catalyzed C-H activation.

After initial investigations, we became aware that the Knowles group was working on the generation of nitrogen radicals via photoredox catalysis (Scheme 3.2.4).[18] The mechanism for the generation of nitrogen radicals is different from our proposal. In their case, a proton-coupled electron transfer event (concerted deprotonation and oxidation) is proposed. In our proposal, deprotonation of the N-H bond must first take place to allow for oxidation. After communication with the Knowles group, we realized that they conceived the same idea for remote alkylation of C-H bonds with nitrogen radicals. Therefore, the work described in this chapter was conducted independently but published concurrently with the Knowles group.

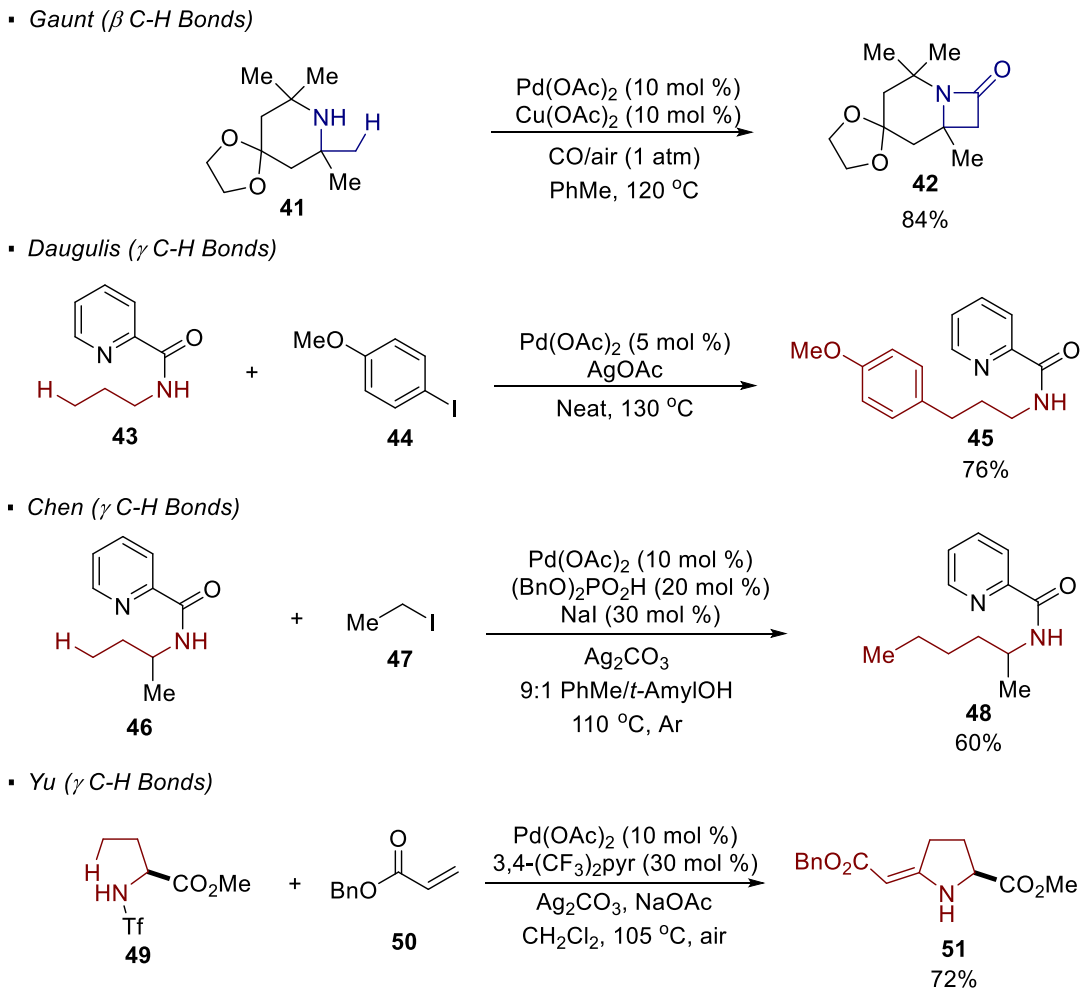

Scheme 3.2.3: Pd-Catalyzed β and γ Activation of Amine Derivatives

While preparing our work for publication, the Chen group reported the generation of an oxygen radical from the reduction of an N-O bond for the remote alkylation of δ C-H bonds through 1,5 HAT (Scheme 3.2.5).[19] Mechanistically, the catalytic cycle begins with the reduction of the N-O bond and ends with oxidation. In contrast, the photocatalyst oxidizes the amidyl anion and gets regenerated upon reduction. In addition, the protocol from Chen allows for access to functionalized alcohols with an activated N-O bond. Our chemistry, on the other hand, benefits the derivatization of nitrogen-containing molecules from an N-H bond.

- *Knowles (2015)*

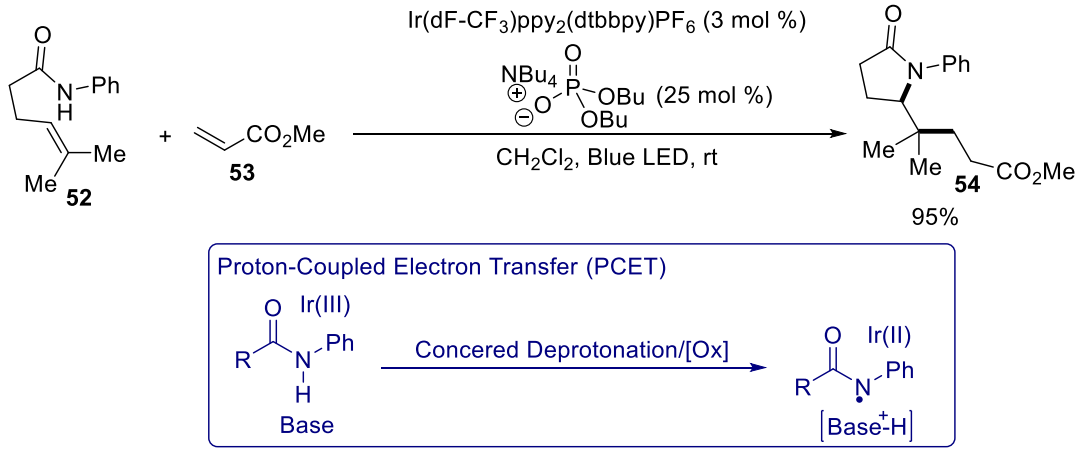

Scheme 3.2.4: Generation of Nitrogen Radical through PCET

3.2.2 Optimization of Reaction Conditions

Next, we focused on reaction optimization. The challenge was to shut down the undesired α-aminyl radical anion pathway. We reasoned that a weaker electron-withdrawing group on the nitrogen disfavors the deprotonation event after the formation of the nitrogen radical. This would prevent the formation of the undesired α-radical anion. Although strong base is needed, we found that a better yield of the δ C-H functionalized product (**60**) is obtained when the Tf

group is replaced by a less electron-withdrawing trifluoroacetyl (tfa) group (**59**) (Scheme 3.2.6). Consistent with our proposal, the desired δ C-H functionalized product was obtained in moderated yield with trifluoroacetamide **62** bearing no α-substitution. On the other hand, a tosyl group on the nitrogen leads to only slight decomposition. No conversion is observed with all other amides bearing less acidic N-H bonds in the forms of dilfuoroacetamide, pentafluorobenzamide and benzamide. These results are consistent with our proposal in which the deprotonated amidyl anion is required for the generation of nitrogen radicals.

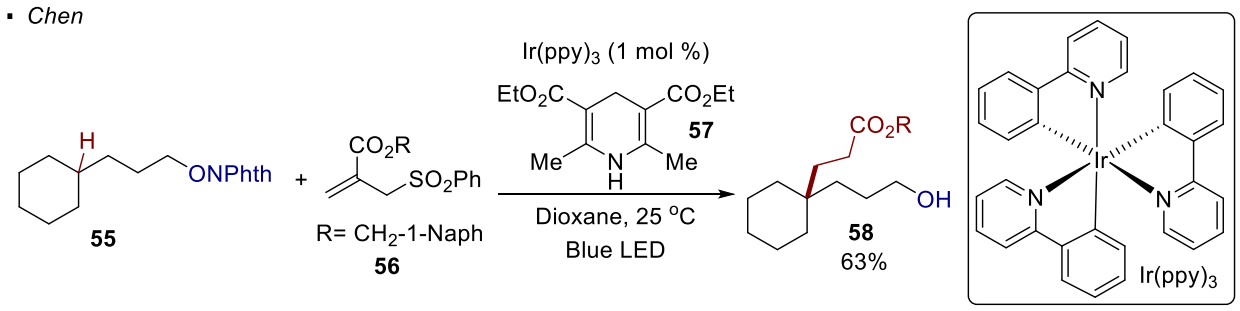

Scheme 3.2.5: Generation of Oxygen Radical from N-O Bond for C-H Alkylation through 1,5 HAT

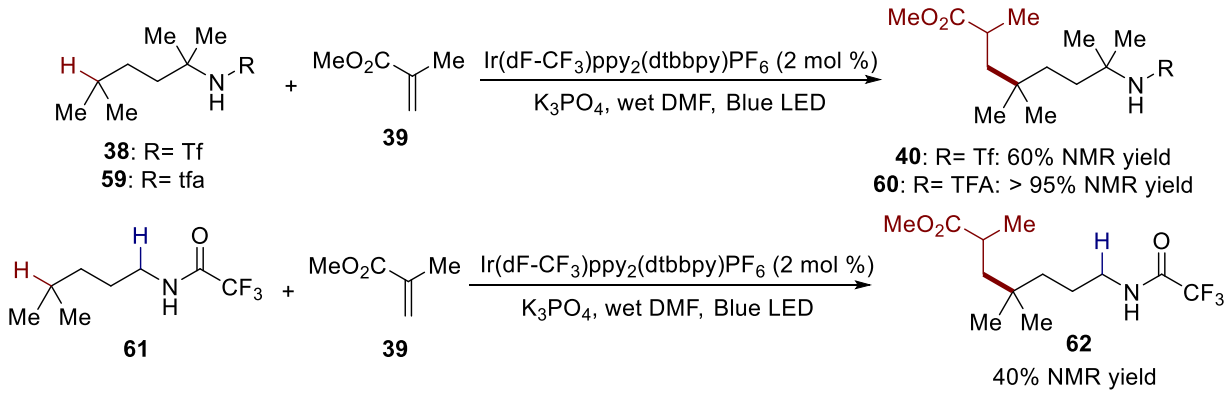

Scheme 3.2.6: Remote Alkylation with Trifluoroacetamides

In the optimization studies with trifluoroacetamide **61**, while most available photocatalysts do not afford any product, the reaction is highly sensitive to solvent (Scheme

3.2.7). In general, polar aprotic solvents (DMF, DMSO, MeCN and acetone) give satisfactory yields. Undesired Michael addition between polar protic solvents (e.g. MeOH and EtOH) and the alkene prevents their use. The use of solvents that bear C-H bonds activated by oxygen results in a messy reaction. This is presumably due to hydrogen transfer between the nitrogen radical and the solvents. $PhCF_3$ is identified to be the most optimal solvent. Any base weaker than K_3PO_4, such as K_2CO_3, K_2HPO_4, KH_2PO_4, or KOAc, does not result in any conversion (Scheme 3.2.7). This observation is consistent with our proposal that deprotonation of the N-H bond is required. The use of a stronger base in NaOH leads to decomposition of the alkene. This was evident by the observed color change of the reaction mixture upon addition of NaOH in the absence of a photocatalyst. Efforts to improve the yield by altering concentration were successful. The yield improves with a higher concentration at 0.03 M to 0.2 M (Scheme 3.2.7). No further increase in yield is observed when concentration reaches 0.2 M. With $PhCF_3$ as solvent and K_3PO_4 as base at a concentration of 0.4 M, the desired C-H functionalization product can be isolated in 75% yield.

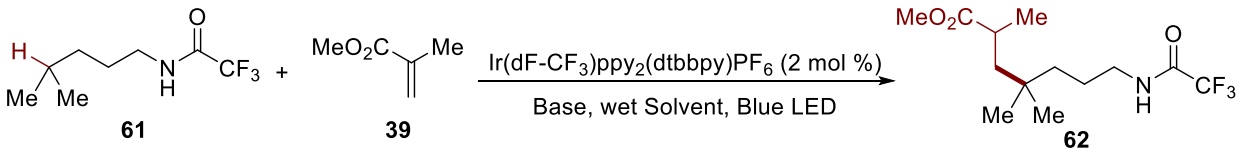

Solvent ***(K_3PO_4, 0.1 M)***	***Base*** ***($PhCF_3$, 0.1 M)***	***Concentration*** ***($PhCF_3$, K_3PO_4)***
DMF: 40%	K_2CO_3: 0%	**0.4 M: >90% (75%)**
DMSO: 40%	KH_2PO_4: 0%	0.2 M: >90% (72%)
Acetone: 48%	K_2HPO_4: 0%	0.13 M: 78%
MeCN: 65%	KOAc: 0%	0.10 M: 71%
$CHCl_3$: 56%	Na_3PO_4: 65%	0.05 M: 22%
DCE: 54%	**K_3PO_4: 71%**	0.03 M: 0%
Dioxane, THF, DME: messy	NaOH: 0%	
PhMe, PhH: 0%		
$PhCF_3$: 71%		

Scheme 3.2.7: Optimization of Reaction Conditions

3.2.3 Reaction Scope

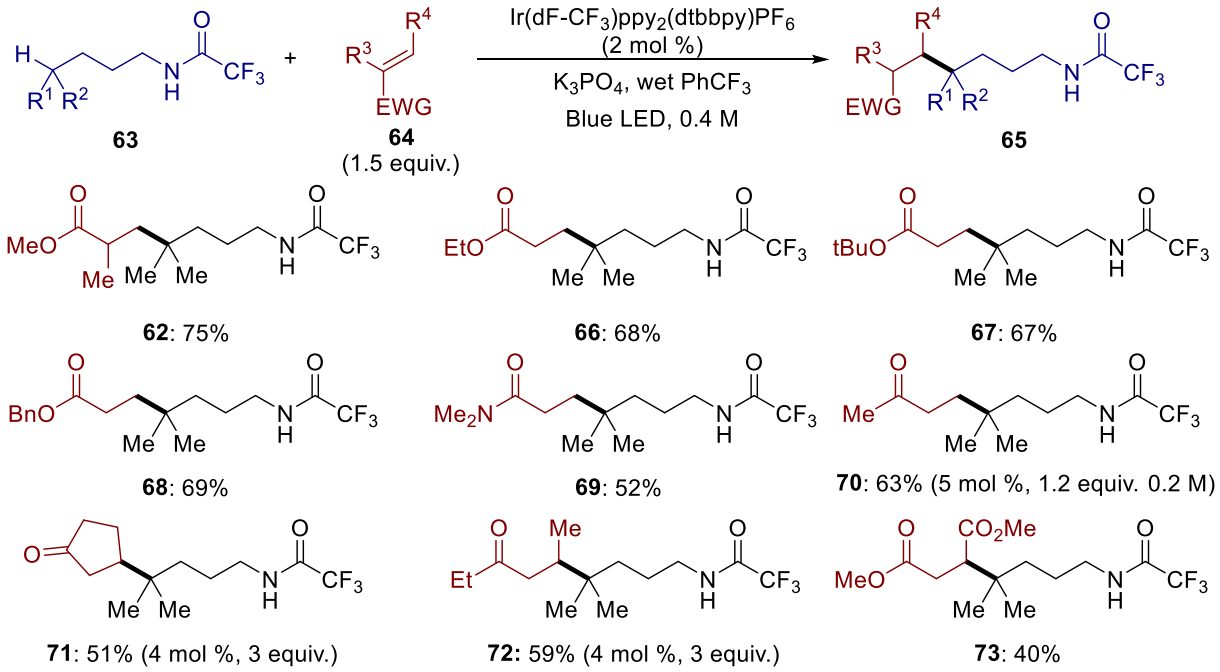

Scheme 3.2.8: Alkene Scope

For the alkene scope, the use of ethyl and *tert*-butyl acrylates shows that α-substitution on the electrophilic alkene is not required for reactivity as **66** and **67** are obtained in good yields (Scheme 3.2.8). The presence of highly activated benzylic C-H bonds are tolerated as alkylation with benzyl acrylate gives **68** in 69% yield. Less reactive *N*,*N* dimethyl acrylamide provides the desired C-H functionalization product **69** in satisfactory yield. A higher catalyst loading and less equivalents of methyl vinyl ketone were required in order to obtain a good yield of **70**. Altering the reaction conditions for this particular entry is necessary to favor the oxidation of the amidyl anion by the excited photocatalyst over aza-Michael addition. β-substituted enones, regardless of the alkene geometry, are competent coupling partners at higher catalyst loadings and alkene equivalents as **71** and **72** were provided in 51% and 59% yields, respectively. **73** can be obtained

with dimethyl maleate albeit in moderate yield. In contrast to the traditional Hoffmann-Loffler-Freytag reaction, an array of products can be accessed by switching the alkene reaction partner.

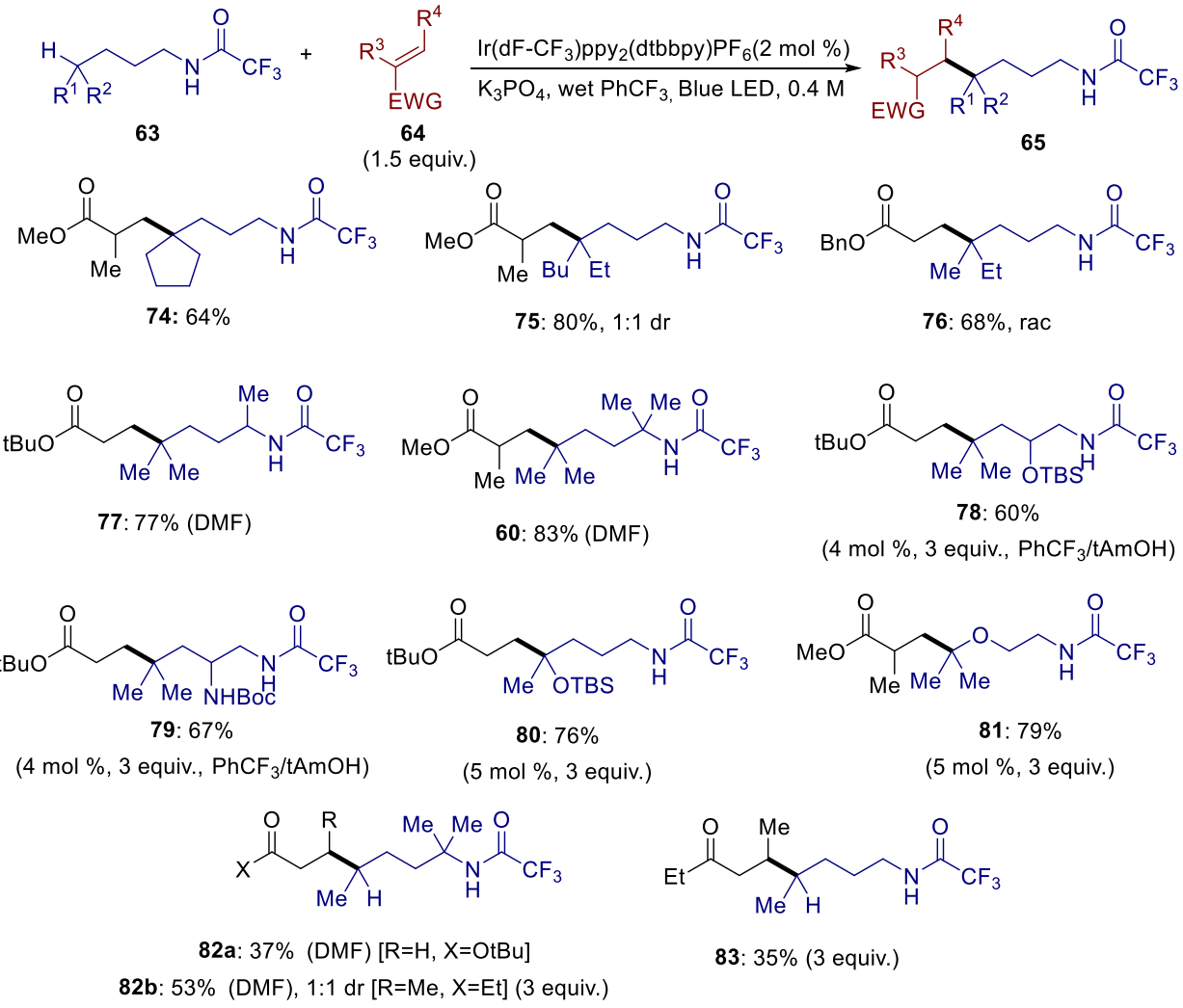

Scheme 3.2.9: Amide Scope

A variety of amides were also tolerated (Scheme 3.2.9). Substrates bearing more hindered tertiary C-H bonds were converted to their corresponding alkylated products (**74** and **75**) in modest to good yield. There is no diastereo control in the latter case. Incorporation of enantiomerically enriched substrates results in complete racemization as observed in the formation of product **76**. This stereochemical outcome is consistent with the proposed radical

mechanism. α-Substituted amides are competent substrates when a more polar solvent is used. Thus, amides **77** and **60** are obtained in excellent yields with DMF. Poor conversion is observed with $PhCF_3$. It is believed that the decreased acidity of the amide is accounted for through the use of a more polar solvent. For β-substituted amides, $PhCF_3$/*tert*-Amyl alcohol and higher catalyst loadings are needed. Protected alcohols are tolerated as **78** is obtained in good yield. The less acidic N-H bond of the carbamate in amide **79** does not alter the outcome of the reaction. This compatibility opens up the possibility of having multiple amine functionalities in the molecule of interest. With high catalyst loadings and equivalents of alkene, substrates with more electron-rich tertiary C-H bonds can be activated in order to promote alkylation. This is reflected through the acquisition of amides **80** and **81**. A limitation of the method, however, is mitigated reactivity with secondary C-H bonds. Alkylation with *tert*-butyl acrylate proceeds in moderate yield to give **82a**. A higher yield of **82b** can be obtained with a β-substituted enone. Nevertheless, the two methyl groups at the α-position to the amide are important for the reactivity as **83** is formed in a lower yield than **82b**.

We were also interested in the functionalization of amides that possess multiple reactive C-H bond sites (tertiary C-H bonds or those activated by heteroatoms). Excellent selectivity for the tertiary C-H bond δ to the nitrogen was observed with amide **84** (Scheme 3.2.10). The remote tertiary C-H bond in **86** remains intact. This indicates that an intramolecular HAT is responsible for the generation of the alkyl radical. With reactive C-H bonds at both the δ and ε positions, there is potential competition between 1,5 and 1,6 HAT. For amide **87**, the δ position can be selectively alkylated to yield **88** in 54% yield. 26% of the starting material is also recovered. This poor conversion could be attributed to the electron-withdrawing oxygen. This oxygen can slow

down the HAT or the trapping of the alkyl radical by rendering it less nucleophilic. When the reaction is carried out to full conversion with amide **89**, a mixture of mono- and dialkylated products are obtained. On other hand, when the reaction is stopped at ~50% conversion, selective alkylation at the δ position affords **90**. After isolation, **90** can be re-subjected with another alkene to yield ε-alkylated product **91**. Although the yields for this sequential 1,5- 1,6 HAT are moderate, there are currently no methods that incorporate two different alkenes into two inert C-H bonds at different positions of the molecule.

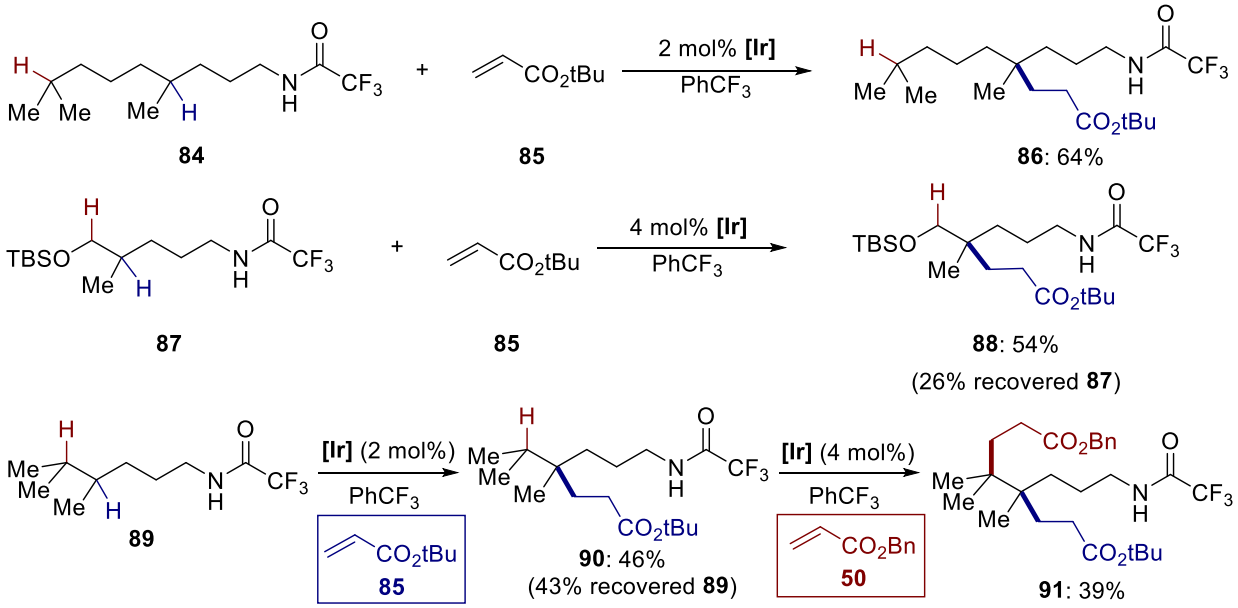

Scheme 3.2.10: Functionalization of Amides with Multiple C-H Bonds

3.2.4 Application to Medicinally-Relevant Molecules

After studying the scope of the reaction, this method was applied to the derivatization of medicinally relevant molecules (Scheme 3.2.11). An analogue of Pregabalin, a drug used to combat nerve and muscle pain,[20] can be successfully obtained via alkylation at the C-H bond δ to

the nitrogen in **92**. Steroid **94**, which bears 7 tertiary C-H bonds, can be alkylated at the δ position to give compound **95** while other C-H bonds remain intact.

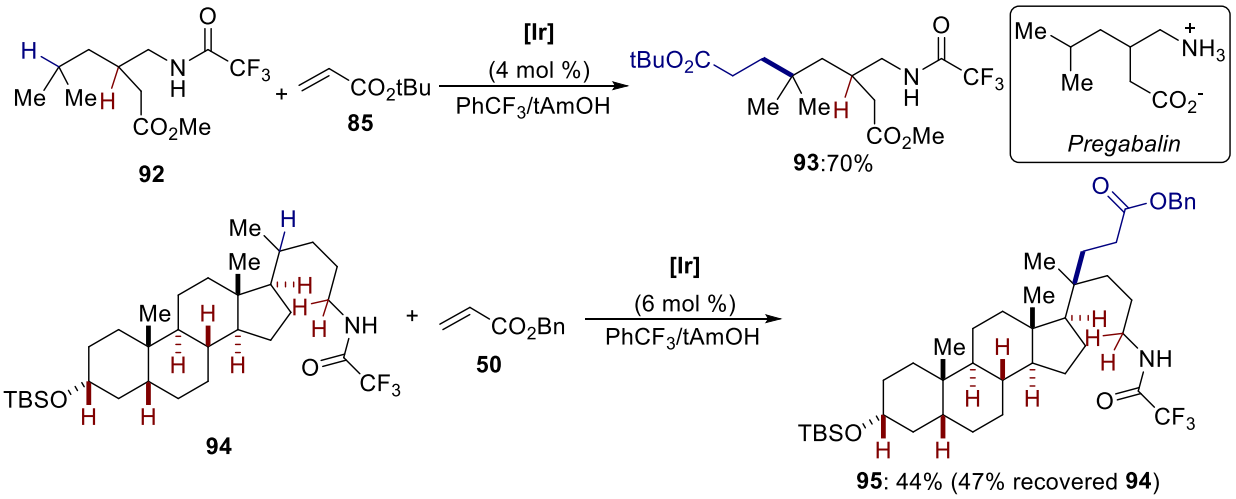

Scheme 3.2.11: Functionalization of Medicinally-Relevant Molecules

3.3 Mechanistic Studies

3.3.1 Chain Propagation vs. Closed Catalytic Cycle

The reaction can proceed through a closed catalytic cycle or a chain propagation pathway. In a closed catalytic cycle, the photocatalyst is involved in the formation of each molecule of the C-H functionalization product (Figure 3.3.1). The catalytic cycle begins with the oxidation of the N-H bond of amide **IC** by the photocatalyst. A 1,5 hydrogen atom transfer forms the alkyl radical **IIIC** that is trapped by an electrophilic alkene. The cycle is then closed upon reduction of the final radical intermediate **IVC**. As for the chain propagation mechanism, the intermediate nitrogen radical **IIC** can be formed without the participation of the photocatalyst. For instance, the final radical intermediate **IVC** can translocate the radical to substrate **IC** by abstracting a hydrogen atom or by taking an electron (Figure 3.3.1). The resulting nitrogen radical can lead to the

functionalization of the C-H bond. This obviates the involvement of the photocatalyst in the formation of each molecule of the product.

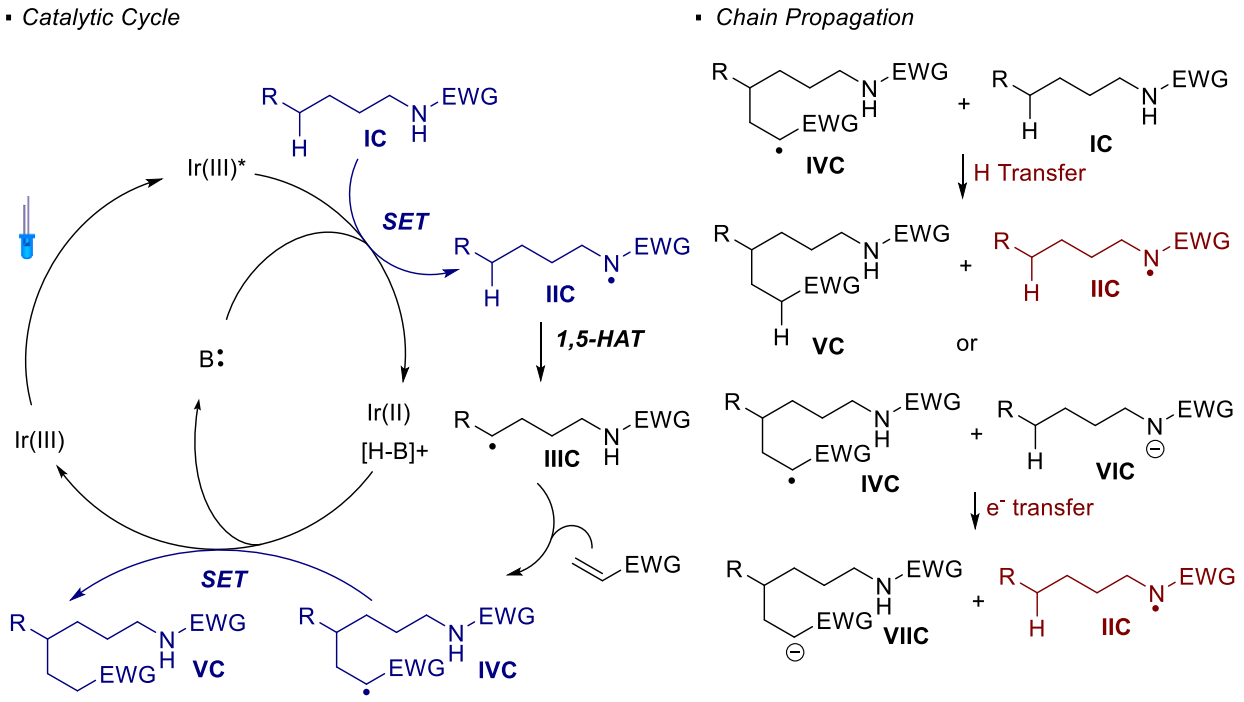

Figure 3.3.1: Catalytic Cycle vs. Chain Propagation

To differentiate a closed catalytic cycle versus a chain propagation mechanism, the quantum yield of the reaction was measured and determined to be 0.11 (Scheme 3.3.1). After the absorption of a photon, the photocatalyst can undergo relaxation and other unproductive pathways. Therefore, a quantum yield of less than 1 does not necessarily lead to the conclusion that a closed catalytic cycle is operative. To seek more evidence for a closed catalytic cycle, ON/OFF responses to light were studied (Figure 3.3.2). In the event of chain propagation, light is only required to initiate the formation of the first nitrogen radical. Thus, the reaction theoretically still proceeds when light is removed. Our result shows that the reaction occurred only in the presence of light. No conversion is observed in the dark. The reactivity is recovered

once the reaction is exposed to light. This ON/OFF response is consistent with a closed catalytic cycle.

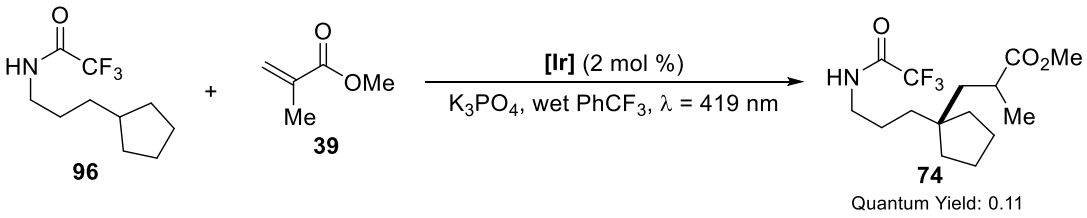

Scheme 3.3.1: Quantum Yield for Amide-Directed C-H Functionalization

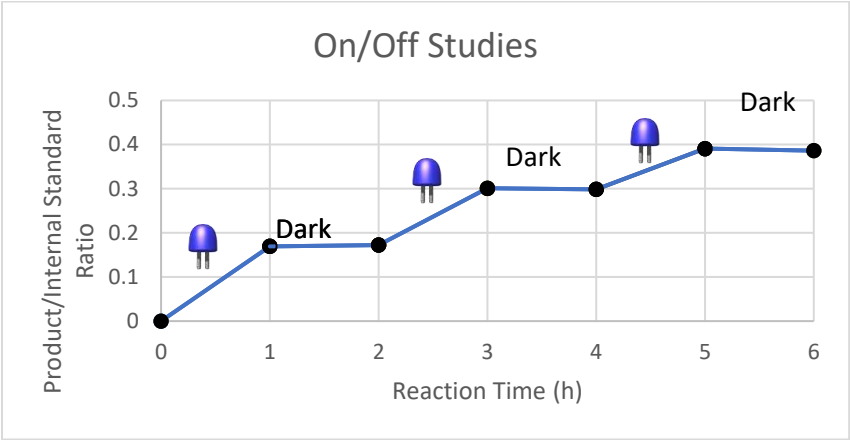

Figure 3.3.2: On/Off Response to Light

It is also believed that chain propagation is unlikely if the bond strengths and pKa's of potential intermediates is considered (Scheme 3.3.2). The first possibility of chain propagation involves a direct electron transfer to the final α-radical intermediate **ID** from amidyl anion **IID**. This is unlikely as the C-H bond α to an ester (95 kcal/mol)[21] is 15 kcal/mol weaker than an amidyl N-H bond (110 kcal/mol).[22] The resulting α anion (pKa= 29.5 in DMSO) is substantially less stable than the initial amidyl anion (pKa= 17.2 in DMSO)[23]. The second possibility is that α-radical **ID** abstracts hydrogen from the N-H bond of the neutral amide (**VD**). This is unlikely since the α-radical would have to abstract a hydrogen from the weaker tertiary C-H bond (95 kcal/mol).[24]

Consequently, the α C-H bond (95 kcal/mol) formed would be much weaker than the amidyl N-H bond (110 kcal/mol) that is being broken. The last possibility is that α-radical **ID** abstracts a hydrogen directly from the tertiary C-H bond δ to the amide through intermolecular HAT. This is disproved because the remote tertiary C-H bond of **84** remains intact. This remote tertiary C-H bond is more electron-rich and should be cleaved in an intermolecular HAT. Therefore, our analysis, along with quantum yield and the response to light, suggests a closed catalytic cycle.

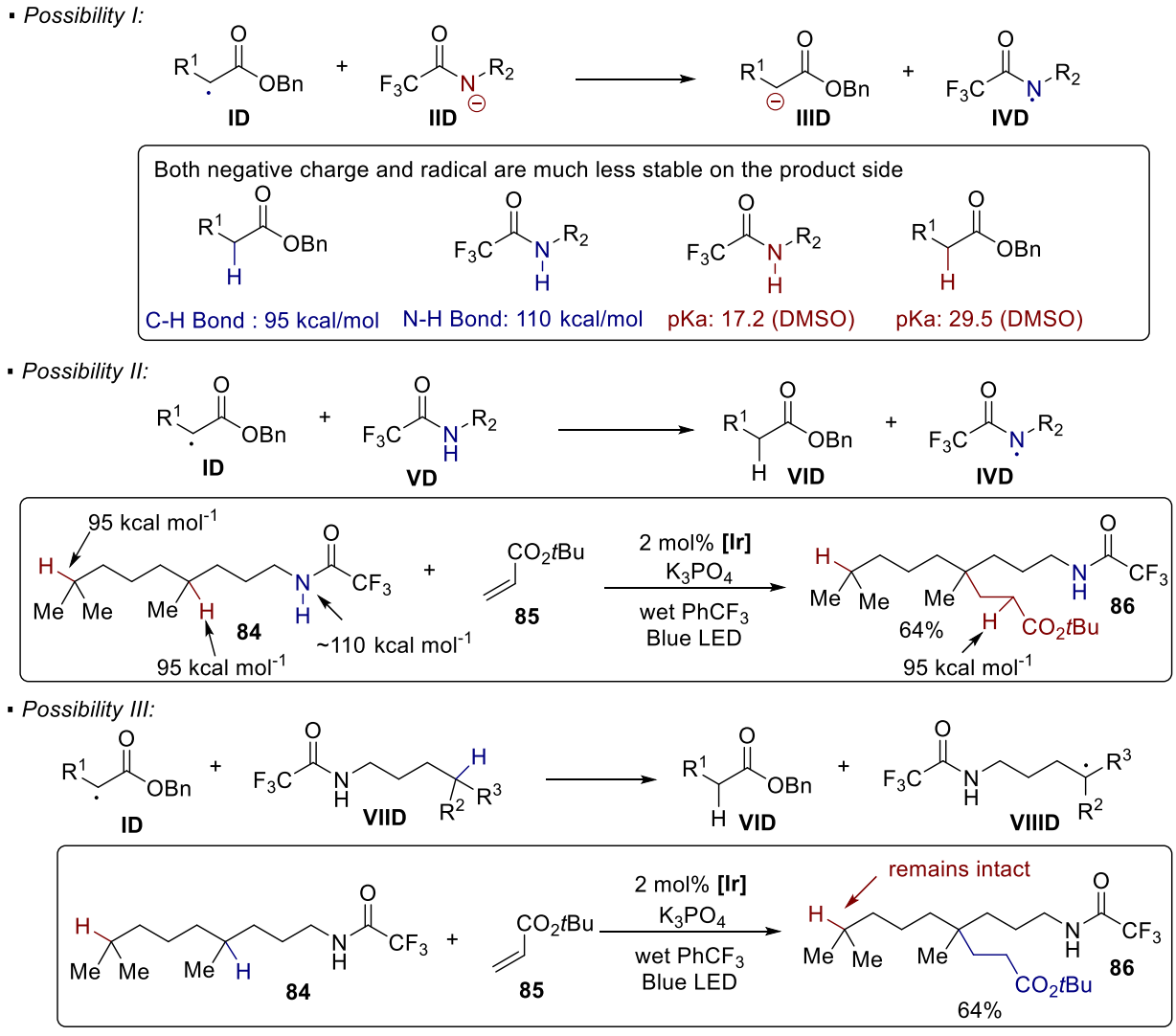

Scheme 3.3.2: Evidence against Potential Chain Propagation Steps

3.3.2 Mechanism for the Generation of the Nitrogen Radical

There are three possible mechanisms for the generation of the nitrogen radical (Figure 3.3.3). The first one involves the stepwise oxidation of the neutral amide followed by deprotonation. The second proposed mechanism features a stepwise deprotonation followed by oxidation of the amidyl anion. The third mechanistic pathway involves a concerted deprotonation and oxidant event (i.e. proton-coupled electron transfer, PCET).

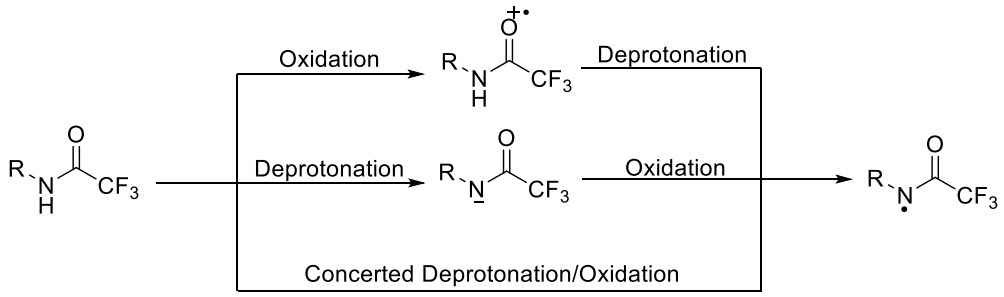

Figure 3.3.3: Three Mechanisms for the Generation of Nitrogen Radicals

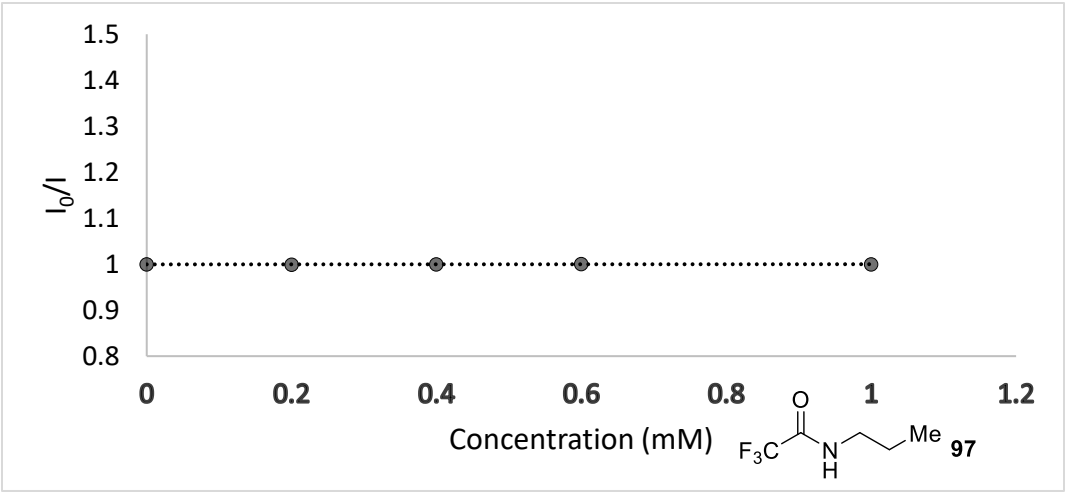

Figure 3.3.4: No Quenching of Ir Photocatalyst by Neutral Amide

Cyclic Voltammetry and Stern-Volmer studies[25] were performed to probe the mechanism. The neutral trifluoroacetamide has an E_p > 2.0 V vs. SCE in MeCN. This is well beyond the excited

Ir photocatalyst's oxidation potential ($E_{1/2}$ = +1.21 V vs. SCE in MeCN)[26]. Stern-Volmer studies also indicate that the excited Ir photocatalyst cannot be quenched by neutral trifluoroacetamide **97** (Figure 3.3.4). This rules out a stepwise oxidation/deprotonation event en route to the nitrogen radical.

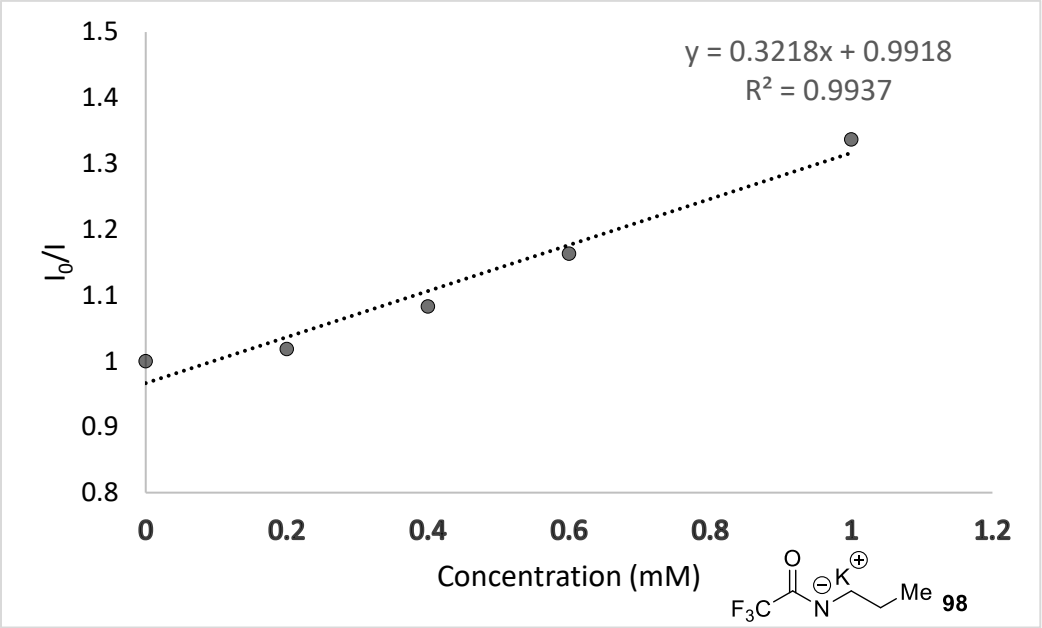

Figure 3.3.5: Quenching of Ir Photocatalyst with Amidyl Anion

The potassium salt of the trifluoroacetamide (**98**) was prepared via deprotonation of trifluoroacetamide **97** with KH under anhydrous conditions. CV studies suggest that **98** (E_p = +0.77 V vs. MeCN) can be oxidized by the excited Ir photocatalyst. The oxidation of **98** by the excited photocatalyst is supported by Stern-Volmer studies in which linearity between concentration and intensity is observed (Figure 3.3.5).

The quenching of the excited state Ir photocatalyst suggests the possibility of a stepwise deprotonation/oxidation event. However, this does not rule out a concerted PCET mechanism. The Knowles group reasoned that large acidity differences between the amide and base (>20)

and the short photocatalyst life-time favor the PCET over the stepwise deprotonation/ oxidation mechanisms in their hydroamination chemistry.[18] In our case, similar pKa's of the trifluoroacetamide (pKa: 13.8 in H_2O)[27] and K_3PO_4 (pKa: 12.3 in H_2O) suggest that invoking a PCET mechanism is unnecessary but do not provide evidence to differentiate the two mechanisms.

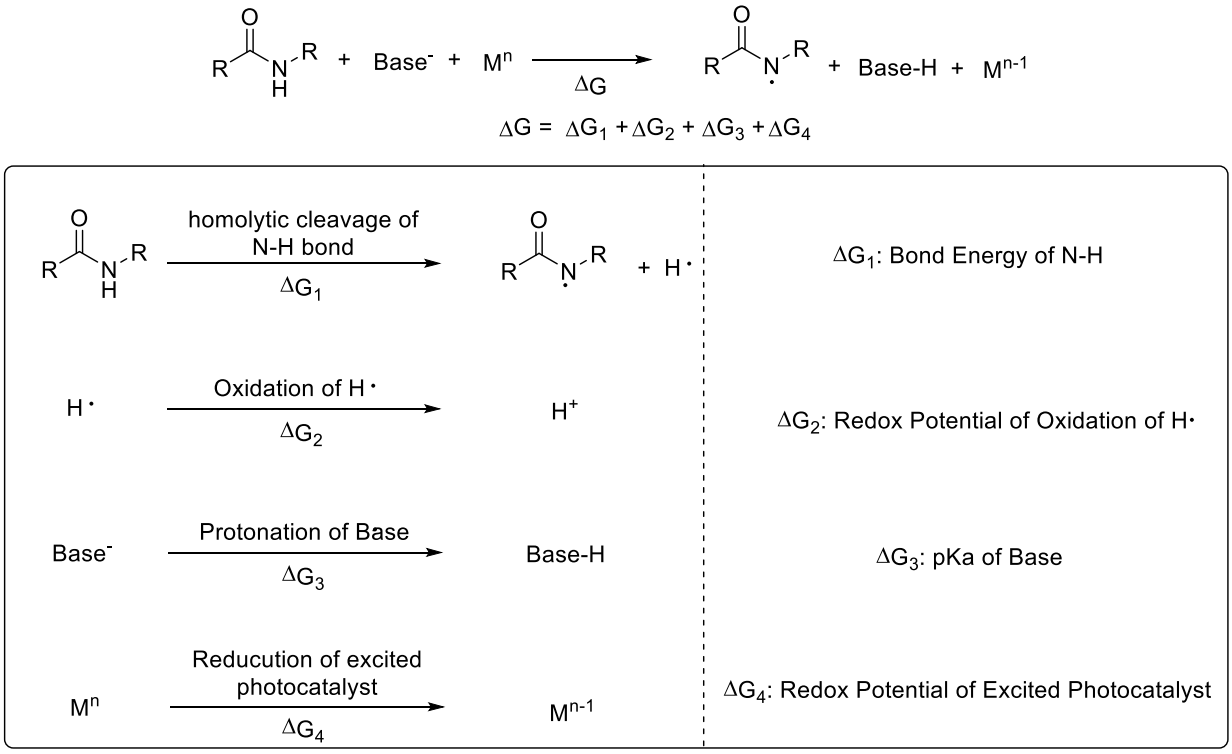

Figure 3.3.6: Consideration of Free Energy Change for Generation of Nitrogen Radical

To gather more mechanistic insight, the free energy change (ΔG) associated with the generation of nitrogen radicals from the amide is considered (Figure 3.3.6). This process can be broken down into several elementary steps: homolytic cleavage of the N-H bond, oxidation of a hydrogen atom to a proton, protonation of the base with H^+, and the reduction of the excited Ir photocatalyst. As a result, the ΔG for the generation of the nitrogen radical can be predicted by the sum of these steps ($\Delta G_1+\Delta G_2+\Delta G_3+\Delta G_4$).

These bond dissociation free energies (BDFEs) have been successfully used to predict the feasibility of a proton-coupled electron-transfer process, as described by the Knowles group.[18] With the same photocatalyst and base, any change in ΔG comes from the N-H bond strength, which varies with the identity of the amide. Weaker N-H bond strength associated with a weaker electron-withdrawing group on the nitrogen in the amide should theoretically lead to a less positive (or more negative) ΔG. This, in turn, will make the generation of the nitrogen radical more favorable. However, our experimental results obtained when going from trifluoroacetamide **61** (pka of CF_3CO_2H=0.2)[28] to difluoroacetamide **99** (pKa of CF_2HCO_2H=1.1)[29] and pentafluorobenzamide **101** (pKa of $C_6F_5CO_2H$=1.7)[30] contradict these predictions. The use of difluoroactamide **99** and pentafluorobenzamide **101** results in no remote alkylation, which can only be explained by a kinetic argument (Scheme 3.3.3). While it is not trivial to offer an explanation in the case of a PCET mechanism, the decrease in acidity of the N-H bond, while having no effect on overall ΔG, could stop deprotonation. This would result in no generation of nitrogen radical in the stepwise deprotonation/oxidation mechanism, presenting a valid kinetic argument for the lack of reactivity with amides **99** and **101**.

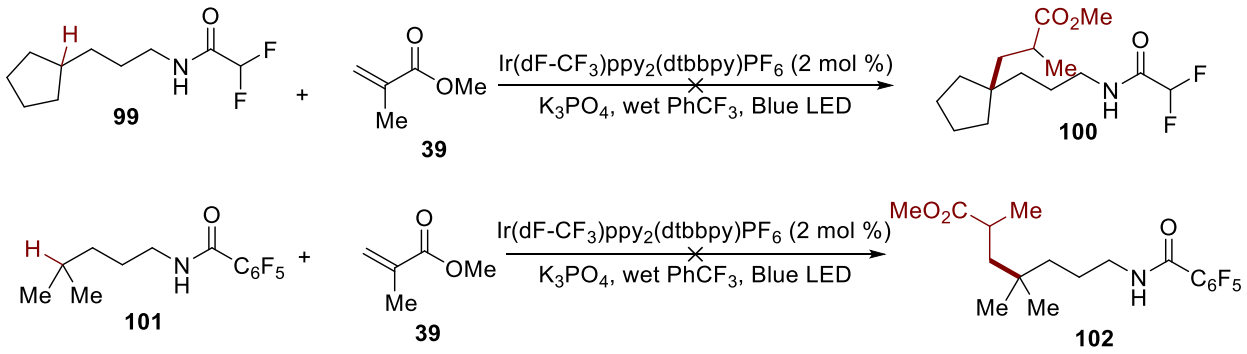

Scheme 3.3.3: Incompetent Amides with Weaker Electron-withdrawing Groups

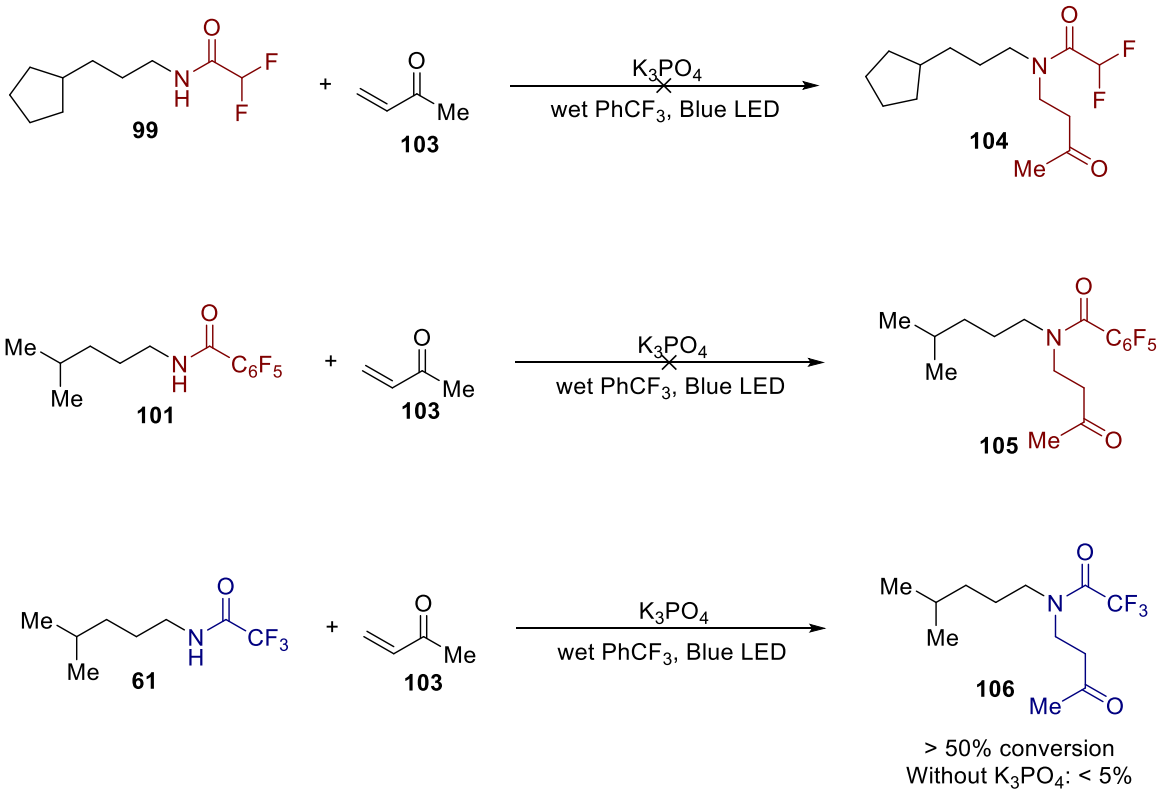

Scheme 3.3.4: Studies of the Presence of Amidyl Anion under Reaction Conditions

To probe whether there is an appreciable amount of the corresponding amidyl anions, difluoroactamide **99** and pentafluorobenzamide **101**, were treated with methyl vinyl ketone **103** and K_3PO_4 in wet $PhCF_3$ (Scheme 3.3.4). There is no conversion of these amides to aza-Michael products, indicating that no significant amounts of amidyl anions are present. As discussed earlier, these two amides are not competent substrates for photocatalytic C-H functionalization. For trifluoroacetamide **61**, the formation of the aza-Michael adduct (**106**) with methyl vinyl ketone (**103**) in the presence of no photocatalyst shows that there is an appreciable amount of the amidyl anion. Thus, there appears to be parallel reactivity between C-H functionalization and aza-Michael addition. This parallel reactivity implicates that amidyl anions are needed for successful C-H functionalization. This also offers an explanation for the contradictory experimental

observations as well as the trends predicted from BDFEs. Therefore, we believe that a stepwise deprotonation/oxidation event is responsible for the generation of nitrogen radicals in our C-H functionalization chemistry.

3.4 Future Directions

3.4.1 Extension to Formation of Various C-X Bonds

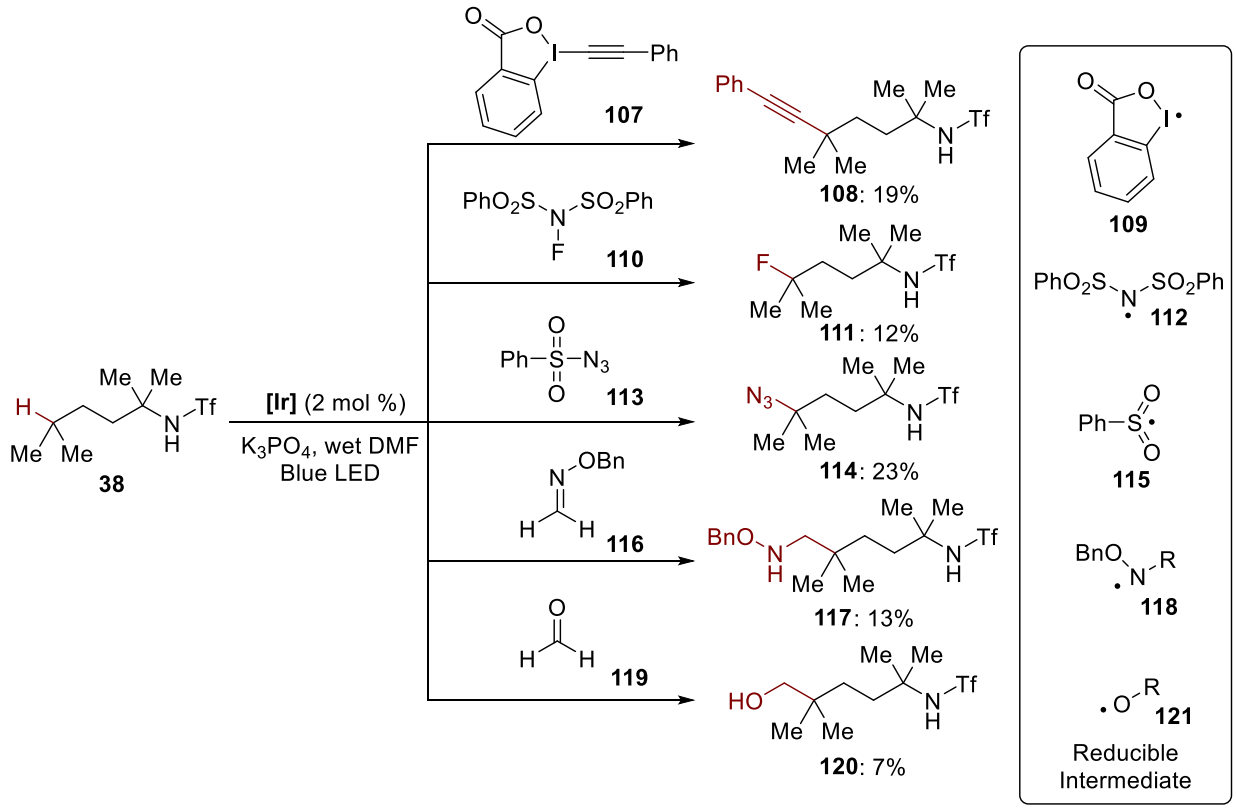

Scheme 3.4.1: Various C-X Bond Formation at Inert C-H Bonds

A unified protocol combining 1,5 HAT with photoredox catalysis to functionalize the δ C-H bond amides will be pursued. The proposed mechanism for the aforementioned C-C bond formation implies that any reagent which reacts with an alkyl radical to generate a reducible intermediate can potentially be applied for a variety of C-X bond formations. We tested this

hypothesis and found out that alkynlyation with benziodoxolone (**107**),[31] fluorination with NFSI (**110**), azidation with $PhSO_2N_3$ (**113**), aminomethylation with oxime (**116**), hydroxymethylation with paraformaldehyde (**119**)[32] are possible. Scheme 3.4.1 shows the preliminary results for these transformations and their reducible intermediates. The optimization of these transformations are currently being pursued by Dr. Keith Barbato, a postdoctoral researcher in the Rovis Group.

3.4.2 Functionalization of Other C-H Bonds Relative to Nitrogen

- *MacMillan (Tertiary and Secondary Amines)*

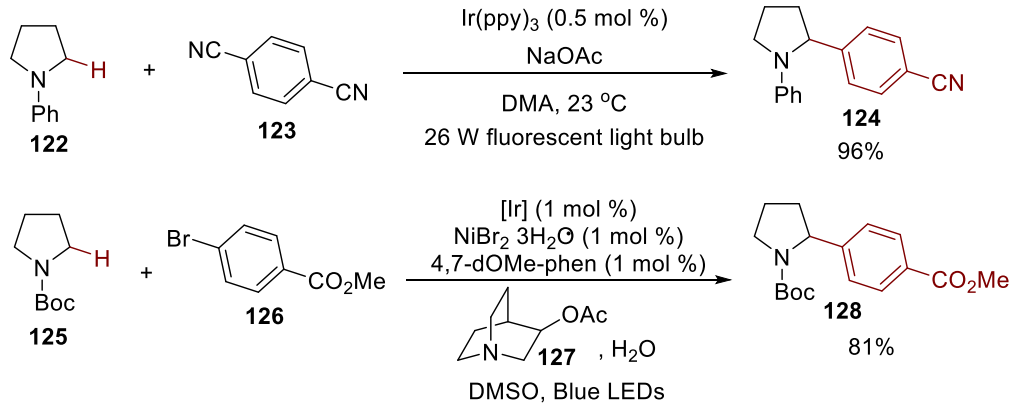

- *MacMillan (Carboxylic Acid Activating Group for Primary Amines)*

- *Takasu, Yamada (Halide Activating Group for Primary Amines)*

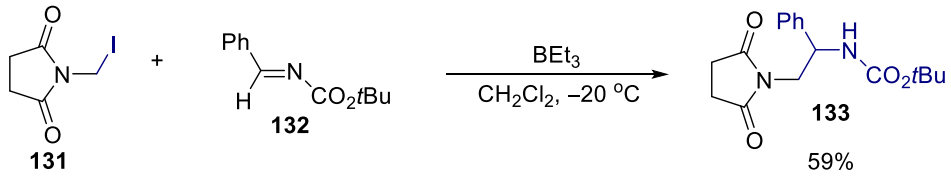

Scheme 3.4.2: Limitation of α-aminyl Radical from Primary Amines

We plan to develop a general protocol for the functionalization of C-H bonds α to aliphatic amines. The directing group on the nitrogen would determine the site-selectivity. The serendipitous discovery of α-functionalization of primary amines bearing highly electron-withdrawing groups provides a good starting point for these investigations (Scheme 3.2.2). While α-aminyl radicals from secondary[33] and tertiary amines[34] can be generated via cleavage of a C-H bond, the current-state-of-the-art approach for primary amines requires an activating group such as a carboxylic acid[35] or halide[36] (Scheme 3.4.2). These prerequisite groups greatly limit the reaction scope since they are not trivial to install.

3.4.3 γ Functionalization of Carbonyl Compounds

We also plan to extend the amide-directed remote alkylation with photoredox catalysis to functionalize the γ-position of carbonyl groups (Scheme 3.4.3). Currently, transition-metal catalyzed C-H activation approaches functionalize the β-position of carbonyl groups.[37] Only few examples of γ C-H functionalization have been reported. In Corey and Chen's reports, the bulky NPhth group is required to favor the formation of the palladacycle from the γ C-H bonds.[38] The protocols developed by Yu are applicable only for carbonyl compounds without β C-H bonds.[39] We aim to advance this research field by providing a more general protocol, in order to broaden both substrate scope and functionalities that can be incorporated for γ-functionalization of carbonyl compounds with a 1,5 HAT as the key step. As exemplified the amide-directed C-H functionalization, various transformations, such as alkylation, fluorination, azidation and aminomethylation of the γ C-H bonds are feasible.

- *Proposed*

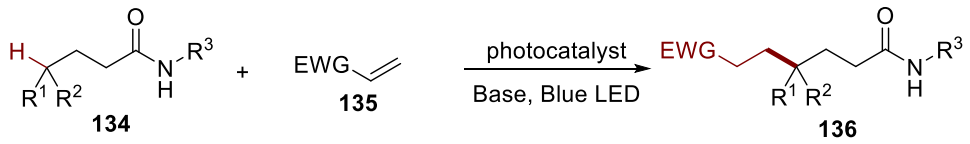

- *Corey (bulky α substitution)*

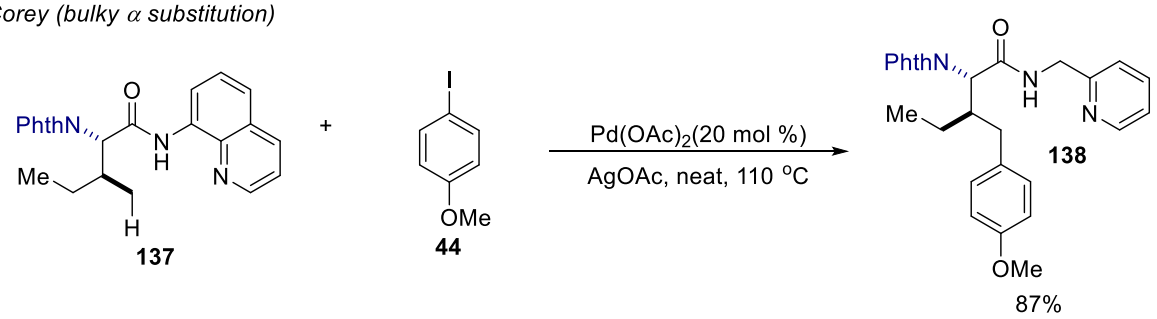

- *Chen (bulky α substitution)*

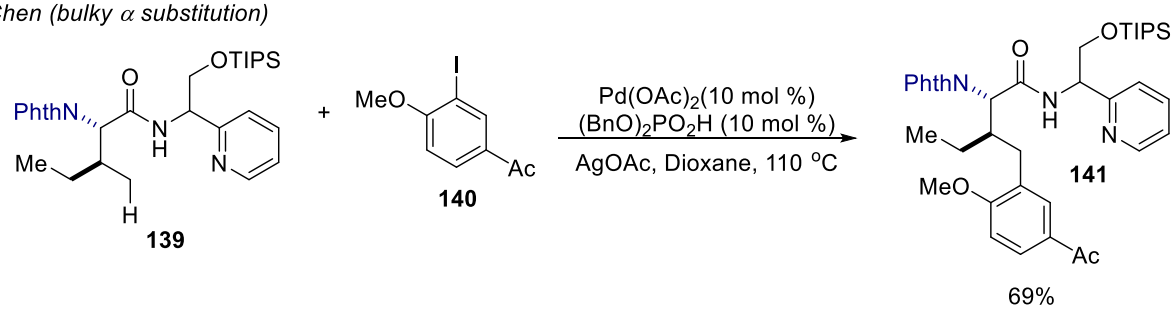

- *Yu (no β C-H Bonds)*

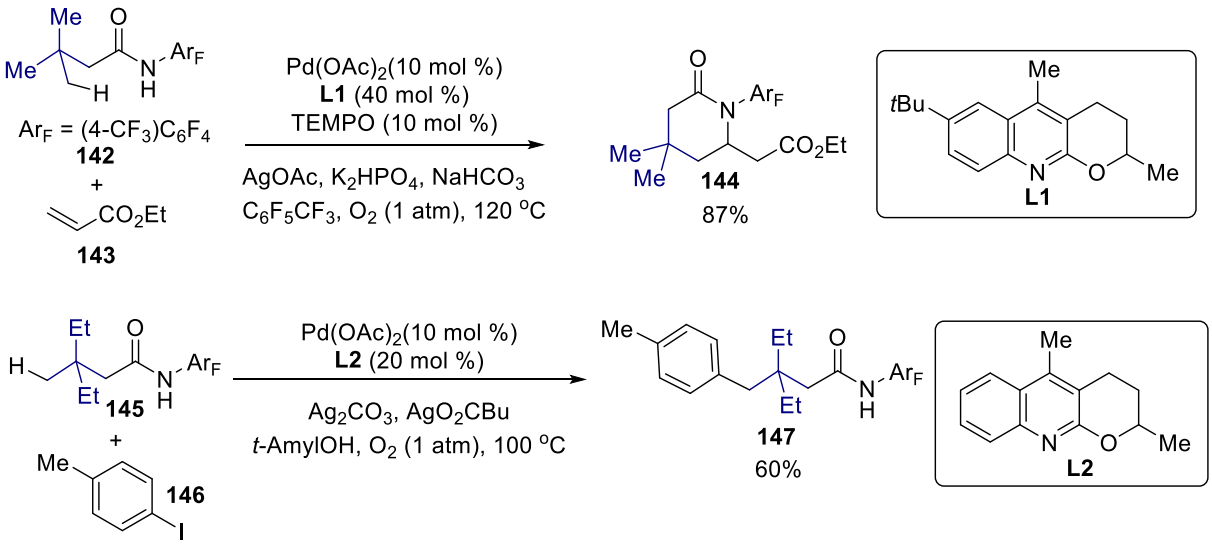

Scheme 3.4.3: Limited Examples of γ-Functionalization of Carbonyl Groups

Our mechanistic studies indicate that the N-H bond has to be acidified by a strong electron-withdrawing group. This will provide access to the aminyl anion allowing for oxidation

to the nitrogen radical. We therefore began our investigation with amide **148**, which bears an electron-withdrawing trifluoromethyl group. Unfortunately, no desired product (**151**) is obtained when subjected to standard reaction conditions (Scheme 3.4.4). It is speculated that the formation of a radical-anion may compete with 1,5 HAT due to the potential stabilization of **IIIE** by the captodative effect.[40] We attempted to stop this putative pathway through increased sterics. Unfortunately, only decomposition of the amide (**149**) was observed. A control experiment with sulfonamides **154** and **156** shows that sterics has a minimal effect on the formation of the radical-anion. As a result, alkylated products **155** and **157** are formed in similar yield. Guided by this finding, we designed amide **150** in order to shut down the possibility of a radical-anion pathway. Indeed, the use of amide **150** results in the formation of the desired γ alkylated product **153** in minimal yield.

The successful formation of C-H functionalization product from **150**, but not **148** and **149**, suggests the significance to have a specially-designed group on nitrogen that lacks α C-H bond to shut down the undesired formation of radical anion. To this end, we acidified the N-H bond with a sulfonyl group (Scheme 3.4.5). Unfortunately, the use of **158** results in no reaction. We attributed this lack of reactivity to decreased reducing power of the amidyl anion. Therefore, we investigated the use of amide **159**, which bears a milder electron-withdrawing acetyl group on nitrogen. Gratifyingly, the remote alkylation between **39** and **160** is successful as product **161** is provided in moderate yield. Currently, Dr. Devin Chen, a postdoctoral researcher in the Rovis group, is working on reaction optimization and eventual substrate development.

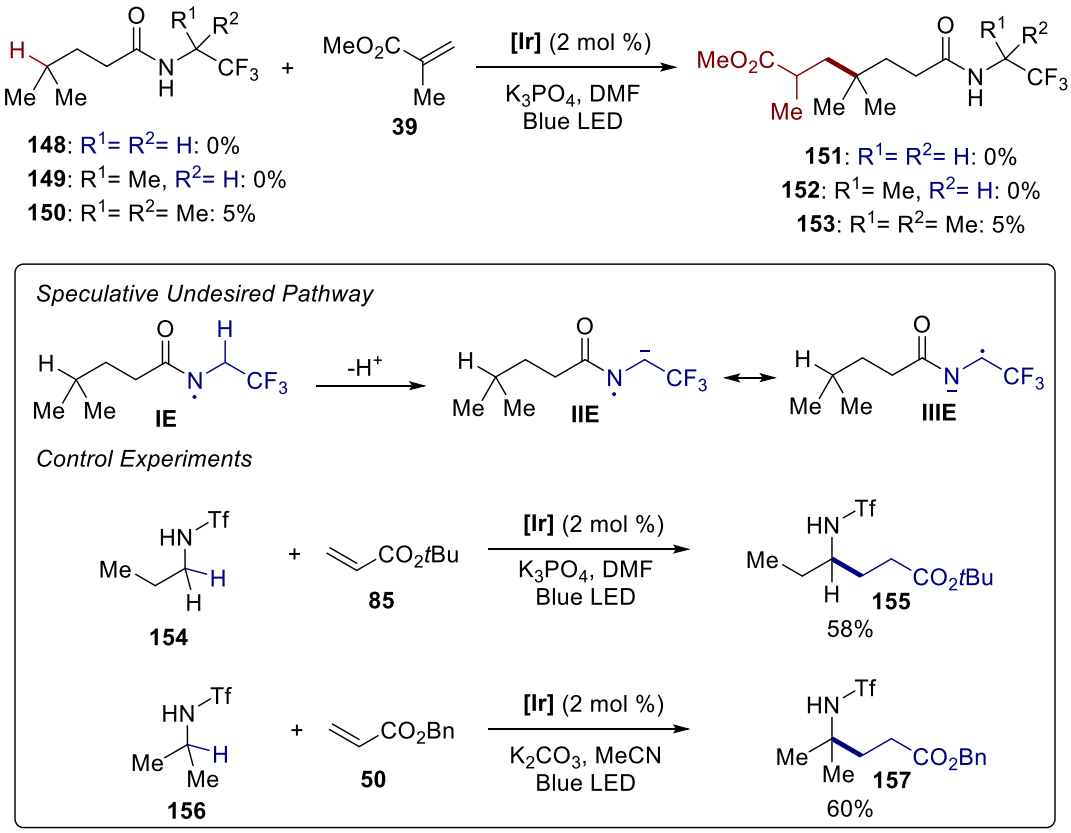

Scheme 3.4.4: Significance of the Lack of α-CH Bonds to Nitrogen

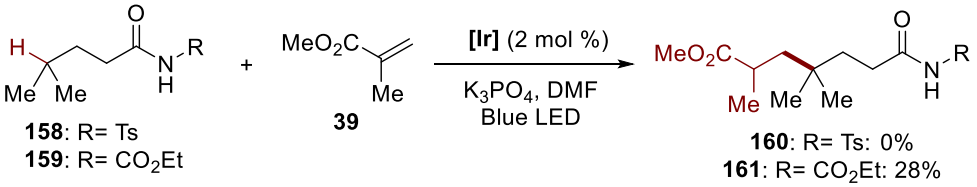

Scheme 3.4.5: Preliminary Results for γ-Functionalization of Carbonyl Groups

3.5 Summary

A photoredox-catalyzed protocol for nitrogen-directed C-C bond formations at inert C-H bonds is developed. The reaction features an N-H bond for the generation of the nitrogen radical and a subsequent 1,5 HAT for the generation of an alkyl radical. Preliminary results suggest that fluorination, azidation, hydroxymethylation, aminomethylation and alkynylation of inert C-H

bonds can also be achieved via 1,5 HAT. In addition, this strategy can also be extended to γ functionalization of carbonyl groups. Results will be reported in due course.

REFERENCES

1. Guimond, N.; Gouliaras, C.; Fagnou, K. *J. Am. Chem. Soc.* **2010**, *132*, 6908-6909.

2. Mochida, S.; Umeda, N.; Hirano, K.; Satoh, T.; Miura, M. *Chem. Lett.* **2010**, *39*, 744-746.

3. Hyster, T. K.; Rovis, T. *J. Am. Chem. Soc.* **2010**, *132*, 10565-10569.

4. Archambeau, A.; Rovis, T. *Angew. Chem. Int. Ed.* **2015**, *54*, 13337-13340.

5. Vitaku, E.; Smith, D. T.; Njardarson, J. T. *J. Med. Chem.* **2014**, *57*, 10257-10274.

6. Cekovic, Z. *J. Serb. Chem. Soc.* **2005**, *70*, 287-318.

7. Hofmann, A. W. *Ber. Dtsch. Chem. Ges.* **1879**, *12*, 984-990.

8. (a) Hernandez, R.; Rivera, A.; Salazar, J. A.; Suarez, E. *J. Chem. Soc. Chem. Commun.* **1980**, 958-959; (b) Carrau, R.; Hernandez, R.; Suarez, E. *J. Chem. Soc. Perkin Trans. 1* **1987**, 937-943; (c) de Armas, P.; Francisco, C. G.; Hernandez, R.; Salazar, J. A.; Suarez, E. *J. Chem. Soc. Perkin Trans. 1* **1988**, 3255-3265; (d) Betancor, C.; Concepcion, J. I.; Hernandez, R.; Salazar, J. A.; Suarez, E. *J. Org. Chem.* **1983**, *48*, 4430-4432; (e) de Armas, P.; Carrau, R.; Concepcion, J. I.; Francisco, C. G.; Hernandez, R.; Suarez, E. *Tetrahedron Lett.* **1985**, *26*, 2493-2496.

9. (a) Faulkner, A.; Race, N. J; Scott, J. S.; Bower, J. F. *Chem. Soc.* **2014**, *5*, 2416-2421; (b) Race, N. J.; Faulkner, A.; Shaw, M. H.; Bower, J. F. *Chem. Soc.* **2016**, *7*, 1508-1513.

10. Nikishin, G. I.; Troyansky, E. I.; Lazareva, M. I. *Tetrahedron* **1985**, *41*, 4279-4288.

11. Zard, S. Z. *Chem. Soc. Rev.* **2008**, *37*, 1603-1618.

12. (a) Yang, M.; Su, B.; Wang, Y.; Chen, K.; Jiang, X. Zhang, Y.-F.; Zhang, X.-S.; Chen, G.; Cheng, Y.; Cao, Z.; Guo, Q.-Y.; Wang, L.; Shi, Z-.J. *Nature Commun.* **2014**, *5*, 4707; (b) Zhou, T.; Luo, F.-X.; Yang, M.-Y.; Shi, Z.-J. *J. Am. Chem. Soc.* **2015**, *137*, 14586-14589.

13. (a) Chu, L.; Ohta, C.; Zuo, Z.; MacMillan, D. W. C. *J. Am. Chem. Soc.* **2014**, *136*, 10886-10889; (b) Ventre, S.; Pentronijevic, F. R.; MacMillan, D. W. C. *J. Am. Chem. Soc.* **2015**, *137*, 5654-5657.

14. (a) McNally, A.; Haffemayer, B.; Collins, B. S. L.; Gaunt, M. J. *Nature* **2014**, *510*, 129-133; (b) Smalley, A. P.; Gaunt, M. J. *J. Am. Chem. Soc.* **2015**, *137*, 10632-10641; (c) He, C.; Gaunt, M. J. *Angew. Chem. Int. Ed.* **2016**, *54*, 15840-15844.

15. Zaitsev, V. G.; Shabashov, D.; Daugulis, O. *J. Am. Chem. Soc.* **2005**, *127*, 13154-13155.

16. Zhang, S.-Y.; He, G.; Nack, W. A.; Zhao, Y.; Li, Q.; Chen, G. *J. Am. Chem. Soc.* **2013**, *135*, 2124-2127.

17. Jiang, H.; He, J.; Liu, T.; Yu, J.-Q. *J. Am. Chem. Soc.* **2016**, *138*, 2055-2059.

18. (a) Choi, G. J.; Knowles, R. R. *J. Am. Chem. Soc.* **2015**, *137*, 9226-9229; (b) Miller, D. C.; Choi, G. J.; Orbe, H. S.; Knowles, R. R. *J. Am. Chem. Soc.* **2015**, *137*, 13492-13495.

19. Zhang, J.; Li, Y.; Zhang, F.; Hu, C.; Chen, Y. *Angew. Chem. Int.* **2016**, *55*, 1872-1875.

20. Tassone, D. M.; Boyce, E.; Guyer, J.; Nuzum, D. *Clin. Ther.* **2007**, *29*, 26-48.

21. Cain, E. N.; Solly, R. K. *J. Am. Chem. Soc.* **1973**, *95*, 4791-4796.

22. Gomes, J. R. B.; Riberiro da Silva, M. D. M. C.; Ribeiro da Silva, M. A. V. *J. Phys. Chem. A.* **2004**, *108*, 2119-2130.

23. Bordwell, F. G. *Acc. Chem. Res.* **1988**, *21*, 456-463.

24. Blanksby, S. J.; Ellison, G. B. *Acc. Chem. Res.* **2003**, *36*, 255-263.

25. Turro, N. J. *Modern Molecular Photochemistry*. **1978**, Benjamin/Cummings, Menlo Park, CA.

26. Lowry, M. S.; Goldsmith, J. I.; Slinker, J. D.; Rohl, R.; Pascal, R. A. Jr.; Maliaras, G. G.; Bernhard, S. *Chem. Mater.* **2005**, *17*, 5712-5719.

27. Li, J. J.; Corey, E. J. *Named Reactions for Functional Group Transformation.* **2007**, 423-437, Wiley, New York.

28. Eidman, K. F.; Nichols, P. J. Trifluoroacetic acid. *E-EROS Encyclopedia of Reagents for Organic Synthesis.* **2004***,* Wiley, New York.

29. D'Anna, F.; Frenna, V.; Ghelfi, F.; Macaluso, G.; Marullo, S.; Spinelli, D. *J. Phys. Chem. A* **2010**, *114*, 10969-10974.

30. Stetzenbach, K. J.; Jensen, S. L.; Thomposon, G. M. *Environ. Sci. Technol.* **1982**, *16*, 250-254.

31. Liu, X.; Wang, Z.; Cheng, X.; Li, C. *J. Am. Chem. Soc.* **2012**, *134*, 14330-14333.

32. Kawamoto, T.; Fukuyama, T.; Ryu, I. *J. Am. Chem. Soc.* **2012**, *134*, 875-877.

33. Shaw, M. H.; Shurtleff, V. W.; Terett, J. A.; Cuthbertson, J. D.; MacMillan, D. W. C. *Science* **2016**, *352*, 1304-1308.

34. Noble, A.; MacMillan, D. W. C. *J. Am. Chem. Soc.* **2014**, *136*, 11602-11605.

35. Zuo, Z.; MacMillan, D. W. C. *J. Am. Chem. Soc.* **2014**, *136*, 5257-5260.

36. Fujii, S.; Konishi, T.; Matsumoto, Y.; Tamaoka, Y.; Takasu, K.; Yamada, K.-i. *J. Org. Chem.* **2014**, *79*, 8128-8133.

37. (a) He, J.; Takise, R.; Fu, H.; Yu, J.-Q. *J. Am. Chem. Soc.* **2015**, *137*, 4618-4621; (b) He, J.; Shigenari, T.; Yu, J.-Q. *Angew. Chem. Int. Ed.* **2015**, *54*, 6545-6549; (c) Zhu, R.-Y.; He, J.; Wang, X.-C.; Yu, J.-Q. *J. Am. Chem. Soc.* **2014**, *136*, 13194-13197.

38. (a) Reddy, B. V. S.; Reddy, L. R.; Corey, E. J. *Org. Lett.* **2006**, *8*, 3391-3394; (b) He, G.; Zhang, S.-Y.; Nack, W. A.; Pearson, R.; Rabb-Lynch, J.; Chen, G. *Org. Lett.* **2014**, *16*, 6488-6491; (c) Li, S.; Zhu, R.-Y.; Xiao, K.-J.; Yu, J.-Q. *Angew. Chem. Int. Ed.* **2016**, *55*, 4317-4321.

39. Li, S.; Chen, G.; Feng, C.-G.; Gong, W.; Yu, J.-Q. *J. Am. Chem. Soc.* **2014**, *136*, 5267-5270.

40. Viehe, H. G.; Janousek, Z.; Merenyi, R. *Acc. Chem. Res.* **1985**, *18*, 148-154.

APPENDIX ONE: CHAPTER 1 EXPERIMENTAL

A.1.1 General Procedure

All reactions were carried out under an atmosphere of argon in over-dried glassware. Dichloromethane, diethyl ether and toluene were degassed with argon and passed through a column of neutral alumina and a column of Q5 reactant. All other solvents were freshly distilled. Unless otherwise stated, flash column chromatography was performed on Silicycle Inc. silica gel 60 (230-400 mesh). Florisil (<200 mesh, fine powder, activated magnesium silicate) was also used when the products were acid-sensitive. Thin layer chromatography was performed on Silicycle Inc. 0.25 mm silica gel 60-F plates. Visualization was accomplished with UV light (254 nm), anisaldehyde or potassium permanganate. ^{1}H NMR and ^{13}C NMR spectra were obtained in CDCl3 at ambient temperature and chemical shifts are expressed in parts per million (δ, ppm). Mass spectra were obtained on an Agilent Technologies 6130 Quadropole Mass Spec (LRMS, ESI + APCI). Infrared spectra were collected on a Nicolet iS-50 FT-IR spectrometer.

Ligands **L9**-**14**[1] and **L16**[2] were synthesized according to previously reported procedures. Other ligands are commercial. All nitro-alkenes[3] are either known compounds or commercially available.

A.1.2 Synthesis of 1-Azadienes and Imines

Unless otherwise stated, all 1-azadienes and imines were synthesized with this procedure: A solution of enal or aldehyde (1 equiv.), aniline (1 equiv.) and anhydrous $MgSO_4$ in Et_2O or PhMe (2.5 mL per mmol of enal) was stirred at rt overnight. The mixture was filtered to remove $MgSO_4$.

The solvent was removed under *vacco* to afford 1-azadiene (>90% yields in all cases) which could be used without further purification. 1-azadienes sometimes were purified by recrystallization from absolute EtOH or by flash chromatography on silica gel (EtOAc/hexane with 1% NEt_3 as an additive).

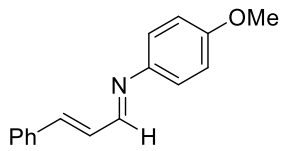

58

The spectral data is identical to those reported in the literature.[4]

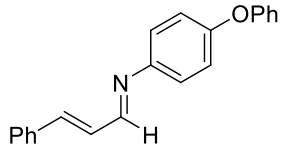

78

^{1}H NMR ($CDCl_3$, 400 MHz): 8.30 (dd, *J*=6.6, 1.6, 1H), 7.55 (d, *J*=7, 2H); 7.42-7.33 (m, 5H), 7.21 (d, *J*=6.6, 2H), 7.14-7.09 (m, 3H), 7.05-7.02 (m, 4H); ^{13}C NMR ($CDCl_3$, 100 MHz): 160.7, 157.3, 155.7, 147.0, 143.7, 135.6, 129.8, 129.5, 128.9, 128.6, 127.5, 123.3, 122.3, 119.5, 118.8; Molecular Weight $[M+H]^+$: 300.1 (expected), 300.1 (found); IR (cm^{-1}): 3058, 3038, 2979, 2946, 2873, 1628, 1603, 1594, 1588, 1489.

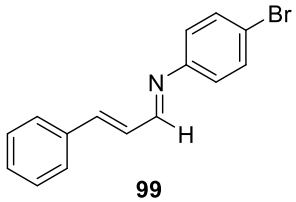

99

^{1}H NMR ($CDCl_3$, 400 MHz): 8.24 (d, *J*= 8.6, 1H), 7.54 (d, *J*= 8.2, 2H), 7.49 (d, *J*= 8.6, 2H), 7.43-7.35 (m, 3H), 7.18 (d, *J*= 16.0, 1H), 7.12-7.04 (m, 3H); ^{13}C NMR ($CDCl_3$, 100 MHz): 162.0, 150.7, 144.7, 135.4, 132.2, 129.8, 129.0, 128.3, 127.6, 122.6, 110.5; Molecular Weight $[M+H]^+$:286.02, 288.02 (expected), 286.1, 288.1 (found); IR (cm^{-1}): 3079, 3058, 3038, 3022, 2999, 2975, 2922, 2875, 2850, 1625, 1602, 1591, 1572, 1483, 1448.

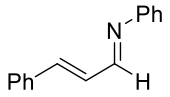

100

The spectral data is identical to those reported in the literature.[5]

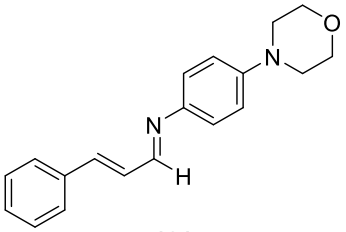

101

^{1}H NMR ($CDCl_3$, 400 MHz): 8.32 (dd, *J*= 5.8, 2.7, 1H), 7.53 (d, *J*= 7.0, 2H), 7.41-7.32 (m, 3H), 7.22 (d, *J*= 9.0, 2H), 7.12-7.11 (m, 2H), 6.93 (d, *J*= 9.0, 2H), 3.88-3.86 (m, 4H), 3.19-3.17 (m, 4H); ^{13}C NMR ($CDCl_3$, 100 MHz): 158.8, 150.0, 143.7, 142.6, 135.9, 129.3, 128.94, 128.88, 127.3, 122.1, 116.0, 66.9, 49.3; Molecular Weight $[M+H]^+$: 293.2 (expected), 293.2 (found); IR (cm^{-1}): 3026, 2859, 2888, 2854, 2836, 1623, 1606, 1574, 1507, 1488, 1447.

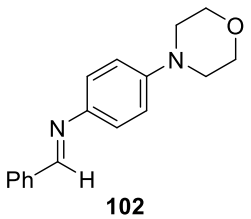

102

^{1}H NMR ($CDCl_3$, 400 MHz): 8.50 (s, 1H), 7.92-7.87 (m, 2H), 7.49-7.44 (m, 3H), 7.26 (d, *J*= 8.6, 2H), 6.95 (d, *J*= 9.0, 2H), 3.90-3.86 (m, 4H), 3.21-3.16 (m, 4H); ^{13}C NMR ($CDCl_3$, 100 MHz): 157.8, 149.9, 144.1, 136.6, 130.9, 128.7, 128.5, 122.1, 116.1, 66.9, 49.4; Molecular Weight $[M+H]^+$: 267.2 (expected), 267.2 (found); IR (cm^{-1}): 3057, 3036, 2956, 2886, 2855, 2830, 1622, 1601, 1588, 1571, 1507, 1447.

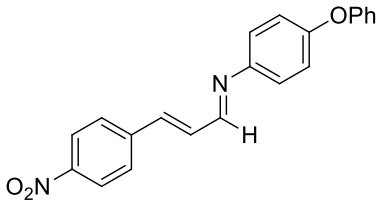

^{1}H NMR ($CDCl_3$, 400 MHz): 8.33 (d, *J*=7.8, 1H), 8.25 (d, *J*=8.7, 2H), 7.67 (d, 9.0, 2H), 7.36 (dd, *J*= 8.0, 8.0, 2H), 7.25-7.19 (m, 4H), 7.15-7.11 (m, 1H), 7.06-7.02 (m, 4H); ^{13}C NMR ($CDCl_3$, 100 MHz): 159.1, 157.0, 156.5, 147.9, 146.3, 141.9, 140.1, 132.7, 129.8, 127.9, 124.3, 123.5, 122.5, 119.4, 119.0; Molecular Weight $[M+H]^+$: 345.12 (expected), 345.2 (found); IR (cm^{-1}): 3097, 3069, 3055, 3040, 2926.0, 2874, 1622, 1594.

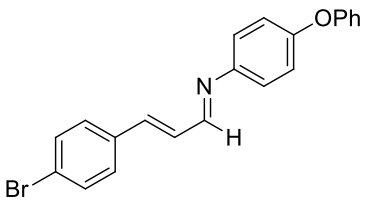

^{1}H NMR ($CDCl_3$, 400 MHz): 8.28 (dd, *J*= 6.9, 1.5, 1H), 7.53 (d, *J*= 8.6, 2H), 7.40-7.32 (m, 4H), 7.20 (d, *J*= 6.6, 2H), 7.13-7.08 (m, 3H), 7.04-7.01 (m, 4H); ^{13}C NMR ($CDCl_3$, 100 MHz): 160.1, 157.2, 155.9, 146.8, 142.1, 134.6, 132.1, 129.8, 129.3 128.8, 123.6, 123.3, 122.31, 119.5, 118.8; Molecular Weight $[M+H]^+$: 378.05, 380.05 (expected), 378.1, 380.1 (found); IR (cm^{-1}): 3058, 3038, 2954, 2931, 2871, 1739, 1708, 1629, 1598, 1586, 1548.

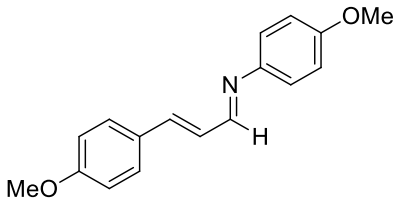

The spectral data is identical to those reported in the literature.[6]

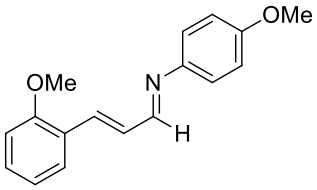

^{1}H NMR ($CDCl_3$, 400 MHz): 8.31 (d, *J*=9.0, 1H); 7.58 (dd, *J*=7.9, 1.6, 1H), 7.48 (d, *J*= 16.0, 1H); 7.32 (dd, *J*= 7.9,1.6, 1H), 7.22-7.14 (m, 3H); 6.98 (dd, *J*= 7.5,7.5, 1H); 6.94-6.90 (m, 3H), 3.90 (s, 3H), 3.83 (s, 3H); ^{13}C NMR ($CDCl_3$, 100 MHz): 160.6, 158.2, 157.5, 144.8, 138.3, 130.6, 129.3, 127.6, 124.7, 122.2, 120.9, 114.4, 111.1, 55.50, 55.47; Molecular Weight $[M+H]^+$: 268.13 (expected), 268.2 (found); IR (cm^{-1}): 3036, 2999, 2943, 2906, 2835, 1620, 1607, 1502, 1386, 1464, 1438.

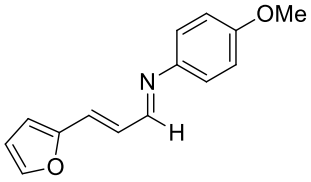

^{1}H NMR ($CDCl_3$, 400 MHz): 8.21 (d, *J*= 8.6, 1H), 7.48 (d, *J*= 1.6, 1H), 7.19 (d, *J*= 8.6, 2H), 6.98 (dd, *J*= 15.7, 9.0, 1H), 6.93-6.86 (m, 3H), 6.54 (d, *J*= 3.5, 1H), 6.46 (dd, *J*= 3.6, 1.5, 1H); 3.82 (s, 3H); 158.9, 158.3, 152.1, 144.7, 144.0, 129.4, 126.9, 122.2, 114.4, 112.16, 112.16, 55.5; Molecular Weight $[M+H]^+$: 228.1 (expected), 228.1 (found); IR (cm^{-1}): 3039, 2999, 2946, 2906, 2859, 2835, 1610, 1628, 1549, 1501, 1465, 1488, 1441.

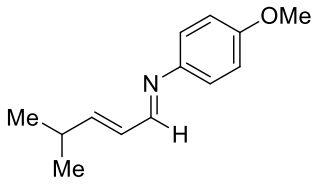

Although the imine obtained was not pure, it could not be purified due to its instability. ^{1}H NMR ($CDCl_3$, 400 MHz): 8.07 (d, *J*= 7.4, 1H); 7.11 (d, *J*= 8.6, 2H), 6.88 (d, *J*= 8.6, 2H), 3.79 (s, 3H), 2.53 (sep, *J*= 6.6, 1H), 1.10(d, *J*= 6.6, 6H); ^{13}C NMR ($CDCl_3$, 100 MHz): 160.5, 158.0, 154.2, 144.8, 128.5, 122.0, 114.3, 55.4, 31.4, 21.6; Molecular Weight $[M+H]^+$: 204.1 (expected), 204.1 (found); IR (cm^{-1}): 3035, 2958, 2931, 2906, 2858, 2834, 1642. 1608, 1577.

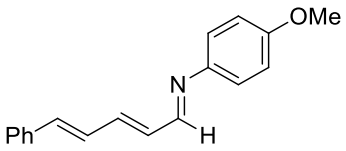

^{1}H NMR ($CDCl_3$, 400 MHz): 8.21 (d, *J*= 9.4, 1H), 7.48 (d, *J*= 7.5, 2H), 7.36 (dd, *J*= 7.2, 7.2, 2H), 7.31-7.27 (m, 1H), 7.19 (d, *J*= 8.6, 2H), 7.03-6.89 (m, 4H), 6.80 (d, *J*=14.5, 1H), 6.65 (dd, *J*= 14.5, 9, 1H), 3.82 (s, 3H); ^{13}C NMR ($CDCl_3$, 100 MHz): 159.3, 158.4, 144.7, 143.0, 137.4, 136.5, 132.5, 128.8, 128.6, 127.8, 127.0, 122.2, 114.4, 55.5; Molecular Weight $[M+H]^+$: 264.14 (expected), 264.2 (found); IR (cm^{-1}): 3055, 3032, 3023, 3001, 2955, 936, 2909, 2835, 1613, 1597, 1575, 1565, 1502, 1487, 1466, 1441.

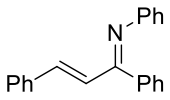

Aniline (0.465 g, 5.0 mmol, 1 equiv.) and chalcone (1.04 g, 5.0 mmol, 1 equiv.) was dissolved in DCM (15 mL). NEt_3 (1.39 mL, 10 mmol, 2 equiv.) was added. At 0 ^{o}C, $TiCl_4$ (0.55 mL, 5.0 mmol, 1 equiv.) was added dropwise. The mixture was allowed to warm to rt and stirred for

16 h. The reaction was quenched with H_2O. The aqueous layer was extracted with DCM three times. The combined organic layer was washed with brine, dried over Na_2SO_4 and filtered. Solvent was removed under *vacco*. The crude product was purified by flash column chromatography (6%-17% EtOAc/hex). Recrystallization from hexane afforded pure *N*,1,3-triphenylprop-2-en-1-imine (0.570 g, 40%) as a mixture of geometric isomers.

^{1}H NMR: all the peaks appear in the aromatic region and cannot be assigned; ^{13}C NMR ($CDCl_3$, 100 MHz): 167.1, 150.9, 141.6, 139.4, 135.7, 131.7, 129.9, 129.3 128.9, 128.8, 128.3, 127.5, 123.9, 121.9, 120.8; Molecular Weight $[M+H]^+$: 284.1 (expected), 284.1 (found); IR (cm^{-1}): 3057, 3025, 1621, 1585, 1574, 1493, 1481, 1448.

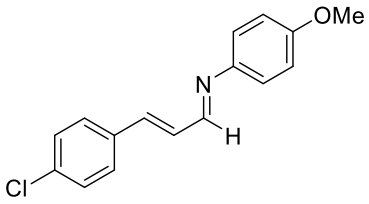

^{1}H NMR ($CDCl_3$, 400 MHz): 8.25 (dd, *J*=6.1, 2.2, 1H), 7.43-7.41 (m, 2H), 7.34-7.32 (m,2H), 7.19-7.17(m, 2H), 7.05-7.03 (m, 2H), 6.91-6.89 (m, 2H), 3.80(s, 3H); ^{13}C NMR ($CDCl_3$, 100 MHz): 159.0, 158.5, 144.4, 141.3, 135.1, 134.2, 129.3, 129.1, 128.5, 122.2, 114.4, 77.3, 77.0, 76.7, 55.5; Molecular Weight $[M+H]^+$: 272.1 (expected), 272.1 (found); IR (cm^{-1}): 3091, 3051, 3008, 2961, 2933, 2838, 1629, 1606, 1579,1562, 1504, 1490, 1439.

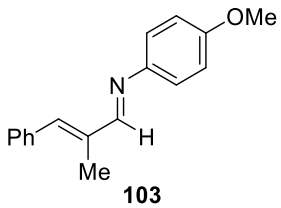

103

^{1}H NMR ($CDCl_3$, 400 MHz): 8.21 (s, 1H), 7.48 (d, *J*= 7.5, 2H), 7.42 (t, *J*= 7.7, 2H), 7.32 (t, *J*= 7.3, 1H), 7.18 (d, *J*= 8.6, 2H), 6.97 (s, 1H), 6.93 (d, *J*= 9.0, 2H), 3.83 (s, 3H), 2.30 (s, 3H); ^{13}C NMR ($CDCl_3$, 100 MHz): 163.6, 158.0, 145.2, 140.8, 137.6, 136.6, 129.5, 128.4, 127.9, 122.1, 114.3, 55.5, 13.2; Molecular Weight $[M+H]^+$: 252.14 (expected), 252.2 (found); IR (cm^{-1}): 3162, 3052, 3032, 2998, 2953, 2910, 2866, 2835, 1609, 1502, 1465, 1442.

A.1.3 Procedure for Ligand Screening

A solution of $Zn(OTf)_2$ (0.015 mmol, 10 mol %), the ligand (0.015 mmol, 10 mol %) and MS 4Å in PhMe (0.5 mL) in a vial was stirred at rt for 15 mins. A solution of nitro-alkene (0.225 mmol, 1.5 equiv.) in PhMe (0.5 mL) in a vial was added to the zinc complex. The vial containing nitro-alkene was rinsed with 0.5 mL and then 0.2 mL PhMe to ensure complete transfer of the nitro-alkene. 1-Azadiene (0.15 mmol, 1 equiv.) was added. The vial was sealed with a cap. The mixture was stirred for 16 h at the temperature specified. MeOH (1 mL) was added at rt. $NaCNBH_3$ (0.225 mmol, 1.5 equiv.) and $ZnCl_2$ (0.225 mmol, 1.5 equiv.) were added. The mixture was stirred until all [4+2] cycloadduct was consumed. The reaction was quenched with sat. $NaHCO_3$. The aqueous and organic layers were separated. The aqueous layer was extracted with Et_2O twice. The combined organic layer was dried over anhydrous Na_2SO_4 and filtered. The solvent was removed under *vacco*. The yield was determined by ^{1}H NMR using 1,3,5-trimethoxybenzene as an internal standard.

A.1.4 Mechanistic Experiments and Origin of Electronic Effect of Ligands

Control Experiment with 1,4-diphenyldiene*:* A solution of $Zn(OTf)_2$ (5.5 mg, 0.015 mmol, 10 mol %), ligand **L14** (7.4 mg, 0.015 mmol, 10 mol %) and MS 4Å in PhMe was stirred for 15 min.

A solution of 1,4-diphenylbutadiene **72** (30.9 mg, 0.15 mmol, 1 equiv.), nitroalkene **67** (29.4 mmol, 0.225 mmol, 1.5 equiv.) in PhMe (1 mL) was added. The mixture was stirred at rt overnight. The mixture was filtered through florisil. The solvent was removed under *vacco*. TLC and NMR analysis indicated there was no reaction.

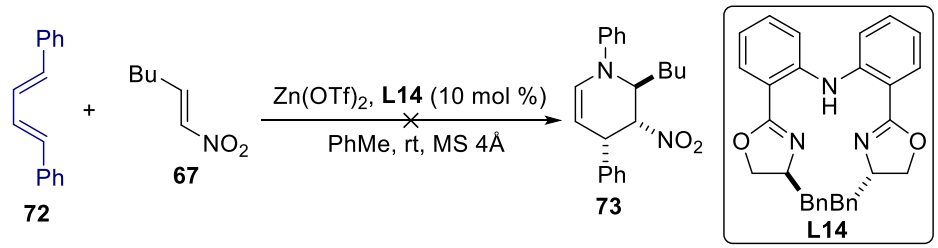

Control Experiments with thiourea catalyst: To a solution of thiourea **76**[7] (11.5 mg, 0.02 mmol, 20 mol %) and MS 4Å in PhMe (0.5 mL), a solution of 1-azadiene **58** (23.7 mg, 0.1 mmol, 1 equiv.) and nitroalkene **67** (19.4 mg, 0.15 mmol, 1.5 equiv.) in PhMe (0.5 mL) was added. The mixture was stirred at rt overnight. MeOH was added. $NaCNBH_3$ and $ZnCl_2$ were added. The mixture was stirred for 2 h. The reaction was quenched with sat. $NaHCO_3$. The aqueous and organic layers were separated. The aqueous layer was extracted with Et_2O twice. The combined organic layer was dried over anhydrous Na_2SO_4 and filtered. The yield of **68** was determined by NMR spectroscopy with 1,3,5-trimethoxy- benzene as an internal standard.

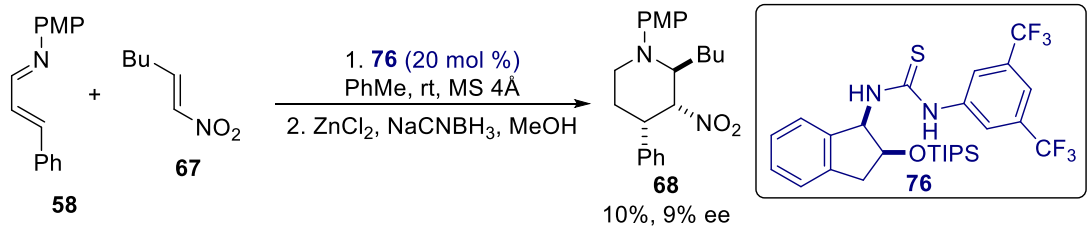

A solution of $Zn(OTf)_2$ (5.5 mg, 0.015 mmol, 10 mol %), **L29** (7.7 mg, 0.015 mmol, 10 mol %) and MS 4Å in PhMe (0.5 mL) was stirred at rt for 15 min. A solution of diphenylmethanimine

74 (27.3 mg, 0.15 mmol, 1 equiv.) and nitroalkene **75** (29.3, mg, 0.23 mmol, 1.5 equiv.) in PhMe (0.5 mL). 0.5 mL of PhMe was used to rinse the remaining diphenylmethanimine **74** and nitroalkene **75** to the reaction mixture. The mixture was stirred at rt for 24 h. The mixture was filtered through florisil. Solvent was removed under *vacco*. *N*-(diphenylmethylene)-1-nitrohexan-2-amine **77** was obtained in 90% yield by ^{1}H NMR spectroscopy with 1,3,5-trimethoxybenzene as an internal standard.

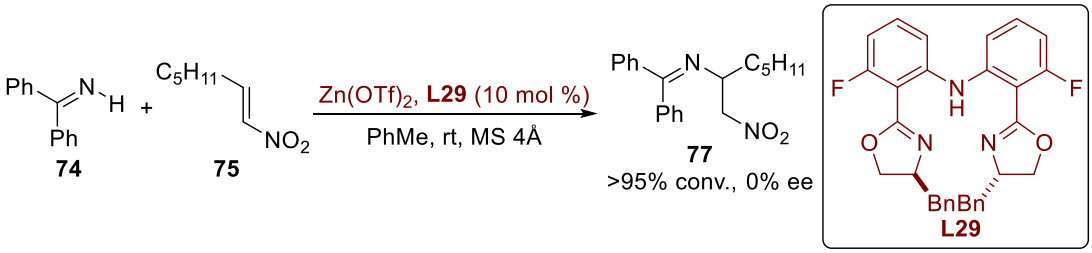

Synthesis of Deuterated Nitro-alkene and 1-Azadiene:

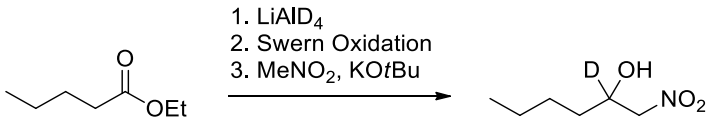

To a solution of LAD (1.29 g, 30.7 mmol, 1.9 equiv.) in Et_2O (35 mL) was added ethyl pentenoate (2.4 mL, 16.1 mmol, 1 equiv.) dropwise. The reaction mixture was stirred at rt for 1h and then reflux for 1h. The mixture was cooled to rt. Sodium sulfate decahydrate was added slowly until no gas bubbles were observed. The mixture was filtered. Solvent was removed under *vacco* to give a mixture of deuterated pentan-1-ol and water. DCM was added. The mixture was dried over anhydrous Na_2SO_4 and filtered. Solvent was removed under *vacco*. The crude deuterated pentan-1-ol was used without further purification. To a solution of $(COCl)_2$ (2.2 mL, 26.0 mmol, 1.6 equiv.) in DCM (41.5 mL) was added DMSO (3.7 mL, 52.1 mmol 3.2 equiv.)

dropwise at –78°C. The mixture was stirred for 15 min. A solution of the crude pentan-1-ol described previously in DCM (6.2 mL) was added slowly. The mixture was stirred for 30 min. NEt_3 (7.25 mL, 52.1 mmol, 3.2 equiv.) was added slowly. The mixture was stirred for 2 h and then allowed to warm to rt. The mixture was quenched with sat. NH_4Cl and extracted with DCM three times. The combined organic layer was washed with water twice and brine, dried over anhydrous Na_2SO_4 and filtered. Solvent was removed under *vaccu*. The crude pentanal was dissolved in THF (8 mL) and *t*BuOH (8 mL). Nitromethane (1.4 mL, 25.8 mmol, 1.6 equiv.) was added. At 0 °C, K*t*OBu (0.387 g, 3.45 mmol, 0.21 equiv.) was added. The mixture was stirred at rt overnight. The mixture was quenched with sat. NH_4Cl. The organic layer and aqueous layer were separated. The aqueous layer was extracted with Et_2O three times. The combined organic layer was washed with brine, dried over Na_2SO_4 and filtered. Solvent was removed under *vacco*. Flash column chromatography (10-18% EtOAc/hex) afforded pure deuterated 1-nitrohexan-2-ol (1.015g, 43% over 3 steps). ^1H NMR ($CDCl_3$, 300 MHz): 4.45-4.33 (m, 2H), 2.46 (br, 1H), 1.58-1.32 (m, 6H), 0.92 (t, *J*= 7.3, 3H). The ^1H NMR spectrum has all the signals of non-deuterated 1-nitrohexan-2-ol[8] except the peak at 4.35-4.27 ppm.

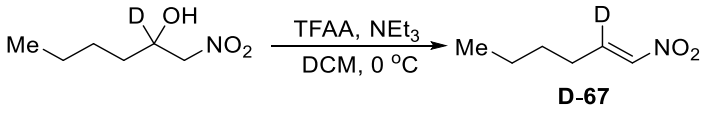

D-67

To a solution of deuterated 1-nitrohexan-2-ol (901.3 mg, 6.08 mmol, 1 equiv.) was added TFAA (0.888 mL, 6.39 mmol, 1.05 equiv.) at 0 °C dropwise. NEt_3 (1.865 mL, 13.4 mmol, 2.20 equiv.) was added dropwise at 0 °C. The mixture was allowed to stirred at the same temperature for 15 min. At 0 °C, the mixture was quenched with sat. NH_4Cl. The organic and aqueous layers were separated. The aqueous layer was extracted with DCM twice. The combined organic layer was

washed with NH_4Cl three times, dried over Na_2SO_4, and filtered. Solvent was removed under *vacco*. Pure deuterated (E)-1-nitrohex-1-ene **D-67** (366.4 mg, 41%) was obtained by flash chromatography (10% Et_2O/hex) and then vacuum distillation. ^1H NMR ($CDCl_3$, 400 MHz): 6.98-6.97 (m, 1H), 2.27 (t, *J*= 7.5, 2H), 1.54-1.47 (m, 2H), 1.43-1.33 (m, 2H), 0.94 (t, *J*= 7.3, 2H). The ^1H NMR spectrum has all the signals of non-deuterated (E)-1-nitrohex-1-ene except the peak at 7.31-7.22 ppm.

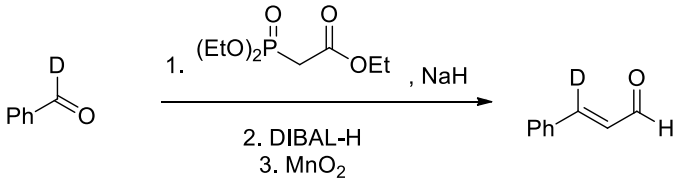

To a solution of ethyl 2-(diethoxyphosphoryl)acetate (2.0125 g, 8.977 mmol, 1.05 equiv.) in THF (24 mL) was added NaH (0.384 g, 60% in mineral oil, 9.6 mmol, 1.1 equiv.) at 0 ^oC. The mixture was stirred for 10 min. Deuterated benzaldehyde (0.885 mL, 8.715 mmol, 1 equiv.) was added dropwise. The mixture was warm to rt and stirred overnight. The mixture was quenched with sat. NH_4Cl. The mixture was extracted with Et_2O three times. The combined organic layer was washed with sat. $NaHCO_3$, brine,, dried over Na_2SO_4 and filtered. Solvent was removed under *vacco*. The crude ester was dissolved in DCM (38. 5mL). At –78 ^oC, DIBAL-H (20.1 mL, 1 M solution in hexane, 20.1 mmol, 2.31 equiv.) was added dropwise. The mixture was stirred at –40 ^oC for 2 h. The mixture was diluted with Et_2O. Rocelle's salt was added. The mixture was stirred at rt overnight. The mixture was extracted with Et_2O three times. The combined organic layer was washed with 1 M HCl, sat. $NaHCO_3$ and brine, dried over Na_2SO_4 and filtered. Solvent was removed under *vacco*. The crude alcohol was dissolved in DCM (48 mL). MnO_2 (6.005 g, 69.7 mmol, 8.00 equiv.) was added. The mixture was stirred at rt overnight. Excess MnO_2 was removed

by filtration. Solvent was removed under *vacco*. Flash column chromatography (5%-20% Et_2O/hex) afforded pure deuterated cinnamaldehyde (881.3 mg, 76% over 3 steps). ^1H NMR ($CDCl_3$, 400 MHz): 9.72 (d, *J*= 7.5, 1H), 7.59-7.56 (m, 2H), 7.45-7.42 (m, 3H), 6.73 (dt(1:1:1 t), 7.9, 2.4, 1H). The ^1H NMR spectrum has all the signals as non-deuterated cinnamaldehyde except the peak at 7.48 ppm.

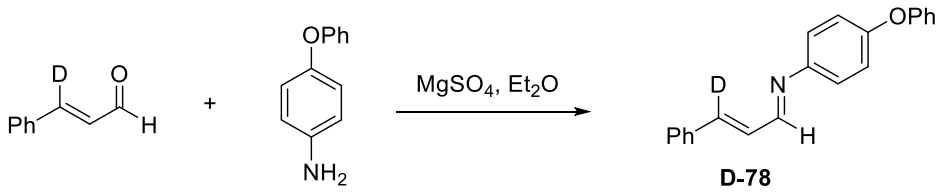

D-78

To a solution of deuterated cinnamaldehyde (221.2 mg, 1.66 mmol, 1 equiv.) and $MgSO_4$ (0.1 g) in Et_2O (4 mL) was added 4-phenoxyaniline (307.7 mg, 1.66 mmol, 1 equiv.) The mixture was stirred at rt overnight. $MgSO_4$ was removed by filtration. Solvent was removed under *vacco*. The deuterated (*E*)-4-phenoxy-N-((*E*)-3- phenylallylidene)aniline (499.3 mg, 100%) **D-78** obtained was pure by ^1H NMR spectroscopy. ^1H NMR ($CDCl_3$, 400 MHz): 8.30 (d, *J*= 9.0, 1H), 7.56-7.53 (d, 2H), 7.42-7.33 (m, 5H), 7.21 (dt, *J*= 8.6, 2.8, 2H), 7.13-7.09 (m, 2H), 7.05-7.01 (m, 4H). The ^1H NMR spectrum has all the signals of non-deuterated (*E*)-4-phenoxy-N-((*E*)-3- phenylallylidene)aniline except the peak at 7.12 ppm.

Studies on Kinetic Isotope Effects:

Deuterated Nitro-alkene: A solution of $Zn(OTf)_2$ (2.8 mg, 0.0077 mmol, 10 mol %), Ligand (0.0077 mmol, 10 mol %) and MS 4Å in PhMe (0.92 mL) was stirred for 15 min. A stock solution of 1:1 nitro-alkene: d_1-nitroalkene was prepared by the addition of 2.7 mL PhMe to a mixture of 129.9 mg nitro-alkene and 130.9 mg d_1-nitro-alkene. 0.1 mL of this stock solution (0.0377 mmol

each, 0.5 equiv. each) was added. The mixture was stirred for 5 min. 1-azadiene **78** (11.3 mg, 0.0377 mmol, 0.5 equiv.) was added. The mixture was stirred for the 16 h. A few drops of NEt_3 was added to prevent hydrolysis of the product. The mixture was filtered through florisil. Solvent was removed under *vacco*. Conversion was determined by ^1H NMR spectroscopy. Pure product was obtained by flash chromatography (5-20% Et_2O/hex, florisil as stationary phase). The ratio of D-product to H-product was determined by ^1H NMR with d_1=25 s, nt= 128. All experiments were repeated and consistent KIE's were obtained.

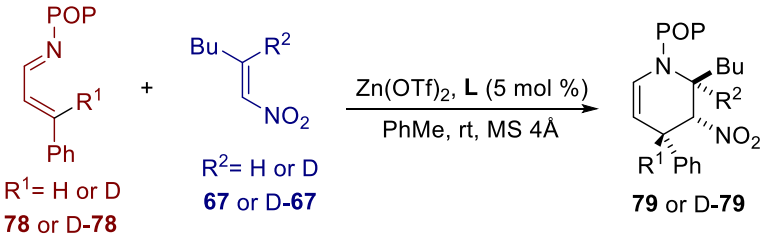

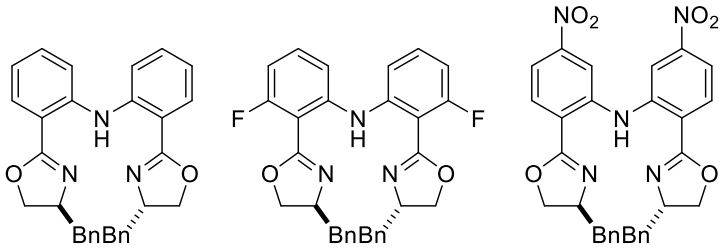

L14 **L29** **L26**

deuterated 1-azadiene	1.00	1.00	1.00
deuterated nitro-alkene	0.89	0.88	0.87

Deuterated 1-azadiene: Both the deuterated and non-deuterated aza-dienes were recrystallized with EtOH before use. A solution of $Zn(OTf)_2$ (5.5 mg, 0.015 mmol, 20 mol %), Ligand (0.015 mmol, 20 mol %) and MS 4Å in PhMe (0.4 mL) was stirred for 15 min. A solution of nitro-alkene **67** (4.9 mg, 0.038 mmol, 0.5 equiv.) in PhMe (0.25 mL) was added. The mixture was stirred for 5 min. A stock solution of 1:1 azadiene: d_1-azadiene was prepared by the addition of 40.0 mL PhMe to a mixture of 499.5 mg azadiene and 501.2 mg d_1-azadiene. 0.91 mL of this stock solution

(0.038 mmol each, 0.5 equiv. each) was added. The mixture was stirred for 16 h. The workup procedure was the same as described before. The ratio of D-product to H-product was determined by ^{1}H NMR with d_1=25 s, nt= 128. In all cases, an 1:1 ratio of the D-product to the H-product was obtained.

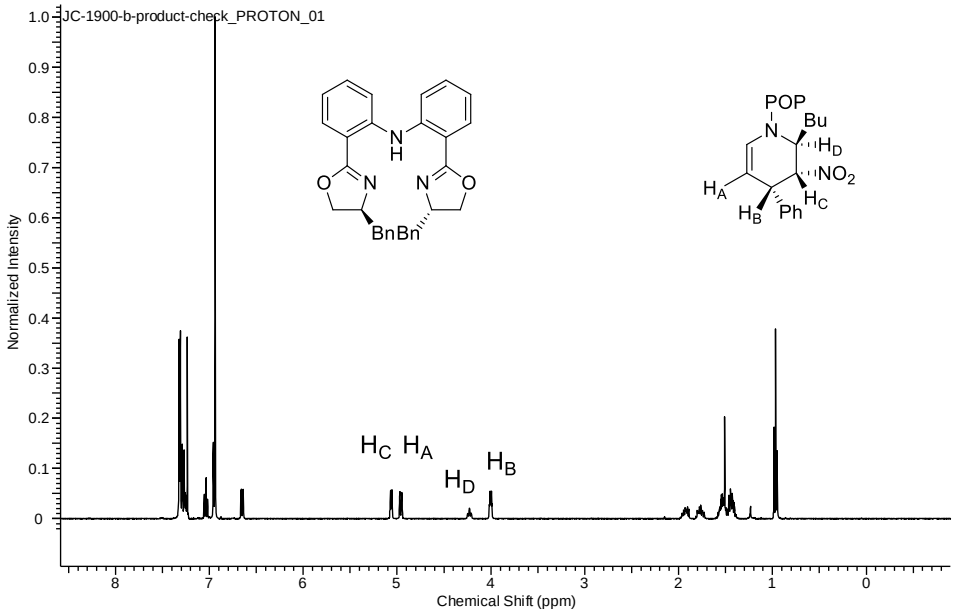

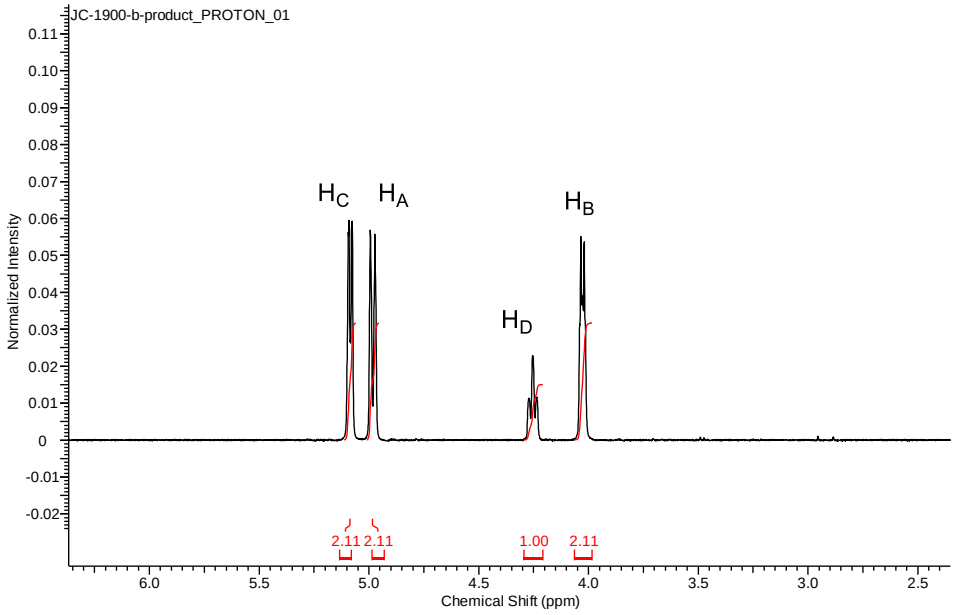

The calculation of KIE with Ligand **L14** is shown below.

$$KIE = \frac{\ln(1 - F)}{\ln[(1 - F)\, R/R_0]}$$

F: conversion based on nitro-alkene = 0.32

$$R_0: \frac{\text{non-deuterated nitro-alkene before reaction}}{\text{deuterated nitro-alkene before reaction}} = 1$$

$$R: \frac{\text{non-deuterated nitro-alkene after reaction}}{\text{deuterated nitro-alkene after reaction}}$$

Assuming initially there are x mmol of deuterated nitroalkene and x mmol of non-deuterated nitroalkene

$$\text{total product} = (x+x)\, F = 1.11\ \text{Product}_H + 1.00\ \text{Product}_H$$
$$\text{Product}_H = 0.9434xF$$
$$\text{Nitroalkene}_{H(\text{after reaction})} = x - \text{Product}_H$$
$$= x - 0.9434xF$$

Similarly,

$$\text{total product} = (x+x)\, F = (1/1.11)\text{Product}_D + 1.00\ \text{Product}_D$$
$$\text{Product}_D = 1.0521xF$$
$$\text{Nitroalkene}_{D(\text{after reaction})} = x - \text{Product}_D$$
$$= x - 1.0532xF$$

$$R = \frac{x - 1.0532xF}{x - 0.9434xF} = 0.9497$$

$$KIE = \frac{\ln(1 - F)}{\ln[(1 - F)\, R/R_0]} = 0.88$$

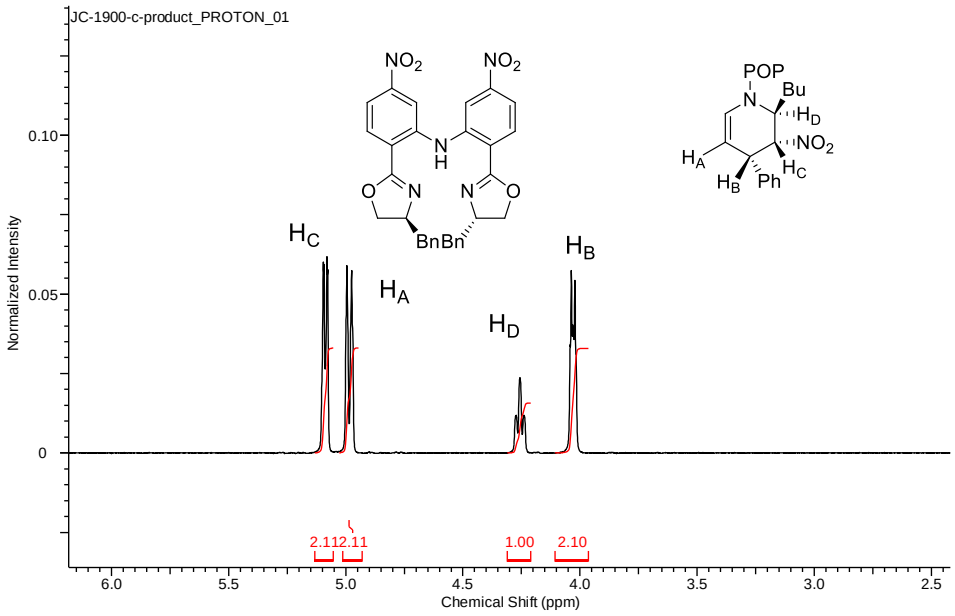
JC-1900-c-product_PROTON_01
Normalized Intensity
Chemical Shift (ppm)
H_C
H_A
H_D
H_B
2.11
2.11
1.00
2.10
POP
Bu
H_D
NO_2
H_A
H_C
H_B
Ph
NO_2
NO_2
N
H
O
N
N
O
BnBn

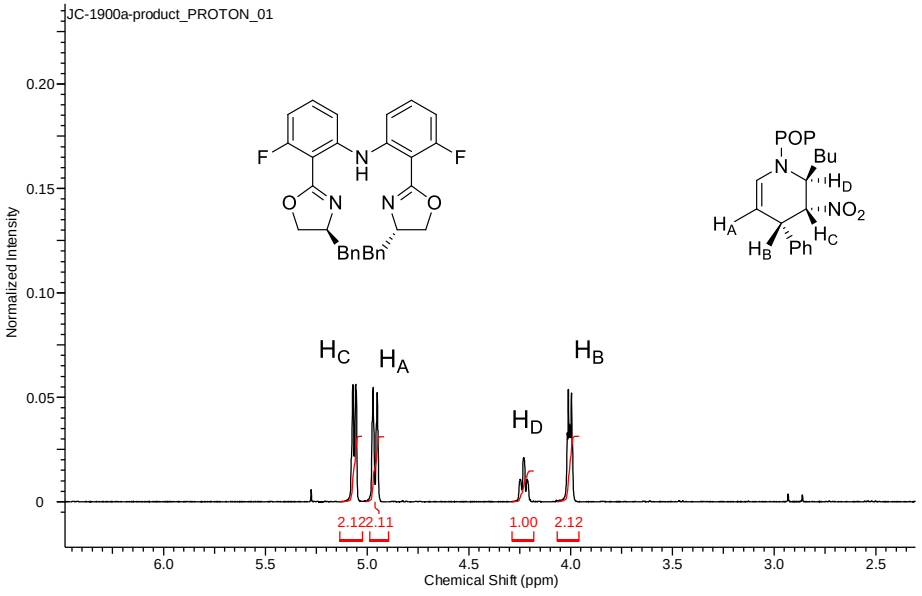
JC-1900a-product_PROTON_01
Normalized Intensity
Chemical Shift (ppm)
H_C
H_A
H_D
H_B
2.12
2.11
1.00
2.12
POP
Bu
H_D
NO_2
H_A
H_C
H_B
Ph
F
F
N
H
O
N
N
O
BnBn

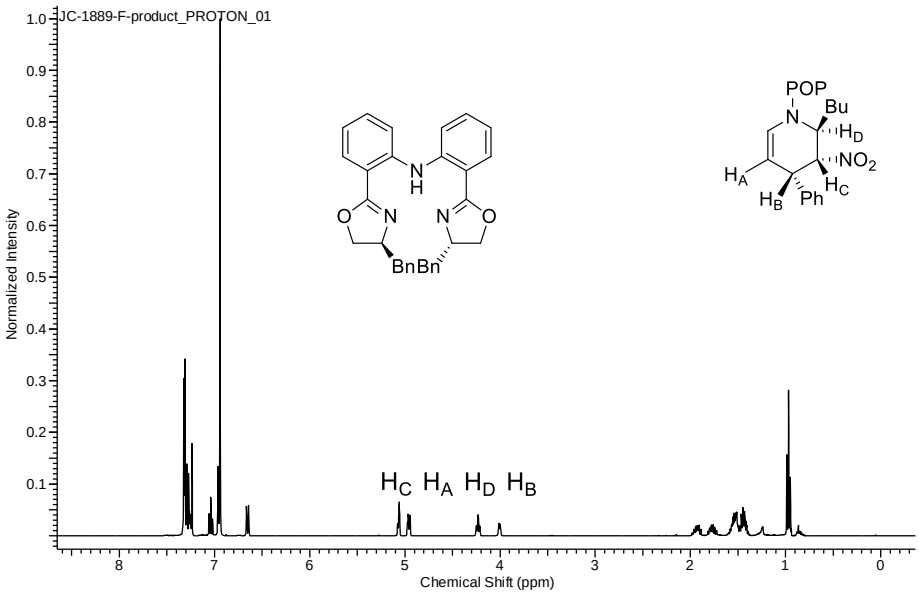
JC-1889-F-product_PROTON_01
Normalized Intensity
Chemical Shift (ppm)
H
N
O
N
N
O
BnBn
POP
N
Bu
H_D
NO_2
H_A
H_B
Ph
H_C
H_C H_A H_D H_B

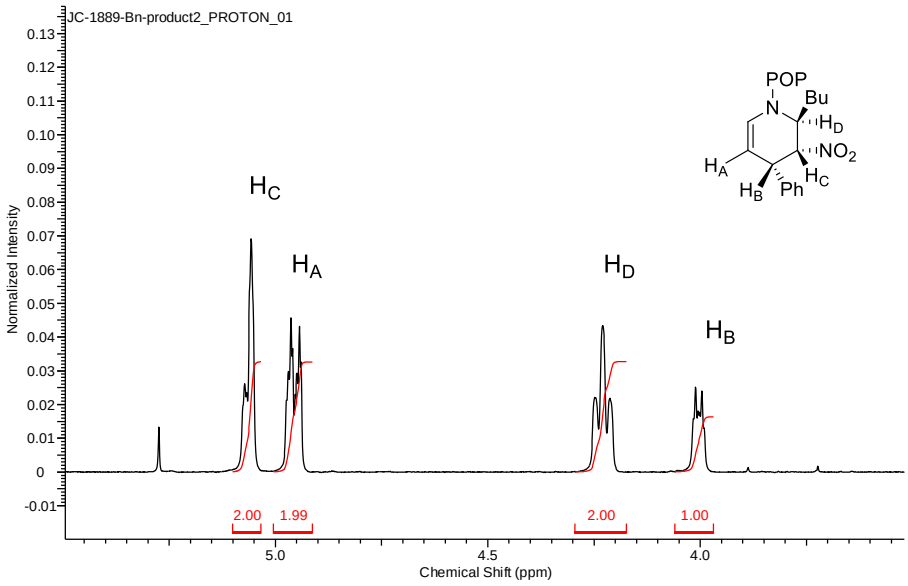
JC-1889-Bn-product2_PROTON_01
Normalized Intensity
Chemical Shift (ppm)
POP
N
Bu
H_D
NO_2
H_A
H_B
Ph
H_C
H_C
H_A
H_D
H_B
2.00
1.99
2.00
1.00

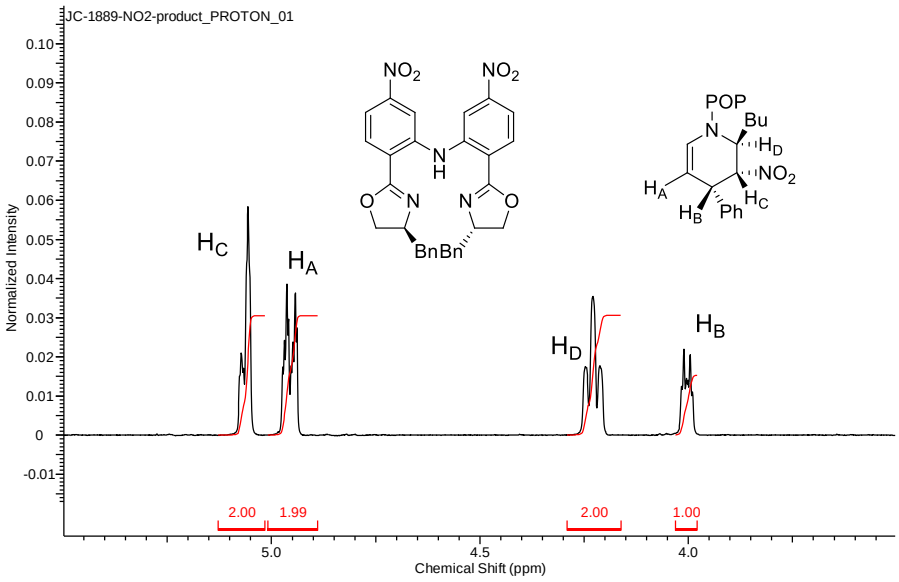
JC-1889-NO2-product_PROTON_01
Normalized Intensity
Chemical Shift (ppm)
H_C
H_A
H_D
H_B
2.00
1.99
2.00
1.00
NO_2
NO_2
BnBn
POP
Bu
H_D
NO_2
H_A
H_C
H_B
Ph

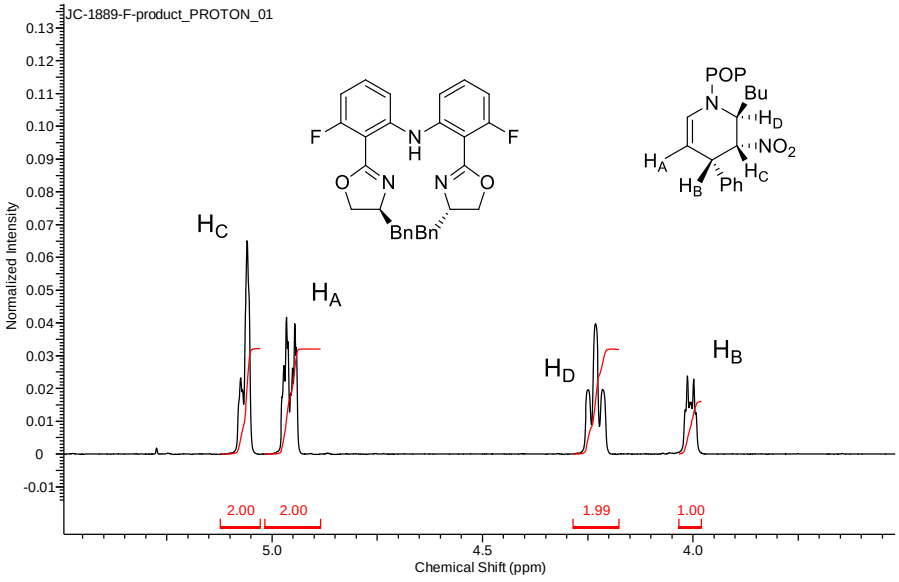
JC-1889-F-product_PROTON_01
Normalized Intensity
Chemical Shift (ppm)
H_C
H_A
H_D
H_B
2.00
2.00
1.99
1.00
F
F
BnBn
POP
Bu
H_D
NO_2
H_A
H_C
H_B
Ph

Effect of 1-Azadiene on Zn-catalyzed Michael Addition:

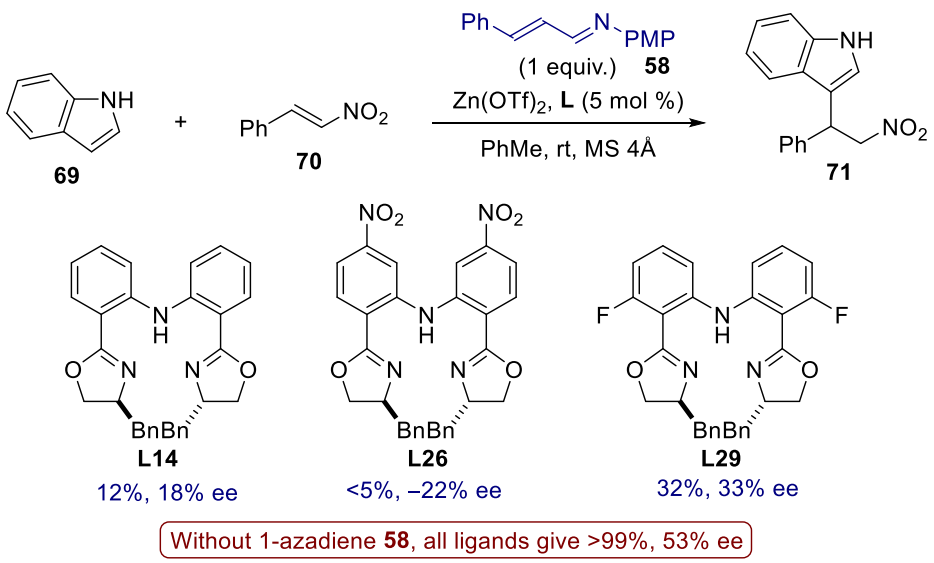

Without 1-azadiene **58**: A solution of $Zn(OTf)_2$ (2.8 mg, 0.0077 mmol, 5 mol %), Ligand (0.0077 mmol, 5 mol %) and MS 4Å in PhMe (0.92 mL) was stirred at rt for 15 min. Nitro-styrene **70** (23.0 mg, 0.15 mmol, 1 equiv.) was added. The mixture was stirred for 5 min. Indole **69** (18.1 mg, 0.15 mmol, 1 equiv.) was added. The mixture was stirred at rt for 18-20 h. Solvent was removed under *vacco*. The yield of **71** was determined by ^{1}H NMR spectroscopy with 1,3,5-methoxybenzene as an internal standard. The crude product was either purified by flash column chromatography (10-25% EtOAc/hex) or filtration through silica gel before HPLC analysis. The spectral data are identical to those previously reported.[9] HPLC conditions: IB column, 70:30 Hex: IPA, 0.8 mL/min, t_1=14.6 min (minor enantiomer), t_2= 16.0 min (major enantiomer).

With 1-azadiene **58**: A solution of $Zn(OTf)_2$ (2.8 mg, 0.0077 mmol, 5 mol %), Ligand (0.0077 mmol, 5 mol %) and MS 4Å in PhMe (0.92 mL) was stirred at rt for 15 min. Nitro-styrene **70** (23.0 mg, 0.15 mmol, 1 equiv.) and 1-azadiene **58** (36.6 mg, 0.15 mmol, 1 equiv.) was added. The mixture was stirred for 5 min. Indole **69** (18.1 mg, 0.15 mmol, 1 equiv.) was added. The mixture

was stirred at rt for 18-20 h. Solvent was removed under *vacco*. The yield of **71** was determined by ^{1}H NMR spectroscopy with 1,3,5-methoxybenzene as an internal standard. The crude product was either purified by flash column chromatography (10-25% EtOAc/hex). Same HPLC conditions were applied as described above.

A.1.5 Optimization of [4+2] Cycloaddition with Ligand L29

A solution of $Zn(OTf)_2$ (10 or 20 mol %), Ligand **L29** (10 or 20 mol %) and MS 4Å in PhMe (0.4 or 0.8 mL) in a vial was stirred at rt for 15 mins. A solution of nitro-alkene **67** (1.5 or 3 equiv. in PhMe (0.15 or 0.3 mL) in a vial was added to the zinc complex. The vial containing nitro-alkene **67** was rinsed with 0.15 or 0.3 mL twice to ensure complete transfer of the nitro-alkene **67**. The mixture was cooled to the specified temperature. 1-Azadiene **78** (0.15 mmol, 1 equiv.) was added. The vial was sealed with a cap. The mixture was stirred at the specified temperature until no 1-azadiene **78** was detected by TLC. The mixture was warmed to rt and MeOH (1 mL) was added. $NaCNBH_3$ (0.60 mmol, 4 equiv.) and $ZnCl_2$ (0.60 mmol, 4 equiv.) were added. The mixture was stirred until all [4+2] cycloadduct was consumed. The reaction was quenched with sat. $NaHCO_3$. The aqueous and organic layers were separated. The aqueous layer was extracted with Et_2O twice. The combined organic layer was dried over anhydrous Na_2SO_4 and filtered. The solvent was removed under *vacco*. The crude piperidine **79** was purified by flash column chromatography.

A.1.6 Procedure for [4+2] Cycloaddition under Optimized Conditions

A solution of $Zn(OTf)_2$ (0.03 mmol, 20 mol %), Ligand **R** (0.03 mmol, 20 mol %) and MS 4Å in PhMe (0.4 mL) in a vial was stirred at rt for 15 mins. A solution of nitro-alkene (0.45 mmol, 3 equiv.) in PhMe (0.15 mL) in a vial was added to the zinc complex. The vial containing nitro-alkene

was rinsed with 0.15 mL twice to ensure complete transfer of the nitro-alkene. The mixture was cooled to −78 °C. 1-Azadiene (0.15 mmol, 1 equiv.) was added. The vial was sealed with a cap and put into a freezer at −38 °C. The mixture was stirred until no 1-azadiene was detected by TLC. The mixture was warmed to rt and MeOH (1 mL) was added. $NaCNBH_3$ (0.60 mmol, 4 equiv.) and $ZnCl_2$ (0.60 mmol, 4 equiv.) were added. The mixture was stirred until all [4+2] cycloadduct was consumed. The reaction was quenched with sat. $NaHCO_3$. The aqueous and organic layers were separated. The aqueous layer was extracted with Et_2O twice. The combined organic layer was dried over anhydrous Na_2SO_4 and filtered. The solvent was removed under *vacco*. The crude piperidine was purified by flash column chromatography.

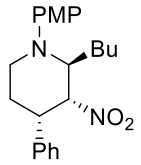

68

^{1}H NMR ($CDCl_3$, 400 MHz): 7.37-7.30 (m, 4H), 7.26 (t, *J*= 7.1, 1H), 6.85-6.80 (m, 4H), 4.94-4.91 (m, 1H), 4.38 (dd, *J*= 7.3, 7.3, 1H), 3.77 (s, 3H), 3.52 (ddd, *J*= 12.5, 4.0, 1.6, 1H), 3.37-3.26 (m, 2H), 2.94 (qd, *J*= 12.9, 5.1, 1H), 1.97-1.90 (m, 1H), 1.82-1.69 (m, 2H), 1.40-1.27 (m, 4H), 0.91-0.87 (m, 3H); ^{13}C NMR ($CDCl_3$, 100 MHz): 153.5, 144.2, 139.8, 128.6, 127.4, 127.2, 119.0, 114.5, 87.9, 62.9, 55.6, 42.4, 37.9, 29.0, 26.1, 24.1, 22.5, 13.9; Molecular Weight $[M+H]^+$: 369.22 (expected); 369.3 (found); IR (cm^{-1}): 3028.5, 2955, 2930, 2859, 2832, 1546, 1510; $[\alpha]^{20}_D$= −95.4° (c= 1.00, $CHCl_3$); HPLC (IB column, gradient elution: 100% H_2O at 0 min to 5% H_2O in MeCN at 58 min, 1 mL/min): 44.0 min, 46.1 min (major).

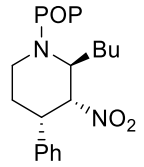

79

^{1}H NMR ($CDCl_3$, 400 MHz): 7.38-7.26 (m, 7H), 7.04 (dd, *J*= 7.4, 7.4, 1H), 6.97-6.93 (m, 4H), 6.86 (d, *J*= 9.0, 2H), 4.95-4.91 (m, 1H), 4.48 (dd, *J*= 7.3, 7.3, 1H), 3.64 (dd, *J*= 12.6, 3.9, 1H), 3.40-3.29 (m, 2H), 2.95 (qd, *J*= 12.5, 5.1, 1H), 1.98-1.91 (m, 1H), 1.84-1.87 (m, 2H), 1.40-1.32 (m, 4H), 0.93-0.90 (m, 3H); ^{13}C NMR ($CDCl_3$, 100 MHz): 158.5, 149.4, 146.7, 139.6, 129.6, 128.6, 127.4, 127.3, 122.3, 120.6, 118.3, 117.6, 87.9, 62.2, 42.0, 38.1, 29.0, 26.9, 23.9, 22.5, 13.9; Molecular Weight $[M+H]^+$: 431.23 (expected), 431.3 (found); IR (cm^{-1}): 3061, 3039, 2956, 2930, 2860, 1588, 1546, 1488, 1467; $[\alpha]^{20}_D$= +3.9° (c= 0.92, $CHCl_3$); HPLC (IB column, gradient elution: 100% H_2O at 0 min to 5% H_2O in MeCN at 28 min, 1 mL/min): 26.7 min, 27.5 min (major).

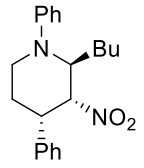

109

^{1}H NMR ($CDCl_3$, 400 MHz): 7.38-7.22 (m, 7H), 6.88 (d, *J*= 8.2, 2H), 6.82 (t, *J*= 7.3, 1H), 4.98-4.91 (m, 1H), 4.56 (dd, *J*=7.4, 7.4, 1H), 3.74 (dd, *J*= 12.9, 3.9, 1H), 3.39 (dt, *J*= 13.3, 4.2, 1H), 3.32 (td, *J*= 12.7, 3.1, 1H), 2.95 (qd, *J*=12.9, 5.0, 1H), 1.97-1.90 (m, 1H), 1.84-1.79 (m, 2H), 1.41-1.33 (m, 4H), 0.91 (t, *J*= 6.9, 3H); ^{13}C NMR ($CDCl_3$, 100 MHz): 150.2, 139.6, 129.2, 128.6, 127.4, 127.3, 119.3, 116.6, 87.8, 61.4, 41.5, 38.3, 28.9, 27.3, 23.9, 22.5, 13.9; Molecular Weight $[M+H]^+$: 339.21 (expected), 339.3 (found); IR (cm^{-1}): 3026, 2956, 2930, 1597, 1546, 1466; $[\alpha]^{20}_D$= +23.4° (c= 1.00,

$CHCl_3$); HPLC (IB column, gradient elution: 100% H_2O at 0 min to 5% H_2O in MeCN at 28 min): 25.0 min, 26.3 min (major).

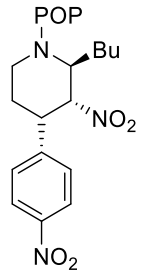

110

^{1}H NMR ($CDCl_3$, 400 MHz): 8.22 (d, *J*= 9.0, 2H), 7.50 (d, *J*= 8.6, 2H), 7.32-7.27 (m, 2H), 7.04 (t, *J*= 7.4, 1H), 6.97-6.93 (m, 4H), 6.86 (dt, *J*= 6.7, 3.0, 2H), 4.95-4.91 (m, 1H), 4.56 (dd, *J*= 7.2, 7.2, 1H), 3.62 (dd, *J*= 12.9, 3.9, 1H), 3.47 (dt, *J*= 13.3, 4.0, 1H), 3.35 (td, *J*= 12.6, 3.2, 1H), 2.91 (qd, *J*=13.0, 4.9, 1H), 2.05-1.98 (m, 1H), 1.88-1.74 (m, 2H), 1.43-1.30 (m, 4H), 0.93-0.89 (m, 3H); ^{13}C NMR ($CDCl_3$, 100 MHz): 158.3, 149.9, 147.4, 147.1, 146.3, 129.6, 128.3, 123.8, 122.5, 120.6, 118.7, 117.7, 87.3, 62.4, 41.8, 37.9, 29.0, 26.7, 24.0, 22.5, 13.9; Molecular Weight $[M+H]^+$: 476.22 (expected), 476.3 (found); IR (cm^{-1}): 3040, 2957, 2931, 2860, 1599, 1589, 1547, 1489; $[\alpha]^{20}_D$= −29.1° (c= 1.00, $CHCl_3$); HPLC (OC column, 85:15 hex: EtOAc, 1 mL/min): 31.1 min, 33.7 min (major).

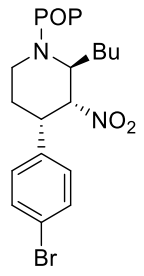

111

^{1}H NMR ($CDCl_3$, 400 MHz): 7.48 (d, *J*=8.2, 2H), 7.32-7.27 (m, 2H), 7.19 (d, *J*= 8.6, 2H), 7.04 (dd, *J*= 7.4, 7.4, 1H), 6.97-6.92 (m, 4H), 6.85 (d, *J*= 6.6, 1H), 4.88-4.86 (m, 1H), 4.48 (dd, *J*= 7.5, 7.5, 1H), 3.62 (dd, *J*=12.9, 4.3, 1H), 3.35-3.27 (m, 2H), 2.89 (qd, *J*= 12.9, 5.1, 1H), 1.94-1.88 (m, 1H), 1.85-1.72 (m, 2H), 1.41-1.27 (m, 4H), 0.92-0.89 (m, 3H); ^{13}C NMR ($CDCl_3$, 100 MHz): 158.4, 149.6, 146.5, 138.7, 131.7, 129.6, 129.1, 122.4, 121.2, 120.6, 118.4, 117.61, 87.6, 62.2, 41.9, 37.6, 29.0, 26.9, 23.9, 22.5, 13.9; Molecular Weight $[M+H]^+$: 509.1, 511.1 (expected), 509.2, 511.2 (found); IR (cm $^{-1}$): 3040, 2956, 2929, 2869, 2860, 1606, 1589, 1546, 1488, 1467; $[\alpha]^{20}_D$= +24.4° (c=1.00, $CHCl_3$); HPLC (IB column, 95:5 hex: EtOAc, 1 mL/min): 9.8 min (major), 11.1 min.

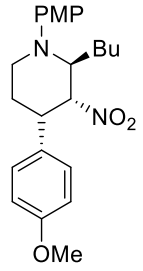

112

^{1}H NMR ($CDCl_3$, 400 MHz): 7.22 (d, *J*=8.8, 2H), 6.88 (d, *J*=8.8, 2H), 6.82-6.81 (m, 4H), 4.88-4.85 (m, 1H), 4.34 (dd, 7.1, 7.1, 1H), 3.79 (s, 3H), 3.77 (s, 3H), 3.52 (dd, 12.6, 3.6, 1H), 3.32-3.25 (m, 2H), 2.90 (qd, *J*= 12.9, 5.1, 1H), 1.92-1.85 (m, 1H), 1.79-1.70 (m, 2H), 1.40-1.26 (m, 4H), 0.91-0.86 (m, 3H); ^{13}C NMR ($CDCl_3$, 100 MHz): 158.6, 153.4, 144.3, 131.7, 128.4, 118.9, 114.5, 114.0, 88.1, 62.8, 55.6, 55.3, 42.4, 37.4, 29.1, 26.2, 24.4, 22.5, 13.9; Molecular Weight $[M+H]^+$: 399.23 (expected), 399.3 (found); IR (cm^{-1}): 3038, 2994, 2955, 2931, 2869, 2860, 1612, 1583, 1508, 1464; $[\alpha]^{20}_D$= −10.8° (c= 1.00, $CHCl_3$); HPLC (IC column, 85:15 hex: EtOAc, 1 mL/min): 13.7 min (major), 19.9 min.

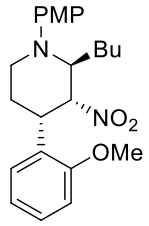

113

^{1}H NMR ($CDCl_3$, 400 MHz): 7.38 (d, *J*= 7.4, 1H), 7.25 (td, *J*= 7.3,1.6, 1H), 6.99 (t, *J*= 7.4, 1H), 6.88-6.80 (m, 5H), 5.16 (m, 1H), 4.38 (ddd, *J*= 9.8, 4.7, 1.6, 1H), 3.86 (s, 3H), 3.77 (s, 3H), 3.71 (ddd, *J*= 13.3, 3.7, 3.7, 1H), 3.48 (ddd, *J*=12.1, 4.7, 1.6, 1H), 3.31 (ddd, *J*= 12.1, 12.1, 3.1, 1H), 2.93 (qd, *J*= 12.9, 5.5, 1H), 1.94-1.84 (m, 1H), 1.79-1.75 (m, 1H), 1.42-1.29 (m, 4H), 0.91 (t, *J*= 6.9, 3H); ^{13}C NMR ($CDCl_3$, 100 MHz): 156.4, 153.4, 144.4, 128.8, 128.1, 127.6, 120.8, 119.1, 114.4, 109.8, 85.1, 63.1, 55.6, 55.2, 42.8, 32.0, 28.8, 25.4, 24.0, 22.5, 14.0; Molecular Weight $[M+H]^{+}$: 399.22 (expected), 399.3 (found); IR (cm^{-1}): 3040, 2954, 2932, 2868, 2835, 1601, 1584, 1545, 1510, 1492, 1464; $[\alpha]^{20}_{D}$= +14,2° (c= 1.00, $CHCl_3$); HPLC (IA column, 90:10 hex: EtOAc, 1 mL/min): 6.3 min, 7.5 min (major).

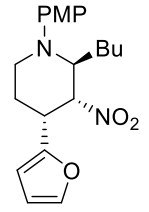

114

^{1}H NMR ($CDCl_3$, 400 MHz): 7.32 (d, *J*=1.6, 1H), 6.82-6.80 (m, 4H), 6.34 (dd, *J*=3.1, 1.9, 1H), 6.18 (d, *J*= 3.1, 1H), 5.07-5.05 (m, 1H), 4.39 (ddd, *J*= 7.2, 7.2,1.9, 1H), 3.76 (s, 3H), 3.44-3.39 (m, 2H), 3.27 (td, *J*= 12.1, 3.1, 1H), 2.66 (qd, *J*= 12.9, 5.5, 1H), 2.06-1.99 (m, 1H), 1.71-1.65 (m, 2H), 1.35-1.23 (m, 4H), 0.87-0.84 (m, 3H); ^{13}C NMR ($CDCl_3$, 100 MHz):153.8, 153.7, 144.19, 144.20, 119.3, 114.5, 110.6, 105.9, 84.4, 62.6, 55.6, 41.2, 32.9, 28.9, 25.9, 23.8, 22.4, 13.8; Molecular

Weight $[M+H]^+$: 359.2 (expected), 359.2 (found); IR (cm^{-1}): 3040, 2956, 2932, 2861, 2833, 1548, 1509, 1465; $[\alpha]^{20}_D = -36.6^o$ (c= 1.00, $CHCl_3$); HPLC (IB column, gradient elution: 100% H_2O at 0 min to 5% H_2O in MeCN at 28 min, 1 mL/min): 23.4 min, 24.4 min (major).

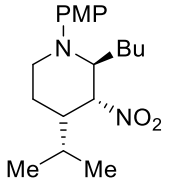

115

^1H NMR ($CDCl_3$, 400 MHz): 6.80-6.75 (m, 4H), 4.77-4.74 (m, 1H), 4.30 (ddd, *J*= 7.4, 7.4, 1.2, 1H), 3.75 (s, 3H), 3.34 (dd, *J*= 12.6, 4.7, 1H), 3.10 (ddd, *J*= 12.6, 12.6, 3.6, 1H), 2.16 (qd, *J*= 12.9, 5.5, 1H), 1.90-1.79 (m, 2H), 1.60-1.54 (m, 2H), 1.52-1.44 (m, 1H), 1.32-1.15 (m, 4H), 1.01 (d, *J*= 6.7, 3H), 0.96 (d, *J*= 6.6, 3H), 0.85-0.82 (m, 3H); ^{13}C NMR ($CDCl_3$, 100 MHz): 153.2, 144.4, 118.7, 114.4, 84.8, 62.9, 55.6, 42.2, 40.2, 29.1, 28.9, 25.8, 24.2, 22.4, 21.2, 20.5, 13.7; Molecular Weight $[M+H]^+$: 335.23 (expected), 335.3 (found); IR (cm^{-1}): 3039, 2958, 2933, 2870, 2833, 1545, 1509, 1455, 1442; $[\alpha]^{20}_D = -35.2^o$ (c= 1.00, $CHCl_3$); HPLC (IA column, 95:5 hex: EtOAc, 1 mL/min): 5.0 min, 5.4 min (major).

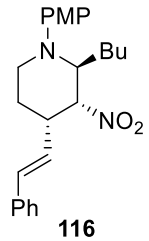

116

^1H NMR ($CDCl_3$, 400 MHz): 7.38-7.23 (m, 5H), 6.84-6.80 (m, 4H), 6.55 (d, *J*= 16.0, 1H), 6.39 (dd, *J*= 16.0, 7.4, 1H), 4.70-4.66 (m, 1H), 4.35 (td, *J*= 6.7, 1.6, 1H), 3.77 (s, 3H), 3.39-3.32 (m, 1H), 3.20 (td, *J*=12.1, 3.1, 1H), 2.95-2.87 (m, 1H), 2.49 (qd, *J*= 12.4, 5.1, 1H), 1.84-1.76 (m, 1H), 1.68-

1.63 (m, 2H), 1.35-1.22 (m, 4H), 0.85 (t, *J*= 6.9, 3H); ^{13}C NMR ($CDCl_3$, 100 MHz): 153.7, 144.3, 136.7, 132.2, 129.2, 128.6, 127.7, 126.3, 119.5, 114.5, 87.4, 62.5, 55.6, 42.4, 36.9, 28.7, 26.2, 26.1, 22.5, 13.9; Molecular Weight $[M+H]^+$: 395.23 (expected), 395.3 (found); IR (cm^{-1}): 3080, 3025, 2955, 2930, 2859, 2832. 1544, 1509, 1464; $[\alpha]^{20}_D$= –60.6.° (c= 1.00, $CHCl_3$); HPLC (IC column, 95:5 hex: EtOAc, 1 mL/min): 12.4 min (major), 23.0 min (major).

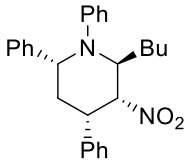

117

^{1}H NMR ($CDCl_3$, 400 MHz): 7.35-7.23 (m, 7H), 7.18 (t, *J*= 7.5, 2H), 7.12-7.05 (m, 3H), 6.85-6.81 (m, 3H), 5.12-5.07 (m, 1H), 4.34 (dt, *J*= 9.4, 3.5, 1H), 4.65 (dd, *J*= 11.3, 3.9, 1H), 3.54 (dt, *J*= 13.3, 3.9, 1H), 2.92 (q, *J*= 12.8, 1H), 2.21 (dt, *J*= 13.3, 4.0, 1H), 1.98-1.89 (m, 1H), 1.82-1.74 (m, 1H), 1.38-1.19 (m, 4H), 0.86 (t, *J*= 6.5, 3H); ^{13}C NMR ($CDCl_3$, 100 MHz): 148.8, 144.0, 139.5, 128.6, 128.3, 128.2, 127.3, 127.3, 127.2, 126.7, 125.3, 122.4, 87.9, 66.2, 57.7, 37.7, 35.3, 29.0, 24.7, 22.4, 13.8; Molecular Weight $[M+H]^+$: 415.24 (expected), 415.3 (found); IR (cm^{-1}): 3086, 3061, 3027, 3003, 2956, 2930, 2870, 1597, 1584, 1547, 1492, 1465, 1452; $[\alpha]^{20}_D$= –81.8° (c= 1.00, $CHCl_3$); HPLC (IB column, gradient elution: 100% H_2O at 0 min to 5% H_2O in MeCN at 58 min, 1 mL/min): 47.0 min, 47.4 min (major).

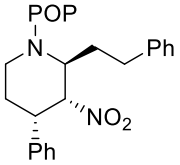

118

^{1}H NMR ($CDCl_3$, 400 MHz): 7.36-7.25 (m, 8H), 7.23-7.17 (m, 4H), 7.05 (t, *J*= 7.3, 1H), 6.96 (d, *J*= 7.8, 2H), 6.92 (d, *J*= 9.0, 2H), 6.78 (d, *J*= 9.0, 2H), 4.93-4.91 (m, 1H), 4.52 (t, *J*= 6.9, 1H), 3.68 (dd, *J*= 12.5, 3.5, 1H), 3.38-3.31 (m, 2H), 2.95 (qd, *J*= 12.9, 5.1, 1H), 2.80-2.67 (m, 2H), 2.23-2.09 (m, 2H), 1.97-1.91 (m, 1H);^{13}C NMR ($CDCl_3$, 100 MHz): 158.5, 149.5, 146.4, 140.5, 139.4, 129.6, 128.8, 128.6, 128.4, 127.31, 127.28, 126.5, 122.4, 120.6, 118.3, 117.6; Molecular Weight $[M+H]^+$: 479.23 (expected), 479.3 (found); IR (cm^{-1}): 3060, 3026, 2927, 2855, 1601, 1588, 1547, 1506, 1488; $[\alpha]^{20}_D$= −2.2° (c= 1.00, $CHCl_3$); HPLC (IA column, 99:1 hex: EtOAc, 1 mL/min): 27.8 min, 32.6 min (major).

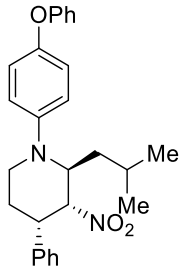

119

^{1}H NMR ($CDCl_3$, 400 MHz): 7.38-7.27 (m, 7H), 7.05 (t, *J*= 7.5, 1H), 6.98-6.94 (m, 4H), 6.87 (d, *J*= 9.0, 2H), 4.93-4.91 (m, 1H), 4.58-4.54 (m, 1H), 3.61 (dd, *J*= 12.5, 3.5, 1H), 3.41-3.28 (m, 2H), 2.96 (qd, *J*= 12.9, 5.5, 1H), 1.99-1.92 (m, 1H), 1.73-1.60 (m, 3H), 0.97-0.96 (m, 6H); ^{13}C NMR ($CDCl_3$, 100 MHz): 158.5, 149.5, 146.4, 139.6, 129.6, 128.6, 127.4, 127.3, 122.4, 120.6, 118.6, 117.6, 88.02, 60.3, 42.1, 37.9, 35.9, 25.4, 24.0, 23.2, 22.0; Molecular Weight $[M+H]^+$: 431.23 (expected), 431.3 (found); $[\alpha]^{20}_D$= −11.5° (c= 0.59, $CHCl_3$); IR (cm^{-1}): 3060, 3039, 2956, 2929, 2868, 1588, 1547, 1520, 1488, 1468, 1451; HPLC (IB column, gradient elution: 100% H_2O at 0 min to 5% H_2O in MeCN at 58 min, 1 mL/min): 48.1 min, 49.5 min (major).

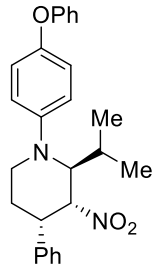

120

^{1}H NMR ($CDCl_3$, 400 MHz): 7.37-7.33 (m, 2H), 7.31-7.25 (m, 5H), 7.03 (dd, *J*= 7.5, 7.5, 1H), 6.96-6.89 (m, 4H), 6.80 (d, *J*= 9.0, 2H), 5.09-5.07 (m, 1H), 4.18 (d, *J*= 11.0, 1H), 3.87 (dd, *J*=13.7, 5.1, 1H), 3.42-3.34 (m, 2H), 2.98 (qd, *J*= 12.9, 5.1, 1H), 2.55-2.42 (m, 1H), 1.90-1.83 (m, 1H), 1.21 (d, *J*= 6.7, 3H), 0.96 (d, *J*= 6.6, 3H); ^{13}C ($CDCl_3$, 100 MHz): 158.7, 148.2, 147.7, 139.7, 129.5, 128.7, 127.4, 127.3, 122.1, 120.8, 117.4, 116.4, 86.5 67.7, 41.8, 38.7, 28.4, 23.2, 20.7, 20.6; Molecular Weight $[M+H]^+$: 417.22 (expected), 417.3 (found); IR (cm^{-1}): 3060, 3040, 2962, 2928, 2870, 1588, 1546, 1488; $[\alpha]^{20}_D$= +42.6° (c= 1.00, $CHCl_3$); HPLC (IB column, gradient elution: 100% H_2O at 0 min to 5% H_2O in MeCN at 28 min, 1 mL/min): 26.13 min, 26.8 min (major).

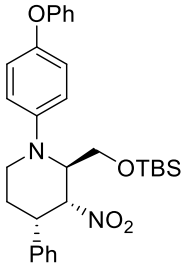

121

^{1}H NMR ($CDCl_3$, 400 MHz): 7.38-7.27 (m, 7H), 7.04 (t, *J*= 7.5, 1H), 6.98-6.89 (m, 5H), 5.39-5.36 (m, 1H), 4.57 (dd, *J*= 8.9, 5.0, 1H), 4.07 (dd, *J*= 10.0, 10.0, 1H), 3.88 (dd, *J*= 10.2, 5.1, 1H), 3.69 (ddd, *J*= 12.5, 4.7, 1.6, 1H), 3.48 (dt, *J*= 13.3, 5.5, 1H), 3.34 (td, *J*= 12.3, 3.1, 1H), 2.93 (qd, *J*= 13.1, 5.1, 1H), 1.98 (dd, *J*= 12.5, 2.3, 1H), 1.11-1.04 (m, 15H); ^{13}C NMR ($CDCl_3$, 100 MHz): 158.5, 149.5,

146.1, 139.6, 129.6, 128.7, 127.29, 127.25, 122.3, 120.8, 117.9, 117.5, 85.6, 62.5, 58.8, 43.6, 38.4, 23.8, 18.00, 17.98, 11.8; $[\alpha]^{20}_{D}$= +7.8° (c= 1.00, $CHCl_3$); HPLC (IC column, 88:12 hex: EtOAc, 1 mL/min): 5.5 min (major), 5.8 min.

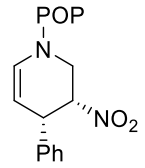

122

51 is unstable to be purified. Reductive workup with $ZnCl_2$, $NaCNBH_3$ and MeOH leads to decomposition.

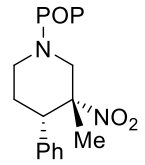

123

^{1}H NMR (C_6D_6, 400 MHz): 7.22 (d, *J*= 7.0, 2H), 7.15-7.12 (m, 2H), 7.08-7.04 (m, 3H), 6.99 (d, *J*= 7.8, 2H), 6.92 (d, *J*= 9.0, 2H), 6.83 (t, *J*= 7.3, 2H), 6.66 (d, *J*= 9.0, 2H), 3.88 (dd, *J*= 12.9, 1.5, 1H), 3.15-3.11 (m, 1H), 2.66 (qd, *J*= 12.7, 4.7, 1H), 2.27-2.21 (m, 3H), 1.41 (dq, *J*= 13.3, 3.2, 1H), 1.08 (s, 3H); ^{13}C NMR (C_6D_6, 100 MHz): 158.8, 150.8, 147.4, 138.5, 130.2, 129.6, 127.3, 122.3, 120.52, 120.51, 119.3, 117.7, 88.0, 62.4, 49.89, 49.88, 27.7, 23.6; Molecular Weight $[M+H]^+$: 389.2 (expected), 389.2 (found); IR (cm^{-1}): 3060, 3029, 2930, 2868, 1588, 1538, 1505, 1487, 1463, 1451; $[\alpha]^{20}_{D}$= +19.8° (c= 0.96, $CHCl_3$); HPLC (IB column, 98:2 hex: EtOAc, 1 mL/min): 13.3 min, 16.0 min (major).

A.1.7 Functionalization of Cycloadducts

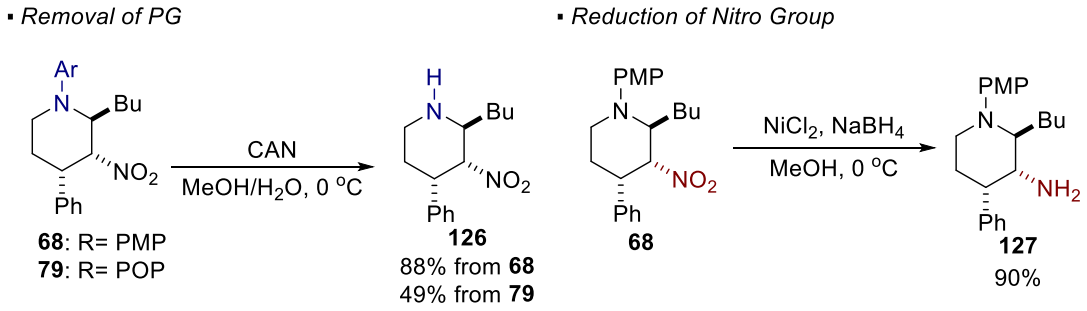

Removal of PG in **68**: To a solution of (2*R*,3*S*,4*R*)-2-butyl-1-(4-methoxyphenyl) -3-nitro-4-phenylpiperidine **68** (13.8 mg, 0.0375 mmol) in MeCN/H_2O (4:1, 0.95 mL) was added CAN (125.8 mg, 0.229 mmol, 6 equiv.) at 0 °C. The mixture was stirred at 0 °C for 3 h. The mixture was diluted with Et_2O and H_2O, and basified with solid K_2CO_3. The organic and aqueous layers were separated. The aqueous layer was extracted with EtOAc twice. The combined organic layer was dried over Na_2SO_4 and filtered. The solvent was removed under *vacco*. Flash chromatography (1:5:95 to 1:70:30 NEt_3:EtOAc:hexane) afforded (2R,3S,4R)-2-butyl-3-nitro-4-phenylpiperidine **126** (8.6 mg, 88%) as a yellow solid. ^{1}H NMR ($CDCl_3$, 400 MHz): 7.35-7.31 (m, 2H), 7.28-7.24 (m, 1H), 7.19 (d, *J*= 7.1, 2H), 4.69 (dd, *J*= 4.3, 0.8, 1H), 3.35-3.28 (m, 2H), 3.14 (ddd, *J*= 14.5, 4.7, 2.4, 1H), 2.96-2.89 (m, 1H), 2.49 (qd, *J*= 12.8, 4.7, 1H), 1.90-1.81 (m, 2H), 1.68 (dq, *J*= 13.3, 3.4, 1H), 1.64-1.52 (m, 2H), 1.45-1.36 (m, 3H), 0.96 (t, *J*= 7.1, 3H); ^{13}C NMR ($CDCl_3$, 100 MHz): 139.7, 128.8, 127.5, 127.3, 89.2, 56.2, 39.9, 39.4, 30.5, 29.0, 25.0, 22.5, 14.0; Molecular Weight $[M+H]^+$: 263.2 (expected), 263.2 (found); IR (cm^{-1}): 3086, 3061, 3028, 2954, 2931, 2869, 1541, 1495, 1465, 1452.

Removal of PG in **79**: To a solution of (2*R*,3*S*,4*R*)-2-butyl-3-nitro-1-(4-phenoxyphenyl) -4-phenylpiperidine **79** (19.2 mg, 0.0446 mmol) in MeCN/H_2O (4:1, 1.10 mL) was added CAN (146.7 mg, 0.2676 mmol, 6 equiv.) at 0 °C. The mixture was stirred at 0 °C for 2 h. The mixture was

diluted with Et_2O and H_2O, and basified with solid K_2CO_3. The organic and aqueous layers were separated. The aqueous layer was extracted with EtOAc twice. The combined organic layer was dried over Na_2SO_4 and filtered. The solvent was removed under *vacco*. Flash chromatography (1:5:95 to 1:50:50 NEt_3:EtOAc:hexane) afforded (2R,3S,4R)-2-butyl-3-nitro-4-phenylpiperidine **126** (5.7 mg, 49%) as a yellow solid.

Reduction of Nitro Group: To a solution of (2*R*,3*S*,4*R*)-2-butyl-1-(4-methoxyphenyl) -3-nitro-4-phenylpiperidine **68** (21.1 mg, 0.0573 mmol) in MeOH (1.35 mL) was added nickel(II) chloride hexahydrate (32.3 mg, 0.143 mmol, 2.5 equiv.) at 0 ^oC. $NaBH_4$ (33.9 mg, 0.946 mmol, 16.5 equiv.) was added in portions. The mixture was stirred at 0 ^oC for 60 mins. The mixture was quenched with H_2O and then 10% HCl. The mixture was neutralized with 2M NaOH. The aqueous layer was saturated with solid NaCl and extracted with EtOAc fourteen times. The combined organic layer was dried over Na_2SO_4 and filtered. The solvent was removed under *vacco*. Flash chromatography (1:5:95 to 1:50:50 NEt_3:EtOAc:hexane) afforded (2*R*,3*S*,4*R*)-2-butyl-1-(4-methoxyphenyl)-4-phenyl- piperidin-3-amine **127** (17.4 mg, 90%) as a yellow solid.

^1H NMR ($CDCl_3$, 400 MHz): 7.39-7.35 (d, 2H), 7.29-7.23 (m, 5H), 3.77 (s, 3H), 3.39-3.29 (m, 1H), 3.22-3.09 (m, 2H), 2.25 (qd, *J*= 12.8, 4.4, 1H), 1.82-1.70 (m, 2H), 1.65-1.50 (m, 2H), 1.35-1.20 (m, 4H), 0.85 (t, *J*= 6.8, 3H); ^{13}C NMR ($CDCl_3$, 100 MHz): 152.9, 145.7, 143.2, 128.6, 127.7, 126.4, 118.7, 114.4, 64.5, 55.6, 53.2, 42.7, 40.0, 29.4, 25.3, 23.2, 22.8, 14.0; Molecular Weight $[M+H]^+$: 339.24 (expected), 339.3 (found); IR (cm^{-1}): 3450, 3058, 3025, 2952, 2929, 2858, 1601, 1510, 1464.

A.1.8 Synthesis of New Ligands

General Procedure A for Sandmeyer reaction:

Anthranilic acid (1 equiv.) was dissolved in AcOH (0.6 mL per mmol of anthranilic acid), HBr (48% in H_2O, 0.4 mL per mmol of anthranilic acid) and H_2O (0.4 mL per mmol of anthranilic acid. The mixture was cooled with ice-water bath saturated with NaCl. $NaNO_2$ (1 equiv.) in H_2O (0.2 mL per mmol of $NaNO_2$) was added dropwise while cooling. After addition, the mixture was stirred at 0 ^oC for 2.5-3 h. While the resulting diazonium salt was still at 0 ^oC, it was added to CuBr (1 equiv.) in HBr (48% in H_2O, 0.5 mL per mmol of CuBr) at rt. The mixture was stirred at 65 ^oC for 2.5-3 h. The mixture was diluted with H_2O and extracted with EtOAc three times. The organic layer was washed with H_2O several times until no more precipitate was formed when H_2O was added. The organic layer was washed with brine, dried over Na_2SO_4, filtered. The solvent was removed under vacco. 2-bromobenzoic acid was obtained as a white or pale yellow solid. The product was analytically pure and used without further purification.

General Procedure B for Ullmann Coupling:

2-bromobenzoic acid (1 equiv.), anthranilic acid (1.1 equiv.), copper powder (0.2 equiv.), Cu_2O (0.1 equiv.), K_2CO_3 (3 equiv.) in DMF (1.50 mL per mmol of 2-bromobenzoic acid) was refluxed overnight. The reaction mixture was cool to rt. H_2O was added to dissolve the product. Copper powder and copper salt were removed by filtration through celite. The filtrate was acidified by conc. HCl until pH <3. The mixture was filtered and the solid was collected and dried under vacuum. The product obtained was usually pure and used without further purification.

General Procedure C1 for the Formation of Bis(hydroxy-amide):

Dibenzoic acid (1 equiv.) in $SOCl_2$ (1.48 mL per mmol of dibenzoic acid) was refluxed for 3-5 h. The excess $SOCl_2$ was removed under vacco. The resulting di(acid chloride) was dissolved in DCM (8.7 mL per mmol of dibenzoic acid). (If the di(acid) was not completely dissolved, more DCM was added.) This solution was added to a solution of amino alcohol (2-2.2 equiv.), NEt_3 (2 equiv.) in DCM (1.4mL per mmol of amino alcohol) at 0 ^{0}C. The reaction mixture was stirred at rt overnight. Sat. NH_4Cl solution was added. The organic layer was washed with 1M HCl, sat. $NaHCO_3$, H_2O and brine. The organic layer was dried over Na_2SO_4 and filtered. The solvent was removed under vacco. Bis(hydroxy-amide) was obtained was a solid.

General Procedure C2 for the Formation of Bis(hydroxy-amide):

To a solution of amino alcohol (2.2 equiv.), EDCl hydrochloride salt (2.3 equiv.), HOBt (2.3 equiv.) in DCM (23 mL per mmol of dibenzoic acid) was added dibenzoic acid (1 equiv.). The reaction mixture was stirred at rt for 2 overnights. The reaction mixture was quenched with H_2O. The organic layer was washed with 1M NaOH and brine. The organic layer was dried over Na_2SO_4 and filtered. The solvent was removed under vacco. Flash chromatography afforded bis(hydroxy-amide) as a while or yellow solid.

General Procedure D for the Formation of Bisoxazolines:

To a solution of hydroxy-amide (1 equiv.), NEt_3 (8 equiv.), either DMAP or 4-pyrrolidinopyridine (10 mol %) in DCM (13.9 mL per mmol of bis(hydroxy-amide)) was added a solution of TsCl (2-2.2 equiv.) in DCM (2.3 mL per mmol of TsCl) at 0 ^{o}C. The reaction mixture was

stirred at rt for at least two overnights. The reaction was quenched with sat. NH_4Cl. The organic layer was washed with H_2O and brine, and was dried over Na_2SO_4 and filtered. The solvent was removed under vacco. Flash chromatography afforded bisoxazoline as a while or yellow solid.

General Procedure E for Esterification of Dibenzoic acids:

To a solution of dibenzoic acid in MeOH (2.65 mL per mmol of dibenzoic acid) was added conc. H_2SO_4 (0.265 mL per mmol of dibenzoic acid) dropwise. The reaction mixture was reflux overnight. The solvent was removed under *vacco*. H_2O was added. Solid Na_2CO_3 was added until no more gas bubbles were observed. The mixture was extracted with EtOAc three times. The organic layer was washed with brine, dried over Na_2SO_4 and filtered. The solvent was removed under vacco to afford diester as a solid. The product was analytically pure and used without further purification.

*Synthesis of Ligand **L15**:*

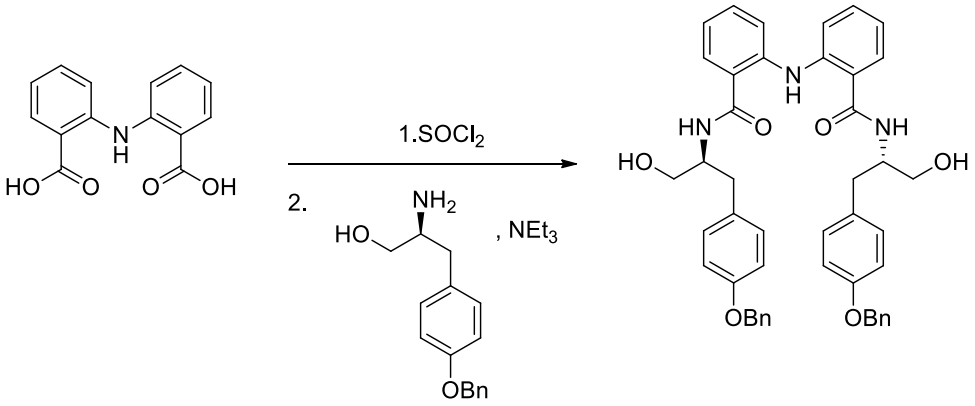

General Procedure C1: 2,2'-azanediyldibenzoic acid (0.75 g) afforded 2,2'-azanediylbis(N-((S)-1-(4-(benzyloxy)phenyl)-3-hydroxypropan-2-yl)benzamide) (2.20 g) in 100% yield. It was used without further purification.

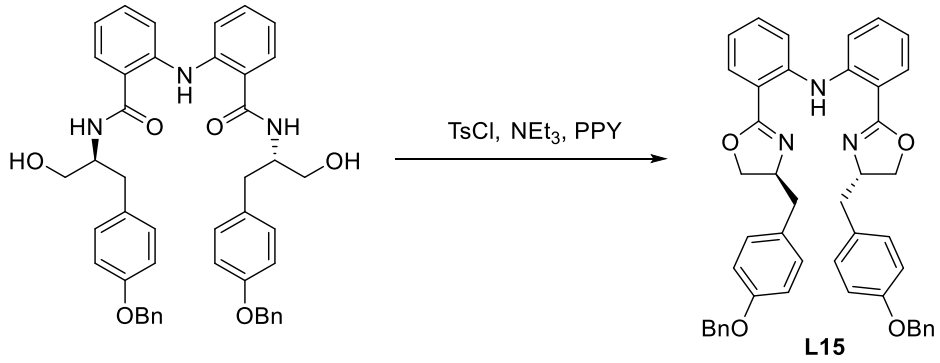

General Procedure D with 4-pyrrolidinopyridine: 2,2'-azanediylbis(N-((S)-1-(4-(benzyloxy)phenyl)-3-hydroxypropan-2-yl)benzamide) (150.0 mg) afforded bis(2-((S)-4-(4-(benzyloxy)benzyl)-4,5-dihydrooxazol-2-yl) phenyl)amine **L15** (86.4 mg, 61%). Flash chromatography: 1:20:80- 1:80:20 NEt_3: EtOAc: hexane. ^1H NMR ($CDCl_3$, 400 MHz): 10.98 (br, 1H), 7.82 (dd, *J*= 7.9, 1.6, 2H), 7.48 (d, *J*= 8.6, 2H), 7.42-7.28 (m, 12H), 7.09 (d, *J*= 8.2, 4H), 6.90 (t, *J*= 7.5, 2H), 6.81 (d, *J*= 8.2, 4H), 4.99 (s, 4H), 4.45-4.37 (m, 2H), 4.23 (t, *J*= 8.6, 2H), 3.96 (t, *J*= 7.9, 2H), 3.05 (dd, *J*= 13.7, 5.9, 2H), 2.68 (dd, *J*= 13.7, 7.8, 2H); ^{13}C NMR ($CDCl_3$, 100 MHz): 162.9, 157.4, 143.2, 137.1, 131.3, 130.5, 130.4, 130.3, 128.5, 127.9, 127.5, 119.7, 118.1, 115.7, 114.7, 110.0, 70.6, 69.9, 68.3, 40.9; Molecular Weight $[M+H]^+$: 700.3 (expected), 700.4 (found); IR (cm^{-1}): 3028, 2892, 1640, 1608, 1580, 1510, 1457; $[\alpha]^{20}_D$= +14.4° (c= 0.25, $CHCl_3$).

*Synthesis of Ligand **L17:***

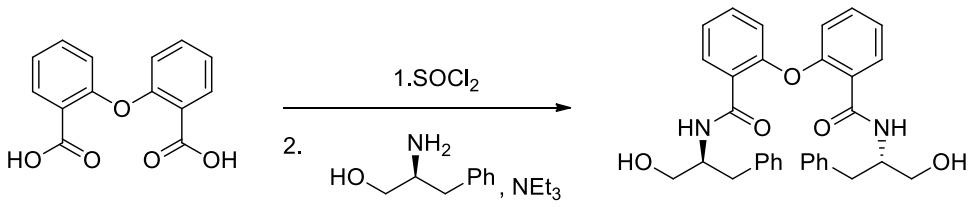

General Procedure C1: 2,2'-oxydibenzoic acid[10] (1.08 g) afforded 2,2'-oxybis(N-((S)-1-hydroxy-3-phenylpropan-2-yl)benzamide) (2.03 g) in 93% yield. It was used without further purification.

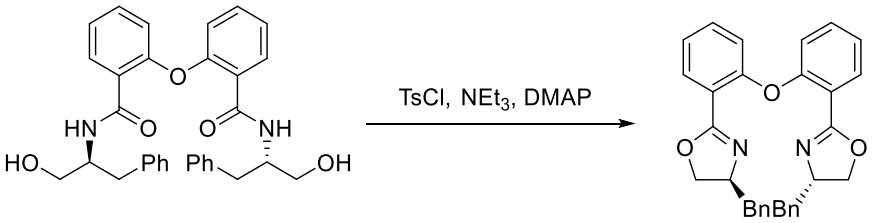

L17

General Procedure D with DMAP: 2,2'-oxybis(*N*-((*S*)-1-hydroxy-3-phenylpropan-2-yl)benzamide) (1.70 g) afforded (4*S*,4'*S*)-2,2'-(oxybis(2,1-phenylene))bis(4-benzyl- 4,5-dihydrooxazole) **L17** (1.46 g, 92%). Flash chromatography: 1:30:70- 1:70:30 NEt_3: EtOAc: hexane. ^1H NMR ($CDCl_3$, 400 MHz): 7.85 (dd, *J*= 7.8, 1.6, 2H), 7.39 (td, *J*= 7.8, 1.9, 2H), 7.28-7.24 (m, 4H), 7.21-7.13 (m, 8H), 6.94 (d, *J*= 8.3, 2H), 4.50-4.43 (m, 2H), 4.19 (t, *J*= 9.0, 2H), 3.99 (dd, *J*= 7.8, 7.8, 2H), 3.11 (dd, *J*= 13.7, 5.1, 2H), 2.55 (dd, *J*= 13.7, 8.6, 2H); ^{13}C NMR ($CDCl_3$, 100 MHz): 162.7, 155.7, 138.1, 132.2, 131.4, 129.3, 128.4, 126.4, 123.2, 120.2, 119.7, 71.8, 67.6, 41.7; Molecular Weight $[M+H]^+$: 489.2 (expected), 489.3 (found); IR (cm^{-1}): 3061, 3026, 3000, 2922, 2898, 2855, 1640, 1602, 1581, 1485, 1474, 1464, 1448; $[\alpha]^{20}_D$= –41.0° (c= 0.68, $CHCl_3$).

*Synthesis of Ligand **L18:***

To a solution of dimethyl 2,2'-azanediyldibenzoate[11] (5.24 g, 1 equiv.) in DMF (154 mL) was added NaH (2.35 g, 60% in mineral oil, 3.2 equiv.) in portions. MeI (6.85 mL, 6 equiv.) was

added dropwise. The mixture was stirred at rt overnight. An additional NaH (0.73 gm 60% in mineral oil, 1 equiv.), followed by MeI (2.3 mL, 2 equiv.), was added. The mixture was stirred for 2 h. The reaction was quenched with H_2O. The mixture was extracted with EtOAc three times. The organic layer was washed with H_2O several until no DMF remained in the organic layer. The organic layer was washed with brine twice, dried over Na_2SO_4 and filtered. The solvent was removed under *vacco*. The crude product was dissolved in EtOH (91.8 mL). A solution of KOH (4.12 g, 4 equiv.) was added. The mixture was refluxed overnight. The mixture was cooled to 0 ^oC and acidified with 2M HCl. EtOH was removed under *vacco*. The mixture was extracted with EtOAc five times. The organic layer was washed with H_2O, dried over Na_2SO_4 and filtered. The solvent was removed under *vacco* to afford 2,2'-(methylazanediyl)dibenzoic acid (4.98 g, 100%) as a pale brown solid. It was used without further purification.

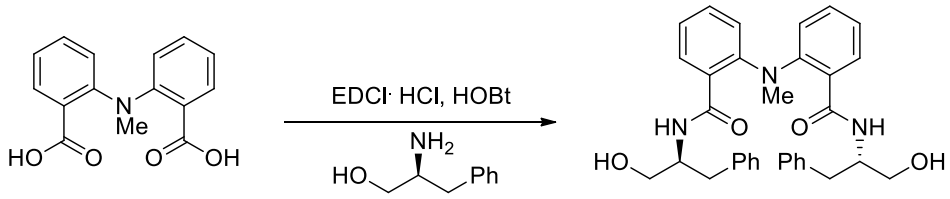

General Procedure C2: 2,2'-(methylazanediyl)dibenzoic acid (1.0065 g) afforded 2,2'-(methylazanediyl)bis(N-((*S*)-1-hydroxy-3-phenylpropan-2-yl)benzamide) (0.8188 g) in 41% yield. Flash chromatography: EtOAc-2% MeOH/DCM. ^1H NMR (DMSO, 400 MHz): 7.58 (br, 2H), 7.38 (d, *J*= 7.4, 2H), 7.30 (td, *J*= 7.8, 1.5, 2H), 7.24-7.16 (m, 10H), 7.03 (t, *J*= 7.5, 2H), 6.88 (d, *J*= 8.2, 2H), 4.22-4.13 (m, 2H), 3.39 (s, 3H), 3.05-2.72 (m, 10H); ^{13}C NMR ($CDCl_3$, 100 MHz): 168.7, 147.9, 138.0, 131.2, 130.01, 129.99, 129.2, 128.5, 126.4, 123.1, 122.0, 63.76, 53.2, 42.2, 36.7;; Molecular

Weight $[M+Na]^+$: 560.3 (expected), 560.4 (found); IR (cm^{-1}): 3399 (br), 3260 (br), 3064, 3028, 2930, 2877, 1620, 1596, 1562, 1545, 1495; $[\alpha]^{20}_D$= –37.6° (c= 1.00, $CHCl_3$).

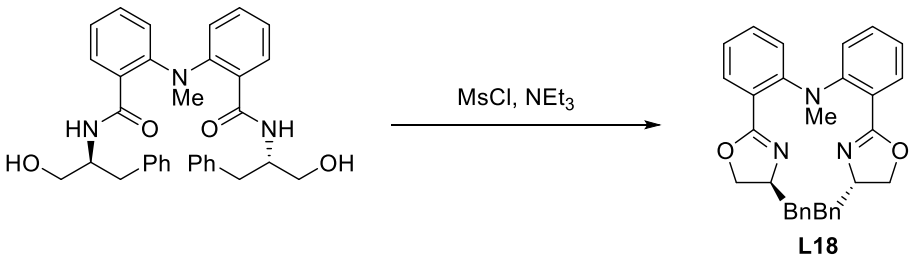

L18

To a solution of 2,2'-(methylazanediyl)bis(N-((*S*)-1-hydroxy-3-phenylpropan-2-yl) benzamide) (148.5 mg, 1 equiv.), NEt_3 (0.175 mL, 4.4 equiv.) in DCM (3 mL) was added MsCl (0.048 mL, 2.2 equiv.) dropwise at 0 °C. The mixture was stirred at rt for 2 overnights. The mixture was quenched with sat. NH_4Cl. The organic layer was washed with sat. $NaHCO_3$ and brine, dried over Na_2SO_4 and filtered. The solvent was removed under *vacco*. Flash chromatography (1:30:70-1:70:30 NEt_3: EtOAc: hexane) afforded 2-((S)-4-benzyl-4,5-dihydrooxazol-2-yl)-N-(2-((S)-4-benzyl-4,5- dihydrooxazol -2-yl)phenyl)-N-methylaniline **L18** (108.0 mg, 78%) as a pale yellow solid.

^1H NMR ($CDCl_3$, 400 MHz): 7.59 (dd, *J*= 7.9, 1.6, 2H), 7.39 (td, *J*= 7.9, 1.6, 2H), 7.28-7.24 (m, 4H), 7.20-7.17 (m, 2H), 7.16-7.11 (m, 6H), 7.02 (t, *J*= 7.7, 2H), 4.22-4.14 (m, 2H), 3.88 (t, *J*= 9.0, 2H), 3.72 (t, *J*= 8.0, 2H), 3.31 (s, 3H), 2.99 (dd, *J*= 13.7, 4.7, 2H), 2.33 (dd, *J*= 13.7, 9.0, 2H); ^{13}C NMR ($CDCl_3$, 100 MHz): 164.3, 148.6, 138.2, 131.8, 131.3, 129.2, 128.4, 126.3, 123.1, 121.9, 121.7, 71.3, 67.1, 42.7, 41.4; Molecular Weight $[M+H]^+$: 502.3 (expected), 502.3 (found); IR (cm^{-1}): 3060, 3026, 2956, 2893, 2810, 1649, 1595, 1571, 1485, 1463; $[\alpha]^{20}_D$= +10.4° (c= 0.81, $CHCl_3$).

*Synthesis of Ligand **L19***

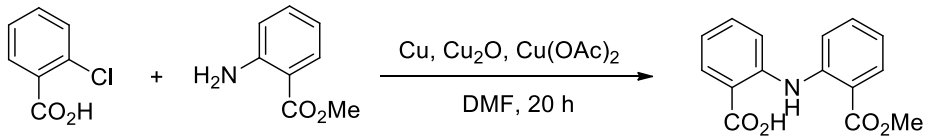

A solution of 2-chlorobenzoic acid (4.04 g, 1 equiv.), methyl 2-aminobenzoate (4.3 mL, 1.32 equiv.), Cu (190 mg, 12 mol %), Cu_2O (140 mg, 4 mol %) and $Cu(OAc)_2$ (360 mg, 8 mol %) in DMF (120 mL) was refluxed for 20 h. After cooling to rt, the mixture was filtered through a short pad of silica gel. The silica gel was washed with EtOAc. EtOAc in the filtrate was removed under *vacco*. 0.1M HCl (120 mL) was added. The mixture was diluted with H_2O until no more solid was formed. The mixture was filtered. The solid was washed with H_2O and dried under vacuum. The solid was re-dissolved in EtOAc. The organic layer was washed with 1M HCl, H_2O and brine, dried over Na_2SO_4, and filtered. The solvent was removed under *vacco*. Flash chromatography (5% EtOAc/hex- 1% NEt_3/EtOAc) afforded 2-((2-(methoxycarbonyl)phenyl)amino) benzoic acid[12] (1.60 g, 23%).

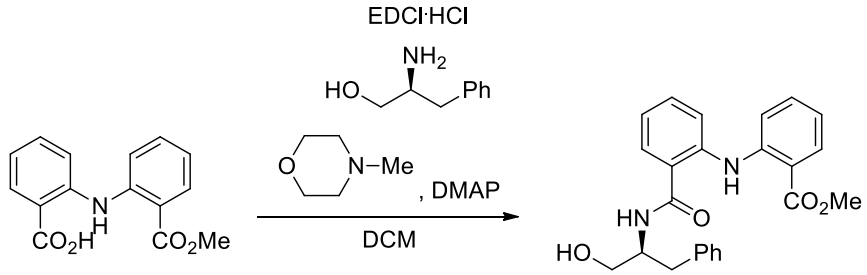

To a solution of 2-((2-(methoxycarbonyl)phenyl)amino)benzoic acid (298.4 mg, 1 equiv.), EDCI·HCl (244 mg, 1.15 equiv.), DMAP (6.8 mg, 5 mol %) in DCM (19.4 mL) was added *N*-methylmorpholine (0.2 mL, 1.65 equiv.). (*S*)- phenylalaninol (192 mg, 1.15 equiv.) was added. The

mixture was stirred at rt for 2 days. The mixture was quenched with sat. NH_4Cl, washed with 1M HCl, sat. $NaHCO_3$ and brine, dried over Na_2SO_4 and filtered. The solvent was removed under *vacco*. Flash chromatography (1:50:50-1:85:15 NEt_3:EtOAc:hexane) afforded (S)-methyl 2-((2-((1-hydroxy-3-phenylpropan-2-yl) arbamoyl)phenyl)amino)benzoate as a solid (282.5 mg, 63%). ^1H NMR ($CDCl_3$, 400 MHz): 10.15 (br, 1H), 7.98 (dd, *J*= 7.8, 1.5, 1H), 7.55 (dd, *J*= 7.4, 1.6, 1H), 7.41 (d, *J*= 7.8, 1H), 7.36-7.31 (m, 2H), 7.25-7.15 (m, 5H), 7.01 (t, *J*= 7.1, 1H), 6.86-6.80 (m, 2H), 4.41-4.34 (m, 1H), 3.93 (s, 3H), 3.69 (d, *J*= 11.0, 1H), 3.58 (dd, *J*= 10.6, 2.7, 1H), 2.88 (dd, *J*= 7.4, 2.7, 2H), 2.60 (br, 1H); ^{13}C NMR ($CDCl_3$, 100 MHz): 168.3, 168.1, 146.2, 140.2, 137.6, 133.8, 131.7, 131.6, 129.2, 129.1, 128.6, 126.8, 126.6, 122.7, 121.6, 118.9, 116.0, 114.9, 64.0, 52.9, 52.1, 36.9; Molecular Weight $[M+Na]^+$: 427.2 (expected), 427.2 (found); $[\alpha]^{20}_D$= −325.6° (c= 1.00, $CHCl_3$); IR (cm^{-1}): 3303 (br), 3062, 3027, 3002, 2949, 2877, 1694, 1650, 1634, 1594, 1578, 1509, 1482, 1446.

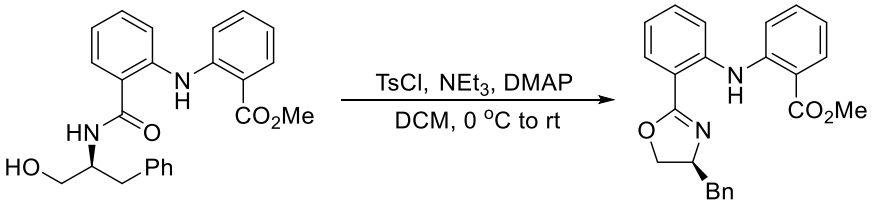

L19

To a solution of (*S*)-methyl 2-((2-((1-hydroxy-3-phenylpropan-2-yl)carbamoyl)phenyl) amino)benzoate (208.6 mg, 1 equiv.), NEt_3 (0.29 mL, 4 equiv.), DMAP (3.2 mg, 5 mol %) in DCM (7mL) was added a solution of TsCl (108.2 mg, 2 equiv.) in DCM (2 mL) at 0 °C. The reaction mixture was stirred at rt for two overnights. The reaction was quenched with sat. NH_4Cl. The organic layer was washed with H_2O and brine, and was dried over Na_2SO_4 and filtered. The solvent was removed under vacco. Flash chromatography (1:10:90 to 1:15:85 NEt_3/EtOAc/Hexane) afforded (S)-methyl 2-((2-(4-benzyl-4,5-dihydrooxazol-2-yl)phenyl)amino)benzoate **L19** as a solid

(167.8 mg, 84%). ^{1}H NMR ($CDCl_3$, 400 MHz): 11.04 (br, 1H), 8.00 (dd, *J*= 7.8, 1.5, 1H), 7.81 (dd, *J*= 7.8, 1.5, 1H), 7.56 (d, *J*= 8.2, 1H), 7.47 (d, *J*= 8.2, 1H), 7.38 (td, *J*= 7.8, 1.6, 1H), 7.31-7.18 (m, 6H), 6.94 (t, *J*=7.6, 1H), 6.87 (t, *J*= 7.7, 1H), 4.74-4.67 (m, 1H), 4.32 (t, *I*= 8.8, 1H), 4.08 (t, *J*= 7.8, 1H), 3.82 (s, 3H), 3.22 (dd, *J*= 14.1, 5.8, 1H), 2.82 (dd, *J*= 13.6, 8.2, 1H); ^{13}C NMR ($CDCl_3$, 100 MHz): 167.2, 163.1, 144.0, 143.3, 138.1, 133.0, 131.9, 131.4, 130.3, 129.3, 128.4, 126.4, 120.2, 119.3, 119.1, 118.7, 116.8, 114.4, 70.5, 68.3, 51.8, 41.9; Molecular Weight $[M+H]^+$: 387.2 (expected), 387.2 (found); IR (cm^{-1}): 3177 (br), 3061, 3026, 2949, 2898, 2842, 1709, 1637, 1604, 1580, 1518, 1453; $[\alpha]^{20}_D$= +51.6° (c= 0.55, $CHCl_3$).

*Synthesis of Ligand **L21**:*

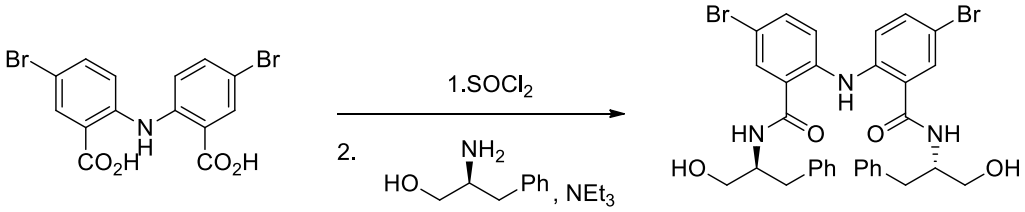

General Procedure C1: 6,6'-azanediylbis(3-bromobenzoic acid)[9] (1.07 g) afforded 6,6'-azanediylbis(N-((S)-1-hydroxy-3-phenylpropan-2-yl)-3-bromobenzamide) as a red solid (1.76 g) in 100% yield. It was used without further purification.

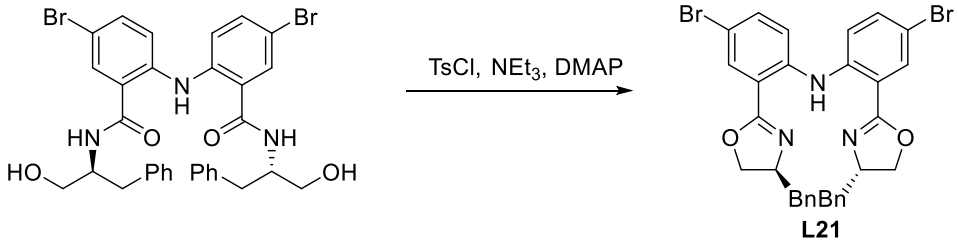

L21

General Procedure D with DMAP: 6,6'-azanediylbis(N-((S)-1-hydroxy-3- phenylpropan-2-yl)-3-bromobenzamide) (249.2 mg) afforded bis(2-((S)-4- benzyl-4,5-dihydrooxazol-2-yl)-3-

bromophenyl)amine **L21** (186.9 mg) in 79% yield. Flash chromatography: 1:20:80 NEt_3: EtOAc: hexane. ^1H NMR ($CDCl_3$, 400 MHz): 11.01 (br, 1H), 7.95 (d, *J*= 2.4, 2H), 7.39 (d, *J*= 8.6, 2.4, 2H), 7.31 (d, *J*= 9.0, 2H), 7.24-7.15 (m, 10H), 4.45-4.38 (m, 2H), 4.24 (t, *J*= 8.8, 2H), 3.98 (t, *J*= 7.9, 2H), 3.10 (dd, *J*= 13.7, 5.9, 2H), 2.73 (d, *J*= 13.7, 7.9, 2H); ^{13}C NMR ($CDCl_3$, 100 MHz): 161.7, 141.8, 137.8, 134.1, 132.9, 129.3, 128.4, 126.4, 119.6, 117.4, 111.8, 70.8, 68.3, 41.7; Molecular Weight $[M+H]^+$: 646.05 (expected), 646.2 (found); IR (cm^{-1}): 3132, 3083, 3061, 3026, 3000, 2959, 2896, 1641, 1596, 1574, 1502, 1454, 1473; $[\alpha]^{20}_D$= +42.8° (c= 1.00, $CHCl_3$).

*Synthesis of Ligand **L23**:*

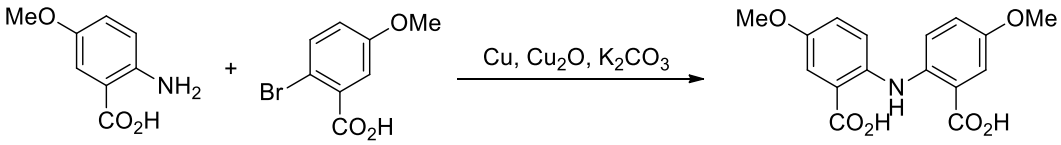

General Procedure B: 2-bromo-5-methoxybenzoic acid (2.01 g) afforded 6,6'-azanediylbis(3-methoxybenzoic acid) (2.38 g) as a green solid in 86% yield. ^1H NMR (DMSO, 400 MHz): 13.00 (br, 2H), 10.27 (br, 1H), 7.36 (d, *J*= 2.7, 2H), 7.26 (d, *J*= 9, 2H); 7.05 (dd, *J*= 9.0, 2.7, 2H), 3.73 (s, 6H); ^{13}C NMR (DMSO, 100 MHz): 168.6, 152.5, 138.6, 121.0, 119.6, 118.6, 115.2, 55.9; Molecular Weight $[M-H]^-$: 316.1 (expected), 316.1 (found); IR (cm^{-1}): 3417, 3358, 1673, 1619, 1597, 1566, 1525, 1461.

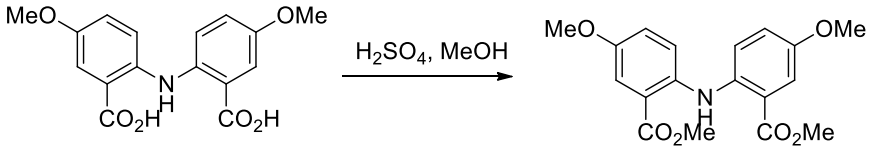

General Procedure E: 6,6'-azanediylbis(3-methoxybenzoic acid) (0.3047 g) afforded dimethyl 6,6'-azanediylbis(3-methoxybenzoate) (0.3182 g) as a brown solid in 96% yield. ^1H NMR

($CDCl_3$, 400 MHz): 10.48 (br, 1H), 7.46 (d, *J*= 2.8, 2H), 7.36 (d, *J*= 9.0, 2H), 6.98 (dd, *J*= 9.4, 2.8, 2H), 3.93 (s, 6H), 3.80 (s, 6H); ^{13}C NMR ($CDCl_3$, 100 MHz):167.5, 152.5, 138.9, 121.2, 119.1, 117.2, 114.5, 55.7, 52.1; Molecular Weight $[M+H]^+$: 346.13 (expected), 346.2 (found); IR (cm^{-1}):3329, 2998, 2950, 2909, 2834, 1699, 1614, 1586, 1570, 1508.

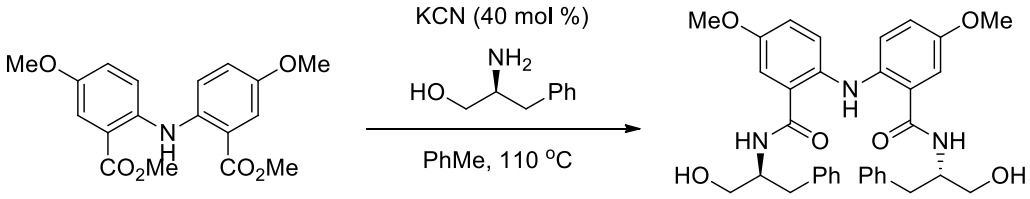

A solution of dimethyl 6,6'-azanediylbis(3-methoxybenzoate) (257.0 mg, 1 equiv.), (*S*)-phenylalaninol (318.4 mg, 2.6 equiv.), KCN (21.1 mg, 40 mol %) in PhMe (2.5 mL) was refluxed overnight. After cooling to rt, H_2O was added. The mixture was extract with DCM three times. The organic layer was washed with H_2O and brine. The organic layer was dried over Na_2SO_4 and filtered. The solvent was removed under vacco. The mixture was re-dissolved in DCM and washed with 1M HCl, sat. $NaHCO_3$, H_2O and brine. The organic layer was dried over Na_2SO_4 and filtered. The solvent was removed under vacco to afford 6,6'-azanediylbis(N-((S)-1-hydroxy-3-phenyl propan-2-yl)-3-methoxybenzamide) as a yellow solid (318.8 mg, 67%). It was used without further purification.

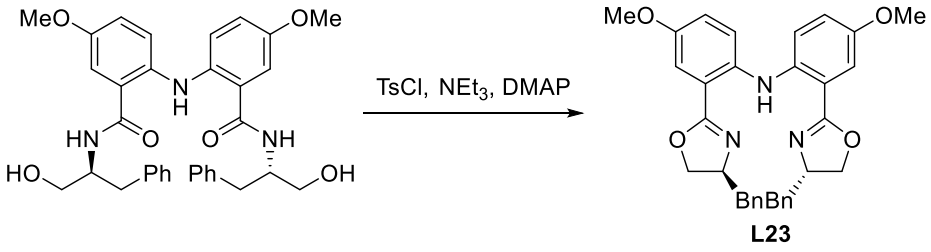

General Procedure D with DMAP 6,6'-azanediylbis(N-((*S*)-1-hydroxy-3- phenylpropan-2-yl)-3-methoxybenzamide) (291.0 mg) afforded bis(2-((*S*)-4-benzyl-4,5-dihydrooxazol-2-yl)-4-methoxyphenyl) amine **L23** (242.7 mg) in 89% yield. Flash chromatography: 1:20:80- 1:70:30 NEt_3: EtOAc: hexane. ^1H NMR ($CDCl_3$, 400 MHz): 10.34 (br, 1H), 7.33 (d, *J*= 3.2, 2H), 7.29 (d, *J*= 9.0, 2H), 7.25-7.16 (m, 10 H), 6.92 (dd, *J*= 9.0, 2.8, 2H), 4.56-4.48 (m, 2H), 4.22 (t, *J*= 8.9, 2H), 3.99 (t, *J*= 8.0, 2H), 3.81 (s, 6H), 3.18 (dd, *J*= 13.7, 5.5, 2H); 2.71 (dd, *J*= 14.1, 8.6, 2H); ^{13}C NMR ($CDCl_3$, 100 MHz): 163.1, 152.7, 138.1, 137.9, 129.3, 128.4, 126.4, 119.9, 119.1, 116.1, 133.6, 70.7, 68.1, 55.8, 41.8; Molecular Weight $[M+H]^+$: 548.3 (expected), 548.3 (found); IR (cm^{-1}): 3300 (br), 3084, 3060, 3026, 2998, 2931, 2899, 2834, 1642, 1606, 1512, 1463, 1455; $[\alpha]^{20}_D$= +53.0° (c= 0.56, $CHCl_3$).

*Synthesis of Ligand **L25**:*

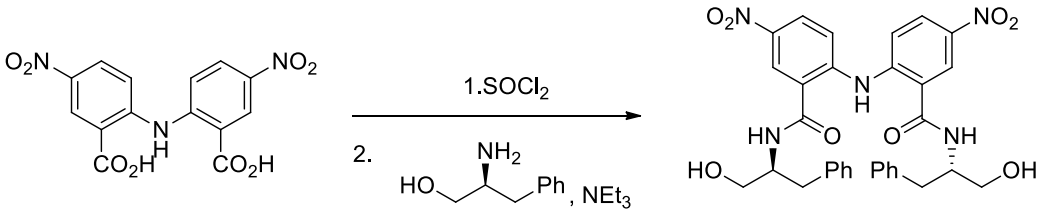

General Procedure C1: 6,6'-azanediylbis(3-nitrobenzoic acid[9] (504.0 mg) afforded 6,6'-azanediylbis(N-((S)-1-hydroxy-3-phenylpropan-2-yl)-4-nitrobenzamide) as a red solid (435.9 mg) in 49% yield. It was used without further purification.

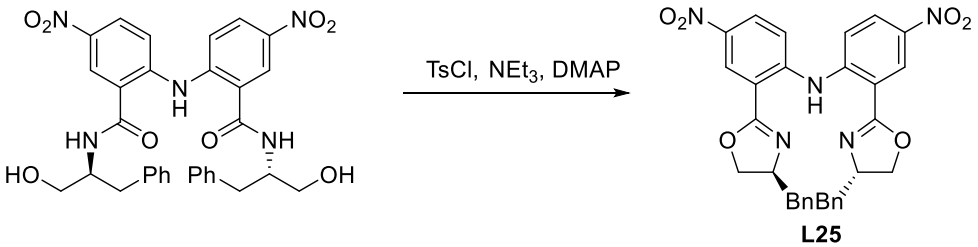

L25

General Procedure D with DMAP: 6,6'-azanediylbis(N-((S)-1-hydroxy-3- phenylpropan-2-yl)-3-nitrobenzamide) (228.9 mg) afforded bis(2-((S)-4- benzyl-4,5-dihydrooxazol-2-yl)-3-nitrophenyl)amine **L25** (169.1 mg) in 78% yield. Flash chromatography: 1:20:80- 1:60:40 NEt_3: EtOAc: hexane. ^1H NMR ($CDCl_3$, 400 MHz): 12.45 (s, 1H), 8.80 (d, *J*= 2.7, 2H), 8.24 (dd, *J*= 9.4, 2.7, 2H), 7.62 (d, *J*= 9.4, 2H), 7.19-7.15 (m, 6H), 7.12-7.10 (m, 4H), 4.31 (dd, *J*= 8.8, 8.8, 2H), 4.21-4.13 (m, 2H), 4.00 (dd, *J*= 8.0, 8.0, 2H), 2.94 (dd, *J*= 13.7, 7.0, 2H), 2.75 (dd, *J*= 13.7, 6.7, 2H); ^{13}C NMR ($CDCl_3$, 100 MHz): 160.5, 146.7, 141.0, 137.8, 129.3, 128.2, 126.9, 126.7, 126.5, 117.8, 116.0, 71.1, 68.8, 41.8; Molecular Weight $[M+H]^+$: 578.20 (expected), 578.3 (found); IR (cm^{-1}): 3086, 3061, 3026, 2917, 1647, 1615, 1574, 1541, 1513, 1501, 1473, 1463, 1454; $[\alpha]^{20}_D$= –319.2° (c= 1.00, $CHCl_3$).

*Synthesis of Ligand **L26**:*

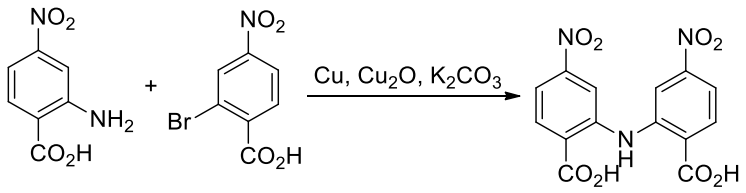

General Procedure B: 2-bromo-4-nitrobenzoic acid (1.42 g) afforded 6,6'-azanediylbis(4-nitrobenzoic acid) (0.87 g) in 43% yield. ^1H NMR (400 MHz, DMSO): 8.25 (d, *J*= 2.4, 2H), 8.14 (d, *J*= 8.8, 2H), 7.77 (dd, *J*= 8.8, 2.3, 2H); ^{13}C NMR (100 MHz, DMSO): 167.6, 150.8, 143.8, 133.9, 115.39, 115.38, 112.3; Molecular Weight $[M-H]^-$: 346.0 (expected), 346.0 (found); IR (cm^{-1}): 3250, 3127, 1672, 1587.

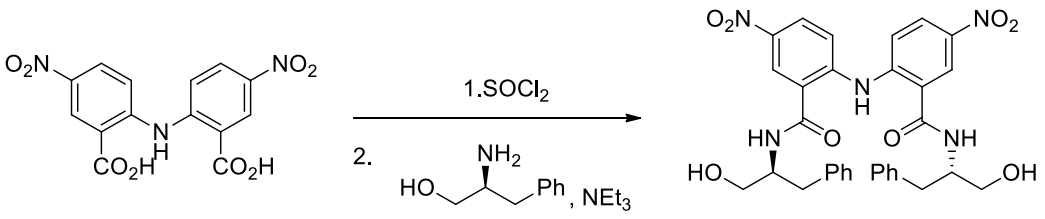

General Procedure C1: 6,6'-azanediylbis(4-nitrobenzoic acid) (300.5 mg) afforded 6,6'-azanediylbis(N-((S)-1-hydroxy-3-phenylpropan-2-yl)-4-nitrobenzamide) as an orange solid (487.6 mg) in 92% yield. It was used without further purification.

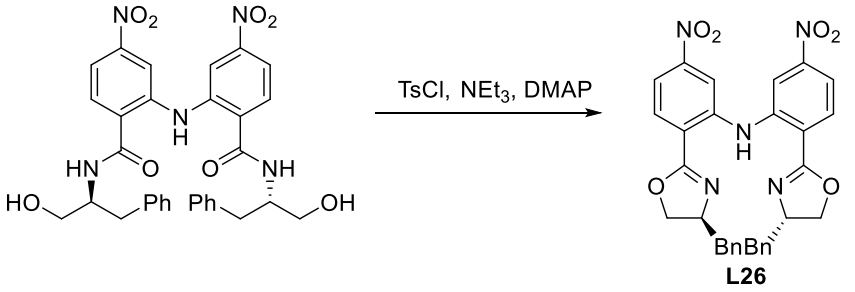

L26

General Procedure D with DMAP: 6,6'-azanediylbis(N-((S)-1-hydroxy-3- phenylpropan-2-yl)-4-nitrobenzamide) (265.2 mg) afforded bis(2-((S)-4- benzyl-4,5-dihydrooxazol-2-yl)-4-nitrophenyl)amine **L26** (168.8 mg) in 68% yield. Flash chromatography: 1:10:90- 1:80:20 NEt_3: EtOAc: hexane. ^1H NMR ($CDCl_3$, 400 MHz): 11.72 (br, 1H), 8.32 (d, *J*= 2.3, 2H), 8.02 (d, *J*= 8.6, 2H), 7.80 (dd, *J*= 8.6, 1.9, 2H), 7.20-7.17 (m, 6H), 7.15-7.12 (m, 4H), 4.38-4.28 (m, 4H), 4.02 (t, *J*= 6.9, 2H), 3.02 (dd, *J*= 13.7, 5.8, 2H), 2.76 (dd, *J*= 13.7, 6.7, 2H); ^{13}C NMR ($CDCl_3$, 100 MHz): 161.1, 149.8, 143.0, 137.7, 131.7, 129.3, 128.3, 126.5, 120.8, 114.9, 112.3, 71.0, 68.6, 41.7; Molecular Weight $[M-H]^-$: 576.3 (expected), 576.3 (found); IR (cm^{-1}): 3170, 3105, 3086, 3063, 3028, 2957, 2900, 1637, 1597, 1533, 1497, 1473, 1454, 1415; $[\alpha]^{20}_D$= +116.8° (c= 0.76, $CHCl_3$).

*Synthesis of Ligand **L27**:*

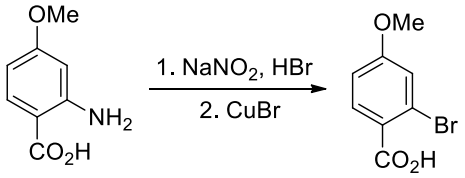

General Procedure A: 2-amino-4-methoxybenzoic acid (1.5055 g) afforded 2-bromo-4-methoxybenzoic acid[13] (1.8755 g) in 90% yield.

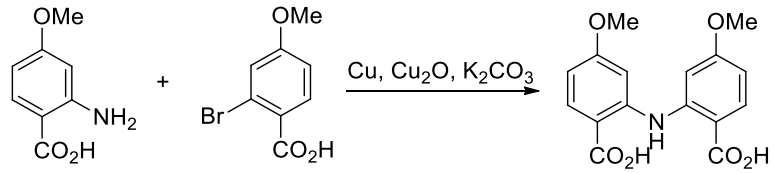

General Procedure B: 2-bromo-4-methoxybenzoic acid (1.00g) afforded 2,2'-azanediylbis(4-methoxybenzoic acid) (1.24 g) as a black solid in 90% yield. ^{1}H NMR (DMSO, 400 MHz): 12.65 (br, 2H), 10.98 (br, 1H), 7.86 (d, *J*=9.0, 2H), 7.00 (d, *J*= 2.0, 2H), 6.53 (dd, *J*= 9.0, 2.4, 2H), 3.74 (s, 6H); ^{13}C NMR (DMSO, 100 MHz): 168.4, 163.6, 145.8, 134.2, 110.7, 107.5, 102.1, 55.8; Molecular Weight $[M-H]^{-}$: 316.1 (expected), 316.1 (found); IR (cm^{-1}): 3370, 3350, 1668, 1611, 1563, 1525, 1446.

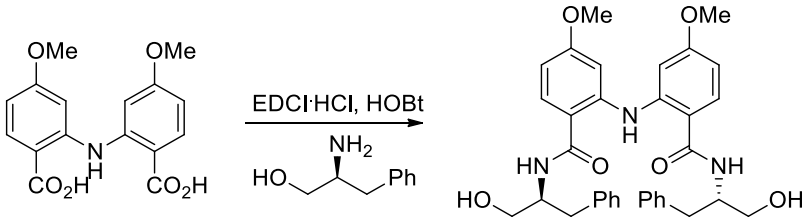

General Procedure C2: 2,2'-azanediylbis(4-methoxybenzoic acid) (99.8 mg) afforded 2,2'-azanediylbis(N-((S)-1-hydroxy-3-phenylpropan-2-yl)-4-methoxybenzamide) (109.6 mg) in 60% yield. Flash chromatography: 50% Hexane/EtOAc- 3.5% MeOH/EtOAc, florisil as stationary phase.

^{1}H NMR ($CDCl_3$, 400 MHz): 9.66 (br, 1H), 7.45 (d, *J*= 8.6, 2H), 7.24-7.15 (m, 10H), 6.83 (d, *J*= 7.8, 2H), 6.69 (d, *J*= 2.8, 2H), 6.45 (dd, *J*= 8.6, 2.3, 2H), 4.36-4.28 (m, 2H), 3.71 (s, 6H), 3.66 (dd, *J*= 11.4, 3.5, 2H), 3.55 (dd, *J*= 11.3, 4.7, 2H), 2.87 (d, *J*= 7.4, 4H), ^{13}C NMR ($CDCl_3$, 100 MHz): 168.3, 162.6, 143.7, 137.8, 130.7, 129.3, 128.5, 126.5, 116.4, 107.6, 104.2, 63.5, 55.3, 52.8, 37.1; Molecular Weight $[M+Na]^+$: 606.3 (expected), 606.3 (found); IR (cm^{-1}): 3299 (br), 3085, 3060, 3026, 3002, 2935, 2872, 1620, 1602, 1573, 1513, 1496, 1449; $[\alpha]^{20}_D$= –99.8° (c= 0.95, $CHCl_3$).

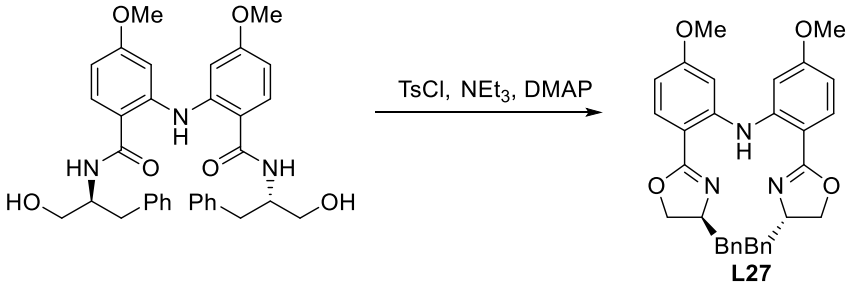

L27

General Procedure D with DMAP: 2,2'-azanediylbis(N-((S)-1-hydroxy-3- phenylpropan-2-yl)-4-methoxybenzamide) (80.0 mg) afforded bis(2-((S)-4- benzyl-4,5-dihydrooxazol-2-yl)-5-methoxyphenyl) amine **L27** (42.8 mg) in 57% yield. Flash chromatography: 50% EtOAc/hexane, florisil (<200 mesh) as stationary phase. ^{1}H NMR ($CDCl_3$, 400 MHz): 10.98 (br, 1H), 7.77 (d, *J*= 8.6, 2H), 7.24-7.16 (m, 10H), 7.04 (d, *J*= 2.3, 2H), 6.49 (dd, *J*= 9.0, 2.3, 2H), 4.47-4.39 (m, 2H), 4.19 (t, *J*= 8.7, 2H), 3.94 (t, *J*= 7.9, 2H), 3.78 (s, 6H), 3.14 (dd, *J*= 13.6, 5.4, 2H), 2.69 (dd, *J*= 13.6, 8.3, 2H); ^{13}C NMR ($CDCl_3$, 100 MHz): 162.9, 162.2, 144.6, 138.3, 131.9, 129.3, 128.4, 126.3, 109.0, 106.7, 102.9, 70.5, 68.0, 55.3, 41.9; Molecular Weight $[M+H]^+$: 548.3 (expected), 548.3 (found); IR (cm^{-1}): 3060, 3025, 3000, 2957, 2917, 1639, 1612, 1576, 1503, 1464, 1452, 1442; $[\alpha]^{20}_D$= +65.6° (c= 0.50, $CHCl_3$).

*Synthesis of Ligand **L28**:*

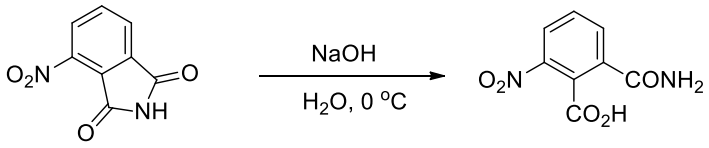

To a solution of 4-nitroisoindoline-1,3-dione (15.03 g, 1 equiv.) in H_2O (180 mL) was added NaOH (21 mL, 30% w/w in H_2O) at 0 °C dropwise. The mixture was stirred at 0 °C for 2 h. conc. HCl (13.5 mL) was added at 0 °C. The mixture was stirred at 0 °C for 30 mins. The mixture was filtered. The residue was washed with cold water and dried under vacuum. 2-carbamoyl-6-nitrobenzoic acid was obtained as a pale yellow solid (11.9 g, 72%). ^{1}H NMR (DMSO, 400 MHz): 7.67 (br, 1H), 7.71 (t, *J*= 7.8, 1H), 7.91 (d, *J*= 7.8, 1H), 8.12 (d, *J*= 7.8, 1H), 8.13 (br, 1H), 13.57 (br, 1H); ^{13}C NMR (DMSO, 100 MHz): 125.8, 129.6, 130.7, 133.0, 137.2, 147.5, 166.4, 167.8; Molecular Weight $[M-H]^-$: 209.0 (expected), 209.0 (found); IR (cm^{-1}): 3481, 3431, 3269 (br), 1719, 1646, 1614.

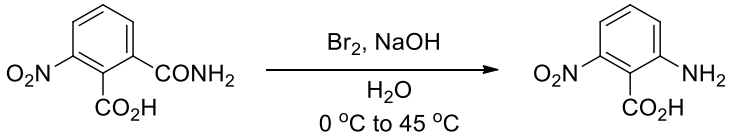

At 0 °C, Br_2 (2.9 mL, 2 equiv.) was dissolved in H_2O (26 mL) and NaOH (22.5 mL, 30% w/w in H_2O). A solution of 2-carbamoyl-6-nitrobenzoic acid (11.70 g, 1 equiv.) in H_2O (40 mL) and NaOH (7.5 mL, 30% w/w in H_2O) was added at 0 °C. The mixture was stirred at 45 °C for 45 mins. When mixture was cooled to 0 °C, conc. HCl (10 mL) was added dropwise. The mixture was stirred for 15 mins at 0 °C. The mixture was filtered. The residue was washed with cold water and dried under vacuum. 2-amino-6-nitrobenzoic acid was obtained as a yellow solid (8.49 g, 84%). ^{1}H NMR

(DMSO, 400 MHz): 7.29 (t, *J*= 8.0, 1H), 7.00 (d, *J*=8.0, 1H), 6.88 (d, *J*=8.0, 1H); ^{13}C NMR (DMSO, 100 MHz): 106.1, 110.7, 120.6, 132.3, 150.4, 151.9, 166.9; Molecular Weight $[M-H]^-$: 181.0 (expected), 181.0 (found); IR (cm^{-1}): 3462, 3361, 2967 (br), 1668, 1618.

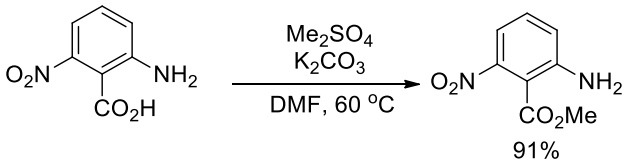

To a solution of 2-amino-6-nitrobenzoic acid (598.3 mg, 1 equiv.), K_2CO_3 (455.3 mg, 1 equiv.) in DMF (9.2 mL) was added Me_2SO_4 dropwise. The mixture was stirred at 60 °C overnight. The mixture was diluted with Et_2O and EtOAc. Water was added. The mixture was extracted with EtOAc three times, wash with H_2O five times and brine once. The mixture was dried over Na_2SO_4 and filtered. The solvent was removed under vacco. Flash chromatography (20% EtOAc/hexane-1:40:60 NEt_3:EtOAc/hexane) afforded methyl 2-amino-6-nitrobenzoate[14] (587.3 mg) in 91% yield.

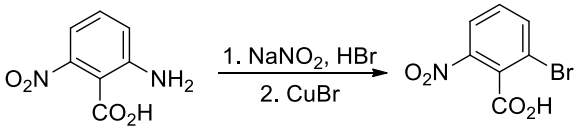

General Procedure A: 2-amino-6-nitrobenzoic acid (2.01 g) afforded 2-bromo-6-nitrobenzoic acid[15] (2.25 g) in 83% yield.

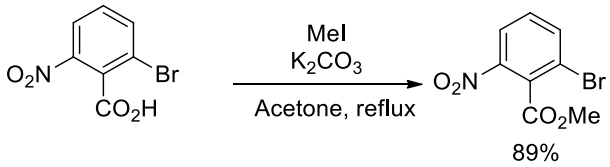

To a solution of 2-bromo-6-nitrobenzoic acid (0.6500 g, 1 equiv.), K_2CO_3 (0.4496 g, 1.2 equiv.) in acetone (9.8 mL was added MeI (0.15 mL, 3.6 equiv.) dropwise. The mixture was

refluxed overnight. H_2O was added. The mixture was extracted with DCM three times. The organic layer was washed with H_2O and brine, dried over Na_2SO_4 and filtered. The solvent was removed under vacco. Flash chromatography (15% EtOAc/hexane) afforded methyl 2-bromo-6-nitrobenzoate[15] (0.6102 g) in 89% yield.

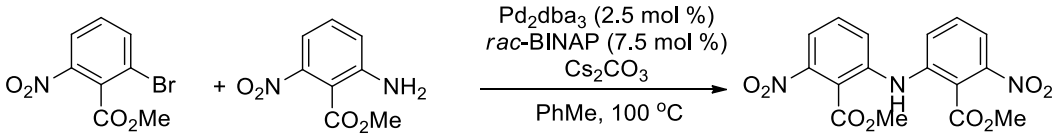

In a glove box, Pd_2dba_3 (22.9 mg, 2.5 mol %), *rac*-BINAP (46.7 mg, 7.5 mol %) and Cs_2CO_3 (0.6513 g, 2 equiv.) were added to a 20 mL flask. The flask was removed from the glove box. methyl 2-bromo-6-nitrobenzoate (259.9 mg, 1 equiv.) and methyl 2-amino-6-nitrobenzoate (235.4 mg, 1.2 equiv.) were added. PhMe (4 mL) was added. The reaction mixture was stirred at 100 °C overnight. After cooling to rt, the solvent was removed under vacco. The sample was dissolved in EtOAc and filtered through silica gel. The solvent was removed under *vacco*. Flash chromatography (30-40% EtOAc/hexane) afforded dimethyl 6,6'-azanediylbis(2-nitrobenzoate) as a brown solid (203.0 mg) in 54% yield. ^1H NMR ($CDCl_3$, 400 MHz): 9.14 (br, 1H), 7.54-7.45 (m, 6H), 3.95 (s, 6H); ^{13}C NMR ($CDCl_3$, 100 MHz): 165.3, 150.2, 142.1, 131.7, 122.3, 117.2, 116.7, 53.5; Molecular Weight $[M+H]^+$: 376.1 (expected), 376.1 (found); IR (cm^{-1}): 3342 (br), 3099, 3008, 2955, 1722, 1608, 1579.

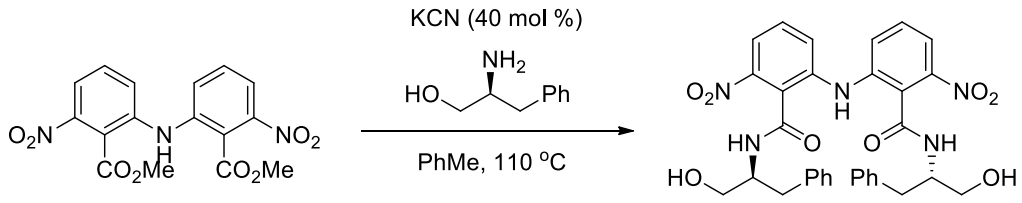

A solution of dimethyl 6,6'-azanediylbis(2-nitrobenzoate) (167.7 mg, 1 equiv.), (*S*)-phenylalaninol (175.7 mg, 2.6 equiv.), KCN (11.6 mg, 40 mol %) in PhMe (2.7 mL) was refluxed for two overnights. After cooling to rt, H_2O was added. The mixture was extract with DCM three times. The organic layer was washed with H_2O, 1M HCl, H_2O and brine. The organic layer was dried over Na_2SO_4 and filtered. The solvent was removed under vacco. Flash chromatography (30% EtOAc/hex- EtOAc) afforded 6,6'-azanediylbis(N-((S)-1-hydroxy-3-phenylpropan-2-yl)-2-nitrobenzamide) (43.5 mg) contaminated with a trace amount of impurities in 16% yield.

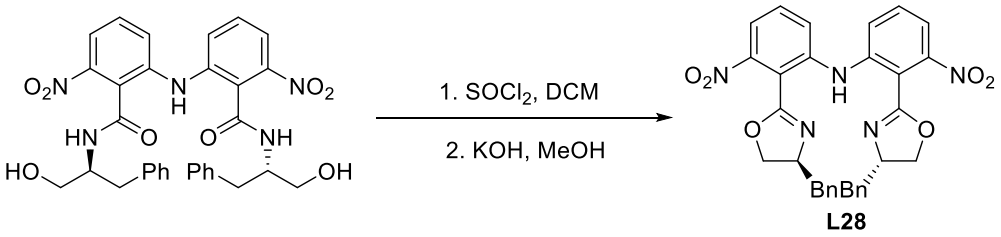

L28

To a solution of 6,6'-azanediylbis(N-((S)-1-hydroxy-3-phenylpropan-2-yl)-2-nitrobenzamide) (43.5 mg, 1 equiv.) in DCM (0.285 mL) was added $SOCl_2$ (0.37 mL, 7.2 equiv.) at 0 ^oC dropwise. The mixture was stirred at rt overnight. The excess $SOCl_2$ and DCM were removed under vacco. A solution of KOH (8.0 mg, 2 equiv.) in MeOH (0.435 mL) was added. The mixture was stirred at rt overnight. H_2O was added. The mixture was extracted with DCM three times. The organic layer was washed with brine, dried over Na_2SO_4 and filtered. The solvent was removed under vacco. Flash chromatography (1:30:70-1:60:40 NEt_3:EtOAc:hexane) afforded bis(2-((S)-4-benzyl-4,5-dihydrooxazol-2-yl)-3-nitrophenyl)amine **L28** (17.1 mg) as a yellow solid in 42% yield. ^1H NMR ($CDCl_3$, 400 MHz): 7.70 (dd, *J*= 6.3, 3.1, 2H), 7.44-7.40 (m, 4H), 7.26-7.24 (2H, m), 7.20-7.16 (m, 4H), 7.11-7.07 (m, 2H), 6.03 (d, *J*= 9.0, 2H), 4.75-4.69 (m, 2H), 3.85 (dd, *J*= 11.3, 3.9, 2H), 3.60 (dd, *J*= 11.3, 2.8, 2H), 3.10 (dd, *J*= 13.7, 6.2, 2H), 2.96 (13.7, 8.6, 2H); ^{13}C NMR ($CDCl_3$,

100 MHz): 164.1, 147.8, 141.2, 136.6, 130.6, 129.3, 128.6, 126.7, 123.1, 122.4, 117.7, 51.1, 46.3, 36.8; Molecular Weight [M–H]$^{-}$: 576.2 (expected), 576.0 (found); IR (cm^{-1}): 3365 (br), 3274 (br), 3061, 3028, 2925, 2854, 1652, 1609, 1577, 1532, 1452; $[\alpha]^{20}_{D}$= –79.7^{o} (c= 0.63, $CHCl_3$).

*Synthesis of Ligand **L29**:*

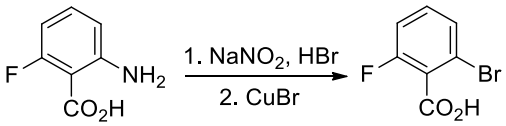

General Procedure A: 2-amino-6-fluorobenzoic acid (4.53 g) afforded 2-bromo-6-fluorobenzoic acid[16] (5.55 g) in 87% yield.

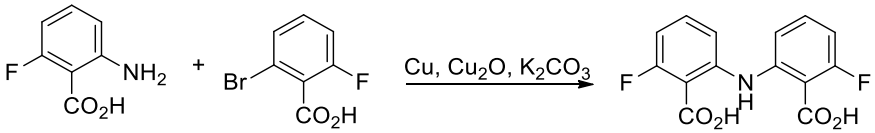

General Procedure B: 2-bromo-6-fluorobenzoic acid (1.50 g) afforded 6,6'-azanediylbis(2-fluorobenzoic acid) (1.40 g) as a pale brown solid in 70% yield. ^{1}H NMR (DMSO, 400 MHz): 13.67 (br, 2H), 9.79 (br, 2H), 7.42-7.36 (m), 7.15 (d, *J*=8.2, 2H), 6.82 (dd, *J*= 10.2, 8.7, 2H);^{13}C NMR (DMSO, 100 MHz): 166.6 (s), 161.6 (d, *J*= 250), 143.77 (d, *J*=4), 133.36 (d, *J*= 12), 114.46 (d, *J*= 3), 110.88 (d, *J*= 16), 108.77 (d, *J*= 23); Molecular Weight [M–H]$^{-}$: Expected: 292.0, Found: 292.0; IR (cm^{-1}): 2980 (br), 2978, 2864, 1675, 1623, 1592.

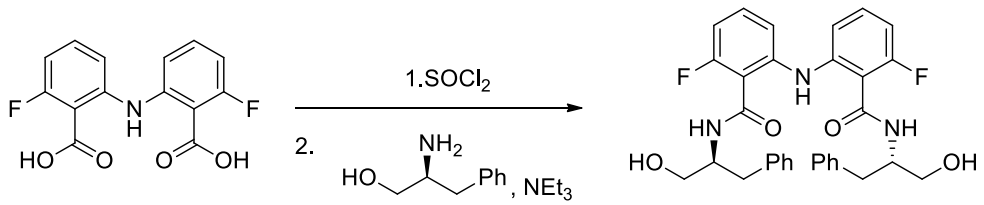

General Procedure C1: 6,6'-azanediylbis(2-fluorobenzoic acid) (0.5000 g) afforded 6,6'-azanediylbis(2-fluoro-N-((S)-1-hydroxy-3-phenylpropan-2-yl)benzamide) (0.9000 g) as a yellow solid in 94% yield. It was used without further purification.

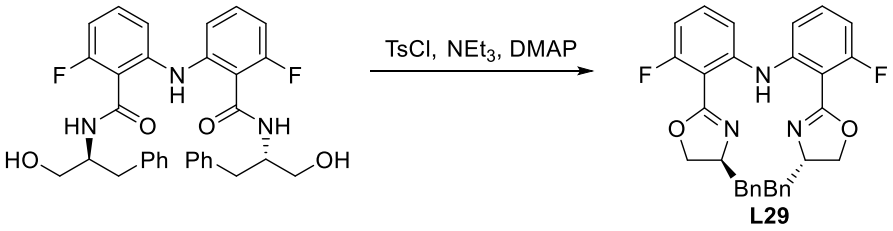

L29

General Procedure D with DMAP: 6,6'-azanediylbis(2-chloro-N-((*S*)-1-hydroxy-3-phenylpropan-2-yl)benzamide) (0.5600 g) afforded bis(2-((*S*)-4-benzyl-4,5- dihydrooxazol-2-yl)-3-fluorophenyl) amine **L29** (0.3699 g) in 71% yield. Flash Chromatography: 1:10:90-1:55:45 NEt_3:EtOAc:hexane. ^1H NMR ($CDCl_3$, 400 MHz): 10.49 (br, 1H), 7.28-7.13 (m, 14H), 6.69 (dd, *J*= 10.1, 8.3, 2H), 4.64-4.56 (m, 2H), 4.31 (t, *J*= 9.0, 2H), 4.10 (t, *J*= 7.9, 2H), 3.22 (dd, *J*= 13.7, 5.1, 2H), 2.75 (dd, *J*= 13.6, 8.6, 2H), ^{13}C NMR ($CDCl_3$, 100 MHz): 163.4 (s), 160.9 (s), 160.3 (d, *J*= 1.5), 144.3 (d, *J*= 4.6), 137.6 (s), 131.7 (d, *J*= 11.4), 128.9 (d, *J*= 68.7), 126.5 (s), 114.1 (d, *J*= 3.1), 108.0 (d, *J*= 22.9), 106.6 (d, *J*= 15.3); 71.3 (s), 67.4 (s), 41.7 (s); Molecular Weight $[M+H]^+$: 524.22 (expected), 524.3 (found); IR (cm^{-1}): 3250 (br), 3083, 3062, 3026, 2922, 2899, 2852, 1632, 1608, 1578, 1519, 1495, 1458; $[\alpha]^{20}_D$= +39.0° (c= 1.00, $CHCl_3$).

*Synthesis of Ligand **L30**:*

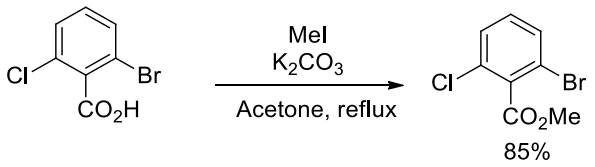

To a solution of 2-bromo-6-chlorobenzoic acid (2.002 g, 1 equiv.), K_2CO_3 (1.41 g, 1.2 equiv.) in acetone (30.8 mL) was added MeI (1.90 mL, 3.6 equiv.) dropwise. The mixture was refluxed overnight. H_2O was added. The mixture was extracted with DCM three times. The organic layer was washed with H_2O and brine, dried over Na_2SO_4 and filtered. The solvent was removed under vacco. Flash chromatography (8-12% EtOAc/hexane) afforded methyl 2-bromo-6-chlorobenzoate[17] (1.7988 g) as a solid in 85% yield.

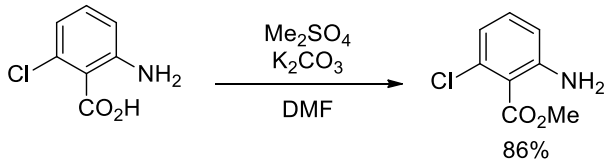

To a solution of 2-amino-6-chlorobenzoic acid (2.98 g, 1 equiv.), K_2CO_3 (2.41 g, 1 equiv.) in DMF (48 mL) was added Me_2SO_4 (1.655 mL, 1 equiv.) dropwise. The mixture was stirred at rt overnight. H_2O was added. The mixture was extracted with EtOAc three times. The organic layer was washed with H_2O several times until no more DMF remained, washed with brine, dried over Na_2SO_4 and filtered. The solvent was removed under vacco. Flash chromatography (12% EtOAc/hexane-1:40:60 NEt_3/EtOAc/hexane) afforded methyl 2-amino-6-chlorobenzoate (2.79 g) as a brown oil in 86% yield. ^{1}H NMR (DMSO, 400 MHz): 3.92 (s, 3H), 4.87 (br, 2H), 6.57 (d, *J*= 8.2, 1H), 6.74 (d, *J*=7.8, 1H); 7.07 (t, *J*= 8.0, 1H); ^{13}C NMR (DMSO, 100 MHz); Molecular Weight $[M+H]^+$: 186.0 (expected), 186.0 (found); IR (cm^{-1}): 1609, 1702, 2952, 3001, 3381, 3482.

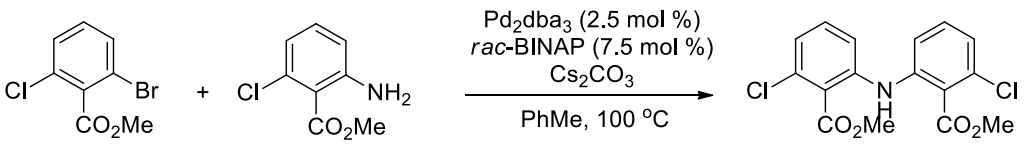

In a glove box, Pd_2dba_3 (68.7 mg, 2.5 mol %), *rac*-BINAP (140.1 mg, 7.5 mol %) and Cs_2CO_3 (1.368 g, 1.4 equiv.) were added to a 50 mL flask. The flask was removed from the glove box. Methyl 2-bromo-6-chlorobenzoate (0.7508 g, 1 equiv.) and methyl 2-amino-6-chlorobenzoate (0.6682 g, 1.2 equiv.) were added. PhMe (12 mL) was added. The reaction mixture was stirred at 100 ^oC overnight. After cooling to rt, the solvent was removed under vacco. The sample was dissolved in EtOAc and filtered through silica gel. The solvent was removed under vacco. Flash chromatography (10-12% EtOAc/hexane) afforded dimethyl 6,6'-azanediylbis(2- chlorobenzoate) as a pale yellow solid (0.6200 g) in 58% yield. ^1H NMR ($CDCl_3$, 400 MHz): 8.21 (br, 1H), 7.32 (t, *J*= 8.0, 2H), 7.18 (d, *J*= 8.0, 2H), 7.09 (d, *J*=8.0, 2H); ^{13}C NMR ($CDCl_3$, 100 MHz): 166.7, 142.7, 133.5, 131.5, 123.1, 122.0, 116.7, 52.6; Molecular Weight $[M+H]^+$: 354.03, 356.03 (expected), 354.1, 356.1 (found); IR (cm^{-1}): 2800 (br), 1737, 1705, 1597.

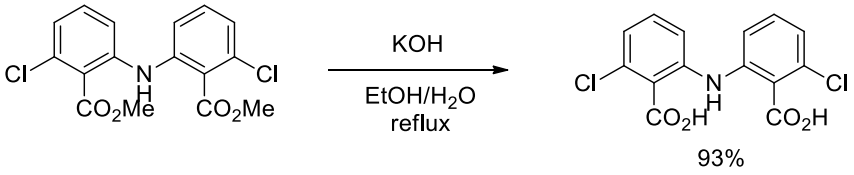

A mixture of dimethyl 6,6'-azanediylbis(2-chlorobenzoate) (0.3539 g, 1 equiv.), KOH (0.2244 g, 4 equiv.) in EtOH (5 mL) and H_2O (5 mL) was refluxed with stirring for 26 h. Additional KOH (0.1122 g, 2 equiv.) was added. The mixture was reflux with stirring for overnight. After cooling to rt, the mixture was diluted with H_2O (20 mL) and acidified with 1M HCl until pH < 3. Filtration afforded analytically pure 6,6'-azanediylbis(2-chlorobenzoic acid) (0.3026 g) as a pale yellow solid in 93% yield. ^1H NMR (DMSO, 400 MHz): 8.49 (br, 1H), 7.21-7.15 (m, 4H), 6.99 (dd, *J*= 6.5, 2.7, 2H), 3.98 (s, 6H); ^{13}C NMR (DMSO, 100 MHz): 167.5, 142.02, 131.9, 131.7, 124.3, 123.1,

117.6; Molecular Weight [M−H]$^-$: 324.0 (expected), 324.0 (found); IR (cm^{-1}): 3309, 2970, 2853, 2750 (br), 1665, 1564.

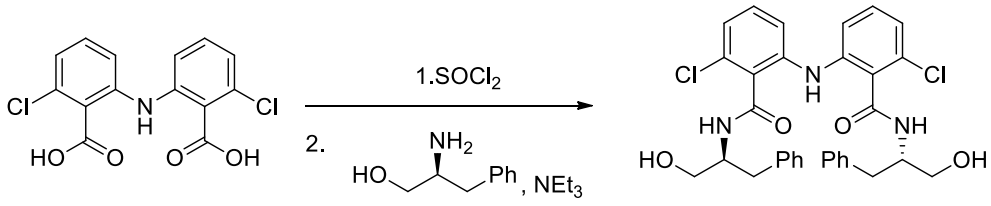

General Procedure C: 6,6'-azanediylbis(2-chlorobenzoic acid) (0.1483 g) afforded 6,6'-azanediylbis(2-chloro-N-((*S*)-1-hydroxy-3-phenylpropan-2-yl)benzamide) (0.0950 g) as a yellow solid in 35% yield. Flash Chromatography: 50-80% EtOAc/hexane. ^{1}H NMR (CD_3OD, 400 MHz): 7.27-7.24 (m, 4H), 7.21 (d, *J*= 7.8, 2H), 7.14 (d, *J*= 7.5, 4H), 7.08-7.05 (m, 4H), 7.00 (d, *J*= 8.3, 2H), 4.35-4.28 (m, 2H), 3.59 (d, *J*= 5.5, 4H), 2.97 (dd, *J*= 13.7, 6.3, 2H), 2.83 (dd, *J*= 13.7, 5.9, 2H);^{13}C NMR (CD_3OD, 100 MHz): 166.6, 141.5, 138.3, 131.4, 130.2, 129.0, 127.9, 127.5, 125.8, 122.1, 117.0, 62.4, 53.3, 36.2; Molecular Weight [M+Na$^+$]: 614.2 (expected), 614.3 (found); IR (cm^{-1}): 3377 (br), 3085, 3061, 3027, 2926, 2874, 1627, 1596, 1586, 1560, 1469; $[\alpha]^{20}_D$= −35.1^o (c= 0.65, MeOH).

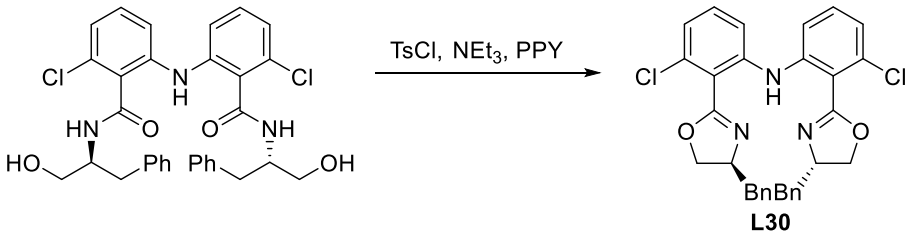

L30

General Procedure D with 4-pyrrolidinopyridine: 6,6'-azanediylbis(2-chloro-N-((*S*)-1-hydroxy-3-phenylpropan-2-yl)benzamide) (0.0629 g) afforded bis(2-((S)-4-benzyl- 4,5-dihydrooxazol-2-yl)-3-chlorophenyl) amine **L30** (0.0292 g) in 49% yield. Flash Chromatography:

1:20:80-1:50:50 NEt_3:EtOAc:hexane. ^1H NMR ($CDCl_3$, 400 MHz): 9.03 (br, 1H), 7.28-7.17 (m, 14H), 7.00 (dd, *J*= 7.0, 1.8, 2H), 4.65-4.57 (m, 2H), 4.34 (t, *J*= 8.8, 2H), 4.13 (t, *J*= 8.0, 2H), 3.23 (dd, *J*= 13.7, 5.5, 2H), 2.78 (dd, *J*= 13.7, 8.6, 2H); ^{13}C NMR ($CDCl_3$, 100 MHz): 161.2, 143.3, 137.7, 134.5, 131.0, 129.3, 128.6, 126.5, 122.4, 118.0, 116.1, 71.7, 67.8, 41.8; Molecular Weight $[M+H]^+$: 556.2 (expected), 556.2 (found); IR (cm^{-1}): 3350 (br), 3061, 3027, 2922, 2898, 2850, 1662, 1573, 1496, 1444; $[\alpha]^{20}_D$= +23.2° (c= 0.48, $CHCl_3$).

*Synthesis of Ligand **L31**:*

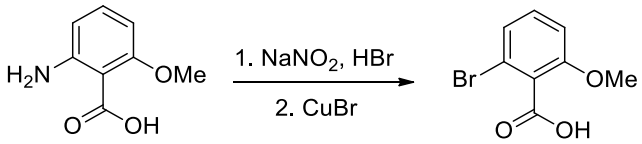

General Procedure A: 2-amino-6-methoxybenzoic acid (2.01 g) afforded 2-bromo-6-methoxybenzoic acid[18] (1.83 g) in 66% yield.

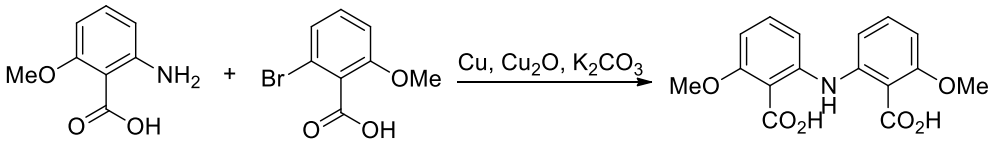

General Procedure B: 2-bromo-6-methoxybenzoic acid (0.8002 g) afforded 6,6'-azanediylbis(2-methoxybenzoic acid) (0.4889 g) as a brown solid in 45% yield. ^1H NMR (DMSO, 400 MHz): 13.05 (br, 2H), 8.52 (br, 1H), 7.26 (t, *J*= 8.5, 2H), 6.82 (d, *J*= 8.3, 2H), 6.63 (d, *J*= 8.2, 2H), 3.77 (s, 6H); ^{13}C NMR (DMSO, 100 MHz): 168.5, 158.4, 142.2, 131.8, 113.5, 111.0, 104.7, 56.3; Molecular Weight $[M-H]^-$: 316.1 (expected), 316.1 (found); IR (cm^{-1}): 3400, 3195, 1710, 1691, 1678, 1602, 1579, 1516, 1458, 1434.

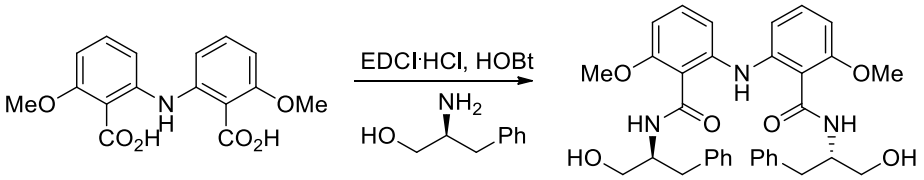

General Procedure C2: 6,6'-azanediylbis(2-methoxybenzoic acid) (0.2023 g) afforded 6,6'-azanediylbis(N-((S)-1-hydroxy-3-phenylpropan-2-yl)-2-methoxybenzamide) as (0.3143 g) as a yellow solid in 84% yield. Flash chromatography: EtOAc-3% MeOH/EtOAc, florisil (<200 mesh) as stationary phase. ^{1}H NMR ($CDCl_3$, 400 MHz): 10.35 (br, 1H), 7.28-7.23 (m, 8H), 7.19-7.14 (m, 4H), 6.97 (d, *J*= 8.2, 2H), 6.95 (br, 2H), 6.42 (d, *J*= 8.3, 2H), 4.42-4.34 (m, 2H), 3.85-3.80 (m, 2H), 3.73 (s, 6H), 3.64-3.56 (m, 4H), 3.01-2.97 (m, 4H);^{13}C NMR ($CDCl_3$, 100 MHz): 167.4, 158.2, 143.9, 137.8, 130.9, 129.4, 128.4, 126.4, 113.2, 111.5, 103.1, 63.7, 55.9, 52.9, 37.2; Molecular Weight $[M+Na]^+$: 606.3 (expected), 606.3 (found); IR (cm^{-1}): 3376 (br), 3084, 3061, 3027, 2928, 2880, 2839, 1630, 1580, 1509, 1460, 1435; $[\alpha]^{20}_D$= −152.8° (c= 1.00, $CHCl_3$).

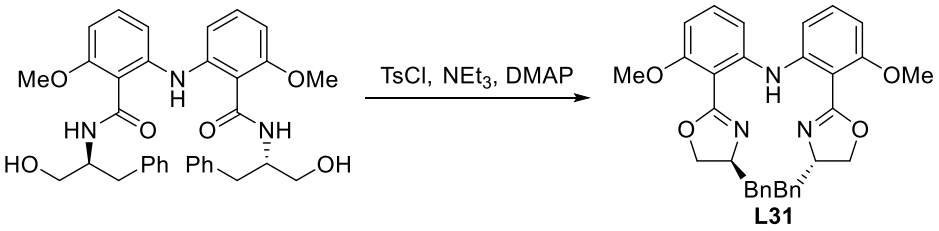

General Procedure D with DMAP: 6,6'-azanediylbis(N-((*S*)-1-hydroxy-3- phenylpropan-2-yl)-2-methoxybenzamide) (0.1504 g) afforded bis(2-((*S*)-4- benzyl-4,5-dihydrooxazol-2-yl)-3-methoxyphenyl) amine **L31** (0.0737 g) in 52% yield. Flash chromatography: 50% EtOAc/hexane, florisil (<200 mesh) as stationary phase. ^{1}NMR ($CDCl_3$, 400 MHz): 9.41 (br, 1H), 7.26-7.16 (m, 12H), 6.98 (d, *J*= 8.2, 2H), 6.49 (d, *J*= 8.2, 2H), 4.63-4.56 (m, 2H), 4.30 (t, *J*= 9.0, 2H), 4.09 (d, *J*= 8.1, 2H), 3.84 s, 6H), 3.27 (dd, *J*= 14.1, 5.1, 2H), 2.76 (dd, *J*= 13.7, 9.0, 2H), ^{13}C NMR ($CDCl_3$, 100 MHz): 161.9,

159.4, 143.8, 138.1, 131.1, 129.2, 128.5, 126.3, 111.1, 107.6, 103.4, 71.3, 67.5, 56.1, 41.8; Molecular Weight $[M+H]^+$: 548.3 (expected), 548.3 (found); IR (cm^{-1}): 3320 (br), 3083, 3061, 3025, 3002, 2958, 2935, 2897, 2837, 1660, 1637, 1581, 1516, 1495, 1465, 1436; $[\alpha]^{20}_D = +36.9^o$ (c= 0.58, $CHCl_3$).

*Synthesis of Ligand **L32**:*

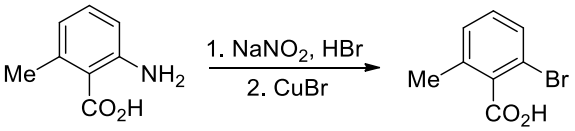

General Procedure A: 2-amino-6-methylbenzoic acid (2.00 g) afforded 2-bromo-6-methylbenzoic acid as a pale brown solid (2.03 g) in 71% yield. ^1H NMR (CD_3OD, 400 MHz): 7.42 (d, *J*=8.2, 1H), 7.23-7.15 (m, 2H); 2.34 (s, 3H); ^{13}C NMR (CD_3OD, 100 MHz): 170.0; 137.1; 136.1; 129.9; 128.7, 117.7, 18.3; Molecular Weight $[M-H^+]$: 212.96, 215.0 (expected), 213.1, 215.0 (found); IR (cm^{-1}): 3061 (br), 3022, 2928, 1720, 1594, 1565.

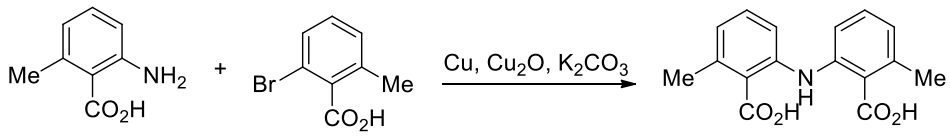

General Procedure B: 2-bromo-6-methylbenzoic acid (1.00 g) afforded 6,6'-azanediylbis(2-methylbenzoic acid) as a dark brown solid (1.09 g) in 82% yield. ^1H NMR (DMSO, 400 MHz): 13.39 (br, 2H), 8.77 (br, 1H), 7.18 (dd, *J*= 7.8, 7.8, 2H), 7.05 (d, *J*= 8.2, 2H), 6.79 (d, *J*= 7.8, 2H), 2.34 (s, 6H); ^{13}C NMR (DMSO, 100 MHz): 170.1, 142.0, 138.0, 130.8, 123.49, 123.47, 116.2, 21.4; Molecular Weight $[M-H]^-$: 284.1 (expected), 284.1 (found); IR (cm^{-1}): 3420, 1674, 1610, 1585, 1462.

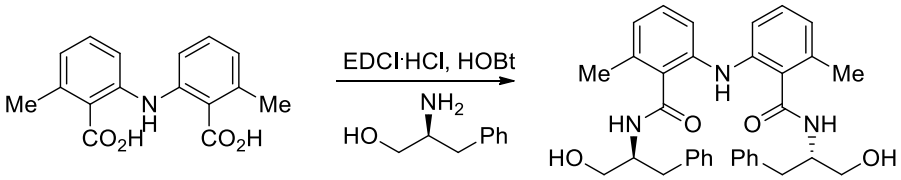

General Procedure C2: 6,6'-azanediylbis(2-methylbenzoic acid) (467.8 mg) afforded 6,6'-azanediylbis(N-((S)-1-hydroxy-3-phenylpropan-2-yl)-2-methylbenzamide) (477.9 mg) as a light brown solid in 53% yield. Flash chromatography: 40-100% Hexane/EtOAc. ^{1}H NMR ($CDCl_3$, 400 MHz): 7.21-7.06 (m, 12H), 6.98 (d, *J*=8.2, 2H), 6.71 (d, *J*= 7.4, 2H), 6.06 (d, *J*=9.0, 2H), 4.44-4.35 (m, 2H), 3.79 (dd, *J*= 11.3, 3.5, 2H), 3.63 (br, 2H), 3.52 (dd, *J*= 11.3, 4.7, 2H), 2.86 (dd, *J*= 13.4, 6.1, 2H), 2.77 (dd, *J*= 14.1, 9, 2H), 2.06 (s, 6H), ^{13}C NMR ($CDCl_3$, 100 MHz): 169.0, 140.1, 137.9, 136.1, 129.6, 129.2, 128.5, 127.7, 126.3, 123.2, 115.9, 63.8, 52.6, 37.2, 19.3; Molecular Weight [M+Na^+]: 574.27 (expected), 574.4 (found); IR (cm^{-1}): 3371 (br), 3277 (br), 3062, 3028, 2924, 2871, 1620, 1598, 1579, 1510, 1463; $[\alpha]^{20}_D$= −144.9° (c= 0.88, $CHCl_3$).

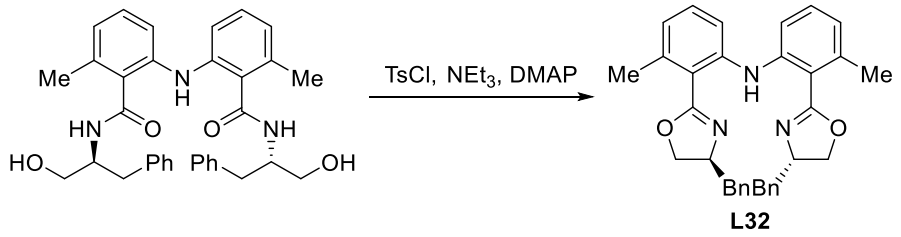

L32

General Procedure D with DMAP: 6,6'-azanediylbis(N-((*S*)-1-hydroxy-3-phenyl propan-2-yl)-2-methylbenzamide) (293.6 mg) afforded bis(2-((*S*)-4-benzyl -4,5-dihydrooxazol-2-yl)-3-methylphenyl)amine **L32** (188.7 mg) in 69% yield. Flash Chromatography: 1:10:90-1:30:70 NEt_3: EtOAc:hexane. ^{1}H NMR ($CDCl_3$, 400 MHz): 9.25 (br, 1H), 7.28-7.12 (m, 14H), 6.74 (d, *J*= 7.0, 2H), 4.65-4.58 (m, 2H), 4.29 (t, *J*= 8.8, 2H), 4.08 (t, *J*= 7.8), 3.22 (dd, *J*= 14.1, 5.5, 2H), 2.77 (dd, *J*= 14.0, 8.6, 2H); 2.34 (s, 6H); ^{13}C NMR ($CDCl_3$, 100 MHz): 163.5, 142.8, 139.0, 137.9, 130.1, 129.3, 128.5,

126.5, 122.6, 117.8, 115.7, 70.9, 67.6, 41.9, 20.9; Molecular Weight $[M+H]^+$: 516.3 (expected), 516.3 (found); IR (cm^{-1}): 3061, 3027, 2963, 2925, 2898, 1655, 1598, 1575, 1516, 1496, 1460; $[\alpha]^{20}_D$= +79.6° (c= 0.66, $CHCl_3$).

A.1.9 Relative Stereochemistry of Cycloadduct from β-substituted nitroalkenes

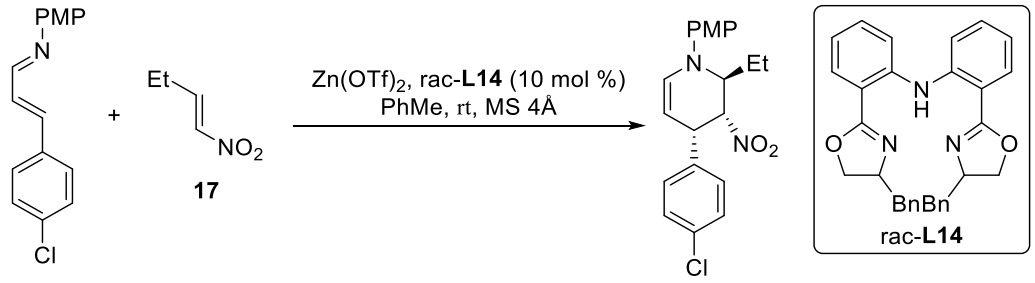

A solution of $Zn(OTf)_2$ (3.6 mg, 0.01 mmol, 10 mol %), rac-**L14** (4.8 mg, 0.005 mmol, 10 mol %), and MS 4Å in PhMe (0.5 mL) in a vial was stirred at rt for 15 mins. A solution of nitro-alkene **17** (15.2 mg, 0.15 mmol, 1.5 equiv.) in PhMe (0.25 mL) in a vial was added to the zinc complex. The vial containing nitro-alkene **17** was rinsed with PhMe (0.25 mL) to ensure complete transfer of the nitro-alkene **17**. (1*E*,2*E*)-3-(4- chlorophenyl)-N-(4-methoxyphenyl)prop-2-en-1-imine (27.5 mg, 0.10 mmol, 1 equiv.) was added. The vial was sealed with a cap. The mixture was stirred at rt for 22 h. The mixture was filtered through florisil. Flash column chromatography (8-10% EtOAc/hex, florisil as stationary phase) afforded (2*S*, 3*R*, 4*S*)-2-ethyl-1-(4- methoxyphenyl)-3-nitro-4-phenylpiperidine (24.1 mg, 64%) as a yellow solid. The relative stereochemistry is established by X-ray crystallography.

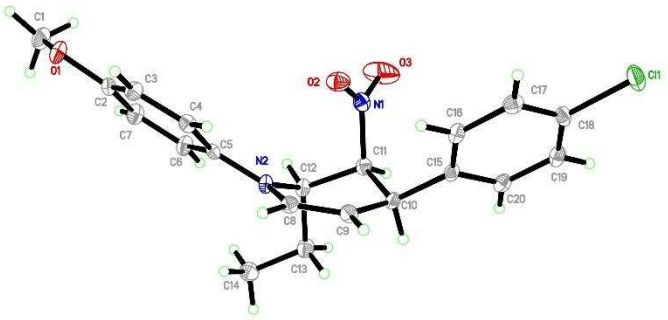

^{1}H NMR ($CDCl_3$, 400 MHz): 7.31-7.26 (m, 5H), 6.96 (d, *J*= 9.0, 2H), 6.84 (d, *J*= 9.0, 2H), 6.62 (d, *J*= 7.9, 1H), 5.05-5.02 (m, 1H), 4.82 (d, *J*= 7.9, 1H), 4.12 (td, *J*= 7.1 2.0, 1H), 4.00-3.97 (m,1H), 3.78 (s, 3H), 2.02-1.91 (m, 1H), 1.83-1.72 (m, 1H), 1.14 (t, *J*= 7.4, 3H); ^{13}C NMR ($CDCl_3$, 100 MHz): 155.1, 140.4, 136.8, 133.4, 130.6, 129.8, 128.7, 119.8, 114.7, 97.1, 84.6, 60.6, 55.6, 37.5, 25.6, 10.4; Molecular Weight $[M+H]^+$: 373.1 (expected), 373.1 (found); IR (cm^{-1}): 3044, 2965, 2934, 2877, 2834m, 1644, 1578, 1547, 1509, 1492, 1463, 1440.

Table 1. Crystal data and structure refinement for R173MP.

Identification code	r173mp
Empirical formula	C20 H21 Cl N2 O3
Formula weight	372.84
Temperature	120 K
Wavelength	0.71073 Å
Crystal system	Monoclinic
Space group	P2(1)/c
Unit cell dimensions	a = 10.6192(7) Å a= 90°.

	b = 12.5451(7) Å	b= 110.242(3)°.
	c = 14.4977(10) Å	g = 90°.
Volume	1812.1(2) $Å^3$	
Z	4	
Density (calculated)	1.367 Mg/m^3	
Absorption coefficient	0.233 mm^{-1}	
F(000)	784	
Crystal size	Not Determined	
Theta range for data collection	2.04 to 26.37°.	
Index ranges	-13<=h<=13, -15<=k<=15, -18<=l<=18	
Reflections collected	29653	
Independent reflections	3703 [R(int) = 0.0514]	
Completeness to theta = 26.37°	100.0 %	
Absorption correction	Semi-empirical from equivalents	
Refinement method	Full-matrix least-squares on F^2	
Data / restraints / parameters	3703 / 0 / 237	
Goodness-of-fit on F^2	1.022	
Final R indices [I>2sigma(I)]	R1 = 0.0368, wR2 = 0.0768	

R indices (all data)	R1 = 0.0577, wR2 = 0.0858
Largest diff. peak and hole	0.260 and -0.254 e.Å^{-3}

Table 2. Atomic coordinates (x 10^4) and equivalent isotropic displacement parameters (Å^{2}x 10^3) for R173MP. U(eq) is defined as one third of the trace of the orthogonalized U^{ij} tensor.

	x	y	z	U(eq)
C(1)	4373(2)	-367(2)	2716(1)	25(1)
C(2)	6536(2)	429(1)	3489(1)	16(1)
C(3)	7921(2)	299(1)	3788(1)	17(1)
C(4)	8770(2)	1015(1)	4433(1)	15(1)
C(5)	8265(2)	1892(1)	4784(1)	13(1)
C(6)	6876(2)	2017(1)	4462(1)	18(1)
C(7)	6018(2)	1290(1)	3831(1)	19(1)
C(8)	10491(2)	2658(1)	5565(1)	15(1)
C(9)	11437(2)	2974(1)	6390(1)	16(1)
C(10)	11150(2)	3308(1)	7291(1)	15(1)
C(11)	9703(2)	3023(1)	7202(1)	15(1)
C(12)	8718(2)	3220(1)	6149(1)	14(1)

C(13)	8637(2)	4421(1)	5929(1)	20(1)
C(14)	7705(2)	4686(1)	4897(1)	23(1)
C(15)	12181(2)	2925(1)	8252(1)	15(1)
C(16)	12885(2)	1981(1)	8299(1)	17(1)
C(17)	13794(2)	1615(1)	9177(1)	18(1)
C(18)	13999(2)	2208(1)	10022(1)	17(1)
C(19)	13343(2)	3160(1)	10001(1)	19(1)
C(20)	12433(2)	3518(1)	9111(1)	16(1)
Cl(1)	15114(1)	1739(1)	11142(1)	26(1)
N(1)	9564(1)	1879(1)	7471(1)	17(1)
N(2)	9136(1)	2624(1)	5437(1)	14(1)
O(1)	5776(1)	-351(1)	2872(1)	21(1)
O(2)	9937(1)	1168(1)	7050(1)	24(1)
O(3)	9054(2)	1713(1)	8090(1)	47(1)

Table 3. Bond lengths [Å] and angles [°] for R173MP:

C(1)-O(1)	1.427(2)	C(15)-C(16)	1.389(2)
C(2)-C(7)	1.380(2)	C(15)-C(20)	1.394(2)

C(2)-O(1)	1.382(2)	C(16)-C(17)	1.384(2)
C(2)-C(3)	1.391(2)	C(17)-C(18)	1.384(2)
C(3)-C(4)	1.382(2)	C(18)-C(19)	1.378(3)
C(4)-C(5)	1.395(2)	C(18)-Cl(1)	1.7480(17)
C(5)-C(6)	1.393(2)	C(19)-C(20)	1.391(2)
C(5)-N(2)	1.410(2)	N(1)-O(3)	1.2162(19)
C(6)-C(7)	1.387(2)	N(1)-O(2)	1.2217(18)
C(8)-C(9)	1.329(2)	C(7)-C(2)-O(1)	124.80(16)
C(8)-N(2)	1.387(2)	C(7)-C(2)-C(3)	119.28(15)
C(9)-C(10)	1.499(2)	O(1)-C(2)-C(3)	115.90(14)
C(10)-C(15)	1.522(2)	C(4)-C(3)-C(2)	120.49(15)
C(10)-C(11)	1.539(2)	C(3)-C(4)-C(5)	121.03(16)
C(11)-N(1)	1.507(2)	C(6)-C(5)-C(4)	117.54(15)
C(11)-C(12)	1.543(2)	C(6)-C(5)-N(2)	121.59(14)
C(12)-N(2)	1.462(2)	C(4)-C(5)-N(2)	120.87(15)
C(12)-C(13)	1.536(2)	C(7)-C(6)-C(5)	121.68(16)
C(13)-C(14)	1.518(2)	C(2)-C(7)-C(6)	119.95(16)
C(9)-C(8)-N(2)	123.73(16)	C(17)-C(16)-C(15)	121.35(16)
C(8)-C(9)-C(10)	123.33(15)	C(16)-C(17)-C(18)	118.79(16)

C(9)-C(10)-C(15)	114.32(14)	C(19)-C(18)-C(17)	121.53(16)
C(9)-C(10)-C(11)	111.08(13)	C(19)-C(18)-Cl(1)	119.16(13)
C(15)-C(10)-C(11)	112.59(13)	C(17)-C(18)-Cl(1)	119.31(14)
N(1)-C(11)-C(10)	112.59(13)	C(18)-C(19)-C(20)	118.92(16)
N(1)-C(11)-C(12)	108.36(13)	C(19)-C(20)-C(15)	120.88(16)
C(10)-C(11)-C(12)	111.19(13)	O(3)-N(1)-O(2)	123.23(15)
N(2)-C(12)-C(13)	111.37(14)	O(3)-N(1)-C(11)	117.57(14)
N(2)-C(12)-C(11)	110.37(13)	O(2)-N(1)-C(11)	119.19(13)
C(13)-C(12)-C(11)	109.44(13)	C(8)-N(2)-C(5)	121.22(13)
C(14)-C(13)-C(12)	112.95(14)	C(8)-N(2)-C(12)	116.42(13)
C(16)-C(15)-C(20)	118.49(15)	C(5)-N(2)-C(12)	121.22(13)
C(16)-C(15)-C(10)	121.17(15)	C(2)-O(1)-C(1)	117.14(13)
C(20)-C(15)-C(10)	120.34(15)		

Table 4. Anisotropic displacement parameters ($Å^2 x\ 10^3$) for R173MP. The anisotropic displacement factor exponent takes the form: $-2p^2[\ h^2 a^{*2} U^{11} + ... + 2\ h\ k\ a^*\ b^*\ U^{12}\ ]$.

U^{11}	U^{22}	U^{33}	U^{23}	U^{13}	U^{12}

C(1)	17(1)	26(1)	25(1)	-4(1)	0(1)	-4(1)
C(2)	16(1)	17(1)	12(1)	-1(1)	2(1)	-1(1)
C(3)	20(1)	14(1)	18(1)	-2(1)	8(1)	3(1)
C(4)	12(1)	17(1)	15(1)	2(1)	5(1)	2(1)
C(5)	14(1)	14(1)	10(1)	2(1)	3(1)	1(1)
C(6)	16(1)	17(1)	19(1)	-5(1)	4(1)	3(1)
C(7)	12(1)	23(1)	20(1)	-2(1)	2(1)	2(1)
C(8)	13(1)	17(1)	16(1)	1(1)	7(1)	-1(1)
C(9)	12(1)	20(1)	17(1)	2(1)	6(1)	-1(1)
C(10)	13(1)	14(1)	15(1)	-1(1)	2(1)	-2(1)
C(11)	16(1)	15(1)	15(1)	-2(1)	6(1)	1(1)
C(12)	12(1)	17(1)	14(1)	-3(1)	4(1)	1(1)
C(13)	21(1)	15(1)	21(1)	-2(1)	3(1)	3(1)
C(14)	23(1)	19(1)	24(1)	2(1)	5(1)	4(1)
C(15)	10(1)	19(1)	15(1)	-1(1)	4(1)	-4(1)
C(16)	14(1)	20(1)	15(1)	-4(1)	4(1)	-3(1)
C(17)	14(1)	18(1)	24(1)	0(1)	7(1)	-1(1)
C(18)	10(1)	27(1)	14(1)	4(1)	2(1)	-4(1)
C(19)	15(1)	26(1)	16(1)	-5(1)	6(1)	-6(1)
C(20)	15(1)	18(1)	18(1)	-3(1)	7(1)	-2(1)

Cl(1)	17(1)	40(1)	17(1)	8(1)	1(1)	-1(1)
N(1)	14(1)	21(1)	16(1)	1(1)	5(1)	1(1)
N(2)	12(1)	17(1)	12(1)	-3(1)	3(1)	1(1)
O(1)	17(1)	21(1)	21(1)	-8(1)	2(1)	-1(1)
O(2)	31(1)	17(1)	27(1)	0(1)	15(1)	2(1)
O(3)	78(1)	36(1)	53(1)	8(1)	55(1)	3(1)

Table 5. Hydrogen coordinates (x 10^4) and isotropic displacement parameters ($Å^2$x 10^3) for R173MP:

	x	y	z	U(eq)
H(1A)	4243	-376	3339	37
H(1B)	3976	-993	2349	37
H(1C)	3957	257	2355	37
H(3)	8277	-273	3552	20
H(4)	9693	910	4636	18
H(6)	6516	2603	4675	21
H(7)	5094	1382	3639	23

H(8)	10753	2447	5043	18
H(9)	12321	2990	6410	19
H(10)	11199	4088	7308	18
H(11)	9442	3483	7651	18
H(12)	7826	2970	6109	17
H(13A)	8326	4787	6400	24
H(13B)	9529	4684	6013	24
H(14A)	7978	4298	4428	34
H(14B)	7743	5437	4782	34
H(14C)	6803	4491	4829	34
H(16)	12743	1588	7728	20
H(17)	14258	981	9200	22
H(19)	13506	3557	10572	23
H(20)	11988	4161	9089	20

A.1.10 Relative Stereochemistry of Cycloadduct from α-methyl nitroethylene

A solution of $Zn(OTf)_2$ (10.9 mg, 0.03 mmol, 10 mol %), rac-**L14** (14.8 mg, 0.03 mmol, 10 mol %), and MS 4Å in PhMe (2.5 mL) in a vial was stirred at rt for 15 mins. A solution of methyl nitro-ethylene **97** (31.3 mg, 0.356 mmol, 1.2 equiv.) in PhMe (0.25 mL) in a vial was added to the

zinc complex. The vial containing nitro-alkene **97** was rinsed with PhMe (0.25 mL) to ensure complete transfer of the nitro-alkene **97**. (*E*)-4-phenoxy-N-((*E*)-3-phenylallylidene)aniline **78** (91.0 mg, 0.304 mmol, 1 equiv.) was added. The vial was sealed with a cap. The mixture was stirred at rt for 12 h. MeOH (2 mL) was added. $NaCNBH_3$ (42 mg, 0.67 mmol, 2.2 equiv.)and $ZnCl_2$ (82.9 mg, 0.61 mmol, 2 equiv.) were added. The mixture was stirred for 3 h. The reaction was quenched with sat. $NaHCO_3$. The aqueous layer was extracted with Et_2O twice. The combined organic layer was washed with brine, drived over Na_2SO_4 and filtered. Solvent was removed under *vacco*. The crude 3-nitropiperidine was dissolved in MeOH (7.2 mL). At 0 ^oC, $NiCl_2$ hexahydrate (180.6 mg, 0.760 mmol, 2.5 equiv.) was added. $NaBH_4$ (189.8 mg, 5.02 mmol, 16.5 equiv.) was added slowly. The mixture was stirred at 0 ^oC for 1.5 h and then at rt overnight. H_2O was added. 10% HCl was added. 15% NaOH was added. The aqueous layer was extracted with EtOAc five times. The combined organic layer was dried over Na_2SO_4 and filtered. Solvent was removed under *vacco*. Flash column chromatography (1:15:85 NEt_3:EtOAc:hex to 1:60:40 NEt_3:EtOAc:hex) afforded (3*R*,4*S*)-3-methyl-3-nitro-1-(4-phenoxyphenyl)-4- phenylpiperidine (43.7 mg, 37% over 3 steps) as a brown oil.

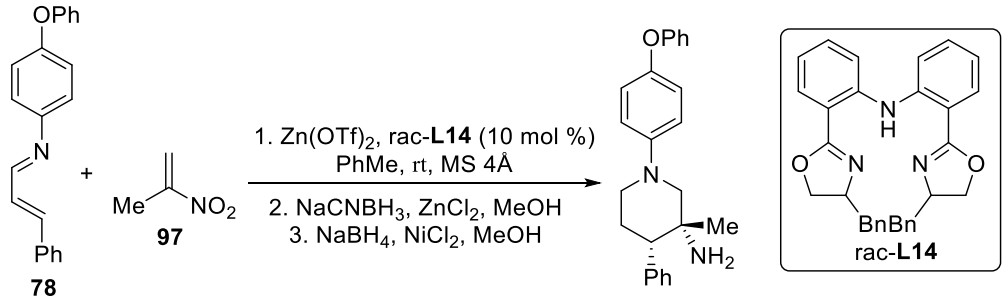

^1H NMR ($CDCl_3$, 400 MHz): 7.35-7.23 (m, 7H), 7.05-6.95 (m, 7H), 3.64 (dt, *J*= 11.4, 2.0, H_F), 3.42 (dd, *J*= 11.3, 1.6, H_A), 2.73 (td, *J*= 12.0, 2.8, H_G), 2.71 (d, *J*= 11.8, H_B), 2.60 (dd, *J*= 12.9, 3.5,

H_C), 2.30 (qd, *J*= 12.8, 1.0, H_E), 1.76 (dq, *J*= 13.6, 3.0, H_D), 1.52 (br, 2H), 0.92 (s, CH_3); ^{13}C NMR ($CDCl_3$, 400 MHz): 158.5, 150.1, 148.8, 141.3, 129.6, 129.1, 128.0, 126.7, 122.4, 120.4, 119.0, 117.7, 65.8, 51.4, 51.1, 50.8, 27.8, 26.9; Molecular Weight $[M+H]^+$: 359.2 (expected), 359.3 (found); IR (cm^{-1}): 3377, 3083, 3058, 3038, 2960, 2924, 2869, 2802, 1588, 1504, 1487, 1460, 1451. The relative stereochemistry was determined by 2D-NOESY NMR.

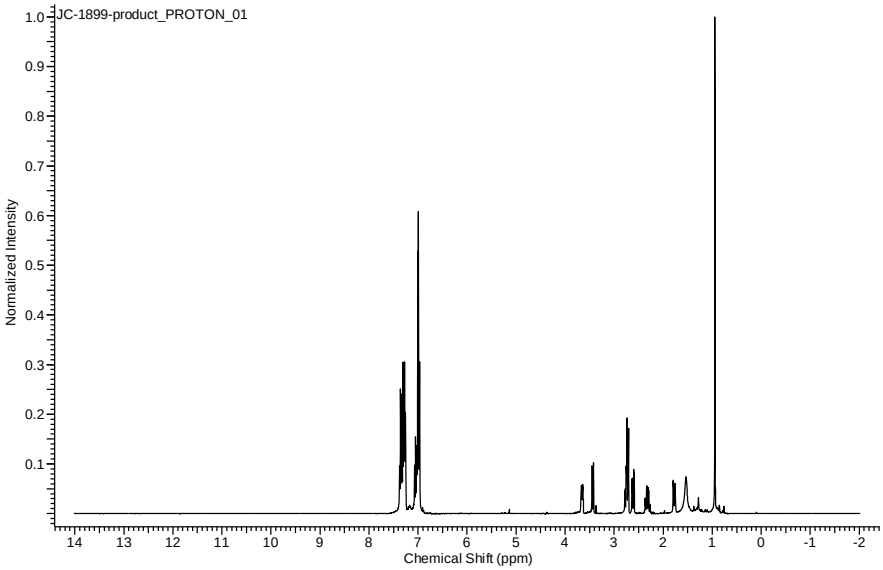

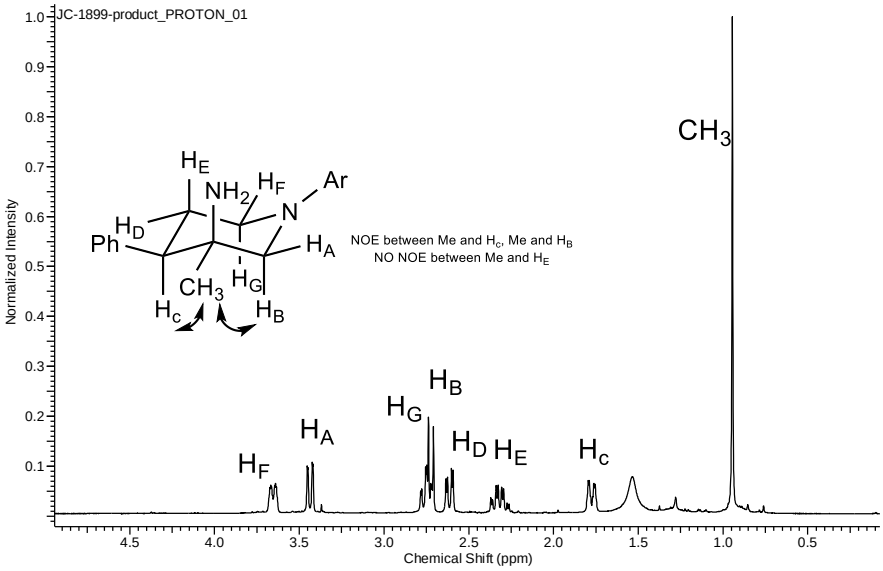

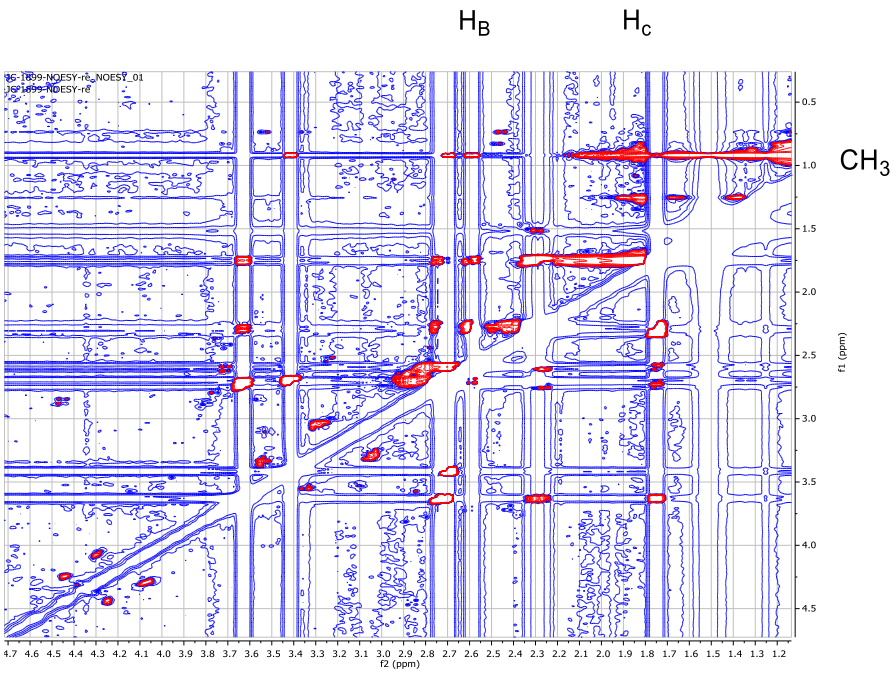
H_B
H_c
CH_3
f2 (ppm)
f1 (ppm)

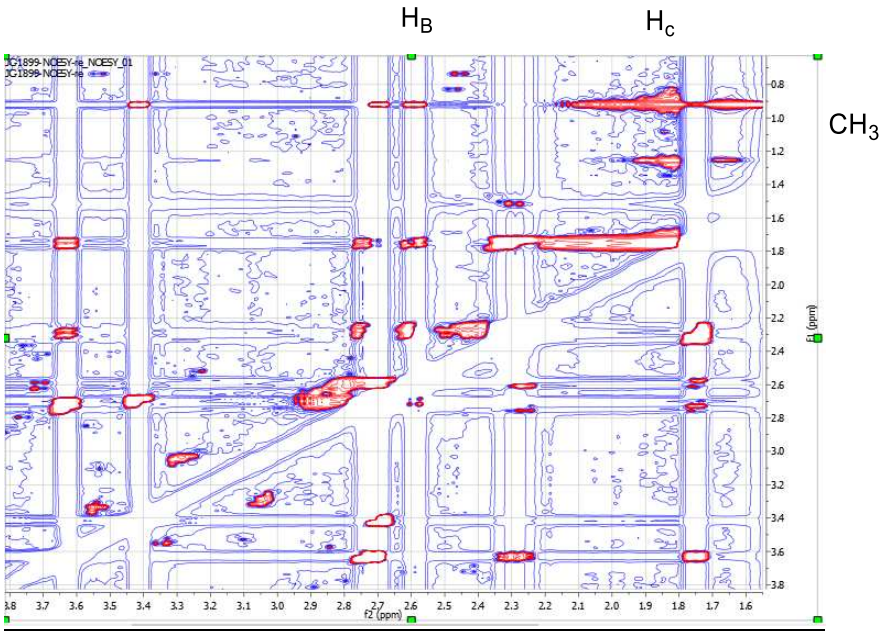
H_B
H_c
CH_3
f2 (ppm)
f1 (ppm)

A.1.11 Absolute Stereochemistry of Cycloadducts

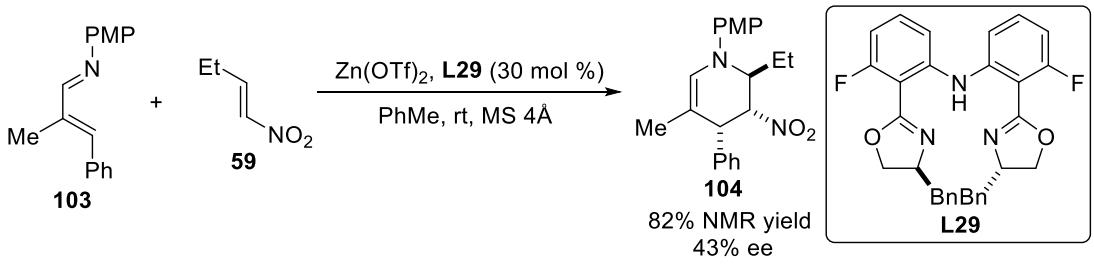

A solution of $Zn(OTf)_2$ (32.7 mg, 0.09 mmol, 30 mol %), and **L29** (46.4 mg, 0.09 mmol, 30 mol %) in PhMe (0.5 mL) in a vial was stirred at rt for 15 mins. A solution of the nitro-alkene **59** (151.7 mg, 1.50 mmol, 5 equiv.) in PhMe (0.5 mL) in a vial was added to the zinc complex. The vial containing nitro-alkene **59** was rinsed with 0.5 mL and then 0.2 mL PhMe to ensure complete transfer of the nitro-alkene **59**. 1-azadiene **103** (73.7 mg, 0.293 mmol, 1 equiv.) was added. After stirring at rt for overnight, the mixture was filtered through florisil. The yield was determined to be 82% by ^{1}H NMR of the crude mixture using 1,3,5-trimethoxybenzene as an internal standard. Pure [4+2] cycloadduct was obtained by flash chromatography (florisil as stationary phase). Its spectral properties are identical to those previously reported. Its optical rotation ($[\alpha] = +198.6^o$, $CHCl_3$, c=1.04) is consistent with that of reported for the absolute structure drawn above[19] ($[\alpha]= +381.7^o$, $CHCl_3$, c=1.0, 99% ee). The absolute stereochemistry is also consistent from that obtained from previously reported asymmetric Michael addition of other nucleophiles to nitro-alkenes with the same antipode of Zn-BOPA complexes.[1b,1c,20]

A.1.12 NMR Spectra

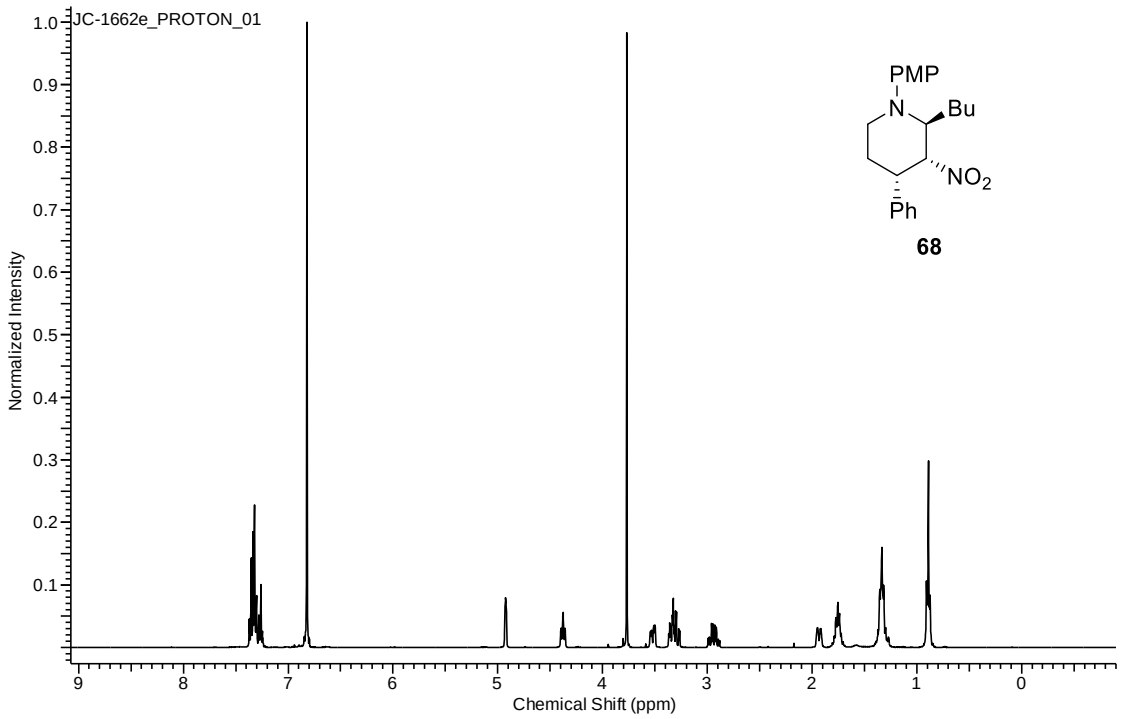

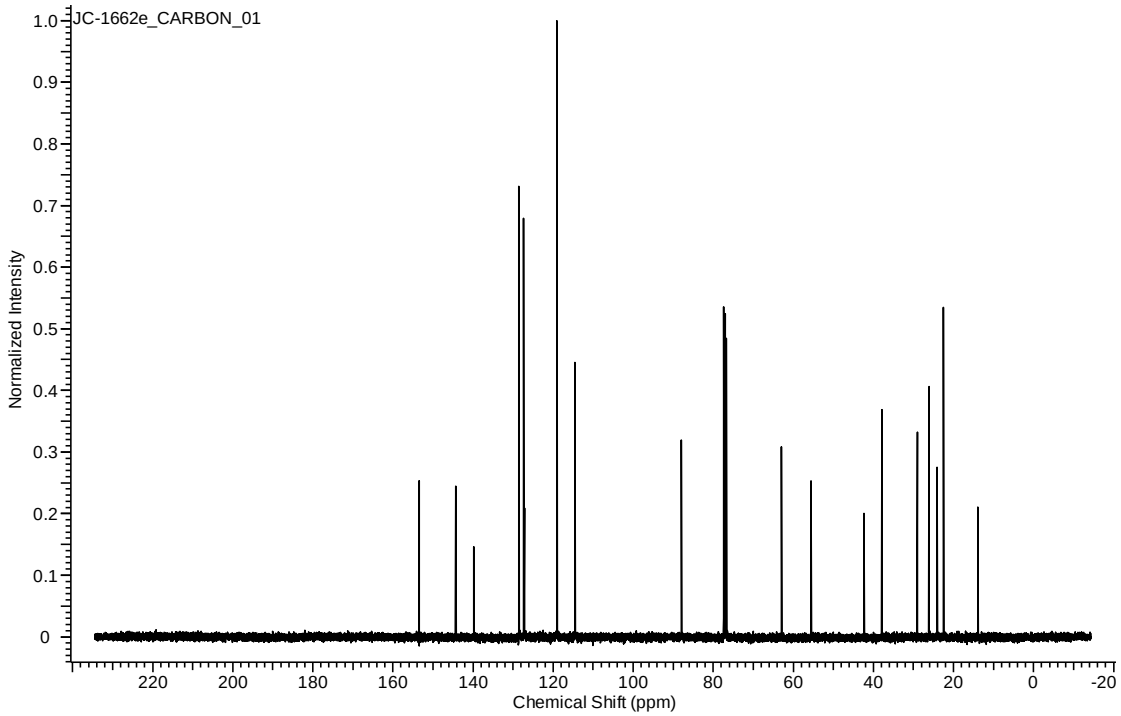

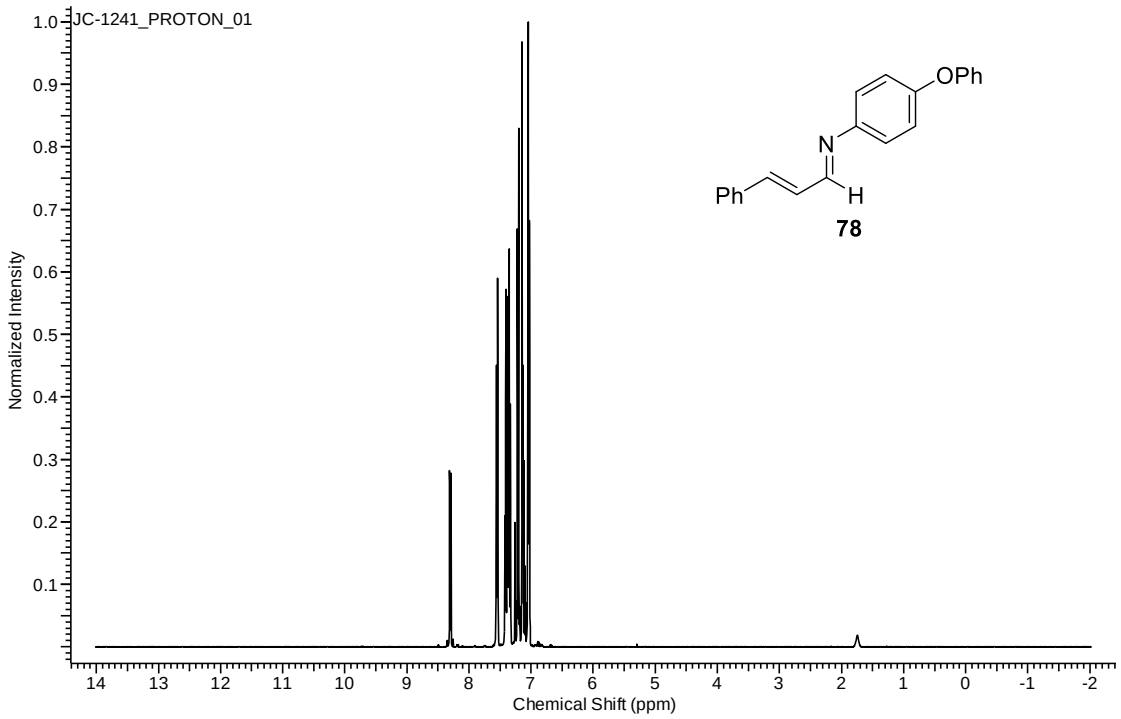
JC-1241_PROTON_01
Normalized Intensity
Chemical Shift (ppm)
OPh
N
H
Ph
78

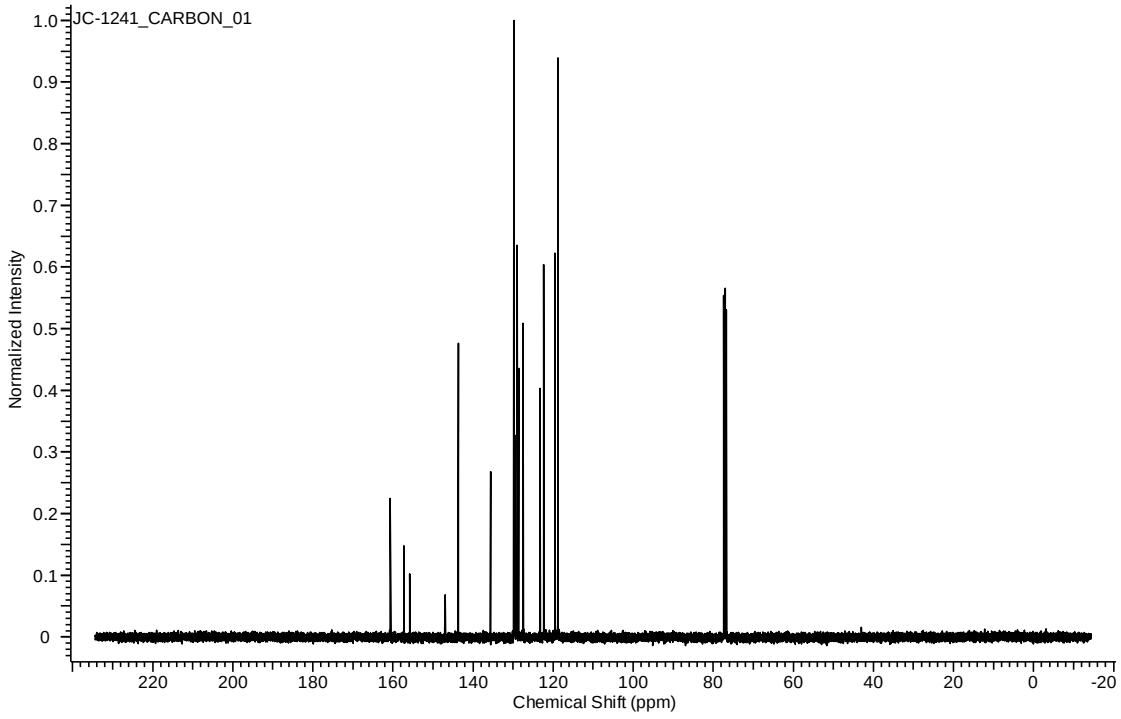
JC-1241_CARBON_01
Normalized Intensity
Chemical Shift (ppm)

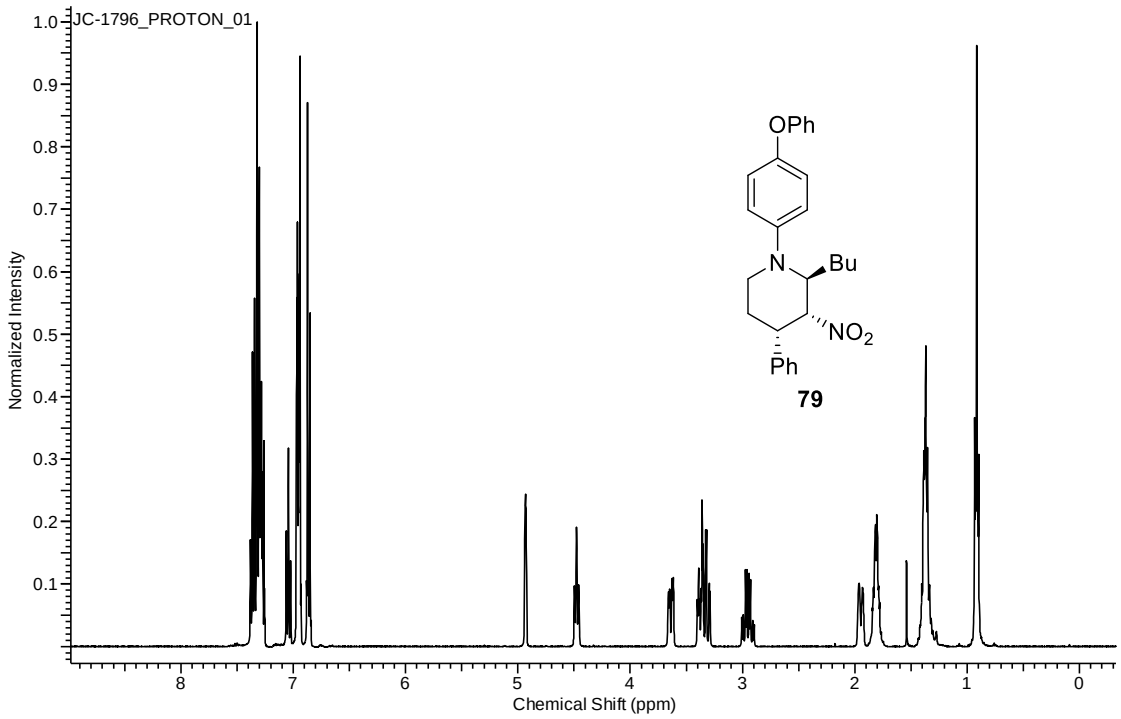
JC-1796_PROTON_01
Normalized Intensity
Chemical Shift (ppm)
OPh
N
Bu
NO2
Ph
79

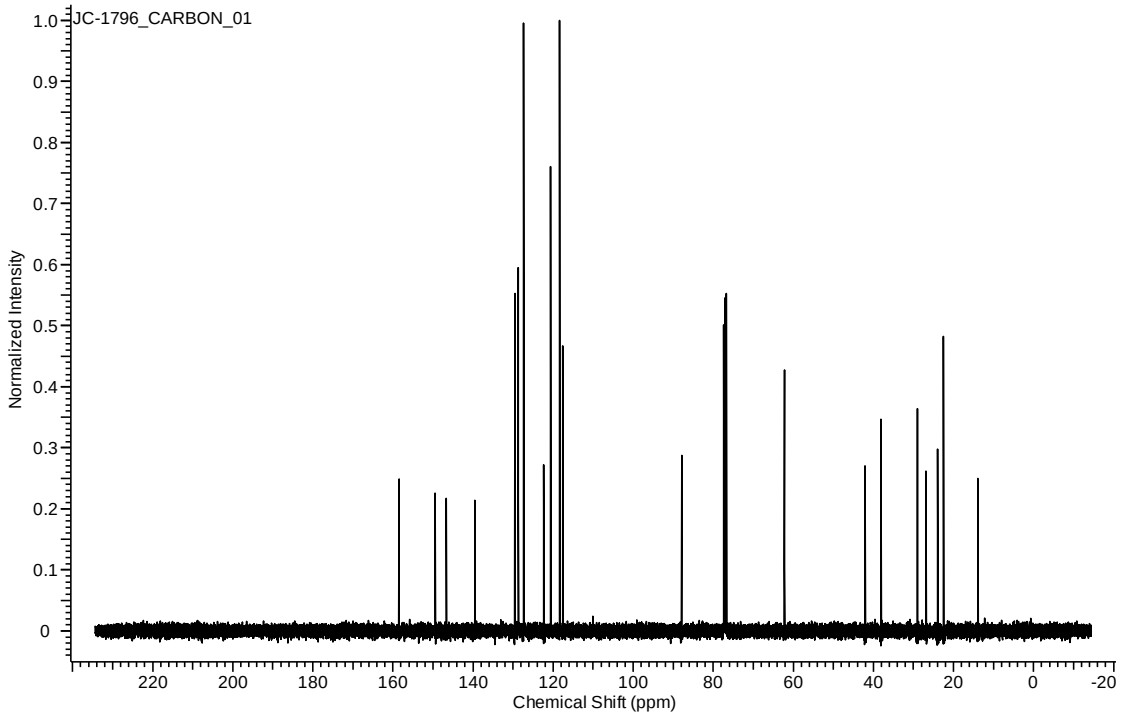
JC-1796_CARBON_01
Normalized Intensity
Chemical Shift (ppm)

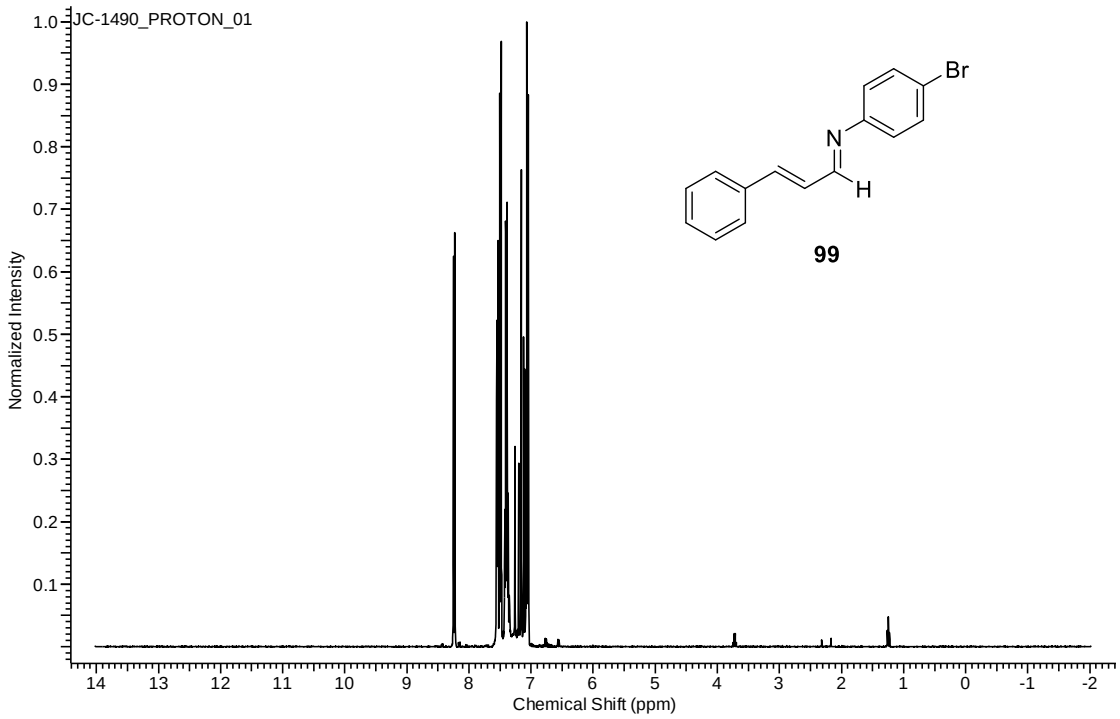
JC-1490_PROTON_01
Normalized Intensity
Chemical Shift (ppm)
Br
N
H
99

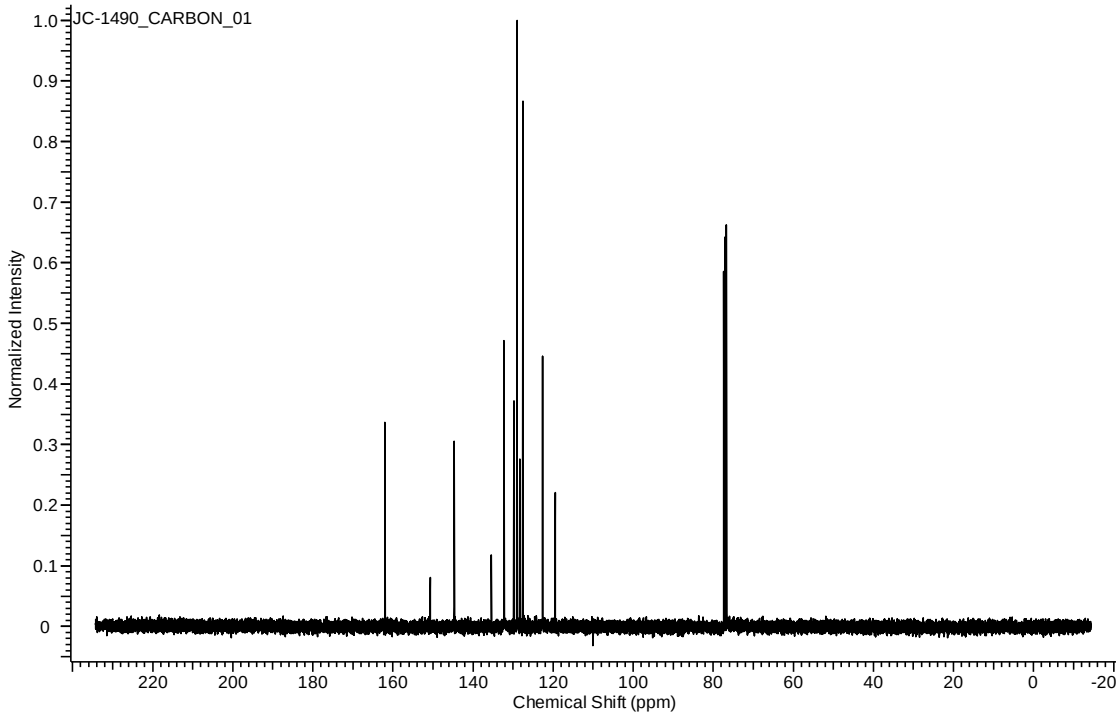
JC-1490_CARBON_01
Normalized Intensity
Chemical Shift (ppm)

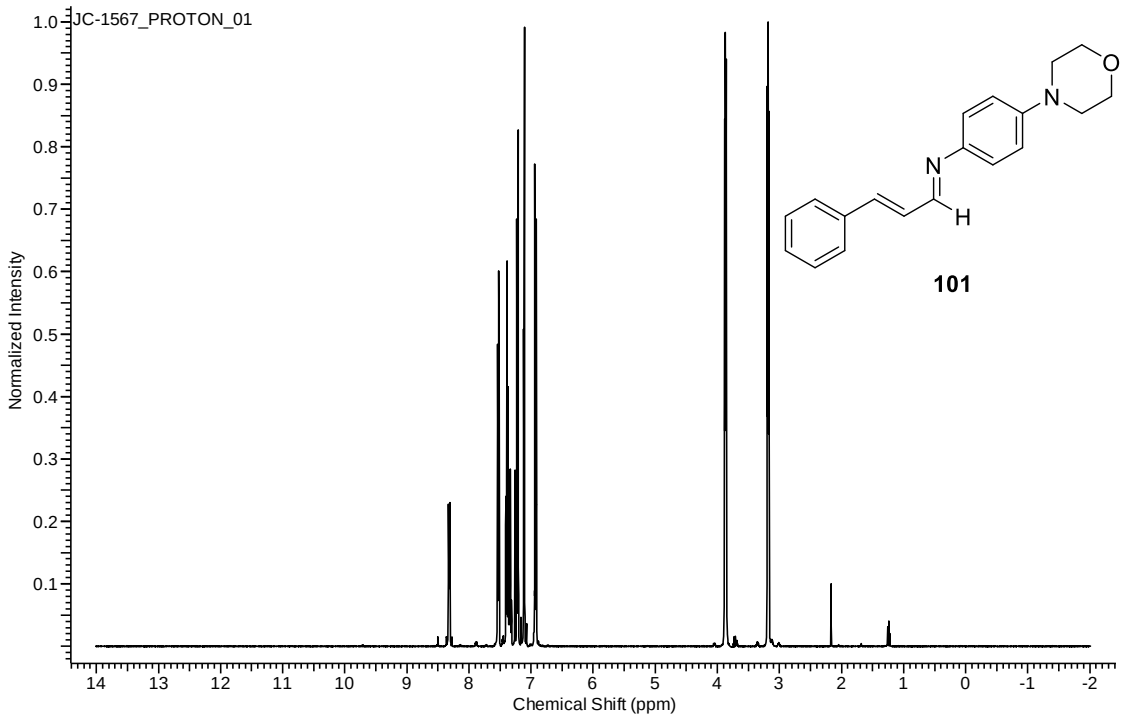
JC-1567_PROTON_01
Normalized Intensity
Chemical Shift (ppm)
O
N
N
H
101

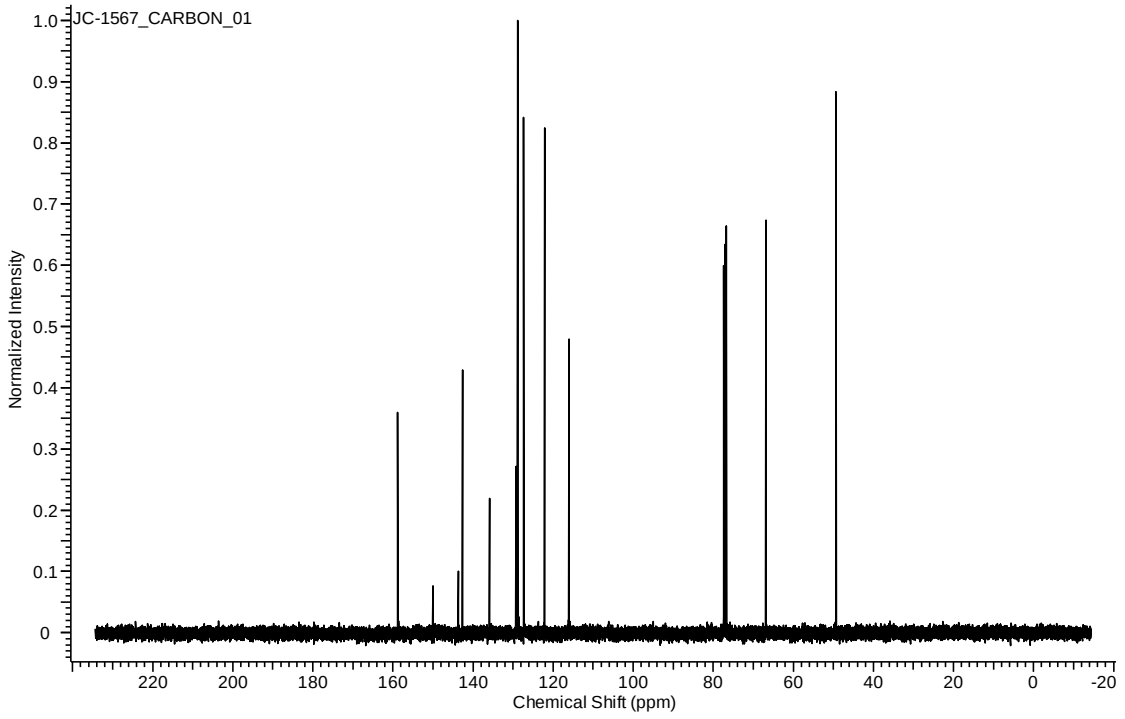
JC-1567_CARBON_01
Normalized Intensity
Chemical Shift (ppm)

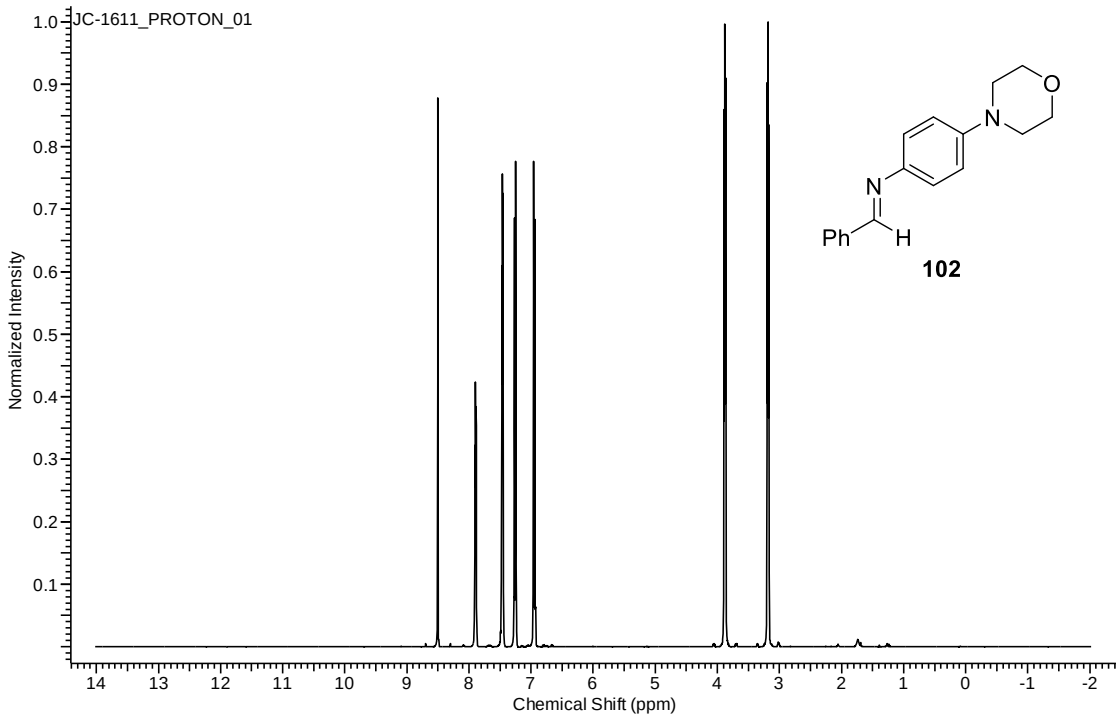
JC-1611_PROTON_01
Normalized Intensity
Chemical Shift (ppm)
O
N
N
Ph
H
102

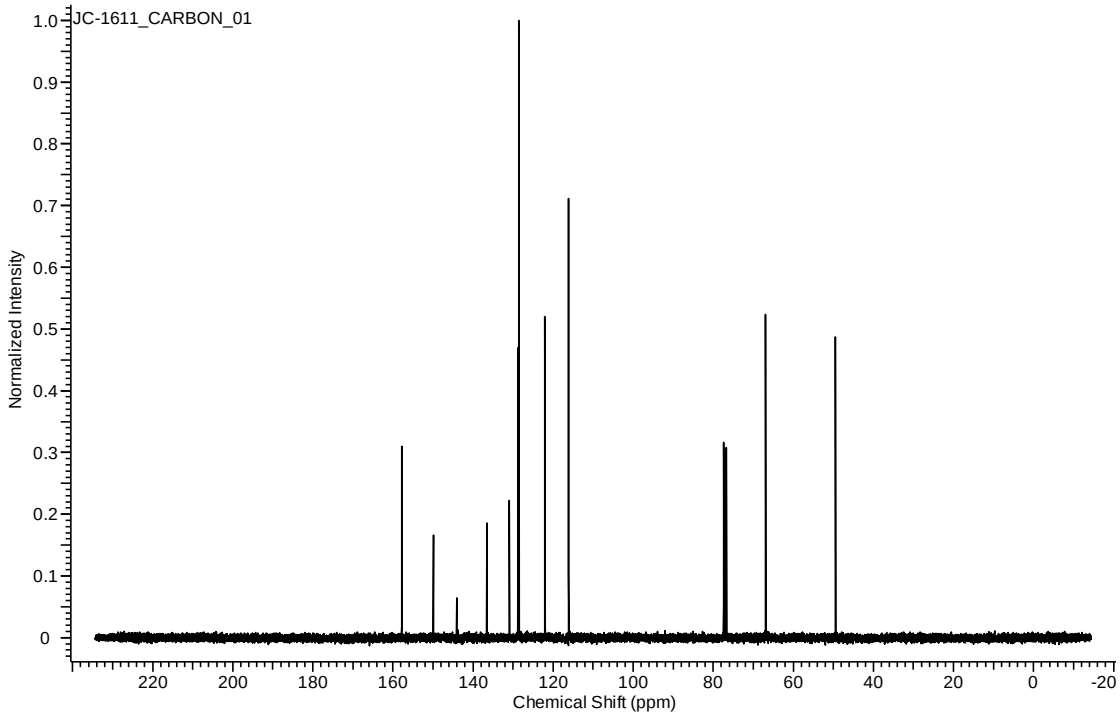
JC-1611_CARBON_01
Normalized Intensity
Chemical Shift (ppm)

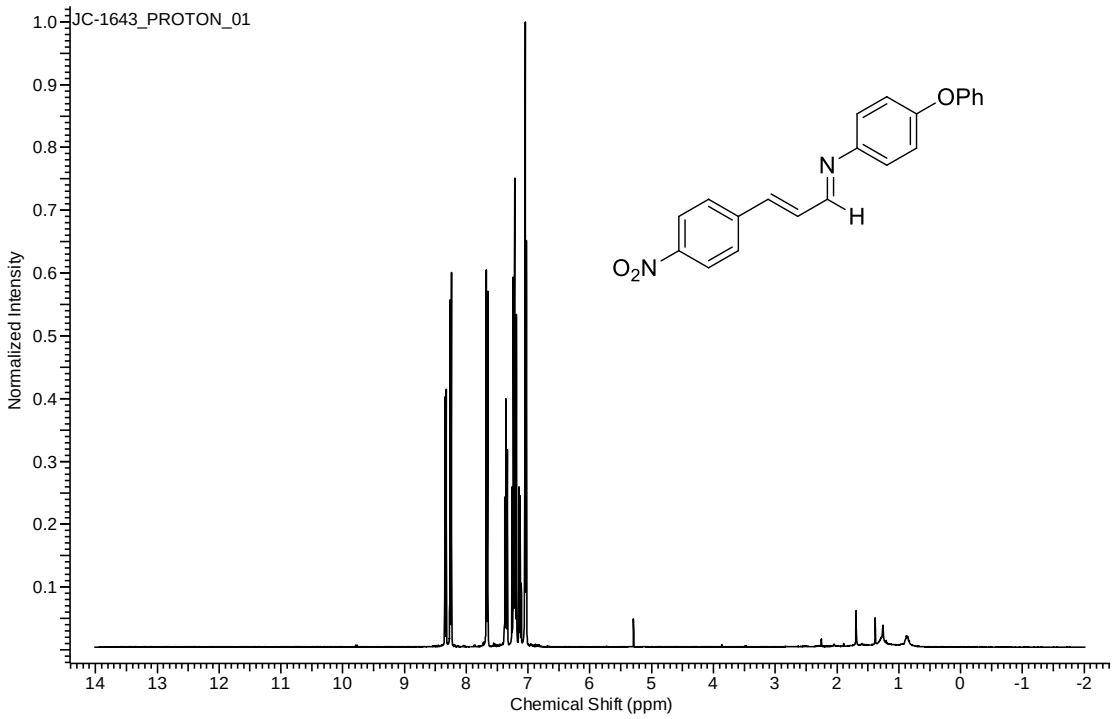
JC-1643_PROTON_01
Normalized Intensity
Chemical Shift (ppm)
OPh
N
H
O2N

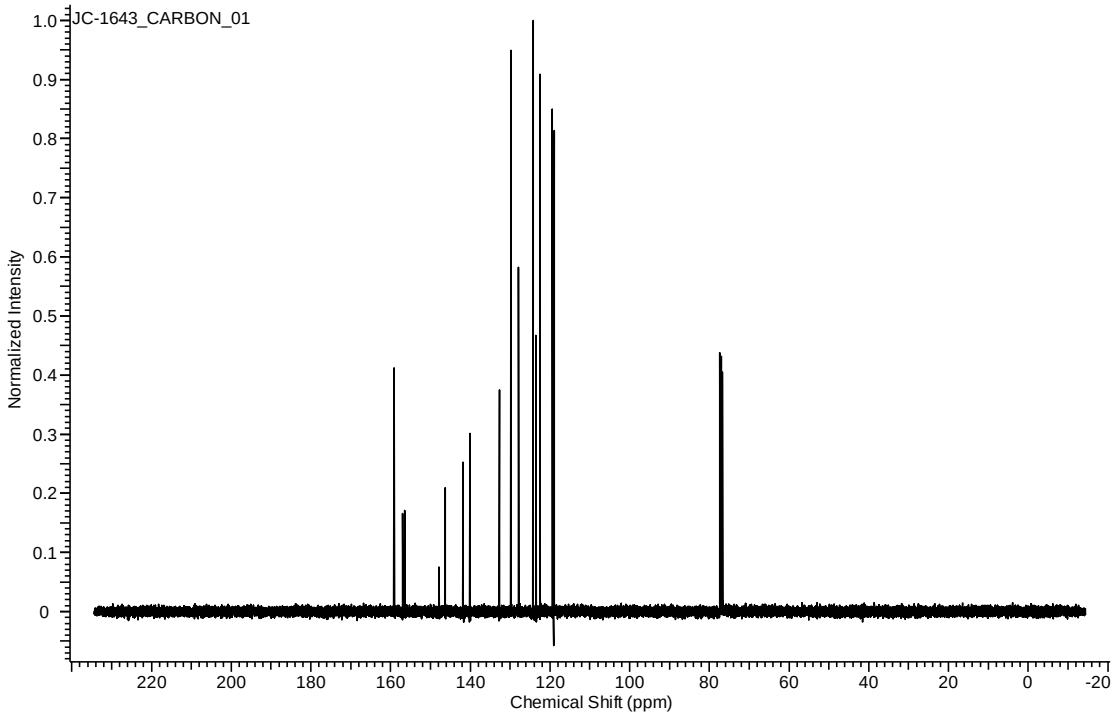
JC-1643_CARBON_01
Normalized Intensity
Chemical Shift (ppm)

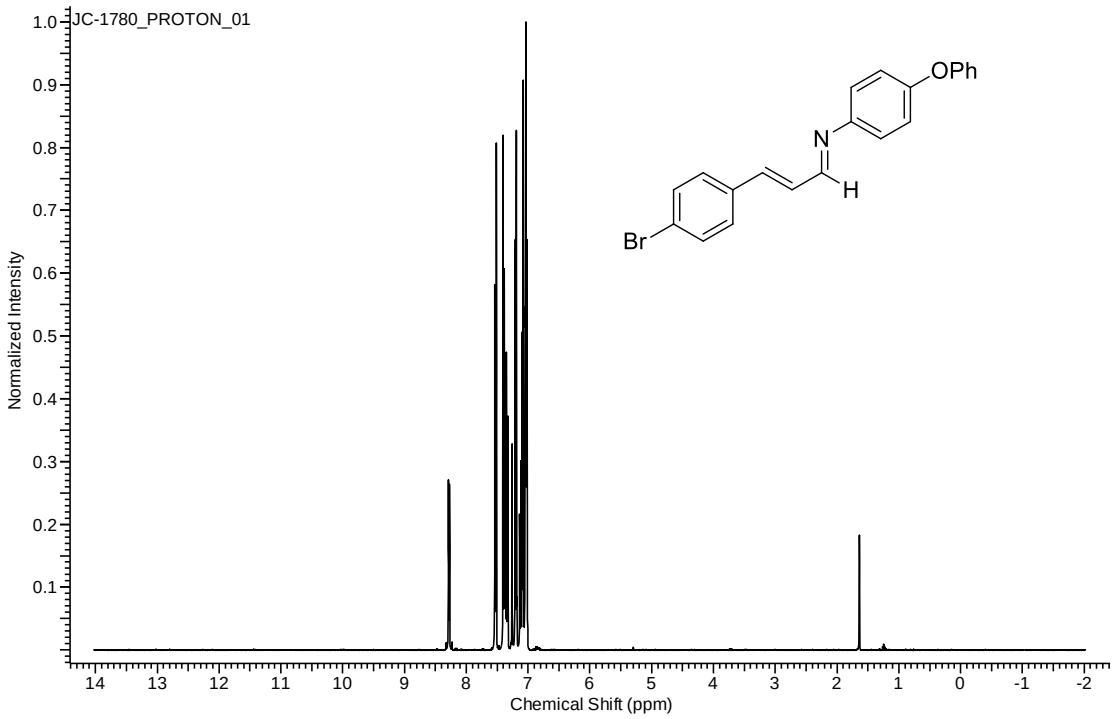
JC-1780_PROTON_01
Normalized Intensity
Chemical Shift (ppm)
OPh
N
H
Br

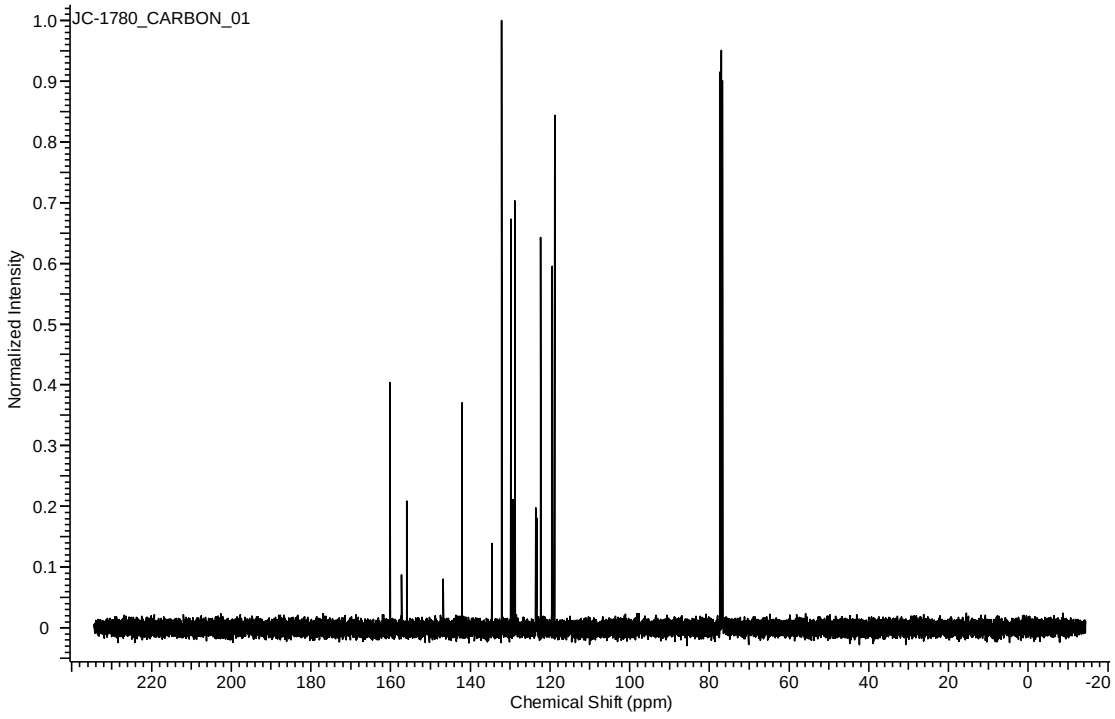
JC-1780_CARBON_01
Normalized Intensity
Chemical Shift (ppm)

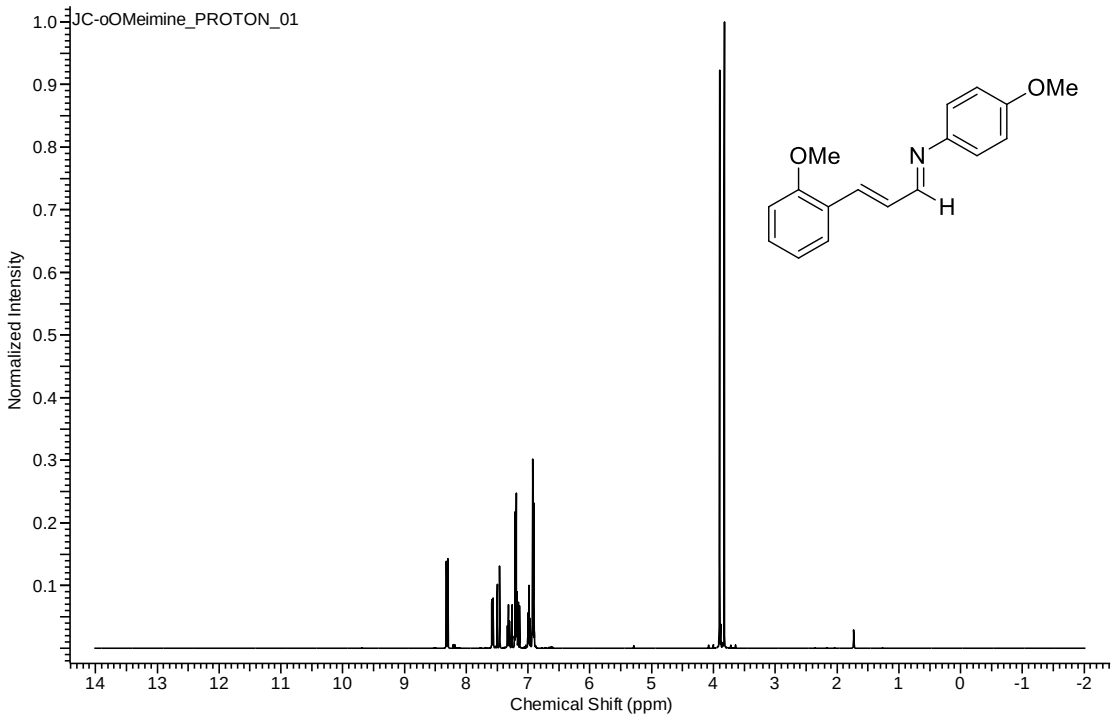
JC-oOMeimine_PROTON_01
Normalized Intensity
Chemical Shift (ppm)
OMe
N
H
OMe

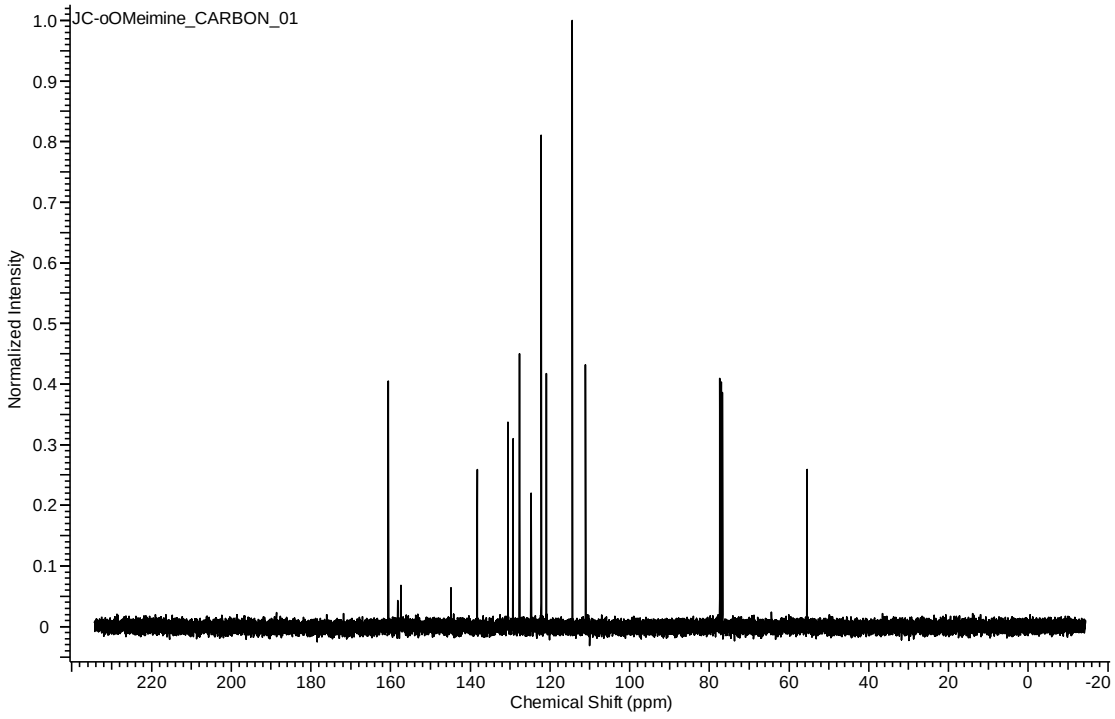
JC-oOMeimine_CARBON_01
Normalized Intensity
Chemical Shift (ppm)

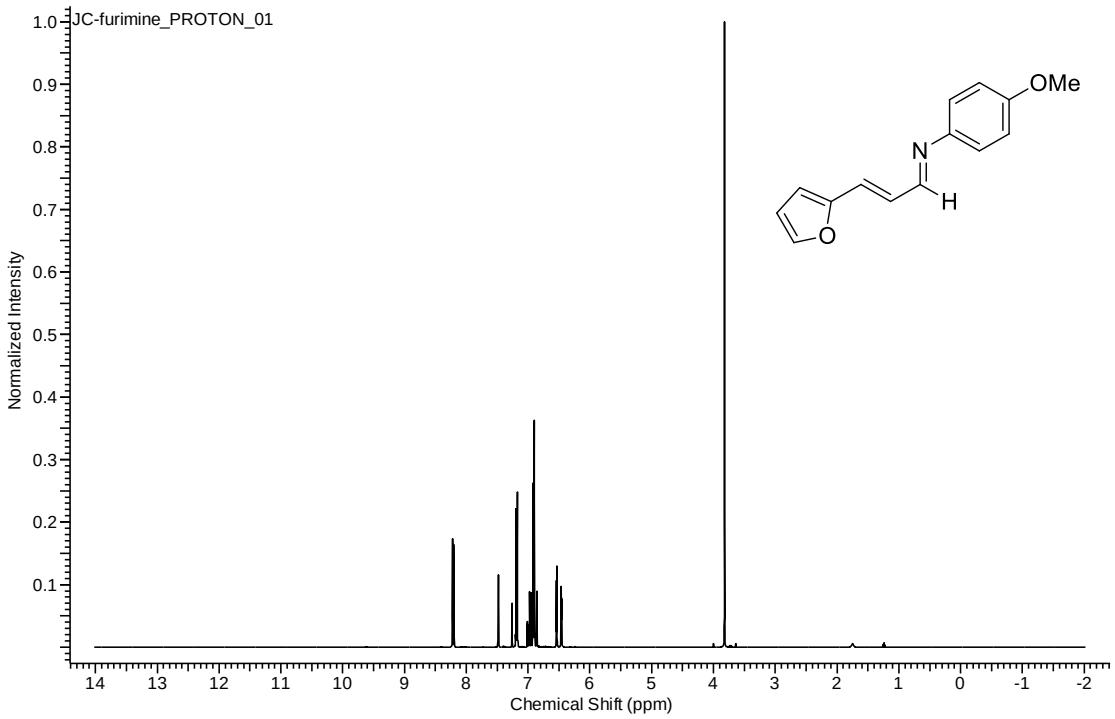
JC-furimine_PROTON_01
Normalized Intensity
Chemical Shift (ppm)
OMe
N
H
O

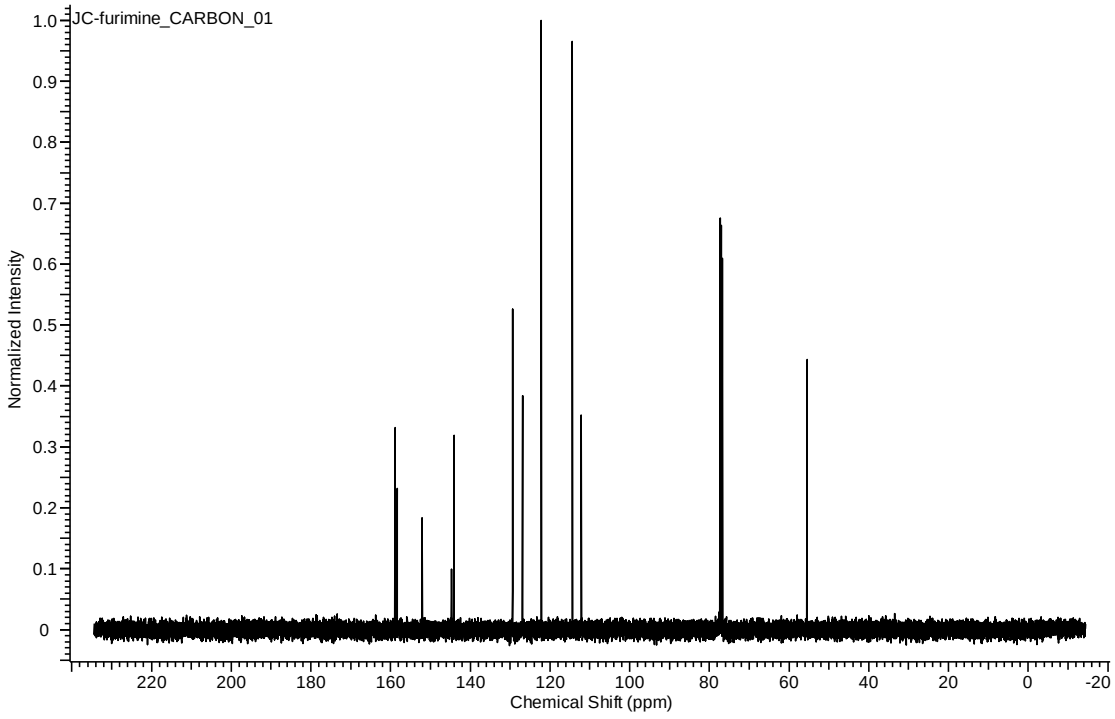
JC-furimine_CARBON_01
Normalized Intensity
Chemical Shift (ppm)

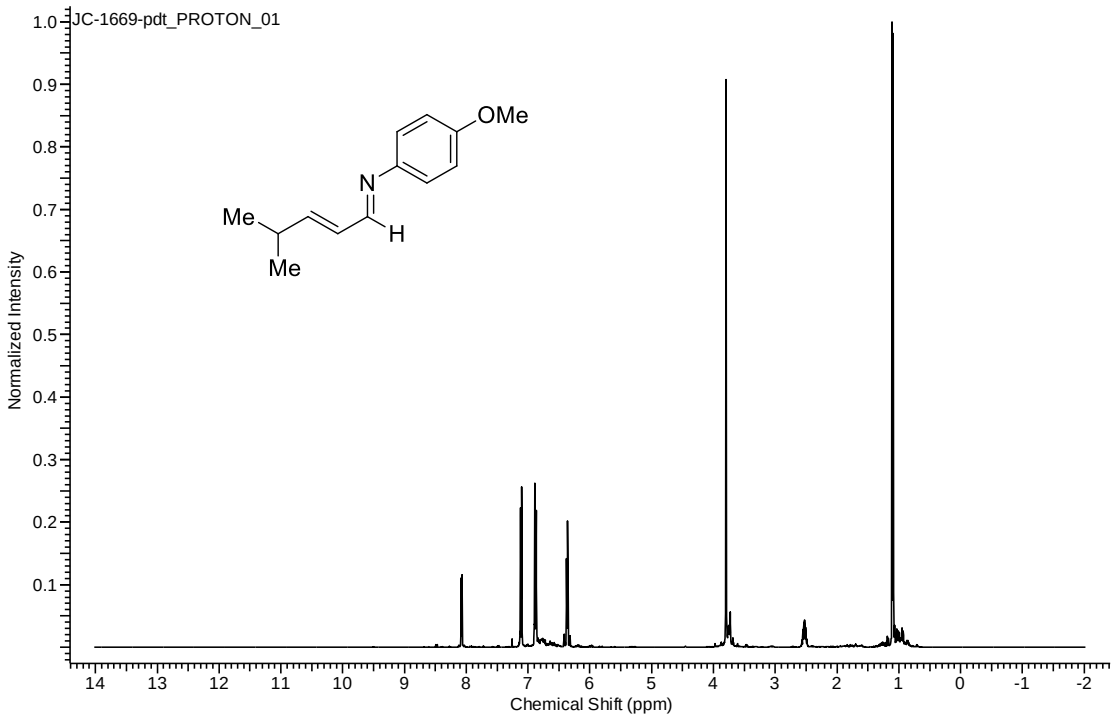
JC-1669-pdt_PROTON_01
OMe
N
H
Me
Me
Normalized Intensity
Chemical Shift (ppm)

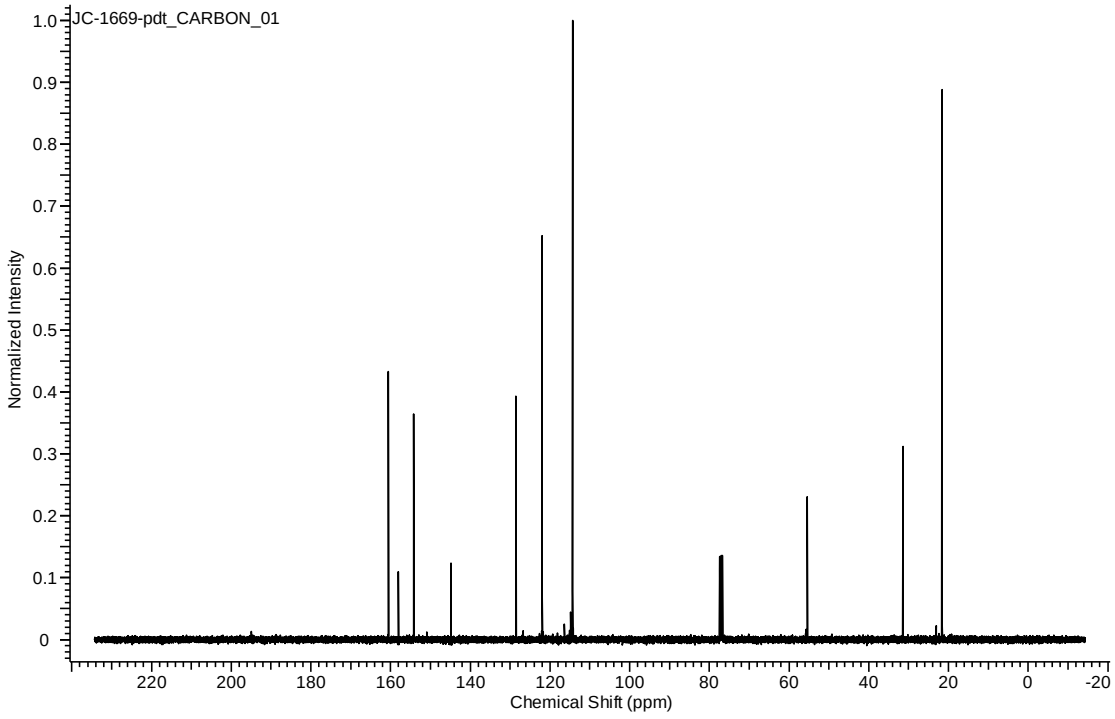
JC-1669-pdt_CARBON_01
Normalized Intensity
Chemical Shift (ppm)

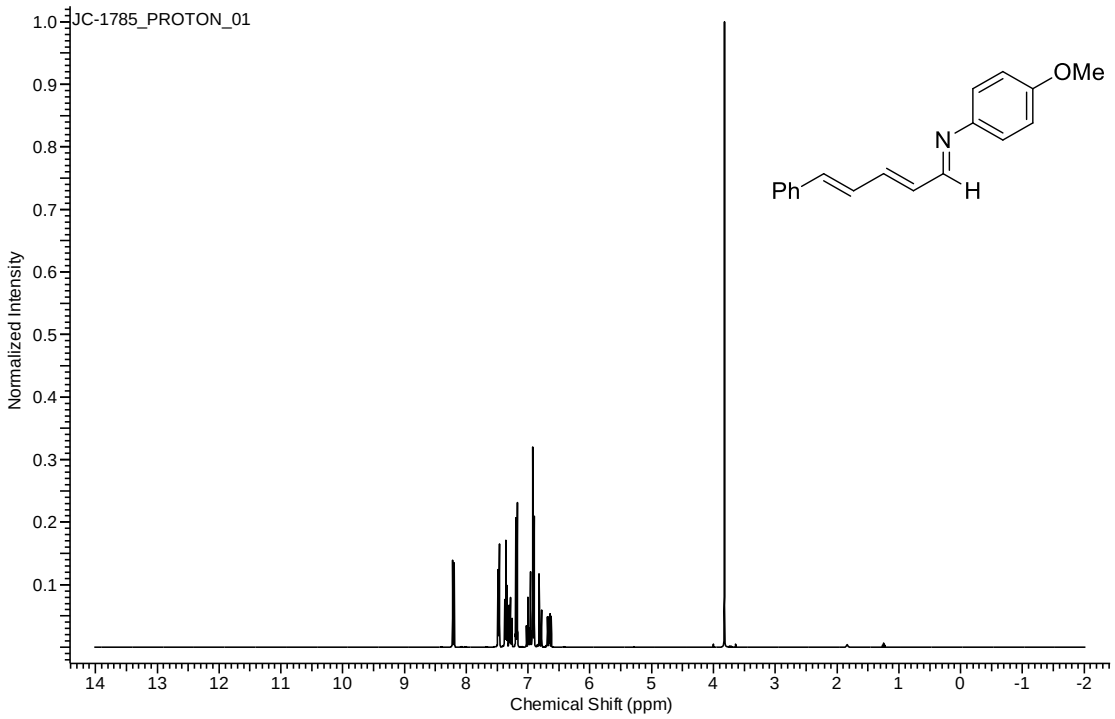
JC-1785_PROTON_01
Normalized Intensity
Chemical Shift (ppm)
OMe
N
Ph
H

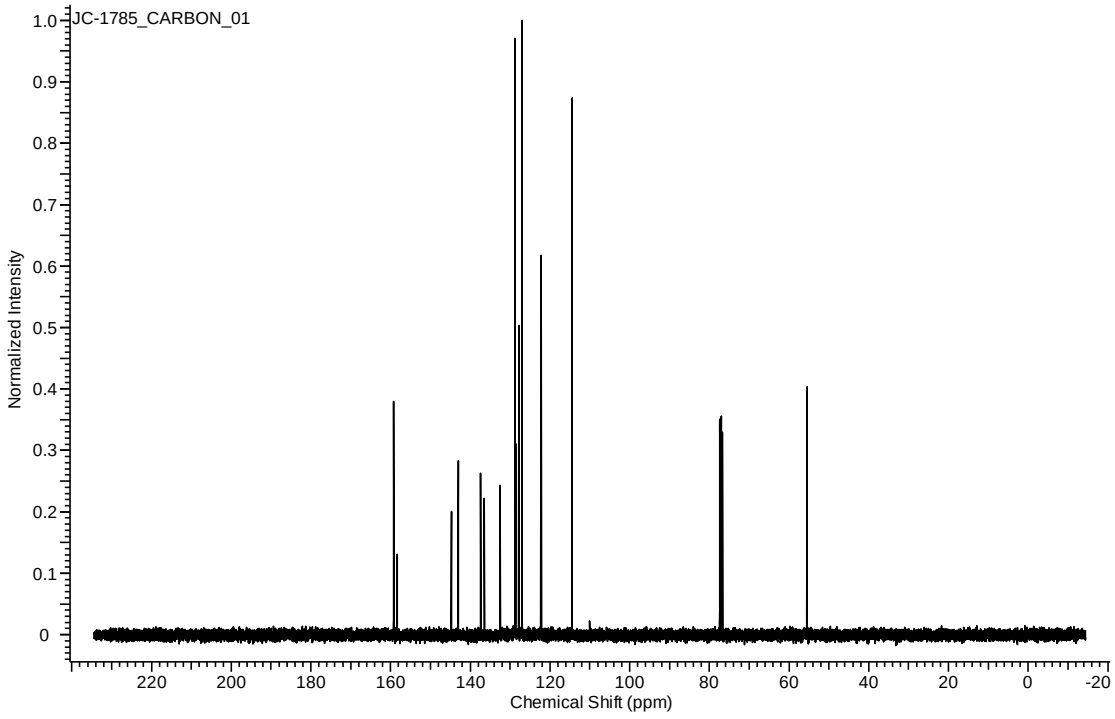
JC-1785_CARBON_01
Normalized Intensity
Chemical Shift (ppm)

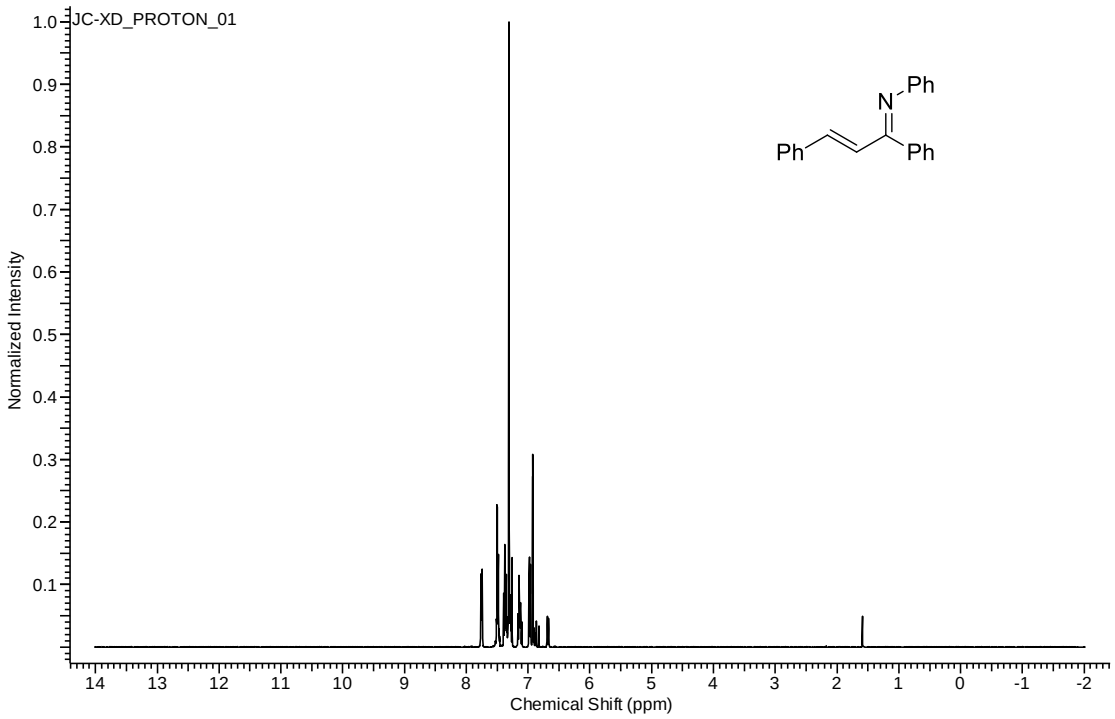
JC-XD_PROTON_01
Normalized Intensity
Chemical Shift (ppm)
N
Ph
Ph
Ph

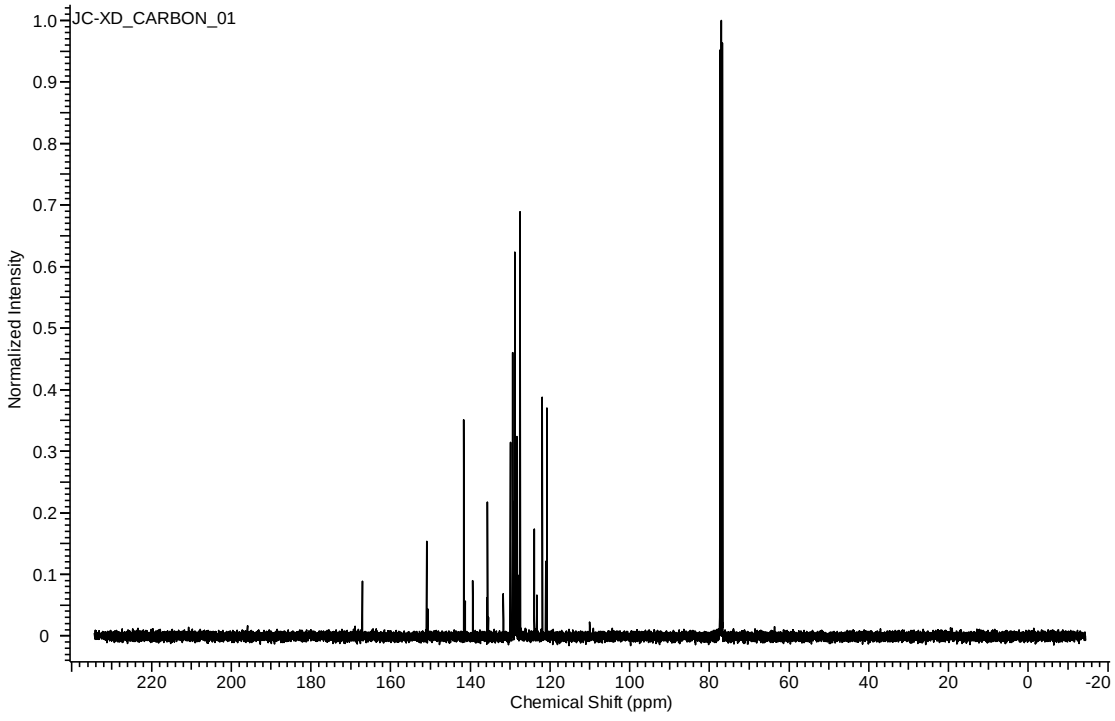
JC-XD_CARBON_01
Normalized Intensity
Chemical Shift (ppm)

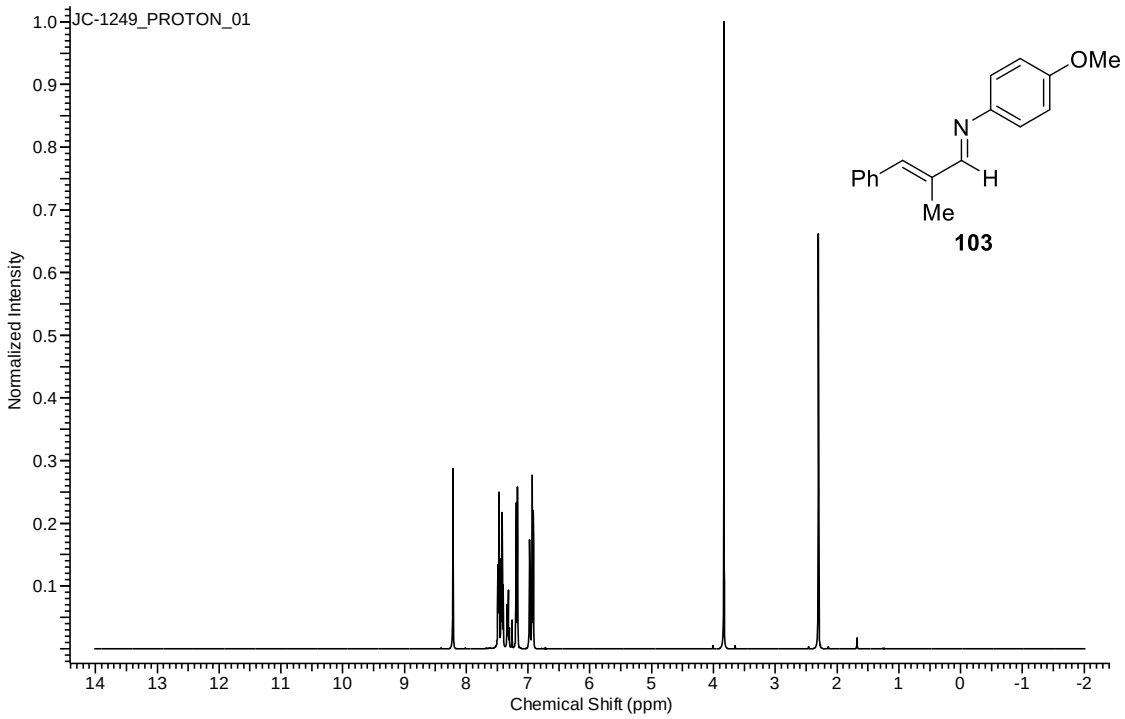
JC-1249_PROTON_01
Normalized Intensity
Chemical Shift (ppm)
OMe
N
Ph
H
Me
103

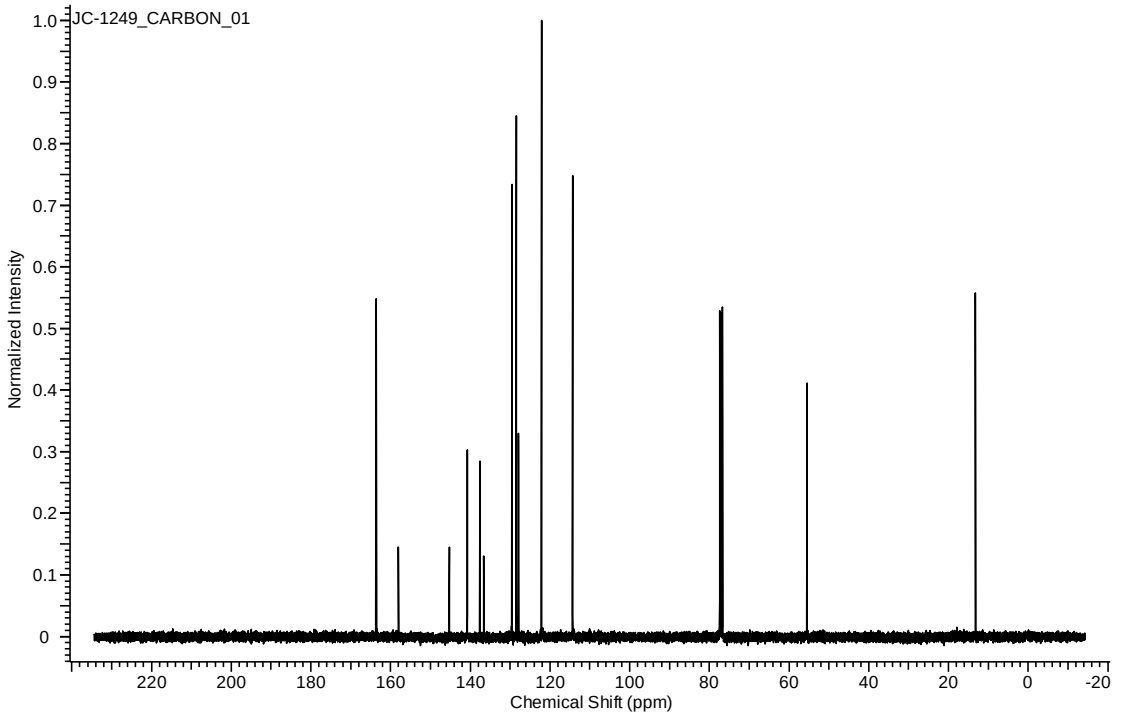
JC-1249_CARBON_01
Normalized Intensity
Chemical Shift (ppm)

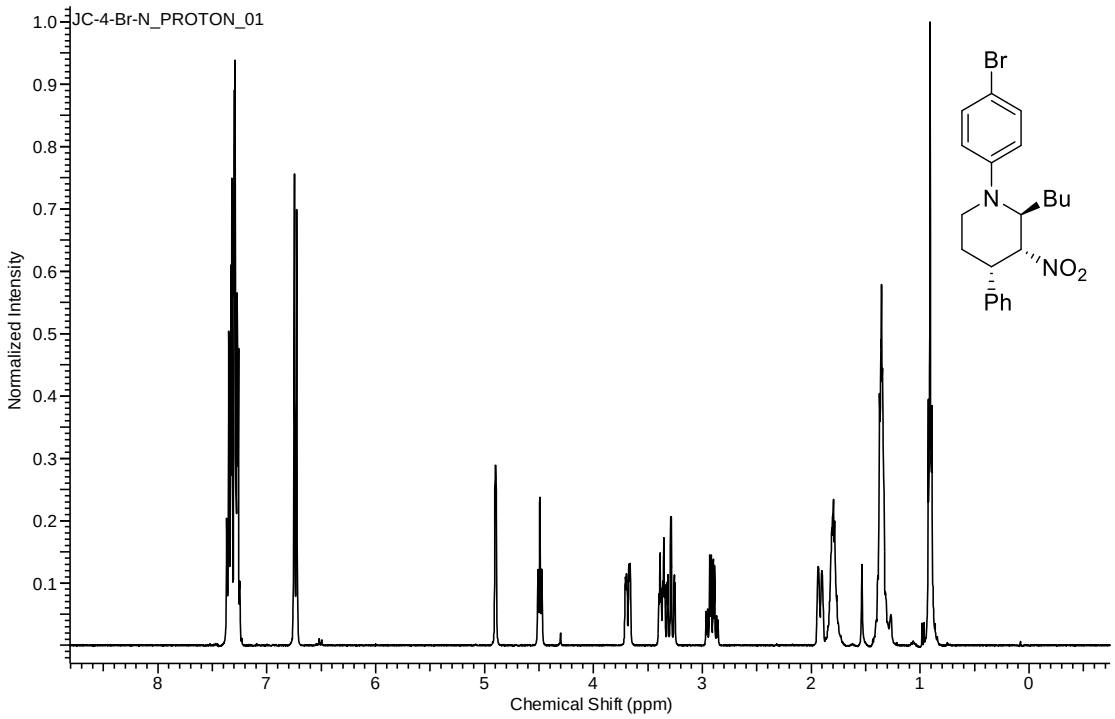
JC-4-Br-N_PROTON_01
Normalized Intensity
Chemical Shift (ppm)
Br
N
Bu
NO2
Ph

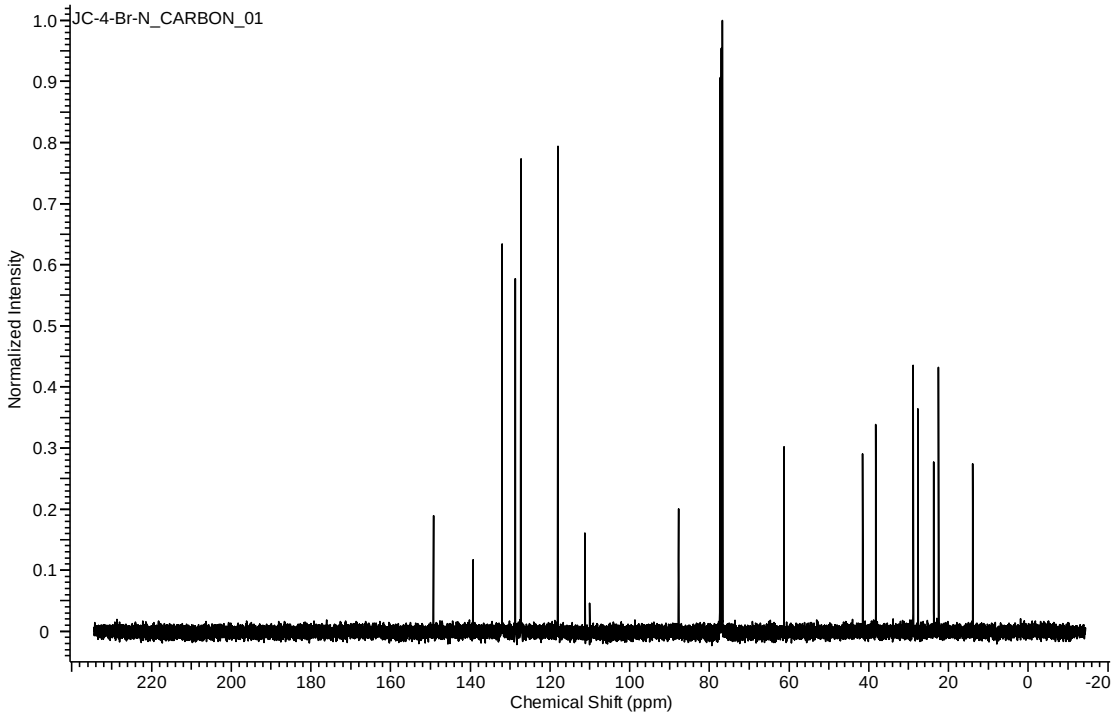
JC-4-Br-N_CARBON_01
Normalized Intensity
Chemical Shift (ppm)

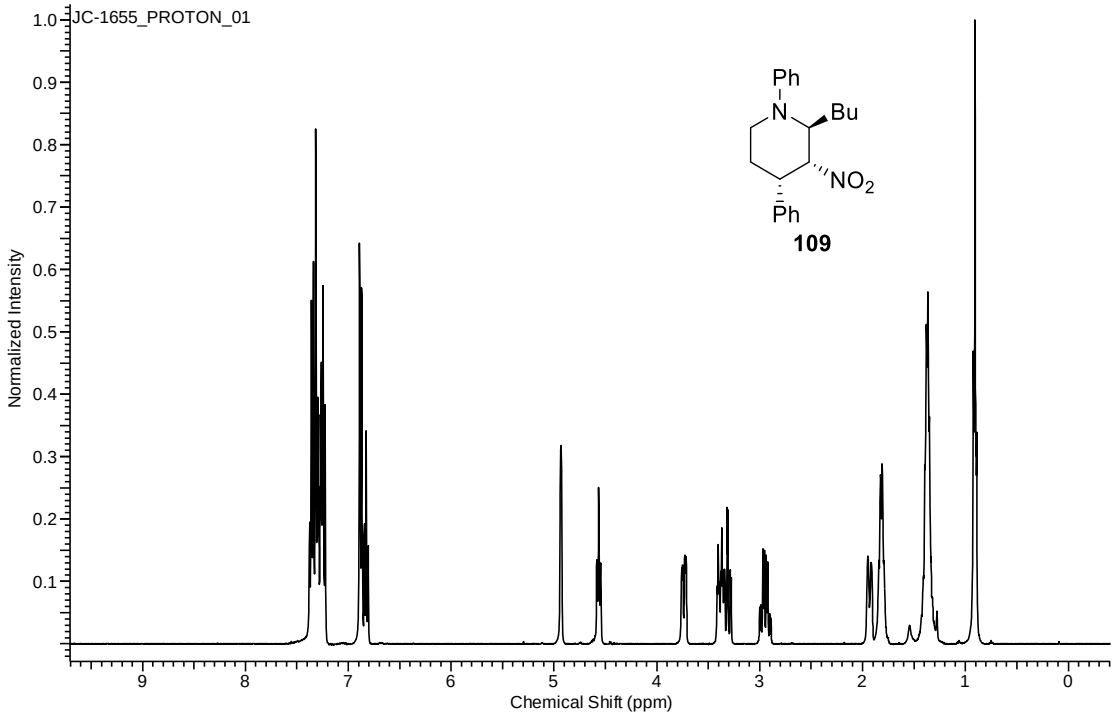
JC-1655_PROTON_01
Normalized Intensity
Chemical Shift (ppm)
Ph
N
Bu
NO2
Ph
109

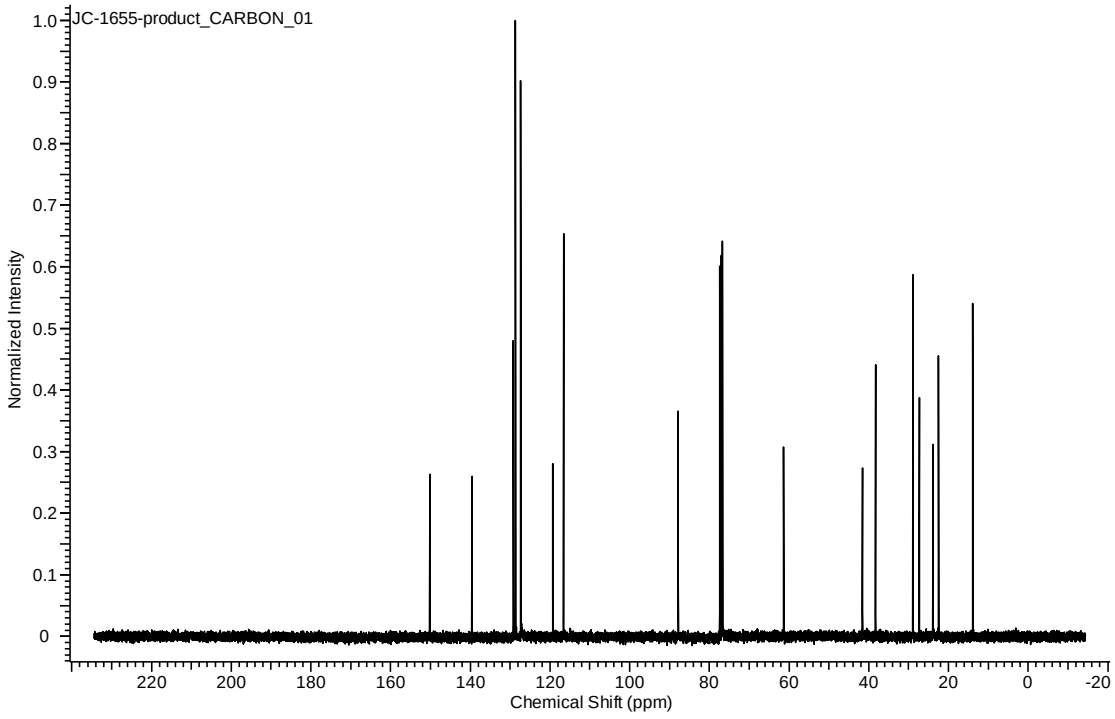
JC-1655-product_CARBON_01
Normalized Intensity
Chemical Shift (ppm)

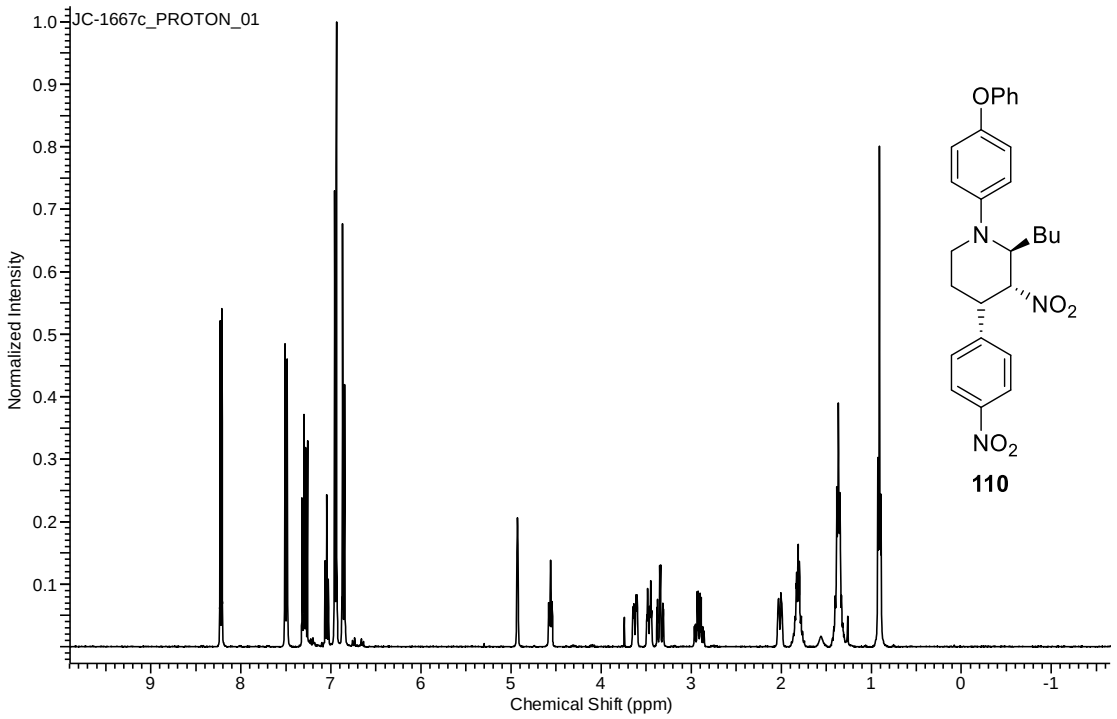
JC-1667c_PROTON_01
Normalized Intensity
Chemical Shift (ppm)
OPh
N
Bu
NO2
NO2
110

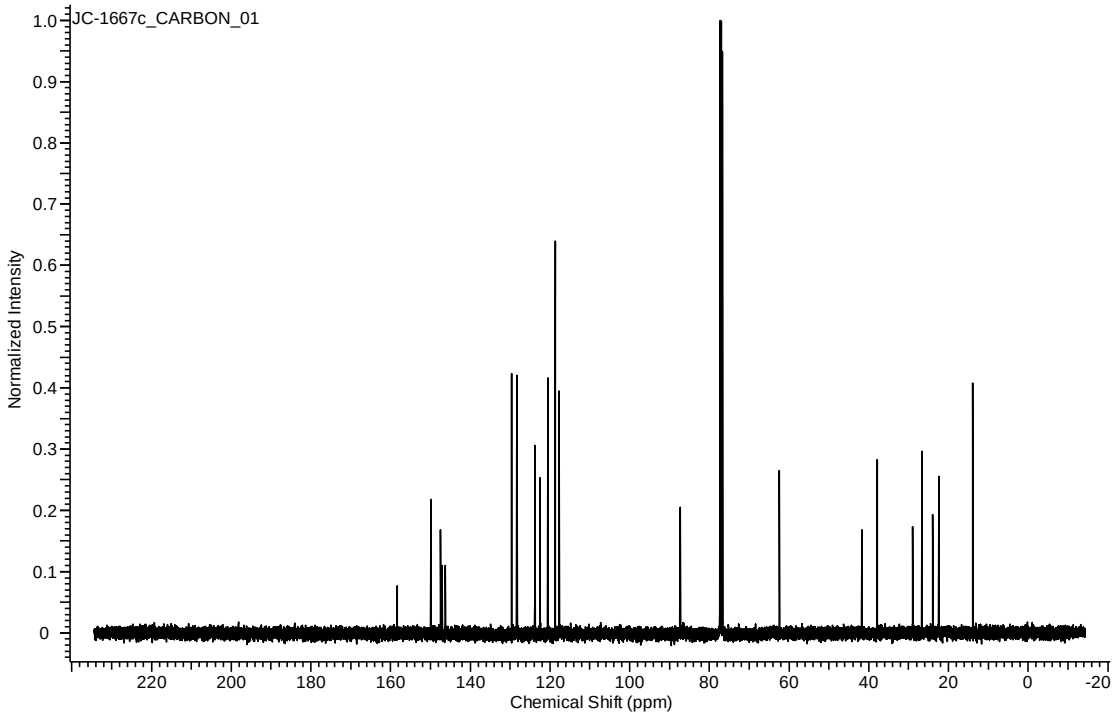
JC-1667c_CARBON_01
Normalized Intensity
Chemical Shift (ppm)

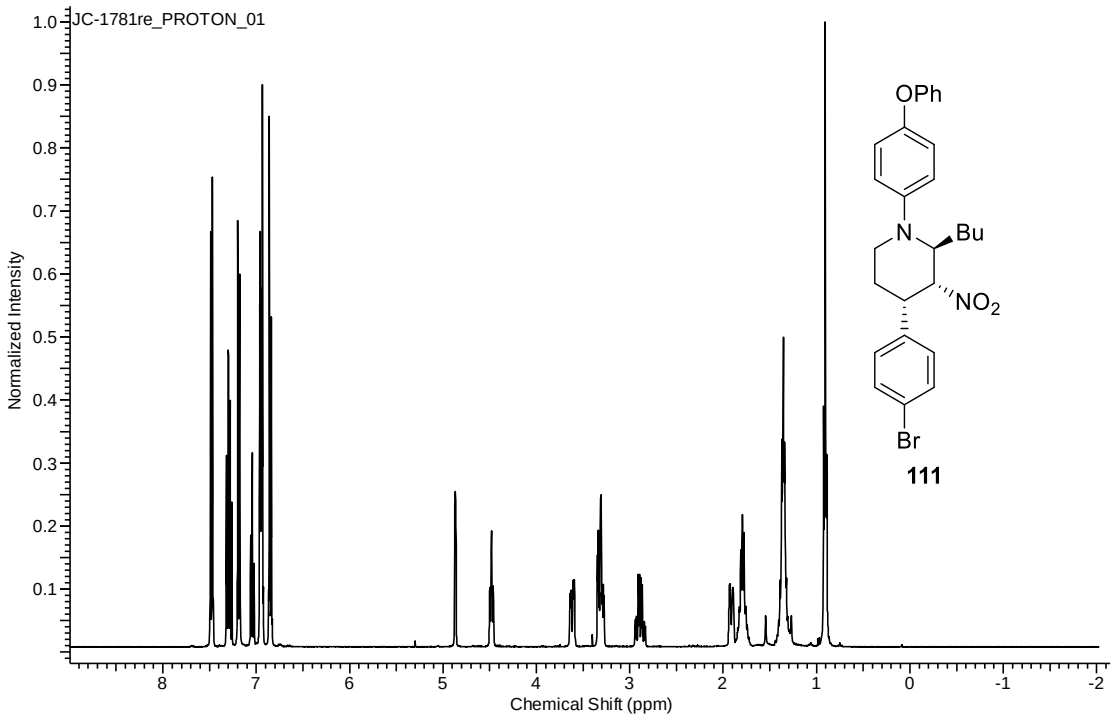
JC-1781re_PROTON_01
Normalized Intensity
Chemical Shift (ppm)
OPh
N
Bu
NO2
Br
111

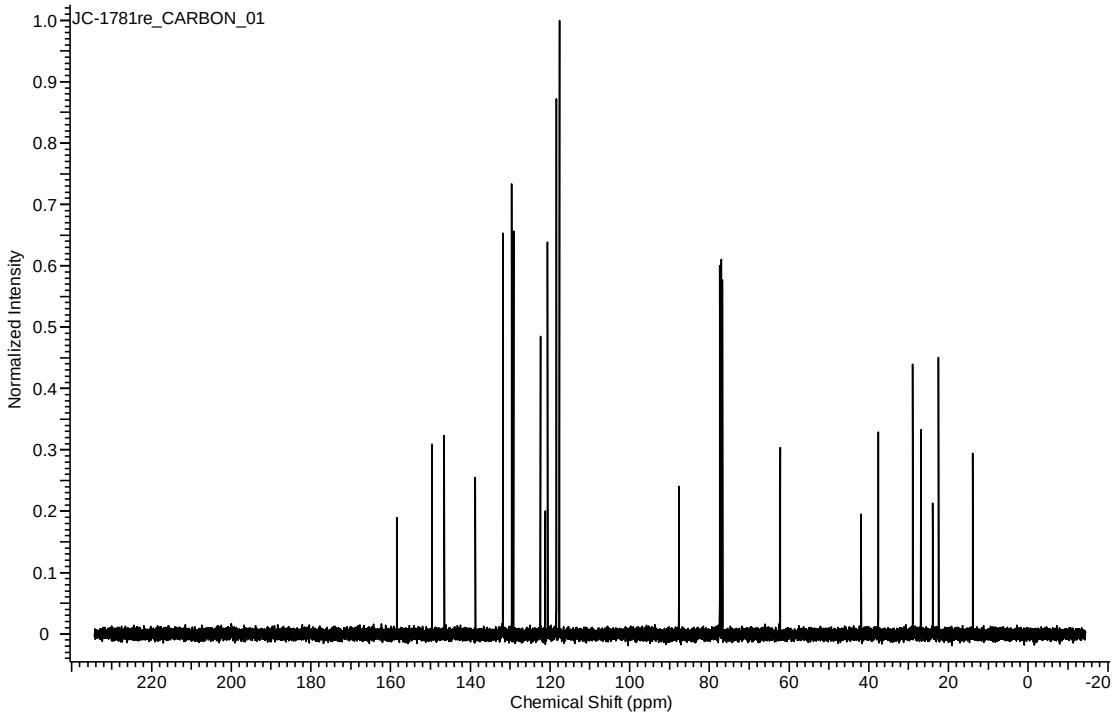
JC-1781re_CARBON_01
Normalized Intensity
Chemical Shift (ppm)

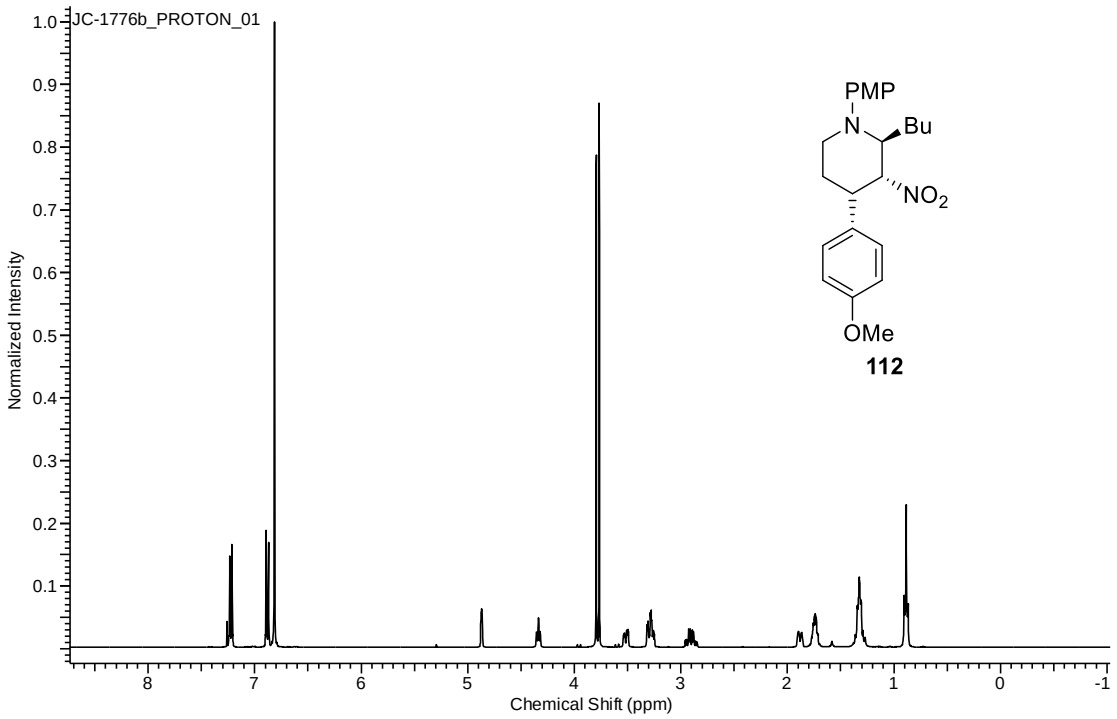
JC-1776b_PROTON_01
Normalized Intensity
Chemical Shift (ppm)
PMP
N
Bu
NO2
OMe
112

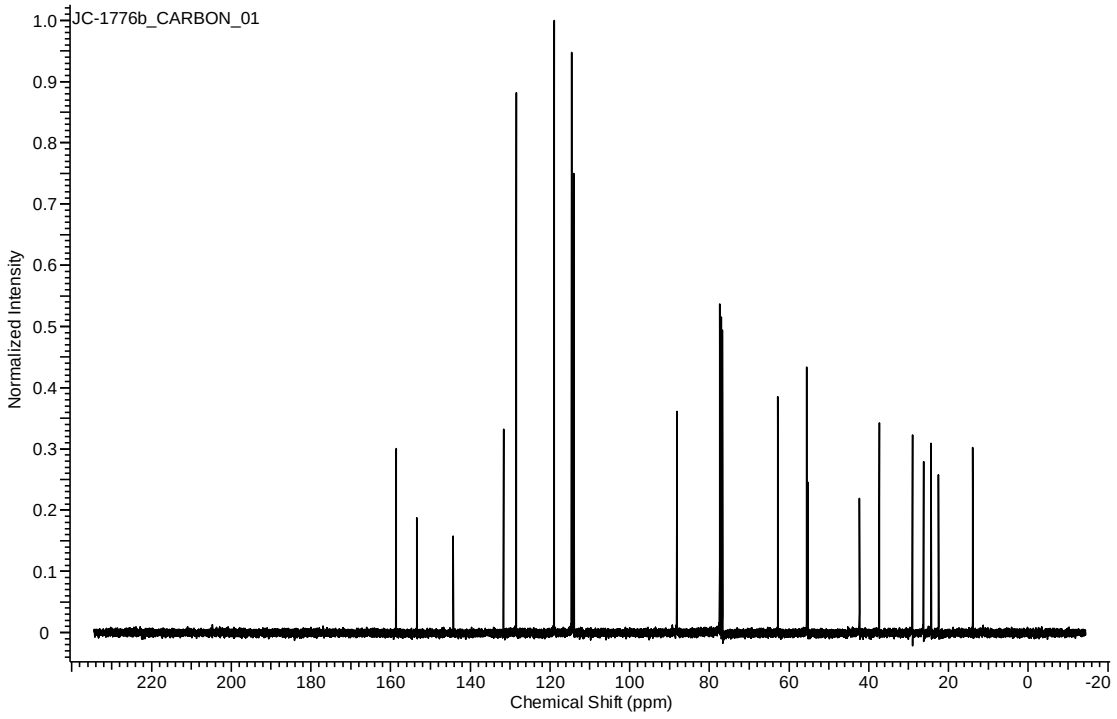
JC-1776b_CARBON_01
Normalized Intensity
Chemical Shift (ppm)

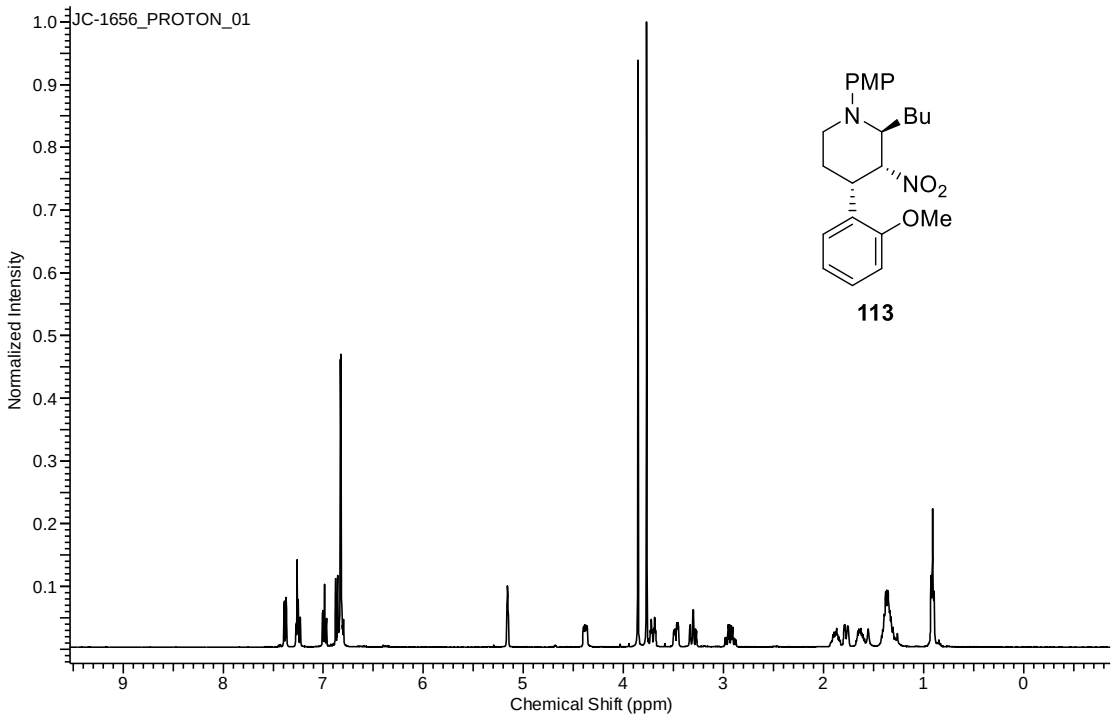
JC-1656_PROTON_01
Normalized Intensity
Chemical Shift (ppm)
PMP
N
Bu
NO2
OMe
113

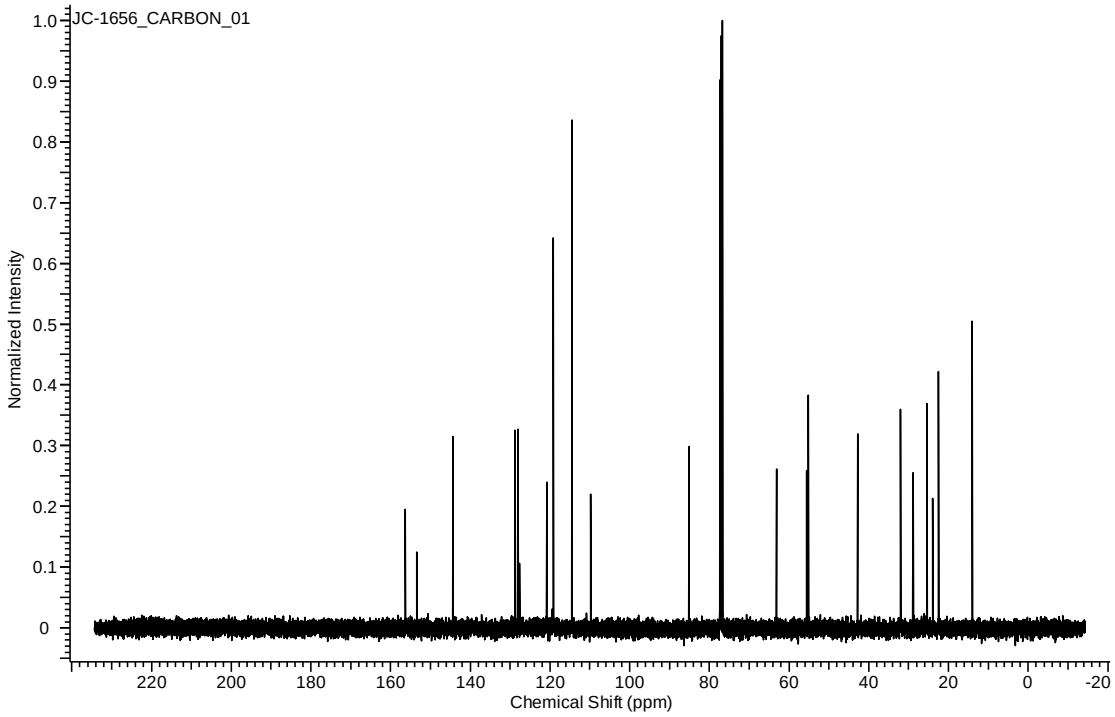
JC-1656_CARBON_01
Normalized Intensity
Chemical Shift (ppm)

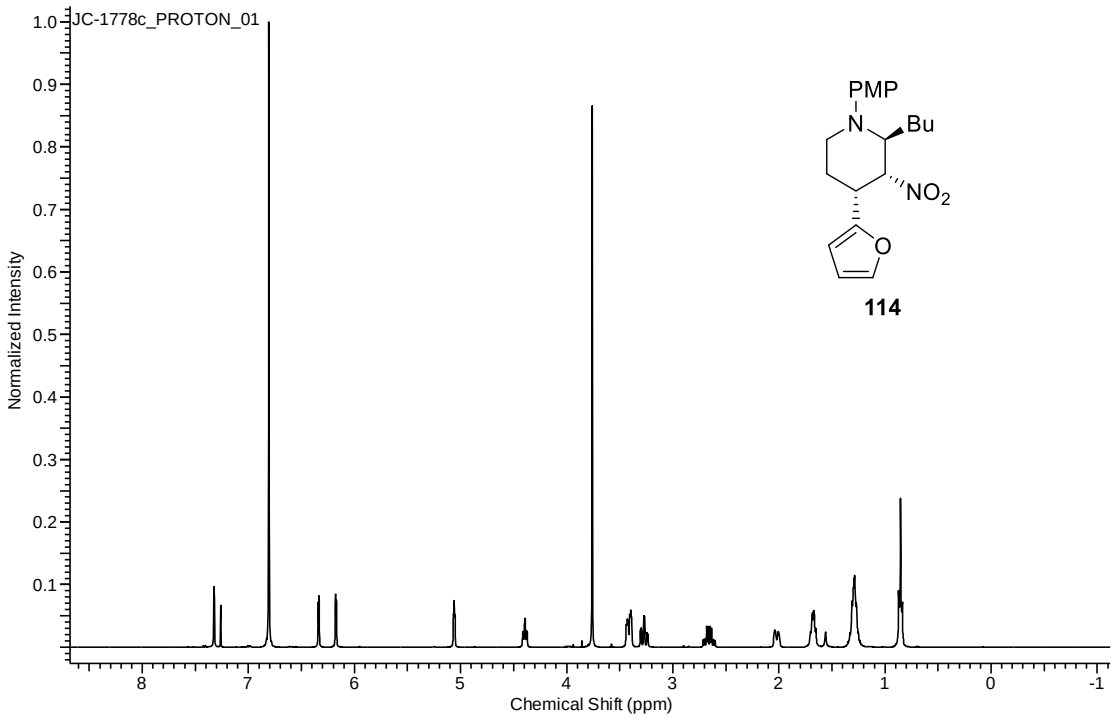
JC-1778c_PROTON_01
Normalized Intensity
Chemical Shift (ppm)
PMP
N
Bu
NO2
O
114

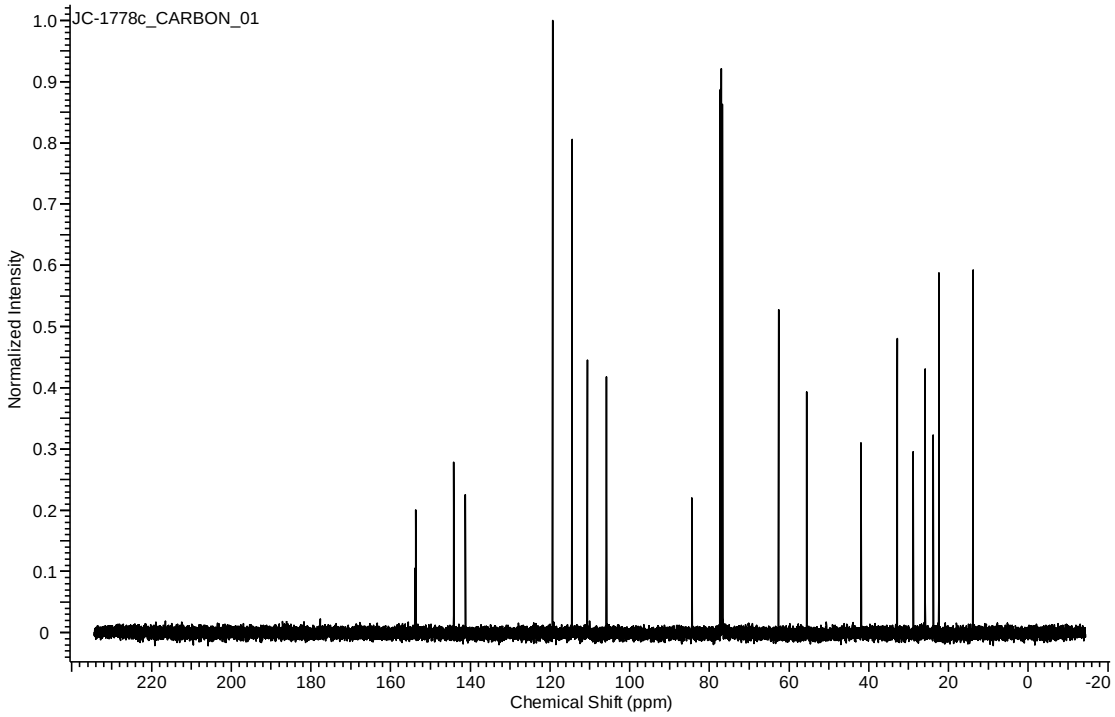
JC-1778c_CARBON_01
Normalized Intensity
Chemical Shift (ppm)

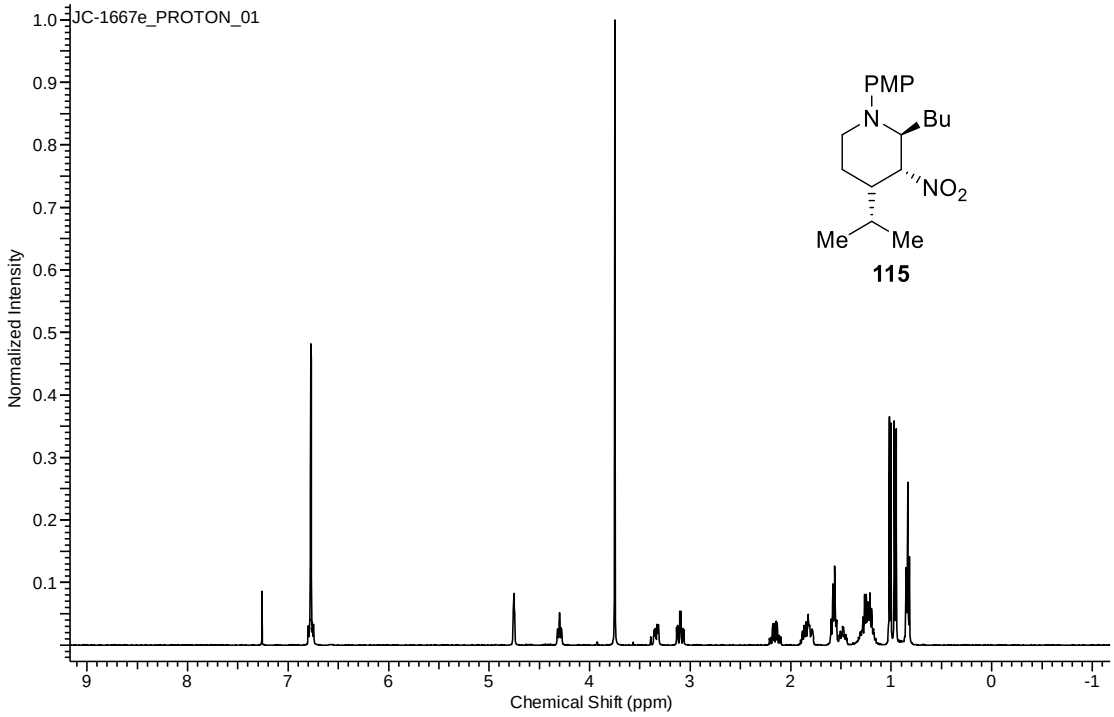
JC-1667e_PROTON_01
Normalized Intensity
Chemical Shift (ppm)
PMP
N
Bu
NO2
Me
Me
115

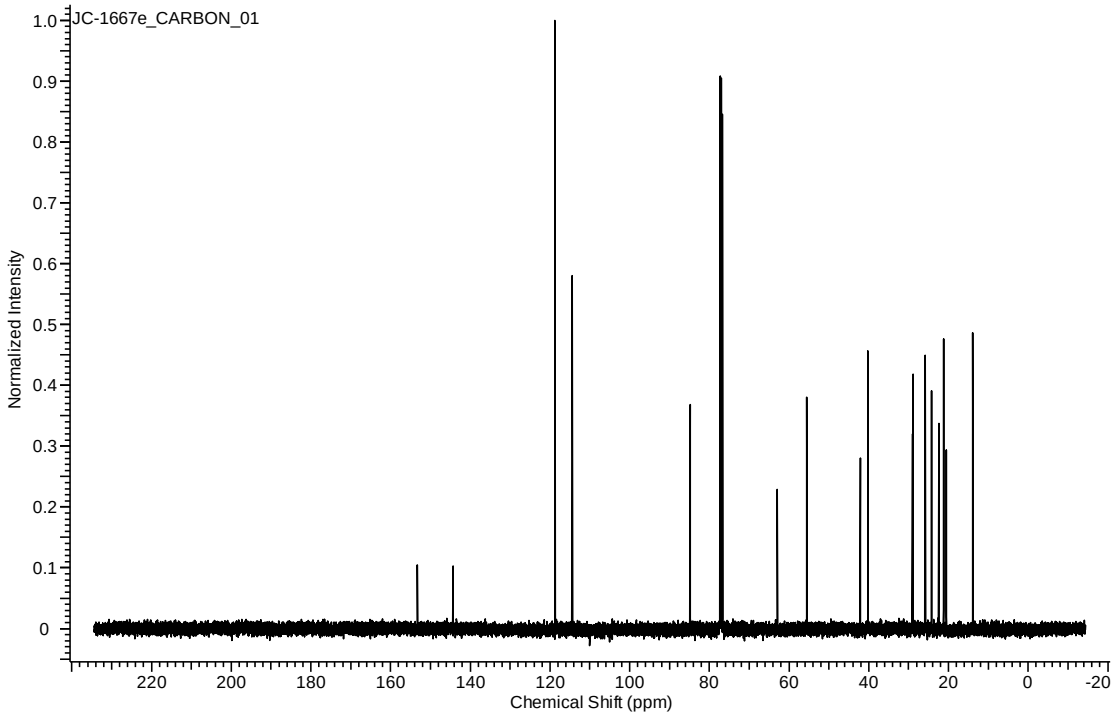
JC-1667e_CARBON_01
Normalized Intensity
Chemical Shift (ppm)

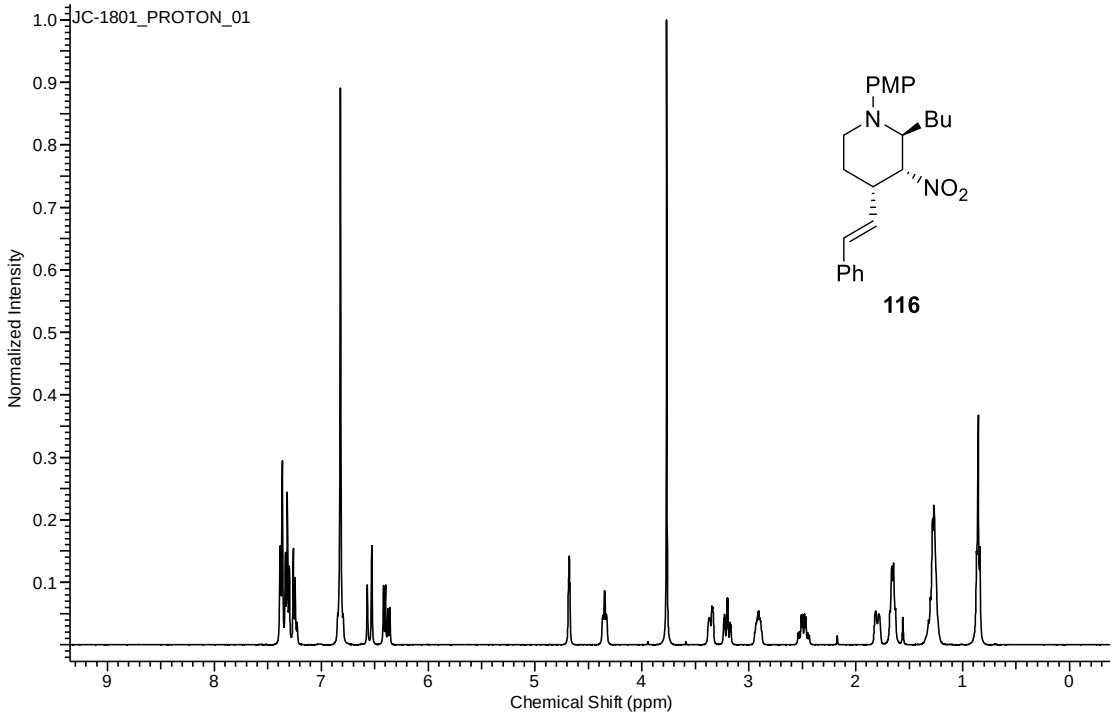
JC-1801_PROTON_01
Normalized Intensity
Chemical Shift (ppm)
PMP
N
Bu
NO2
Ph
116

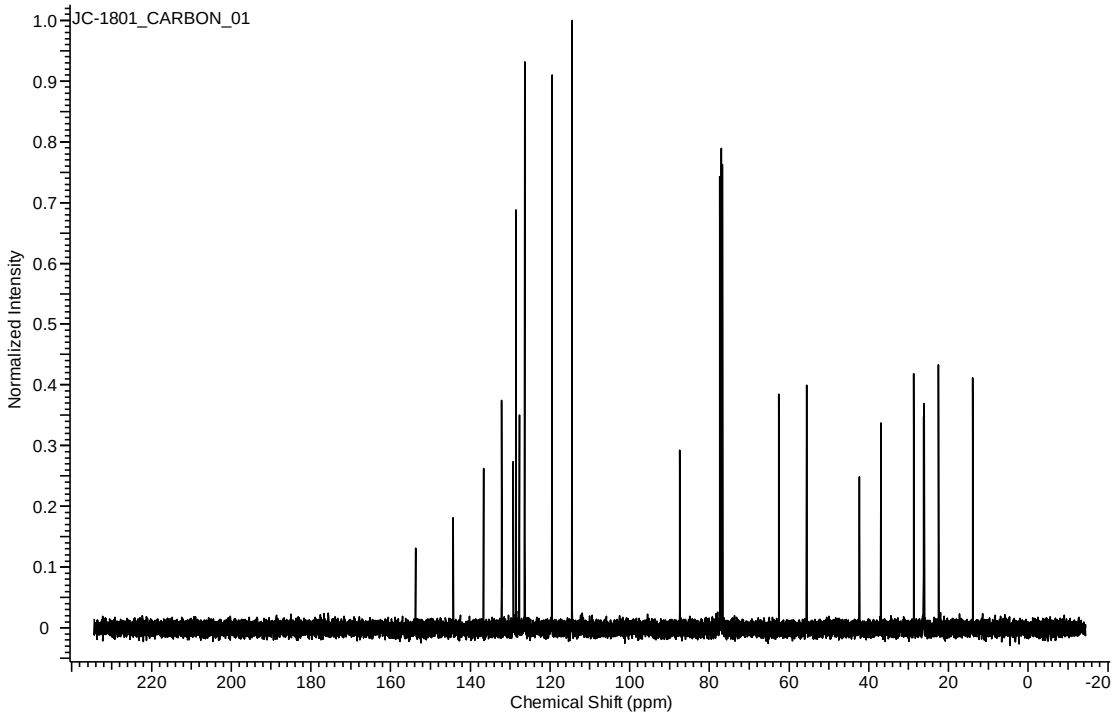
JC-1801_CARBON_01
Normalized Intensity
Chemical Shift (ppm)

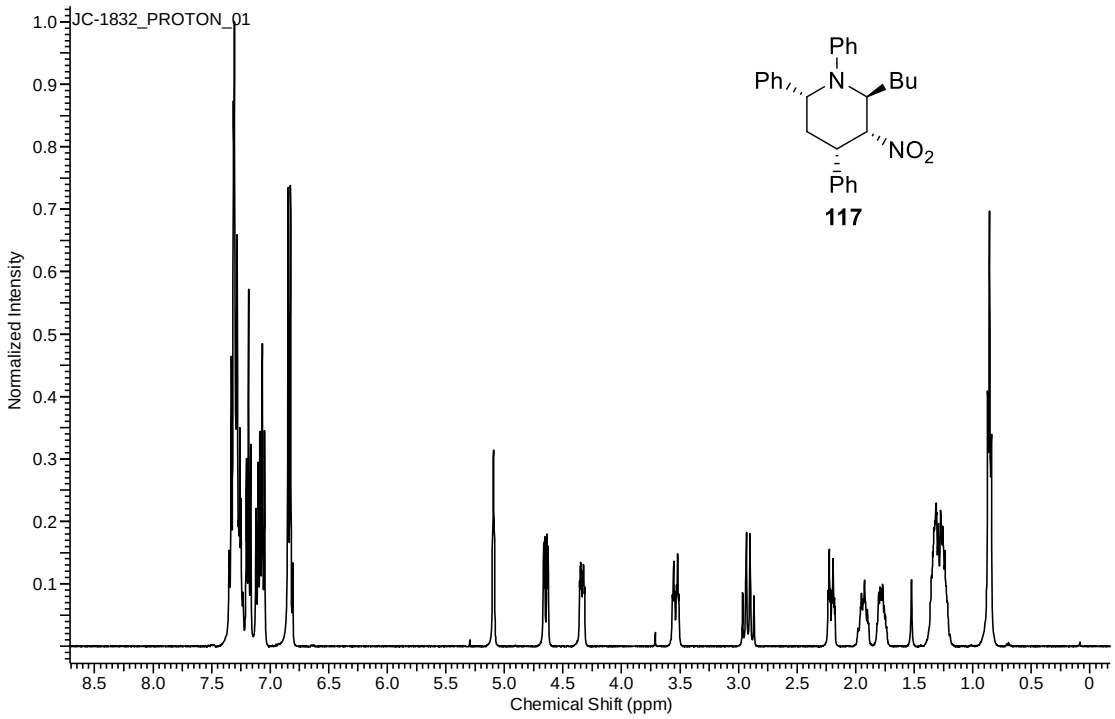
JC-1832_PROTON_01
Normalized Intensity
Chemical Shift (ppm)
Ph
N
Ph
Bu
NO2
Ph
117

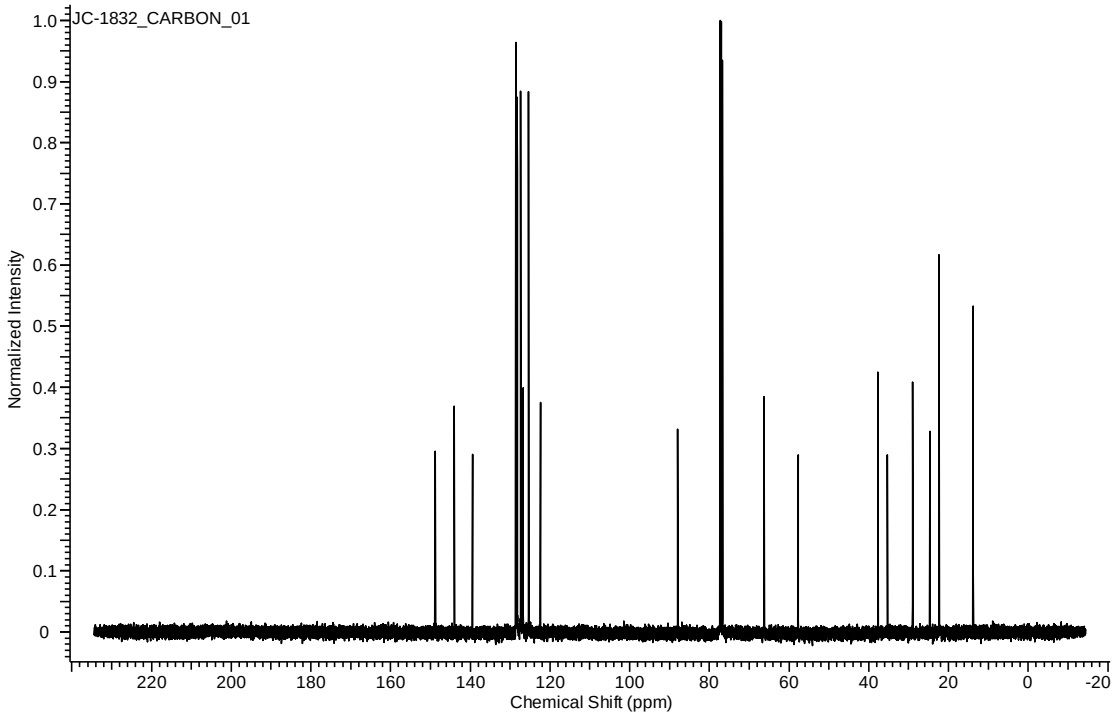
JC-1832_CARBON_01
Normalized Intensity
Chemical Shift (ppm)

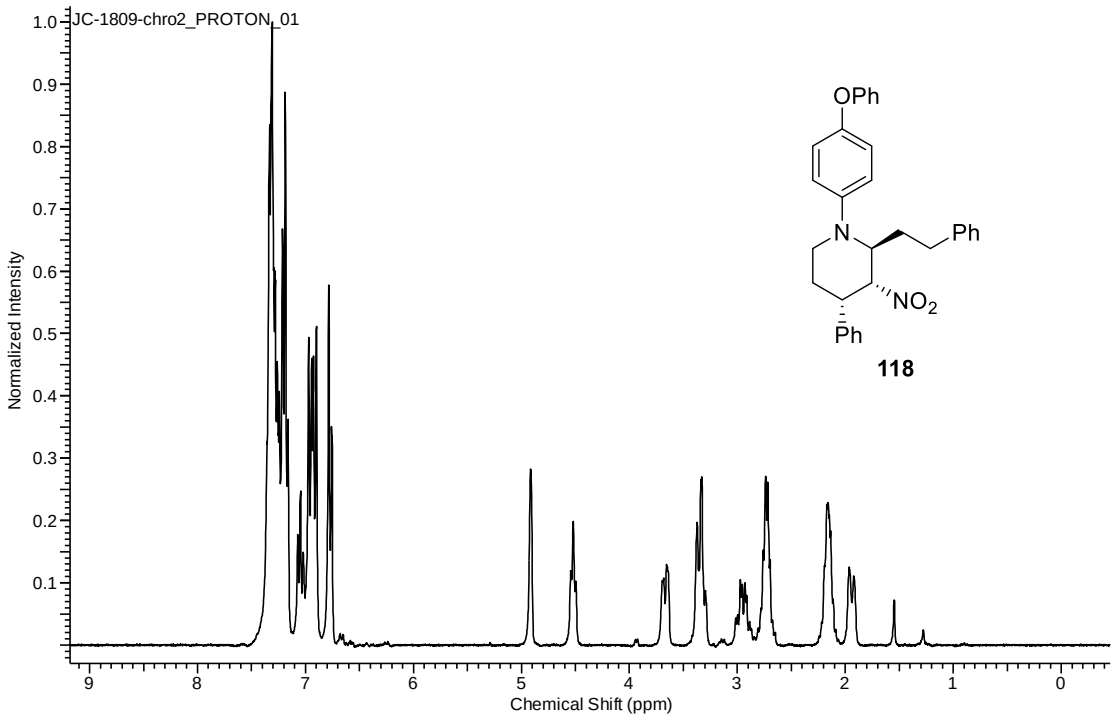
JC-1809-chro2_PROTON_01
Normalized Intensity
Chemical Shift (ppm)
OPh
N
Ph
NO2
Ph

118

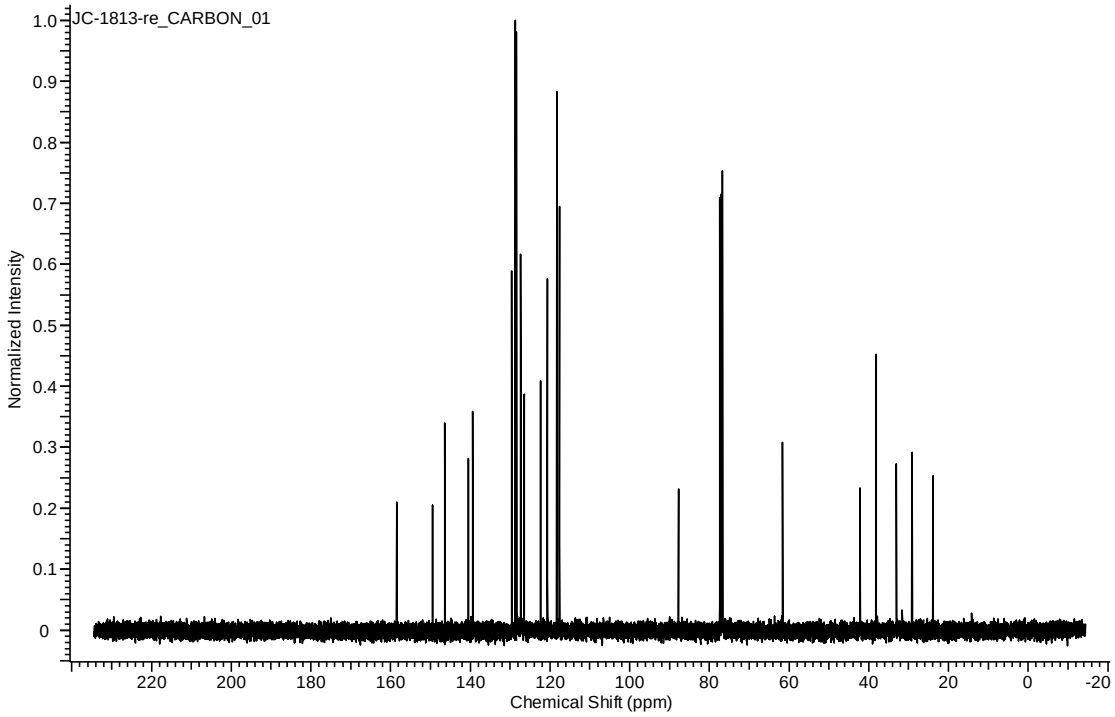
JC-1813-re_CARBON_01
Normalized Intensity
Chemical Shift (ppm)

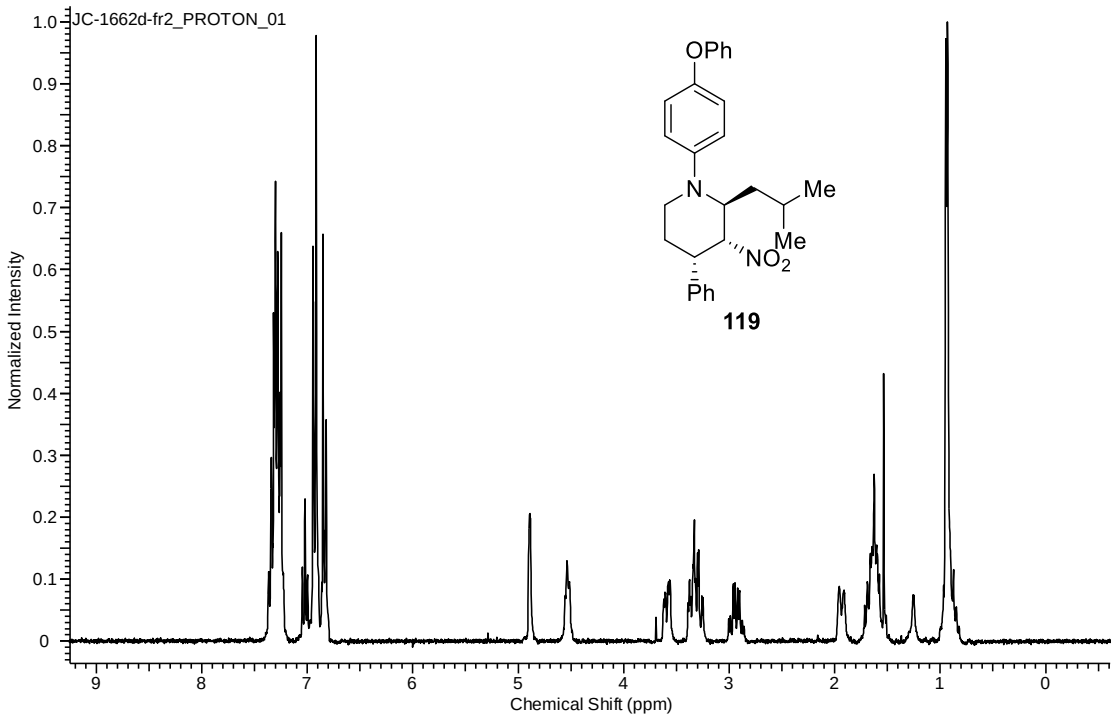
JC-1662d-fr2_PROTON_01
Normalized Intensity
Chemical Shift (ppm)
OPh
N
Me
Me
NO2
Ph
119

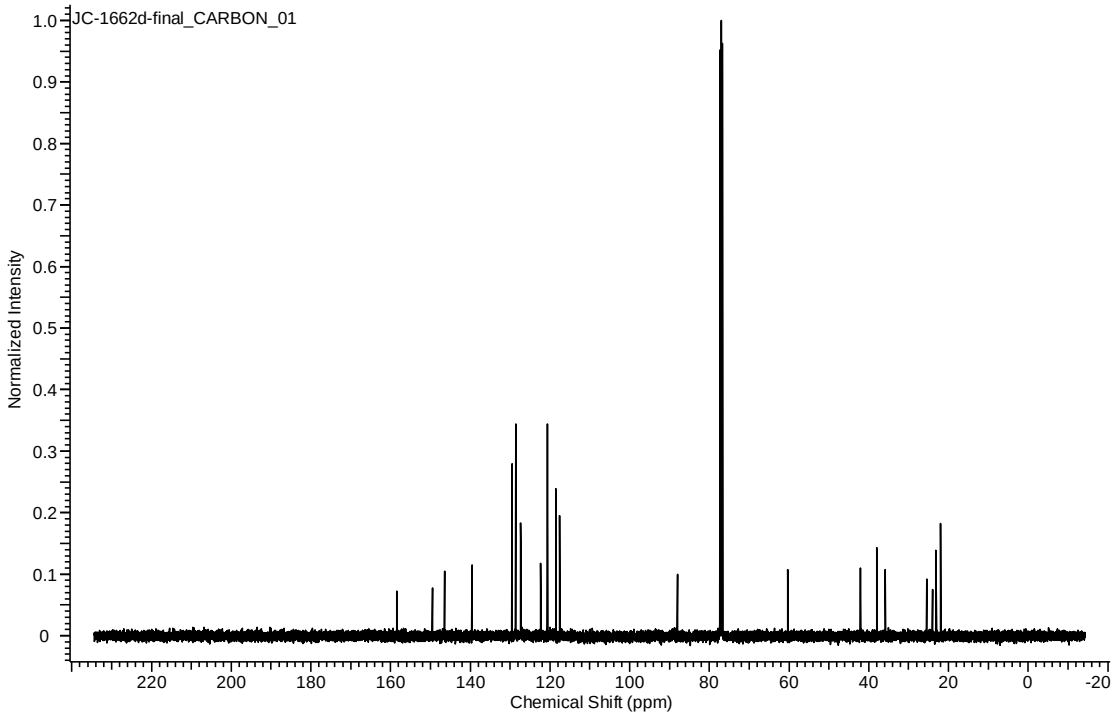
JC-1662d-final_CARBON_01
Normalized Intensity
Chemical Shift (ppm)

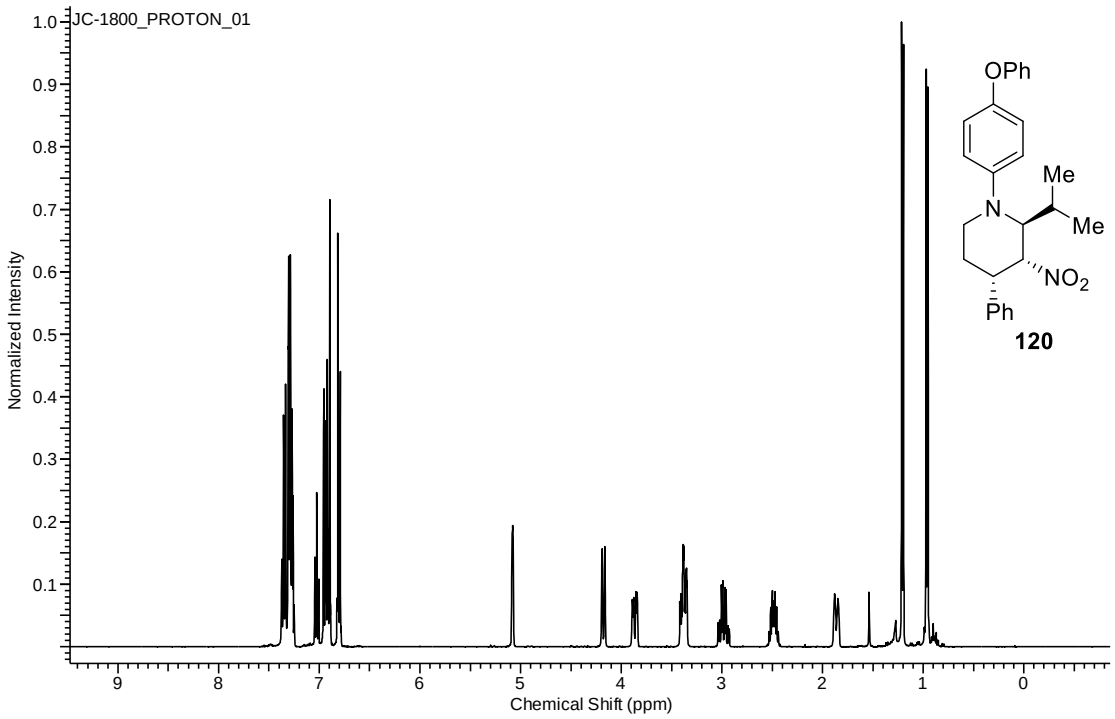
JC-1800_PROTON_01
Normalized Intensity
Chemical Shift (ppm)
OPh
Me
N
Me
NO2
Ph
120

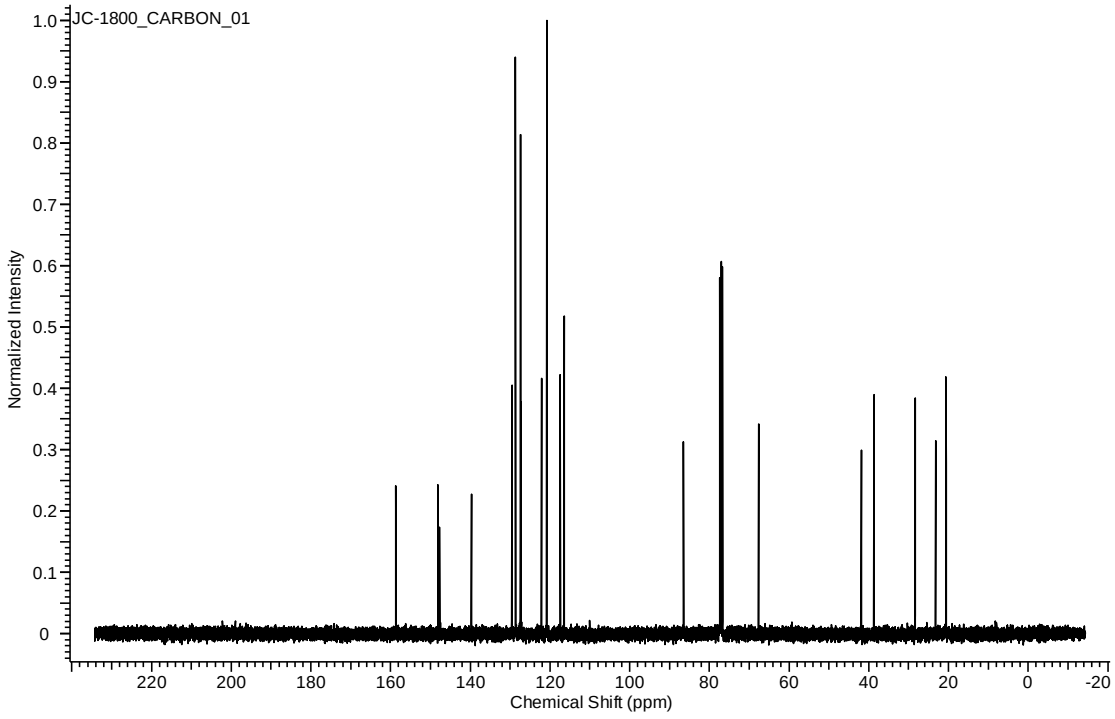
JC-1800_CARBON_01
Normalized Intensity
Chemical Shift (ppm)

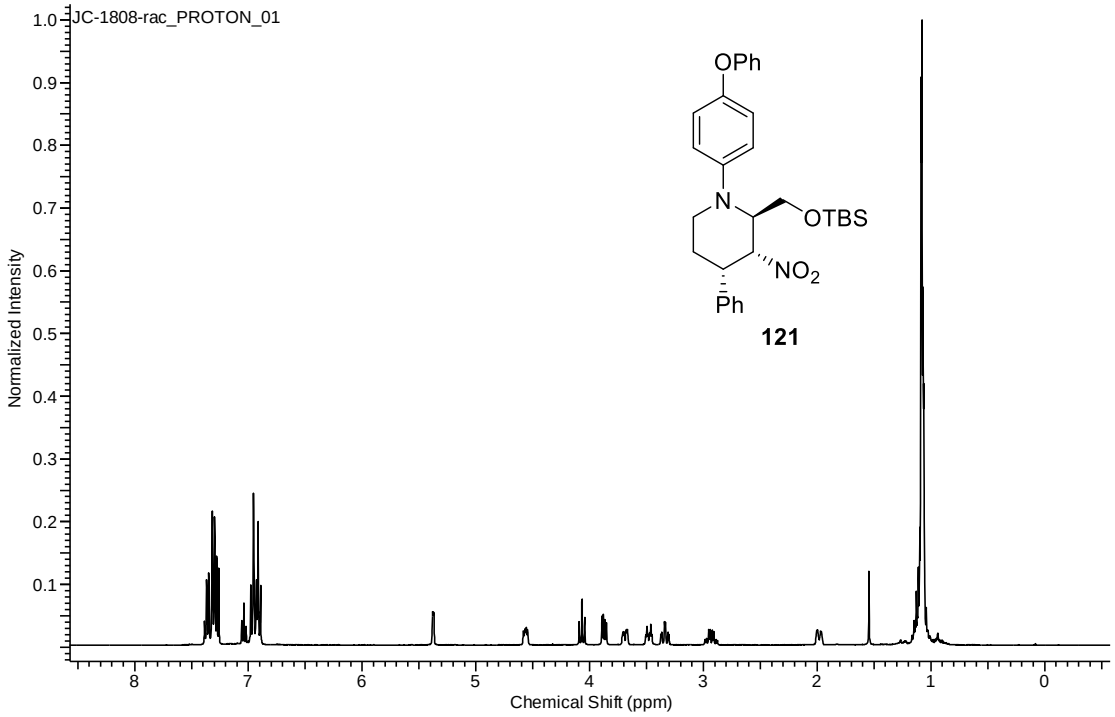
JC-1808-rac_PROTON_01
Normalized Intensity
Chemical Shift (ppm)
OPh
N
OTBS
NO2
Ph
121

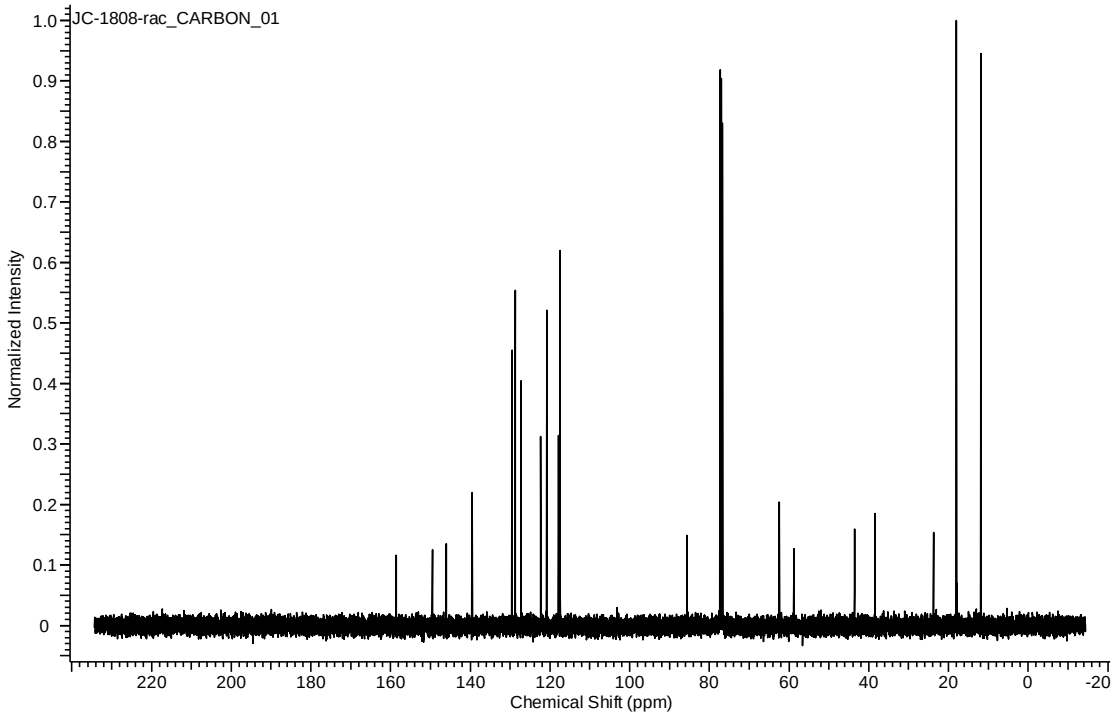
JC-1808-rac_CARBON_01
Normalized Intensity
Chemical Shift (ppm)

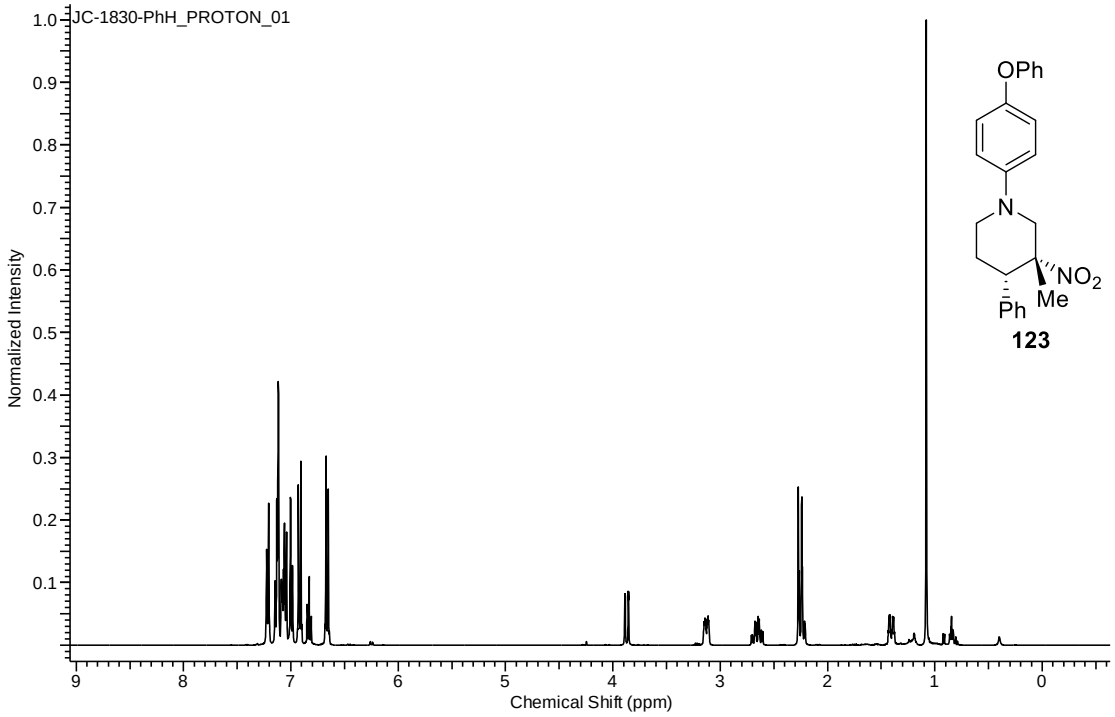
JC-1830-PhH_PROTON_01
Normalized Intensity
Chemical Shift (ppm)
OPh
N
NO2
Me
Ph
123

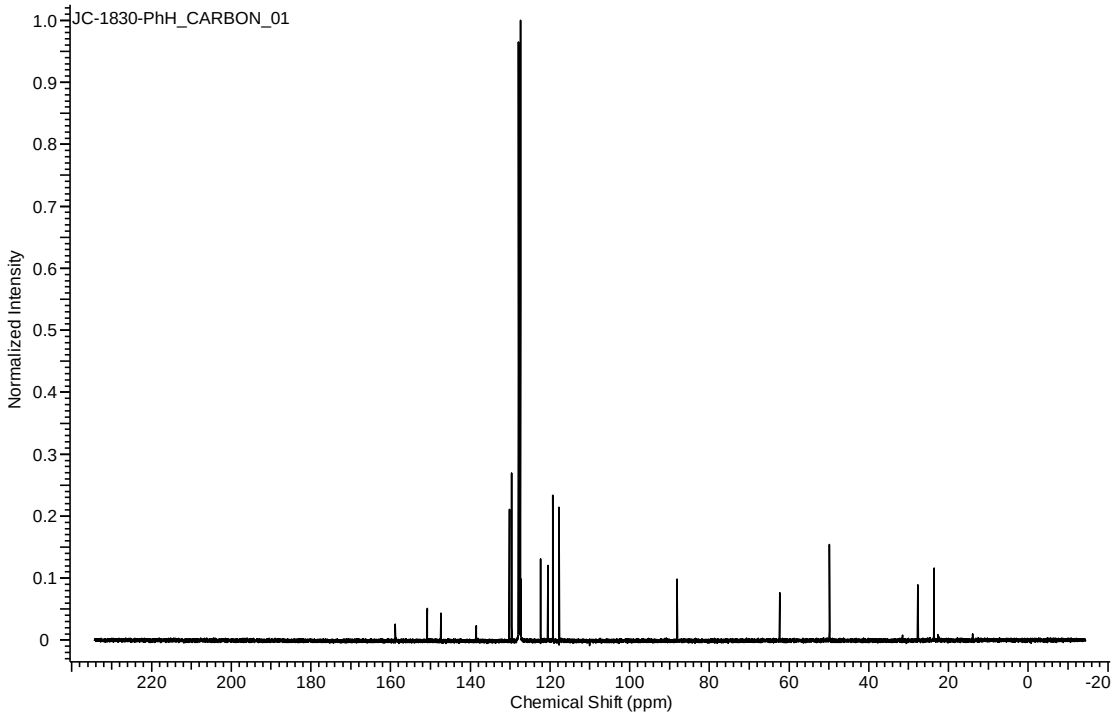
JC-1830-PhH_CARBON_01
Normalized Intensity
Chemical Shift (ppm)

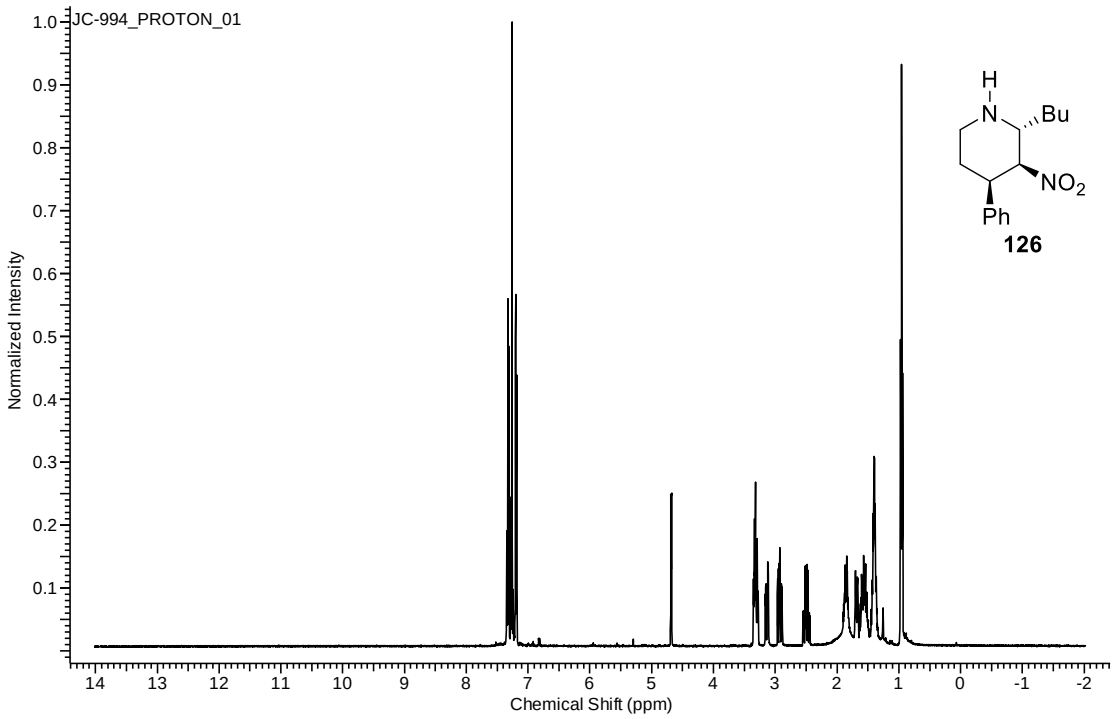
JC-994_PROTON_01
Normalized Intensity
Chemical Shift (ppm)
H
N
Bu
NO2
Ph
126

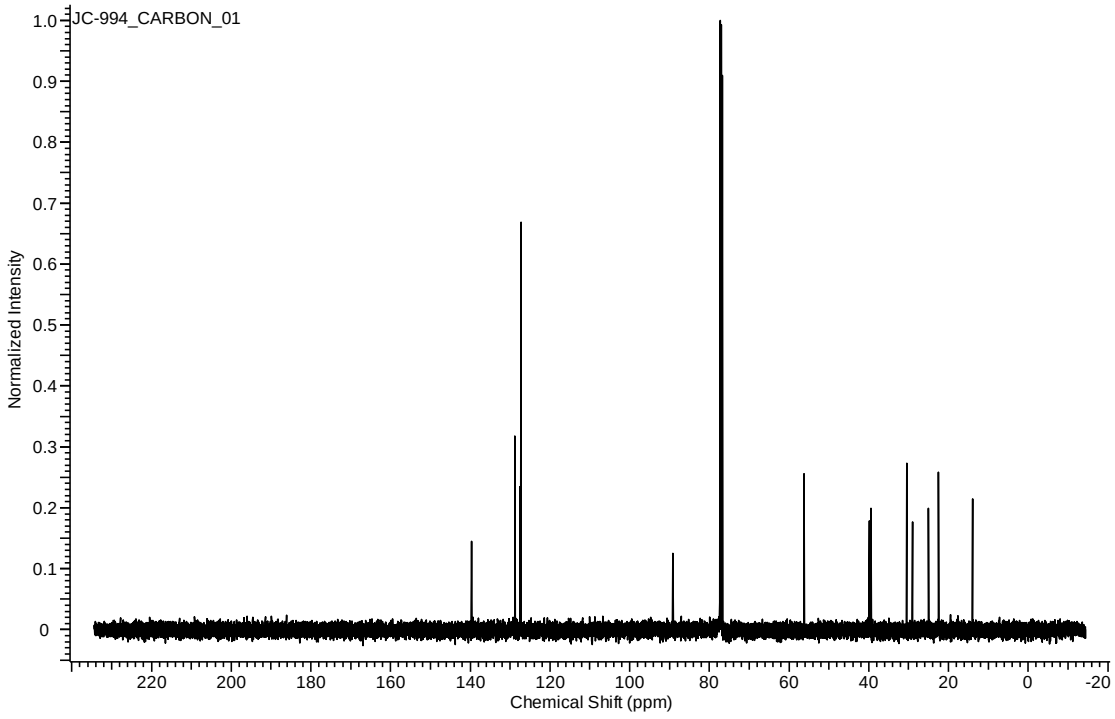
JC-994_CARBON_01
Normalized Intensity
Chemical Shift (ppm)

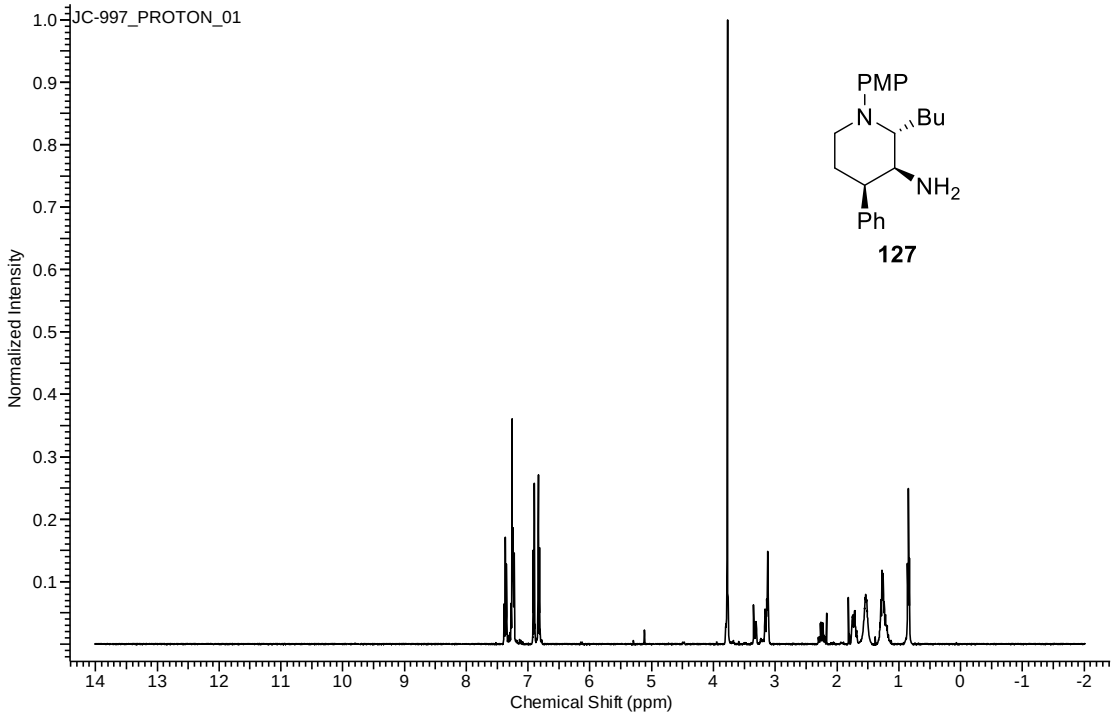
JC-997_PROTON_01
Normalized Intensity
Chemical Shift (ppm)
PMP
N
Bu
NH2
Ph
127

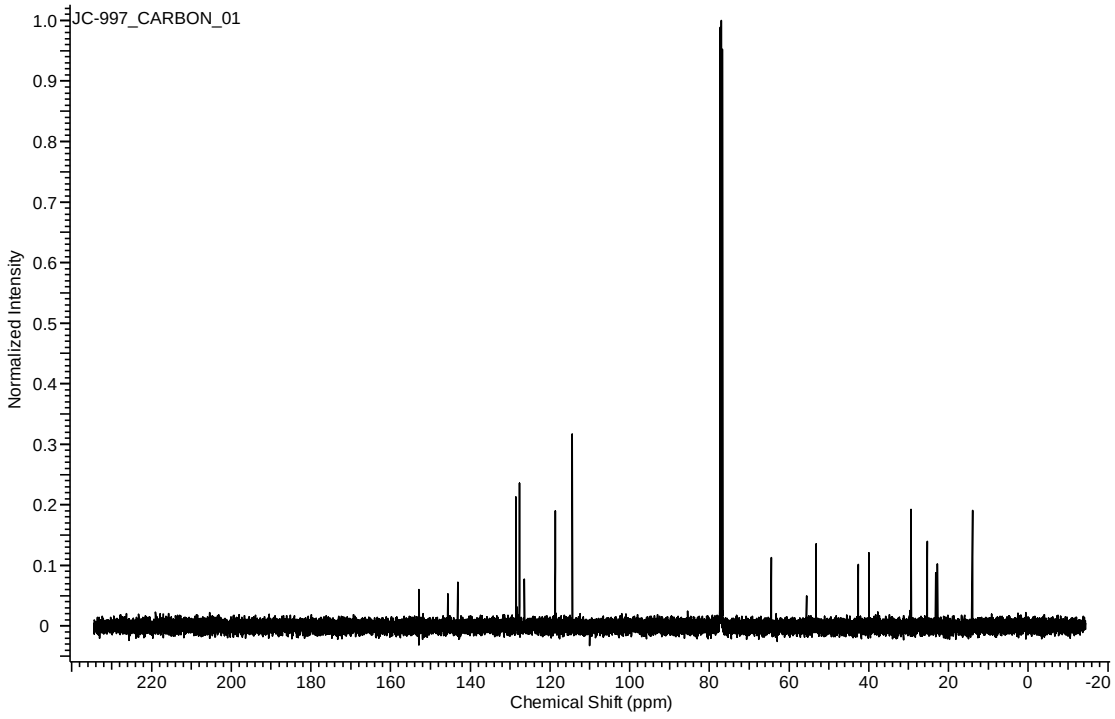
JC-997_CARBON_01
Normalized Intensity
Chemical Shift (ppm)

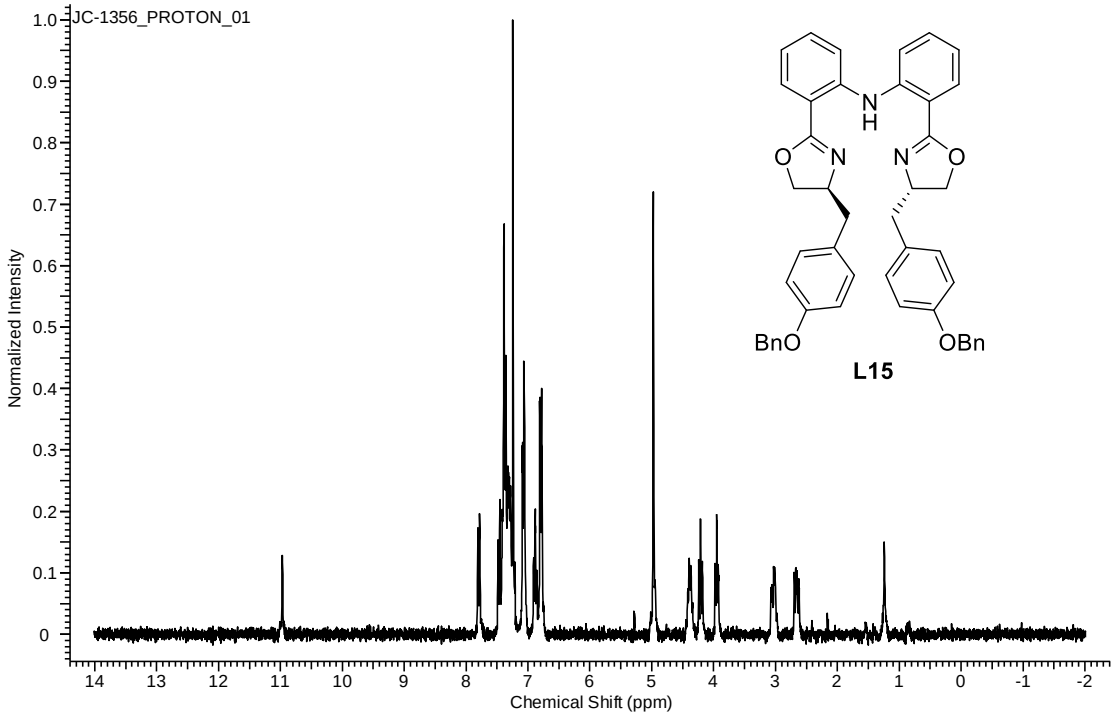
JC-1356_PROTON_01
Normalized Intensity
Chemical Shift (ppm)
BnO
OBn
L15

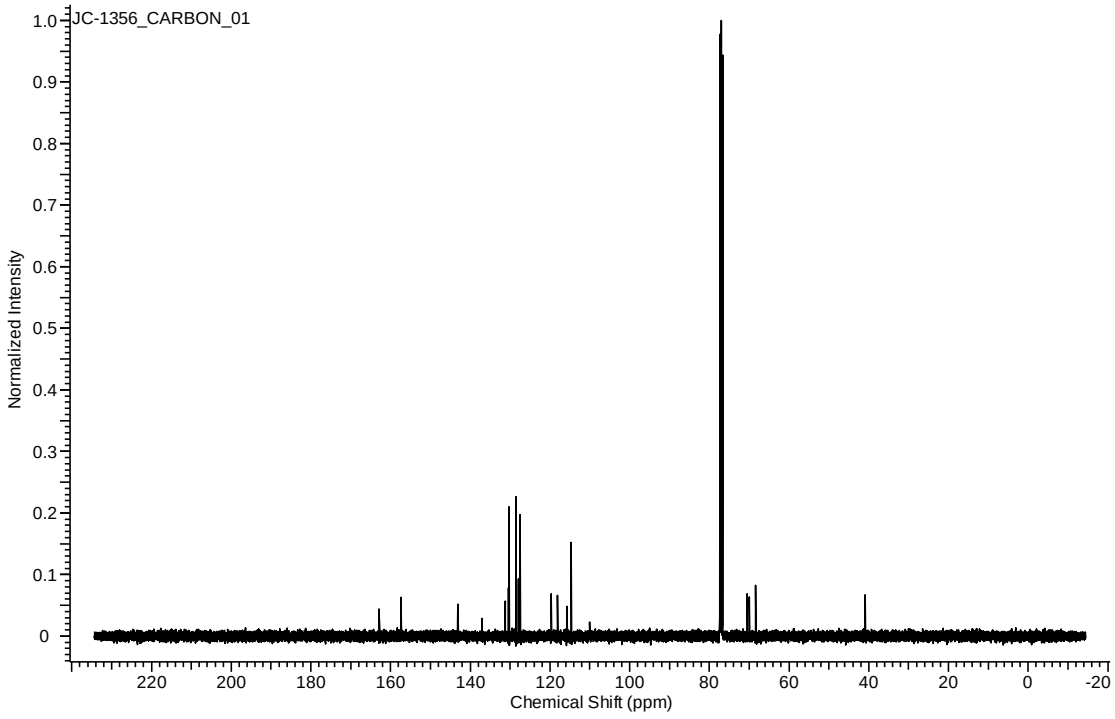
JC-1356_CARBON_01
Normalized Intensity
Chemical Shift (ppm)

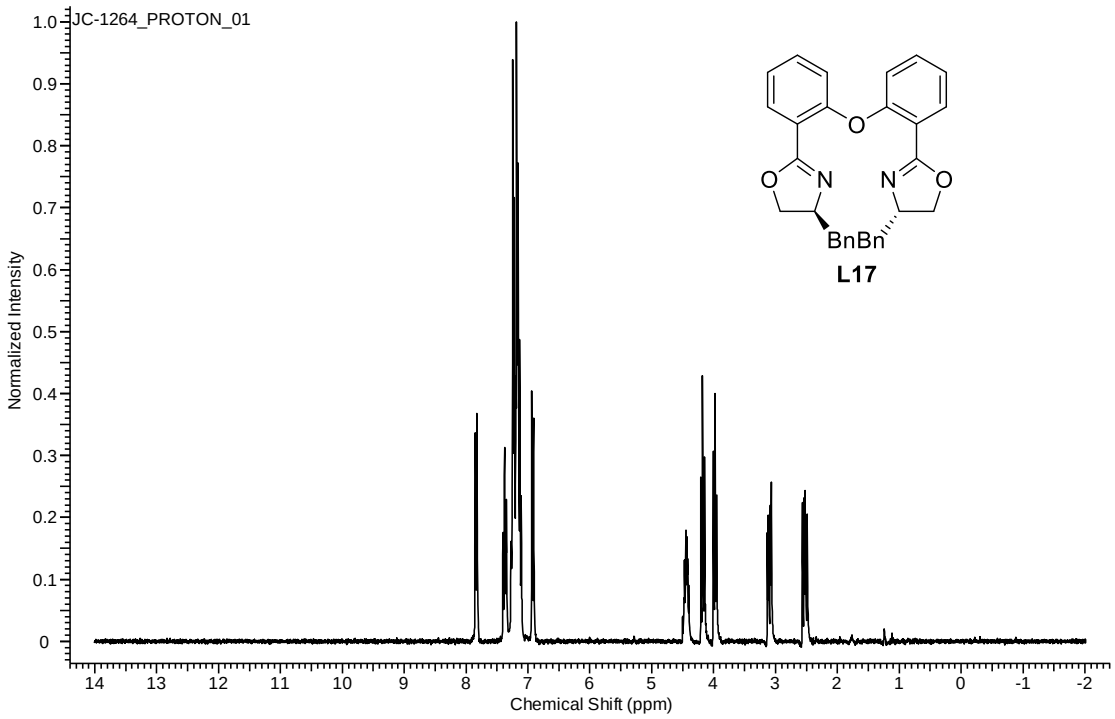
JC-1264_PROTON_01
Normalized Intensity
Chemical Shift (ppm)
BnBn
L17

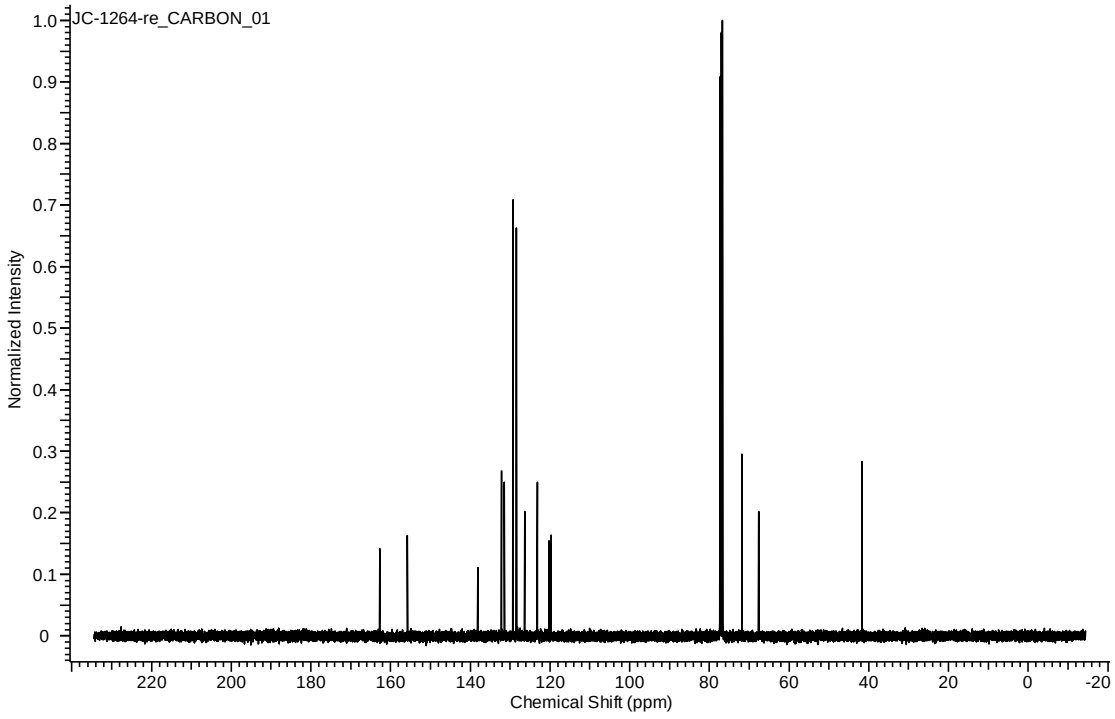
JC-1264-re_CARBON_01
Normalized Intensity
Chemical Shift (ppm)

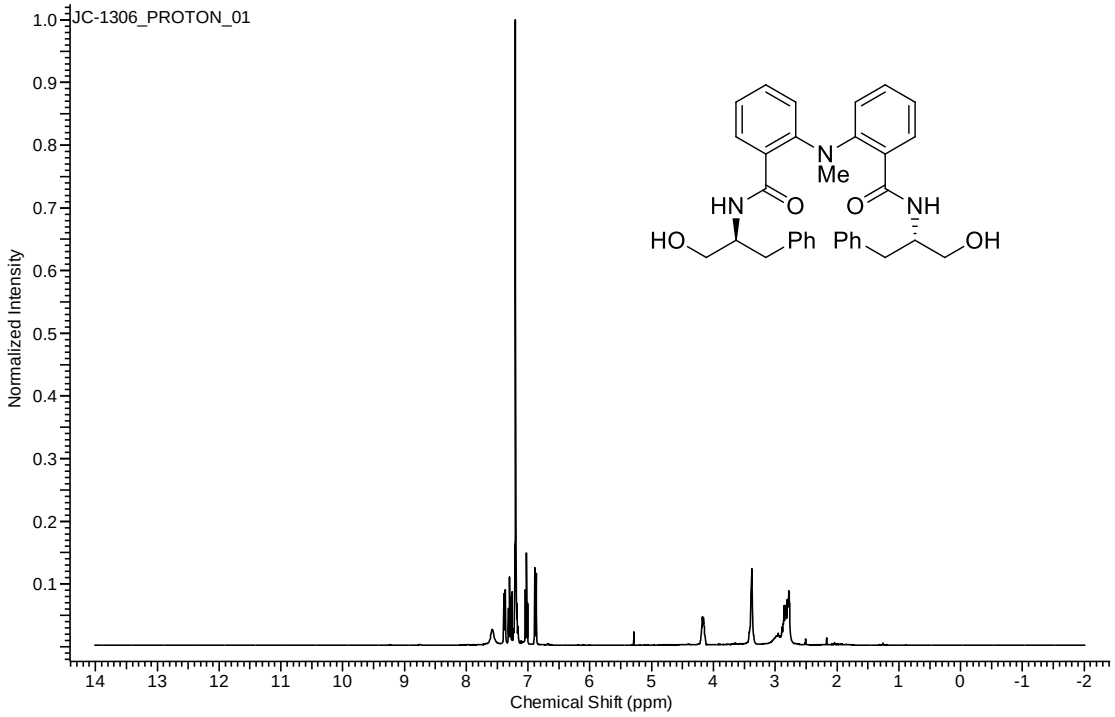
JC-1306_PROTON_01
Normalized Intensity
Chemical Shift (ppm)
N
Me
HN
O
O
NH
HO
Ph
Ph
OH

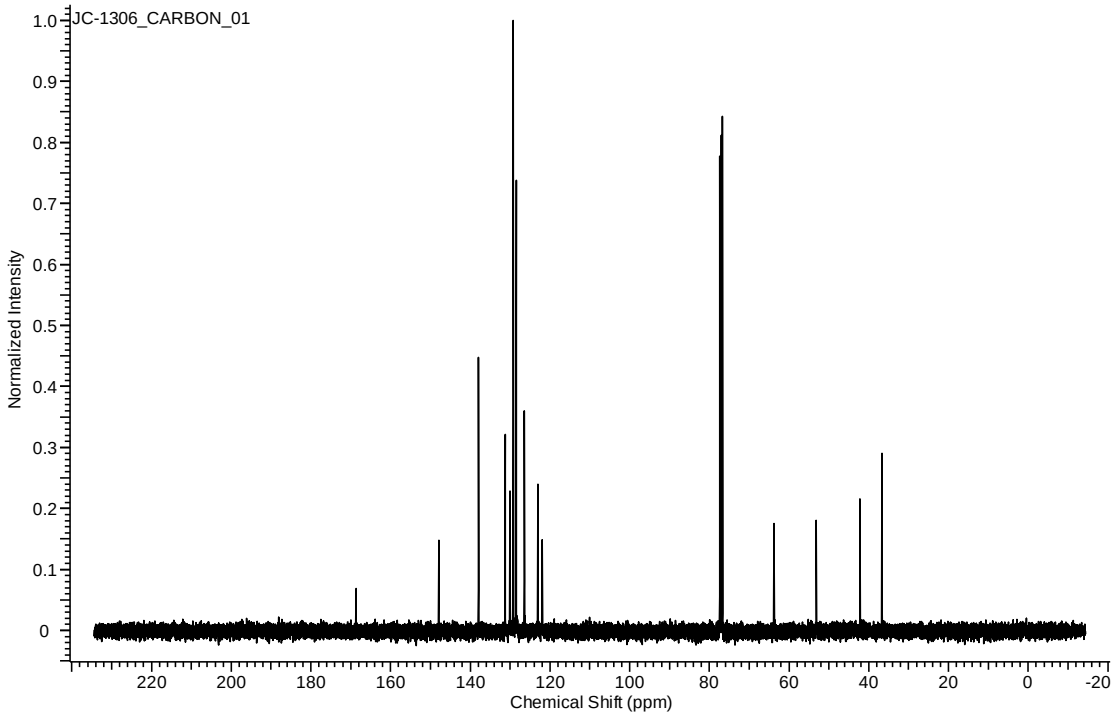
JC-1306_CARBON_01
Normalized Intensity
Chemical Shift (ppm)

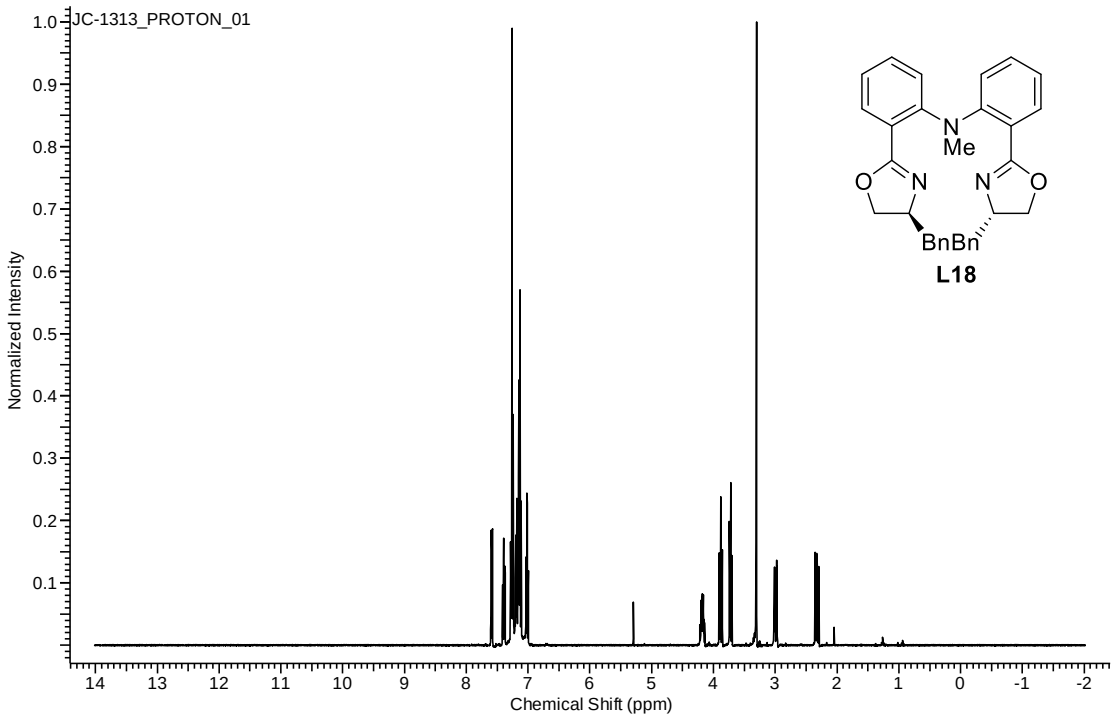
JC-1313_PROTON_01
Normalized Intensity
Chemical Shift (ppm)
N
Me
O
N
N
O
BnBn
L18

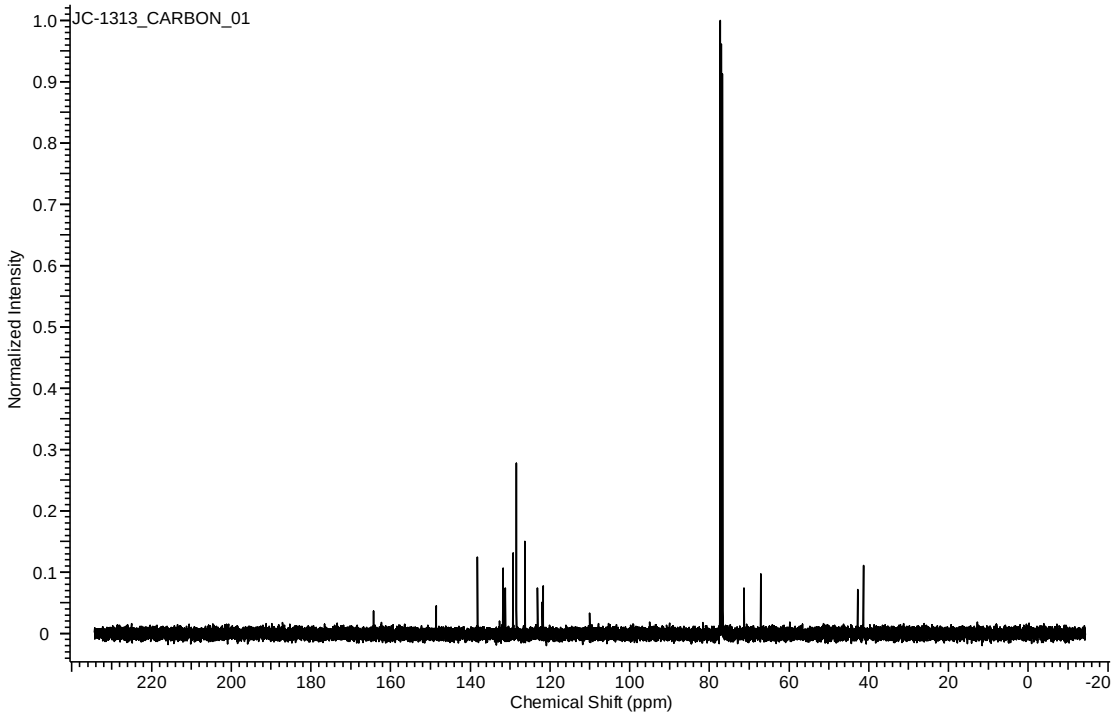
JC-1313_CARBON_01
Normalized Intensity
Chemical Shift (ppm)

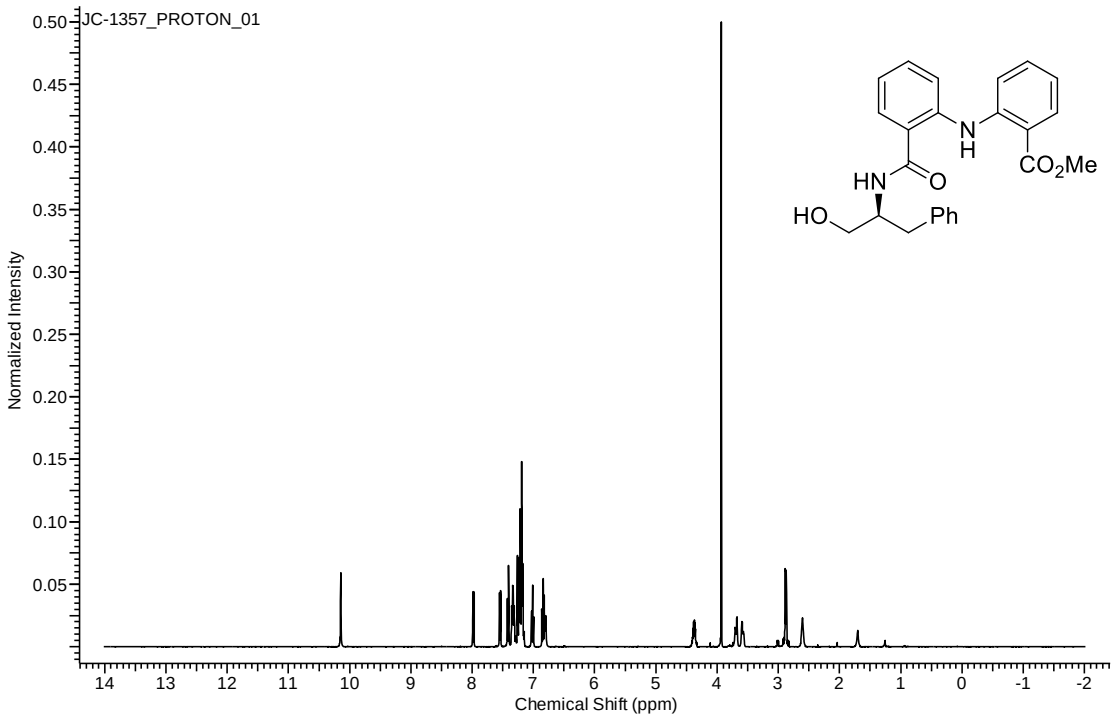
JC-1357_PROTON_01
Normalized Intensity
Chemical Shift (ppm)
HN
O
HO
Ph
N
H
CO2Me

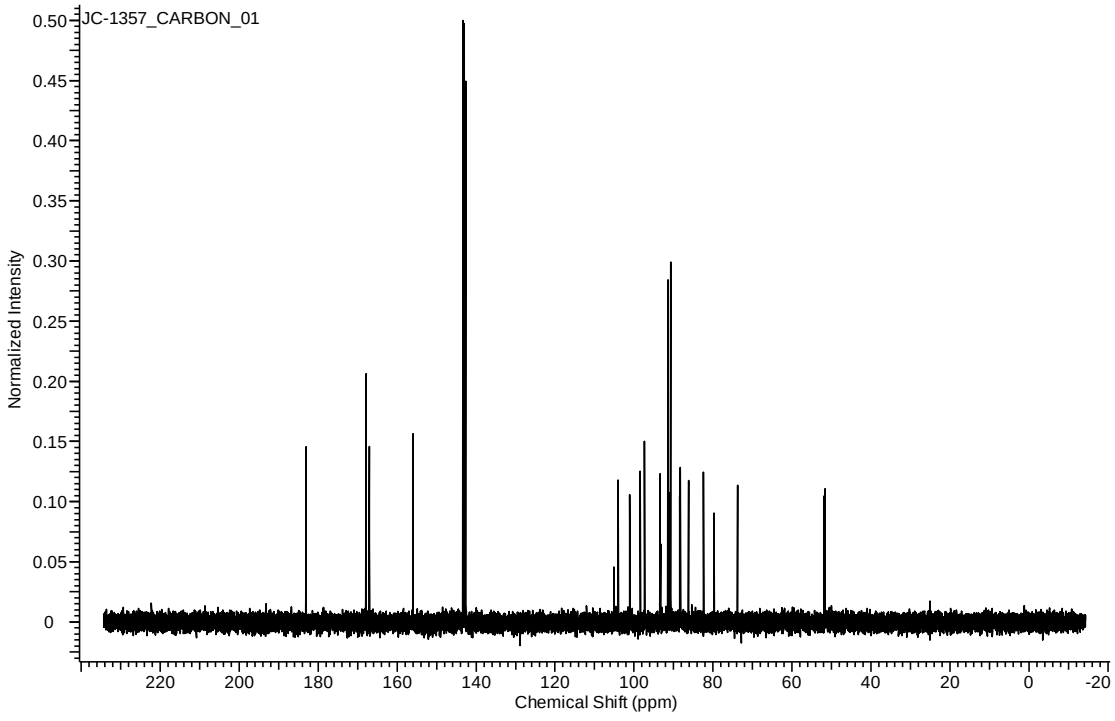
JC-1357_CARBON_01
Normalized Intensity
Chemical Shift (ppm)

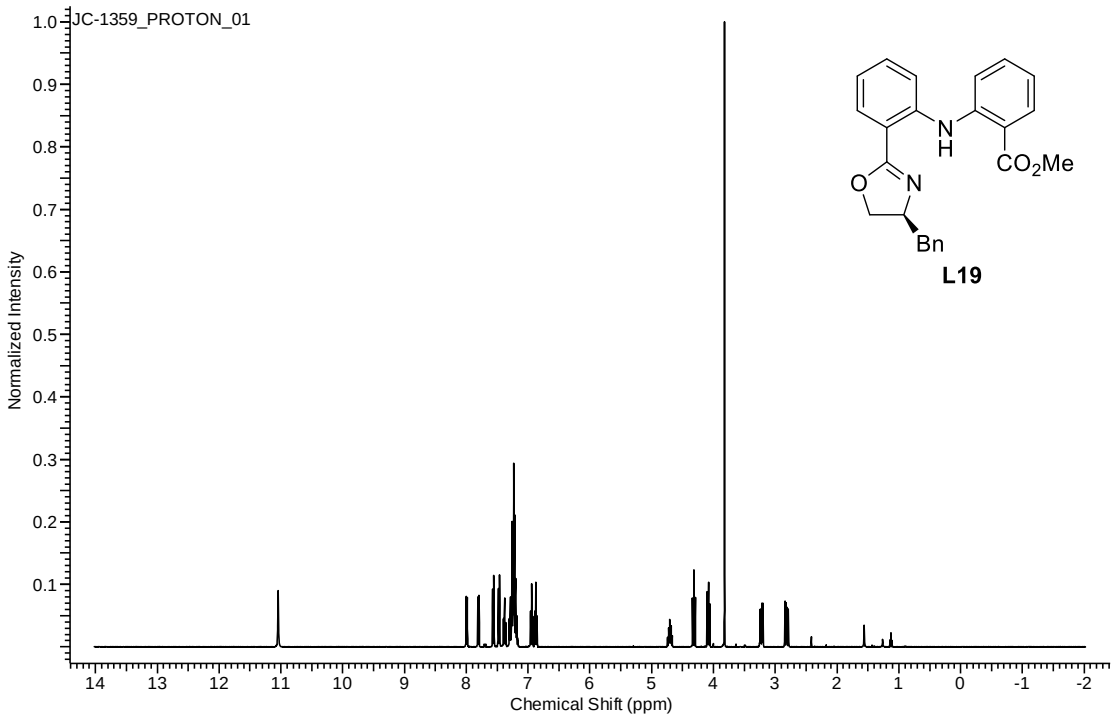
JC-1359_PROTON_01
Normalized Intensity
Chemical Shift (ppm)
N
H
CO2Me
O
N
Bn
L19

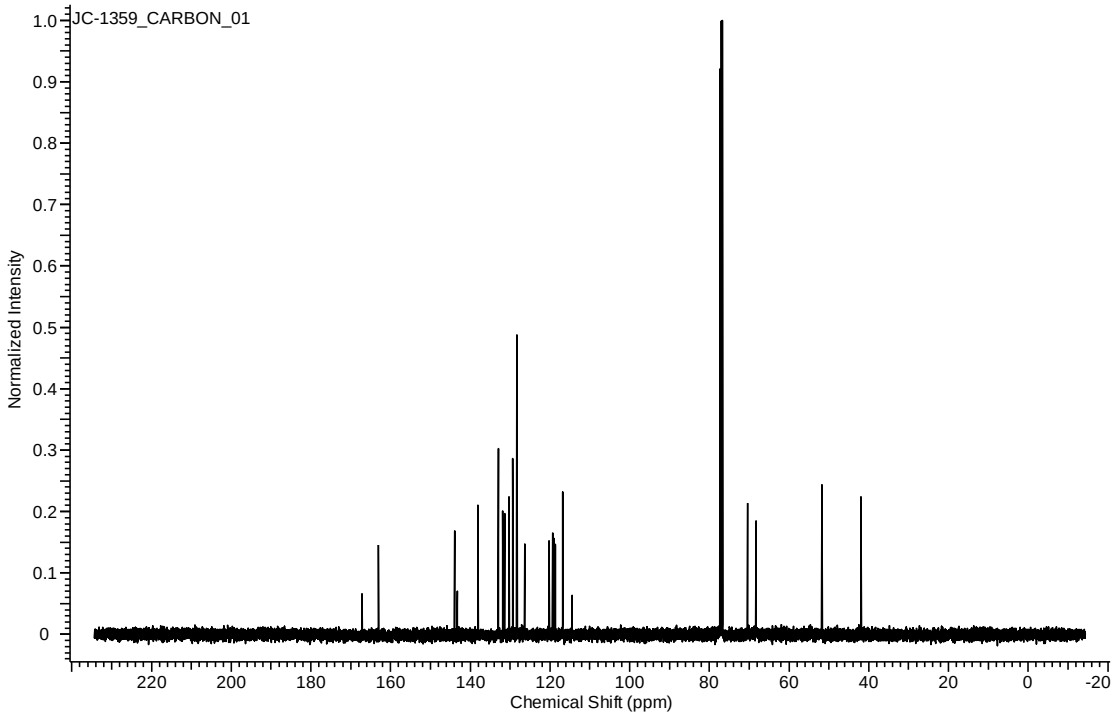
JC-1359_CARBON_01
Normalized Intensity
Chemical Shift (ppm)

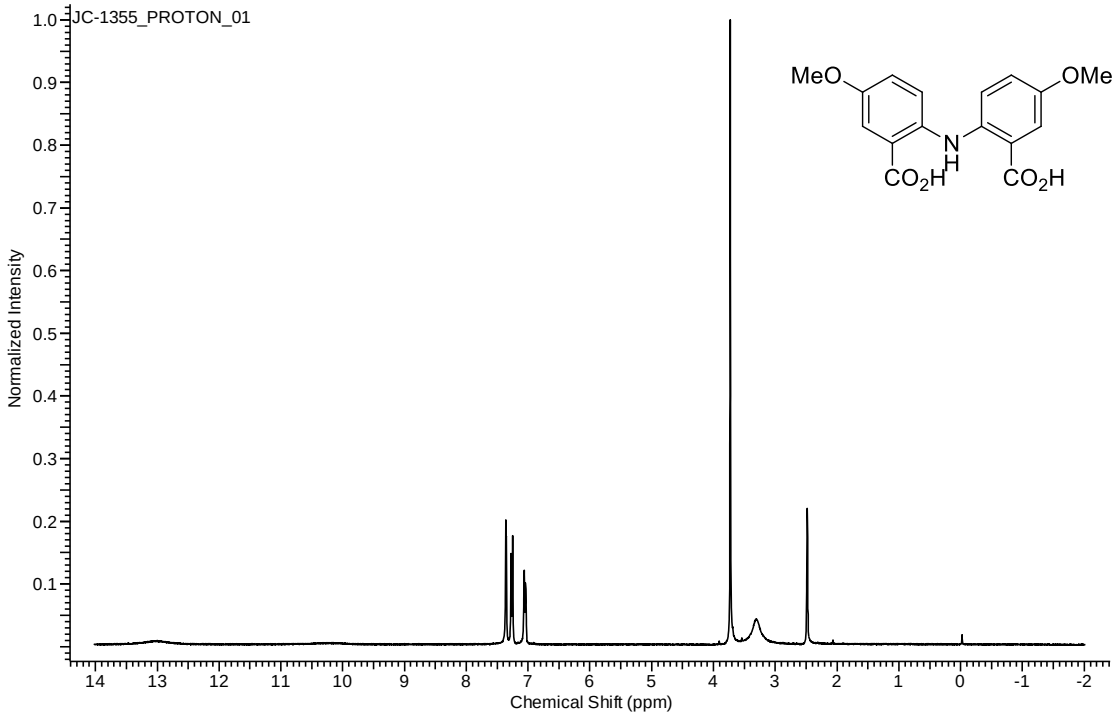
JC-1355_PROTON_01
Normalized Intensity
Chemical Shift (ppm)
MeO
OMe
N
H
CO2H
CO2H

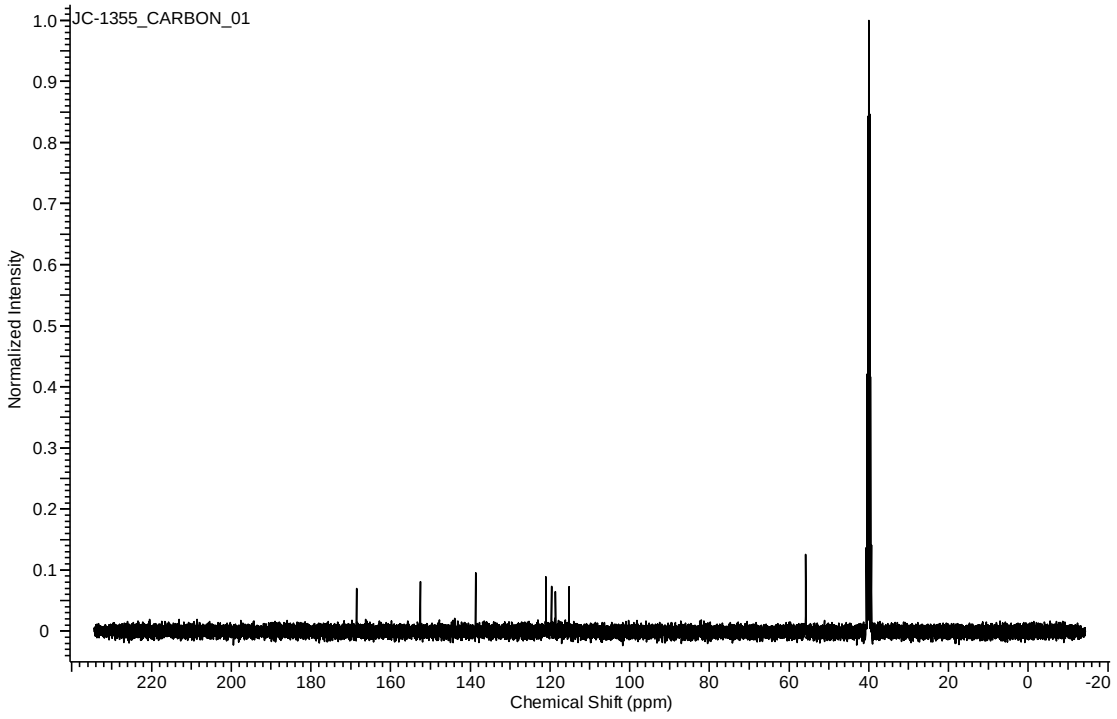
JC-1355_CARBON_01
Normalized Intensity
Chemical Shift (ppm)

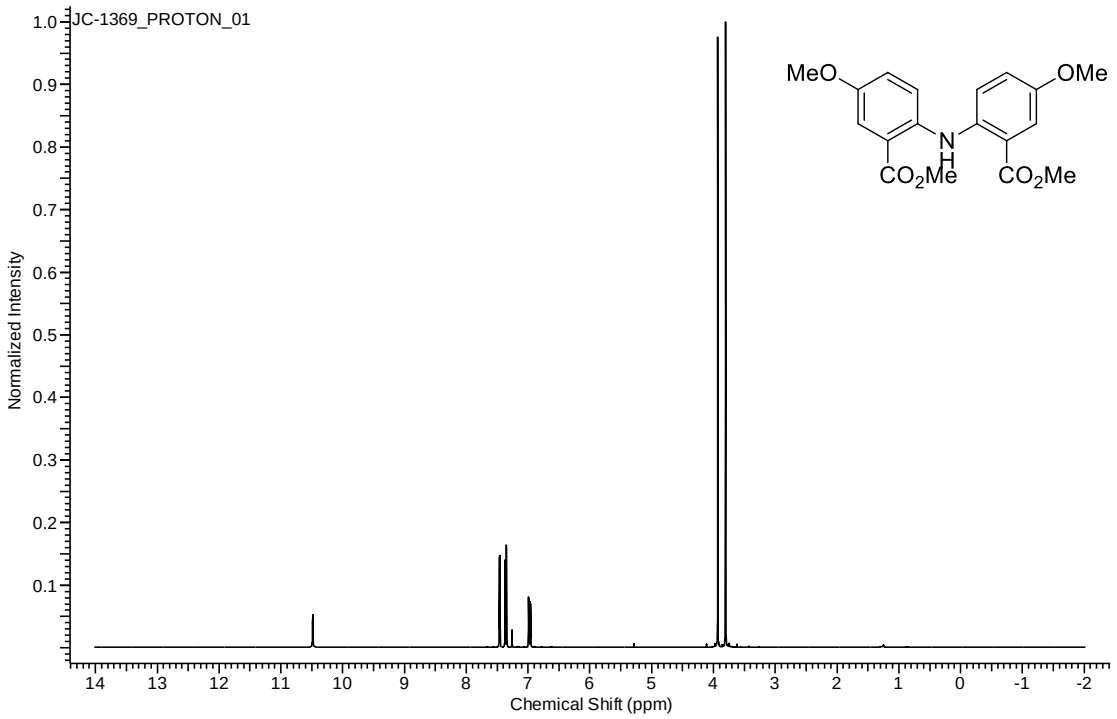
JC-1369_PROTON_01
MeO
OMe
N
H
CO2Me
CO2Me
Normalized Intensity
Chemical Shift (ppm)

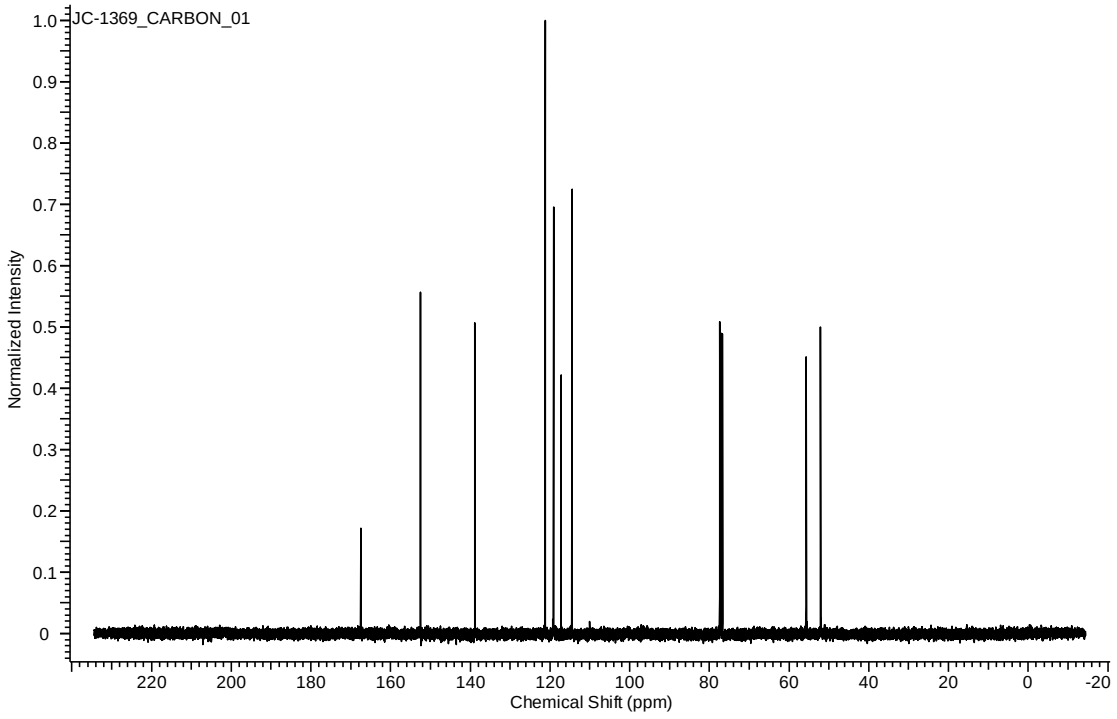
JC-1369_CARBON_01
Normalized Intensity
Chemical Shift (ppm)

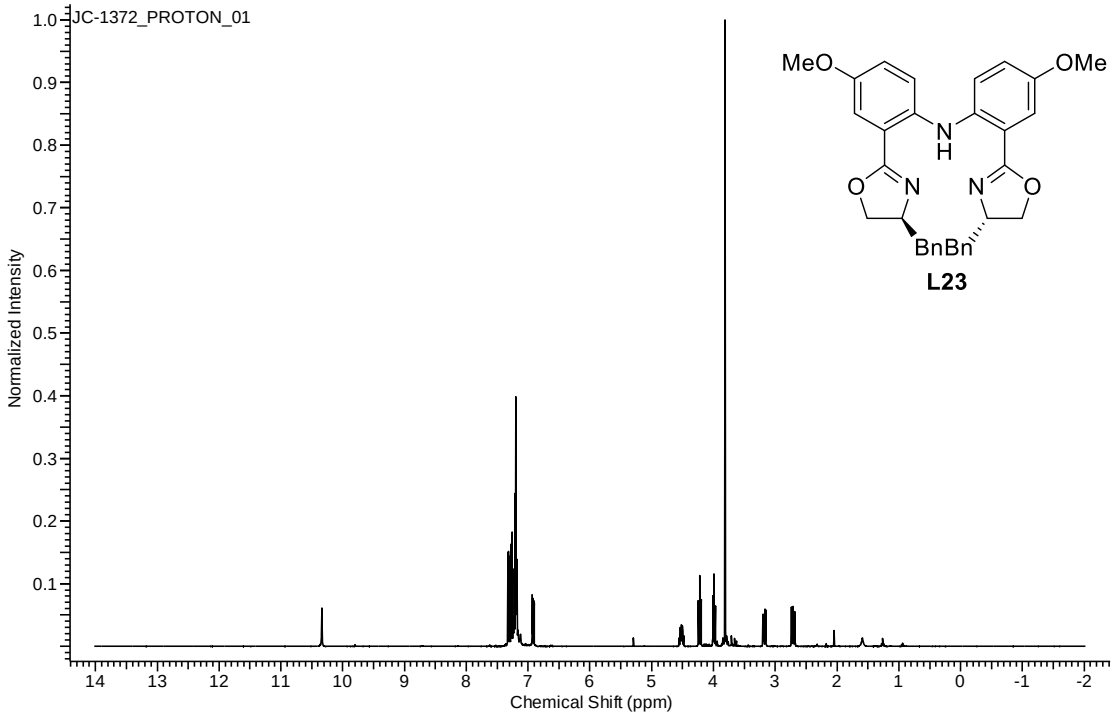
JC-1372_PROTON_01
Normalized Intensity
Chemical Shift (ppm)
MeO
OMe
N
H
O
N
N
O
BnBn

L23

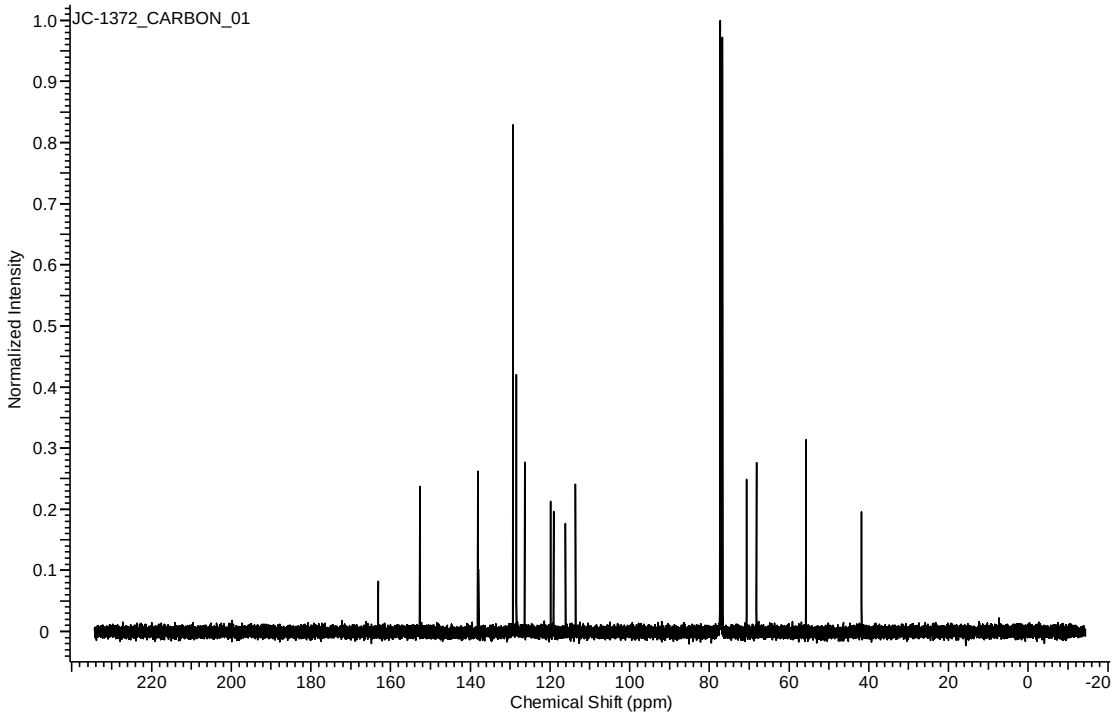
JC-1372_CARBON_01
Normalized Intensity
Chemical Shift (ppm)

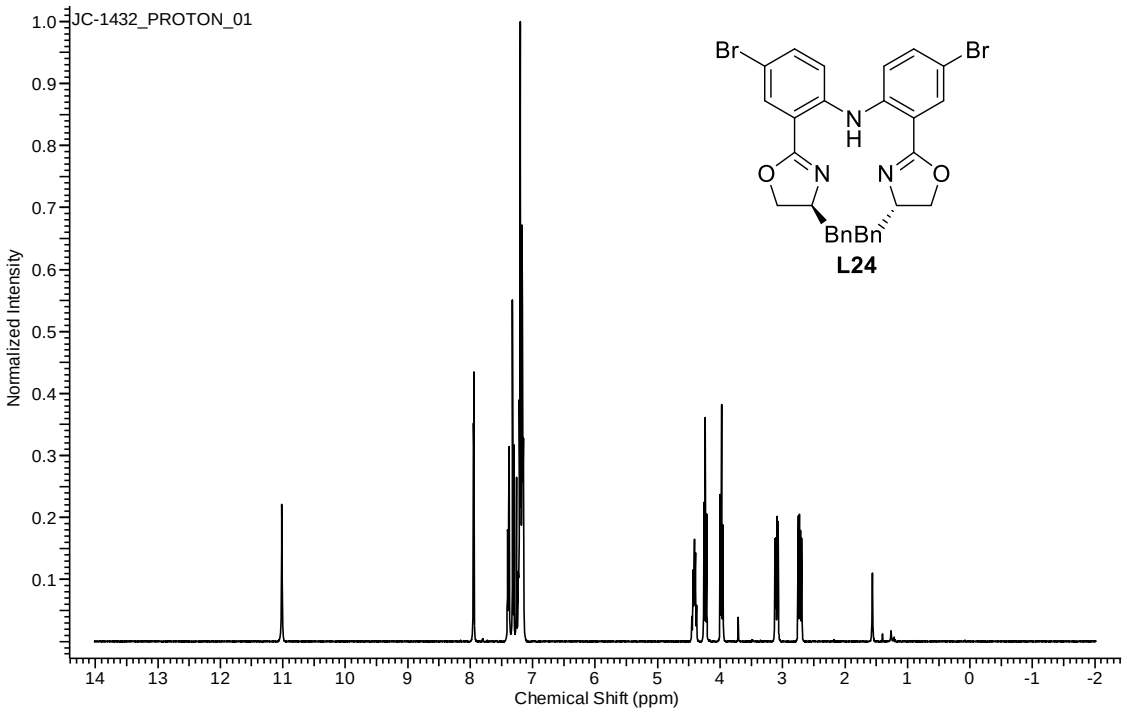
JC-1432_PROTON_01
Normalized Intensity
Chemical Shift (ppm)
Br
Br
N
H
O
N
N
O
BnBn
L24

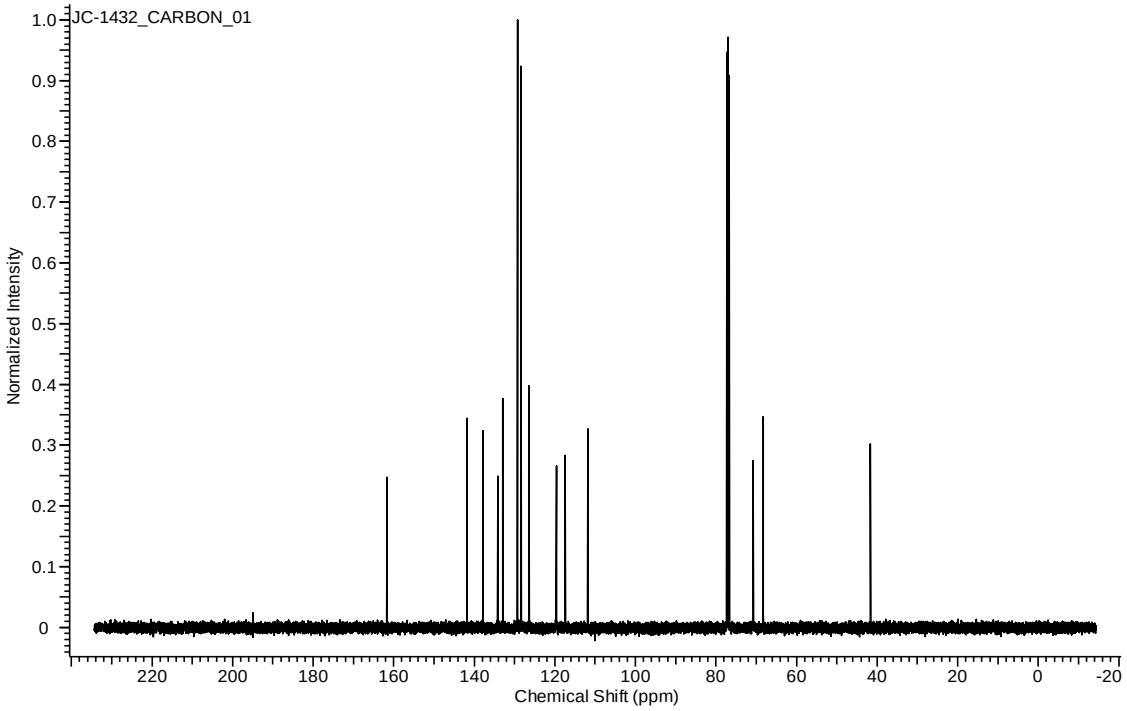
JC-1432_CARBON_01
Normalized Intensity
Chemical Shift (ppm)

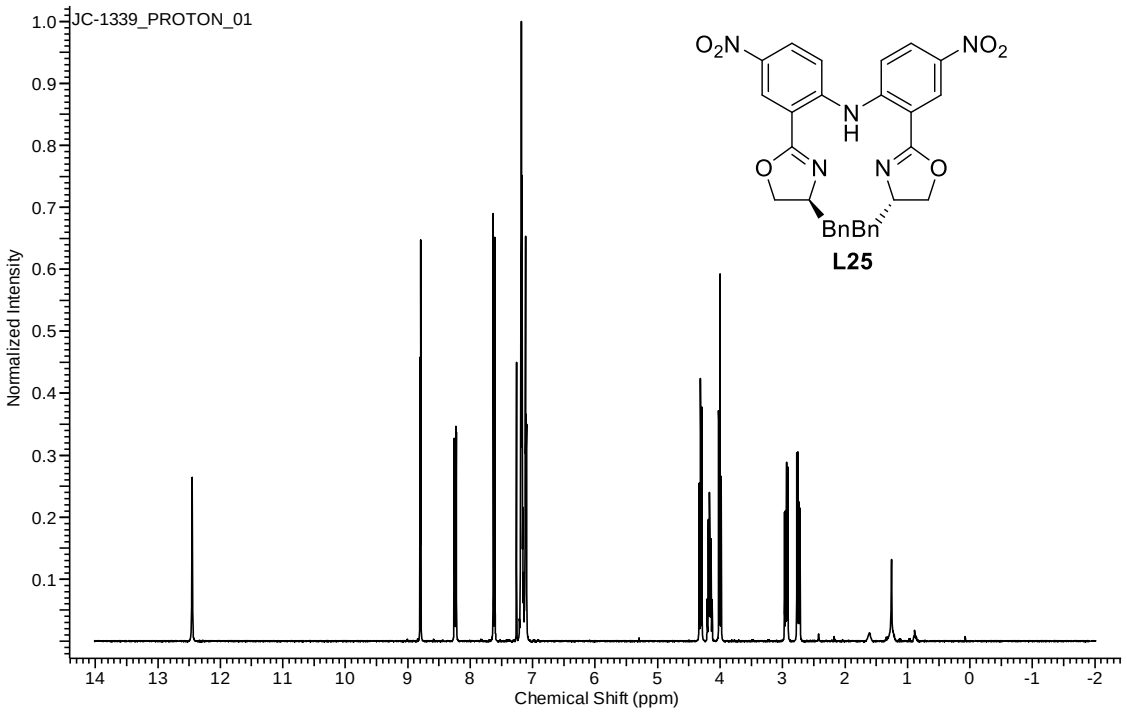
JC-1339_PROTON_01
Normalized Intensity
Chemical Shift (ppm)
O2N
NO2
N
H
O
N
N
O
BnBn
L25

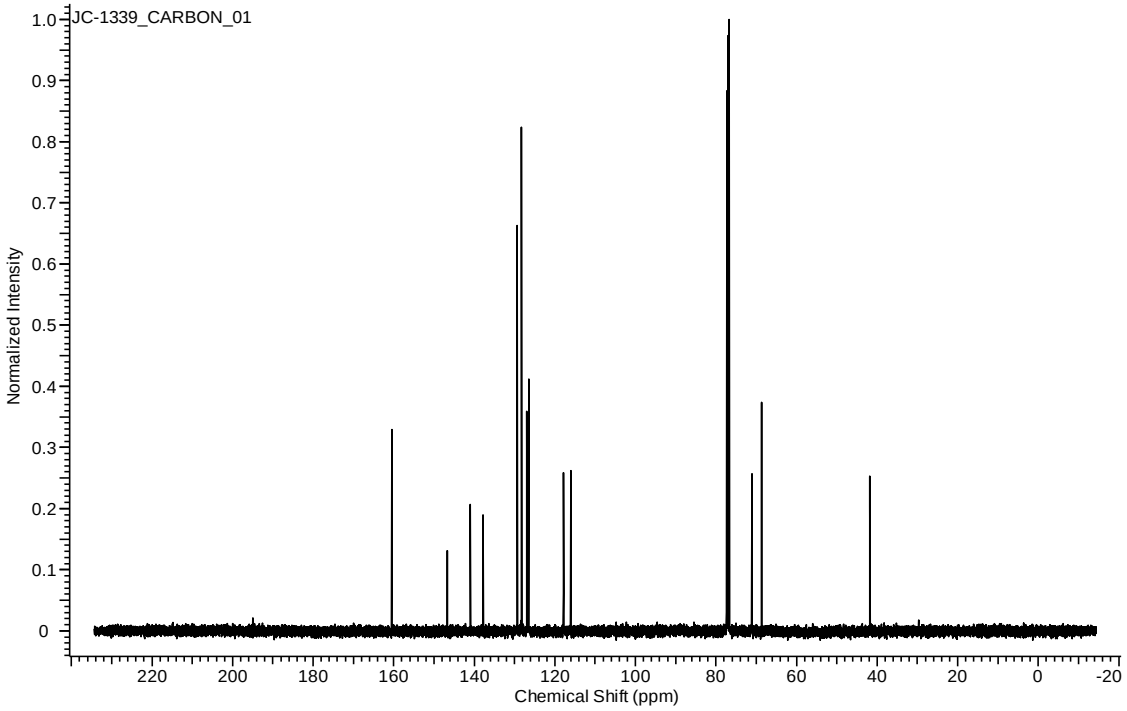
JC-1339_CARBON_01
Normalized Intensity
Chemical Shift (ppm)

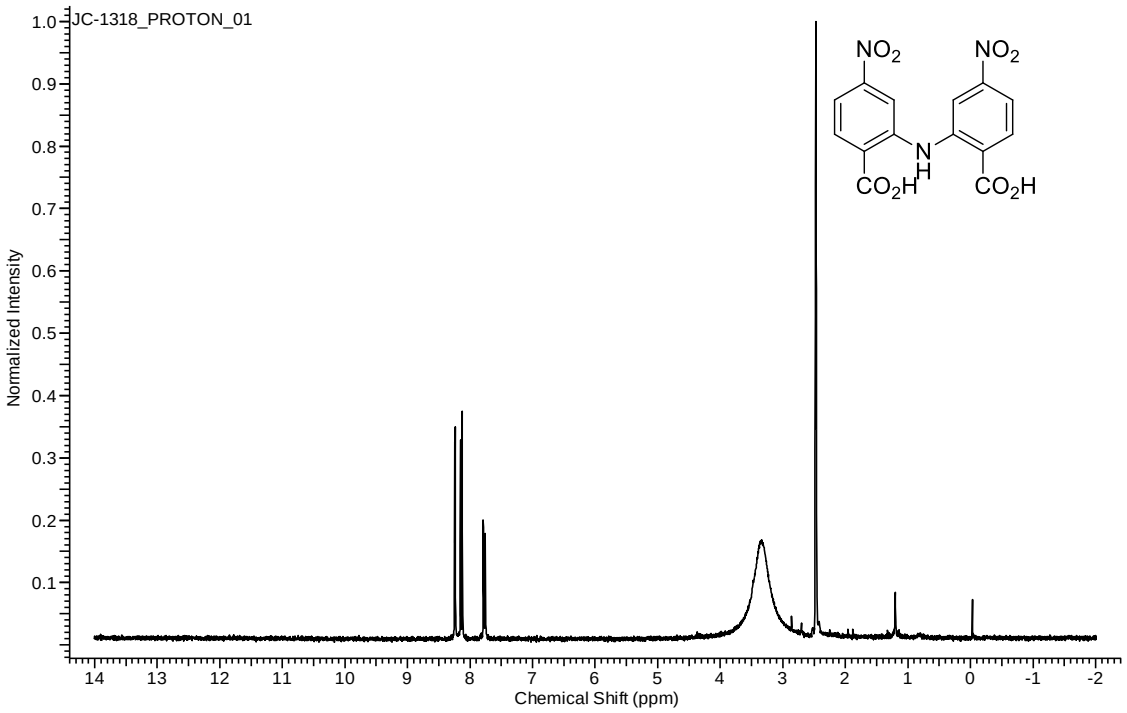
JC-1318_PROTON_01
Normalized Intensity
Chemical Shift (ppm)
NO2
NO2
N
H
CO2H
CO2H

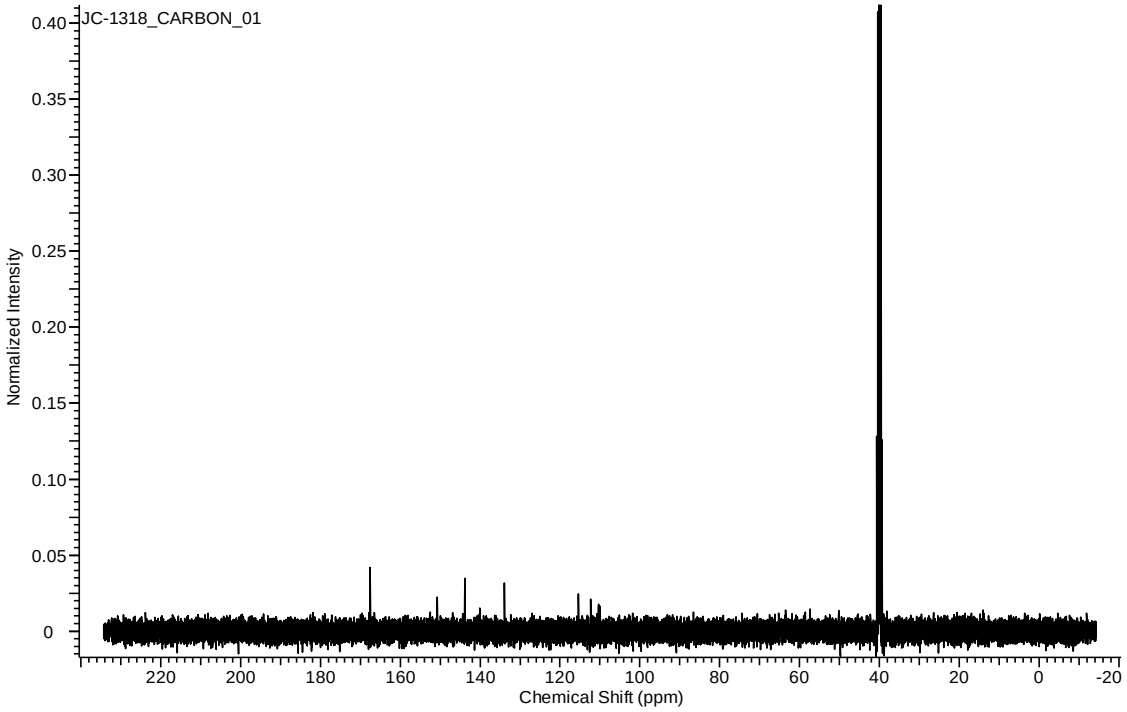
JC-1318_CARBON_01
Normalized Intensity
Chemical Shift (ppm)

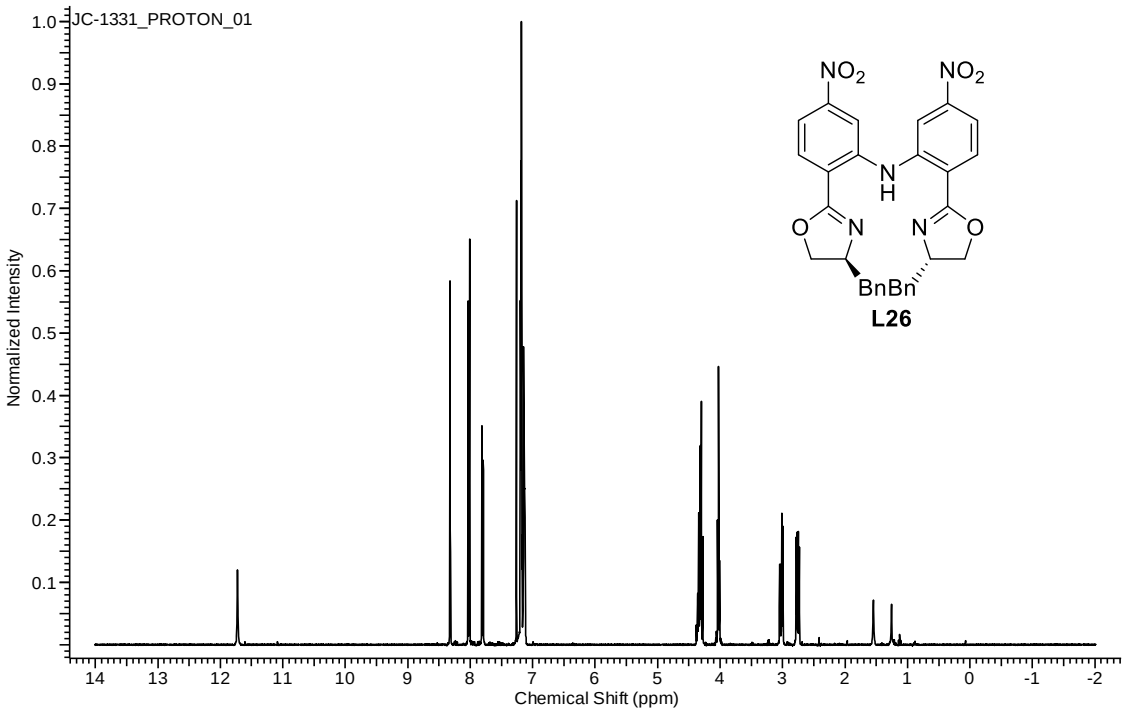
JC-1331_PROTON_01
Normalized Intensity
Chemical Shift (ppm)
NO2
NO2
N
H
O
N
N
O
BnBn
L26

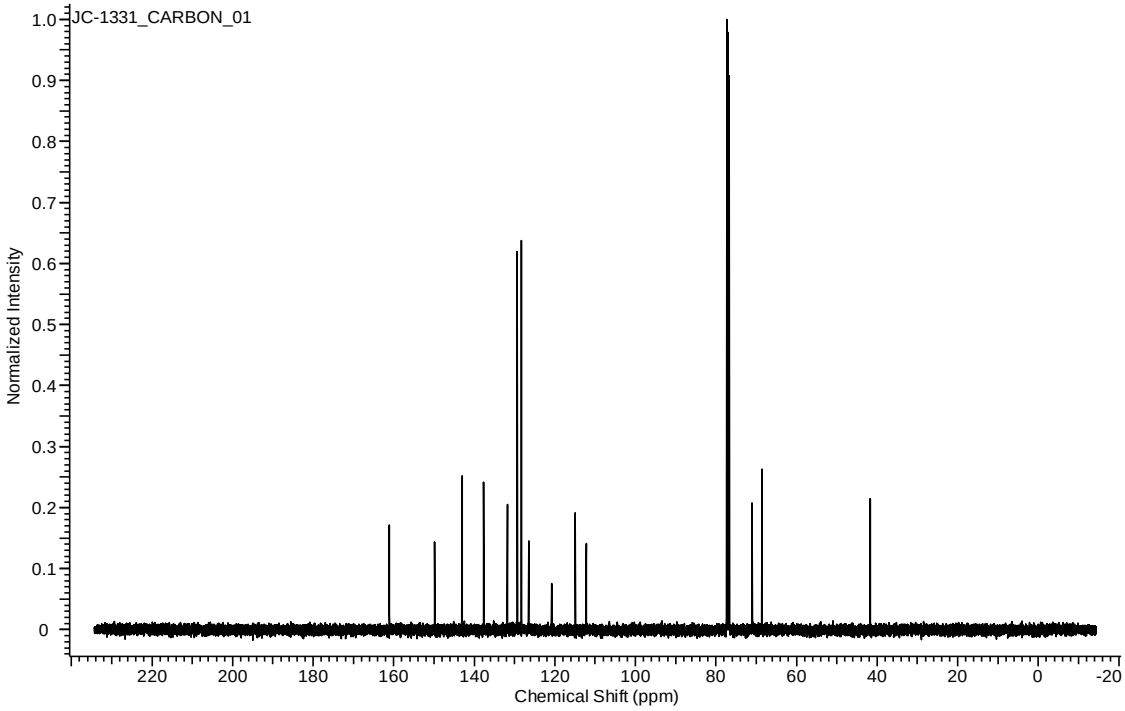
JC-1331_CARBON_01
Normalized Intensity
Chemical Shift (ppm)

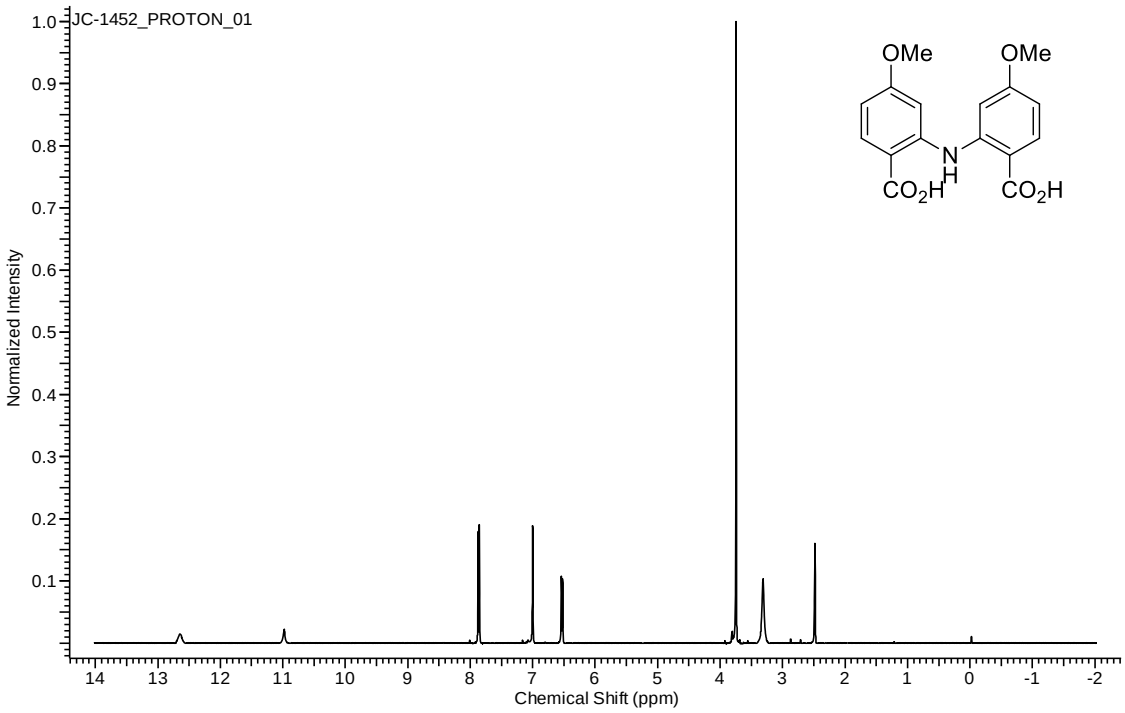
JC-1452_PROTON_01
OMe
OMe
N
H
CO2H
CO2H
Normalized Intensity
Chemical Shift (ppm)

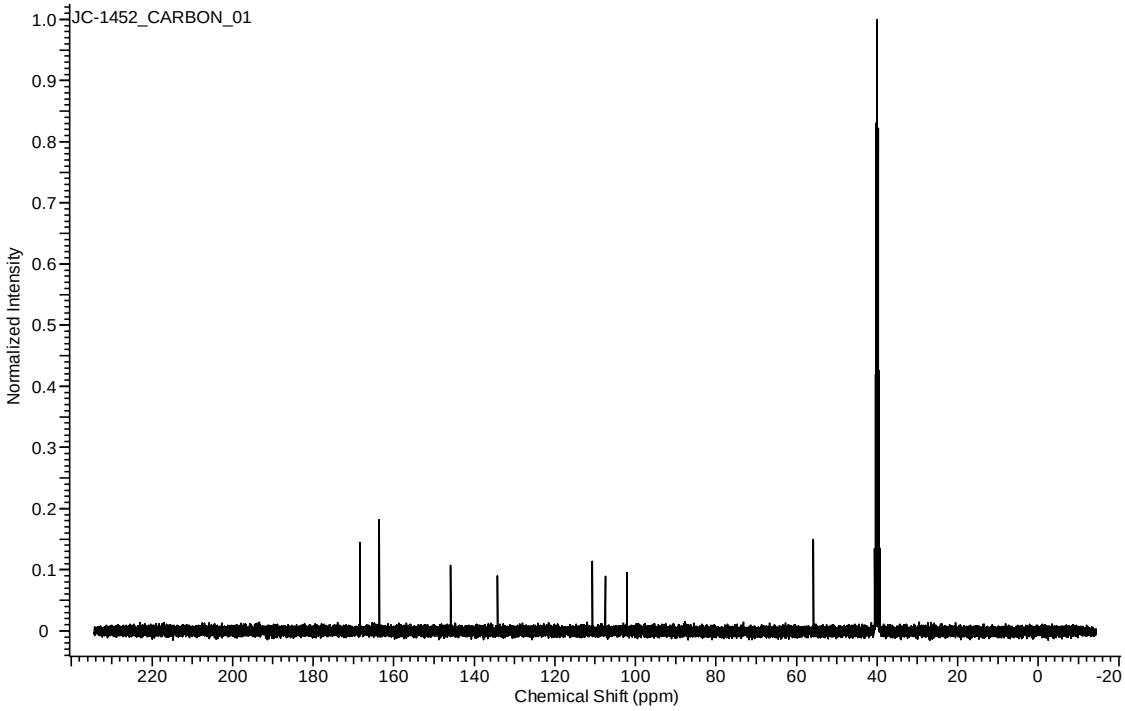
JC-1452_CARBON_01
Normalized Intensity
Chemical Shift (ppm)

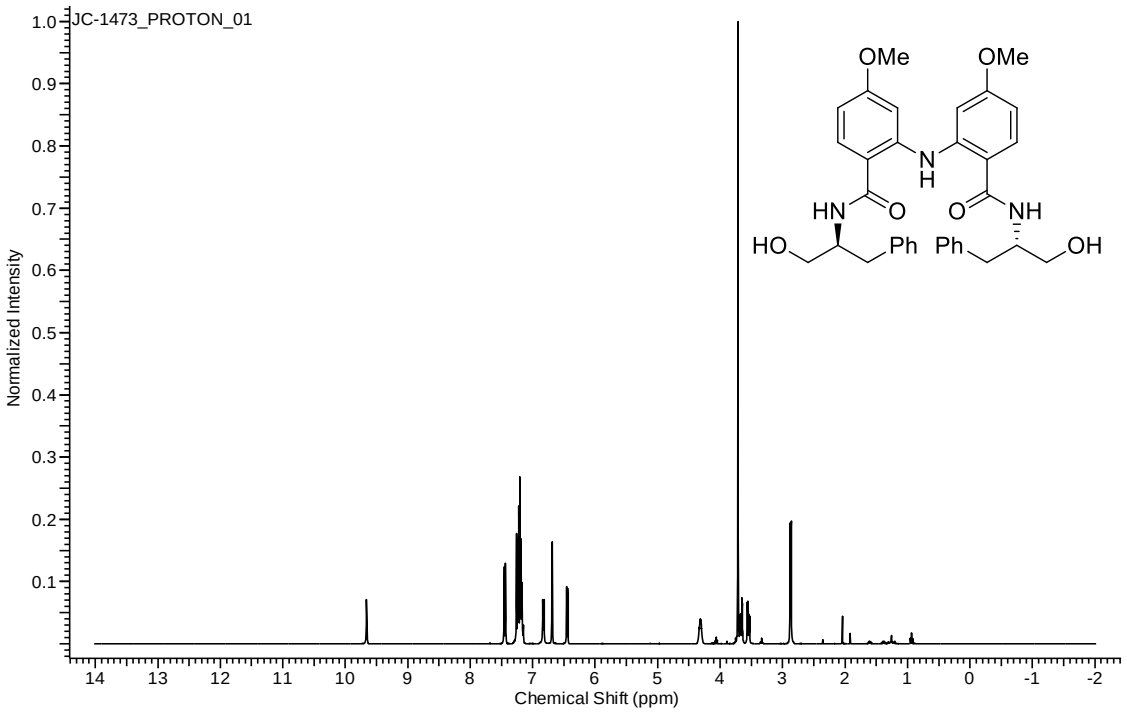
JC-1473_PROTON_01
Normalized Intensity
Chemical Shift (ppm)
OMe
OMe
N
H
HN
O
O
NH
HO
Ph
Ph
OH

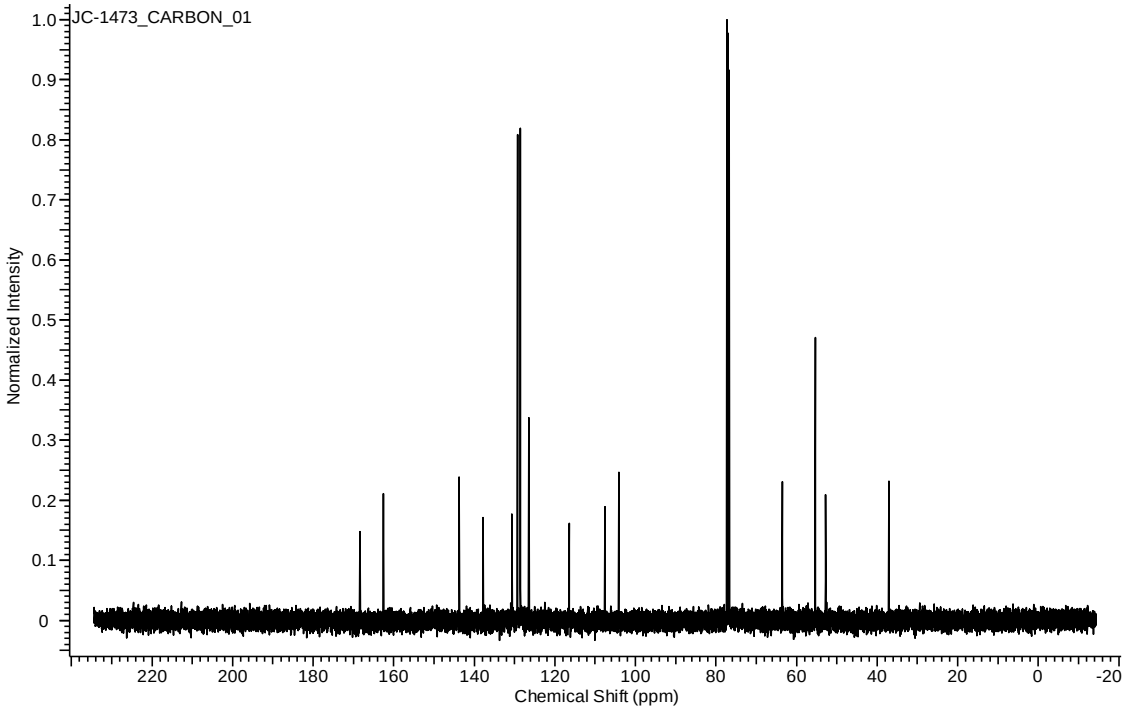
JC-1473_CARBON_01
Normalized Intensity
Chemical Shift (ppm)

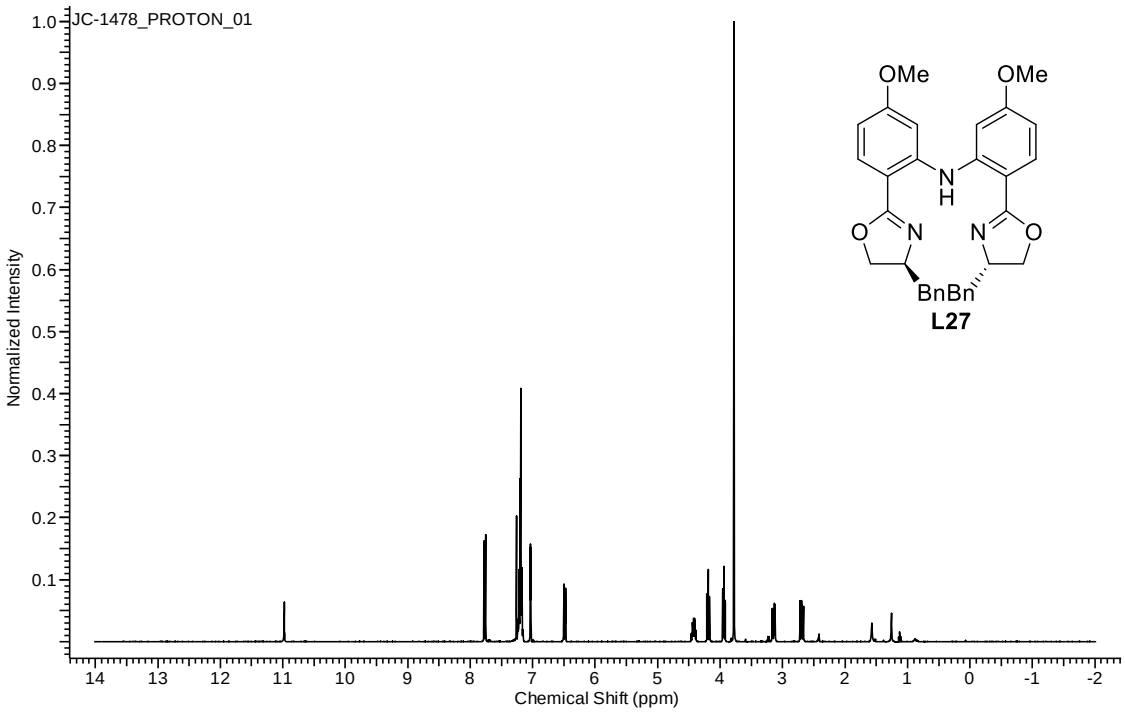
JC-1478_PROTON_01
Normalized Intensity
Chemical Shift (ppm)
OMe
OMe
N
H
O
N
N
O
BnBn
L27

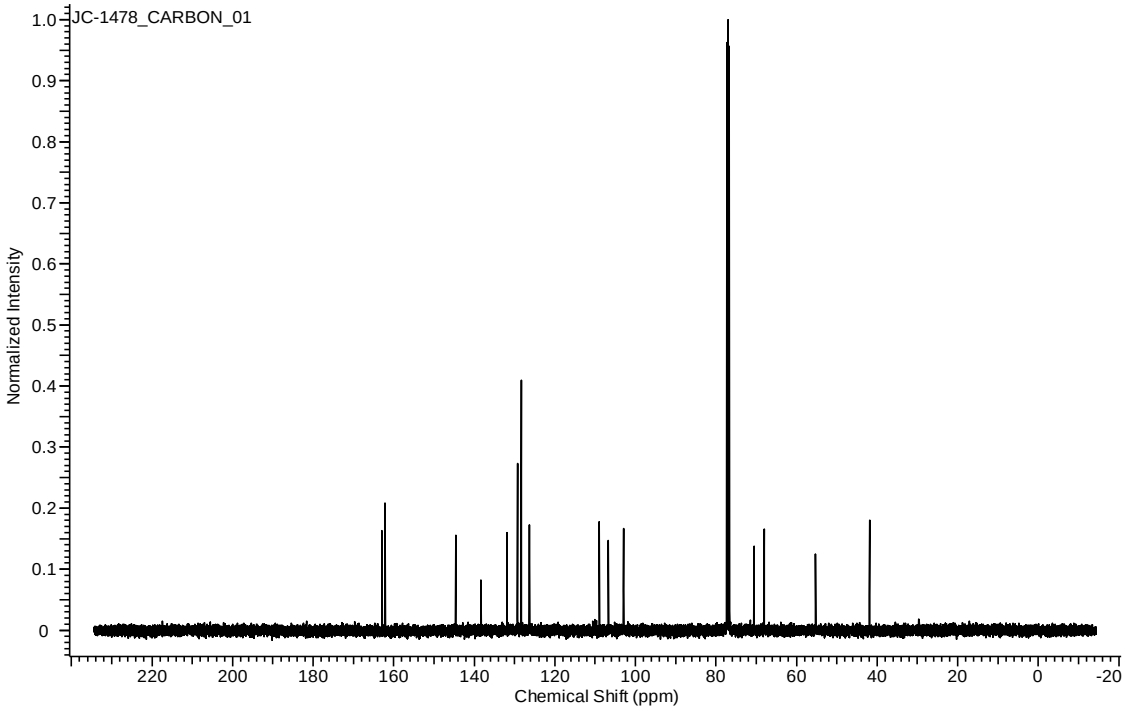
JC-1478_CARBON_01
Normalized Intensity
Chemical Shift (ppm)

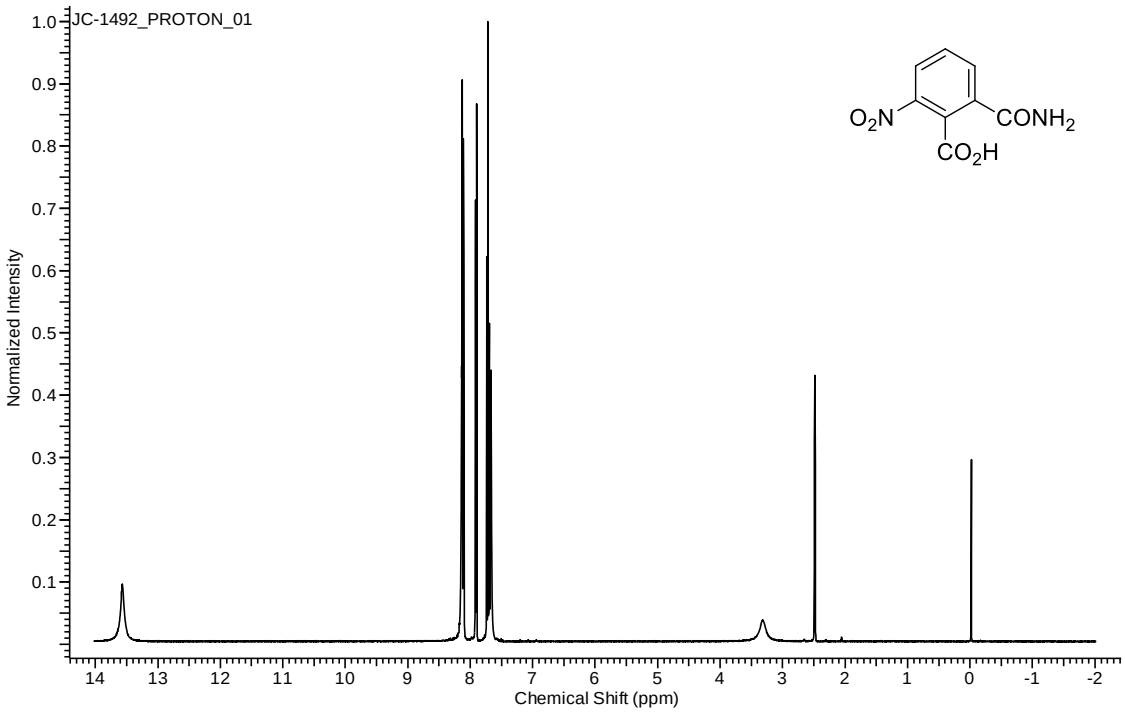
JC-1492_PROTON_01
Normalized Intensity
Chemical Shift (ppm)
O2N
CONH2
CO2H

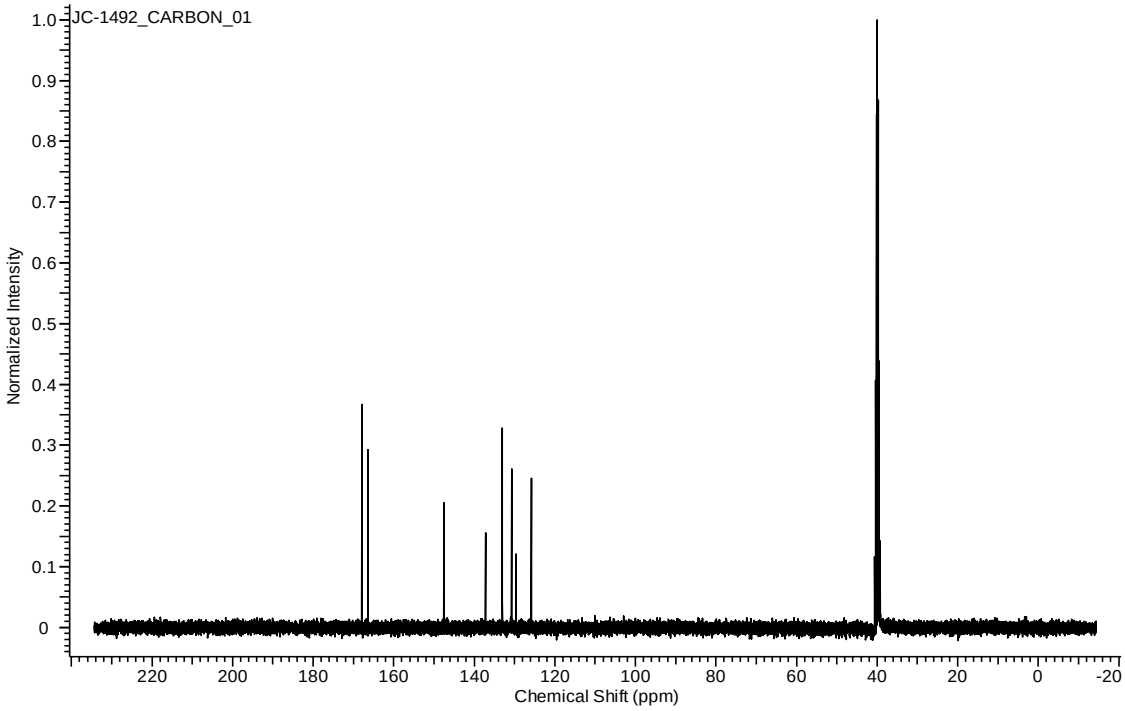
JC-1492_CARBON_01
Normalized Intensity
Chemical Shift (ppm)

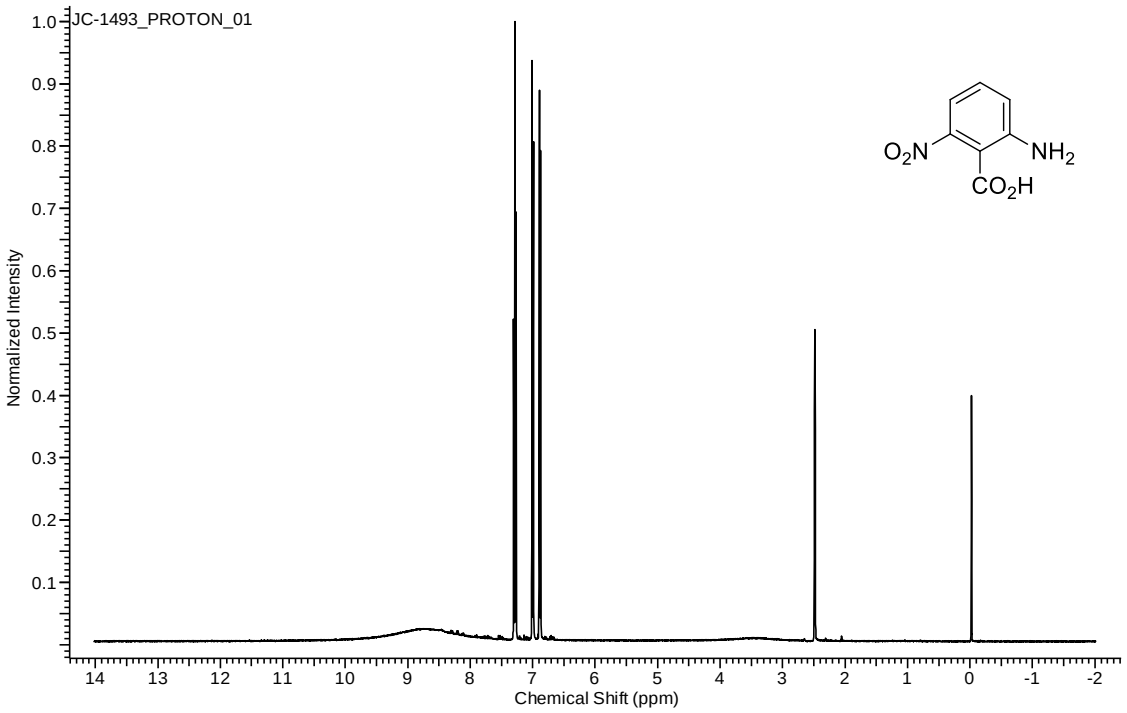
JC-1493_PROTON_01
Normalized Intensity
Chemical Shift (ppm)
O2N
NH2
CO2H

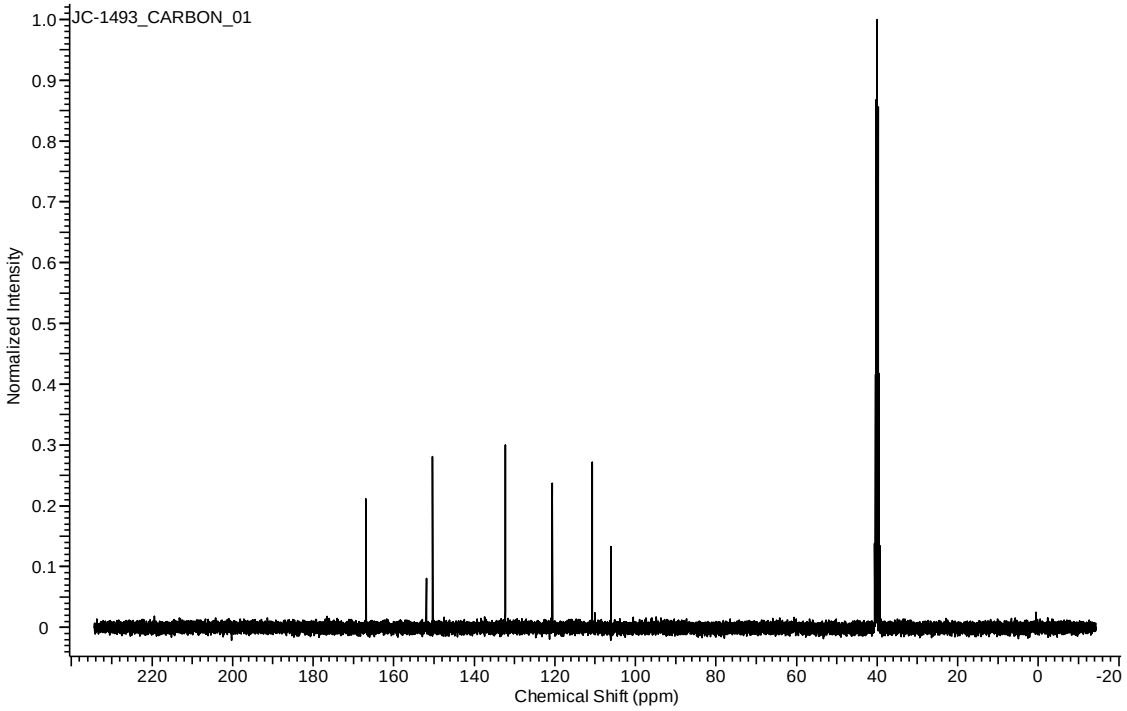
JC-1493_CARBON_01
Normalized Intensity
Chemical Shift (ppm)

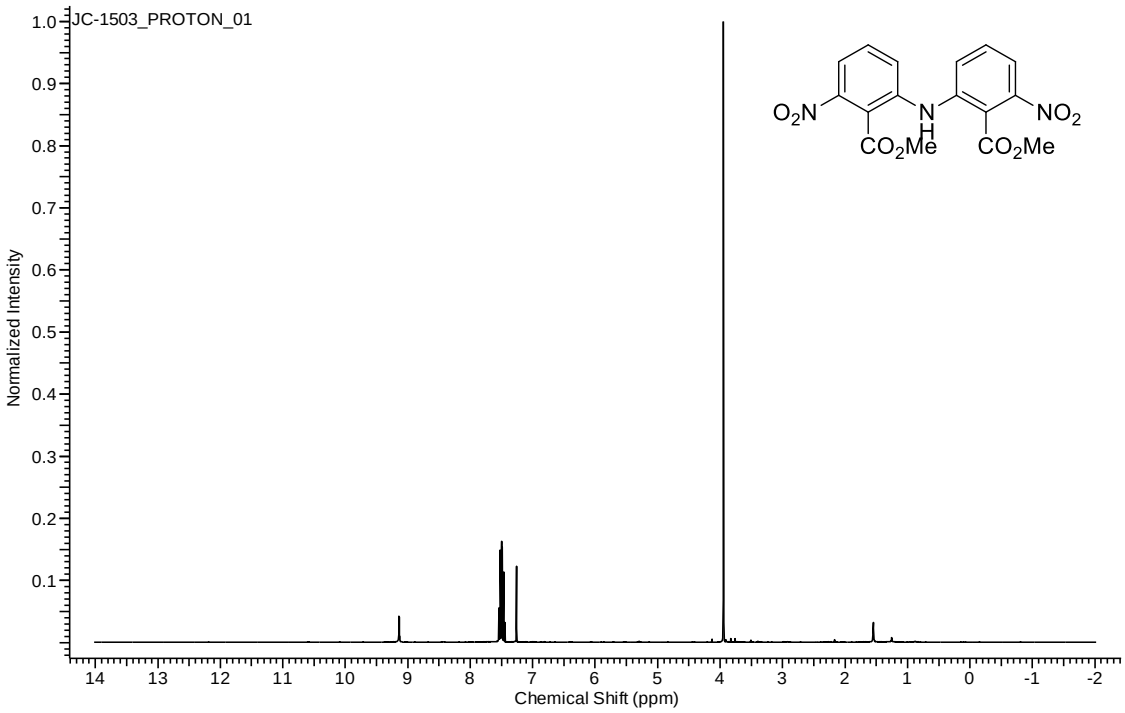
JC-1503_PROTON_01
Normalized Intensity
Chemical Shift (ppm)
O2N
NO2
N
H
CO2Me
CO2Me

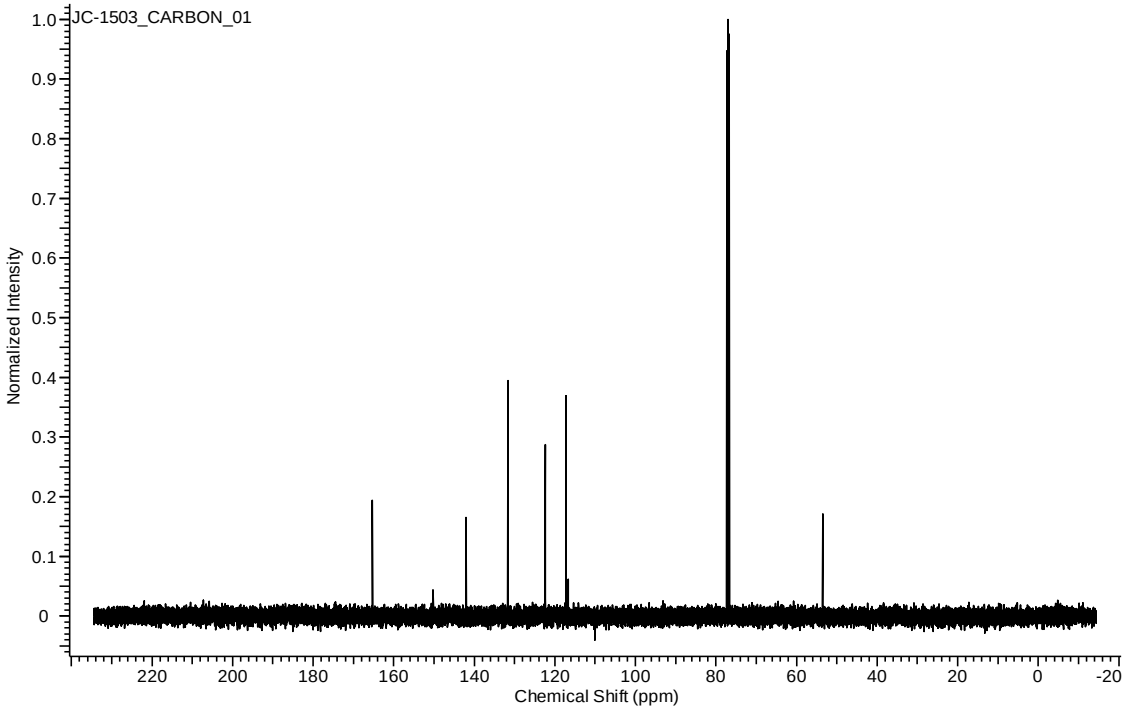
JC-1503_CARBON_01
Normalized Intensity
Chemical Shift (ppm)

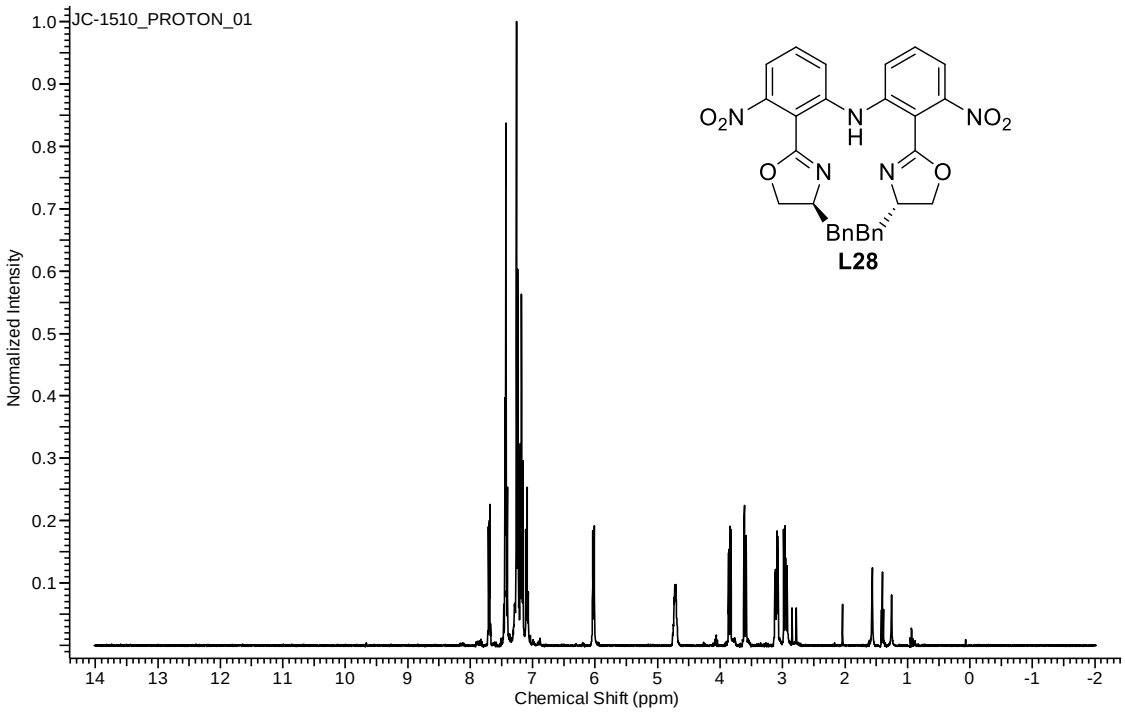
JC-1510_PROTON_01
Normalized Intensity
Chemical Shift (ppm)
O2N
NO2
N
H
O
N
N
O
BnBn

L28

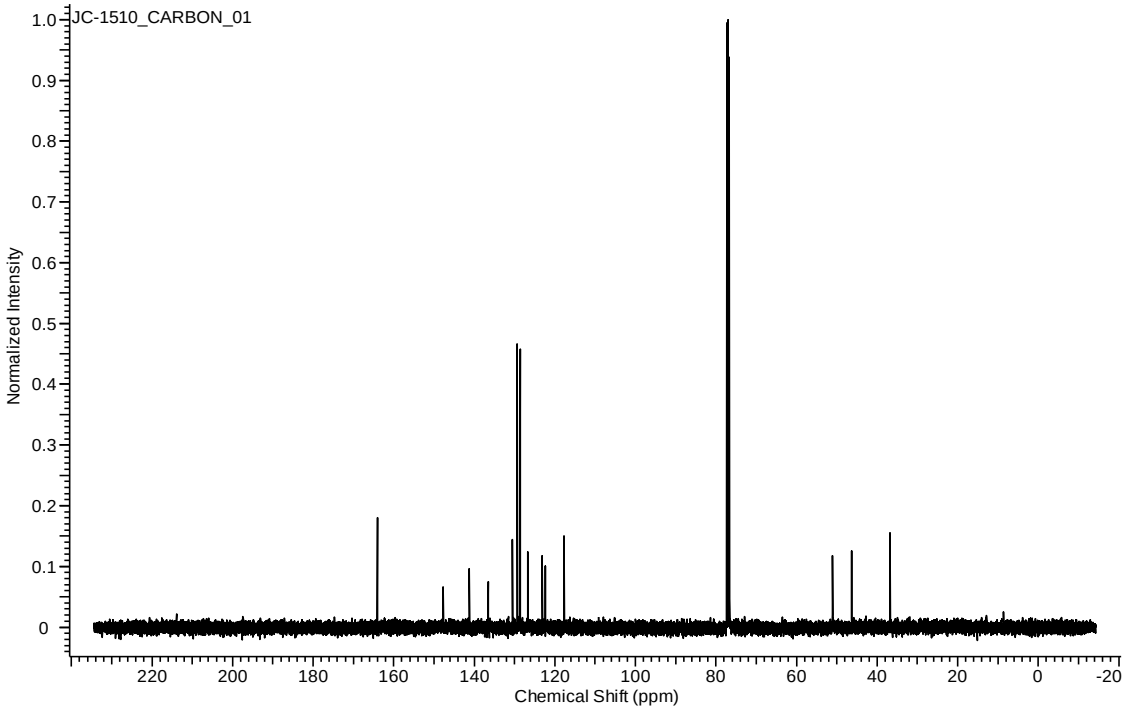
JC-1510_CARBON_01
Normalized Intensity
Chemical Shift (ppm)

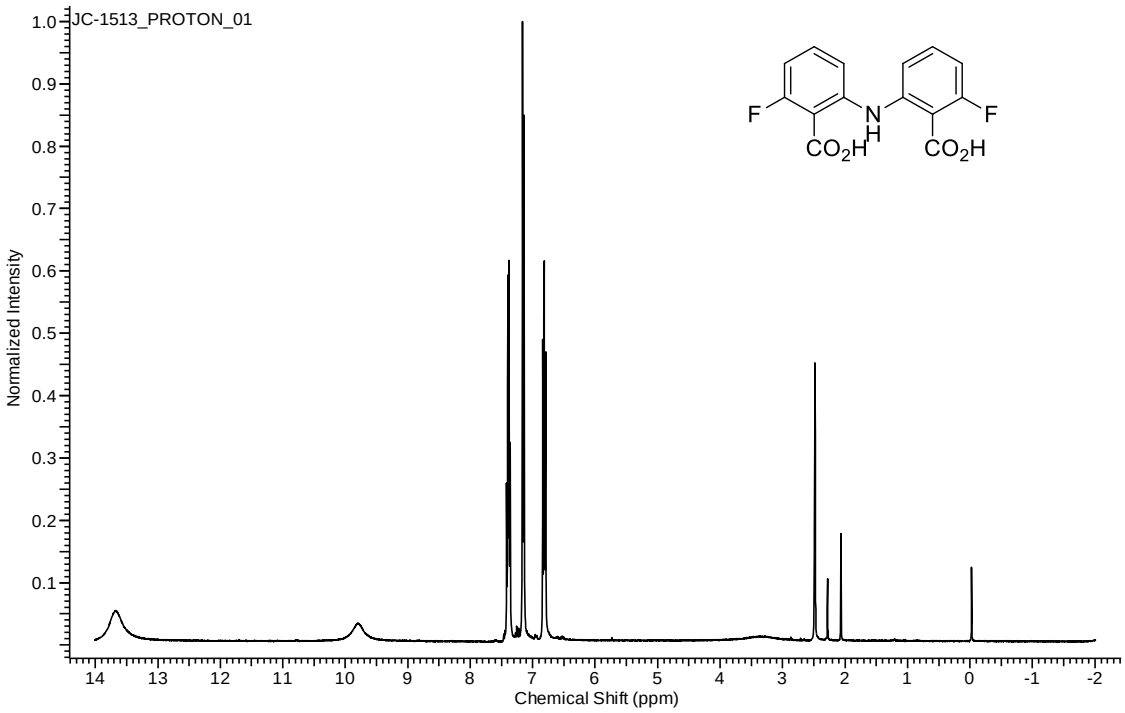
JC-1513_PROTON_01
Normalized Intensity
Chemical Shift (ppm)
F
N
H
F
CO2H
CO2H

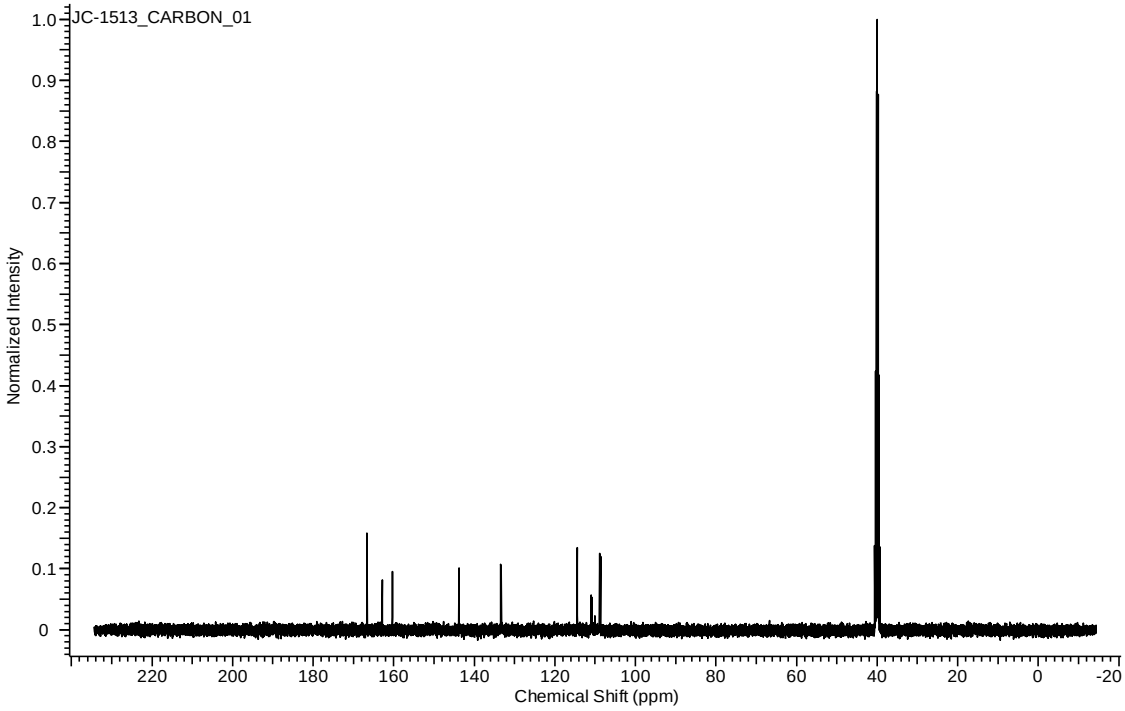
JC-1513_CARBON_01
Normalized Intensity
Chemical Shift (ppm)

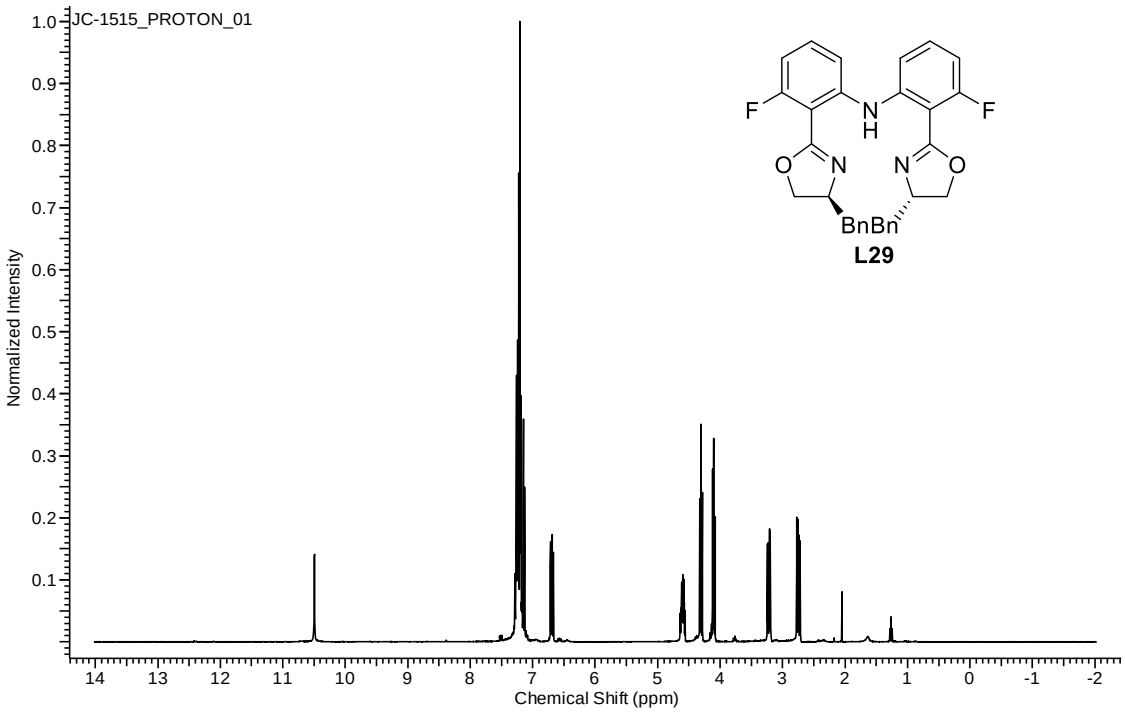
JC-1515_PROTON_01
Normalized Intensity
Chemical Shift (ppm)
F
N
H
F
O
N
N
O
BnBn

L29

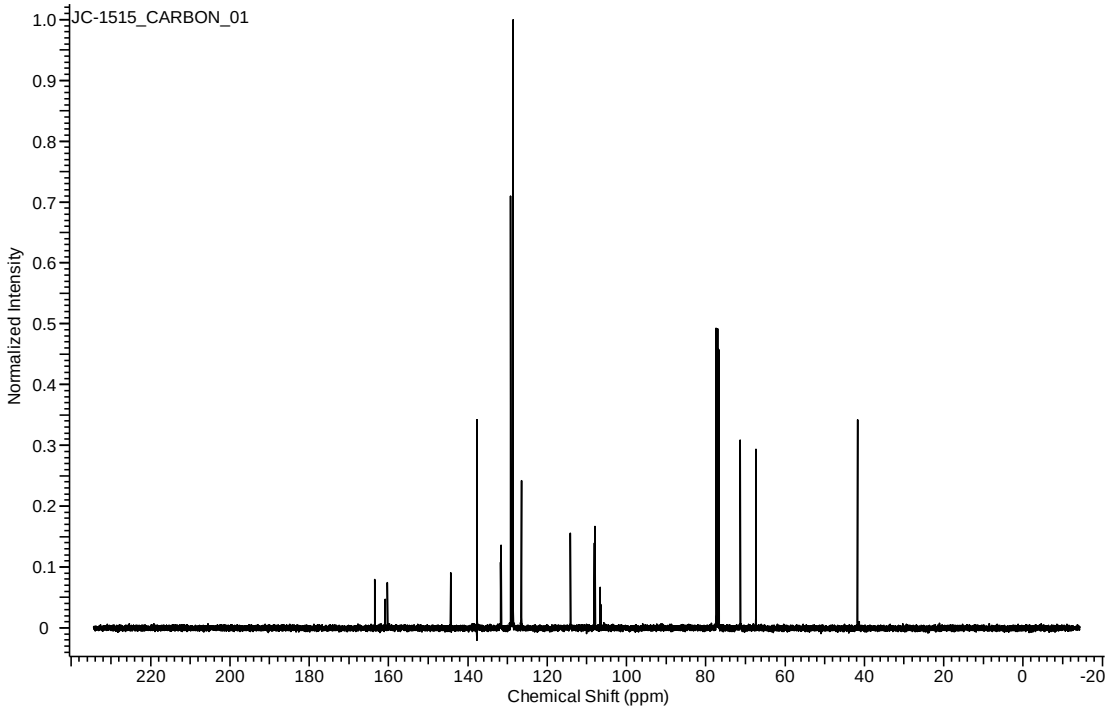
JC-1515_CARBON_01
Normalized Intensity
Chemical Shift (ppm)

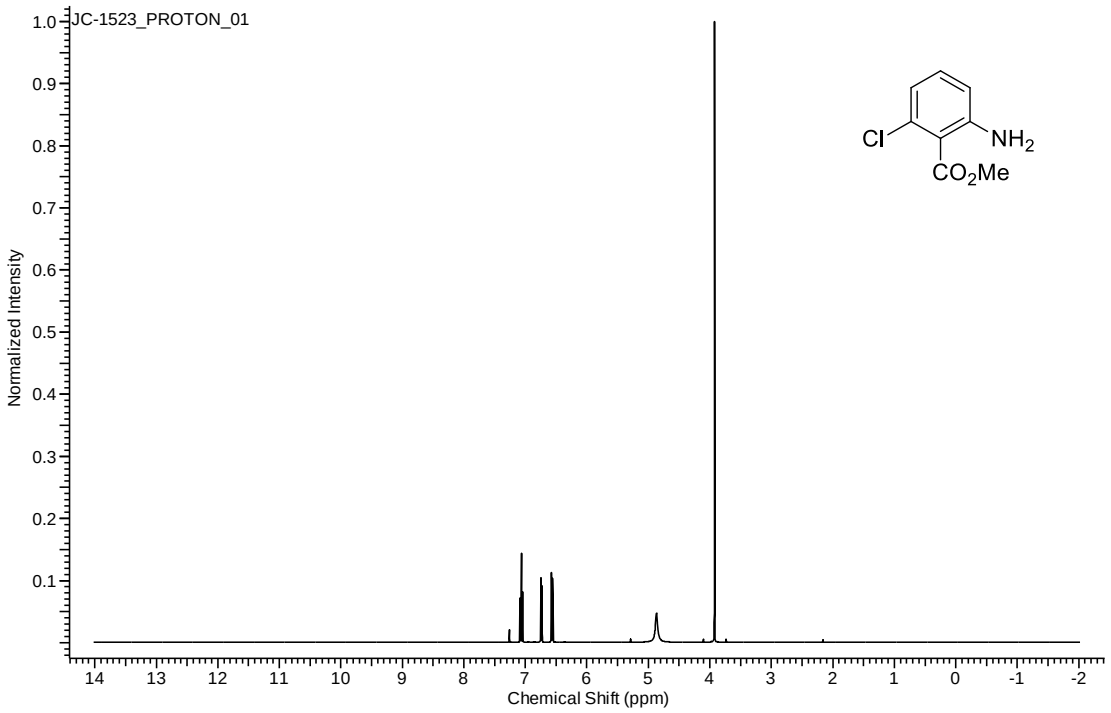
JC-1523_PROTON_01
Normalized Intensity
Chemical Shift (ppm)
Cl
NH2
CO2Me

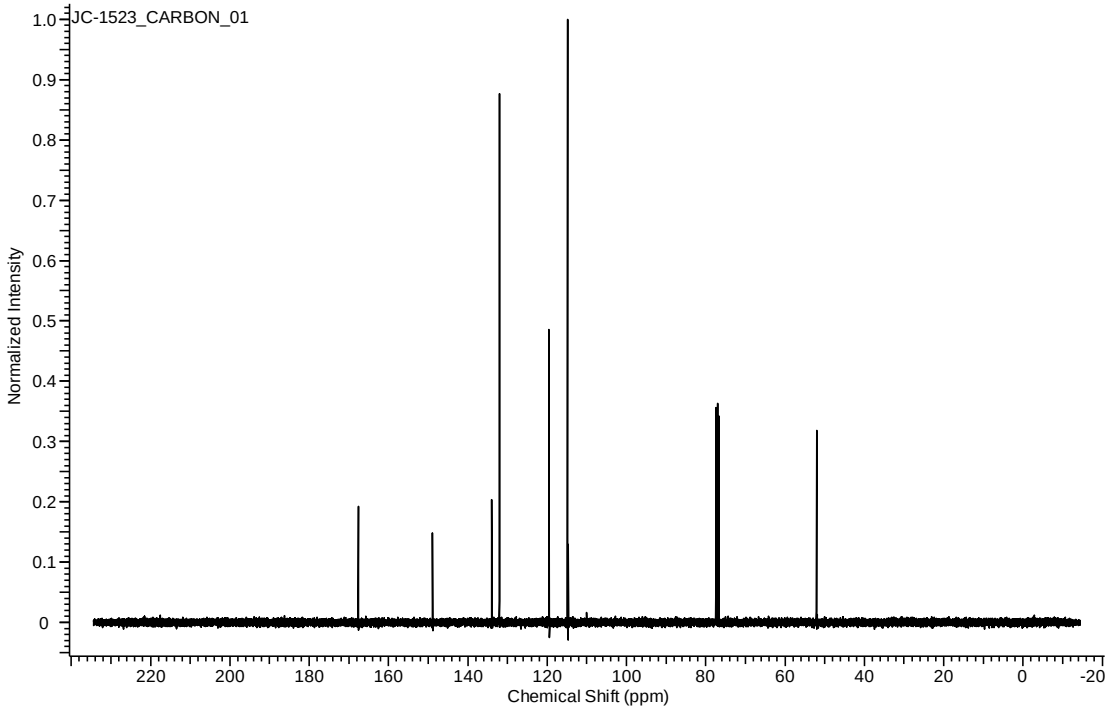
JC-1523_CARBON_01
Normalized Intensity
Chemical Shift (ppm)

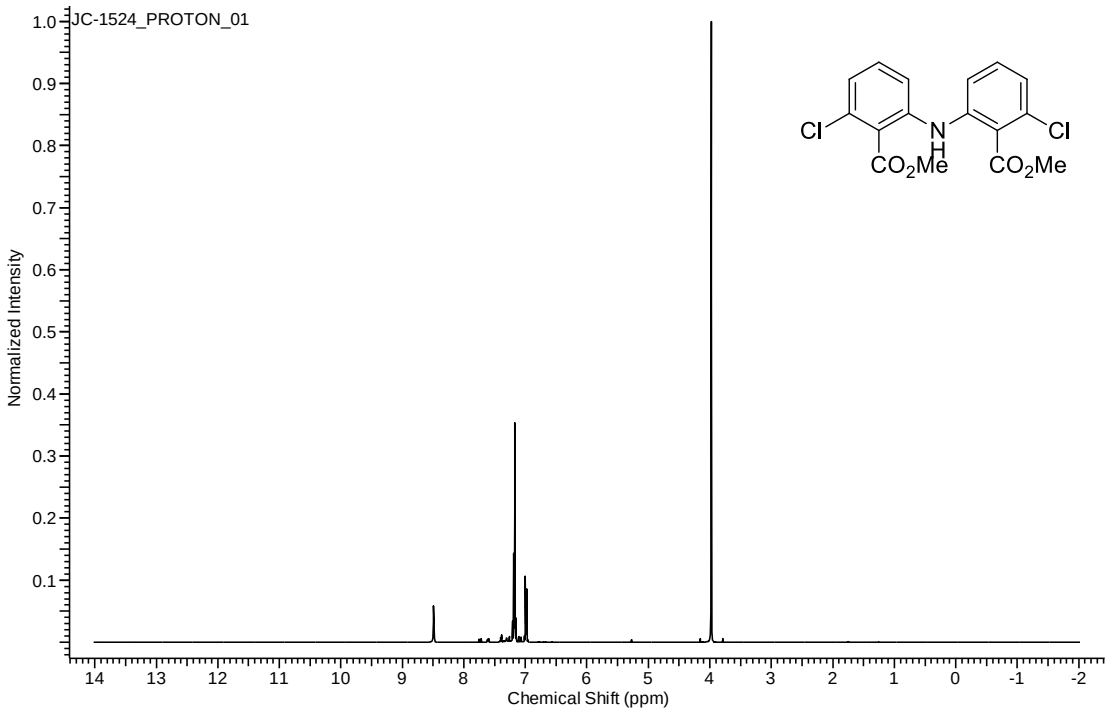
JC-1524_PROTON_01
Normalized Intensity
Chemical Shift (ppm)
Cl
N
H
Cl
CO2Me
CO2Me

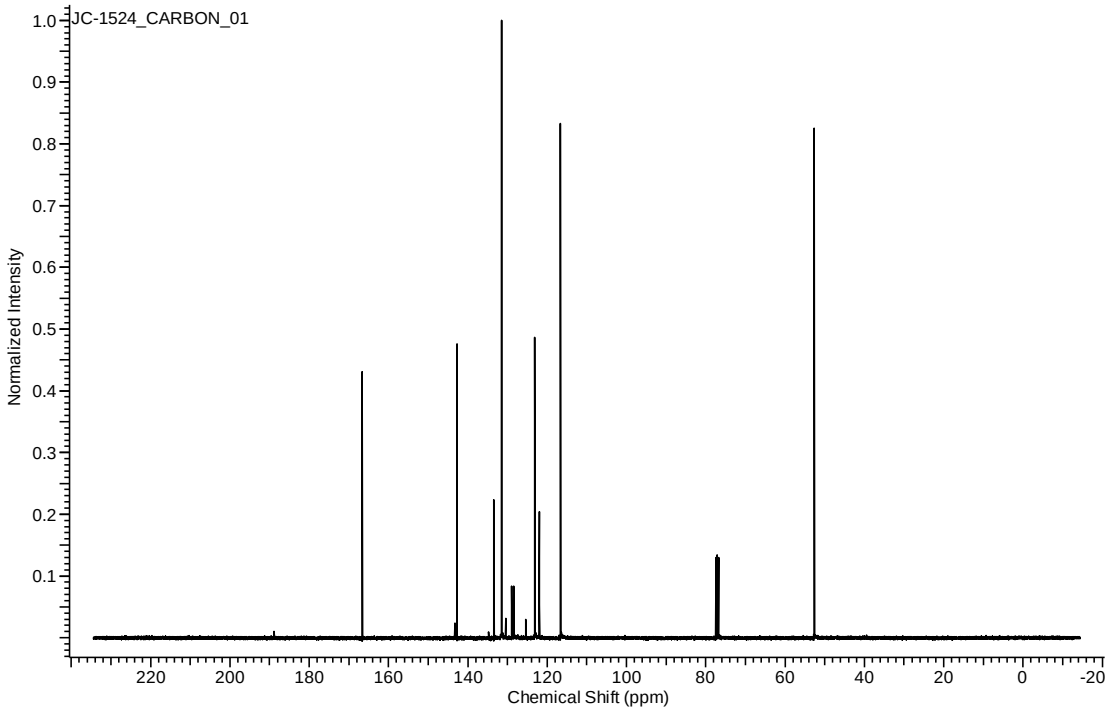
JC-1524_CARBON_01
Normalized Intensity
Chemical Shift (ppm)

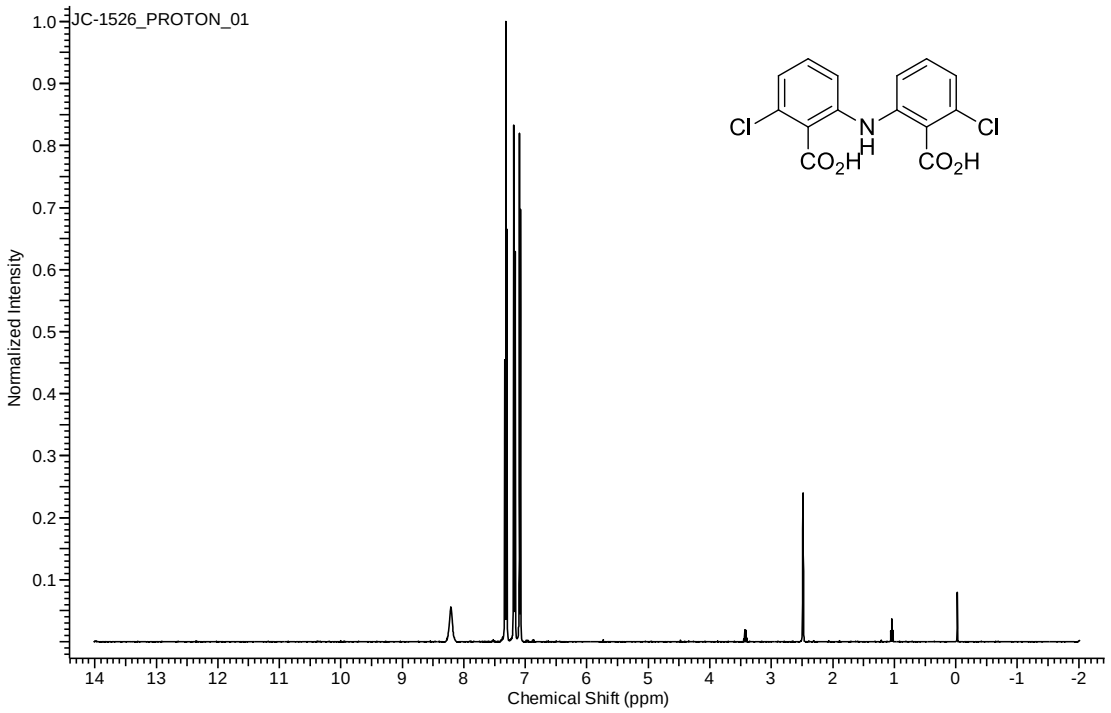
JC-1526_PROTON_01
Normalized Intensity
Chemical Shift (ppm)
Cl
N
H
CO2H
CO2H
Cl

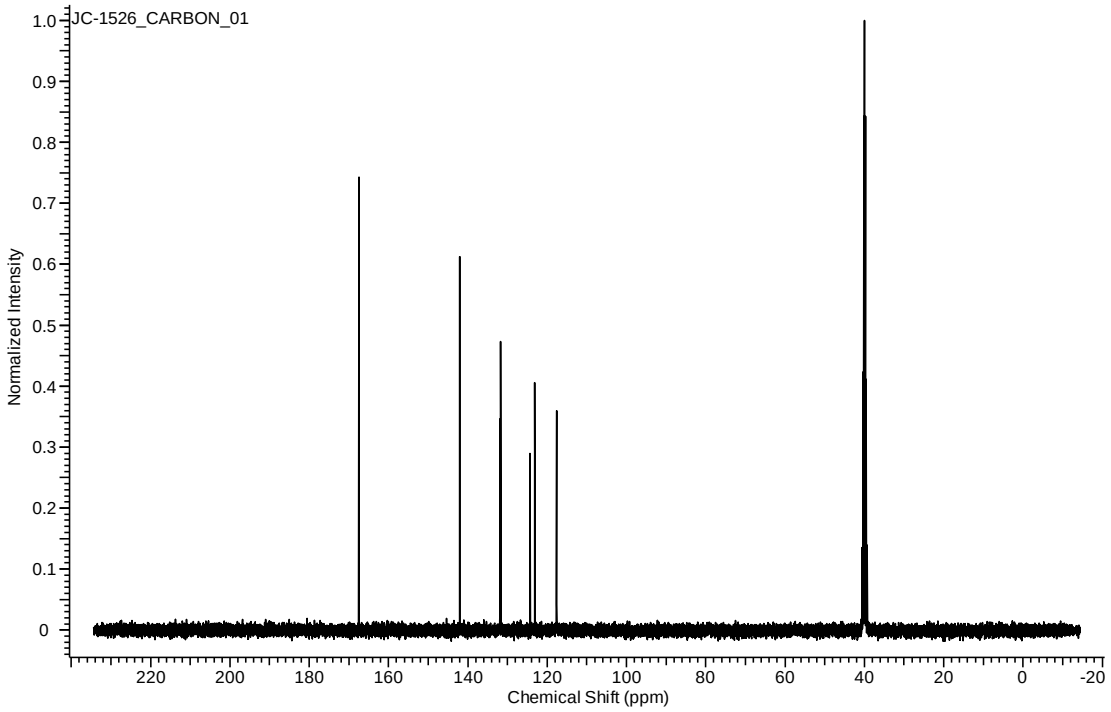
JC-1526_CARBON_01
Normalized Intensity
Chemical Shift (ppm)

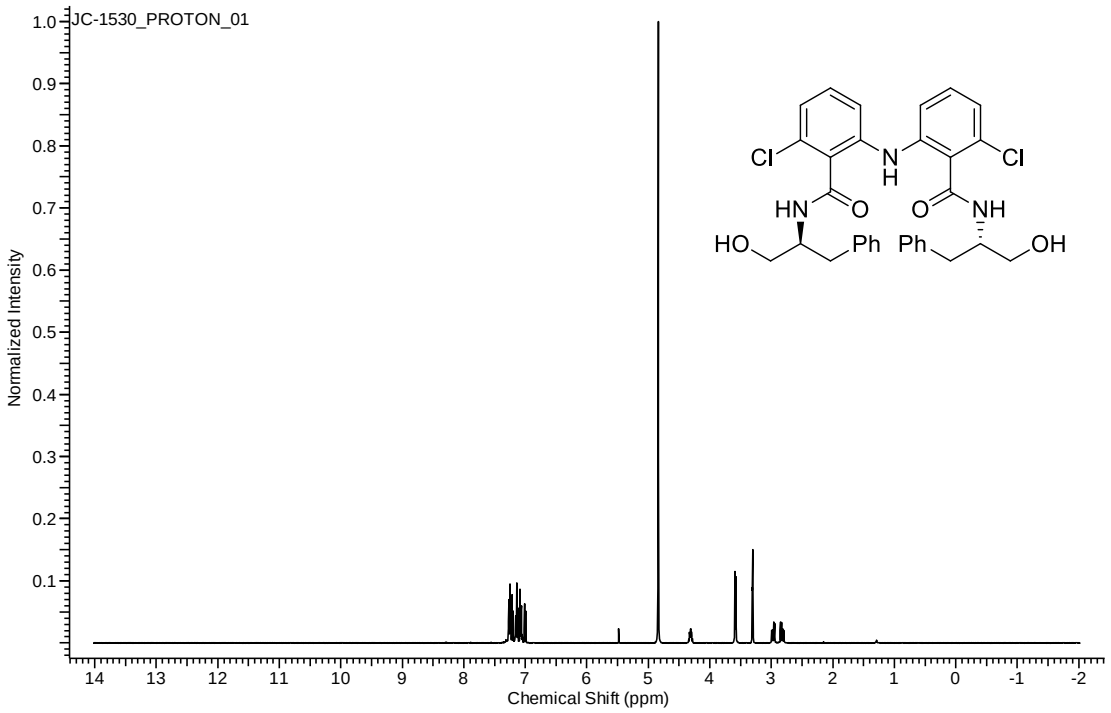
JC-1530_PROTON_01
Normalized Intensity
Chemical Shift (ppm)
Cl
N
H
Cl
HN
O
O
NH
HO
Ph
Ph
OH

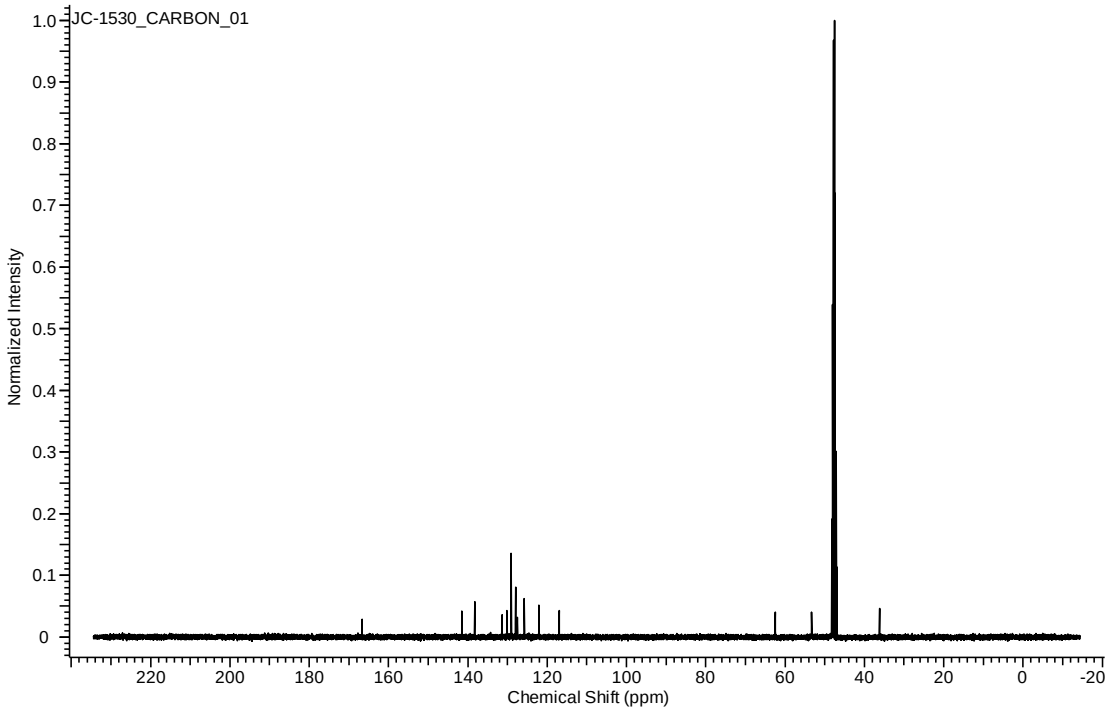
JC-1530_CARBON_01
Normalized Intensity
Chemical Shift (ppm)

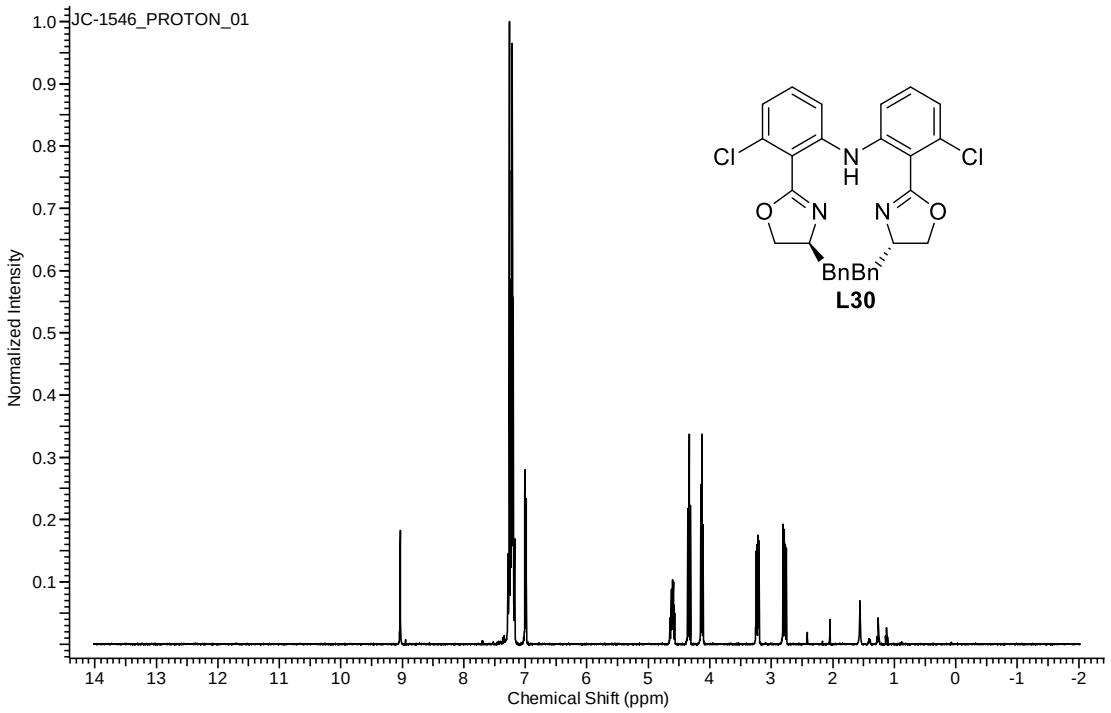
JC-1546_PROTON_01
Normalized Intensity
Chemical Shift (ppm)
Cl
N
H
Cl
O
N
N
O
BnBn
L30

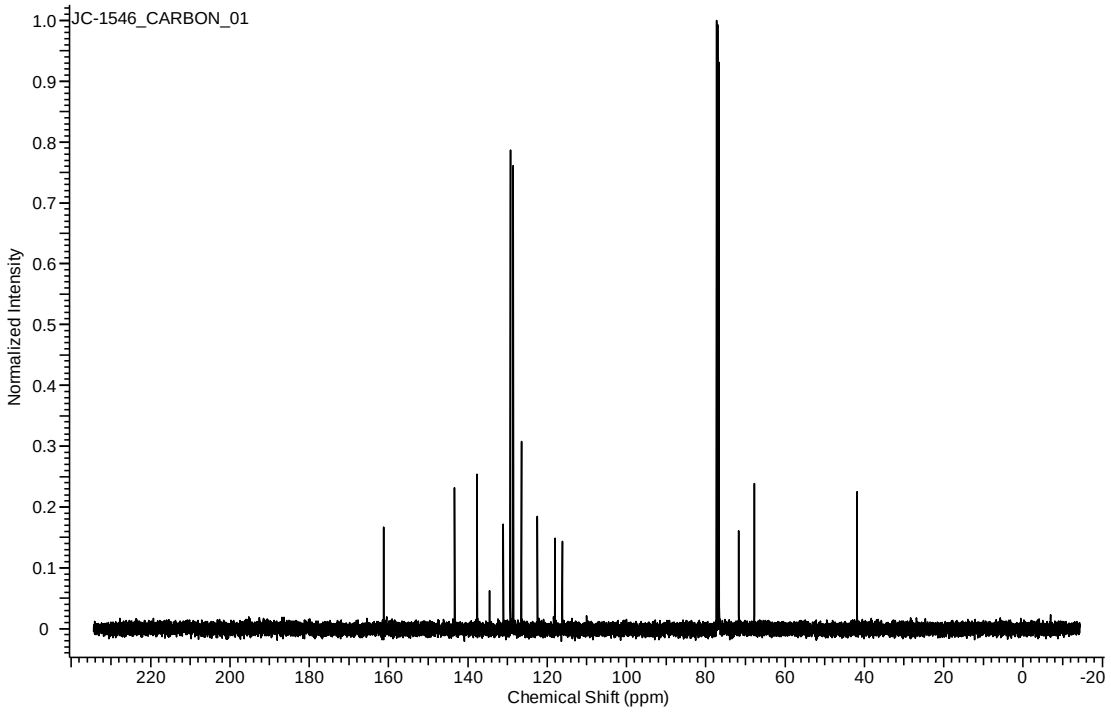
JC-1546_CARBON_01
Normalized Intensity
Chemical Shift (ppm)

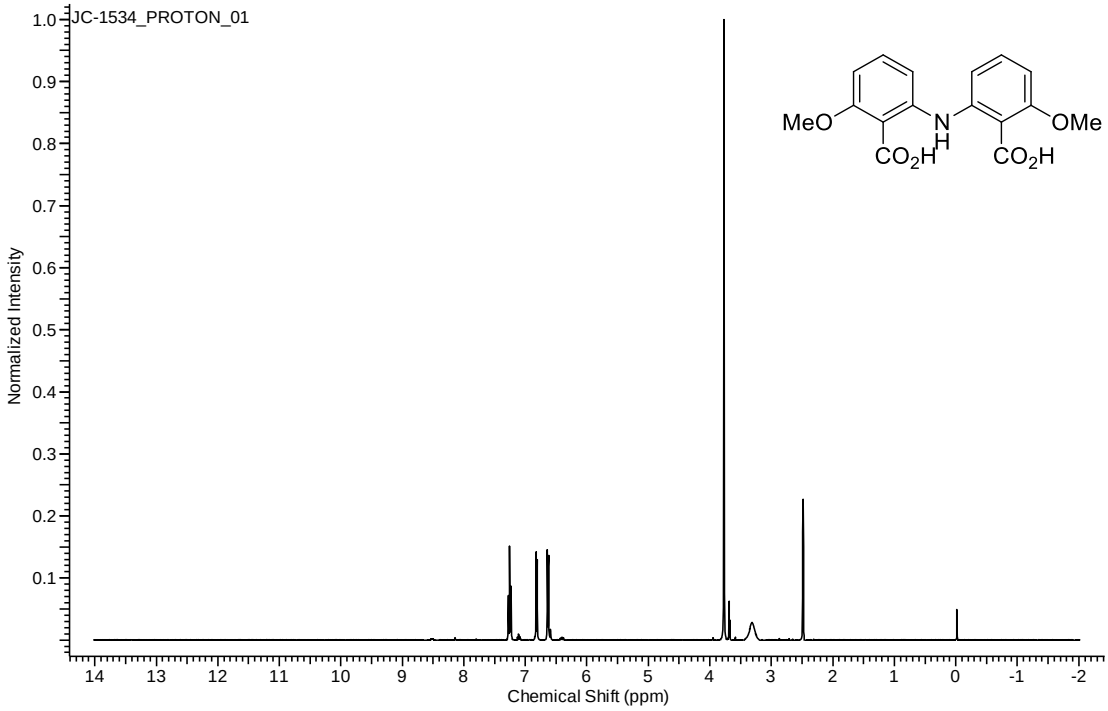
JC-1534_PROTON_01
Normalized Intensity
Chemical Shift (ppm)
MeO
OMe
N
H
CO2H
CO2H

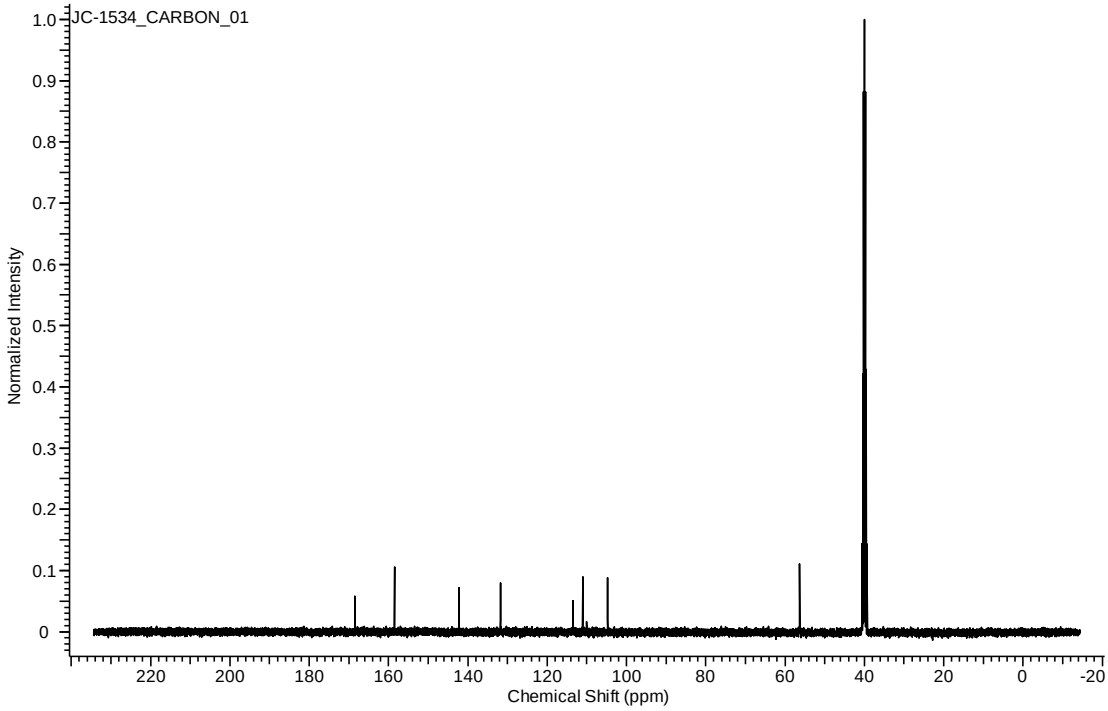
JC-1534_CARBON_01
Normalized Intensity
Chemical Shift (ppm)

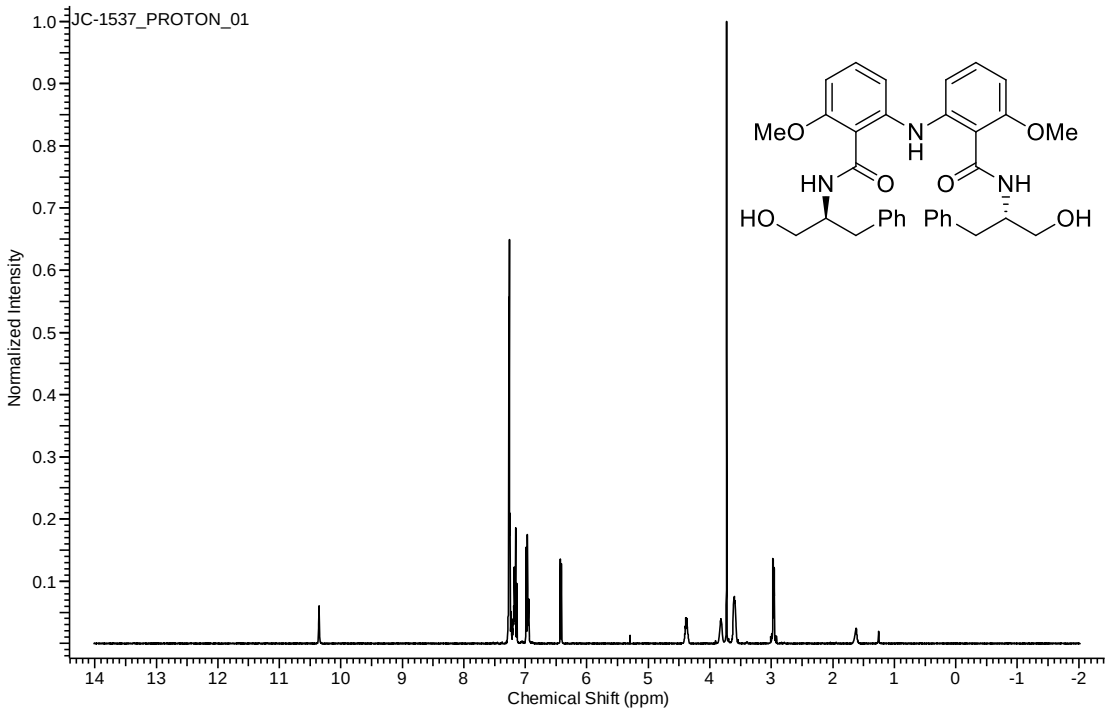
JC-1537_PROTON_01
Normalized Intensity
Chemical Shift (ppm)
MeO
OMe
N
H
HN
O
O
NH
HO
Ph
Ph
OH

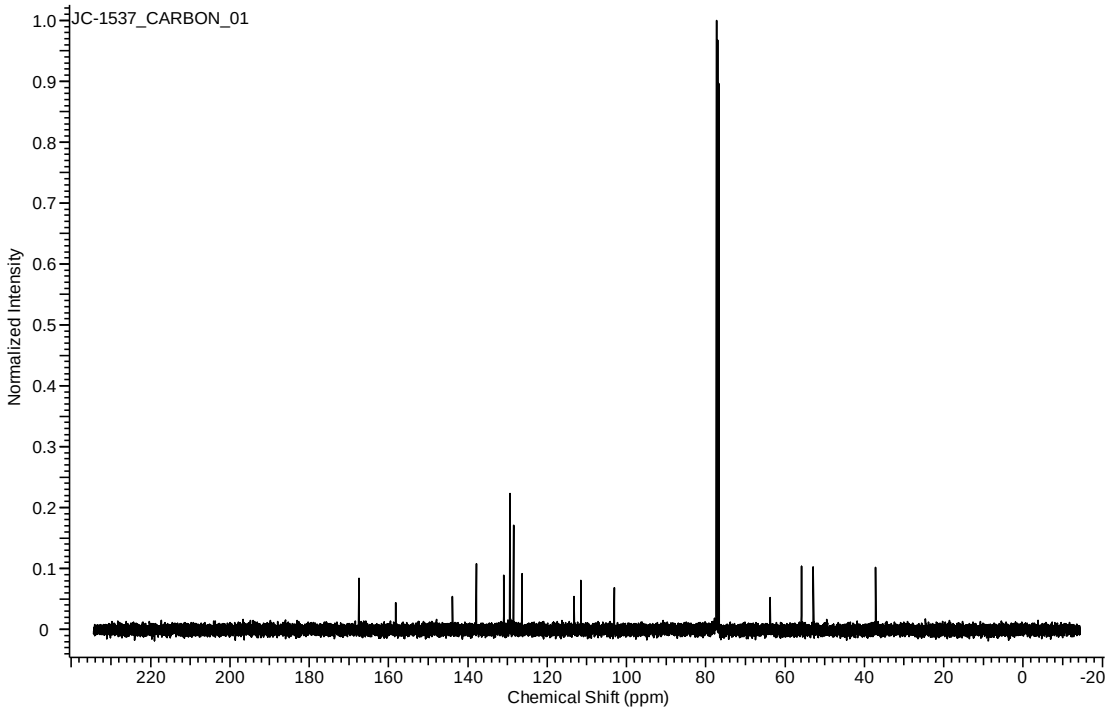
JC-1537_CARBON_01
Normalized Intensity
Chemical Shift (ppm)

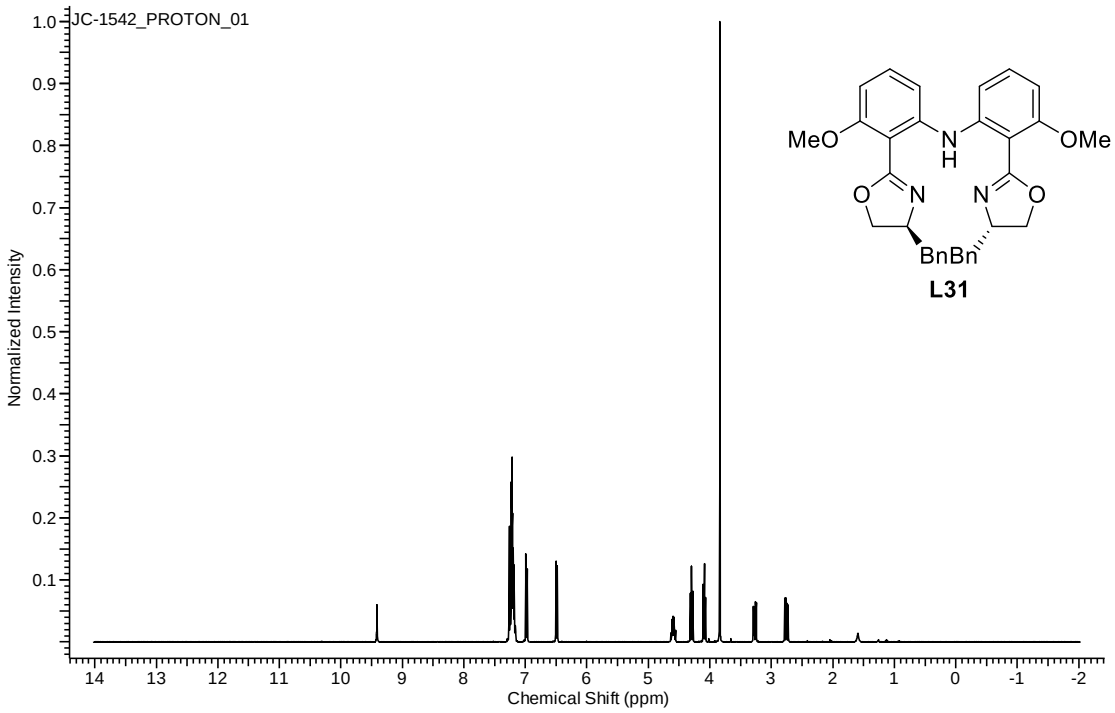
JC-1542_PROTON_01
Normalized Intensity
Chemical Shift (ppm)
MeO
OMe
N
H
O
N
N
O
BnBn
L31

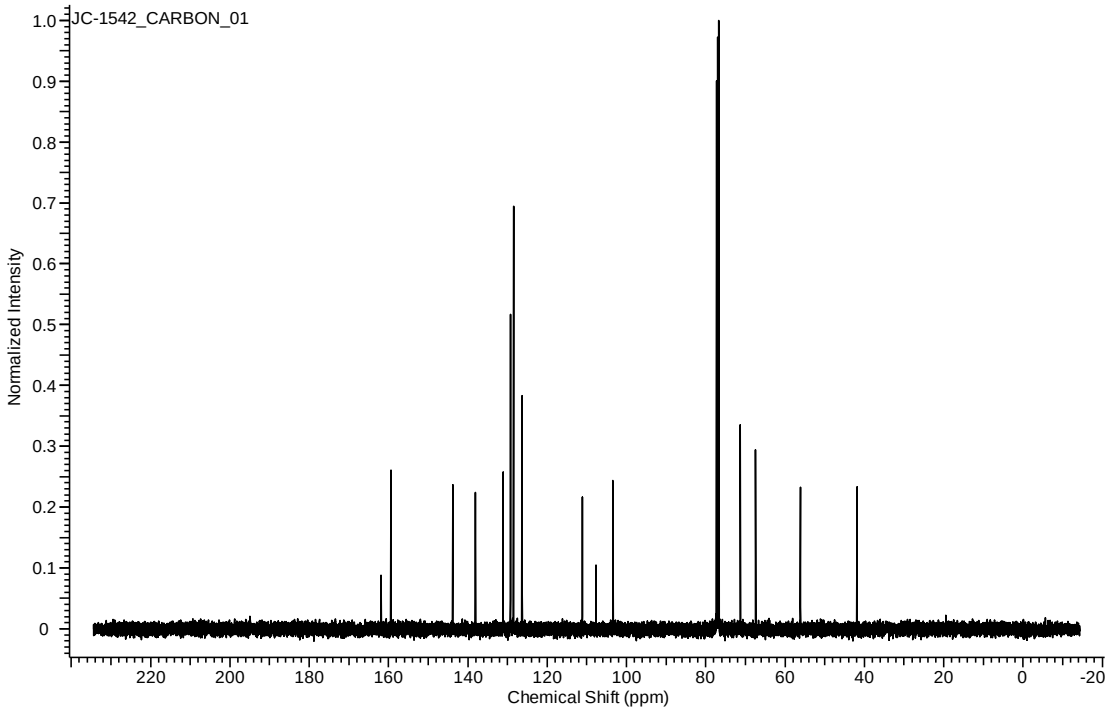
JC-1542_CARBON_01
Normalized Intensity
Chemical Shift (ppm)

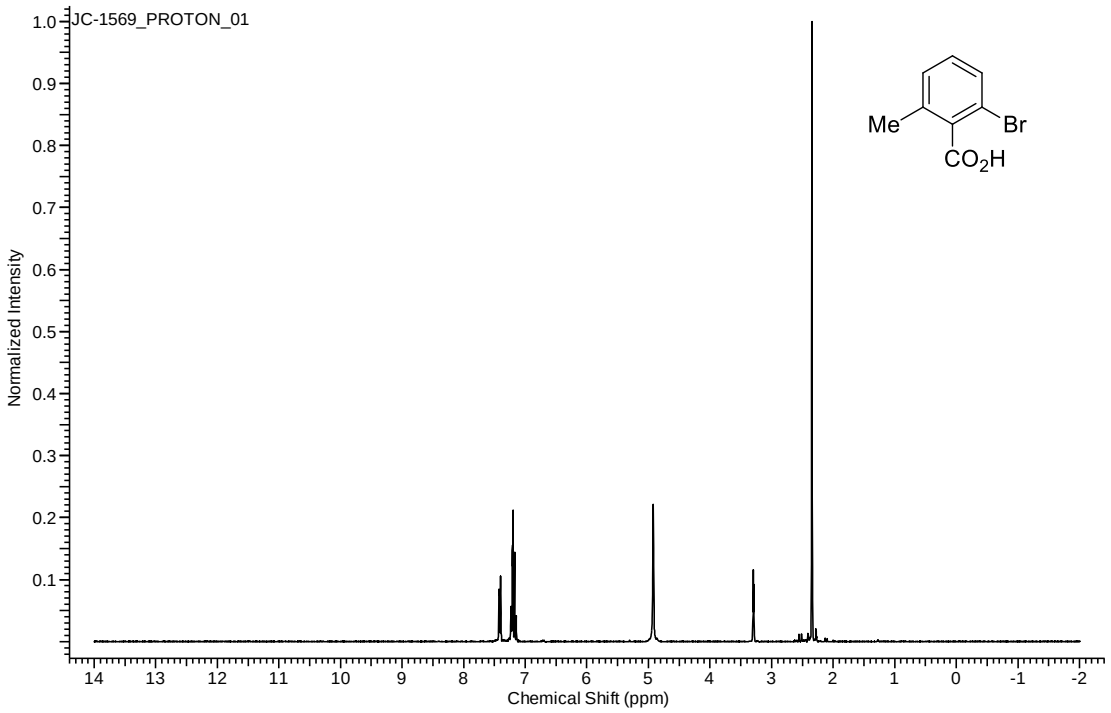
JC-1569_PROTON_01
Normalized Intensity
Chemical Shift (ppm)
Me
Br
CO2H

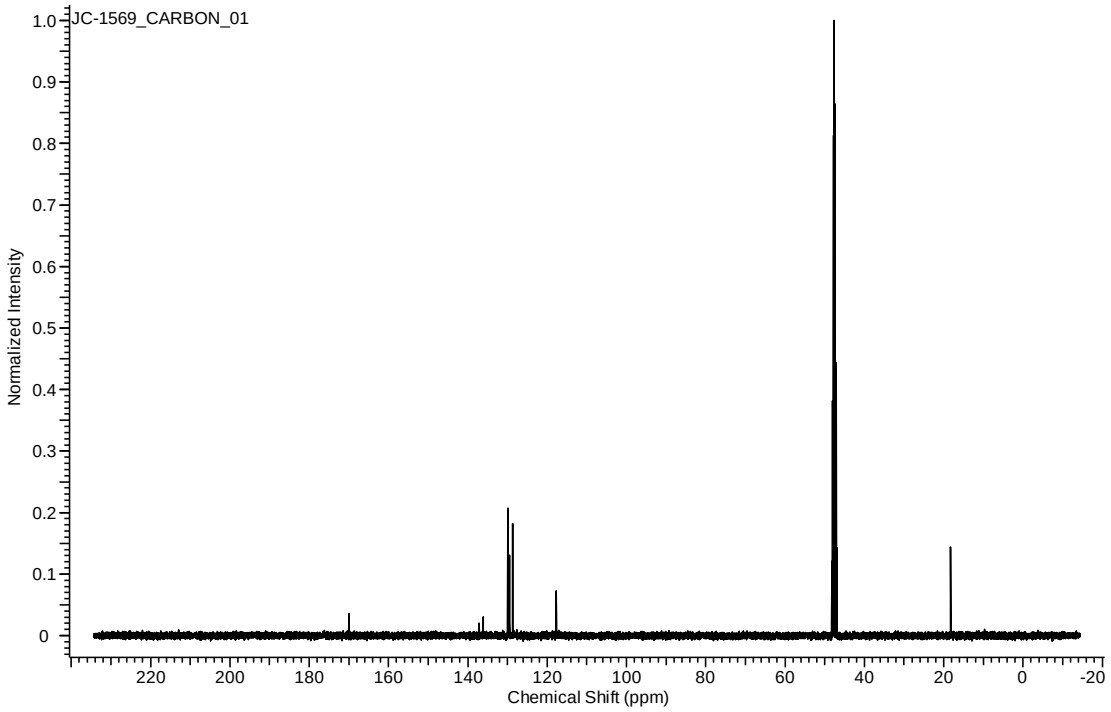
JC-1569_CARBON_01
Normalized Intensity
Chemical Shift (ppm)

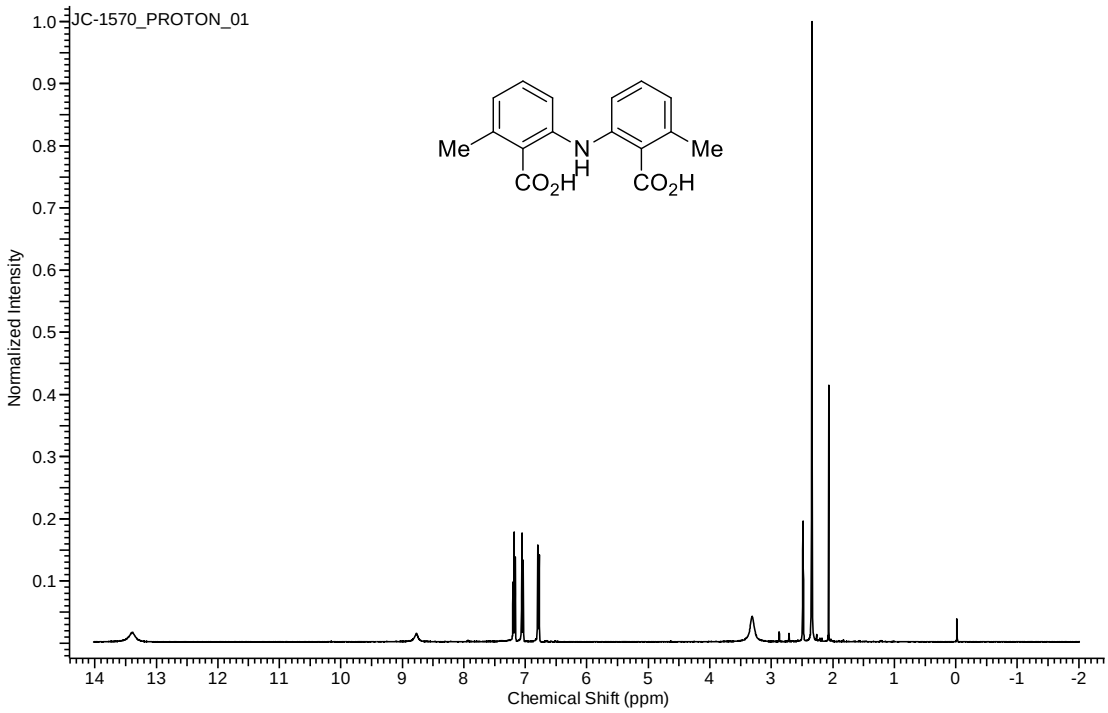
JC-1570_PROTON_01
Me
N
H
Me
CO2H
CO2H
Normalized Intensity
Chemical Shift (ppm)

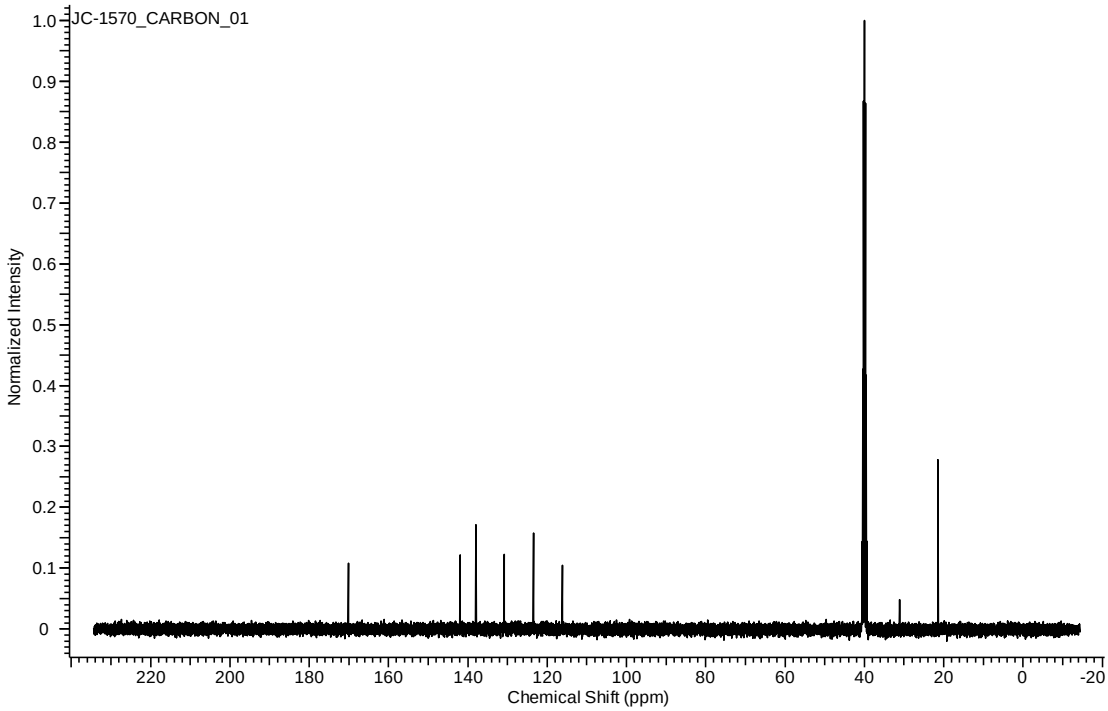
JC-1570_CARBON_01
Normalized Intensity
Chemical Shift (ppm)

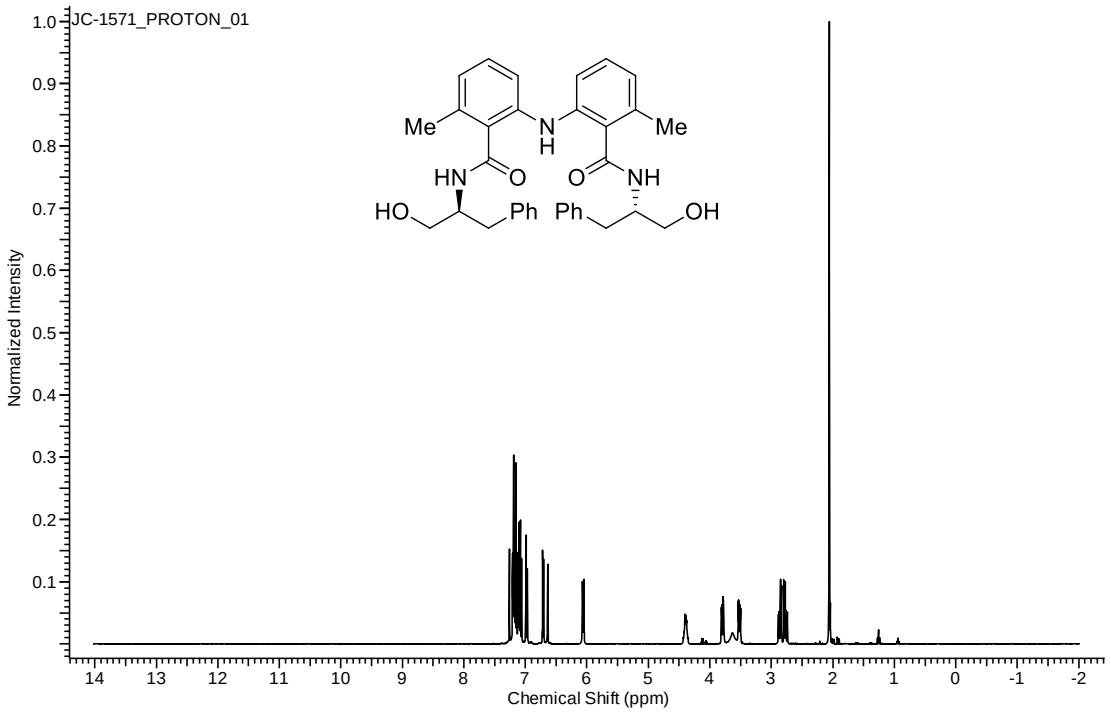
JC-1571_PROTON_01
Normalized Intensity
Chemical Shift (ppm)
Me
N
H
Me
HN
O
O
NH
HO
Ph
Ph
OH

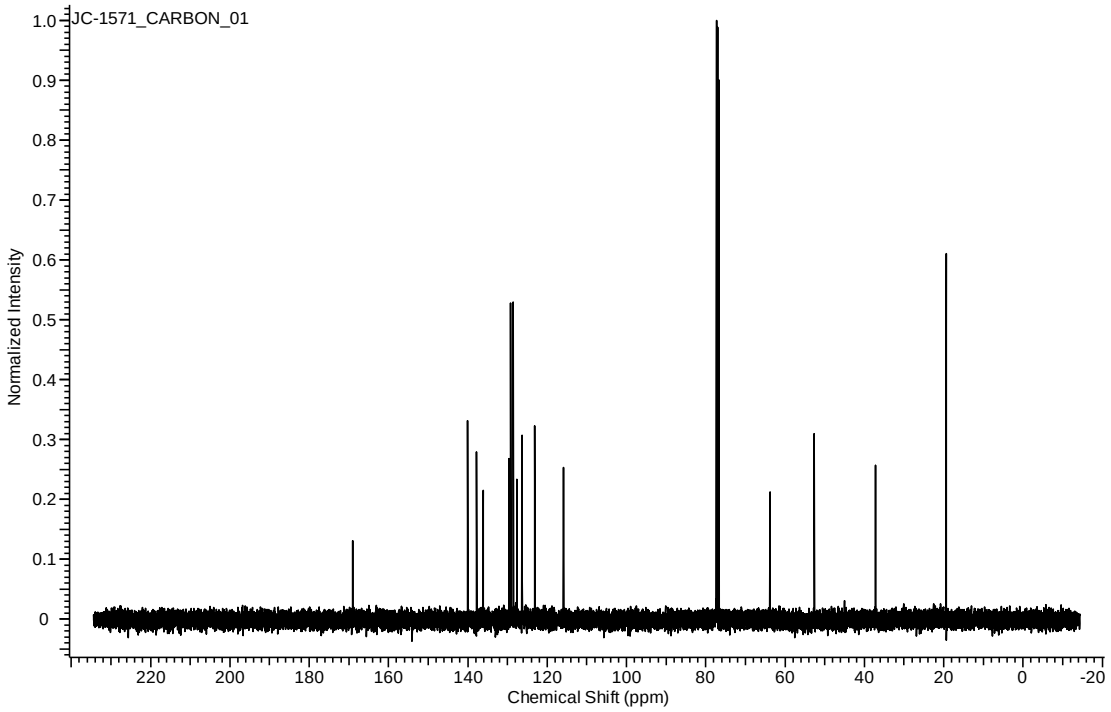
JC-1571_CARBON_01
Normalized Intensity
Chemical Shift (ppm)

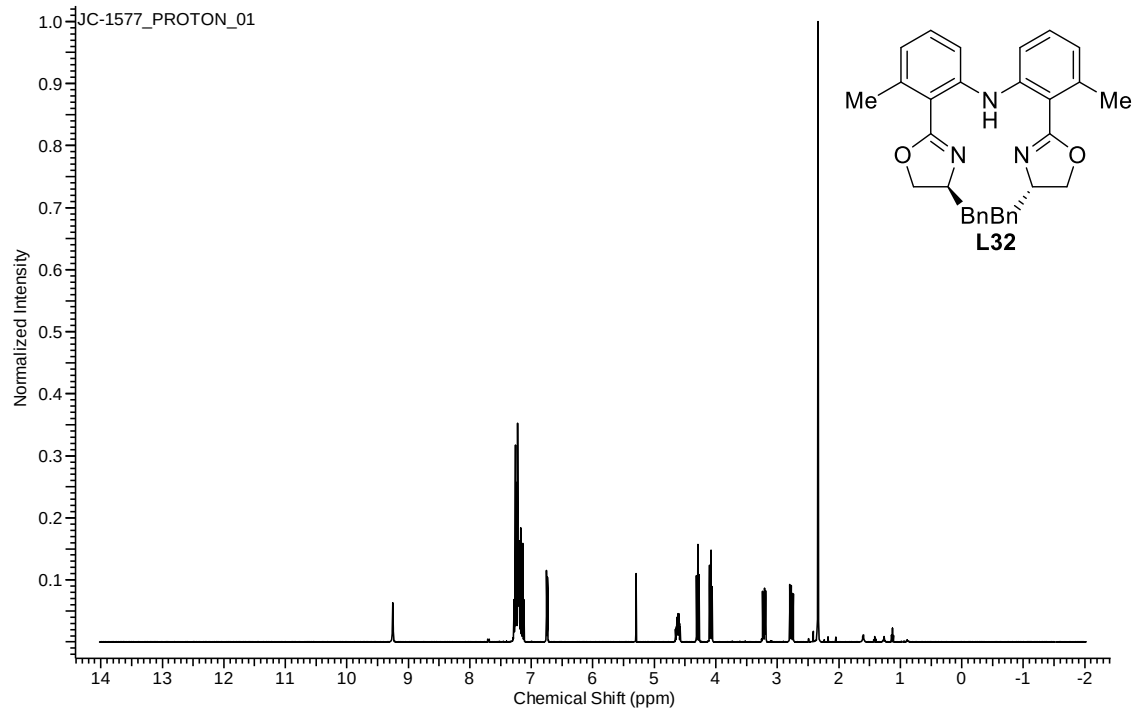
JC-1577_PROTON_01
Normalized Intensity
Chemical Shift (ppm)
Me
N
H
Me
O
N
N
O
BnBn
L32

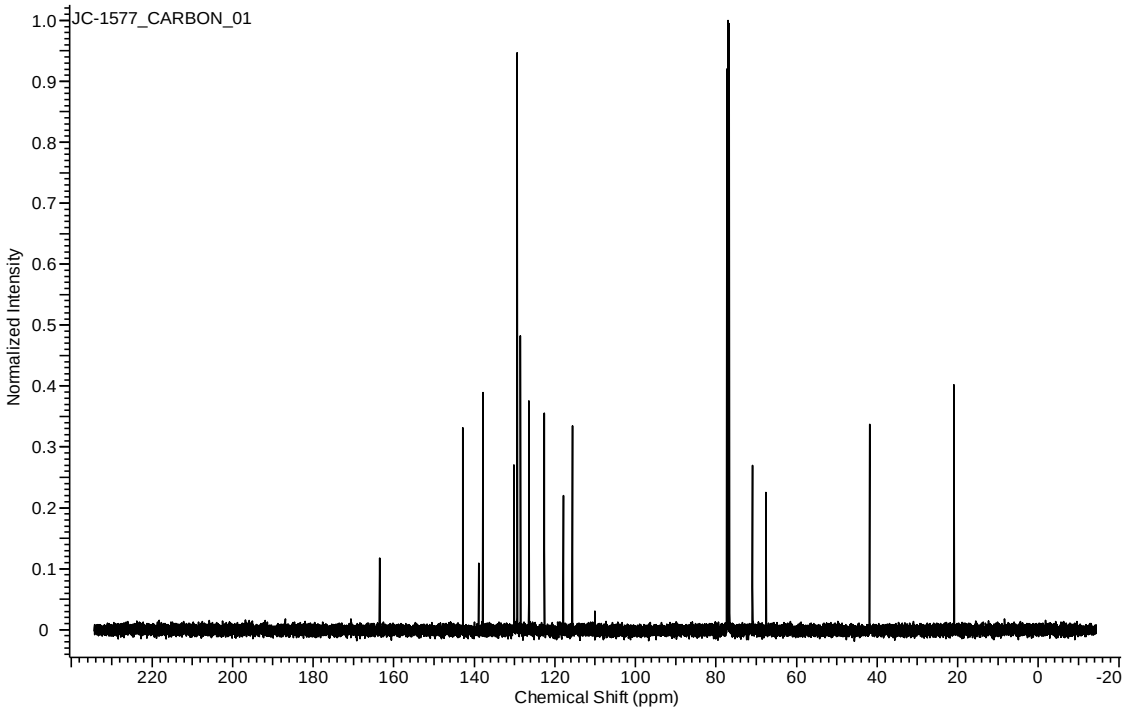
JC-1577_CARBON_01
Normalized Intensity
Chemical Shift (ppm)

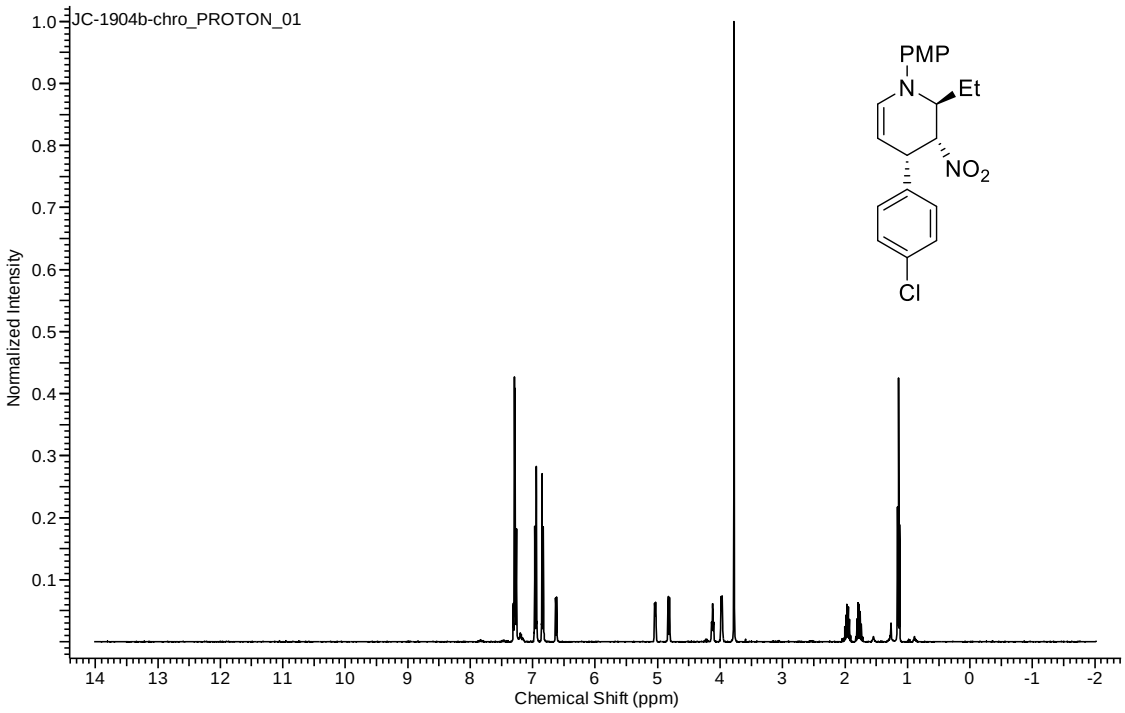
JC-1904b-chro_PROTON_01
PMP
N
Et
NO2
Cl
Normalized Intensity
Chemical Shift (ppm)

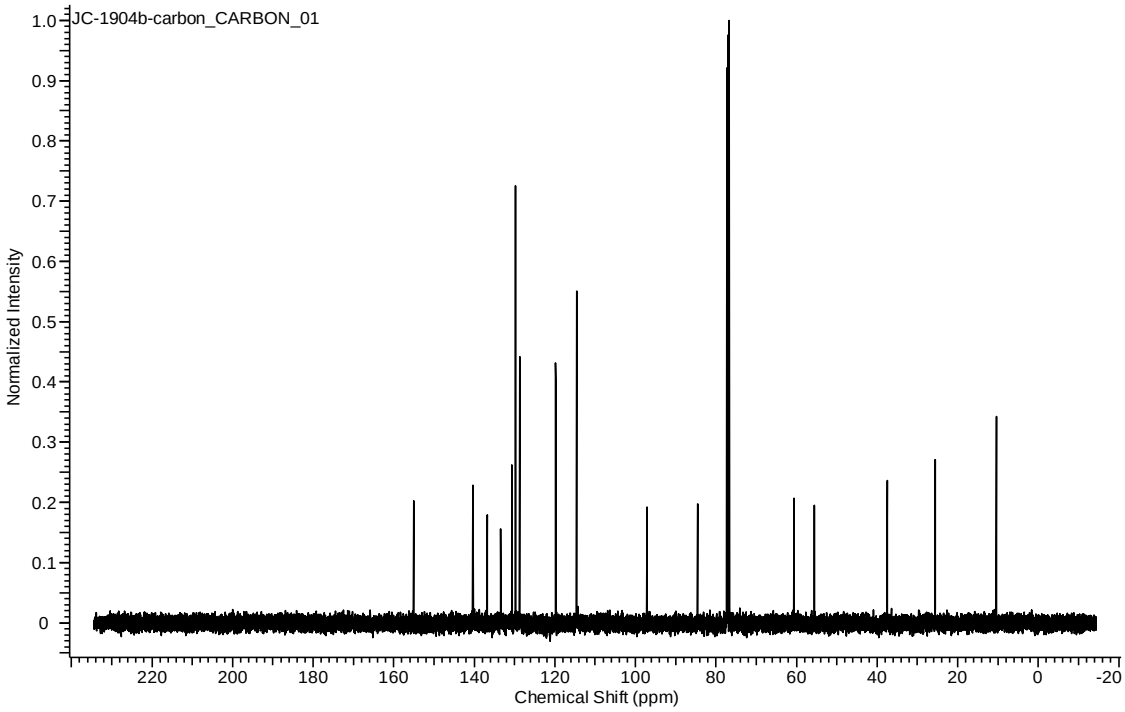
JC-1904b-carbon_CARBON_01
Normalized Intensity
Chemical Shift (ppm)

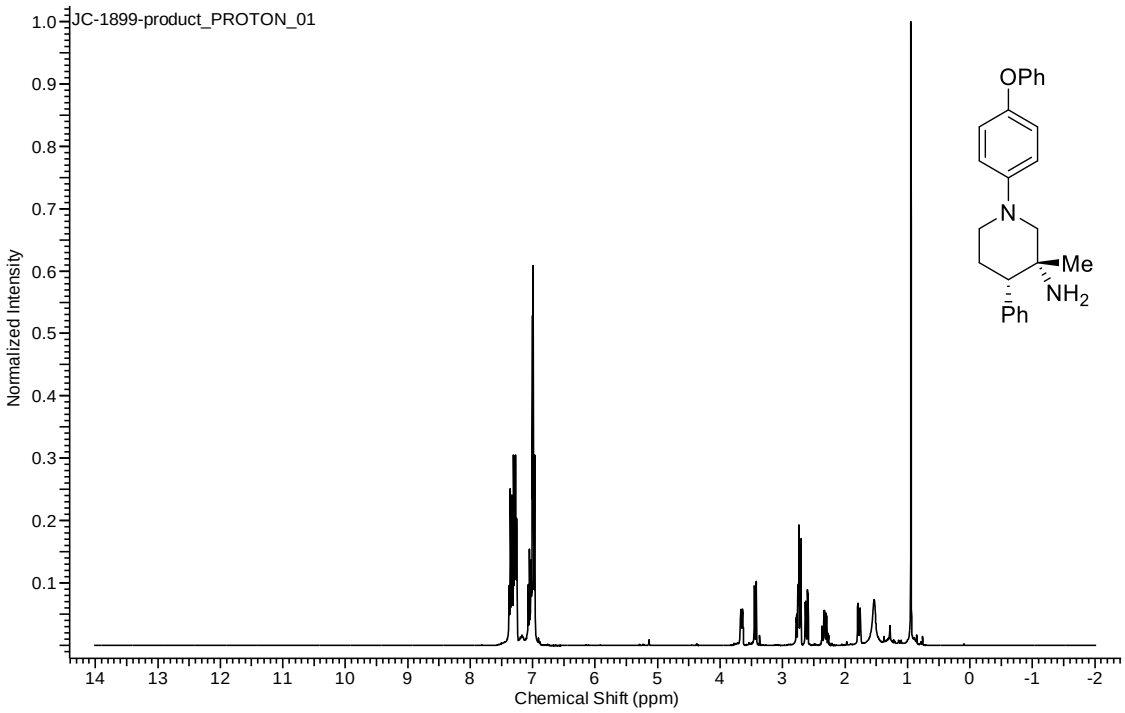
JC-1899-product_PROTON_01
Normalized Intensity
Chemical Shift (ppm)
OPh
N
Me
NH2
Ph

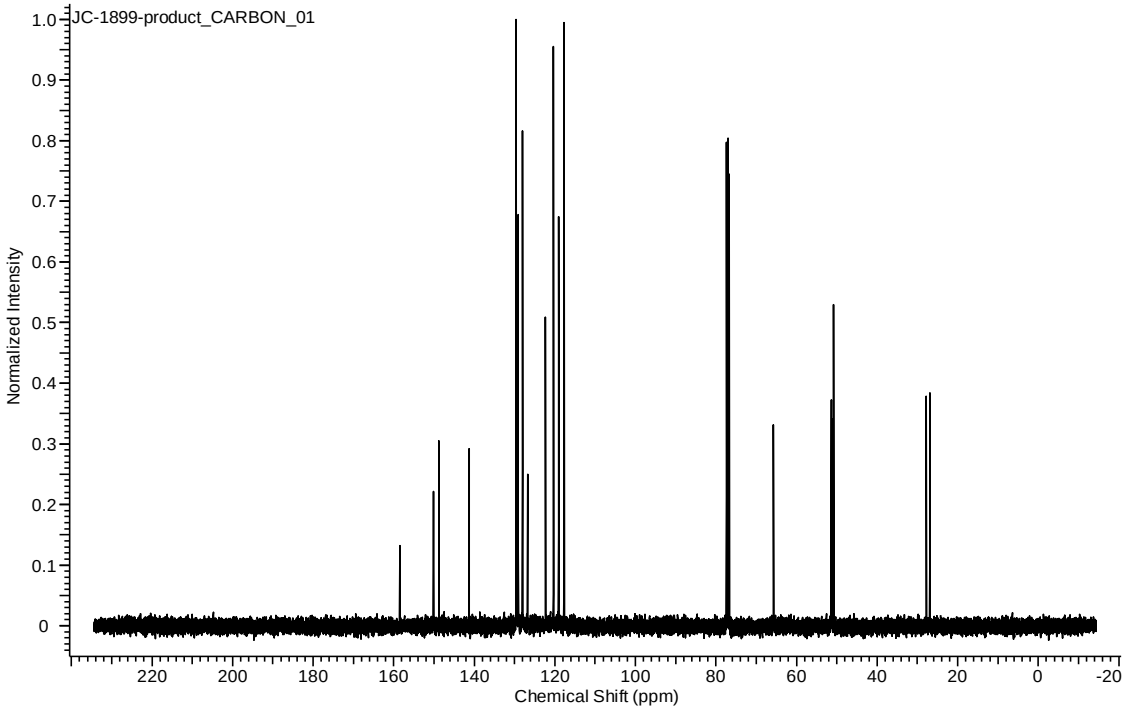
JC-1899-product_CARBON_01
Normalized Intensity
Chemical Shift (ppm)

REFERENCES

1. (a) Lu, S.-F. ; Du, D.-M. ; Zhang, S.-W. ; Xu, J. *Tetrahedron: Asymmetry* **2004**, *15*, 3433-3441; (b) Lu, S.-F., Du, D.-M. ; Xu, J. *Org. Lett.* **2006**, *8*, 2115-2118 ; (c) Liu, H. ; Xu, J. ; Du, D.-M. *Org. Lett.* **2007**, *9*, 4725-4728.
2. Du, X.; Liu, H. ; Du, D.-M. *Tetrahedron : Asymmetry* **2010**, *21*, 241-246.
3. Dhakal, R. C.; Dieter, R. K. *Org. Lett.* **2014**, *16*, 1362-1365.
4. Kronenthanl, D. R.; Han, C. Y.; Taylor, M. K. *J. Org. Chem.* **1982**, *47*, 2765-2768.
5. Eisenberger, P.; Bailey, A. M.; Crudeen, C. M. *J. Am. Chem. Soc.* **2012**, *134*, 17384-17387.
6. Stokes, S.; Bekkam, M.; Rupp, M.; Mead, K. T. *Synlett.* **2012**, 389-392.
7. Lykke, L.; Monge, D.; Nielsen, M.; Jorgensen, K. A. *Chem. Eur. J.* **2010**, *16*, 13330-13334.
8. Panov, I.; Drabina, P.; Padelkova, Z.; Simunek, P.; Sedlak, M. *J. Org. Chem.* **2011**, *76*, 4787-4793.
9. Liu, H; Li, W.; Du, D.-M. *Science in China Series B: Chem.* **2009**, *52*, 1321-1330.
10. Liu, H.; Lu, S.-F.; Xu, J.; Du, D.-M. *Chem. Asian. J.* **2008**, *3*, 1111-1121.
11. Du, G.; Wei, Y.; Zhang, W.; Dong, Y.; Lin, Z.; He. H.; Zhang, S.; Li, X. *Dalton Trans.* **2013**, *42*, 1278-1286.
12. Rewcastle, G. W.; Denny, W. A. *Synthesis* **1985**, 220-222.
13. Moreno-Sanz, G.; Duranti, A.; Melzig, L.; Fiorelli, C.; Ruda, G. F.; Colombano, G.; Mestichelli, P.; Sanchini, S.; Tontini, A.; Mor, M.; Bandiera, T.; Scarpelli, R.; Tarzia, G.; Piomelli, D. *J. Med. Chem.* **2013**, *56*, 5917-5930.
14. Saari, W. S.; Schwering, J. E. *J. Heterocyclic Chem.* **1986**, *23*, 1253-1255.

15. Hawson, A. T.; Hughes, K.; Richardson, S. K.; Sharpe, D. A.; Wadsworth, A. H. *J. Chem. Soc. Perkin Trans. I* **1991**, 1565-1569.

16. Menzel, K.; Dimichele, L.; Mills, P.; Frantz, D. E.; Nelson, T. D.; Kress, M. H. *Synlett* **2006**, 1948-1952.

17. Hickey, R. M.; Allwein, S. P.; Nelson, T. D. Kress, M. H.; Sudah, O. S.; Moment, A. J.; Rodgers, S. D.; Kaba, M.; Fernandez, P. *Org. Process Res. Dev.* **2005**, *9*, 764-767.

18. Sugaya, T.; Mimura, Y.; Kato, N.; Ikuta, M.; Mimura, T.; Kasai, M.; Tomioka, S. *Synthesis* **1994**, 73-76.

19. Lin, H.; Tan, Y.; Liu, W.-J.; Zhang, Z.-C., Sun, X.-W.; Lin, G.-Q. *Chem. Commun.* **2013**, *49*, 4024-4026.

20. (a) Jia, Y.; Yang, W.; Du, D.-M. *Org. Biomol. Chem.* **2012**, *10*, 4739-4746; (b) Peng, J.; Du, D.-M. *Eur. J. Org. Chem.* **2012**. 4042-4051; (c) Peng, J.; Du, D.-M. *Beilstein J. Org. Chem.* **2013**, *9*, 1210-1216.

APPENDIX 2: CHAPTER 3 EXPERIMENTAL

A.2.1 General Procedure

All reactions were carried out under an atmosphere of argon in over-dried glassware. For substrate synthesis, dichloromethane, diethyl ether and toluene were degassed with argon and passed through a column of neutral alumina and a column of Q5 reactant while all other solvents were freshly distilled. Non-distilled solvents were used in the photoredox catalyzed reactions. Unless otherwise stated, flash column chromatography was performed on Silicycle Inc. silica gel 60 (230-400 mesh). Thin layer chromatography was performed on Silicycle Inc. 0.25 mm silica gel 60-F plates. Visualization was accomplished with UV light (254 nm), Seebach's Magic or potassium permanganate. ^{1}H NMR and ^{13}C NMR spectra were obtained in CDCl3 at ambient temperature and chemical shifts are expressed in parts per million (δ, ppm). Mass spectra were obtained on an Agilent Technologies 6130 Quadropole Mass Spec (LRMS, ESI + APCI). Infrared spectra were collected on a Nicolet iS-50 FT-IR spectrometer. All alkenes are commercially available and were distilled prior to use although control experiments show that non-distilled alkenes give the same results in the photoredox catalyzed reactions. $[Ir(dF\text{-}CF_3ppy)_2dtbbpy]PF_6$ were purchased from Aspira Scientific, Inc. (Milpitas, CA) or Strem Chemicals, Inc. (Newburyport, MA). A Kessil blue LED (34W maximum, 24 VDC) was used as the light source for the photoredox catalyzed reactions.

A.2.2 Synthesis of Substrate

General Procedure A: Synthesis of Amides from Carboxylic Acids

To a solution of the carboxylic acid (1 equiv.) in DCM (0.3 M) was added oxalyl chloride (1.1 equiv.) dropwise. DMF (3 drops) was added. The mixture was stirred at rt until no more gas bubbles were observed (within 3-4h). The solvent was removed under reduced pressure. The crude acid chloride was dissolved in THF (2 mL per mmol of acid chloride). This mixture was added to commercial aq. NH_3 (14.8M, 2 mL per mmol of acid chloride) dropwise at 0 ^oC. The mixture was allowed to warm to rt and stir overnight. The mixture was diluted with EtOAc. The organic and aqueous layers were separated. The aqueous layer was extracted with EtOAc twice. The combined organic layer was washed with brine, dried over Na_2SO_4 and filtered. The solvent was removed under reduced pressure to afford the crude amide, which was used without further purification.

General Procedure B: Synthesis of Amines from Amides

To a solution of the crude amide (1 equiv.) in THF (0.3 M) was added LAH (1.9 equiv.) in portions at 0 ^oC. The mixture was allowed to warm to rt and stir overnight. The mixture was cooled to 0 ^oC. Water (1 mL per 1 g LAH) was added slowly. 15% NaOH (1 mL per 1 g LAH) was added slowly. Water (3 mL per 1 g) was added. The mixture was allowed to rt and stirred for 15 mins. The mixture was filtered. The solvent in the filtrate was removed under reduced pressure to afford the crude amine, which was used without further purification.

General Procedure C: Trifluoroacetylation of Amines

To a solution of the amine (1 equiv.) and NEt_3 (2 equiv.) in DCM (0.25 M) was added trifluoroacetic anhydride (1.02 equiv. or 0.95 equiv. if the amine was not purified in the previous step) at 0 °C. The mixture was slowly allowed to warm to rt and stir overnight. The reaction was quenched with sat. NH_4Cl. The aqueous layer was extracted with DCM two time. The combined organic layer was washed with sat. $NaHCO_3$, brine, dried over Na_2SO_4 and filtered. The solvent was removed under reduced pressure. Flash column chromatography afforded the trifluoroacetamide.

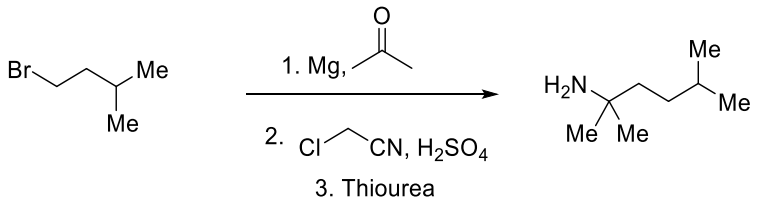

To a solution of acetone (3.20 mL, 43.6 mmol, 1.05 equiv.) in Et_2O (30 mL) was added Grignard reagent in Et_2O (30 mL) freshly prepared from 1-bromo-3-methylbutane(5.0 mL, 41.7 mmol, 1.00 equiv.) and Mg (1.0653 g, 43.8 mmol, 1.05 equiv.) at 0 °C. The reaction was allowed to warm to rt and stirred overnight. The reaction was quenched with sat. NH_4Cl solution. The organic and aqueous layer was separated. The organic layer was extracted with Et_2O twice. The combined organic layer was washed with brine, dried over Na_2SO_4 and filtered. The solvent was removed under reduced pressure to afford 2,5-dimethylhexan-2-ol (3.48 g, 72%). The product was used without further purification.

2,5-dimethylhexan-2-ol (3.44 g, 29.6 mmol, 1 equiv.) and chloroacetonitrile (9.62 mL, 177.6 mmol, 6 equiv.) were dissolved in AcOH (11.3 mL). At 0 °C, concentrated sulfuric acid (12.9

mL, 266.4 mmol, 9 equiv.) was added dropwise. The mixture was stirred at rt for 5 h. The mixture was poured into ice-water. The mixture was extracted with DCM three times. The combined organic layer was washed with sat. Na_2CO_3 twice and brine, dried over Na_2SO_4 and filtered. The solvent was removed under vacuum. Flash column chromatography (15-20% EtOAc/hexane) afforded 2-chloro-*N*-(2,5-dimethylhexan-2-yl)acetamide as a colorless oil (3.97 g, 73%). A solution of 2-chloro-*N*-(2,5-dimethylhexan-2-yl)acetamide (3.96 g, 19.2 mmol, 1 equiv.), thiourea (1.76 g, 23.1 mmol, 1.20 equiv.) in EtOH/AcOH (39 mL/ 8 mL) was refluxed overnight. The mixture was cooled to rt. Solid NaOH was added until pH is larger than 5. The mixture was extracted with DCM three times. The combined organic layer was extracted with 2M HCl three times. The aqueous layer was basified with NaOH solid and extracted with DCM three times. The combined organic layer was dried over Na_2SO_4 and filtered. The solvent was removed under vacuum to afford crude 2,4-dimethylpentan-2-amine (2.51 g, 100%). It was used without further purification.

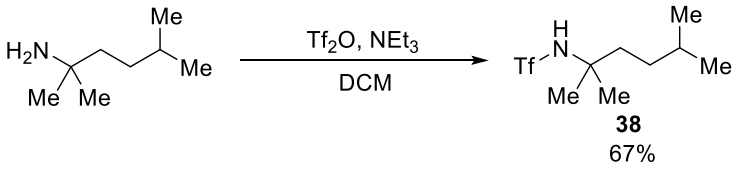

38
67%

To a solution of 2,4-dimethylpentan-2-amine (1.00 g, 7.74 mmol, 1.0 equiv.) and NEt_3 (1.13 mL, 8.11 mmol, 1.05 equiv.) in DCM (15.5 mL) was added Tf_2O (1.30 mL, 7.74 mmol, 1.0 equiv.) dropwise at –78 ^oC. The mixture was stirred at this temperature for 3 h before quenching with sat. NH_4Cl. The organic layer was washed with sat. $NaHCO_3$ and brine, dried over Na_2SO_4 and filtered. Flash column chromatography (3-10% EtOAc/hexane) afforded *N*-(2,5-dimethylhexan-2-yl)-1,1,1-trifluoromethane-sulfonamide **38** (1.36 g, 67% as a colorless oil). The spectral data is consistent with the literature.[1]

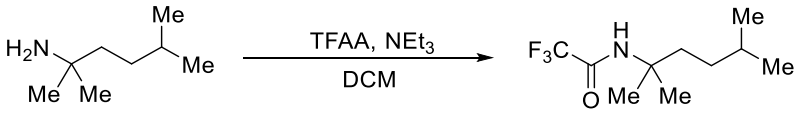

59

69%

By General Procedure C, N-(2,5-dimethylhexan-2-yl)-2,2,2-trifluoroacetamide **59** (361.9 mg, 69%) was synthesized from 2,4-dimethylpentan-2-amine (303.0 mg).

^{1}H NMR ($CDCl_3$, 400 MHz): 6.03 (br, 1H), 1.72-1.68 (m, 2H), 1.49 (septet, *J*= 6.7, 1H), 1.15-1.09 (m, 2H), 0.88-0.86 (d, *J*= 6.7, 6H); ^{13}C NMR ($CDCl_3$, 100 MHz): 156.0 (q, *J*= 35.9), 115.6 (q, *J*= 289.4), 55.3, 37.6, 32.8, 28.3, 26.2, 22.5; ^{19}F NMR ($CDCl_3$, 376 MHz): −76.3; Molecular weight $[M-H]^-$: 224.1 (expected), 224.1 (found); IR (cm^{-1}): 3440, 3314 (br), 3091, 2957, 2934, 2873, 1704, 1652.

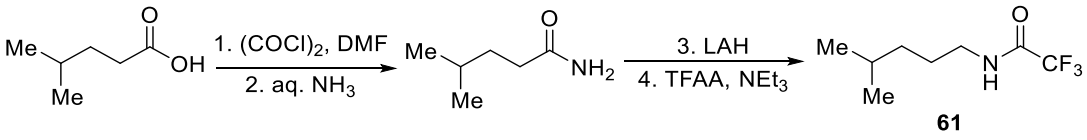

61

By General Procedure A, 4-methylpentan-1-amine (7.00 g, 90%) was synthesized from 4-methylpentanamide (7.50 g). By General Procedure B, 4-methylpentan-1-amine (4.85 g, 79%) was synthesized from 4-methylpentanamide (7.00 g). By General Procedure C, 2,2,2-trifluoro-*N*-(4-methylpentyl)acetamide (2.10 g, 45%) was synthesized from 4-methylpentan-1-amine **61** (2.40 g). Flash column chromatography conditions: 10-15% Et_2O/hexane.

^{1}H NMR ($CDCl_3$, 400 MHz): 6.77 (br, 1H), 3.31 (q, *J*= 6.9, 2H), 1.60-1.52 (m, 3H), 1.22-1.16 (m, 2H), 0.87 (d, *J*= 6.3, 6H); ^{13}C NMR ($CDCl_3$, 100 MHz): 157.3 (q, *J*= 36.9), 115.9 (q, *J*= 287.6), 40.2, 35.7, 27.6, 26.7, 22.3; ^{19}F NMR ($CDCl_3$, 376 MHz): −76.1; Molecular weight $[M-H]^-$: 196.1 (expected), 196.2 (found); IR (cm^{-1}): 3325 (br), 3114, 2959, 2938, 2873, 1703, 1652.

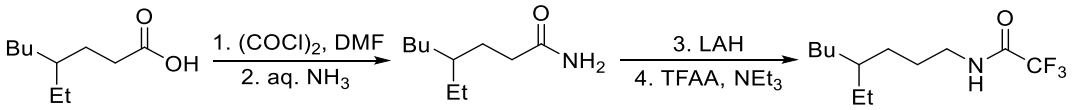

By General Procedure A, 4-ethyloctanamide (1.90 g, 96%) was synthesized from 4-ethyloctanoic acid (2.00 g). By General Procedure B, 4-ethyloctan-1-amine (1.36 g, 92%) was synthesized from 4-ethyloctanamide (1.61 g). By General Procedure C, *N*-(4-ethyloctyl)-2,2,2-trifluoroacetamide (0.946 g, 74%) was synthesized from 4-ethyloctan-1-amine (0.795 g). Flash column chromatography conditions: 7.5-12.5% Et_2O/hexane.

^1H NMR ($CDCl_3$, 400 MHz): 6.71 (br, 1H), 3.32 (q, *J*= 6.8, 2H), 1.56-1.54 (m, 2H), 1.27-1.21 (m, 11H), 0.87 (t, *J*= 6.9, 3H), 0.82 (t, *J*= 7.2, 3H); ^{13}C NMR ($CDCl_3$, 100 MHz): 157.3 (q, *J*= 36.6), 115.9 (q, *J*= 287.9), 40.4, 38.4, 32.6, 30.0, 28.8, 26.1, 25.7, 23.0, 14.0, 10.7; ^{19}F NMR ($CDCl_3$, 376 MHz): −76.1; Molecular weight $[M-H]^-$: 252.2 (expected), 252.2 (found); IR (cm^{-1}):3309 (br), 3105, 2959, 2929, 2873, 2860, 1702, 1650.

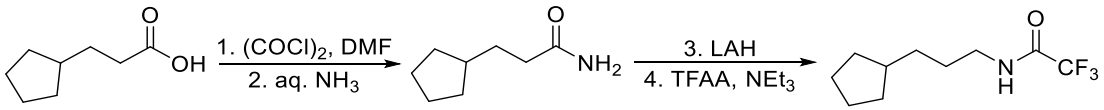

96

By General Procedure A, 3-cyclopentylpropanamide (2.28 g, 97%) was synthesized from 3-cyclopentylpropanoic acid (2.37 g). By General Procedure B, 3-cyclopentylpropan-1-amine (1.52 g, 74%) was synthesized from 3-cyclopentylpropanamide (2.28 g). By General Procedure C, *N*-(3-cyclopentylpropyl)-2,2,2-trifluoroacetamide (380 mg, 43%) was synthesized from 3-cyclopentylpropanamide **96** (500.0 mg). Flash column chromatography conditions: 15-25% Et_2O/hexane.

^{1}H NMR ($CDCl_3$, 400 MHz): 6.83 (br, 1H), 3.32 (q, *J*= 6.9, 2H), 1.77-1.69 (m, 3H), 1.61-1.46 (m, 6H), 1.34-1.28 (m, 2H), 1.07-1.02 (m, 2H); ^{13}C NMR ($CDCl_3$, 100 MHz): 157.3 (q, *J*= 36.9), 115.9, (q, *J*= 287.6), 40.2, 39.6, 33.0, 32.5, 28.1, 25.1; ^{19}F NMR ($CDCl_3$, 376 MHz): −76.1; ; Molecular weight $[M-H]^-$: 222.1 (expected), 222.1 (found); IR (cm^{-1}): 3300 (br), 3105, 2947, 2868, 1701, 1649.

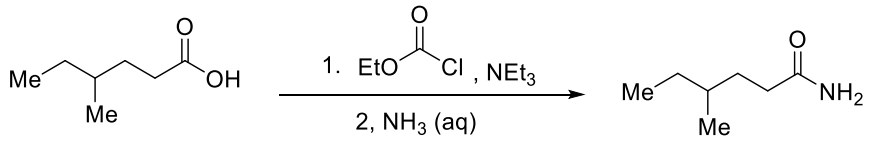

To a solution of 4-methylhexanoic acid (3.04 g, 23.4 mmol, 1 equiv.) and NEt_3 (3.32 mL, 23.8 mmol, 1.02 equiv.) in THF (230 mL) was added ethyl chloroformate (2.27 mL, 23.8 mmol, 1.02 equiv.) dropwise at 0 °C. The mixture was stirred at 0 °C for 1 h. aq. NH_3 (21.5 mL) was added dropwise. The mixture was allowed to warm to rt and stirred overnight. The mixture was extracted with EtOAc three times. The combined organic layer was washed with brine, dried over Na_2SO_4 and filtered. Solvent was removed under vacuum to afford 4-methylhexanamide (2.30 g, 76%) as a white solid. It was used without further purification.

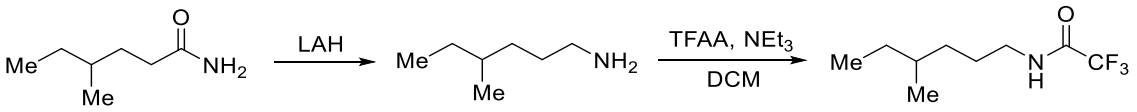

By General Procedure B, 4-methylhexan-1-amine (1.38 g, 76%) was synthesized from 4-methylhexanamide (2.04 g). By General Procedure C, 2,2,2-trifluoro-*N*-(4-methylhexyl)acetamide (0.576 g, 31%) was synthesized from 4-methylhexan-1-amine (1.03 g). Flash column chromatography conditions: 7.5-15% Et_2O/hexane.

^{1}H NMR ($CDCl_3$, 400 MHz): 6.72 (br, 1H), 3.32 (q, *J*= 6.8, 2H), 1.62-1.54 (m, 2H), 1.35-1.28 (m, 3H), 1.17-1.08 (m, 2H), 0.86-0.82 (m, 6H); ^{13}C NMR ($CDCl_3$, 100 MHz): 157.3 (q, *J*=36.6), 115.9 (q, *J*= 287.6), 40.3, 34.0, 33.4, 29.2, 26.4, 18.9, 11.2; ^{19}F NMR ($CDCl_3$, 376 MHz): −76.1; Molecular weight $[M-H]^-$: 210.1 (expected), 210.1 (found); IR (cm^{-1}): 3318 (br), 3109, 2961, 2933, 2876, 1702.

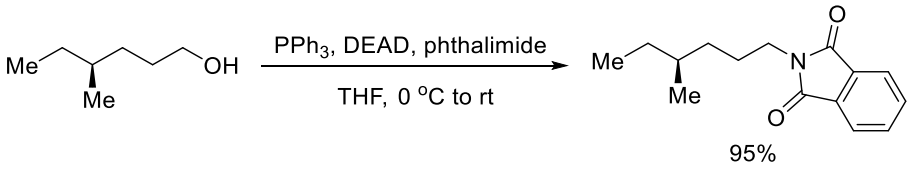

To a solution of commercially available optically active (*S*)-4-methylhexan-1-ol (655.3 mg, 5.64 mmol, 1 equiv.), PPh_3 (1.761 g, 6.77 mmol, 1.2 equiv.) and phthalimide (1.317 g, 6.77 mmol, 1.2 equiv.) in THF (28 mL) was added DEAD (1.05 mL, 6.77 mmol, 1.2 equiv.) at 0 °C dropwise. The mixture was warmed to rt and stirred overnight. Solvent was removed under vacuum. The mixture was filtered through Si gel (50% Et_2O/hex for elution). Flash column chromatography afforded (*S*)-2-(4-methylhexyl)isoindoline-1,3-dione (1.31 g, 95%).

^{1}H NMR ($CDCl_3$, 400 MHz): 7.81-7.79 (m, 2H), 7.69-7,66 (m, 2H), 3.63 (t, *J*= 7.5, 2H), 1.72-1.61 (m, 2H), 1.35-1.28 (m, 3H), 1.14-1.08 (m, 2H), 0.83-0.80 (m, 6H); ^{13}C NMR ($CDCl_3$, 100 MHz): 168.4, 133.8, 132.2, 123.1, 38.3, 34.0, 33.5, 29.3, 26.2, 19.0, 11.3; Molecular weight $[M+H]^+$: 246.2 (expected), 246.2 (found); IR (cm^{-1}): 2958, 2934, 2902, 2873, 1775, 1707, 1615.

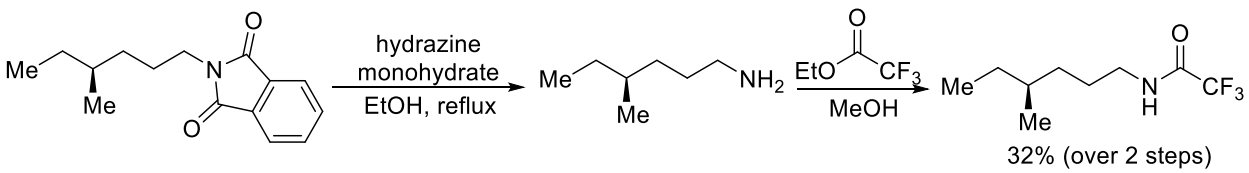

To a solution of (*S*)-2-(4-methylhexyl)isoindoline-1,3-dione (1.20 g, 4.89 mmol, 1 equiv.) in EtOH (58 mL) was added hydrazine monohydrate (0.835 mL, 17.1 mmol, 3.5 equiv.). The mixture was refluxed overnight. The mixture was cooled to rt. H_2O and 1M NaOH was added to dissolve the solid formed. The mixture was extracted with DCM three times. The combined organic layer was washed with brine, dried over Na_2SO_4 and filtered. Solvent was removed under vacuum to afford a 1: 0.63 mixture of (S)-4-methylhexan-1-amine and EtOH (347.4 mg in total). The mixture was dissolved in MeOH (7.2 mL). Ethyl trifluoroacetate (0.190 mL, 1.60 mmol, 1.1 equiv.) was added at 0 °C. The mixture was allowed to warm to rt and stirred overnight. Solvent was removed under vacuum. Flash column chromatography afforded (*S*)-2,2,2-trifluoro-N-(4-methylhexyl)acetamide (325.5 mg, 32% over 2 steps).

^{1}H NMR ($CDCl_3$, 400 MHz): 6.72 (br, 1H), 3.32 (q, *J*= 6.8, 2H), 1.62-1.54 (m, 2H), 1.35-1.28 (m, 3H), 1.17-1.08 (m, 2H), 0.86-0.82 (m, 6H); ^{13}C NMR ($CDCl_3$, 100 MHz): 157.3 (q, *J*=36.6), 115.9 (q, *J*= 287.6), 40.3, 34.0, 33.4, 29.2, 26.4, 18.9, 11.2; ^{19}F NMR ($CDCl_3$, 376 MHz): −76.1; Molecular weight $[M-H]^-$: 210.1 (expected), 210.1 (found); IR (cm^{-1}): 3318 (br), 3109, 2961, 2933, 2876, 1702.

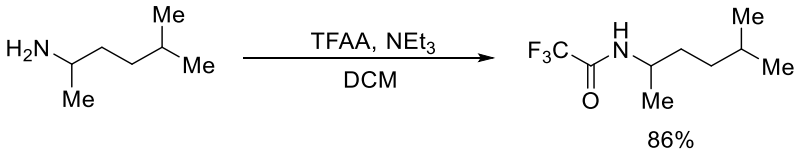

86%

By General Procedure C, 2,2,2-trifluoro-*N*-(5-methylhexan-2-yl)acetamide (3.14 g, 86%) was synthesized from 5-methylhexan-2-amine (2.00 g). Flash column chromatography conditions: 15% Et_2O/hexane.

^{1}H NMR ($CDCl_3$, 400 MHz): 6.54 (br, 1H), 4.00-3.90 (m, 1H), 1.54-1.46 (m, 3H), 1.19-1.14 (m, 5H), 0.86 (d, *J*= 6.7, 6H); ^{13}C NMR ($CDCl_3$, 100 MHz): 156.6 (q, *J*= 36.6), 115.9 (q, *J*= 287.9), 46.8, 34.9, 34.0, 27.8, 22.3, 20.1; ^{19}F NMR ($CDCl_3$, 376 MHz): −76.1; Molecular Weight $[M-H]^-$: 210.1 (expected), 210.1 (found); IR (cm^{-1}): 3233 (br), 257, 2875, 1738, 1714, 1556, 1460, 1436, 1391, 1363, 1275, 1227, 1185, 1144.

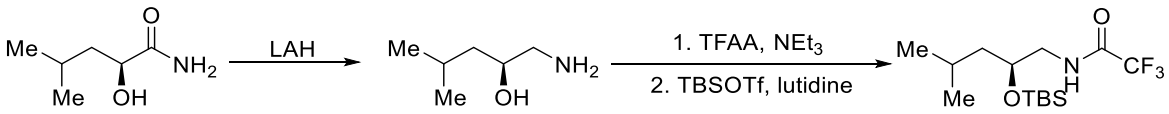

To a solution of the (*S*)-2-hydroxy-4-methylpentanamide[2] (2.54 g, 19.4 mmol, 1 equiv.) in THF (129 mL, 0.15 M) was added LAH (2.20 g, 58.0 mmol, 3 equiv.) in portions at 0 °C. The mixture was refluxed overnight. The mixture was cooled to 0 °C. Water (2.2 mL) was added slowly. 15% NaOH (2.2 mL) was added slowly. Water (6.6 mL) was added. The mixture was allowed to rt and stirred for 15 mins. The mixture was filtered. The solvent in the filtrate was removed under reduced pressure to afford crude (*S*)-1-amino-4-methylpentan-2-ol (2.13 g, 94%), which was used without further purification.

To the crude (*S*)-1-amino-4-methylpentan-2-ol (299.0 mg, 2.55 mmol, 1 equiv.) in DCM (10.2 mL, 0.25 M) was added NEt_3 (0.375 mL, 2.68 mmol, 1.05 equiv.) and TFAA (0.34 mL, 2.42 mmol, 0.95 equiv.) at 0 °C. The mixture was stirred for 30 mins and allowed to warm to rt. The solvent was removed under reduced pressure. The crude product was filtered through Si gel. Flash column chromatography (10-25% EtOAc/hexane) afforded (*S*)-2,2,2-trifluoro-N-(2-hydroxy-4-methylpentyl)acetamide (310.0 mg, 57%) as a white solid.

^{1}H NMR ($CDCl_3$, 400 MHz): 7.36 (br, 1H), 3.84-3.78 (m, 1H), 3.50 (ddd, *J*= 13.7, 6.3, 2.7, 1H), 3.15-3.09 (m, 1H), 2.98 (br, 1H), 1.71 (septet, *J*= 6.7, 1H), 1.42-1.35 (m, 1H), 1.25-1.18 (m, 1H), 0.90 (d, *J*= 6.7, 3H), 0.88 (d, *J*= 6.7, 3H); ^{13}C NMR ($CDCl_3$, 100 MHz): 157.5 (q, *J*= 37.1), 115.5 (q, *J*= 287.4), 67.9, 45.6, 43.4, 24.0, 22.7, 21.5; ^{19}F NMR ($CDCl_3$, 376 MHz): −76.4; Molecular weight $[M-H]^-$: 212.1 (expected), 212.1 (found); IR (cm^{-1}): 3420, 3311 (br), 3104, 2959, 2937, 2874, 1703.

To (*S*)-2,2,2-trifluoro-N-(2-hydroxy-4-methylpentyl)acetamide (200.5 mg, 0.94 mmol, 1 equiv.) in DCM (19 mL, 0.05 M) was added lutidine (0.326 mL, 2.82 mmol, 3 equiv.) At 0 °C, TBSOTf (0.431 mL, 0.188 mmol, 2 equiv.) was added. The mixture was slowly warmed to rt. The mixture was stirred at rt for 3.5 h. The reaction was quenched with sat. NH_4Cl. The organic and aqueous layers were separated. The aqueous layer was extracted with DCM twice. The combined organic layer was washed with sat. $NaHCO_3$ and brine, dried over Na_2SO_4 and filtered. The solvent was removed under reduced pressure. Flash column chromatography (5% EtOAc/hex) afforded (*S*)-N-(2-((*tert*-butyldimethylsilyl)oxy)-4-methylpentyl)-2,2,2-trifluoroacetamide (285.9 mg, 93%).

^{1}H NMR ($CDCl_3$, 400 MHz): 6.58 (br, 1H), 3.93-3.93 (m, 1H), 3.51-3.46 (m, 1H), 3.28-3.22(m, 1H), 1.68-1.55 (m, 1H), 1.42-1.25 (m, 2H), 0.87-0.89 (m, 15H), 0.08 (s, 6H); ^{13}C NMR ($CDCl_3$, 100 MHz): 157.1 (q, *J*= 36.4), 115.9 (q, *J*= 288.1), 68.6, 45.0, 44.4, 25.7, 24.3, 23.0, 22.6, 17.9, −4.5, −4.8; ^{19}F NMR ($CDCl_3$, 376 MHz): −76.1; Molecular weight $[M-H]^-$: 326.2 (expected), 326.2 (found); IR (cm^{-1}): 3434, 3322 (br), 3106, 2957, 2931, 2885, 2859, 170.

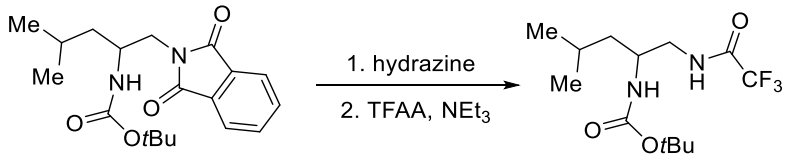

Anhydrous N_2H_4 (100 µL, 3.29 mmol, 2.0 equiv.) was added to a solution of *tert*-butyl (1-(1,3-dioxoisoindolin-2-yl)-4-methylpentan-2-yl)carbamate[3] (570 mg, 1.65 mmol, 1.0 equiv.) in anhydrous EtOH (17 mL) and anhydrous CH_2Cl_2 (3 mL). The reaction mixture was heated at 60 °C for 12 h. The reaction mixture was cooled to room temperature and filtered. The solid was washed with Et_2O. The filtrate was concentrated under reduced pressure. The crude amine was used in the subsequent step without further purification.

TFAA (0.26 mL, 1.82 mmol, 1.1 equiv.) was added dropwise to a solution of crude and Et_3N (0.46 mL, 3.30 mmol, 2.0 equiv.) in anhydrous CH_2Cl_2 (5.5 mL) at 0 °C. The reaction mixture was raised to room temperature. The reaction mixture was stirred at this temperature for 5 h and then diluted with H_2O (5 mL). The phases were separated and the aqueous layer was extracted with CH_2Cl_2 (3 x 5 mL). The combined organic phase was washed with H_2O (10 mL) and brine (10 mL), dried (Na_2SO_4), filtered and concentrated under reduced pressure. The crude product was purified by flash column chromatography (55-65% Et_2O/hexane) to give *tert*-butyl (4-methyl-1-(2,2,2-trifluoroacetamido)pentan-2-yl)carbamate as a white solid (369 mg, 72%).

^{1}H NMR (400 MHz, $CDCl_3$): 8.01 (br, 1H), 7.36 (br, 0.5H, rotamer), 5.30 (br, 0.5H, rotamer), 4.75 (d, *J*= 7.4, 1H), 3.85-3.82 (m, 1H), 3.37-3.23 (m, 2H), 1.67 (septet, *J*= 6.7, 1H), 1.43-1.23 (m, 11H), 0.90-0.87 (m, 6H); ^{13}C NMR (100 MHz, $CDCl_3$): 157.7 (q, *J*= 37.1), 157.2, 115.9 (q, *J*= 287.7), 80.2, 48.2, 46.5, 41.4, 28.1, 24.7, 22.8, 21.8; Molecular weight $[M+Na]^+$: 335.1558 (expected), 335.1543 (found); IR (cm^{-1}): 3340, 2962, 2935, 1695, 1678, 1527, 1188, 1162, 907, 731.

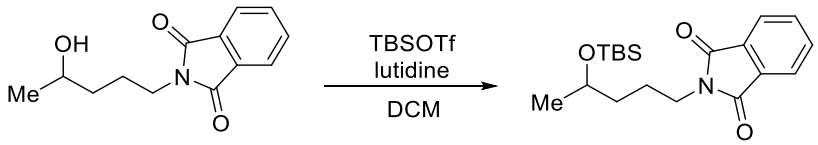

To a solution of 2-(4-hydroxypentyl)isoindoline-1,3-dione[4] (450.0 mg, 1.93 mmol, 1 equiv.) and lutidine (0.70 mL, 6.01, 3.1 equiv.) in DCM (9.5 mL) was added TBSOTf (0.56 mL, 2.44 mmol, 1.26 equiv.) at 0 ^{o}C. The mixture was stirred at rt for 3h. The reaction was quenched with 1 M HCl. The organic and aqueous layer were separated. The organic layer was washed with brine, dried over Na_2SO_4 and filtered. The solvent was removed under vacuum. Flash column chromatography (10-30% Et_2O/hexane) afforded 2-(4-((*tert*-butyldimethylsilyl)oxy)pentyl)-isoindoline-1,3-dione (605 mg, 100%).

^{1}H NMR ($CDCl_3$, 400 MHz): 7.82-7.80 (m, 2H), 7.68-7.66 (m, 2H), 3.79 (sextet, *J*=6.0, 1H), 3.65 (t, *J*= 7.3, 2H), 1.80-1.71 (m, 2H), 1.46-1.38 (m, 2H), 1.08 (d, *J*=5.9, 3H), 0.83 (s, 9H), 0.00 (6H); ^{13}C NMR ($CDCl_3$, 100 MHz): 168.4, 133.8, 132.2, 123.1, 67.8, 38.1, 36.7, 25.9, 24.8, 23.8, 18.1, −4.41, −4.76; Molecular weight $[M-H]^-$: 348.2 (expected), 348.2 (found); IR (cm^{-1}): 3044, 2954, 2929, 2884, 2856, 1775, 1712.

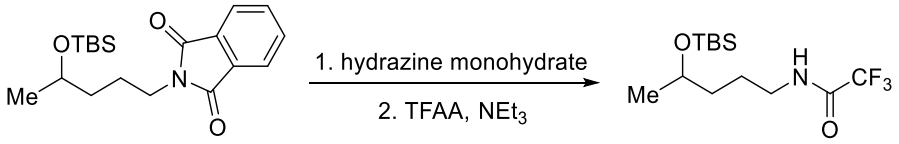

To a solution of 2-(4-((*tert*-butyldimethylsilyl)oxy)pentyl)isoindoline-1,3-dione (589.2 mg, 1.88 mmol., 1 equiv.) in EtOH (23 mL) was added hydrazine monohydrate (0.32 mL, 6.58 mmol, 3.5 equiv.). The mixture was refluxed overnight. The mixture was cooled to rt. Water and 1 M NaOH were added. The mixture was extracted with DCM three times. The combined organic layer was washed with brine, dried over Na_2SO_4 and filtered. The solvent was removed under vacuum to afford crude 4-((*tert*-butyldimethylsilyl)oxy)pentan-1-amine (343.4 mg, 84%).

To a solution of the crude 4-((*tert*-butyldimethylsilyl)oxy)pentan-1-amine (300.8 mg, 1.38 mmol, 1 equiv.), NEt_3 (0.196 mL, 1.41 mmol, 1.02 equiv.) in DCM (7 mL) was added TFAA (0.182 mL, 1.31 mmol, 0.95 equiv.) at 0 ^oC dropwise. The mixture was allowed to warm to rt. The mixture was stirred for 3 h. Solvent was removed under vacuum. The mixture was filtered through Si gel. Flash column chromatography (12-22% Et_2O/hexane) afforded N-(4-((*tert*-butyldimethylsilyl)-oxy)pentyl)-2,2,2-trifluoroacetamide (396.5 mg, 92%).

^1H NMR ($CDCl_3$, 400 MHz): 6.94 (br, 1H), 3.89-3.82 (m, 1H), 3.46-3.38 (m, 1H), 3.31-3.25 (m, 1H), 1.72-1.54 (m, 2H), 1.48-1.43 (m, 2H), 1.12 (d, *J*=6.3, 3H), 0.86 (s, 9H), 0.04 (s, 3H), 0.03 (s, 3H); ^{13}C NMR ($CDCl_3$, 100 MHz): 157.2 (q, *J*= 36.6), 115.9 (q, *J*= 287.6), 67.9, 39.9, 36.3, 25.8, 24.7, 23.3, 18.0, −4.56, −4.90; ^{19}F NMR ($CDCl_3$, 376 MHz): −76.0; Molecular weight $[M-H]^-$: 312.2 (expected), 312.2 (found); IR (cm^{-1}): 3313 (br), 2957, 2931, 2860, 1708, 1558, 1463, 1433, 1371, 1255, 1229, 1184, 1148, 1066, 1005.

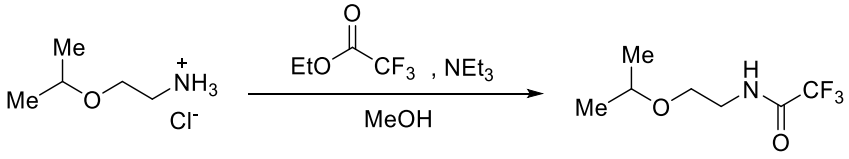

To a solution of 2-isopropoxyethan-1-aminium chloride (2.50 g, 17.9 mmol, 1.0 equiv.) in MeOH (90 mL) was added NEt_3 (2.75 mL, 19.7 mmol, 1.1 equiv.) and then ethyl trifluoroacetate (2.35 mL, 19.7 mmol, 1.1 equiv.). The mixture was stirred at rt overnight. Solvent was removed under reduced pressure. The crude product was filtered through Si gel. Flash column chromatography (25-35% Et_2O/hexane) afforded 2,2,2-trifluoro-*N*-(2-isopropoxyethyl)acetamide (2.90 g, 81%) as a colorless oil.

^{1}H NMR ($CDCl_3$, 400 MHz): 6.94 (br, 1H), 3.55 (septet, *J*= 6.1, 1H), 3.51-3.44 (m, 4H), 1.10 (d, *J*= 6.3, 6H); ^{13}C NMR ($CDCl_3$, 100 MHz): 157.2 (q, *J*= 37.1), 115.8 (q, *J*= 287.6), 72.0, 65.2, 39.9, 21.8; ^{19}F NMR ($CDCl_3$, 376 MHz): −76.3; Molecular weight $[M-H]^-$: 198.1 (expected), 198.1 (found); IR (cm^{-1}): 3317 (br), 3103, 2976, 2937, 2874, 1706, 1553, 1455, 1382, 1371, 1337, 1209, 1151, 1094.

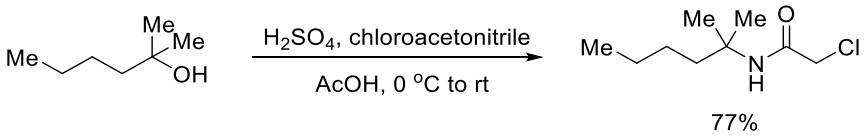

To a solution of 2-methylhexan-2-ol (3.00 g, 25.8 mmol, 1 equiv.) and chloroacetonitrile (9.8 mL, 0.155 mmol, 6.0 equiv.) in AcOH (11.5 mL) was added conc. H_2SO_4 (13.15 mL, 232.2 mmol, 9 equiv.) at 0 °C dropwise. The mixture was allowed to warm to rt and stir for 5 h. The mixture was poured into ice/water mixture. The mixture was extracted with DCM three times. The combined organic layer was washed with sat. Na_2CO3 twice and brine, dried over Na_2SO_4 and filtered. Solvent was removed under vacuum. Flash column chromatography (20% EtOAc/hexane) afforded 2-chloro-*N*-(2-methylhexan-2-yl)acetamide (3,81 g, 77%).

^{1}H NMR ($CDCl_3$, 400 MHz): 6.27 (br, 1H), 3.89 (s, 2H), 1.66-1.62 (m, 2H), 1.30 (s, 6H), 1.27-1.17 (m, 4H), 0.86 (t, *J*= 7.0, 3H); ^{13}C NMR ($CDCl_3$, 100 MHz): 164.7, 54.2, 32.9, 40.0, 26.5, 26.1, 22.9, 14.0; Molecular weight $[M-H]^-$: 190.1 (expected), 190.1 (found); IR (cm^{-1}): 3413, 3296, 3084, 2957, 2932, 2873, 2862, 1657.

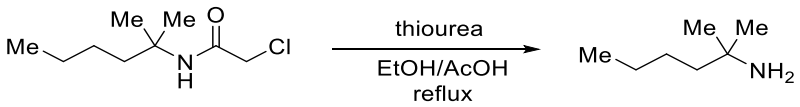

A solution of 2-chloro-*N*-(2-methylhexan-2-yl)acetamide (3.50 g, 18.3 mmol) and thiourea (1.67 g, 21.9 mmol, 1.2 equiv.) in EtOH/AcOH (44 mL, 4.9:1) was refluxed overnight. The mixture was diluted with water. Solid NaOH was added until pH of the solution is less than 5. The mixture was extracted with DCM three times. The combined organic layer was extracted with 2M HCl twice. The combined acidic layer was basified with solid NaOH until pH is higher than 10 and was extracted with DCM three times. The combined organic layer was dried over Na_2SO_4 and filtered. Solvent was removed under vacuum to afford 2-methylhexan-2-amine (705 mg, 34%). It was used without further purification.

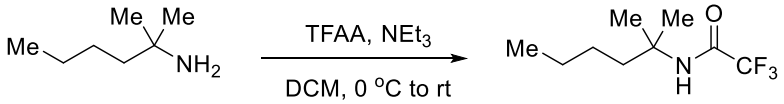

By General Procedure C: 2,2,2-trifluoro-N-(2-methylhexan-2-yl)acetamide (218.7 mg, 48%) was synthesized from 2-methylhexan-2-amine (248.0 mg).

^{1}H NMR ($CDCl_3$, 400 MHz): 6.05 (br, 1H), 1.72-1.68 (m, 2H), 1.35 (s, 6H), 1.31-1.22 (m, 4H), 0.89 (t, *J*= 7.2); ^{13}C NMR ($CDCl_3$, 100 MHz): 156.0 (q, *J*=35.8), 115.6 (q, *J*= 289.3.), 53.5, 39.6, 26.2, 26.0, 22.8, 13.4 ; ^{19}F NMR ($CDCl_3$, 376 MHz): −76.3; Molecular weight $[M-H]^-$: 210.1 (expected), 210.1 (found); IR (cm^{-1}): 3441, 3320, 3095, 2959, 2932, 2865, 1704.

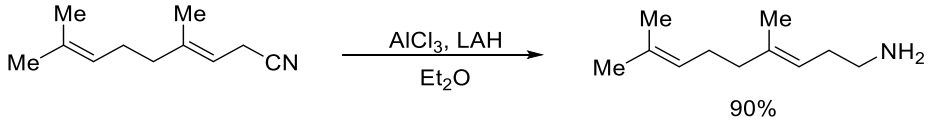

To a solution of LAH (0.226 g, 5.96 mmol, 1 equiv.) in Et_2O (6 mL) was added anhydrous $AlCl_3$ (0.793 g, 5.95 mmol, 1 equiv.) at 0 °C in portions. The mixture was stirred at 10 mins at 0 °C. Homogernanonitrile[5] (0.9711 g, 5.95 mmol, 1 equiv.) in Et_2O (1 mL) was added via cannula. The

mixture was stirred at 0 °C for 1 h and was warmed to rt. The mixture was stirred overnight. The reaction was quenched by 1M NaOH. The mixture was extracted with EtOAc three times. The combined organic layer was washed with brine, dried over Na_2SO_4 and filtered. The solvent was removed under vacuum. Crude (*E*)-4,8-dimethylnona-3,7-dien-1-amine (0.900 g, 90%) was used without further purification.

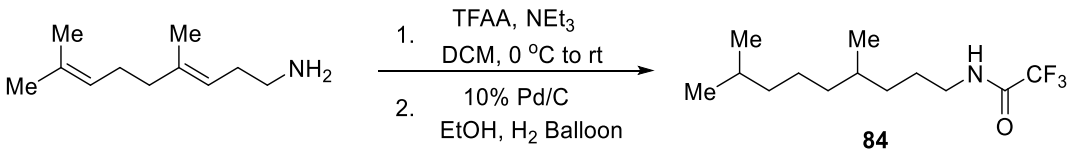

To a solution of (*E*)-4,8-dimethylnona-3,7-dien-1-amine (0.755 g, 4.51 mmol, 1 equiv.) and NEt_3 (0.642 mL, 4.61 mmol, 1.02 equiv.) in DCM (18 mL) was added TFAA (0.595 mL, 4.28 mmol, 0.95 equiv.) dropwise at 0 °C. The mixture was slowly warmed to rt and stirred overnight. The solvent was removed under vacuum. The mixture was filtered through silica gel. Flash column chromatography (4-12% Et_2O/hex) afforded (*E*)-N-(4,8-dimethylnona-3,7-dien-1-yl)-2,2,2-trifluoroacetamide (0.87 g, 73%). To a solution of (*E*)-N-(4,8-dimethylnona-3,7-dien-1-yl)-2,2,2-trifluoroacetamide (509.4 mg, 1.935 mmol, 1 equiv.) in EtOH (17 mL) was added 10% Pd/C (600 mg). The mixture was stirred under a H_2 atmosphere (H_2 balloon) overnight. The mixture was filtered through celite. Flash column chromatography (10-15% Et_2O/hex) afforded *N*-(4,8-dimethylnonyl)-2,2,2-trifluoroacetamide **84** (473.3 mg, 92%).

^{1}H NMR ($CDCl_3$, 400 MHz): 6.62 (br, 1H), 3.32 (q, *J*= 6.9, 2H), 1.66-1.47 (m, 3H), 1.39-1.06 (m, 9H), 0.86-0.84 (m, 9H); ^{13}C NMR ($CDCl_3$, 100 MHz): 157.2 (q, *J*= 36.9), 115.9 (q, *J*= 287.9), 40.3, 39.2, 37.0, 33.8, 32.4, 27.9, 26.5, 24.7, 22.6, 22.5, 19.4; ^{19}F NMR ($CDCl_3$, 376 MHz): −76.1;

Molecular weight [M–H]$^-$: 266.2 (expected), 266.2 (found); IR (cm^{-1}): 3306 (br), 3107, 2954, 2927, 2870, 1701.

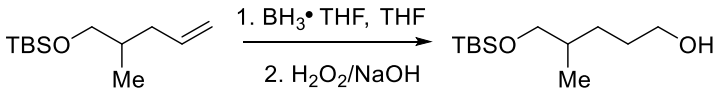

BH_3 (1.0 M in THF, 8.6 mL, 8.61 mmol, 1.0 equiv.) was added dropwise to a solution of *tert*-butyldimethyl((2-methylpent-4-en-1-yl)oxy)silane[6] (1845 mg, 8.61 mmol, 1.0 equiv.) in anhydrous THF (22 mL) at 0 °C. The reaction mixture was stirred at 0 °C for 1 h. A premixed solution of NaOH (2.0 M, 20 mL) and H_2O_2 (30%, 10 mL) was added dropwise to the reaction mixture at 0 °C. The reaction mixture was stirred at 0 °C for 1 h. The reaction was diluted with H_2O (20 mL) and Et_2O (10 mL). The phases were separated and the aqueous layer was extracted with Et_2O (3 x 20mL). The combined organic layer was washed with H_2O (20 mL) and brine (20 mL), dried ($MgSO_4$), filtered and concentrated under reduced pressure. The crude product was purified by flash column chromatography (20-30% EtOAc/hexane) to give 5-((*tert*-butyldimethylsilyl)oxy)-4-methylpentan-1-ol as a colorless oil (1067 mg, 53%). The Spectral data are in accordance with the published values.[7]

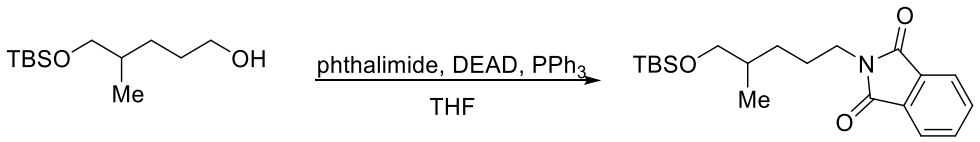

DEAD (0.83 mL, 5.29 mmol, 1.2 equiv.) was added dropwise to a solution of 5-((*tert*-butyldimethylsilyl)oxy)-4-methylpentan-1-ol (1024 mg, 4.41 mmol, 1.0 equiv.), phthalimide (778 mg, 5.29 mmol, 1.2 equiv.) and Ph_3P (1472 mg, 5.29 mmol, 1.2 equiv.) in anhydrous THF (22 mL) at 0 °C. The reaction mixture was allowed to warm to room temperature and was stirred for 12 h. The reaction solvent was removed under reduced pressure. The crude reaction mixture was

suspended in hexane, filtered and concentrated. The crude product was purified by flash column chromatography (3-6% EtOAc/hexane) to give 2-(5-((*tert*-butyldimethylsilyl)oxy)-4-methylpentyl)isoindoline-1,3-dione as a colorless oil (1504 mg, 94%).

^{1}H NMR (400 MHz, $CDCl_3$): 7.86 - 7.78 (m, 2H), 7.73 - 7.67 (m, 2H), 3.67 (t, *J*= 7.3, 2H), 3.41 (dd, J= 9.8, 5.8, 1H), 3.36 (dd, *J*=9.8, 6.2, 1H), 1.79 - 1.54 (m, 3H), 1.17 - 1.06 (m, 1H), 0.86 (d, *J*= 6.7, 3H), 0.85 (s, 9H), 0.00 (s, 6H); ^{13}C NMR (100 MHz, $CDCl_3$): 168.4, 133.8, 132.2, 123.1, 68.0, 38.3, 35.4, 30.2, 26.1, 25.9, 18.3, 16.6, −5.4; Molecular weight $[M+H]^+$: 362.2152 (expected), 362.2143 (found); IR (cm^{-1}): 2961, 2930, 2857, 1711, 1427, 1110, 700.

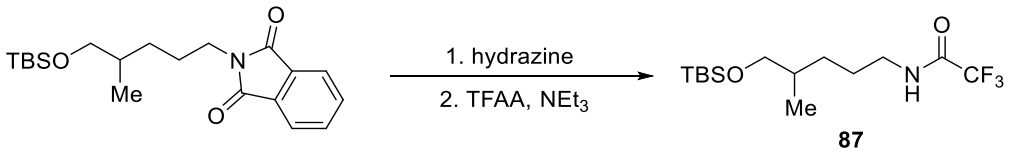

87

Anhydrous N_2H_4 (90 µL, 2.76 mmol, 2.0 equiv.) was added to a solution of 2-(5-((*tert*-butyldimethylsilyl)oxy)-4-methylpentyl)isoindoline-1,3-dione (500 mg, 1.38 mmol, 1.0 equiv.) in anhydrous EtOH (13 mL). The reaction mixture was heated at 60 °C for 2 h. The reaction mixture was cooled to room temperature and filtered. The solid was washed with Et_2O. The filtrate was concentrated under reduced pressure. The crude product was suspended in Et_2O and filtered. The crude amine was used in the subsequent step without further purification.

TFAA (0.21 mL, 1.52 mmol, 1.1 equiv.) was added dropwise to a solution of crude amine and Et_3N (0.38 mL, 2.76 mmol, 2.0 equiv.) in anhydrous CH_2Cl_2 (4.5 mL) at 0 °C. The reaction mixture was allowed to warm to room temperature. The reaction mixture was stirred at this temperature for 5 h and then diluted with H_2O (5 mL). The phases were separated and the aqueous layer was extracted with CH_2Cl_2 (3 x 5 mL). The combined organic phase was washed

with H_2O (10 mL) and brine (10 mL), dried (Na_2SO_4), filtered and concentrated under reduced pressure. The crude product was purified by flash column chromatography (10% EtOAc/hexane) to give N-(5-((*tert*-butyldimethylsilyl)oxy)-4-methylpentyl)-2,2,2-trifluoroacetamide **87** as a colorless oil (405 mg, 90%).

^{1}H NMR (400 MHz, $CDCl_3$): 6.66 (br, 1H), 3.42-3.38 (m, 2H), 3.36-3.31 (m, 2H), 1.67-1.53 (m, 3H), 1.50-1.43 (m, 1H), 1.13-1.09 (m, 1H), 0.87-0.85 (m, 12H), 0.86 (d, J = 6.9, 3H), 0.02 (s, 6H); ^{13}C NMR (100 MHz, $CDCl_3$): 157.2 (q, *J* = 36.7), 115.8 (q, *J* = 287.3), 68.0, 40.3, 35.3, 30.2, 26.4, 25.9, 18.3, 16.5, −5.5, −5.5; ; Molecular weight $[M+H]^+$: 328.1920 (expected), 328.1901 (found); IR (cm^{-1}): 3304, 2955, 2930, 2858, 1701, 1560, 1161, 1093, 834.

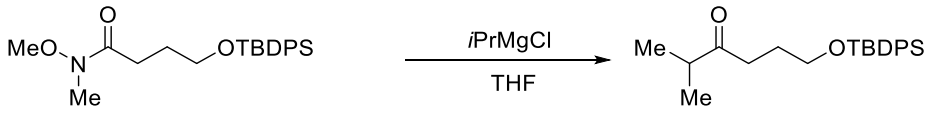

*i*PrMgCl (2.0 M in Et_2O, 12.4 mL, 24.7 mmol, 2.0 equiv.) was added dropwise to a solution of 4-((*tert*-butyldiphenylsilyl)oxy)-N-methoxy-N-methylbutanamide[8] in anhydrous THF (25 mL) at −78 °C. The reaction mixture was stirred at −78 °C for 5 min before being warmed to room temperature. The reaction mixture was stirred at rt for 4 h before being diluted with NH_4Cl (sat. aq., 10 mL) and H_2O (10 ml). The phases were separated and the aqueous layer was extracted with Et_2O (3 x 10 ml). The combined organic layer was washed with H_2O (20 mL) and brine (20 mL), dried ($MgSO_4$), filtered and concentrated under reduced pressure. The crude product was purified by flash column chromatography (5-10% EtOAc/hexane) to give 6-((*tert*-butyldiphenylsilyl)oxy)-2-methylhexan-3-one as a colorless oil (2323 mg, 51%).

^{1}H NMR (400 MHz, $CDCl_3$): 7.69-7.61 (m, 4H), 7.47-7.34 (m, 6H), 3.68 (t, *J*= 6.1, 2H), 2.59 (septet, *J*= 6.1, 1H), 2.58 (t, *J*= 7.2, 2H), 1.87-1.78 (m, 2H), 1.09 (d, *J*= 6H), 1.06 (s, 9H); ^{13}C NMR (100 MHz, $CDCl_3$): 214.6, 135.5, 133.8, 129.6, 127.6, 63.0, 40.9, 36.5, 26.9, 19.2, 18.3; Molecular weight $[M+H]^+$: 369.2250(expected), 369.2238 (found); IR (cm^{-1}): 2961, 2930, 2857, 1711, 1428, 1111, 581.

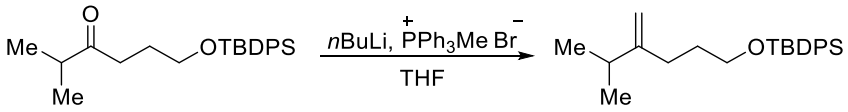

*n*BuLi (1.6 M in hexanes, 12.0 mL, 19.2 mmol, 4.0 equiv.) was added dropwise to a solution of Ph_3MePBr (7186 mg, 20.1 mmol, 4.2 equiv.) in anhydrous THF (40 mL) at 0 °C. The reaction mixture was warmed to room temperature and stirred at this temperature for 1 h. 6-((*tert*-butyldiphenylsilyl)oxy)-2-methylhexan-3-onein anhydrous THF (8 mL) was added dropwise to the reaction mixture. The reaction mixture was heated to 70 °C and stirred at this temperature for 12 h. The reaction mixture was cooled to room temperature and diluted with H_2O (40 mL). The phases were separated and the aqueous layer was extracted with Et_2O (3 x 20 ml). The combined organic layer was washed with H_2O (20 mL) and brine (20 mL), dried ($MgSO_4$), filtered and concentrated under reduced pressure. The crude product was purified by flash column chromatography (2% Et_2O/hexane) to give *tert*-butyl((5-methyl-4-methylenehexyl)oxy)diphenyl-silane as a colorless oil (1764 mg, 100%).

^{1}H NMR (400 MHz, $CDCl_3$): 7.74-7.64 (m, 4H), 7.47-7.33 (m, 6H), 4.74 (s, 1H), 4.66 (s, 1H), 3.69 (t, *J*= 6.4, 2H), 2.22 (septet, *J*= 6.8, 1H), 2.11 (t, *J*= 7.8, 2H), 1.77-1.66 (m, 2H), 1.07 (s, 9H), 1.02 (d, *J*= 6.0, 6H); ^{13}C NMR (100 MHz, $CDCl_3$): 155.7, 135.6, 134.1, 129.5, 127.6, 106.2, 63.7,

33.8, 31.2, 30.5, 26.9, 21.8, 19.2; Molecular weight $[M+H]^+$: 367.2457 (expected), 367.2457 (found); IR (cm^{-1}): 2959, 2931, 2858, 1428, 1107, 690.

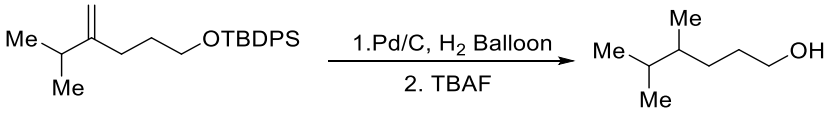

Pd/C (10%, 250 mg) was added to a solution of give *tert*-butyl((5-methyl-4-methylenehexyl)oxy)diphenylsilane (1620 mg, 4.40 mmol, 1.0 equiv.) in EtOH (22 mL). The atmosphere was removed under reduced pressure and replaced with an atmosphere of H_2 (balloon of H_2 with needle running into the reaction mixture); this process was repeated three times. A balloon of H_2 was connected to the reaction flask and the reaction mixture was stirred at room temperature for 12 h. The reaction mixture was filtered through a plug of Celite. The Celite was washed with Et_2O (100 mL) and the filtrate was concentrated under reduced pressure to give the crude TBDPS protected alcohol which was used in the following step without purification.

TBAF (1.0 M in THF, 8.8 mL, 8.80 mmol, 2.0 equiv.) was added dropwise to a solution of crude TBDPS protected alcohol in anhydrous THF (20 mL) at room temperature. The reaction mixture was stirred at this temperature for 3 h before being diluted with NH_4Cl (sat. aq., 10 mL) and H_20 (10 mL). The phases were separated and the aqueous layer was extracted with Et_2O (3 x 10 ml). The combined organic layer was washed with H_2O (20 mL) and brine (20 mL), dried ($MgSO_4$), filtered and concentrated under reduced pressure. The crude product was purified by flash column chromatography (20-50% Et_2O/hexane) to give 4,5-dimethylhexan-1-ol as a colorless oil (559 mg, 98%).

^{1}H NMR (400 MHz, $CDCl_3$): 3.62 (t, *J*= 6.8, 2H), 1.67-1.27 (m, 6H), 1.18-1.07 (m, 1H), 0.86 (d, *J*= 6.9, 3H), 0.81 (d, *J*= 6.8, 3H), 0.80 (d, *J*= 6.9, 3H); ^{13}C NMR (100 MHz, $CDCl_3$): 63.4, 38.4, 32.0, 30.8, 30.1, 20.2, 17.9, 15.3; IR (cm^{-1}): 3317, 2956, 2933, 2871, 1462, 1377, 1058. The molecular weight cannot be observed with MS (EI).

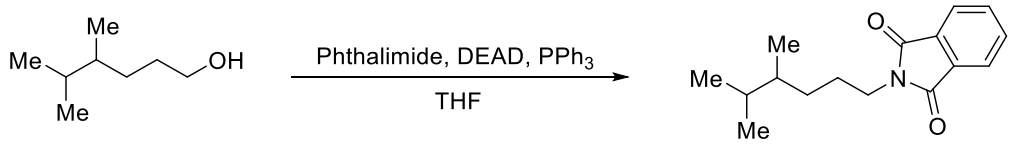

DEAD (0.81 mL, 5.15 mmol, 1.2 equiv.) was added dropwise to a solution of 4,5-dimethylhexan-1-ol (559 mg, 4.29 mmol, 1.0 equiv.), phthalimide (758 mg, 5.15 mmol, 1.2 equiv.) and Ph_3P (1433 mg, 5.15 mmol, 1.2 equiv.) in anhydrous THF (14 mL) at 0 °C. The reaction mixture was allowed to warm to room temperature and was stirred at this temperature for 12 h. The reaction solvent was removed under reduced pressure. The crude reaction mixture was suspended in hexane, filtered and concentrated. The crude product was purified by flash column chromatography (2-10% EtOAc/hexane) to give 2-(4,5-dimethylhexyl)isoindoline-1,3-dione as a colorless oil (1100 mg, 99%).

^{1}H NMR (400 MHz, $CDCl_3$): 7.88-7.76 (m, 2H), 7.74-7.65 (m, 2H), 3.65 (t, *J*= 7.4, 2H), 1.74-1.51 (m, 3H), 1.40-1.28 (m, 2H), 1.19-1.08 (m, 1H), 0.84 (d, *J*= 6.8, 3H), 0.79 (d, *J*= 6.7, 3H), 0.78 (d, *J*= 6.7, 3H); ^{13}C NMR (100 MHz, $CDCl_3$): 168.4, 133.8, 132.2, 123.1, 38.4, 38.2, 31.9, 31.2, 26.6, 20.2, 17.9, 15.2; Molecular weight $[M+H]^+$: 260.1651 (expected), 260.1630 (found); IR (cm^{-1}): 2956, 2871, 1707, 1394, 1361, 717.

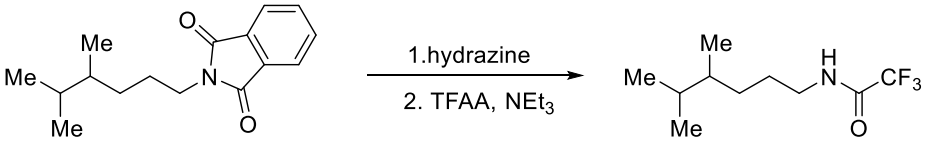

89

Anhydrous N_2H_4 (0.26 mL, 8.33 mmol, 2.0 equiv.) was added to a solution of 2-(4,5-dimethylhexyl)isoindoline-1,3-dione (1080 mg, 4.17 mmol, 1.0 equiv.) in anhydrous EtOH (20 mL). The reaction mixture was heated at 60 °C for 2 h. The reaction mixture was cooled to room temperature, filtered. The solid was washed with Et_2O. The filtrate was concentrated under reduced pressure. The crude amine was used in the subsequent step without further purification.

TFAA (0.65 mL, 4.59 mmol, 1.1 equiv.) was added dropwise to a solution of crude amine and Et_3N (1.10 mL, 8.34 mmol, 2.0 equiv.) in anhydrous CH_2Cl_2 (13 mL) at 0 °C. The reaction mixture was raised to room temperature. The reaction mixture was stirred at this temperature for 5 h and then diluted with H_2O (5 mL). The phases were separated and the aqueous layer was extracted with CH_2Cl_2 (3 x 5 mL). The combined organic phase was washed with H_2O (10 mL) and brine (10 mL), dried (Na_2SO_4), filtered and concentrated under reduced pressure. The crude product was purified by flash column chromatography (10-15% Et_2O/hexane) to give *N*-(4,5-dimethylhexyl)-2,2,2-trifluoroacetamide **89** as a colorless oil (412.5 mg, 44%).

^{1}H NMR ($CDCl_3$, 400 MHz): 6.93 (br, 1H), 3.31 (q, *J*= 6.9, 2H), 1.63-1.46 (m, 3H), 1.38-1.23 (m, 2H), 1.14-1.05 (m, 1H), 0.83 (d, *J*= 7.0, 3H), 0.79 (d, *J*= 2.4, 3H), 0.77 (d, *J*= 2.3, 3H); ^{13}C NMR ($CDCl_3$, 100 MHz): 157.3 (q, *J*= 36.4), 115.9 (q, *J*= 287.6), 40.3, 38.1, 31.8, 31.0, 26.8, 20.0, 17.8, 15.1; ^{19}F NMR ($CDCl_3$, 376 MHz): −76.2 ; Molecular weight $[M-H]^-$: 224.1 (expected), 224.1 (found); IR (cm^{-1}): 3300 (br), 3107, 2959, 2874, 1700.

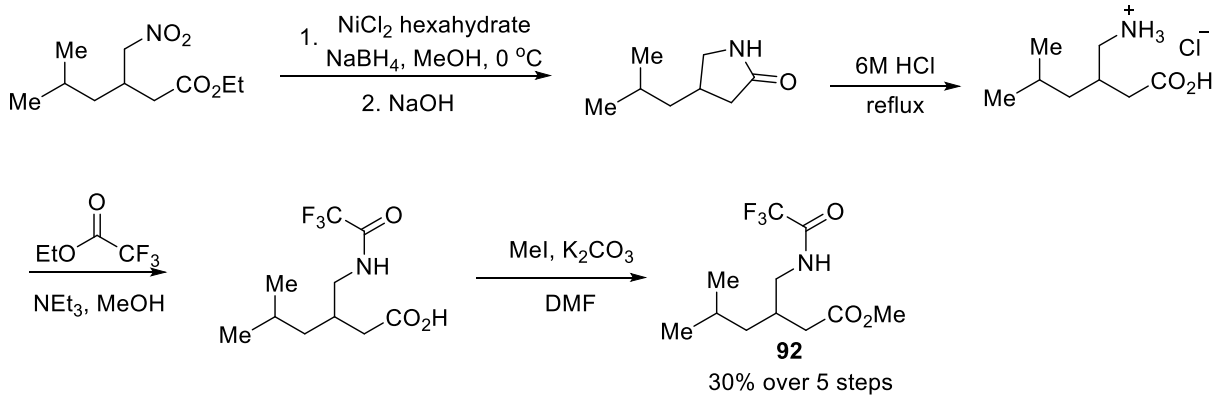

To a solution of ethyl 6-methyl-4-(nitromethyl)heptanoate[9] (1.60 g, 7.3 mmol, 1 equiv.) in MeOH (38.5 mL) was added $NiCl_2$ hexahydrate (1.7282 g,7.3 mmol, 1 equiv.) at 0 °C. $NaBH_4$ (3.0256 g, 80.3 mmol, 11 equiv.) was added in portions and VERY SLOWLY. The mixture was kept at 0 °C for 1 h. 6 M NaOH (9 mL) was added. The mixture was warmed to rt and stirred for 2 h. The mixture was acidified with 2 M HCl. The mixture was extracted with DCM four times. The combined organic layer was dried over Na_2SO_4 and filtered. The solvent was removed under vacuum to afford 4-isobutylpyrrolidin-2-one. The crude lactam was dissolved in 6 M HCl (35 mL). The mixture was refluxed overnight. The solvent was removed under vacuum to afford 2-(2-carboxyethyl)-4-methylpentan-1-aminium chloride. The crude hydrochloride salt was dissolved in MeOH (28 mL). NEt_3 (2.44 mL, 17.5 mmol, 2.4 equiv.) and ethyl trifluoroacetate (1.06 mL, 10.5 mmol, 1.44 equiv.) was added. The mixture was stirred at rt overnight. Solvent was removed under vacuum. The mixture was dissolved in EtOAc. The mixture was washed with 1 M HCl, dried over Na_2SO_4 and filtered. Solvent was removed under vacuum to afford 6-methyl-4-((2,2,2-trifluoroacetamido)methyl)heptanoic acid. The crude carboxylic acid was dissolved in DMF (23 mL). K_2CO_3 (4.837 g, 35.0 mmol, 4.8 equiv.). MeI (2.18 mL, 35.0 mmol, 4.8 equiv.) was added dropwise. The mixture was stirred for 7 h. The mixture was diluted with Et_2O, washed with H_2O

four times and brine twice. It was dried over Na_2SO_4 and filtered. Solvent was removed under vacuum. Flash column chromatography afforded methyl 6-methyl-4-((2,2,2-trifluoroacetamido)methyl)heptanoate **92** (572.9 mg, 30% over 5 steps) as a slightly yellow oil.

^{1}H NMR ($CDCl_3$, 400 MHz): 7.38 (br, 1H), 3.62 (s, 3H), 3.42-3.36 (m, 1H), 3.25-3.18 (m, 1H), 2.37 (dd, *J*= 15.7, 4.7, 1H), 2.26 (dd, *J*= 15.7, 7.8, 1H), 1.64-1.56 (m, 1H), 1.20-1.08 (m, 2H), 0.87 (d, *J*= 6.6, 3H), 0.85 (d, *J*= 6.7, 3H); ^{13}C NMR ($CDCl_3$, 100 MHz): 173.9, 157.5 (q, *J*= 36.6), 115.9 (q, *J*= 287.6), 51.77, 44.0, 41.6, 37.4, 32.5, 25.1, 22.5, 22.3; ^{19}F NMR ($CDCl_3$, 376 MHz): −76.1; Molecular weight $[M-H]^-$: 268.1 (expected), 268.1 (found); IR (cm^{-1}): 3318 (br), 3104, 2957, 2873, 2851, 1705.

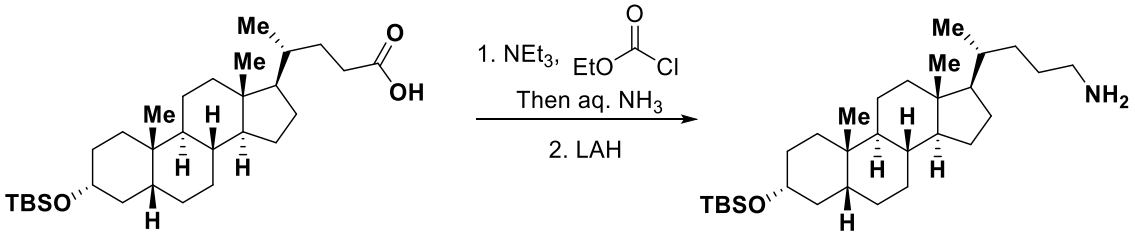

To a solution of TBS-protected lithocholic acid[10] (1.20 g, 2.44 mmol, 1 equiv.) in THF (0.1 M) was added NEt_3 (0.347 mL, 2.49 mmol, 1.02 equiv.) at 0 °C. Ethyl chloroformate (0.238 mL, 2.49 mmol, 1.02 equiv.) was added dropwise. The mixture was stirred at 0 °C for 1 h. aq. NH_3 (2.25 mL, 14.8 M) was added. The mixture was allowed to warm to rt and stir overnight. H_2O was added. The organic and aqueous layers were separated. The aqueous layer was extracted with EtOAc twice. The combined organic layer was washed with brine, dried over Na_2SO_4 and filtered. The Solvent was removed under reduced pressure to yield the amide (1.20 g, 100%) as a white solid. It was used without further purification.

To a solution of the crude amide (1.20 g, 2.44 mmol, 1 equiv.) in THF (16 mL, 0.15 M) was added LAH (0.186 g, 4.88 mmol, 2 equiv.)in portions at 0 °C. The mixture was allowed to warm to rt and stir overnight. The mixture was cooled to 0 °C. Water (0.185 mL) was added slowly. 15% NaOH (0.185 mL) was added slowly. Water (0.555 mL) was added. The mixture was allowed to rt and stirred for 15 mins. The mixture was filtered. The solvent in the filtrate was removed under reduced pressure to afford the crude amine (1.14 g, 98%), which was used without further purification.

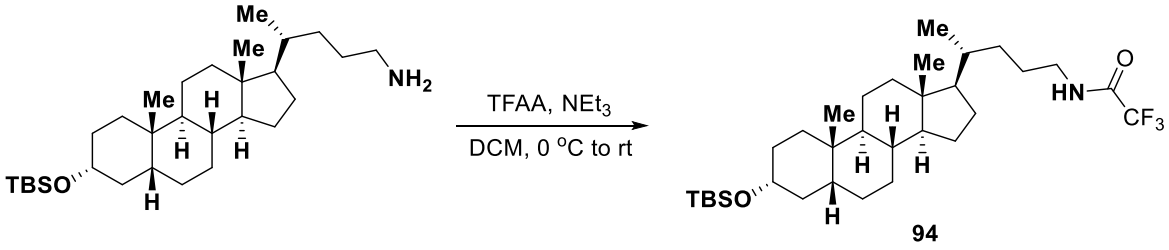

94

By General Procedure C, trifluoroacetamide **94** (304.4 mg, 50%) was synthesized from the crude amine (502.4 mg). Conditions for flash column chromatography: 10-15% Et_2O/hexane.

^{1}H NMR ($CDCl_3$, 400 MHz): 6.42 (br, 1H), 3.60-3.54 (m, 1H), 3.35-3.27 (m, 2H), 1.94-0.88 (m, 43H), 0.62 (s, 3H), 0.05 (s, 6H); ^{13}C NMR ($CDCl_3$, 100 MHz): 157.1 (q, *J*=36.9), 115.1 (q, *J*= 288.0.), 72.8, 56.4, 56.0, 42.7, 42.3, 40.4, 40.2, 40.1, 36.9, 35.8, 35.6, 35.4, 34.6, 32.8, 31.0, 28.2, 27.3, 26.4, 26.0, 25.6, 24.2, 23.4, 20.8, 18.5, 18.3, 12.0, −4.6; ^{19}F NMR ($CDCl_3$, 376 MHz): −76.0; Molecular weight $[M-H]^-$: 570.4 (expected), 570.4 (found); IR (cm^{-1}): 3299, 3103, 2935, 2916, 2883, 2861, 1724, 1700.

A.2.3 Reaction Discovery

To a mixture of the amine (0.1 mmol, 1 equiv.), alkene (0.15 mmol, 1.5 equiv.) and K_3PO_4 (0.2 mmol, 2 equiv.) in a vial was added 3 drops of deionized water (~40 mg), followed by DMF (1.0 mL). Argon was bubbled through the solution for 5 mins. $[Ir(dF\text{-}CF_3pp)_2dtbbp]PF_6$ (0.9 or 1.8 mg, 1 or 2 mol %) was added. Argon was bubbled through the solution for another 10 mins. The vial was then capped and illuminated with a Blue LED for 16h (The distance between the Blue LED and the vial is around 1.5 cm). The mixture was filtered through silica gel. The yield was determined by NMR with 1,3,5-trimethoxybenzene as the standard.

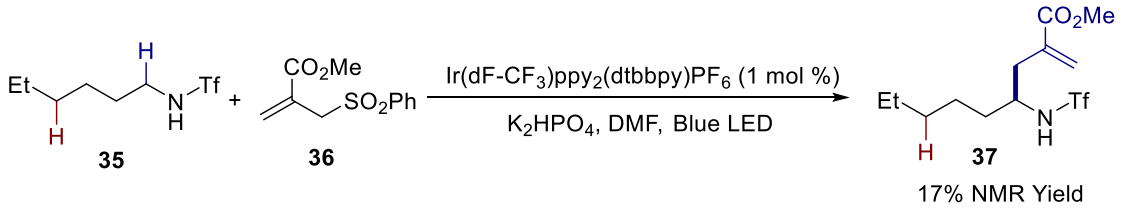

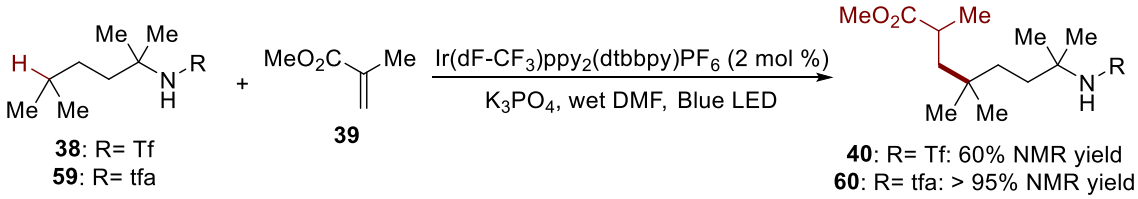

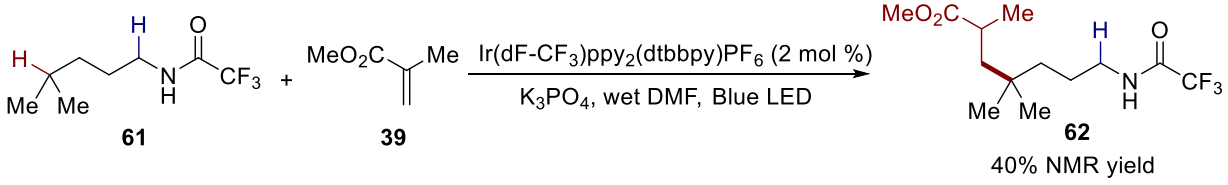

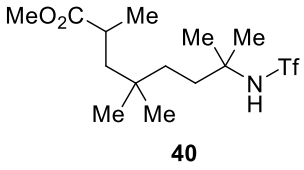

^{1}H NMR ($CDCl_3$, 400 MHz): 5.21 (br, 1H), 3.68 (s, 3H), 2.54-2.46 (m, 1H), 1.90 (dd, *J*= 14.5, 9.4), 1.68-1.58 (m, 1H), 1.52-1.46 (m, 1H), 1.40 (s, 3H), 1.37 (s, 3H), 1.25-1.18 (m, 2H), 1.16 (d, *J*= 7.1, 3H), 1.11 (dd, *J*= 14.0, 9.8), 0.86 (s, 3H), 0.85 (s, 3H); ^{13}C NMR ($CDCl_3$, 100 MHz): 178.8, 119.3 (q, *J*= 321.2), 60.3, 51.9, 44.5, 37.8, 35.5, 34.9, 32.8, 28.9, 27.5, 27.2, 26.6, 20.4; ^{19}F NMR ($CDCl_3$, 376 MHz): −77.8; Molecular weight [M−H]$^-$: 360.2 (expected), 360.1 (found); IR (cm^{-1}): 3232, 2956, 2876, 1738, 1715, 1460, 1435, 1391, 1362, 1275, 1227, 1185, 1143.

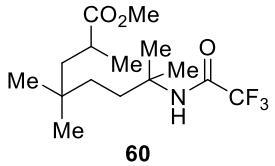

60

^{1}H NMR ($CDCl_3$, 400 MHz): 6.05 (br, 1H), 3.65 (s, 3H), 2.52-2.45 (m, 1H), 1.85 (dd, *J*= 14.1, 9.4, 1H), 1.68-1.64 (m, 2H), 1.37 (s, 3H), 1.36 (s,3H), 1.18-1.10 (m, 6H), 0.83 (s, 3H), 0.82 (s, 3H); ^{13}C NMR ($CDCl_3$, 100 MHz): ; 178.3, 156.0 (q, *J*= 35.9), 115.6 (q, *J*= 289.4), 55.2, 51.6, 45.4, 35.6, 35.6, 34.1, 32.8, 27.0, 26.7, 26.5, 26.1, 20.4; ^{19}F NMR ($CDCl_3$, 376 MHz): −76.1; Molecular weight [M−H]$^-$: 324.2 (expected), 324.2 (found); IR (cm^{-1}): 3332 (br), 3086, 2955, 2875, 1712.

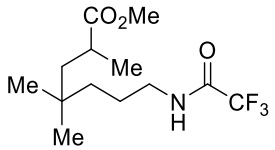

62

^{1}H NMR ($CDCl_3$, 400 MHz): 6.49 (br, 1H), 3.63 (s, 3H), 3.34-3.24 (m,2H), 2.50-2.43 (m,1H), 1.85 (dd, *J*= 14.4, 9.4), 1.18-1.09 (m, 6H), 0.82 (s, 3H), 0.81 (s, 3H); ^{13}C NMR ($CDCl_3$, 100 MHz):178.3, 157.2 (q, *J*= 36.6), 115.9 (q, *J*= 287.9), 51.7, 45.2, 40.6, 38.8, 35.6, 33.0, 27.1, 26.9, 23.6, 20.4; ^{19}F

NMR ($CDCl_3$, 376 MHz): –76.0; Molecular weight $[M–H]^-$: 296.2 (expected), 296.2 (found); IR (cm^{-1}): 3317 (br), 3099, 2955, 2876, 1706.

A.2.4 Optimization of Reaction Conditions

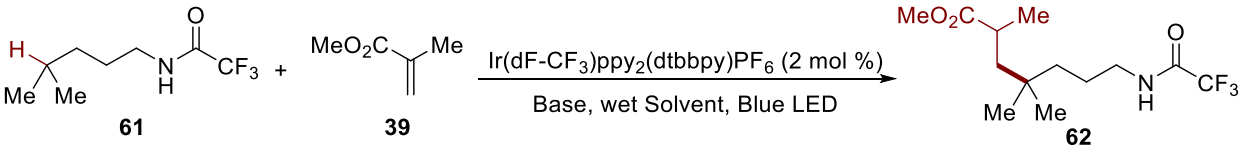

61 **39** **62**

NMR Yield (Isolated Yield)

Solvent ***(K_3PO_4, 0.1 M)***	***Base*** ***($PhCF_3$, 0.1 M)***	***Concentration*** ***($PhCF_3$, K_3PO_4)***
DMF: 40%	K_2CO_3: 0%	**0.4 M: >90% (75%)**
DMSO: 40%	KH_2PO_4: 0%	0.2 M: >90% (72%)
Acetone: 48%	K_2HPO_4: 0%	0.13 M: 78%
MeCN: 65%	KOAc: 0%	0.10 M: 71%
$CHCl_3$: 56%	Na_3PO_4: 65%	0.05 M: 22%
DCE: 54%	**K_3PO_4: 71%**	0.03 M: 0%
Dioxane, THF, DME: messy	NaOH: 0%	
PhMe, PhH: 0%		
$PhCF_3$: 71%		

To a mixture of the amine (0.1 mmol, 1 equiv.), alkene (0.15 mmol, 1.5 equiv.) and Base (0.2 mmol, 2 equiv.) in a vial was added 3 drops of deionized water (~40 mg), followed by the solvent. Argon was bubbled through the solution for 5 mins. $[Ir(dF\text{-}CF_3ppy)_2dtbbp]PF_6$ (0.9 mg, 2 mol %) was added. Argon was bubbled through the solution for another 10 mins. The vial was then capped and illuminated with a Blue LED for 16h (The distance between the Blue LED and the vial is around 1.5 cm). The mixture was filtered through silica gel. The yield was determined by NMR with 1,3,5-trimethoxybenzene as the standard. Yields in brackets refer to isolated yield after column chromatography.

A.2.5 Alkene and Amide Scopes

General Procedure D: Photocatalytic C-C Bond Formation

To a mixture of the amine (0.1 mmol, 1 equiv.), alkene and finely ground K_3PO_4 (0.2 mmol, 2 equiv.) in a vial was added 3 drops of deionized water (~40 mg), followed by the solvent. Argon was bubbled through the solution for 5 mins. $[Ir(dF\text{-}CF_3pp)_2dtbbp]PF_6$ (2-5 mol %) was added. Argon was bubbled through the solution for another 10 mins. The vial was then capped and illuminated with a Blue LED for 16-20 h (The distance between the Blue LED and the vial is around 1.5 cm). The mixture was filtered through silica gel. The product was purified by column chromatography.

Alkene Scope

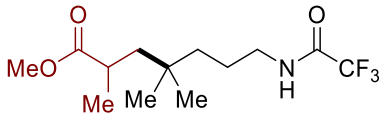

62

By General Procedure D (1.5 equiv. of alkene, 2 mol % Ir photocatalyst, 0.25 mL $PhCF_3$), methyl 2,4,4-trimethyl-7-(2,2,2-trifluoroacetamido)heptanoate **62** (21.5 mg, 75%) was obtained from 2,2,2-trifluoro-*N*-(4-methylpentyl)acetamide (18.9 mg). Flash column chromatography conditions: 15-35% Et_2O/hexane.

^1H NMR ($CDCl_3$, 400 MHz): 6.49 (br, 1H), 3.63 (s, 3H), 3.34-3.24 (m,2H), 2.50-2.43 (m,1H), 1.85 (dd, *J*= 14.4, 9.4), 1.18-1.09 (m, 6H), 0.82 (s, 3H), 0.81 (s, 3H); ^{13}C NMR ($CDCl_3$, 100 MHz):178.3, 157.2 (q, *J*= 36.6), 115.9 (q, *J*= 287.9), 51.7, 45.2, 40.6, 38.8, 35.6, 33.0, 27.1, 26.9, 23.6, 20.4; ^{19}F

NMR ($CDCl_3$, 376 MHz): –76.0; Molecular weight $[M–H]^–$: 296.2 (expected), 296.2 (found); IR (cm^{-1}): 3317 (br), 3099, 2955, 2876, 1706.

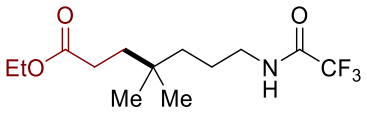

66

By General Procedure D (1.5 equiv. of alkene, 2 mol % Ir photocatalyst, 0.25 mL $PhCF_3$), ethyl 4,4-dimethyl-7-(2,2,2-trifluoroacetamido)heptanoate **66** (19.9 mg, 68%) was obtained from 2,2,2-trifluoro-*N*-(4-methylpentyl)acetamide (19.4 mg). Flash column chromatography conditions: 5-50% Et_2O/hexane.

^1H NMR ($CDCl_3$, 400 MHz): 6.34 (br, 1H), 4.12 (q, *J*= 7.2, 2H), 3.34 (q, *J*= 6.8, 2H), 2.26-2.22 (m, 2H), 1.57-1.53 (m,4H), 1.25 (t, *J*= 7.2, 3H), 1.23-1.19 (m, 2H), 0.87 (s, 6H); ^{13}C NMR ($CDCl_3$, 100 MHz): 174.2, 157.2 (q, *J*= 37.4), 115.9 (q, *J*= 287.7), 60.4, 40.6, 38.5, 36.1, 32.2, 29.5, 26.6, 23.8, 14.2; ^{19}F NMR ($CDCl_3$, 376 MHz): –76.0; Molecular weight $[M–H]^–$: 296.2 (expected), 296.2 (found); IR (cm^{-1}): 3327 (br), 3104, 2959, 2873, 1706.

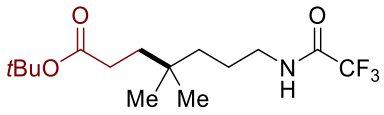

67

By General Procedure D (1.5 equiv. of alkene, 2 mol % Ir photocatalyst, 0.25 mL $PhCF_3$), *tert*-butyl 4,4-dimethyl-7-(2,2,2-trifluoroacetamido)heptanoate **67** (21.4 mg, 67%) was obtained from 2,2,2-trifluoro-*N*-(4-methylpentyl)acetamide (19.3 mg). Flash column chromatography conditions: 20-30% Et_2O/hexane.

^{1}H NMR ($CDCl_3$, 400 MHz): 6.35 (br, 1H), 3.33 (q, *J*= 6.8, 2H), 2.27-2.13 (m, 2H), 1.58-1.48 (m,4H), 1.44 (s, 9H), 1.22-1.18 (m, 2H), 0.86 (s, 6H); ^{13}C NMR ($CDCl_3$, 100 MHz): 173.6, 157.1 (q, *J*= 36.6), 115.8 (q, *J*= 288.0), 80.2, 40.6, 38.6, 36.2, 32.3, 30.7, 28.1, 26.6, 23.8; ^{19}F NMR ($CDCl_3$, 376 MHz): –76.1; Molecular weight $[M-H]^-$: 324.2 (expected), 324.2 (found); IR (cm^{-1}): 3319 (br), 3105, 2960, 2936, 2872, 1727, 1704, 1648, 1557, 1504, 1472, 1457.

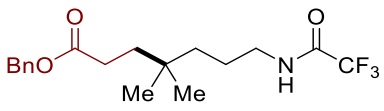

68

By General Procedure D (1.5 equiv. of alkene, 2 mol % Ir photocatalyst, 0.25 mL $PhCF_3$), benzyl 4,4-dimethyl-7-(2,2,2-trifluoroacetamido)heptanoate **68** (21.4 mg, 67%) was obtained from 2,2,2-trifluoro-*N*-(4-methylpentyl)acetamide (19.3 mg). Flash column chromatography conditions: 20-30% Et_2O/hexane.

^{1}H NMR ($CDCl_3$, 400 MHz):7.39-7.32 (m, 5H), 6.36 (br, 1H), 5.11 (s, 2H), 3.31 (q, *J*= 6.8, 2H), 2.32-2.28 (m, 2H), 1.59-1.49 (m, 2H), 1.22-1.19 (m, 2H), 0.86 (s, 6H); ^{13}C NMR ($CDCl_3$, 100 MHz): 174.0, 157.1 (q, *J*= 36.6), 135.9, 128.6, 128.3, 128.3, 115.8 (q, *J*= 287.7), 66.3, 40.6, 28.5, 36.1, 32.3, 29.5, 26.6, 23.8; ^{19}F NMR ($CDCl_3$, 376 MHz): –75.9; Molecular weight $[M-H]^-$: 358.2 (expected), 358.1 (found); IR (cm^{-1}): 3321 (br), 3091, 3035, 2957, 2871, 1704.

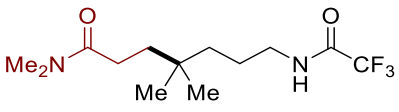

69

By General Procedure D (1.5 equiv. of alkene, 2 mol % Ir photocatalyst, 0.25 mL $PhCF_3$), *N*-(7-((dimethylamino)oxy)-4,4-dimethyl-7-oxoheptyl)-2,2,2-trifluoroacetamide **69** (14.8 mg,

52%) was obtained from 2,2,2-trifluoro-*N*-(4-methylpentyl)acetamide (19.0 mg). Flash column chromatography conditions: 50% Et_2O/hexane – Pure EtOAc.

^{1}H NMR ($CDCl_3$, 400 MHz): 6.79 (br, 1H), 3.33 (q, *J*= 6.6 Hz, 2H), 3.01 (s, 3H), 2.94 (s, 3H), 2.27 (m, 2H), 1.61-1.52 (m, 4H), 1.25-1.20 (m, 2H), 0.88 (s, 6H); ^{13}C NMR ($CDCl_3$, 100 MHz): 173.6, 157.3 (q, *J*= 33.6), 115.9 (q, *J*= 288.2), 40.6, 38.2, 36.0, 32.4, 28.2, 27.0, 23.5; ^{19}F NMR ($CDCl_3$, 376 MHz): 75.8; Molecular weight $[M-H]^-$: 311.2 (expected), 311.2 (found); IR (cm^{-1}): 3254 (br), 3086, 2955, 2871, 1718, 1634.

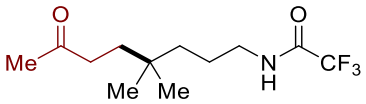

70

By General Procedure D (1.2 equiv. of alkene, 5 mol % Ir photocatalyst, 0.5 mL $PhCF_3$), *N*-(4,4-dimethyl-7-oxooctyl)-2,2,2-trifluoroacetamide **70** (16.3 mg, 63%) was obtained from 2,2,2-trifluoro-*N*-(4-methylpentyl)acetamide (19.1 mg). Flash column chromatography conditions: 40-60% Et_2O/hexane.

^{1}H NMR ($CDCl_3$, 400 MHz): 6.44 (br, 1H), 3.33 (q, *J*= 6.6, 2H), 2.38-2.34 (m, 2H), 2.15 (s, 3H), 1.58-1.45 (m, 4H), 1.20-1.16 (m, 2H), 0.85 (s, 6H); ^{13}C NMR ($CDCl_3$, 100 MHz): 209.3, 157.2 (q, *J*= 36.6), 115.9 (q, *J*= 288.1), 40.6, 38.7, 28.6, 34.8, 32.1, 30.0, 26.7, 23.8; ^{19}F NMR ($CDCl_3$, 376 MHz): –76.0; Molecular weight $[M-H]^-$: 266.1 (expected), 266.2 (found); IR (cm^{-1}): 3313 (br), 3097, 2958, 2872, 1706.

When the reaction was carried out with 1.5 equiv. of alkene, 2 mol % Ir photocatalyst,0.25 mL $PhCF_3$, the desired product was only isolated in low yield (27%). A significant of aza-Michael

addition product (44%) was also obtained. The aza-Michael addition product exists as two rotamers (~1:2), as observed in NMR. Some of the peaks of the two rotamers cannot be distinguished in ^{13}C NMR.

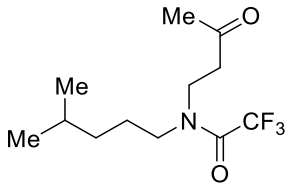

106

^{1}H NMR ($CDCl_3$, 400 MHz): 3.67 (t, *J*= 7.6, 1H, minor rotamer), 3.59 (t, *J*= 6.9, 2H, major rotamer), 3.36 (t, *J*= 8.0, 2H, major rotamer), 3.30 (t, *J*= 7.9, 1H, minor rotamer), 2.82 (t, *J*= 6.9, 2H, major rotamer), 2.77 (t, *J*= 7.5, 1H, minor rotamer), 2.19 (s, 1.5 H, minor rotamer), 2.17 (s, 3H, major rotamer), 1.64-1.50 (m, 4.5H, both rotamers), 1.19-1.13 (m, 3H, both rotamers), 0.90-0.87 (m, 9H, both rotamers); ^{13}C NMR ($CDCl_3$, 100 MHz): 206.5 (major rotamer), 205.4 (minor rotamer), 156.9 (q, *J*= 35.9), 116.4 (q, *J*= 287.4), 49.0 (q, *J*= 3.0, major rotamer)), 47.6, 42.7, 42.6, 41.8 (q, *J*=3.3, minor rotamer), 40.8, 35.7, 35.5, 30.2, 30.2, 27.8, 27.6, 26,7, 24.7, 22.4, 22.4 ; ^{19}F NMR ($CDCl_3$, 376 MHz): −69.21 (major rotamer), −60.29 (minor rotamer); IR (cm^{-1}): 2955, 2933, 2872, 1718, 1685, 1464, 1436; Molecular weight $[M+H]^+$: 268.2 (expected); 268.2 (found).

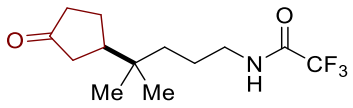

71

By General Procedure D (3 equiv. of alkene, 4 mol % Ir photocatalyst, 0.25 mL $PhCF_3$), 2,2,2-trifluoro-*N*-(4-methyl-4-(3-oxocyclopentyl)pentyl)acetamide **71** (13.5 mg, 51%) was

obtained from 2,2,2-trifluoro-*N*-(4-methylpentyl)acetamide (18.7 mg). Flash column chromatography conditions: 30-70% Et_2O/hexane.

^{1}H NMR ($CDCl_3$, 400 MHz): 6.30 (br, 1H), 3.33 (q, *J*= 6.9, 2H), 2.32 (dd, *J*= 18.4, 8.2, 1H), 2.18-1.91 (m, 5H), 1.63-1.52 (m, 3H), 1.26-1.22 (m, 2H), 0.87 (s, 3H), 0.85 (s, 3H); ^{13}C NMR ($CDCl_3$, 100 MHz): 219.1, 157.2 (q, *J*= 36.6), 115.8 (q, *J*= 287.9), 46.6, 40.1, 40.0, 39.1, 37.8, 34.0, 24.0, 23.9, 23.7, 23.6; ^{19}F NMR ($CDCl_3$, 376 MHz): –76.0; Molecular weight $[M-H]^-$: 278.1 (expected), 278.1 (found); IR (cm^{-1}): 3313 (br), 3097, 2961, 2874, 1706.

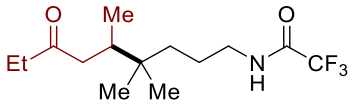

72

By General Procedure D (3 equiv. of alkene, 4 mol % Ir photocatalyst, 0.25 mL $PhCF_3$), 2,2,2-trifluoro-*N*-(4,4,5-trimethyl-7-oxononyl)acetamide **72** (17.4 mg, 59%) was obtained from 2,2,2-trifluoro-*N*-(4-methylpentyl)acetamide (19.7 mg). Flash column chromatography conditions: 30-45% Et_2O/hexane.

^{1}H NMR ($CDCl_3$, 400 MHz): 6.34 (br, 1H), 3.33 (q, *J*= 6.8, 2H), 2.49-2.32 (m, 3H), 2.14 (dd, *J*= 16.0, 10.2, 1H), 1.97-1,91 (m, 1H), 1.61-1.51 (m, 2H), 1.30-1.17 (m, 2H), 1.05 (t, *J*= 7.3, 3H), 0.82 (s, 6H), 0.79 (d, *J*= 6.6, 3H); ^{13}C NMR ($CDCl_3$, 100 MHz): 212.0, 157.2 (q, *J*= 33.8), 115.8 (q, *J*= 287.9),44.9, 40.7, 37.1, 36.7, 36.1, 34.7, 24.2, 23.5, 14.9, 7.8; ^{19}F NMR ($CDCl_3$, 376 MHz): –76.0; Molecular weight $[M-H]^-$: 294.2 (expected), 294.2 (found); IR (cm^{-1}): 3326 (br), 3104, 2965, 2942, 2879, 1703.

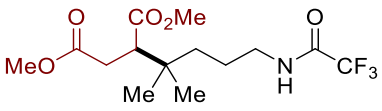

73

By General Procedure D (1.5 equiv. of alkene, 2 mol % Ir photocatalyst, 0.25 mL $PhCF_3$), methyl 3-acetoxy-4,4-dimethyl-7-(2,2,2-trifluoroacetamido)heptanoate **73** (13.7 mg, 40%) was obtained from 2,2,2-trifluoro-*N*-(4-methylpentyl)acetamide (19.8 mg). Flash column chromatography conditions: 45-60% Et_2O/hexane.

^1H NMR ($CDCl_3$, 400 MHz): 6.53 (br, 1H), 3.69 (s, 3H), 3.66 (s, 3H), 3.40-3.27 (m, 2H), 2.84-2.74 (m, 2H), 2.43 (m, 1H), 1.74-1.66 (m, 1H), 1.69-1.54 (m, 1H), 1.36-1.21 (m, 2H), 0.94 (s, 3H), 0.92 (s, 3H); ^{13}C NMR ($CDCl_3$, 100 MHz): 174.3, 172.9, 157.3 (q, *J*= 36.9), 115.8 (q, *J*= 287.9), 51.8, 51.6, 49.1, 40.4, 37.8, 34.9, 32.1, 25.1, 25.0, 23.2; ^{19}F NMR ($CDCl_3$, 376 MHz): –75.9; Molecular weight $[M-H]^-$: 340.1 (expected), 340.2 (found); IR (cm^{-1}): 3335 (br), 3097, 2954, 2915, 2848, 1708.

Amide Scope

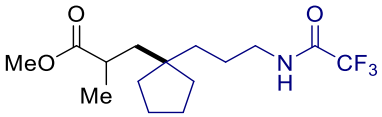

74

By General Procedure D (1.5 equiv. of alkene, 2 mol % Ir photocatalyst, 0.25 mL $PhCF_3$), methyl 2-methyl-3-(1-(3-(2,2,2-trifluoroacetamido)propyl)cyclopentyl)propanoate **74** (19.1 mg, 61%) was obtained from *N*-(3-cyclopentylpropyl)-2,2,2-trifluoroacetamide (21.7 mg). Flash column chromatography conditions: 30-35% Et_2O/hexane.

^{1}H NMR ($CDCl_3$, 400 MHz): 6.58 (br, 1H), 3.66 (s, 3H), 3.39-3.23 (m, 2H), 2.50-2.42 (m, 1H), 1.93 (dd, *J*= 14.5, 9.0, 1H), 1.58-1.23 (m, 13H), 1.16 (d, *J*= 7.0, 3H); ^{13}C NMR ($CDCl_3$, 100 MHz): 178.4, 157.3 (q, *J*= 36.6), 115.9 (q, *J*= 287.6), 51.7, 45.0, 41.7, 40.6, 37.7, 37.6, 36.3, 34.7, 24.1, 24.0, 23.9, 20.2; ^{19}F NMR ($CDCl_3$, 376 MHz): –75.8; Molecular weight $[M-H]^-$: 322.2 (expected), 322.2 (found); IR (cm^{-1}): 3326 (br), 3105, 2951, 2873, 1705.

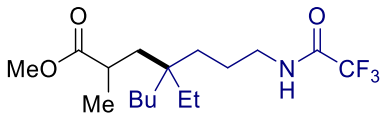

75

By General Procedure D (1.5 equiv. of alkene, 2 mol % Ir photocatalyst, 0.25 mL $PhCF_3$methyl 4-ethyl-2-methyl-4-(3-(2,2,2-trifluoroacetamido)propyl)octanoate **75** (28.3 mg, 81%) was obtained from *N*-(4-ethyloctyl)-2,2,2-trifluoroacetamidetrifluoroacetamide (25.2 mg). Flash column chromatography conditions: 15-30% Et_2O/hexane.

^{1}H NMR ($CDCl_3$, 400 MHz): 6.56 (br, 1H), 3.65 (s, 3H), 3.35-3.21 (m, 2H), 2.48-2.41 (m,1H), 1.82 (dd, *J*= 14.9, 9.4, 1H), 1.53-1.37 (m, 2H), 1.27-1.08 (m, 13H), 0.89 (t, *J*= 7.3, 3H), 0.72 (two overlapped triplet from each diastereomer, *J*= 7.4, 3H);); ^{13}C NMR ($CDCl_3$, 100 MHz): 178.5, 157.2 (q, *J*= 36.6), 115.9 (q, *J*= 287.9), 51.7, 40.7, 39.8, 39.7, 37.7, 35.5, 34.9, 34.9, 33.1, 32.9, 28.3, 28.3, 25.1, 25.0, 23.5, 22.5, 22.4, 20.4, 14.1, 7.4, 7.4; ^{19}F NMR ($CDCl_3$, 376 MHz): –75.9; Molecular weight $[M-H]^-$: 352.2 (expected), 352.2 (found); IR (cm^{-1}): 3322 (br), 3102, 2957, 2932, 2873, 1704.

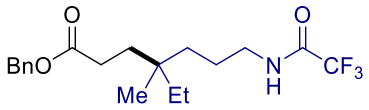

76

By General Procedure D (1.5 equiv. of alkene, 2 mol % Ir photocatalyst, 0.25 mL $PhCF_3$), benzyl 4-ethyl-4-methyl-7-(2,2,2-trifluoroacetamido)heptanoate **76** (25.6 mg, 68%) was obtained from enantiomerically enriched (*S*)-2,2,2-trifluoro-*N*-(4-methylhexyl)acetamide (21.3 mg). Flash column chromatography conditions: 25-35% Et_2O/hexane.

^{1}H NMR ($CDCl_3$, 400 MHz): 7.39-7.31 (m, 5H), 6.31 (br, 1H), 5.11 (s, 2H), 3.31 (q, *J*=6.8, 2H), 2.29-2.24 (m, 2H), 1.58-1.46 (m, 4H), 1.23-1.16 (m,4H), 0.81-0.76 (m, 6H); ^{13}C NMR ($CDCl_3$, 100 MHz): 174.1, 157.1, 135.9, 128.6, 128.2, 115.8, 66.3, 40.6, 35.4, 34.6, 33.3, 31.0, 29.1, 23.9, 23.3, 7.8; ^{19}F NMR ($CDCl_3$, 376 MHz): −75.6; Molecular weight $[M-H]^-$: 372.2 (expected), 372.1 (found); IR (cm^{-1}): 3335 (br), 3091, 3035, 2961, 2877, 1704.

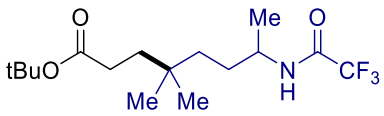

77

By General Procedure D (1.5 equiv. of alkene, 2 mol % Ir photocatalyst, 0.25 mL DMF), *tert*-butyl 4,4-dimethyl-7-(2,2,2-trifluoroacetamido)octanoate (25.6 mg, 77%) **77** was obtained from 2,2,2-trifluoro-*N*-(5-methylhexan-2-yl)acetamide (20.8 mg). Flash column chromatography conditions: 13-25% Et_2O/hexane.

^{1}H NMR ($CDCl_3$, 400 MHz): 6.03 (br, 1H), 3.93 (quintet, *J*= 7.0, 1H), 2.14-2.10 (m, 2H), 1.49-1.42 (m,12H), 1.20-1.15 (m, 6H), 0.82 (s, 6H); ^{13}C NMR ($CDCl_3$, 100 MHz): 173.6, 156.5 (q, *J*= 36.6), 115.9 (q, *J*= 288.2), 80.2, 47.1, 37.6, 36.1, 32.2, 30.8, 30.7, 28.1, 26.7, 20.5; ^{19}F NMR ($CDCl_3$, 376

MHz): –75.8; Molecular weight [M–H]$^-$: 338.2 (expected), 338.2 (found); IR (cm^{-1}): 3311 (br), 3095, 2960, 2935, 2871, 1726, 1699, 1554, 1456, 1391, 1367, 1207, 1157.

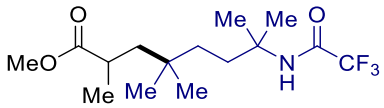

60

By General Procedure D (1.5 equiv. of alkene, 2 mol % Ir photocatalyst, 0.25 mL DMF), methyl 2,4,4,7-tetramethyl-7-(2,2,2-trifluoroacetamido)octanoate **60** (26.2 mg, 83%) was obtained from *N*-(2,5-dimethylhexan-2-yl)-2,2,2-trifluoroacetamide (21.8 mg). Flash column chromatography conditions: 10-25% Et_2O/hexane.

^{1}H NMR ($CDCl_3$, 400 MHz): 6.05 (br, 1H), 3.65 (s, 3H), 2.52-2.45 (m, 1H), 1.85 (dd, *J*= 14.1, 9.4, 1H), 1.68-1.64 (m, 2H), 1.37 (s, 3H), 1.36 (s,3H), 1.18-1.10 (m, 6H), 0.83 (s, 3H), 0.82 (s, 3H); ^{13}C NMR ($CDCl_3$, 100 MHz): ; 178.3, 156.0 (q, *J*= 35.9), 115.6 (q, *J*= 289.4), 55.2, 51.6, 45.4, 35.6, 35.6, 34.1, 32.8, 27.0, 26.7, 26.5, 26.1, 20.4; ^{19}F NMR ($CDCl_3$, 376 MHz): –76.1; Molecular weight [M–H]$^-$: 324.2 (expected), 324.2 (found); IR (cm^{-1}): 3332 (br), 3086, 2955, 2875, 1712.

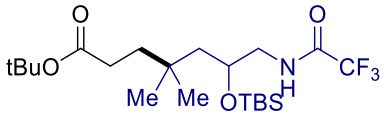

78

By General Procedure D (3 equiv. of alkene, 4 mol % Ir photocatalyst, 0.25 mL 1:1 $PhCF_3$/*t*-amyl alcohol), *tert*-butyl 6-((*tert*-butyldimethylsilyl)oxy)-4,4-dimethyl-7-(2,2,2-trifluoro-acetamido)-heptanoate **78** (25.5 mg, 60%) was obtained from *N*-(2-((*tert*-butyldimethylsilyl)oxy)-4-methylpentyl)-2,2,2-trifluoroacetamide (30.6 mg). Flash column chromatography conditions: 5-15% Et_2O/hexane.

^{1}H NMR ($CDCl_3$, 400 MHz): 6.59 (br, 1H), 3.97 (quintet, *J*= 5.0, 1H), 3.50 (dt, *J*= 13.3, 4.6, 1H), 3.32-3.26 (m, 1H), 2.23-2..11 (m, 2H), 1.59-1.52 (m, 2H), 1.50-1.36 (m, 11H), 0.92-0.89 (m, 15H), 0.11 (s, 3H), 0.09 (s, 3H); ^{13}C NMR ($CDCl_3$, 100 MHz): 173.3, 157.2 (q, *J*= 36.6), 115.6 (q, *J*= 287.6), 80.2, 67.6, 47.2, 46.8, 37.6, 32.0, 30.7, 28.1, 27.2, 26.9, 25.7, 17.8, –4.2, –4.5; ^{19}F NMR ($CDCl_3$, 376 MHz): –75.9; Molecular weight $[M-H]^-$: 454.3 (expected), 454.3 (found); IR (cm^{-1}): 3323 (br), 3096, 2956, 2930, 2858, 1728, 1705.

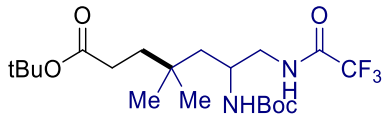

79

By General Procedure D (3 equiv. of alkene, 4 mol % Ir photocatalyst, 0.25 mL 1:1 $PhCF_3$/*t*-amyl alcohol), *tert*-butyl 6-((*tert*-butoxycarbonyl)amino)-4,4-dimethyl-7-(2,2,2-trifluoro-acetamido)heptanoate (28.7 mg, 67%) **79** was obtained from *tert*-butyl (4-methyl-1-(2,2,2-trifluoroacetamido)pentan-2-yl)carbamate (30.2 mg). Flash column chromatography conditions: 30-50% Et_2O/hexane.

^{1}H NMR ($CDCl_3$, 400 MHz): 7.61 (br, 1H), 4.61 (d, *J*= 8.2, 1H), 3.95-3.94 (m, 1H), 3.40-3.22 (m, 2H), 2.17 (t, *J*= 8.3, 2H), 1.63-1.50 (m, 2H), 1.44 (s, 9H), 1.42 (s, 9H), 1.33 (d, *J*= 5.8, 2H), 0.91 (s, 6H); ^{13}C NMR ($CDCl_3$, 100 MHz): 173.3, 157.7 (q, *J*= 40), 156.9, 115.8 (q, *J*= 286), 80.5, 80.3, 47.9, 46.6, 44.1, 36.9, 32.7, 30.6, 28.2, 26.8; ^{19}F NMR ($CDCl_3$, 376 MHz): –76.1; Molecular weight $[M+H]^+$: 285.1 (expected for MW-2BOC+2H), 285.1 (found); IR (cm^{-1}): 3676, 3330 (br), 3109, 2977, 2934, 1707, 1638.

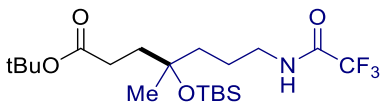

80

By General Procedure D (3 equiv. of alkene, 5 mol % Ir photocatalyst, 0.25 mL $PhCF_3$), *tert*-butyl 4-((*tert*-butyldimethylsilyl)oxy)-4-methyl-7-(2,2,2-trifluoroacetamido)heptanoate **80** (33.4 mg, 76%) was obtained from *N*-(4-((*tert*-butyldimethylsilyl)oxy)pentyl)-2,2,2-trifluoroacetamide (31.0 mg). Flash column chromatography conditions: 7-20% Et_2O/hexane.

^1H NMR ($CDCl_3$, 400 MHz): 6.35 (br, 1H), 3.37-3.32 (m, 2H), 2.25 (t, *J*= 8.0, 2H), 1.74-1.70 (m,2H), 1.66-1.59 (m, 2H), 1.44-1.42 (m, 11H), 1.19 (s, 3H), 0.86 (s, 9H), 0.08 (s, 3H), 0.07 (s, 3H); ^{13}C NMR ($CDCl_3$, 100 MHz): 173.4, 157.2 (q, *J*= 36.6), 115.8 (q, *J*= 287.9), 80.2, 74.5, 40.3, 39.1, 36.9, 30.6, 28.1, 27.3, 25.8, 23.8, 18.2, 2.01; ^{19}F NMR ($CDCl_3$, 376 MHz): −76.0; Molecular Weight $[M-H]^-$: 440.2 (expected), 440.3 (found); IR (cm^{-1}): 3330 (br), 3096, 2955, 2930, 2886, 2857, 1727, 1703, 1555, 1473, 1463, 1392, 1367, 1311, 1253, 1207, 1152, 1122, 1039.

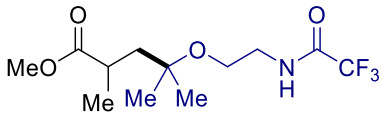

81

By General Procedure D (3.0 equiv. of alkene, 5 mol% Ir photocatalst, 0.25 mL $PhCF_3$), methyl 2,4-dimethyl-4-(2-(2,2,2-trifluoroacetamido)ethoxy)-pentanoate **81** (25.3 mg, 79%) was obtained from 2,2,2-trifluoro-*N*-(2-isopropoxyethyl)acetamide (19.5 mg). First Chromatography: 25-35% Et_2O/hexane, Si gel; Second chromatography: 25-40% Et_2O/hexane, florisil (200 mesh, fine powder, activated magnesium silicate).

^{1}H NMR ($CDCl_3$, 400 MHz): 7.30 (br, 1H), 3.64-3.58 (m, 4H), 3.44-3.34 (m, 2H), 3.30-3.24 (m, 1H), 2.68-2.59 (m, 1H), 2.12 (dd, *J*= 14.1, 11.0, 1H), 1.41 (dd, *J*= 14.0, 2.3, 1H), 1.17-1.14 (m, 9H); ^{13}C NMR ($CDCl_3$, 100 MHz): 178.6, 156.9 (q, *J*= 36.9), 116.0 (q, *J*= 287.6), 74.6, 59.5, 51.5, 46.5, 40.1, 36.0, 26.0, 23.5, 19.2; ^{19}F NMR ($CDCl_3$, 376 MHz): –76.0; Molecular weight $[M-H]^-$: 298.1 (expected), 298.1 (found); IR (cm^{-1}): 3321 (br), 3094, 2975, 2953, 2937, 2879, 1713, 1552, 1462, 1437, 1378, 1367, 1276, 1206, 1148, 1092.

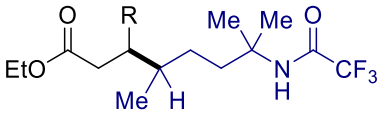

82a

By General Procedure D (1.5 equiv. of alkene, 2 mol % Ir photocatalyst, 0.25 mL DMF), *tert*-butyl 4,7-dimethyl-7-(2,2,2-trifluoroacetamido)octanoate **82a** (12.5 mg, 38%) was obtained from 2,2,2-trifluoro-*N*-(2-methylhexan-2-yl)acetamide (20.4 mg). Flash column chromatography conditions: 10-20% Et_2O/hexane.

^{1}H NMR ($CDCl_3$, 400 MHz): 5.91 (br, 1H), 2.28-2.13 (m, 2H), 1.81-1.60 (m, 3H), 1.44 (s, 9H), 1.41-1.39 (m, 1H), 1.37 (s, 6H), 1.31-1.21 (m,2H), 1.13-1.04 (m,1H), 0.88 (d, *J*=6.3); ^{13}C NMR ($CDCl_3$, 100 MHz): 173.2, 156.0 (q, *J*= 35.9), 115.6 (q, *J*= 289.4), 80.1, 55.3, 37.1, 33.2, 32.6, 31.8, 30.7, 28.1, 26.3, 19.2 ; ^{19}F NMR ($CDCl_3$, 376 MHz): –76.2; Molecular weight $[M-H]^-$: 338.2 (expected), 338.1 (found); IR (cm^{-1}): 3436, 3314 (br), 3084, 2975, 2931, 2872, 1706.

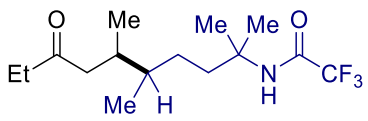

82b

By General Procedure D (3.0 equiv. of alkene, 2 mol % Ir photocatalyst, 0.25 DMF), 2,2,2-trifluoro-N-(2,5,6-trimethyl-8-oxodecan-2-yl)acetamide **82b** (15.8 mg, 53%) was obtained as a 1:1 inseperable mixture of diastereomers from 2,2,2-trifluoro-*N*-(2-methylhexan-2-yl)acetamide (20.4 mg). Flash column chromatography conditions: 15-25% Et_2O/hexane.

^1H NMR ($CDCl_3$, 400 MHz): 6.01 (br, 1H), 5.94 (br, 1H), 2.44-2.32 (m, 6H), 2.27-2.04 (m, 5H), 1.80-1.63 (m, 5H), 1.37 (s, 12H), 1.35-1.20 (m, 4H), 1.04 (t, *J*= 7.5, 6H), 0.85-0.82 (m, 6H), 0.80-0.76 (m, 6H); ^{13}C NMR ($CDCl_3$, 100 MHz): 211.9, 211.6, 156.03 (q, *J*= 35.9), 155.98 (q, *J*= 35.8), 115.6 (q, *J*= 289.4), 55.4, 47.7, 45.7, 37.8, 37.71, 37.66, 37.3, 36.53, 36.51, 33.2, 32.5, 28.6, 27.5, 26.6, 26.40, 26.37, 26.3, 17.3, 16.1, 14.7, 14.4, 7.8; ^{19}F NMR ($CDCl_3$, 376 MHz): −76.13, −76.16; Molecular weight $[M-H]^-$: 308.2 (expected), 308.2 (found); IR (cm^{-1}): 3326 (br), 3086, 2968, 2938, 2878, 1707.

A.2.6 Photoredox-Catalyzed Reactions with Substrates Bearing Multiple Reactive C-H Bonds

General Procedure D: Photocatalytic C-C Bond Formation

To a mixture of the amine (0.1 mmol, 1 equiv.), alkene and finely ground K_3PO_4 (0.2 mmol, 2 equiv.) in a vial was added 3 drops of deionized water (~40 mg), followed by the solvent. Argon was bubbled through the solution for 5 mins. $[Ir(dF\text{-}CF_3pp)_2dtbbp]PF_6$ 2-5 mol %) was added. Argon was bubbled through the solution for another 10 mins. The vial was then capped and illuminated with a Blue LED for 16-20 h (The distance between the Blue LED and the vial is around

1.5 cm). The mixture was filtered through silica gel. The product was purified by column chromatography.

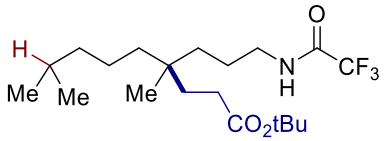

86

By General Procedure D (1.5 equiv. of alkene, 2 mol % Ir photocatalyst, 0.25 mL $PhCF_3$), *tert*-butyl 4,8-dimethyl-4-(3-(2,2,2-trifluoroacetamido)propyl)nonanoate **86** (22.9 mg, 64%) was obtained from *N*-(4,8-dimethylnonyl)-2,2,2-trifluoroacetamide (24.3 mg). Flash column chromatography conditions: 15-25% Et_2O/hexane.

^1H NMR ($CDCl_3$, 400 MHz): 6.35 (br, 1H), 3.33 (q, *J*= 6.8 Hz, 2H),2.13-2.09 (m, 2H), 1.54-1.48 (m, 5H), 1.44(s, 9H), 1.21=1.11 (m, 7H), 0.86 (d, *J*= 6.6, 6H), 0.82 (s, 3H); ^{13}C NMR ($CDCl_3$, 100 MHz): 173.7, 157.1 (q, *J*= 37.1), 115.8 (q, *J*= 287.6), 80.2, 40.6, 39.8, 39.3, 36.0, 34.6, 33.9, 30.3, 28.1, 27.9, 24.5, 23.4, 22.6, 21.1; ^{19}F NMR ($CDCl_3$, 376 MHz): –75.8; Molecular weight $[M-H]^-$: 394.3 (expected), 394.2 (found); IR (cm^{-1}): 3324 (br), 3100, 2956, 2933, 2870, 1728, 1703.

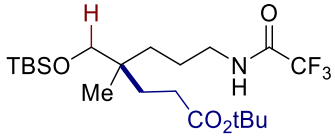

88

By General Procedure D (3.0 equiv. of alkene, 4 mol % Ir photocatalyst, 0.25 mL $PhCF_3$) *tert*-butyl 4-(((*tert*-butyldimethylsilyl)oxy)methyl)-4-methyl-7-(2,2,2-trifluoroacetamido)heptanoate (22.8 mg, 54%) **88** was obtained from *N*-(5-((*tert*-butyldimethylsilyl)oxy)-4-methylpentyl)-2,2,2-trifluoroacetamide (30.2 mg). Some starting material (7.8 mg, 26%) was also

covered. First chromatography: 10-25% Et_2O/hexane. Second chromatography: 10-45% Et_2O/hexane, florisil (200 mesh, fine powder, activated magnesium silicate)

^1H NMR ($CDCl_3$, 400 MHz): 6.29 (br, 1H), 3.34 (q, *J*= 6.5, 2H), 3.25 (s, 2H), 2.17-2.13 (m, 2H), 1.55-1.52 (m, 4H), 1.44 (s, 9H), 1.27-1.24 (m, 2H), 0.88 (s, 9H), 0.79 (s, 3H), 0.02 (s, 6H); ^{13}C NMR ($CDCl_3$, 100 MHz): 173.6, 80.1, 68.9, 40.7, 37.0, 33.4, 31.5, 30.3, 28.1, 25.8, 23.3, 21.5, 18.2, –5.6; ^{19}F NMR ($CDCl_3$, 376 MHz): –75.8; Molecular weight $[M–H]^-$: 454.3 (expected), 454.3 (found); IR (cm^{-1}): 3312 (br), 2955, 2931, 2858, 1728, 1704. The carbons in the trifluoroacetyl group cannot be observed in ^{13}C NMR even after extended NMR time but their presence is supported by ^{19}F NMR.

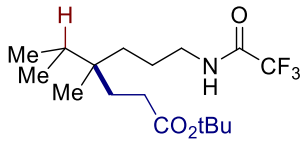

90

By General Procedure D (1.5 equiv. of alkene, 2 mol % Ir photocatalyst, 0.25 mL $PhCF_3$) *tert*-butyl 4-isopropyl-4-methyl-7-(2,2,2-trifluoroacetamido)heptanoate **90** (15.2 mg, 46%) was obtained from *N*-(4,5-dimethylhexyl)-2,2,2-trifluoroacetamide (21.1 mg). Some starting material (9.1 mg, 43%) was also covered. Flash column chromatography conditions: 20-30% Et_2O/hexane.

^1H NMR ($CDCl_3$, 400 MHz): 6.46 (br, 1H), 3.32 (q, *J*= 6.8, 2H), 2.10 (t, *J*= 8.4, 2H), 1.61-1.51 (m, 5H), 1.44 (s, 9H), 1.29-1.18 (m, 2H), 0.83-0.81 (m, 6H), 0.74 (s, 3H); ^{13}C NMR ($CDCl_3$, 100 MHz): 173.8, 157.1 (q, *J*= 36.6), 115.9 (q, *J*= 287.9), 80.2, 40.7, 36.6, 33.5, 33.3, 31.3, 30.2, 28.1, 23.2, 20.6, 17.0; ^{19}F NMR ($CDCl_3$, 376 MHz): –76.0; Molecular weight $[M–H]^-$: 352.2 (expected), 352.2 (found); IR (cm^{-1}): 3318 (br), 3096, 2966, 2878, 1727, 1703.

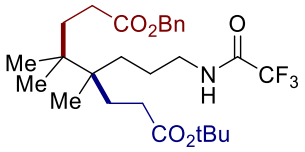

91

By General Procedure D (3.0 equiv. of alkene, 4 mol % Ir photocatalyst, 0.25 mL $PhCF_3$) 1-benzyl 8-(*tert*-butyl) 4,4,5-trimethyl-5-(3-(2,2,2-trifluoroacetamido)propyl)octanedioate **91** (19.3 mg, 39%) was obtained from *tert*-butyl 4-isopropyl-4-methyl-7-(2,2,2-trifluoroacetamido)heptanoate (33.9 mg). Flash column chromatography conditions: 25-45% Et_2O/hexane.

^1H NMR ($CDCl_3$, 400 MHz): 7.37-7.29 (m, 5H), 6.40 (br, 1H), 5.11 (s, 2H), 3.31 (q, *J*= 6.8, 2H), 2.34-2.30 (m, 2H), 2.19-2.15 (m, 2H), 1.67-1.55 (m, 6H), 1.44 (s, 9H), 1.35-1.29 (m, 2H), 0.80 (s, 6H), 0.78 (s, 3H); ^{13}C NMR ($CDCl_3$, 100 MHz): 174.3, 173.6, 157.2 (q, *J*= 36.9), 136.0, 128.6, 128.3, 128.2, 115.8 (q, *J*= 287.9), 80.4, 66.3, 40.9, 40.1, 38.9, 32.3, 32.0, 31.5, 30.0, 29.8, 28.1, 25.3, 21.7, 21.6, 19.4; ^{19}F NMR ($CDCl_3$, 376 MHz): −75.9; Molecular Weight $[M-H]^-$: 514.3 (expected), 514.3 (found); IR (cm^{-1}): 3313 (br), 3095, 3074, 2035, 2974, 2881, 1727.

A.2.7 Application to Biologically Interesting Molecules

General Procedure D: Photocatalytic C-C Bond Formation

To a mixture of the amine (0.1 mmol, 1 equiv.), alkene and finely ground K_3PO_4 (0.2 mmol, 2 equiv.) in a vial was added 3 drops of deionized water (~40 mg), followed by the solvent. Argon was bubbled through the solution for 5 mins. $[Ir(dF\text{-}CF_3ppy)_2dtbbp]PF_6$ (2-5 mol %) was added. Argon was bubbled through the solution for another 10 mins. The vial was then capped and

illuminated with a Blue LED for 16-20 h (The distance between the Blue LED and the vial is around 1.5 cm). The mixture was filtered through silica gel. The product was purified by column chromatography.

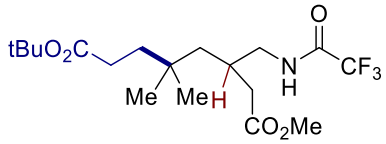

93

By General Procedure D (3.0 equiv. of alkene, 4 mol % Ir photocatalyst, 0.25 mL 1:1 $PhCF_3$/*t*-amyl alcohol) 8-(*tert*-butyl) 1-methyl 5,5-dimethyl-3-((2,2,2-trifluoroacetamido)methyl)-octanedioate **93** (27.2 mg, 70%) was obtained from methyl 5-methyl-3-((2,2,2-trifluoroacetamido)methyl)hexanoate (26.6 mg). The product was purified by flash column chromatography twice. First Chromatography: 30-40% Et_2O/hexane, Si gel; Second chromatography: 25-100% Et_2O/hexane, florisil (200 mesh, fine powder, activated magnesium silicate).

^1H NMR ($CDCl_3$, 400 MHz): 7.09 (br, 1H), 3.69 (s, 3H), 3.44-3.38 (m, 1H), 3.30-3.23 (m, 1H), 2.46 (dd, *J*= 16.0, 4.3, 1H), 2.35 (dd, *J*= 16.0, 7.8, 1H), 2.23-2.14 (m, 3H), 1.55-1.51 (m, 2H), 1.44 (s, 9H), 1.22 (d, *J*= 5.1, 2H), 0.91-0.87 (m, 6H); ^{13}C NMR ($CDCl_3$, 100 MHz): 173.7, 173.3, 157.5 (q, *J*= 37.4), 115.9 (q, *J*= 287.6), 80.3, 51.9, 45.5, 44.0, 39.5, 37.0, 33.2, 30.7, 30.6, 28.1, 26.5, 26.4; ^{19}F NMR ($CDCl_3$, 376 MHz): −76.0; Molecular weight $[M-H]^-$: 396.2 (expected), 396.2 (found); IR (cm^{-1}): 3327 (br), 309, 2956, 2933, 2874, 2853, 1707.

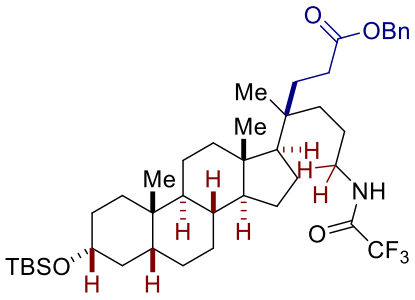

95

By General Procedure D (1.5 equiv. of alkene, 6 mol % Ir photocatalyst, 0.30 mL 1:1 $PhCF_3$/*t*-amyl alcohol) benzyl 4-((3*R*,5*R*,8*R*,9*S*,10*S*,13*S*,14*S*,17*R*)-3-((*tert*-butyldimethylsilyl)oxy)-10,13-dimethylhexadecahydro-1H-cyclopenta[*a*]phenanthren-17-yl)-4-methyl-7-(2,2,2-trifluoro-acetamido)heptanoate **95** (30.9 mg, 44%) was obtained as a pair of diastereomeric mixture (~2:1) from *N*-((*R*)-4-((3*R*,5*R*,8*R*,9*S*,10*S*,13*R*,14*S*,17*R*)-3-((*tert*-butyldimethylsilyl)oxy)-10,13-dimethyl-hexadecahydro-1H-cyclopenta[*a*]phenanthren-17-yl)pentyl)-2,2,2-trifluoroacetamide (21.1 mg). Some starting material (25.0 mg, 47%) was also covered. Flash column chromatography conditions: 5-25% Et_2O/hexane.

^{1}H NMR ($CDCl_3$, 400 MHz): 7.39-7.30 (m, 5H), 6.31 (br, 1H), 5.11 (s, 2H), 3.61-3.53 (m, 1H), 3.37-3.24 (m, 2H), 2.29-2.25 (m, 2H), 1.81-1.59 (m, 5), 1.53-0.89 (m, 39H), 0.73 (s, 3H), 0.05 (s, 6H); ^{13}C NMR ($CDCl_3$, 100 MHz): 174.1, 157.1 (q, *J*=36.6), 136.0, 135.9, 128.55, 128.54, 128.23, 128.21, 128.19, 72.7, 66.3, 66.3, 56.7, 56.6, 56.5, 43.8, 43.8, 42.2, 40.1, 40.9, 40.6, 40.6, 40.2, 43.8, 43.8, 42.2, 41.0, 40.9, 40.6, 40.6, 40.2, 38.5, 38.5, 36.9, 35.7, 35.6, 35.5, 35.3, 35.3, 34.5, 33.5, 33.2, 31.0, 29.3, 29.0, 27.2, 26.2, 26.0, 23.6, 23.5, 23.3, 23.1, 22.9, 22.8, 22.8, 22.7, 20.6, 18.3, 15.0, 14.9, −4.6; ^{19}F NMR ($CDCl_3$, 376 MHz): −75.9; Molecular weight $[M-H]^-$: 732.5 (expected), 732.5 (found); IR (cm^{-1}): 3326 (br), 3091, 3067, 3034, 2927, 2884, 2857, 1705.

A.2.8 Mechanistic Studies

Quantum Yield

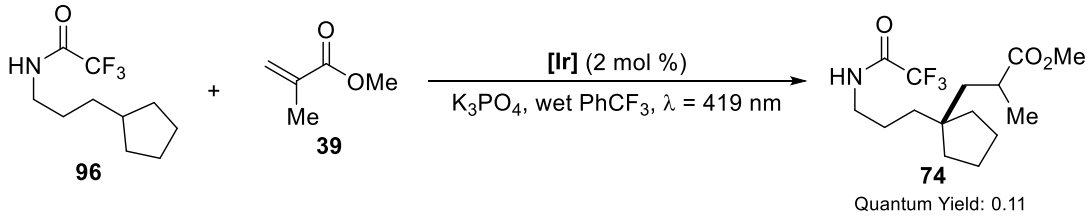

The above reaction was set up in a glove box (44.1 mg of **96**, 2 mol % [Ir] photocatalyst, 1.5 equiv. methyl methacrylate **39**, 2 equiv. K_3PO_4, 0.5 mL $PhCF_3$, 6 drops of H_2O). It was then taken from the glove box and irradiated (λ =419nm) for 2 h (t=7200 s). After irradiation, the sample was filtered through silica gel. After flash column chromatography (20-40% Et_2O/hexane), 1.2 mg of the alkylated product **74** (1.9%) was isolated.

The above experiment was repeated with 44.3 mg starting material. 1.3 mg of the alkylated product (2.0%) was isolated. The average yield of the two experiments is 1.3 mg.

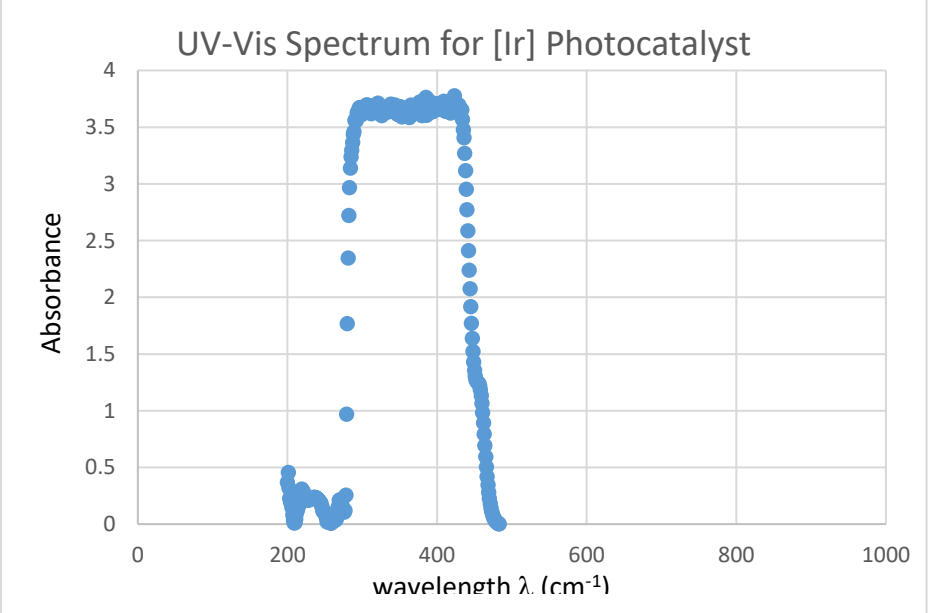

By UV-Vis, all incident light is absorbed by the [Ir] photocatalyst under the reaction conditions (Absorbance > 3 in $PhCF_3$). Therefore, fraction of light absorbed is ~ 1 (f =1).

The photon flux of the spectrophotometer was measured by literature procedures (ferrioxalate actinometry).[11] At 419 nm, it was determined to be 5.2×10^{-9} einstein s^{-1}.

$$\text{Quantum Yield} = \frac{\text{number of moles of product}}{\text{flux x t x f}}$$

$$= \frac{1.3 / 323 / 1000}{5.2 \times 10^{-9} \times 7200 \times 1}$$

$$= 0.11$$

On/Off Studies

The above reaction was set up (43.8 mg of **96**, 2 mol % [Ir] photocatalyst, 1.5 equiv. benzyl acrylate **50**, 2 equiv. K_3PO_4, 0.5 mL $PhCF_3$, 6 drops of H_2O) according to General Procedure D. Mesitylene was added as an internal standard. The reaction mixture was irradiated with a Blue LED for an hour. An aliquot (20 μL) was taken from the reaction mixture and filtered through a short plug of silica gel. The amount of product was determined by HPLC. The reaction mixture was degassed by bubbling argon through for 10 mins. The reaction mixture was covered by aluminum foil and re-subject to the Blue LED. The amount of the product was determined in the same way as before. After degassing, the reaction mixture was unwrapped and irradiated with the Blue LED. The reaction was monitored for 6 hours in total. It was observed that the photoredox-catalyzed reaction demonstrates an On/Off behavior. T. he quantum yield (<1) and the On/Off behavior are consistent with a closed catalytic cycle.

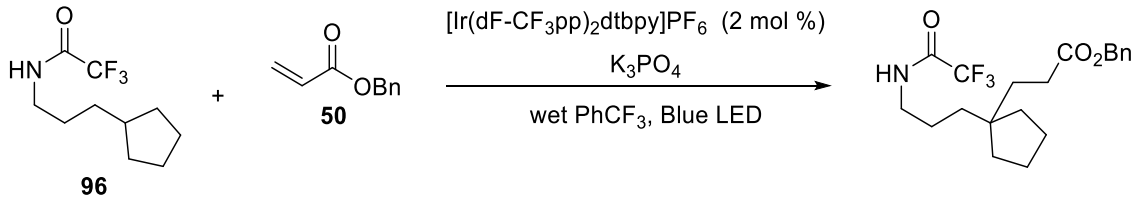

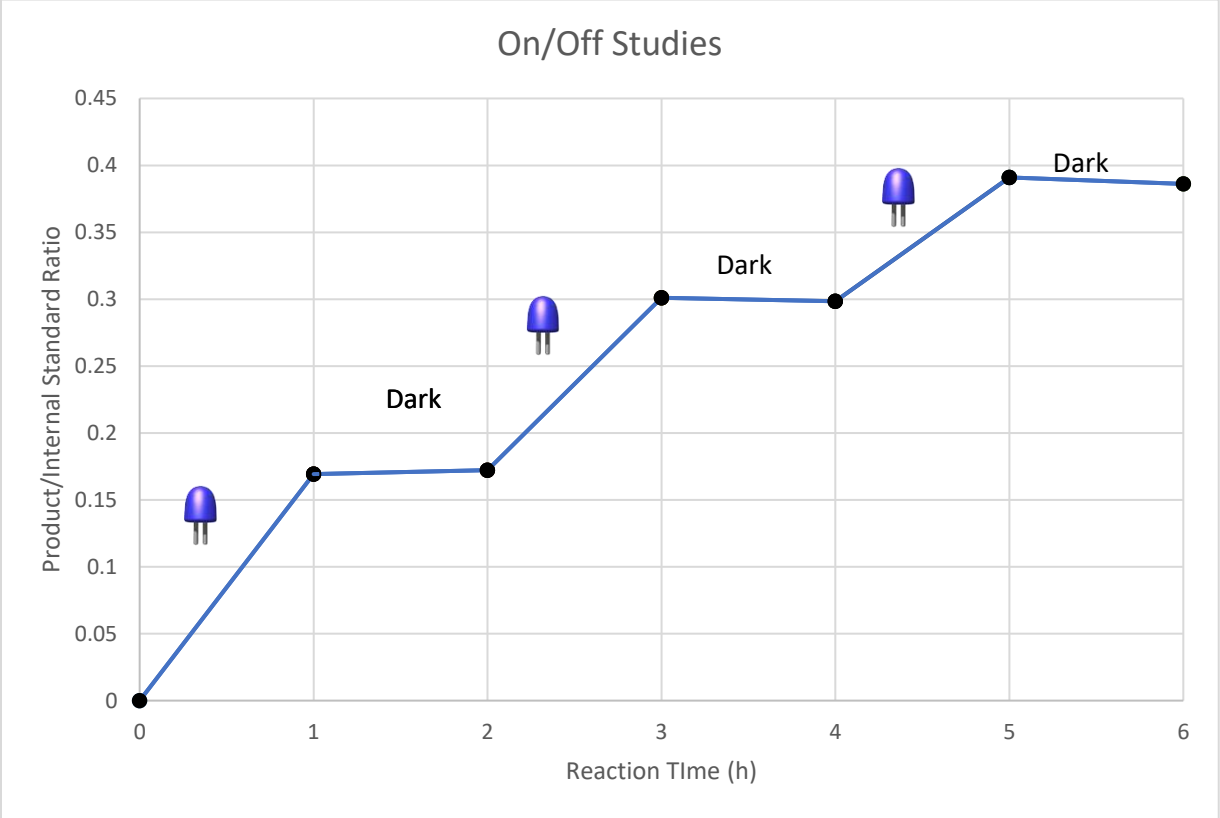

In addition, we believe that chain propagation mechanism is very unlikely by considering the pKa's[12] and bond strength[13,14,15] of the reaction intermediates involved:

▪ *Possibility I:*

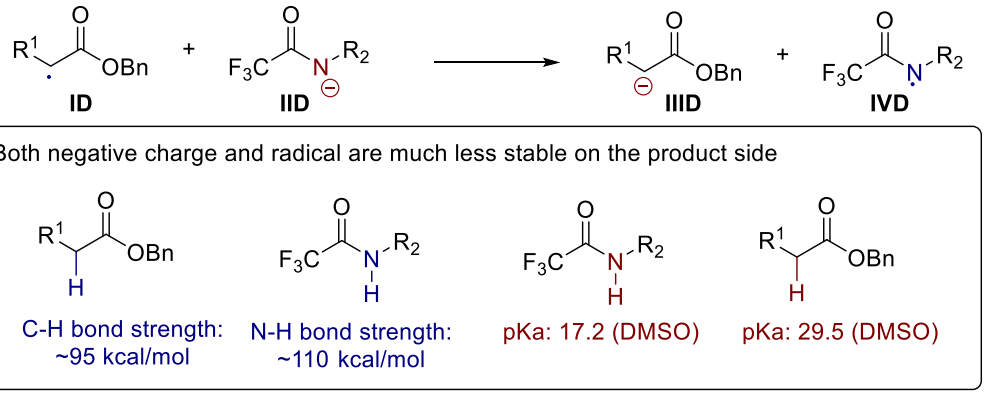

▪ *Possibility II:*

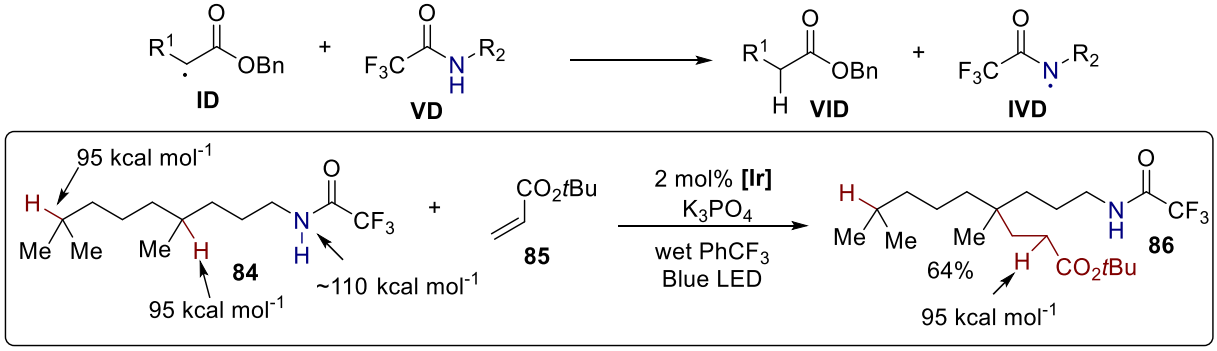

▪ *Possibility III:*

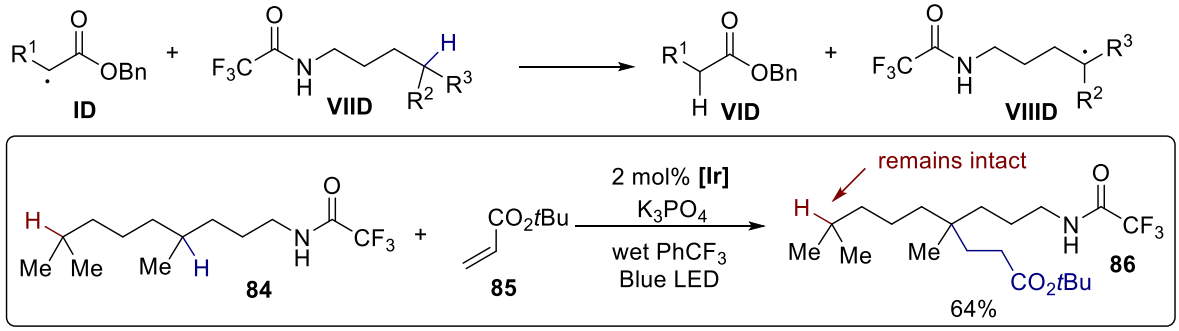

Potential Pathways for the Generation of Nitrogen Radical

a. Possibility of Oxidation/Deprotonation Stepwise Mechanism

Stern-Volmer studies were carried out with Horiba Fluorolog 3 (model number: FL3-11). The standard solutions were prepared in DMF, a competent solvent for the reaction. The

solutions (0.01 mM Ir photocatalyst and varying concentrations of trifluoroacetamide) were irradiated at 380 nm and luminescence was measured at 470 nm.

[trifluroacetamide] (mM)	0	0.2	0.4	0.6	1.0
I_0/I	1	0.99879	0.99963	1.00021	0.99988

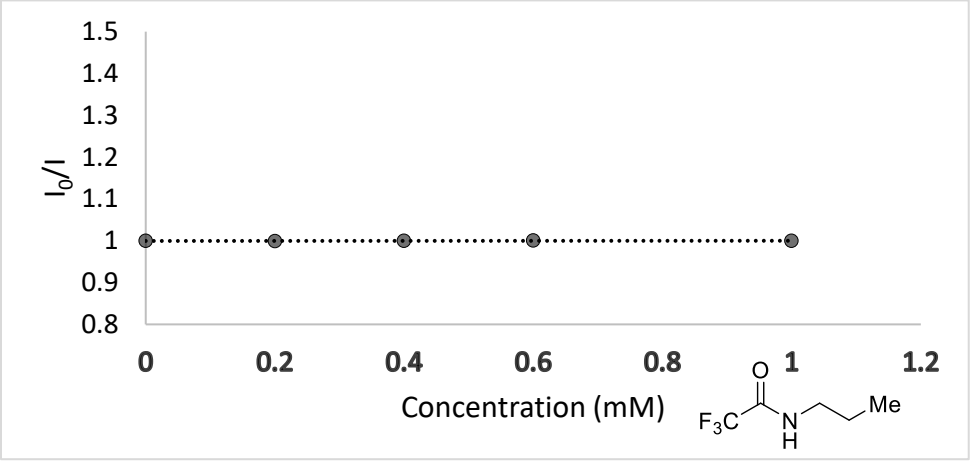

The result shows that the Ir photocatalyst is not quenched by the neutral amide in the absence of a base. This is consistent with CV studies which were obtained with a CH instrument (electrochemical analyzer, CHI1232B, serial number: A3268). A glassy electrode, a Pt mesh counter electron and an Ag/AgCl reference electrode were used and measurement was taken in a 2 mM solution of the amide in MeCN containing 0.1 M NBu_4PF_6. No oxidation was observed even at voltage >2V vs Ag/AgCl (or >1.955 V vs SCE). This suggests that the excited Ir photocatalyst (1.2V vs SCE) cannot oxidize the neutral form of trifluoroacetamide and is consistent with the quenching studies. Thus oxidation/deprotonation stepwise event is unlikely to be responsible for the generation of the nitrogen radical.

b. Discussion about Deprotonation/Oxidation Stepwise and PCET Mechanism

Stern-Volmer studies were also conducted with the potassium salt of trifluoroacetamide. Standard solutions of potassium propyl(2,2,2-trifluoroacetyl)amide and $[Ir(dF\text{-}CF_3pp)_2dtbbp]PF_6$ in anhydrous DMF were prepared by mixing equal amount of potassium hydride and 2,2,2-trifluoro-*N*-propylacetamide in the glove box to make sure there was no water present. The solutions (0.01 mM Ir photocatalyst and varying concentrations of potassium propyl(2,2,2-trifluoroacetyl)amide) were irradiated at 380 nm and luminescence was measured at 470 nm. The plot was obtained by two independent runs (i.e. new standard solutions were prepared for each run):

Run 1

[potassium salt of trifluroacetamide] (mM)	0	0.2	0.4	0.6	1.0
I_0/I	1	1.04686	1.11111	1.19689	1.31199

Run 2

[potassium salt of trifluroacetamide] (mM)	0	0.2	0.4	0.6	1.0
I_0/I	1	0.99000	1.05505	1.14000	1.36214

Average

[potassium salt of trifluroacetamide] (mM)	0	0.2	0.4	0.6	1.0
I_0/I	1	1.108434	1.083081	1.163444	1.33707

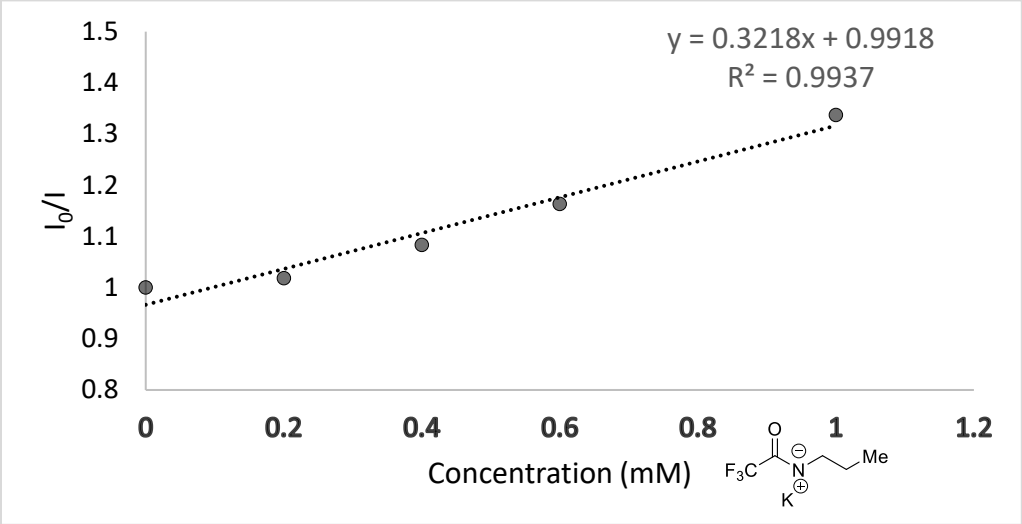

The result shows that the Ir photocatalyst is quenched by the potassium salt of the trifluoroacetamide. This is consistent with CV studies which indicate that the redox potential of the potassium salt of the trifluoroacetamide is 0.80V vs Ag/AgCl (or 0.77 V vs SCE). The potential suggests that the excited state of the photocatalyst (1.2 V vs SCE) can oxidize the potassium salt of trifluoroacetamide.

In addition, the presence of negatively charged nitrogen is evidenced by the formation of aza-Michael addition product with K_3PO_4 in $PhCF_3$ (>50% conversion, see below). No aza-Michael adduct is formed, as determined by ^1H NMR, in the absence of K_3PO_4. Substrates bearing weaker

electron-withdrawing groups on nitrogen, pentafluorobenzoyl and difluoroacetyl groups (pKa of trifluoroacetic acid[16] =0.2, difluoroacetic acid[17] =1.1, pentafluorobenzoic acid[18] =1.7) do not yield the C-H functionalized product under the photocatalyzed conditions nor do they form the aza-Michael addition product with K_3PO_4 in wet $PhCF_3$ (see below). There appears a correlation between the presence of negatively charged nitrogen and the generation of nitrogen radical. Also, the reaction is biphasic and a three-component (Amide, [Ir] photocatalyst and K_3PO_4) transition state is unlikely. This leads us to believe that deprotonation then oxidation stepwise event is responsible for the generation of nitrogen radical.

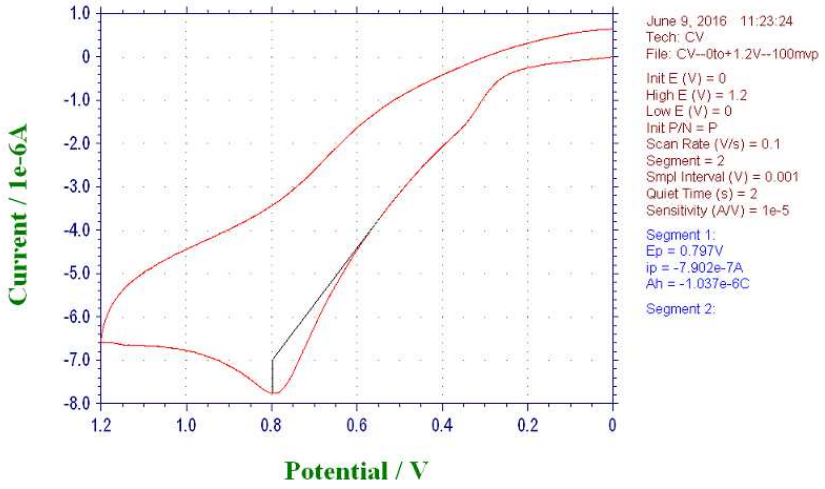

To a mixture of the amine (0.1 mmol, 1 equiv.), methyl vinyl ketone (0.15 mmol, 1.5 equiv.) and K_3PO_4 (0.2 mmol, 2 equiv.) in a vial was added 3 drops of deionized water (~40 mg), followed by $PhCF_3$ (0.25 mL). The vial was then capped and illuminated with a Blue LED for 20 h (The distance between the Blue LED and the vial is around 1.5 cm). The mixture was filtered through silica gel. The conversion was determined by ^1H NMR spectroscopy. The product can be purified by column chromatography (35-60% Et_2O/hexane). The product exists as two rotamers (~1:2), as observed in NMR. Some of the peaks of the two rotamers cannot be distinguished in ^{13}C NMR.

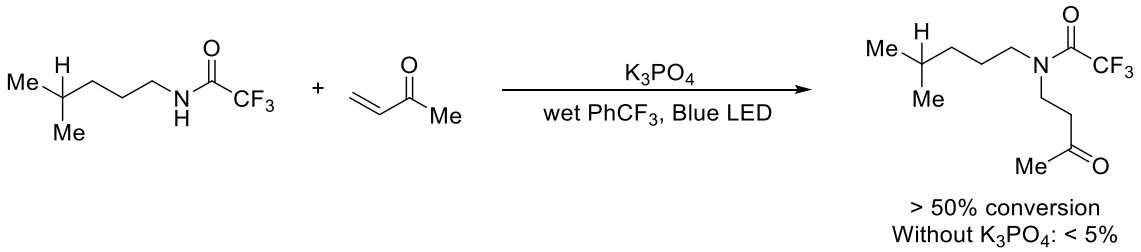

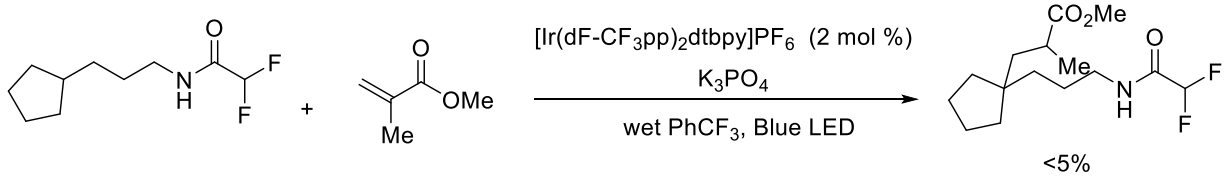

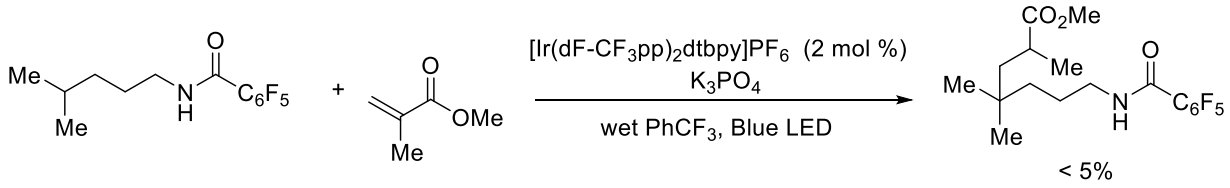

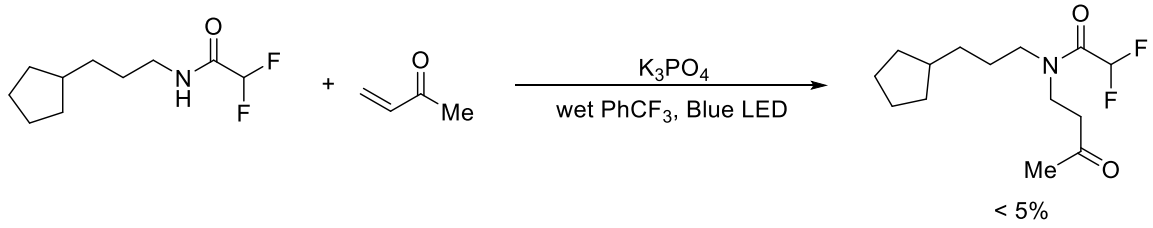

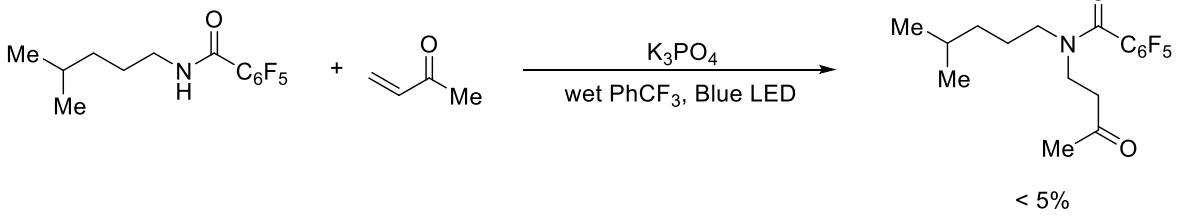

^{1}H NMR ($CDCl_3$, 400 MHz): 3.67 (t, *J*= 7.6, 1H, minor rotamer), 3.59 (t, *J*= 6.9, 2H, major rotamer), 3.36 (t, *J*= 8.0, 2H, major rotamer), 3.30 (t, *J*= 7.9, 1H, minor rotamer), 2.82 (t, *J*= 6.9, 2H, major rotamer), 2.77 (t, *J*= 7.5, 1H, minor rotamer), 2.19 (s, 1.5 H, minor rotamer), 2.17 (s, 3H, major rotamer), 1.64-1.50 (m, 4.5H, both rotamers), 1.19-1.13 (m, 3H, both rotamers), 0.90-0.87 (m, 9H, both rotamers); ^{13}C NMR ($CDCl_3$, 100 MHz): 206.5 (major rotamer), 205.4 (minor

rotamer), 156.9 (q, *J*= 35.9), 116.4 (q, *J*= 287.4), 49.0 (q, *J*= 3.0, major rotamer)), 47.6, 42.7, 42.6, 41.8 (q, *J*=3.3, minor rotamer), 40.8, 35.7, 35.5, 30.2, 30.2, 27.8, 27.6, 26,7, 24.7, 22.4, 22.4 ; ^{19}F NMR ($CDCl_3$, 376 MHz): −69.21 (major rotamer), −60.29 (minor rotamer); IR (cm^{-1}): 2955, 2933, 2872, 1718, 1685, 1464, 1436; Molecular weight $[M+H]^+$: 268.2 (expected); 268.2 (found).

A.2.9 NMR Spectra

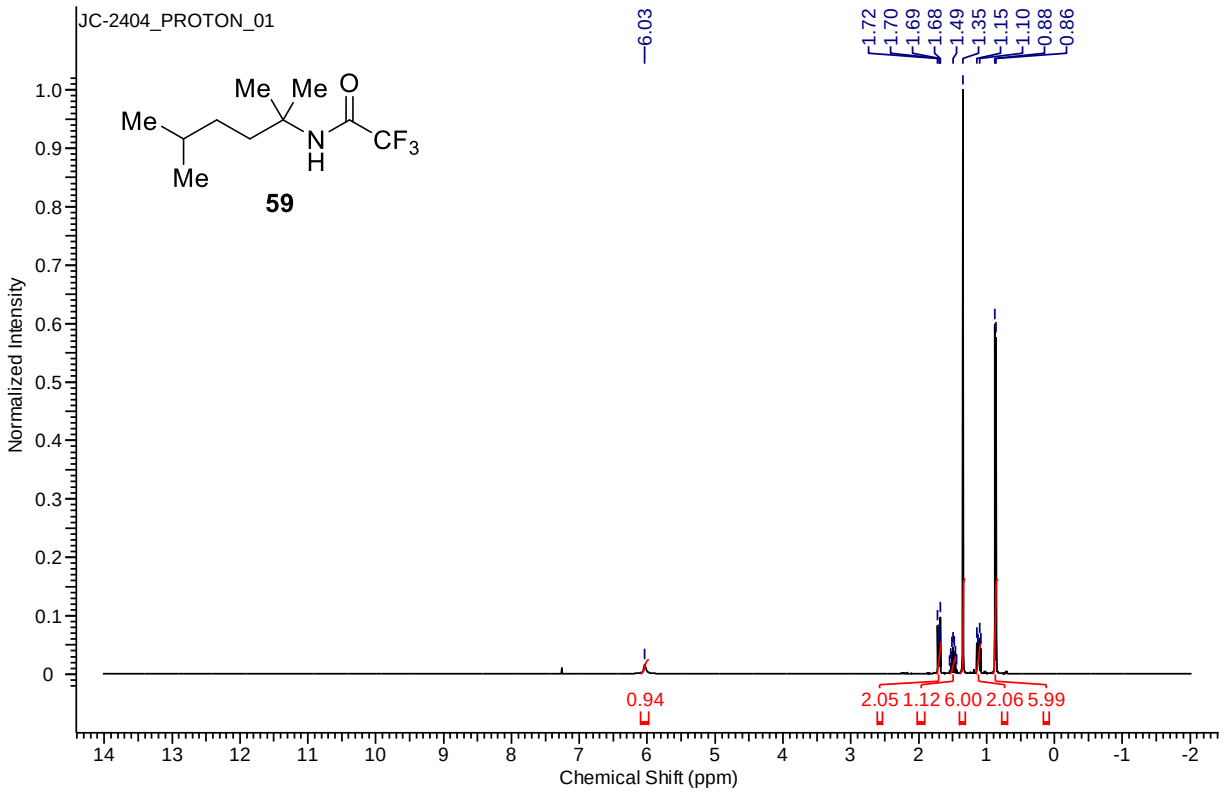

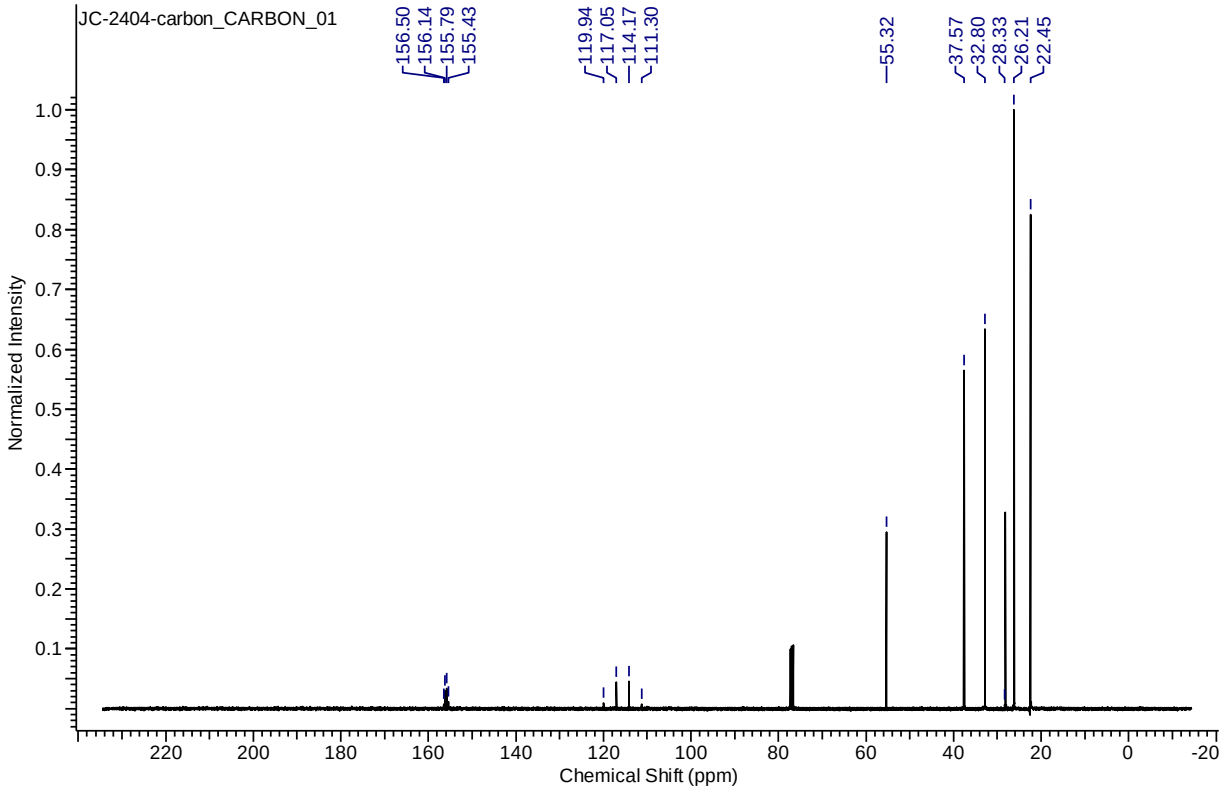

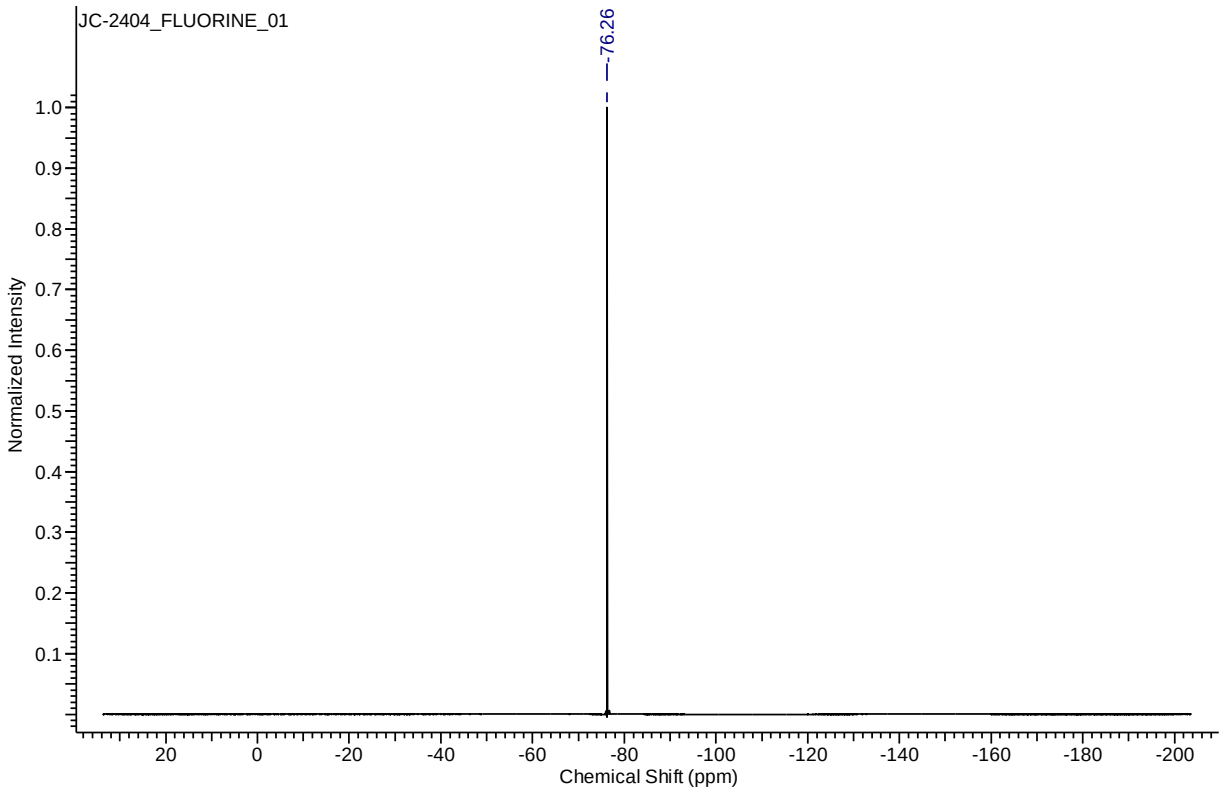
JC-2404_FLUORINE_01
-76.26
Normalized Intensity
Chemical Shift (ppm)

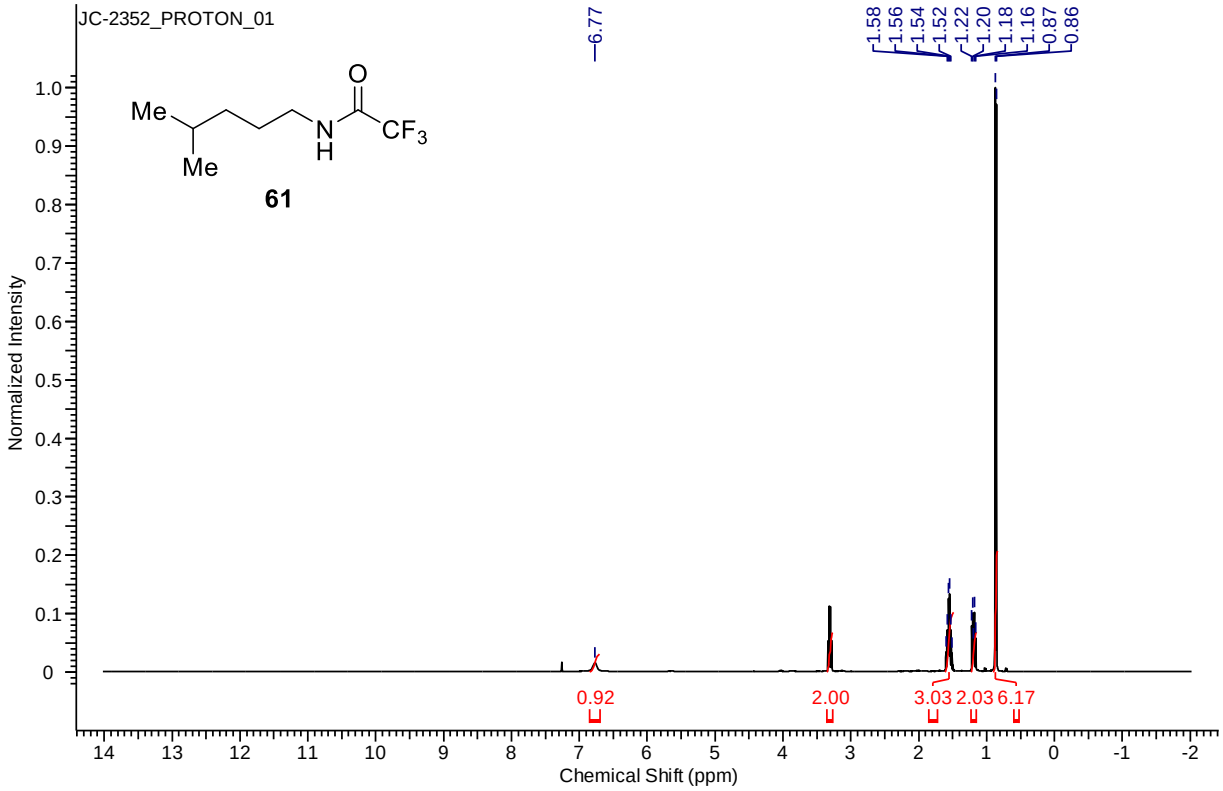
JC-2352_PROTON_01
6.77
1.58
1.56
1.54
1.52
1.22
1.20
1.18
1.16
0.87
0.86
Me
Me
N
H
O
CF3
61
0.92
2.00
3.03
2.03
6.17
Normalized Intensity
Chemical Shift (ppm)

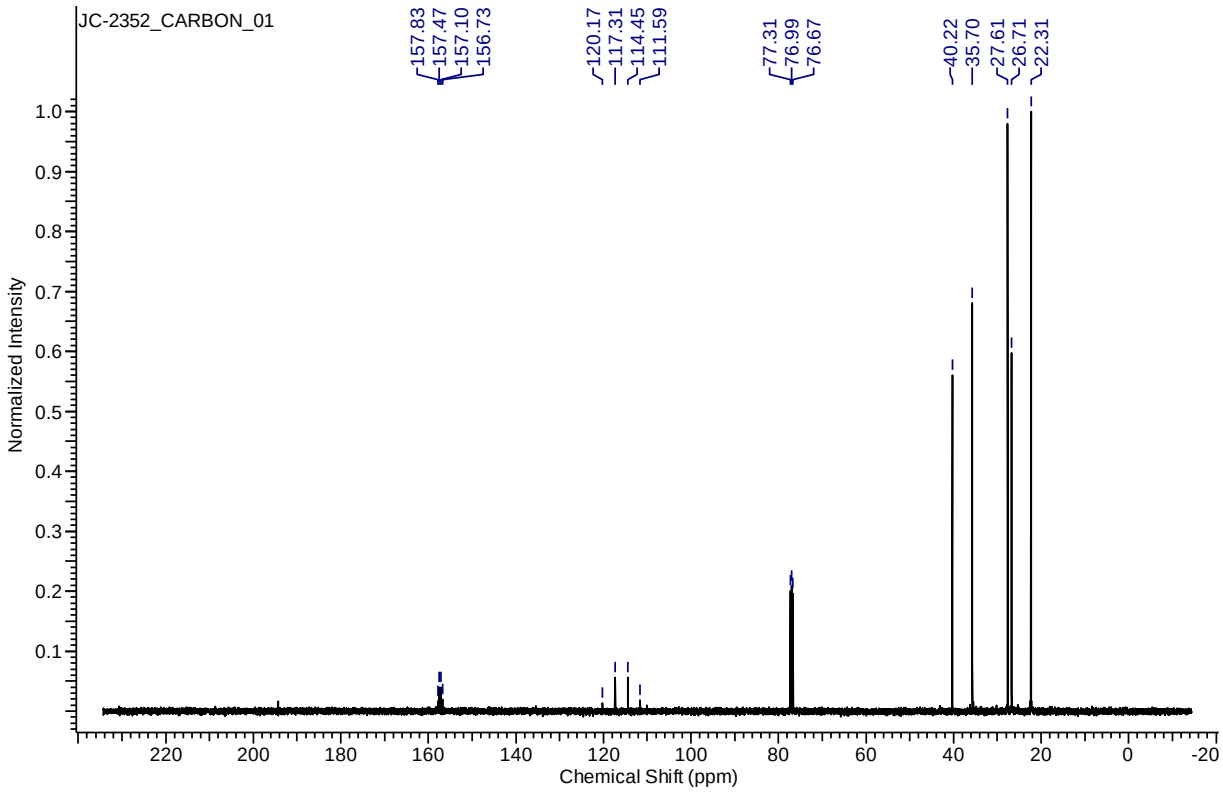
JC-2352_CARBON_01
157.83
157.47
157.10
156.73
120.17
117.31
114.45
111.59
77.31
76.99
76.67
40.22
35.70
27.61
26.71
22.31
Normalized Intensity
Chemical Shift (ppm)

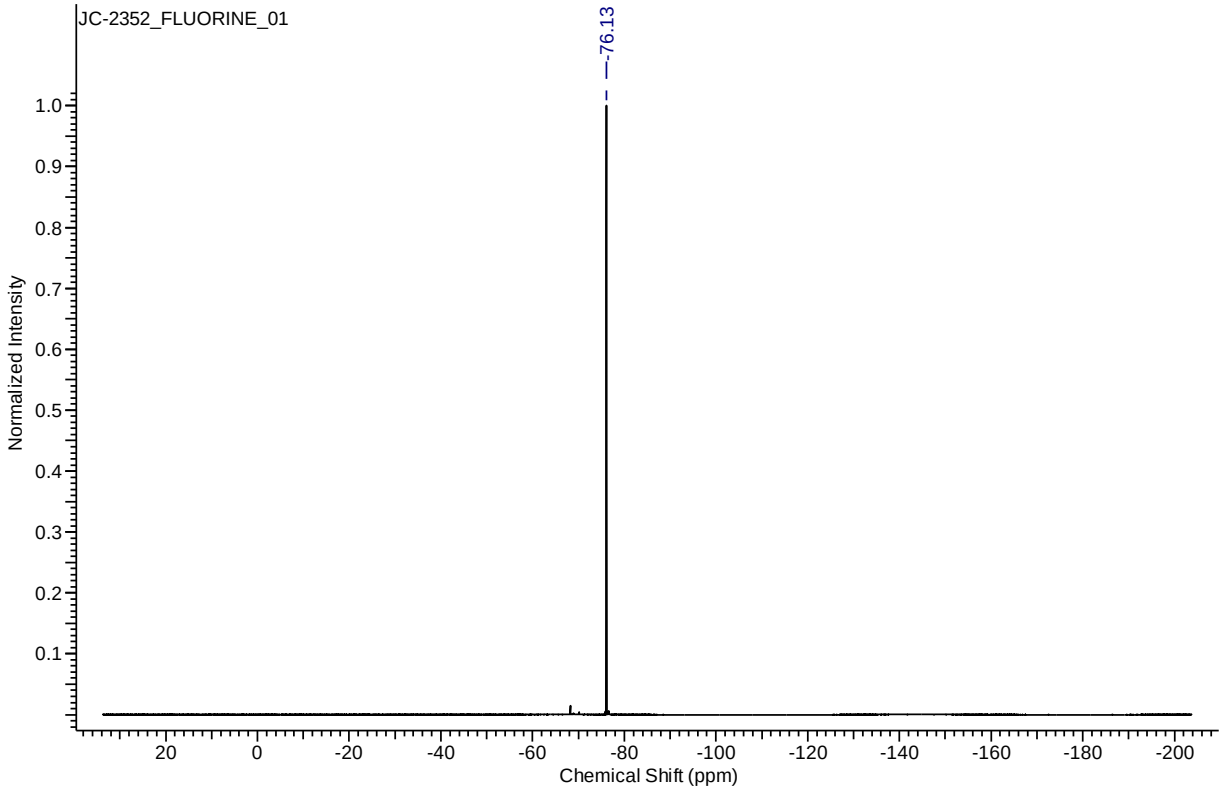
JC-2352_FLUORINE_01
-76.13
Normalized Intensity
Chemical Shift (ppm)

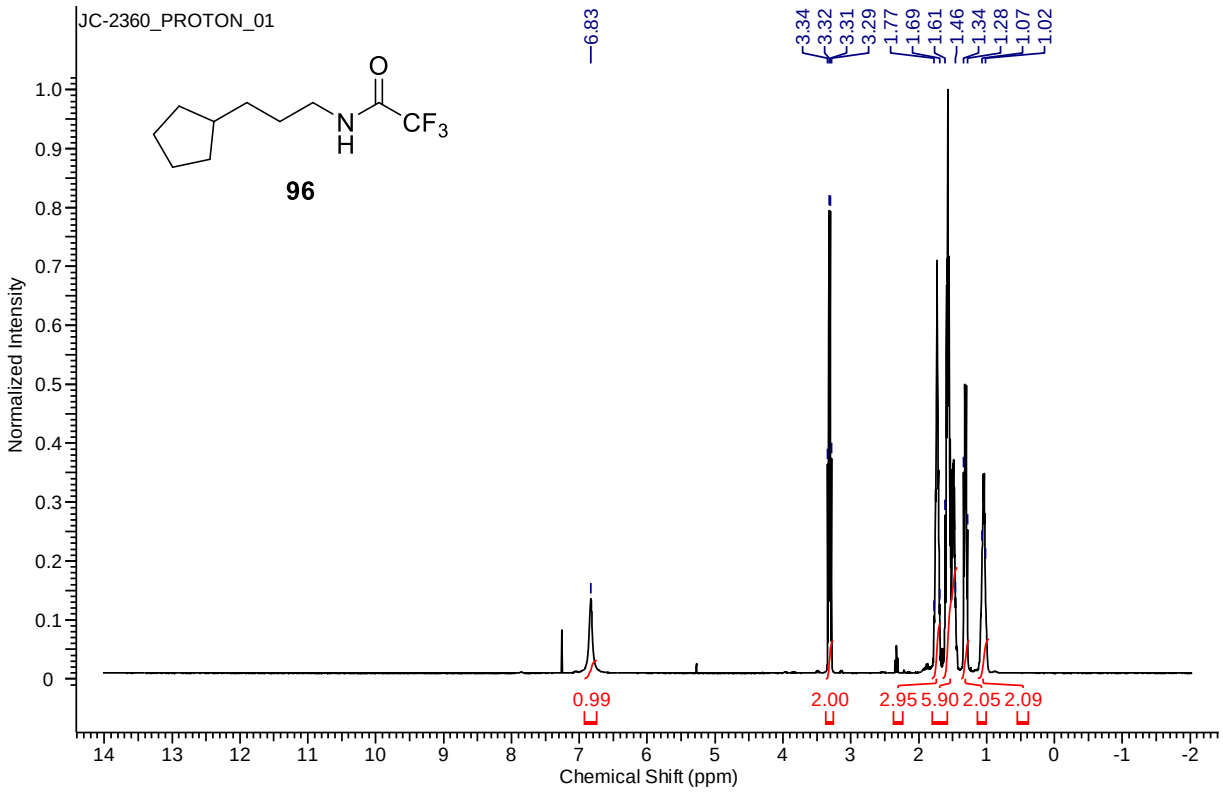
JC-2360_PROTON_01
96
6.83
3.34
3.32
3.31
3.29
1.77
1.69
1.61
1.46
1.34
1.28
1.07
1.02
0.99
2.00
2.95
5.90
2.05
2.09
Normalized Intensity
Chemical Shift (ppm)

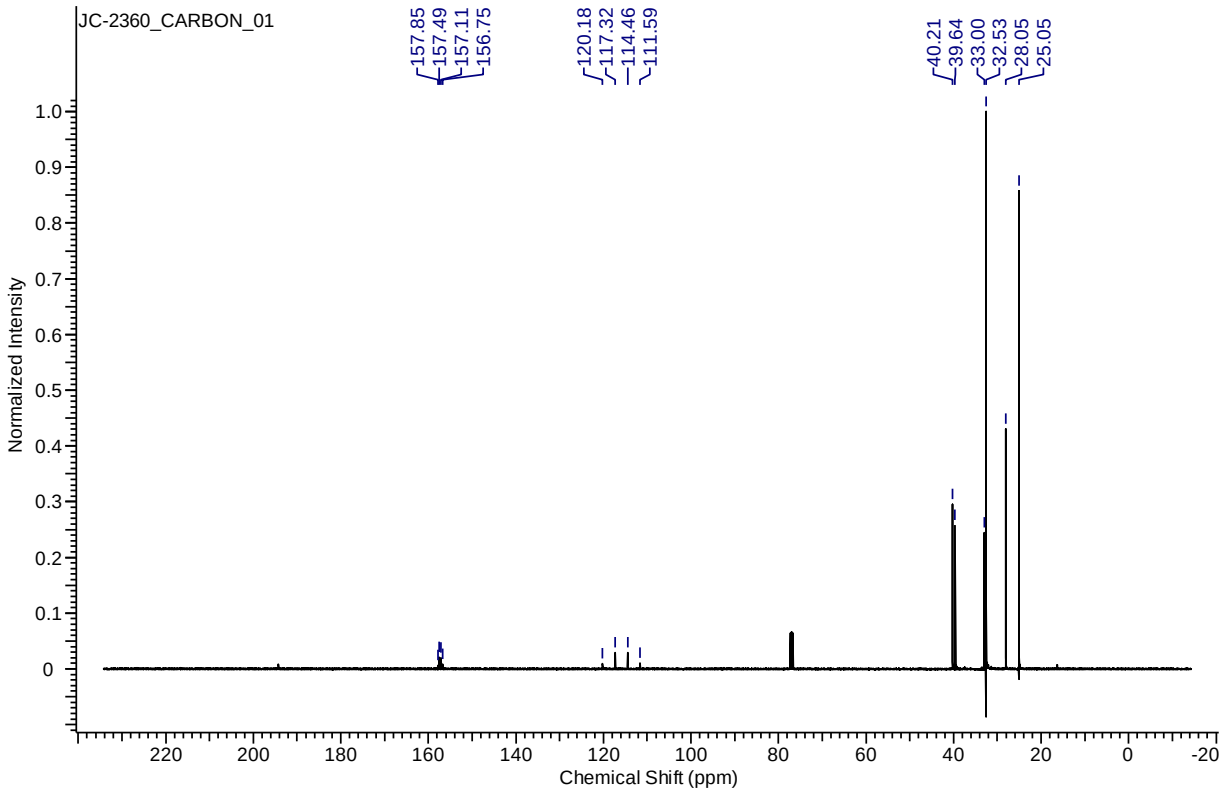
JC-2360_CARBON_01
157.85
157.49
157.11
156.75
120.18
117.32
114.46
111.59
40.21
39.64
33.00
32.53
28.05
25.05
Normalized Intensity
Chemical Shift (ppm)

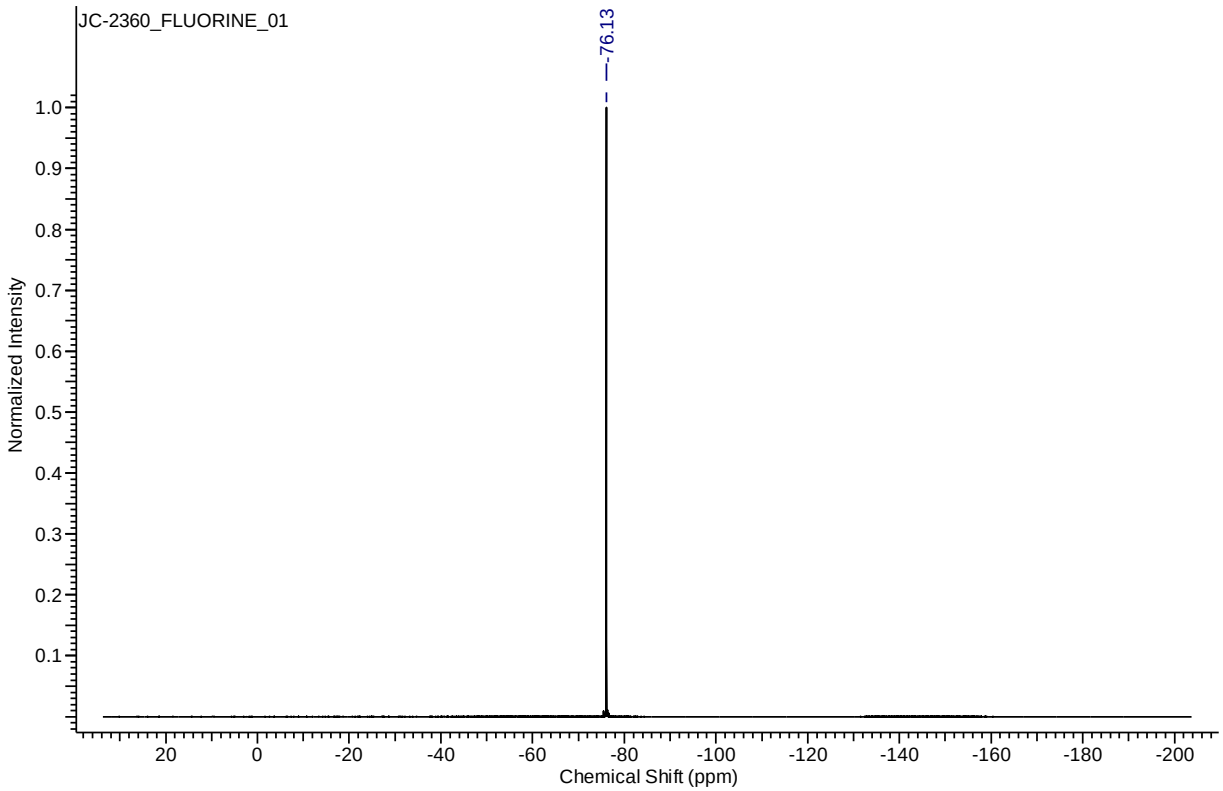
JC-2360_FLUORINE_01
-76.13
Normalized Intensity
Chemical Shift (ppm)

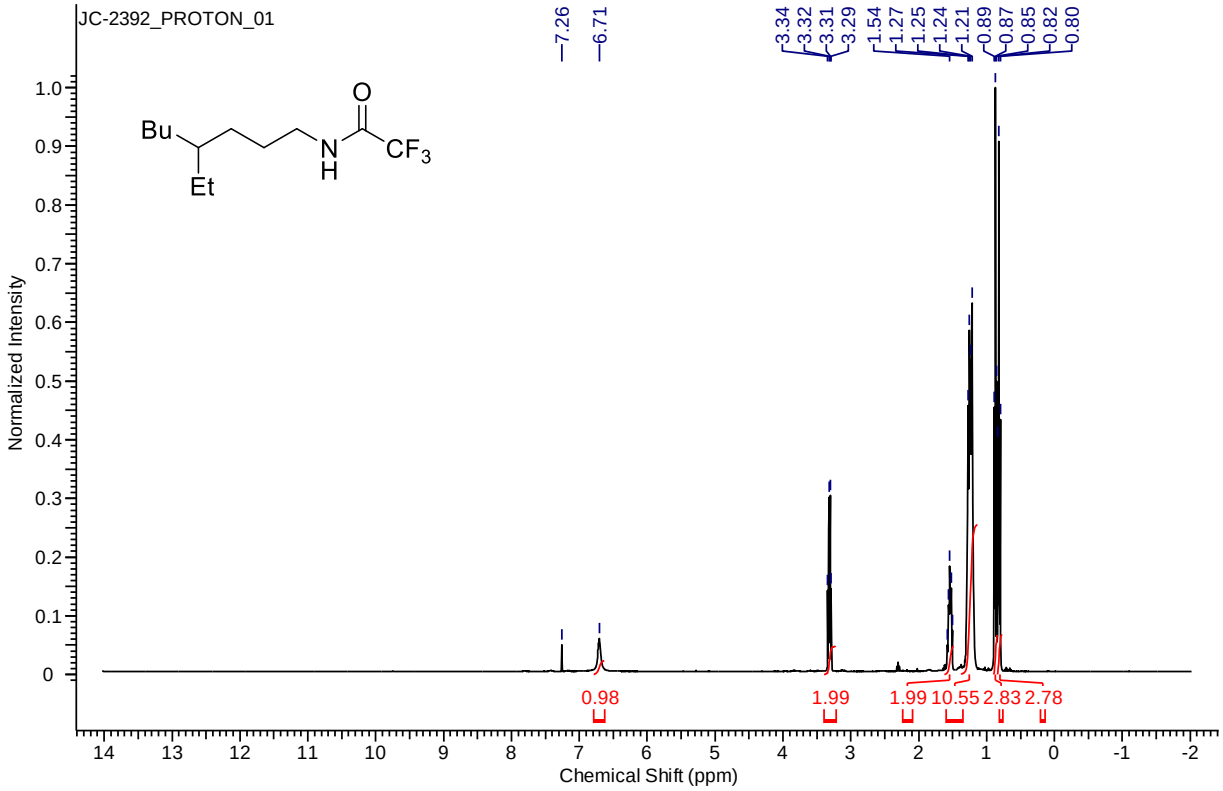
JC-2392_PROTON_01
7.26
6.71
3.34
3.32
3.31
3.29
1.54
1.27
1.25
1.24
1.21
0.89
0.87
0.85
0.82
0.80
Bu
Et
N
H
O
CF3
0.98
1.99
1.99
10.55
2.83
2.78
Normalized Intensity
Chemical Shift (ppm)

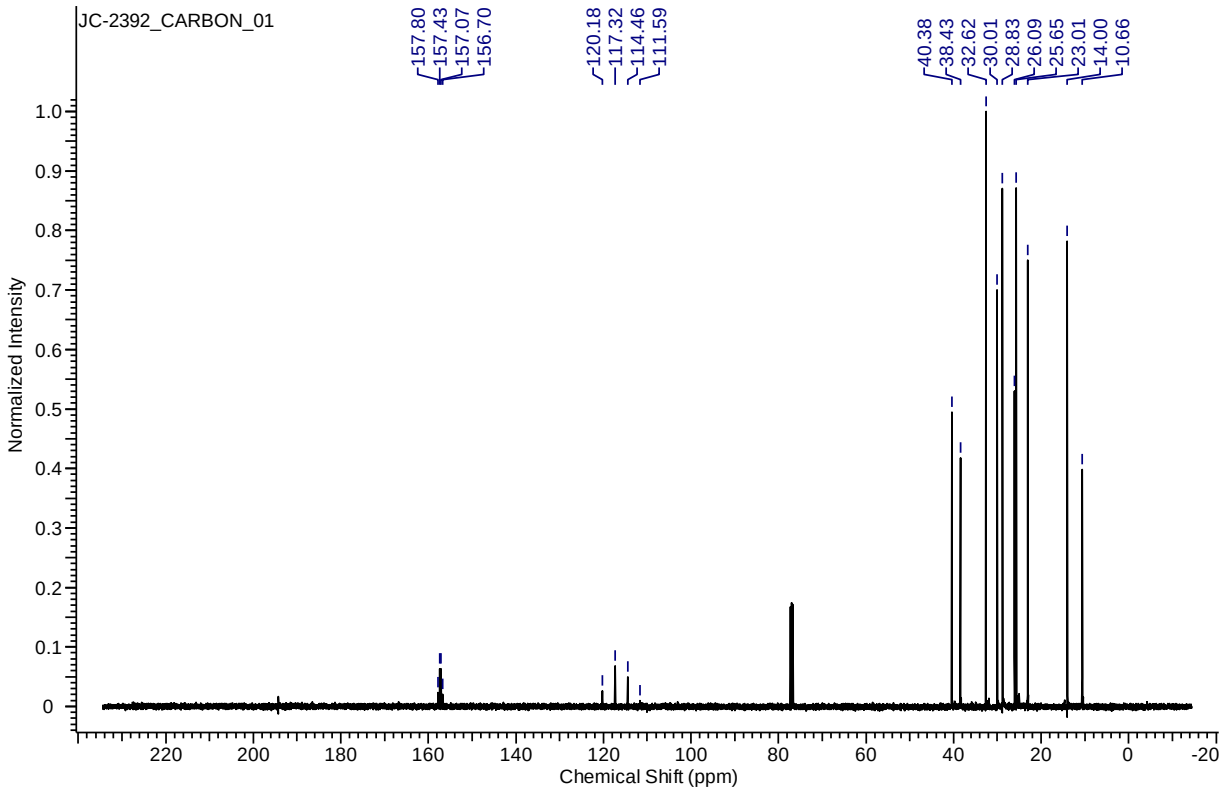
JC-2392_CARBON_01
157.80
157.43
157.07
156.70
120.18
117.32
114.46
111.59
40.38
38.43
32.62
30.01
28.83
26.09
25.65
23.01
14.00
10.66
Normalized Intensity
Chemical Shift (ppm)

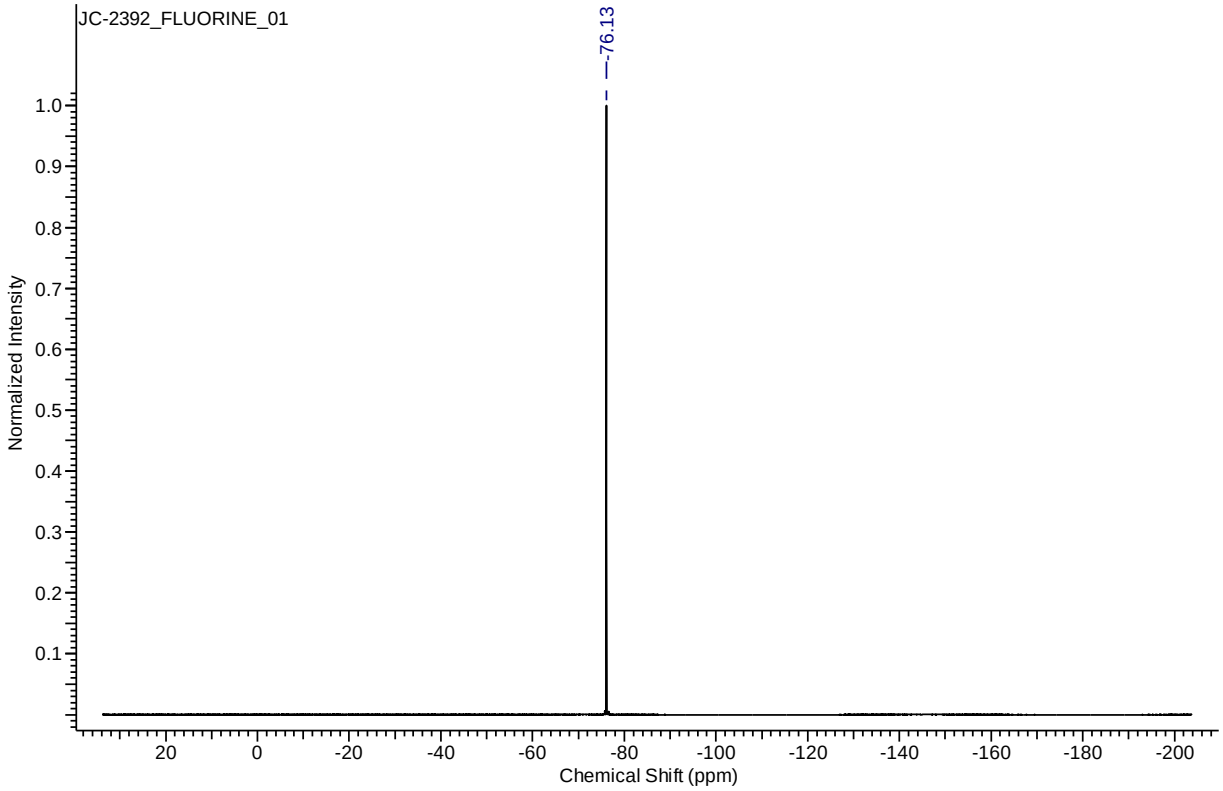
JC-2392_FLUORINE_01
-76.13
Normalized Intensity
Chemical Shift (ppm)

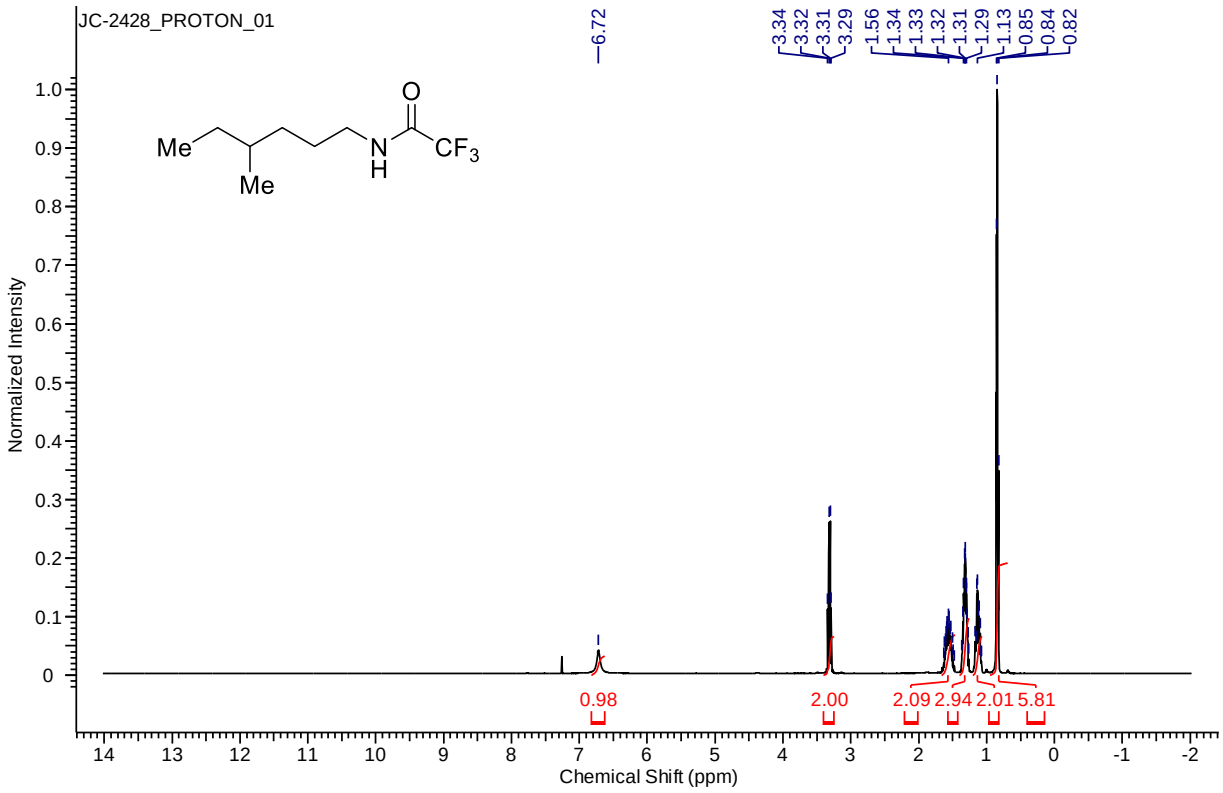
JC-2428_PROTON_01
6.72
3.34
3.32
3.31
3.29
1.56
1.34
1.33
1.32
1.31
1.29
1.13
0.85
0.84
0.82
Me
Me
N
H
O
CF3
0.98
2.00
2.09
2.94
2.01
5.81
Normalized Intensity
Chemical Shift (ppm)

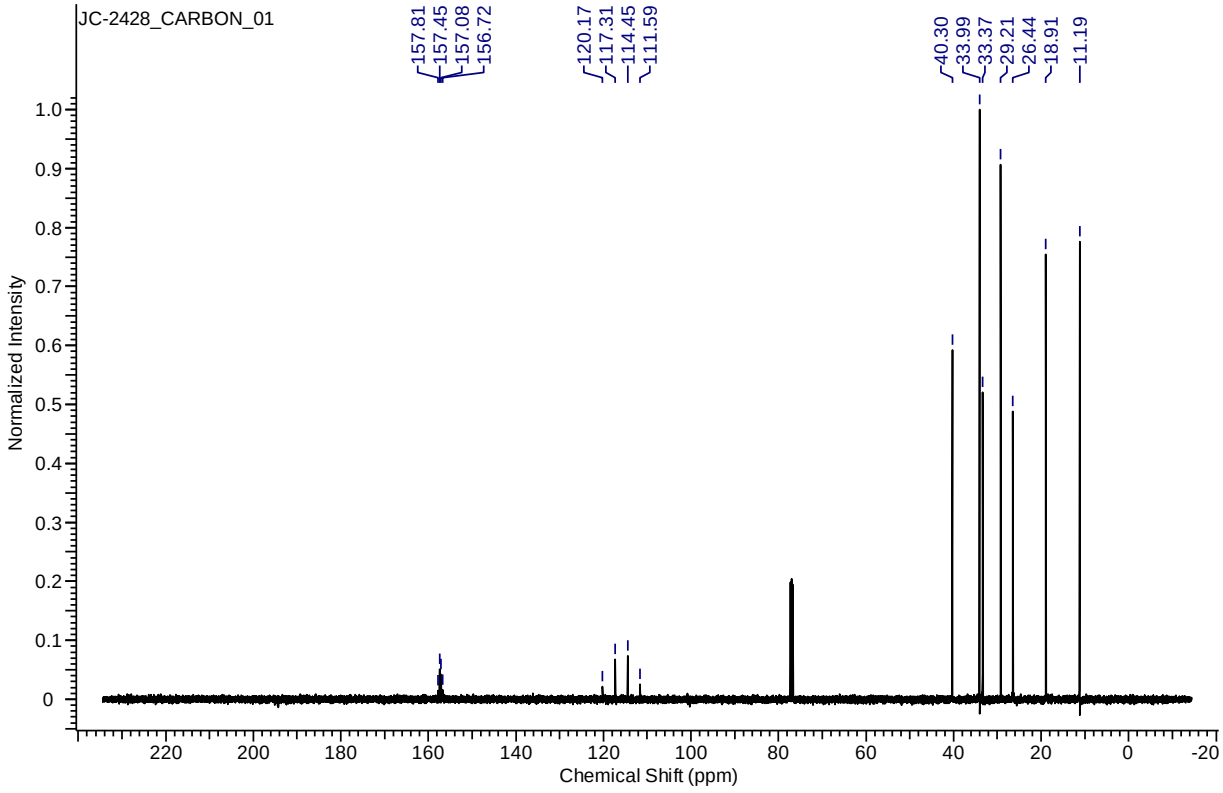
JC-2428_CARBON_01
157.81
157.45
157.08
156.72
120.17
117.31
114.45
111.59
40.30
33.99
33.37
29.21
26.44
18.91
11.19
Normalized Intensity
Chemical Shift (ppm)

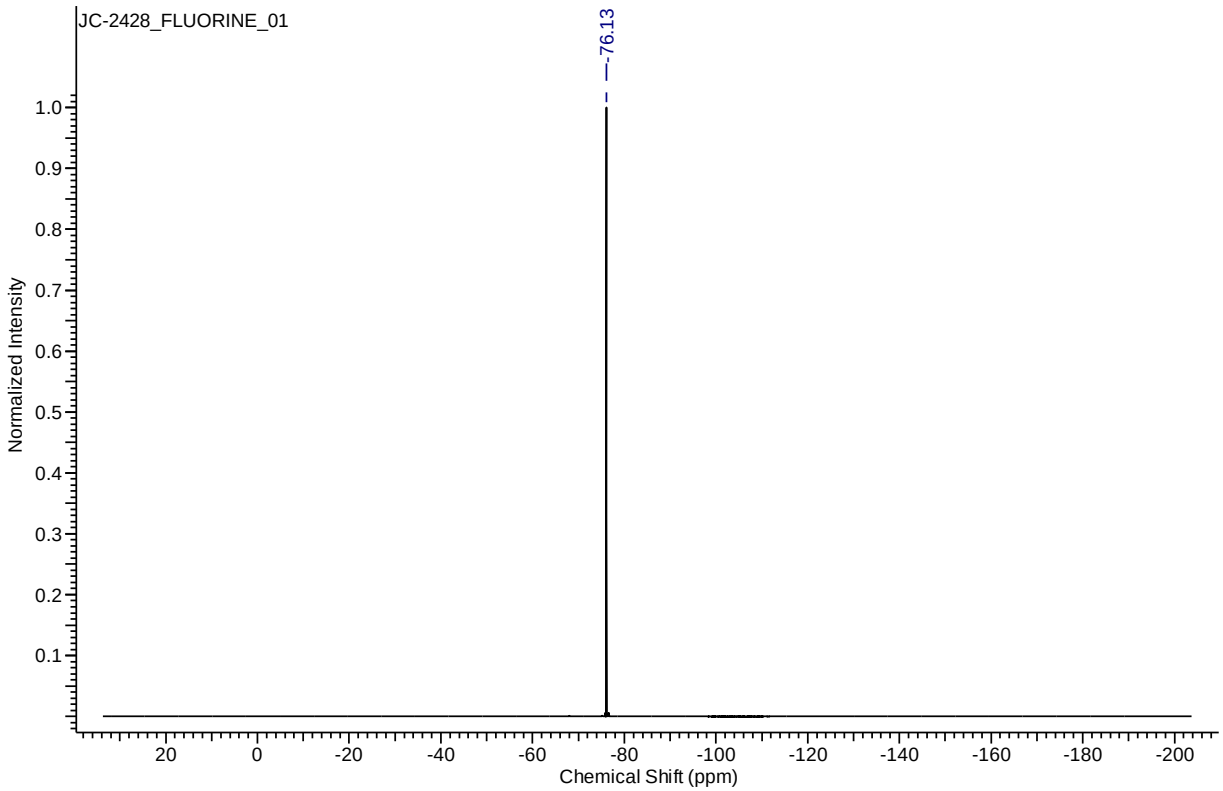
JC-2428_FLUORINE_01
-76.13
Normalized Intensity
Chemical Shift (ppm)

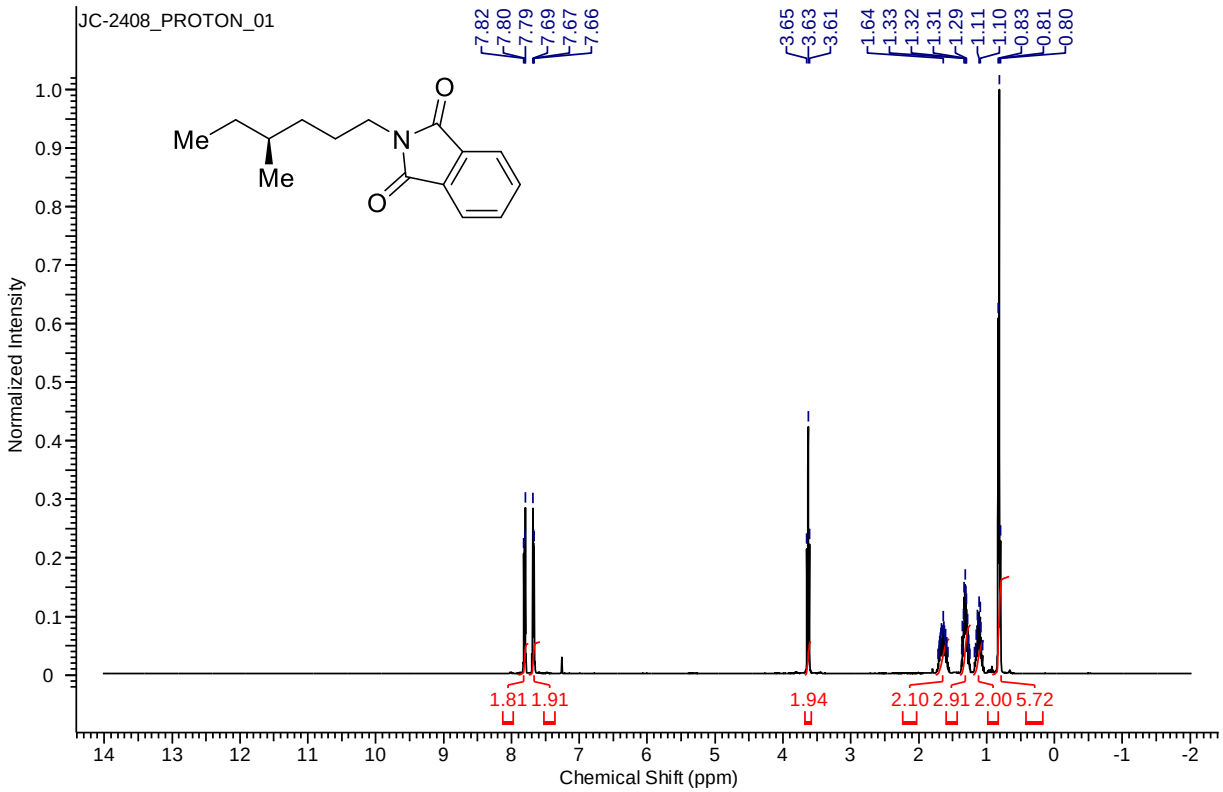
JC-2408_PROTON_01
7.82
7.80
7.79
7.69
7.67
7.66
3.65
3.63
3.61
1.64
1.33
1.32
1.31
1.29
1.11
1.10
0.83
0.81
0.80
Me
Me
N
O
O
1.81
1.91
1.94
2.10
2.91
2.00
5.72
Normalized Intensity
Chemical Shift (ppm)

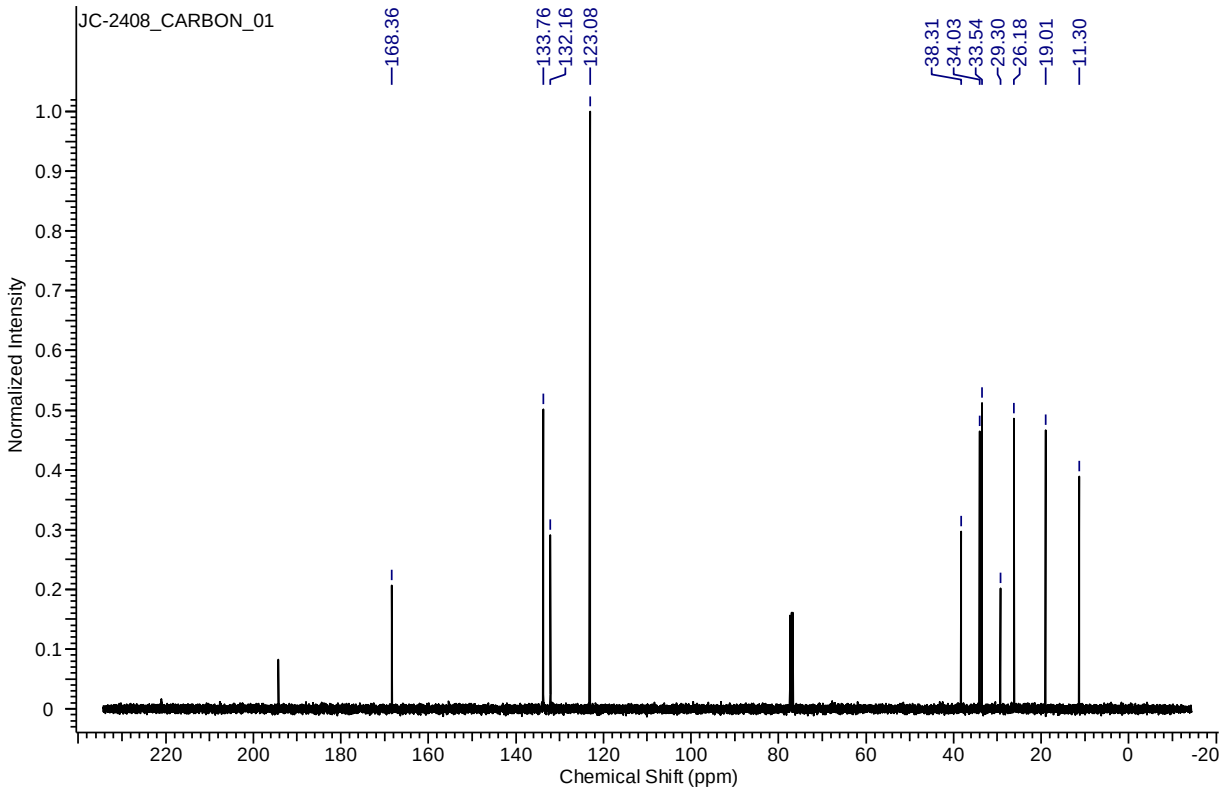
JC-2408_CARBON_01
168.36
133.76
132.16
123.08
38.31
34.03
33.54
29.30
26.18
19.01
11.30
Normalized Intensity
Chemical Shift (ppm)

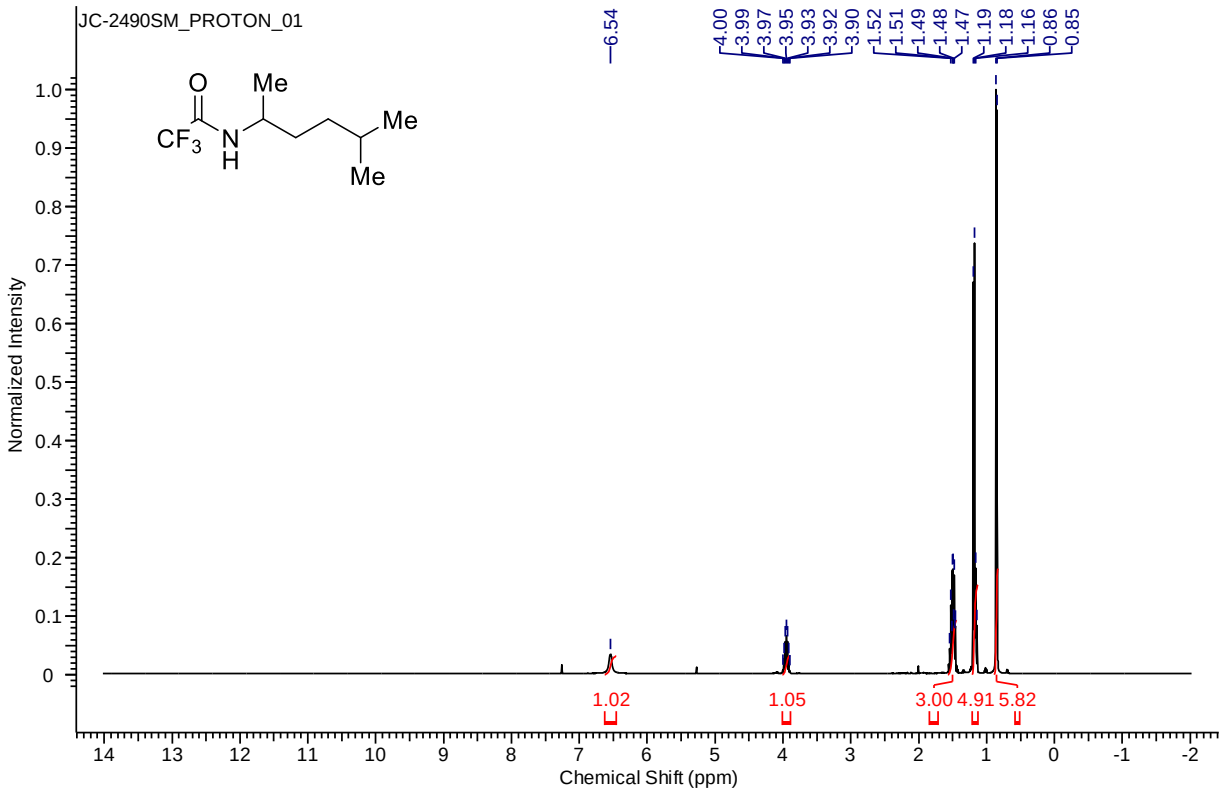
JC-2490SM_PROTON_01
6.54
4.00
3.99
3.97
3.95
3.93
3.92
3.90
1.52
1.51
1.49
1.48
1.47
1.19
1.18
1.16
0.86
0.85
O
Me
CF3
N
H
Me
Me
1.02
1.05
3.00
4.91
5.82
Normalized Intensity
Chemical Shift (ppm)

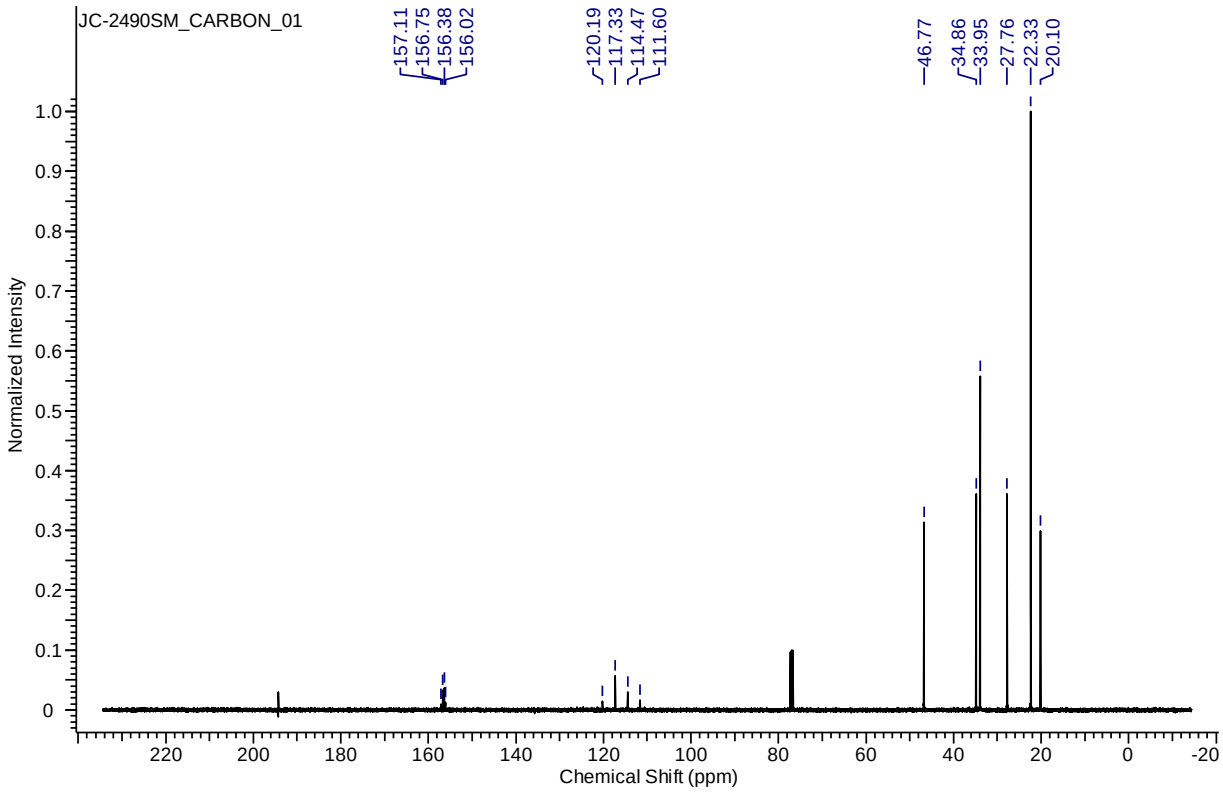
JC-2490SM_CARBON_01
157.11
156.75
156.38
156.02
120.19
117.33
114.47
111.60
46.77
34.86
33.95
27.76
22.33
20.10
Normalized Intensity
Chemical Shift (ppm)

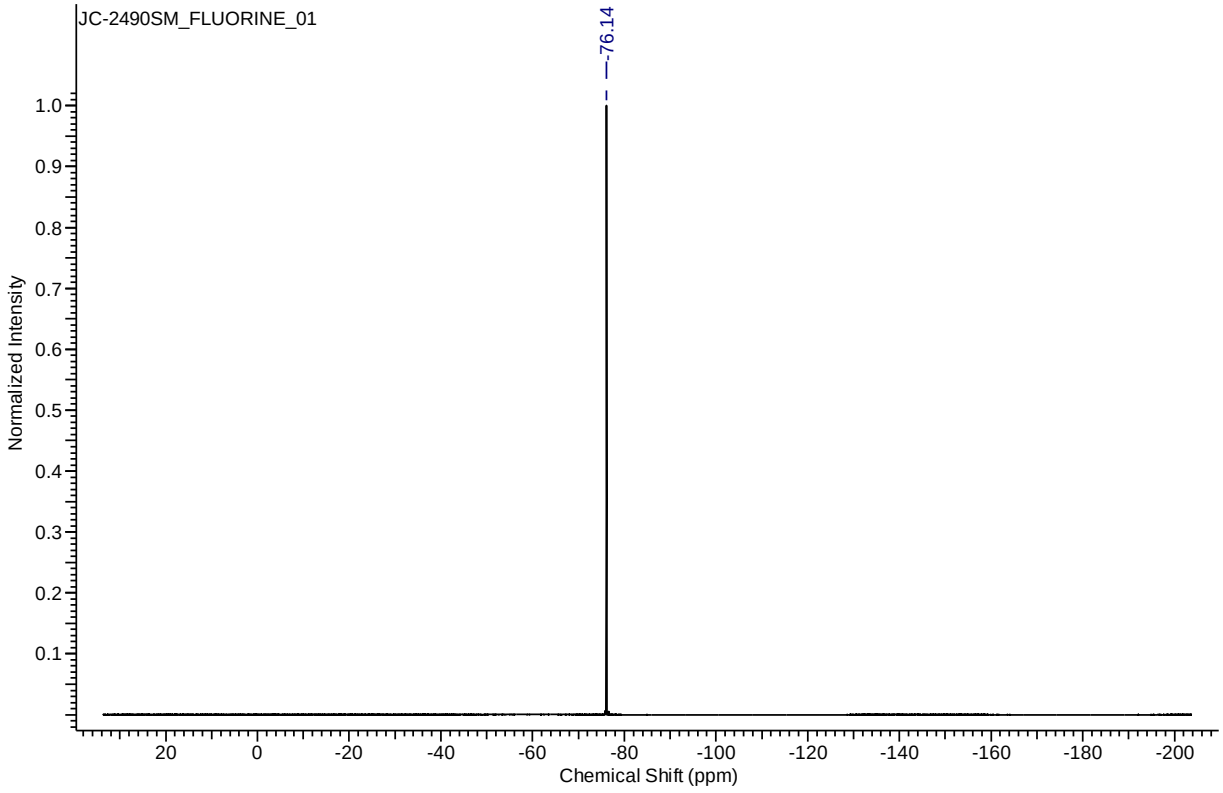
JC-2490SM_FLUORINE_01
-76.14
Normalized Intensity
Chemical Shift (ppm)

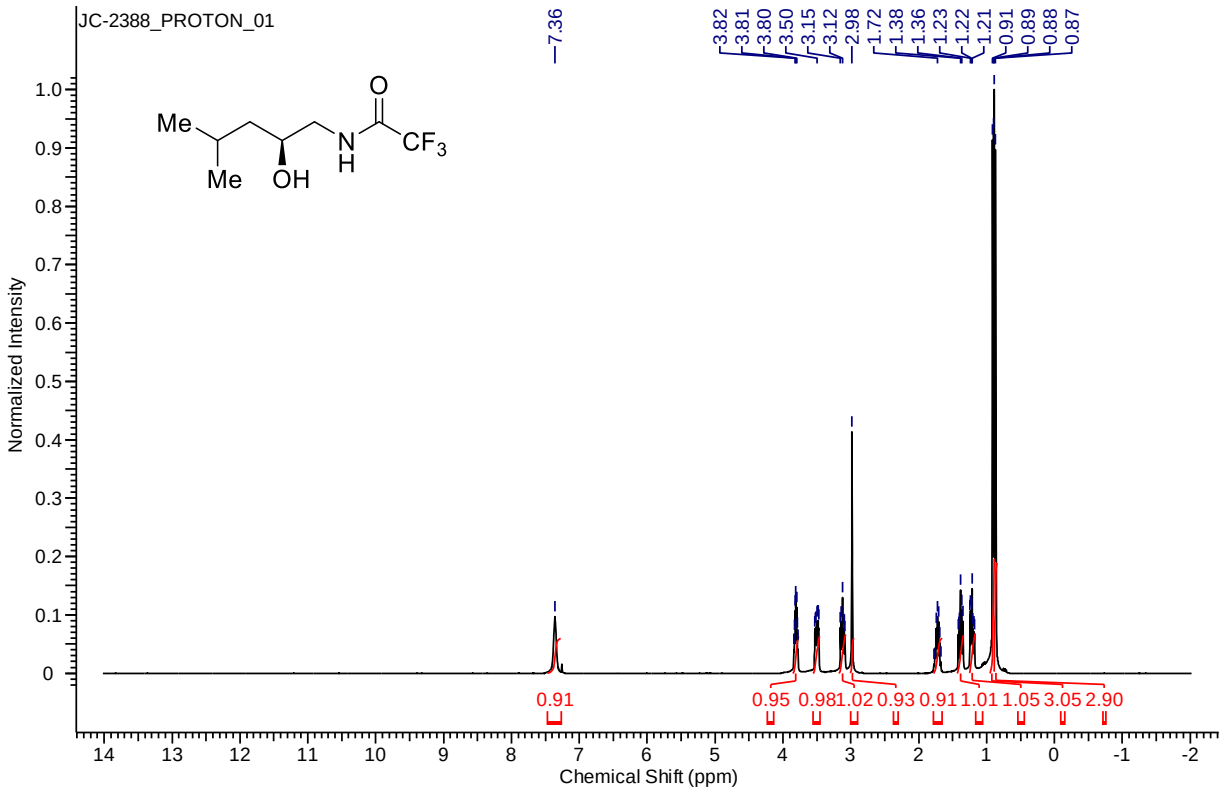
JC-2388_PROTON_01
7.36
3.82
3.81
3.80
3.50
3.15
3.12
2.98
1.72
1.38
1.36
1.23
1.22
1.21
0.91
0.89
0.88
0.87
Me
Me
OH
N
H
O
CF3
Normalized Intensity
Chemical Shift (ppm)
0.91
0.95
0.98
1.02
0.93
0.91
1.01
1.05
3.05
2.90

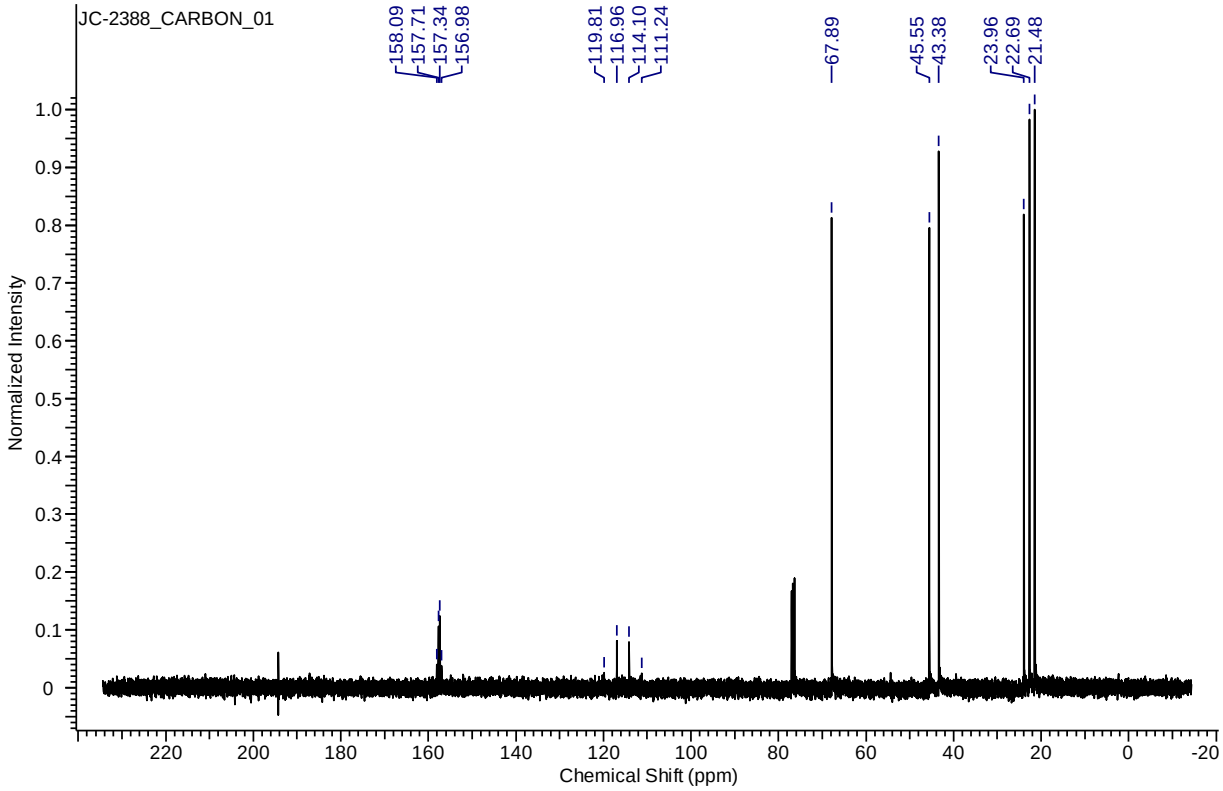
JC-2388_CARBON_01
158.09
157.71
157.34
156.98
119.81
116.96
114.10
111.24
67.89
45.55
43.38
23.96
22.69
21.48
Normalized Intensity
Chemical Shift (ppm)

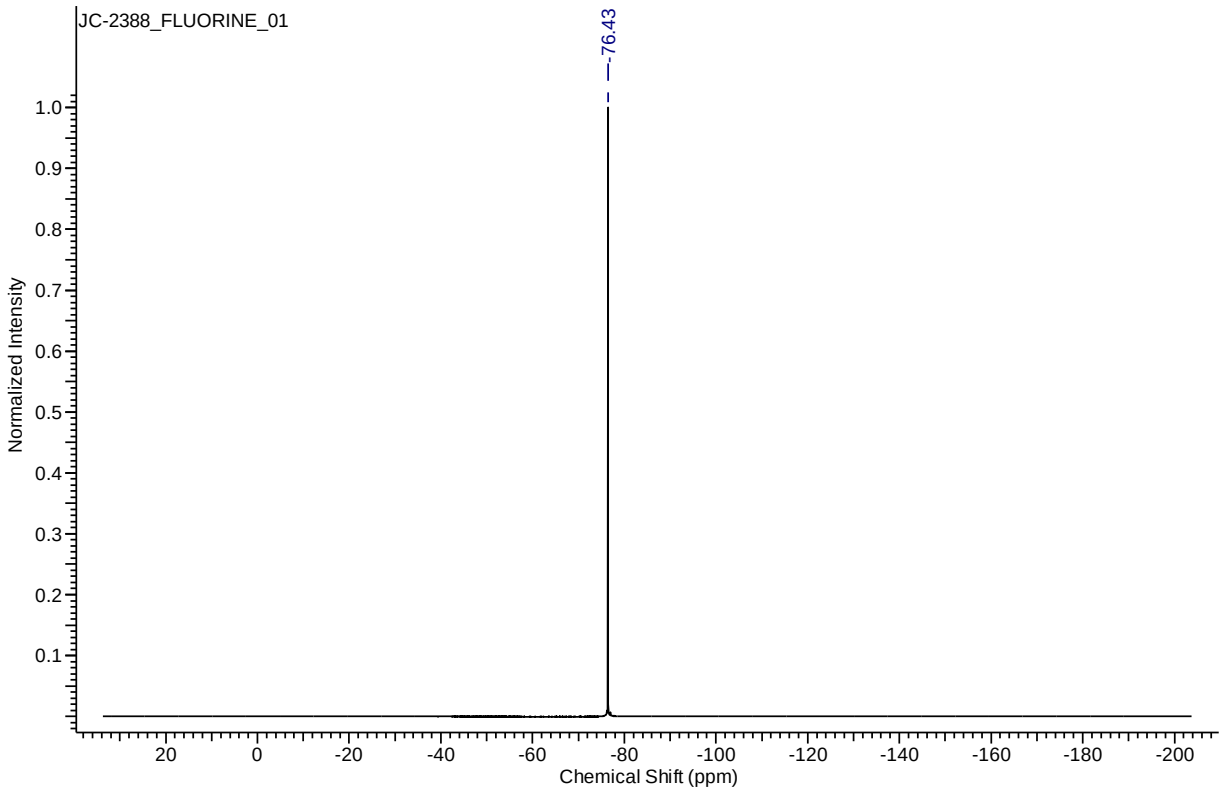
JC-2388_FLUORINE_01
-76.43
Normalized Intensity
Chemical Shift (ppm)

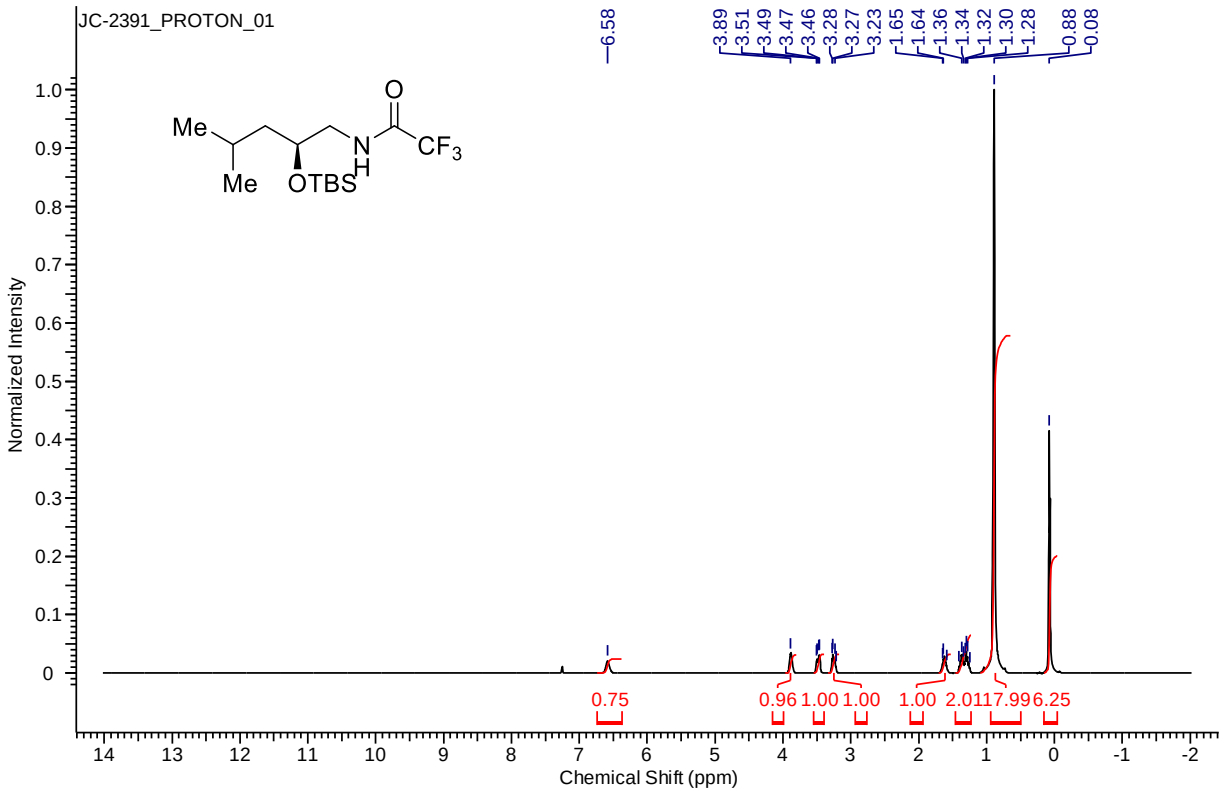
JC-2391_PROTON_01
6.58
3.89
3.51
3.49
3.47
3.46
3.28
3.27
3.23
1.65
1.64
1.36
1.34
1.32
1.30
1.28
0.88
0.08
Me
Me
OTBS
N
H
O
CF3
0.75
0.96
1.00
1.00
1.00
2.01
17.99
6.25
Normalized Intensity
Chemical Shift (ppm)

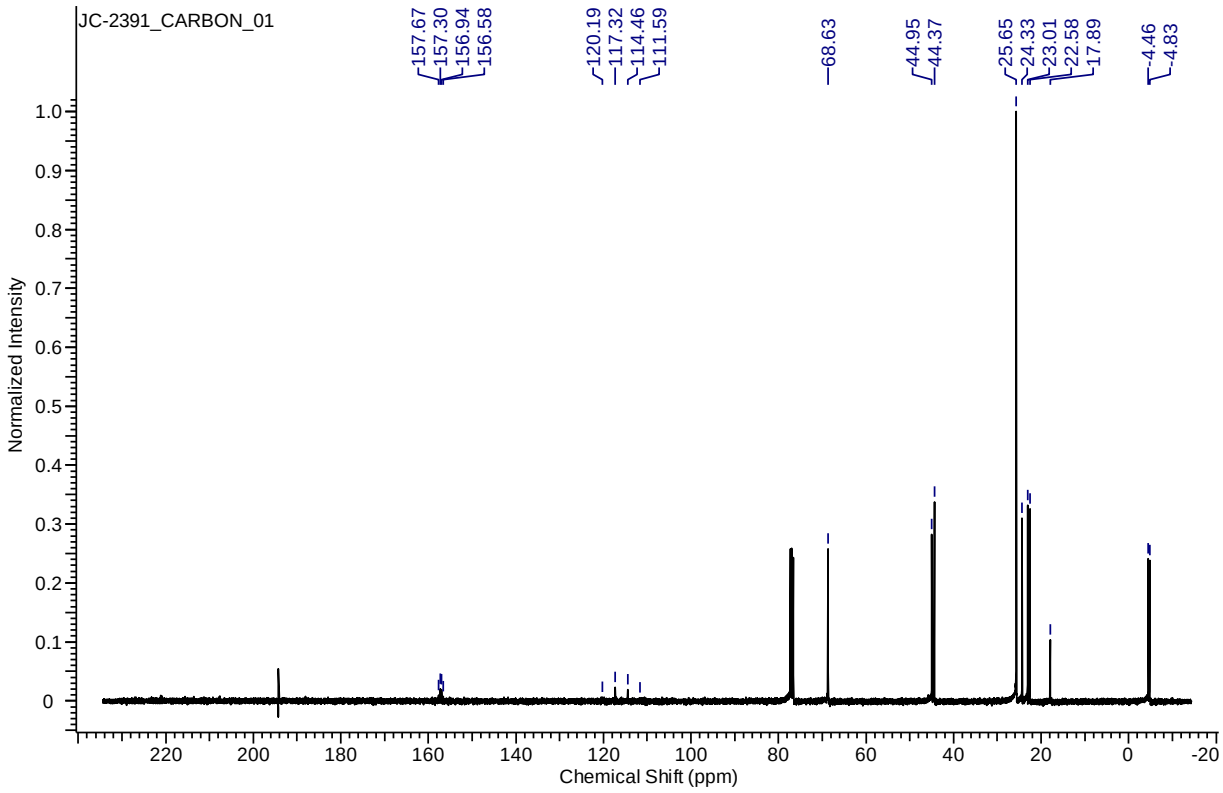
JC-2391_CARBON_01
157.67
157.30
156.94
156.58
120.19
117.32
114.46
111.59
68.63
44.95
44.37
25.65
24.33
23.01
22.58
17.89
-4.46
-4.83
Normalized Intensity
Chemical Shift (ppm)

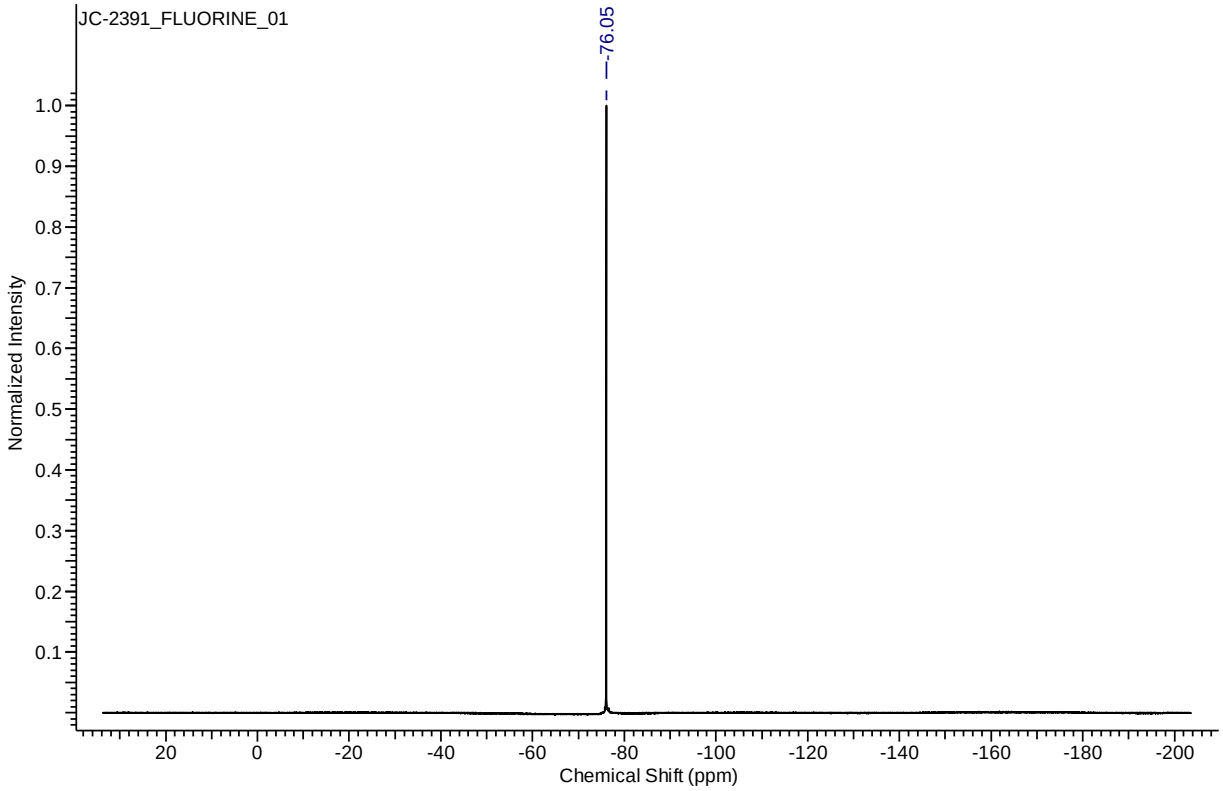
JC-2391_FLUORINE_01
-76.05
Normalized Intensity
Chemical Shift (ppm)

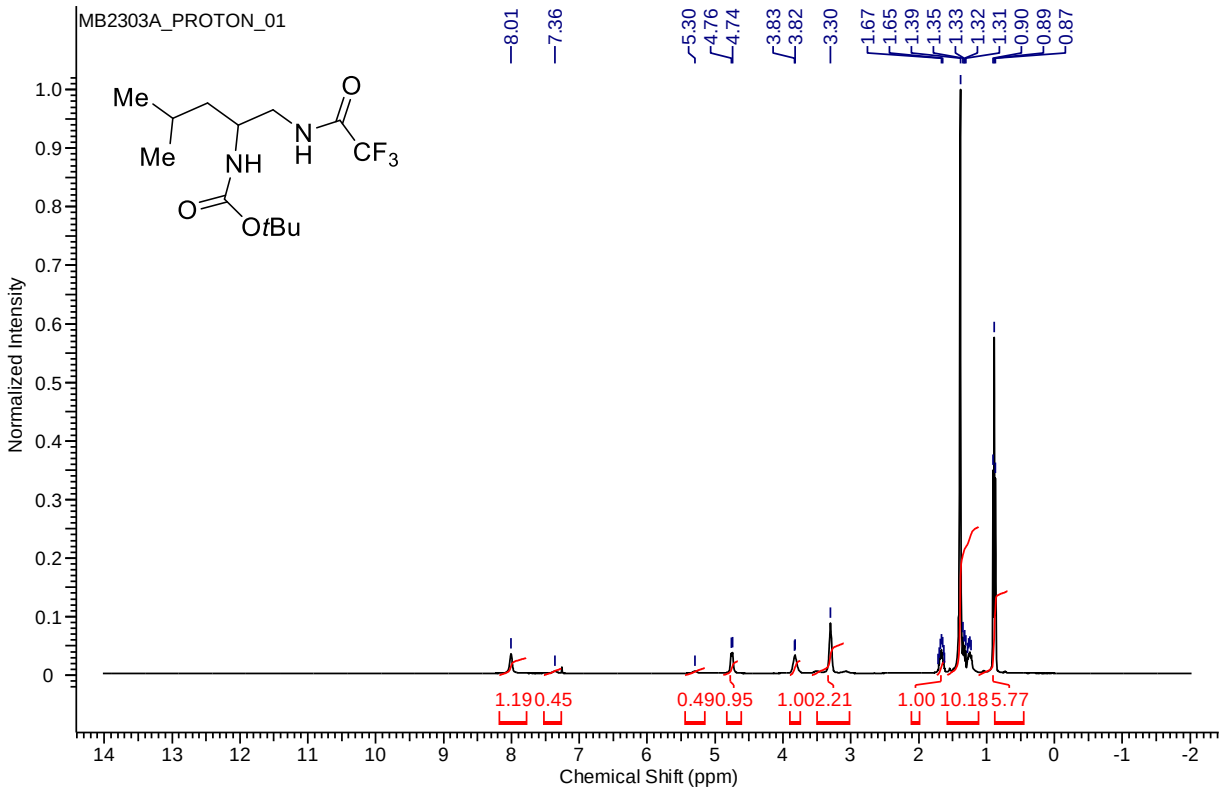
MB2303A_PROTON_01
8.01
7.36
5.30
4.76
4.74
3.83
3.82
3.30
1.67
1.65
1.39
1.35
1.33
1.32
1.31
0.90
0.89
0.87
Me
Me
NH
N
H
O
CF3
O
OtBu
1.19
0.45
0.49
0.95
1.00
2.21
1.00
10.18
5.77
Normalized Intensity
Chemical Shift (ppm)

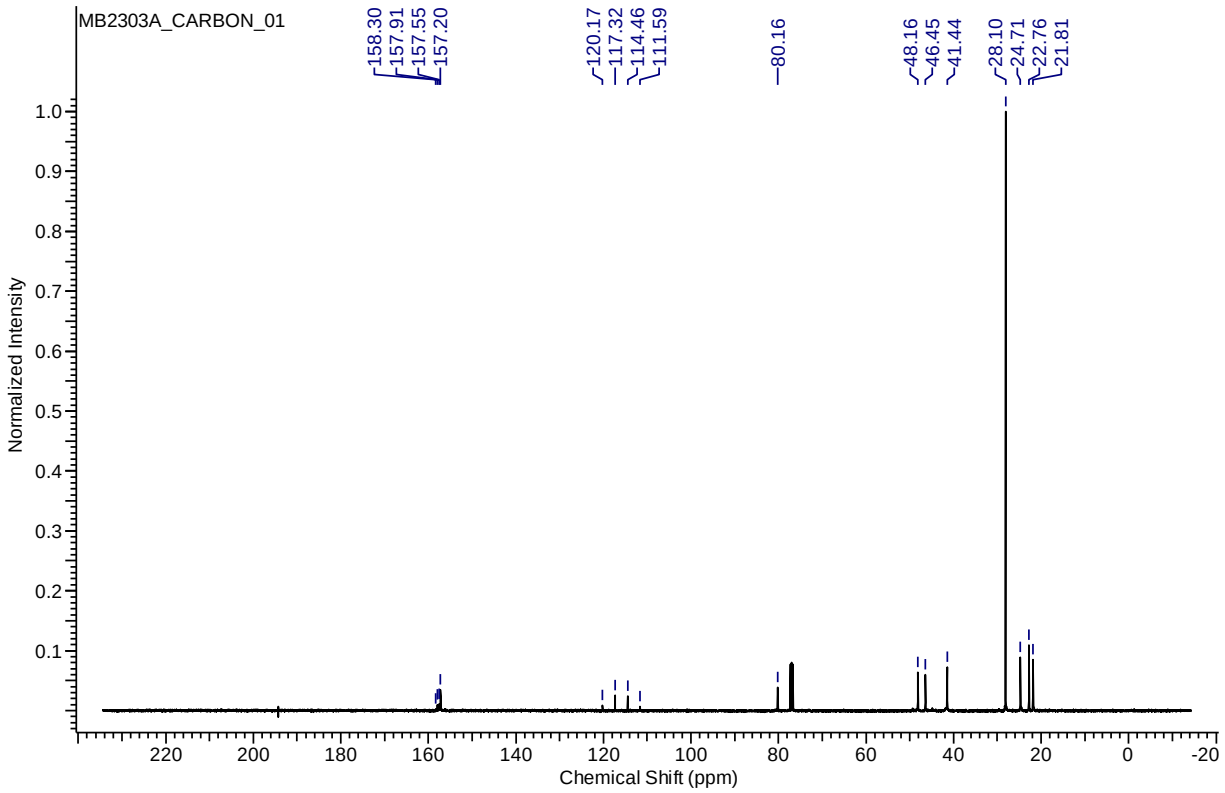
MB2303A_CARBON_01
158.30
157.91
157.55
157.20
120.17
117.32
114.46
111.59
80.16
48.16
46.45
41.44
28.10
24.71
22.76
21.81
Normalized Intensity
Chemical Shift (ppm)

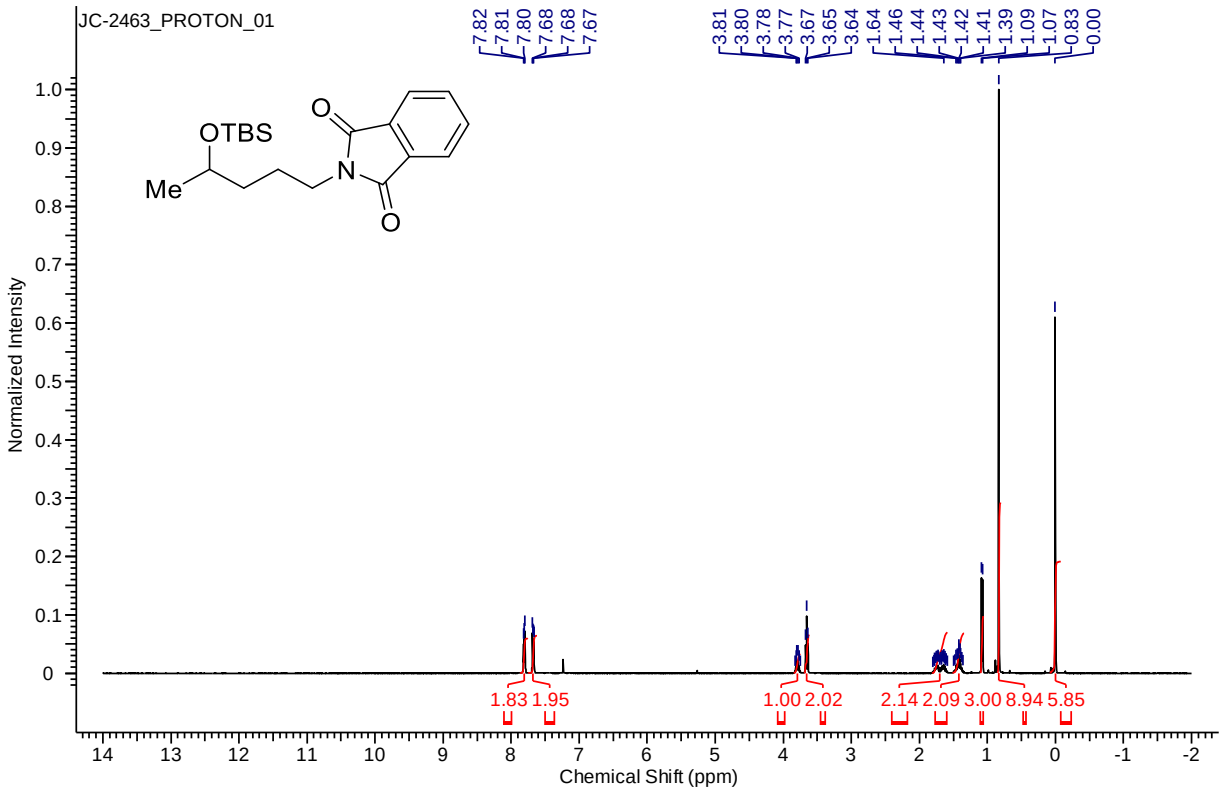
JC-2463_PROTON_01
7.82
7.81
7.80
7.68
7.68
7.67
3.81
3.80
3.78
3.77
3.67
3.65
3.64
1.64
1.46
1.44
1.43
1.42
1.41
1.39
1.09
1.07
0.83
0.00
OTBS
Me
N
O
O
Normalized Intensity
1.83 1.95
1.00 2.02
2.14 2.09 3.00 8.94 5.85
Chemical Shift (ppm)

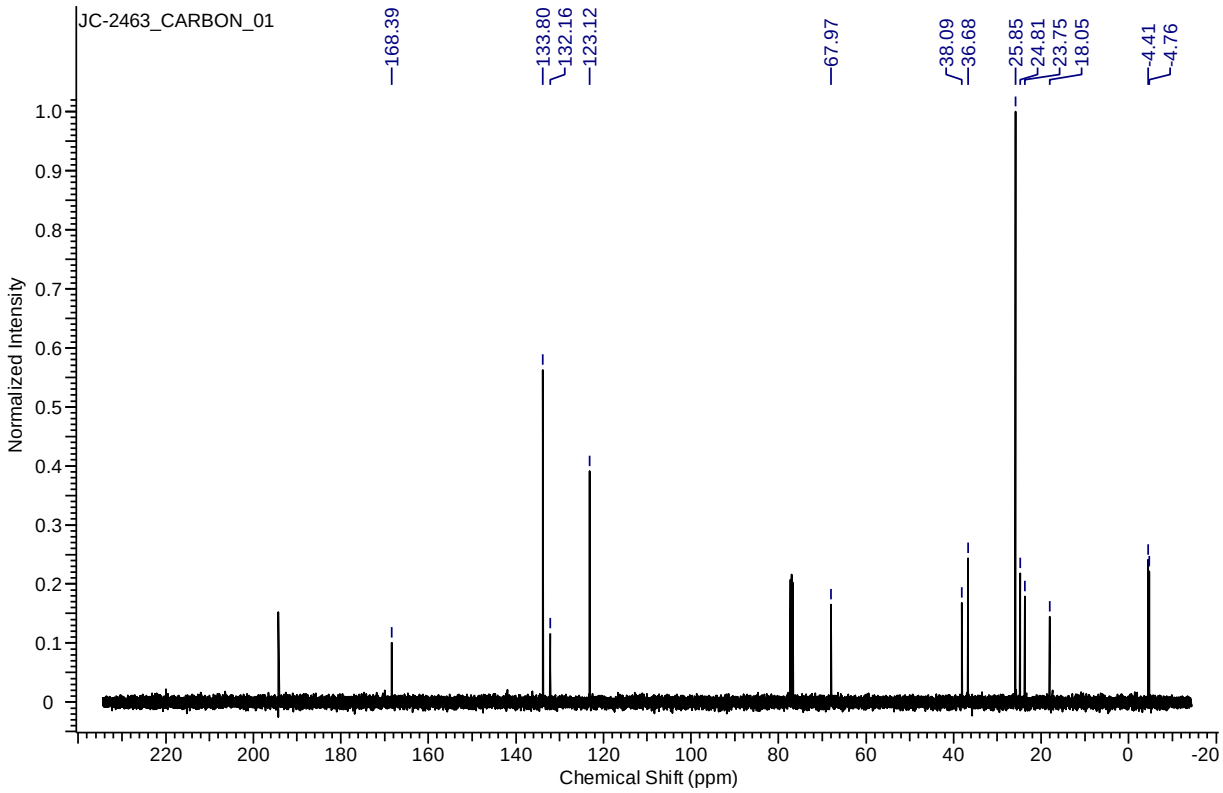
JC-2463_CARBON_01
168.39
133.80
132.16
123.12
67.97
38.09
36.68
25.85
24.81
23.75
18.05
-4.41
-4.76
Normalized Intensity
Chemical Shift (ppm)

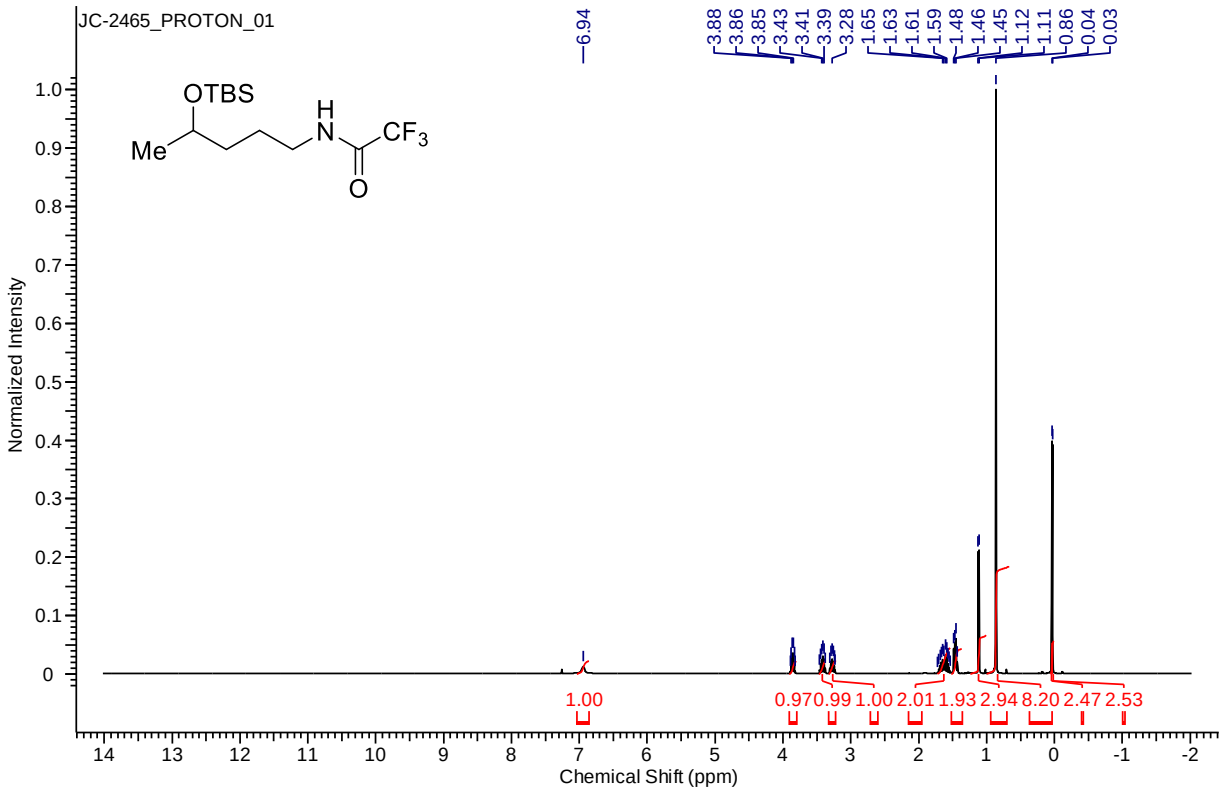
JC-2465_PROTON_01
OTBS
Me
H
N
CF3
O
6.94
3.88
3.86
3.85
3.43
3.41
3.39
3.28
1.65
1.63
1.61
1.59
1.48
1.46
1.45
1.12
1.11
0.86
0.04
0.03
1.00
0.97
0.99
1.00
2.01
1.93
2.94
8.20
2.47
2.53
Normalized Intensity
Chemical Shift (ppm)

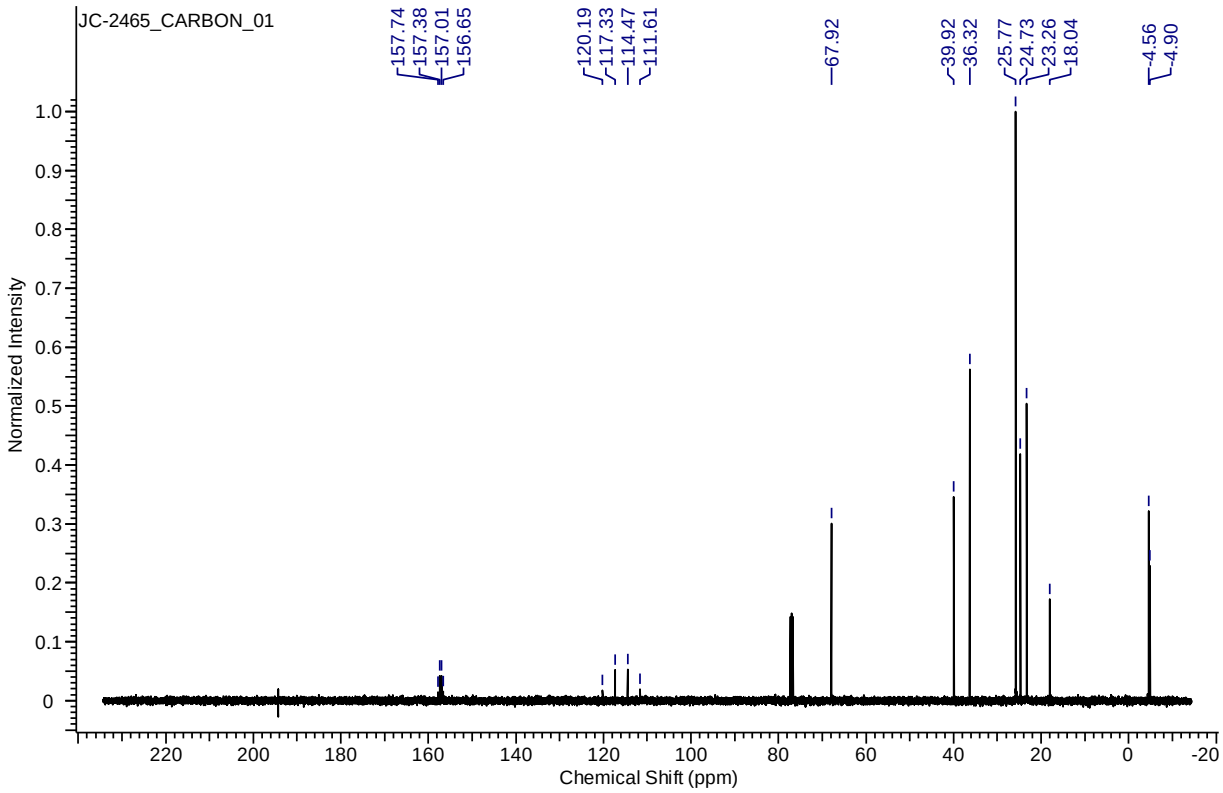
JC-2465_CARBON_01
157.74
157.38
157.01
156.65
120.19
117.33
114.47
111.61
67.92
39.92
36.32
25.77
24.73
23.26
18.04
4.56
4.90
Normalized Intensity
Chemical Shift (ppm)

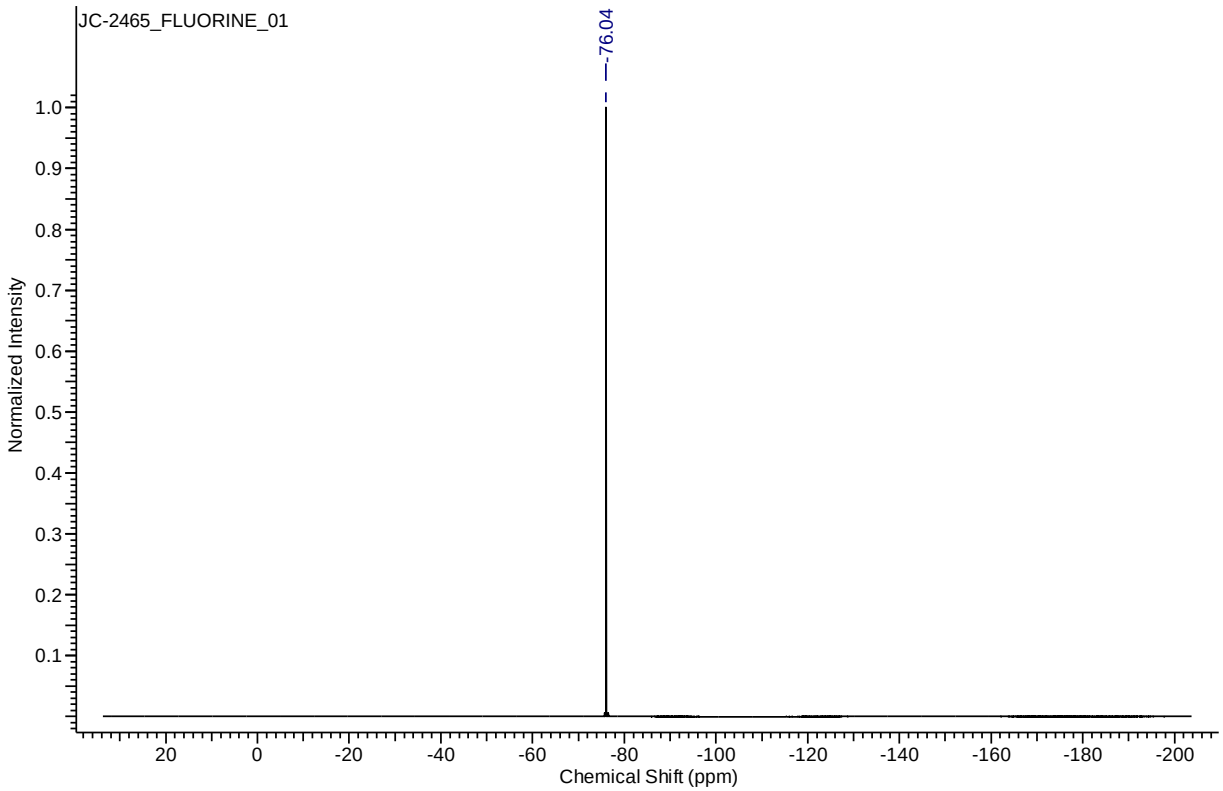
JC-2465_FLUORINE_01
-76.04
Normalized Intensity
Chemical Shift (ppm)

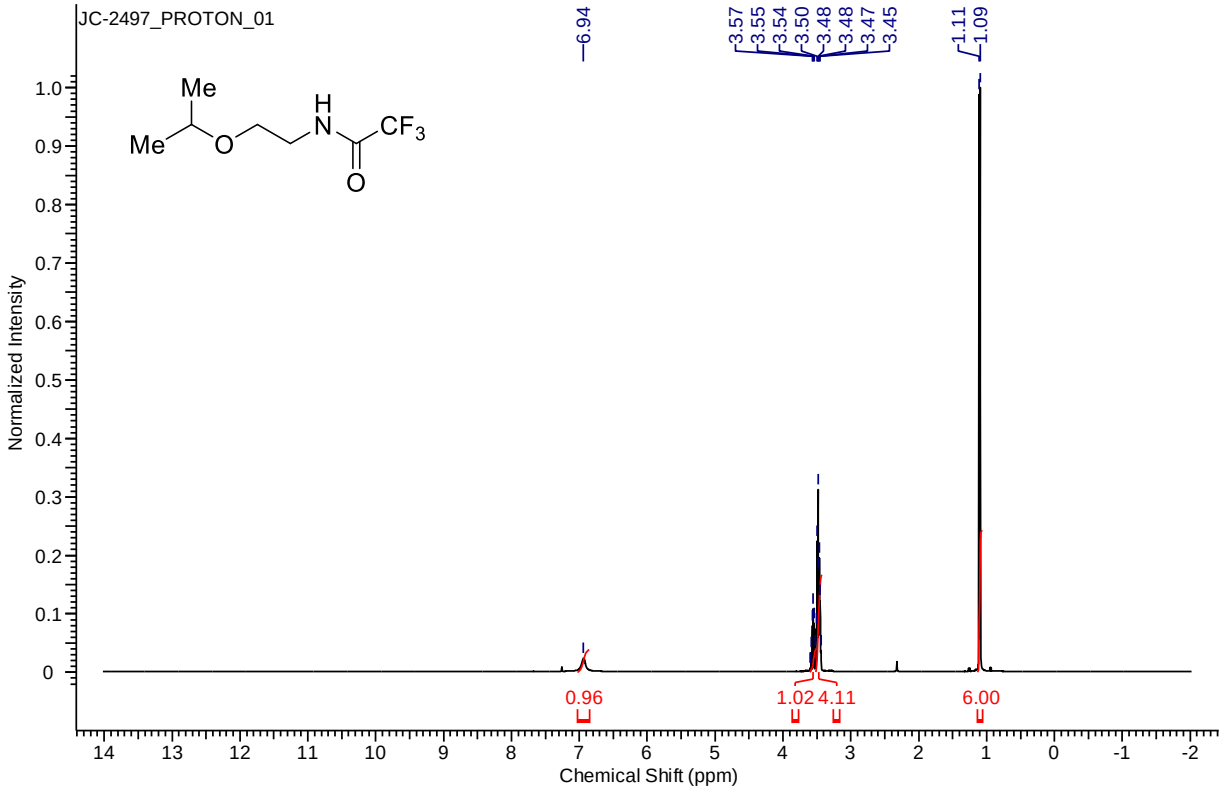
JC-2497_PROTON_01
6.94
3.57
3.55
3.54
3.50
3.48
3.48
3.47
3.45
1.11
1.09
Me
Me
O
H
N
CF3
O
0.96
1.02
4.11
6.00
Normalized Intensity
Chemical Shift (ppm)

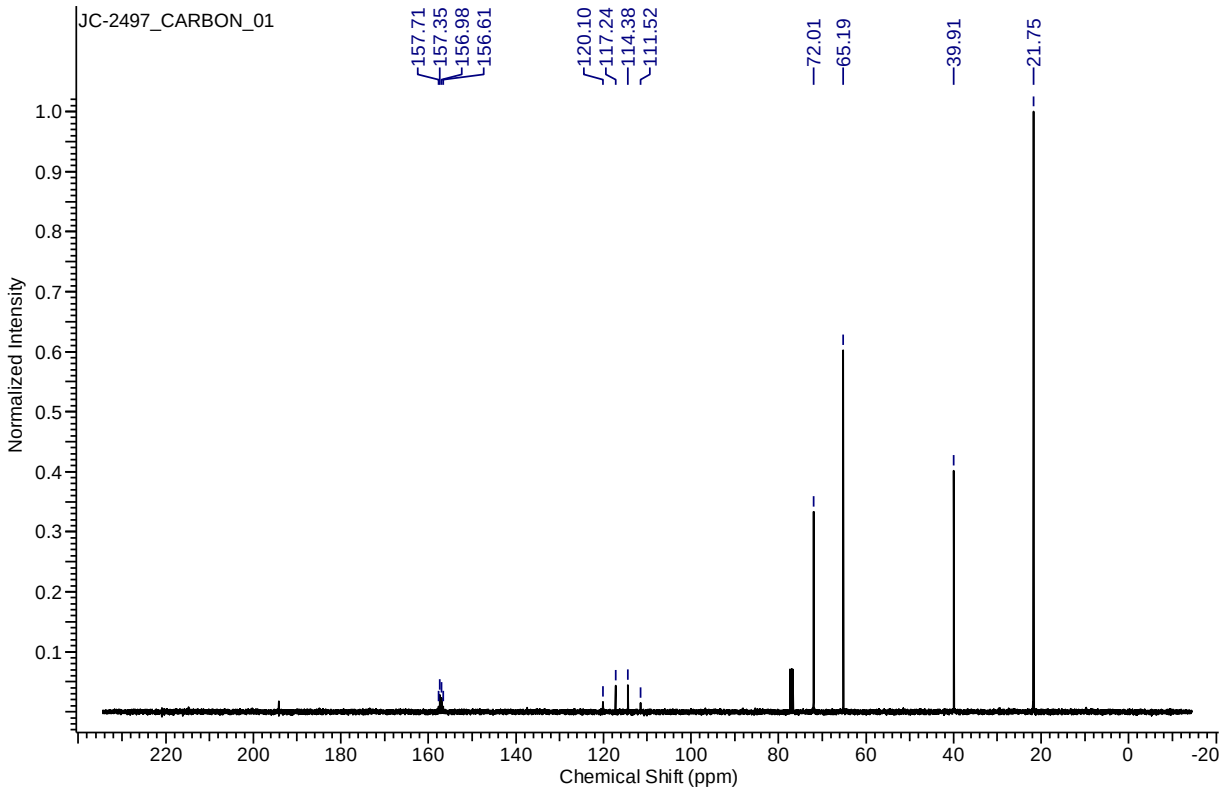
JC-2497_CARBON_01
157.71
157.35
156.98
156.61
120.10
117.24
114.38
111.52
72.01
65.19
39.91
21.75
Normalized Intensity
Chemical Shift (ppm)

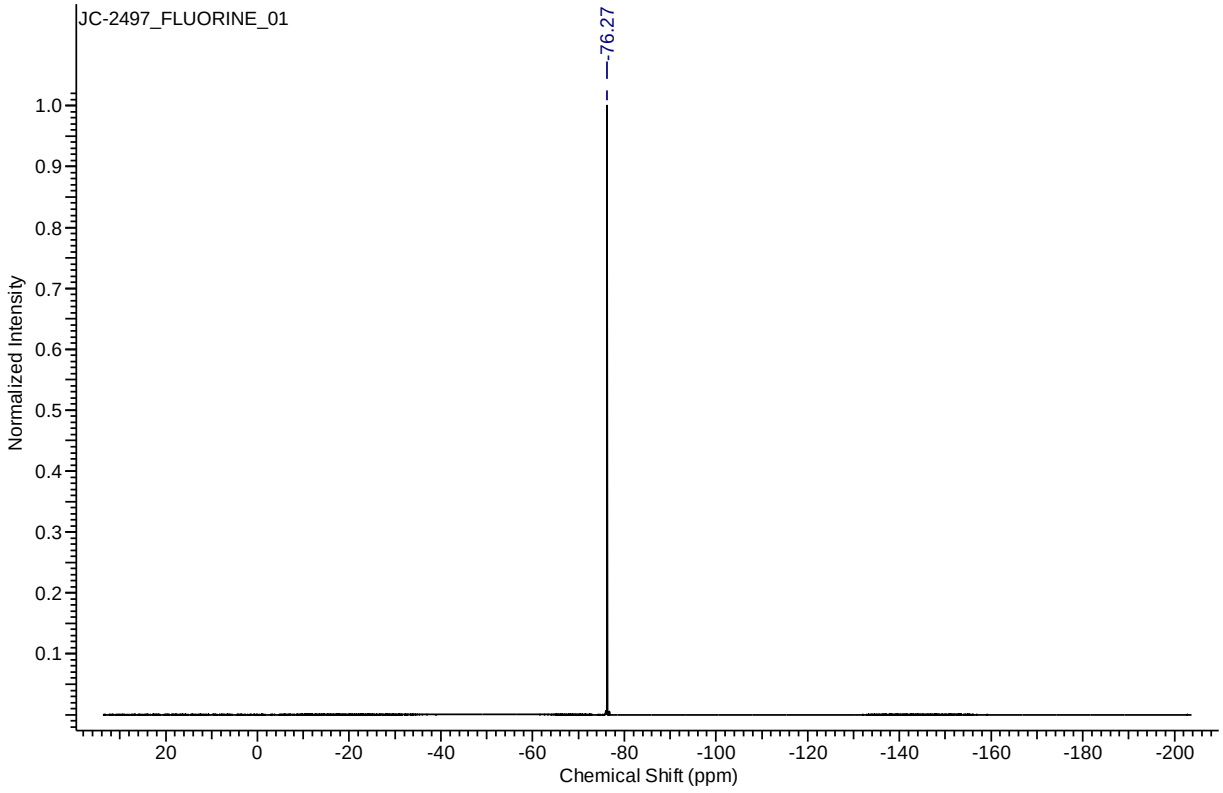
JC-2497_FLUORINE_01
-76.27
Normalized Intensity
Chemical Shift (ppm)

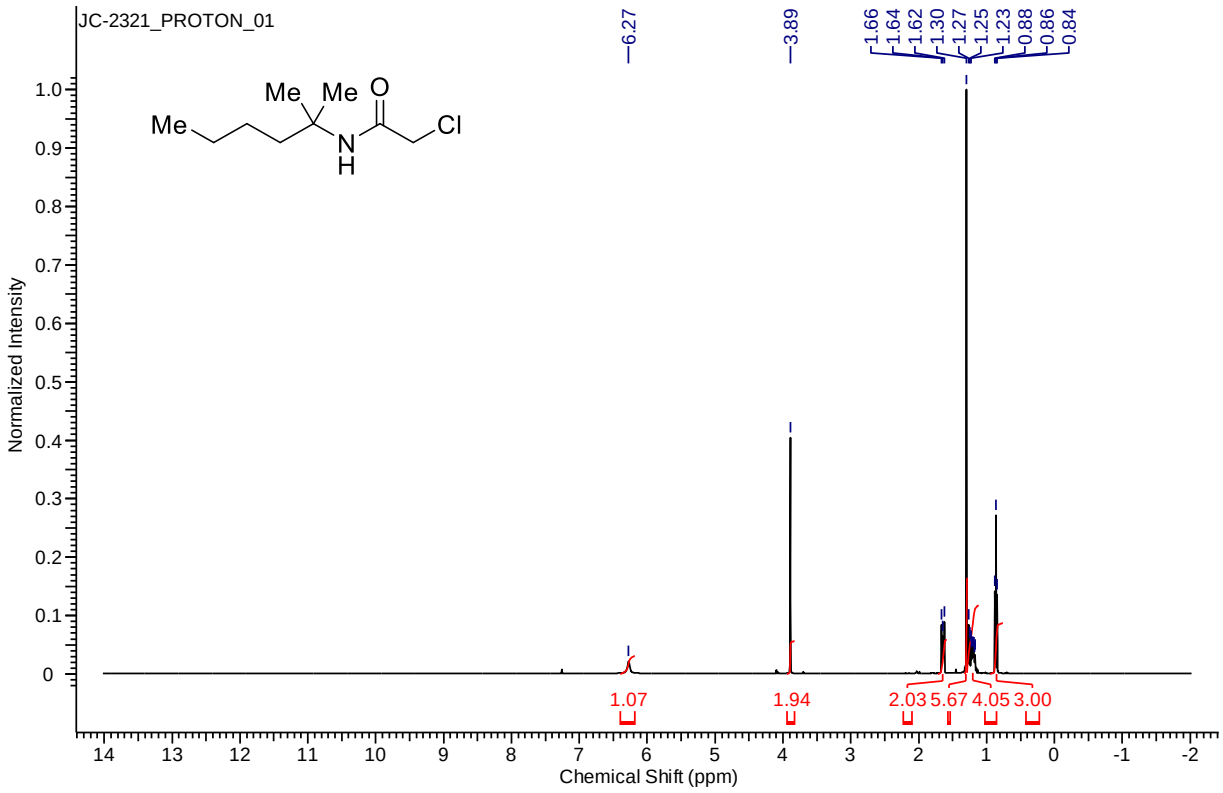
JC-2321_PROTON_01
6.27
3.89
1.66
1.64
1.62
1.30
1.27
1.25
1.23
0.88
0.86
0.84
Me
Me
Me
O
N
H
Cl
1.07
1.94
2.03
5.67
4.05
3.00
Normalized Intensity
Chemical Shift (ppm)

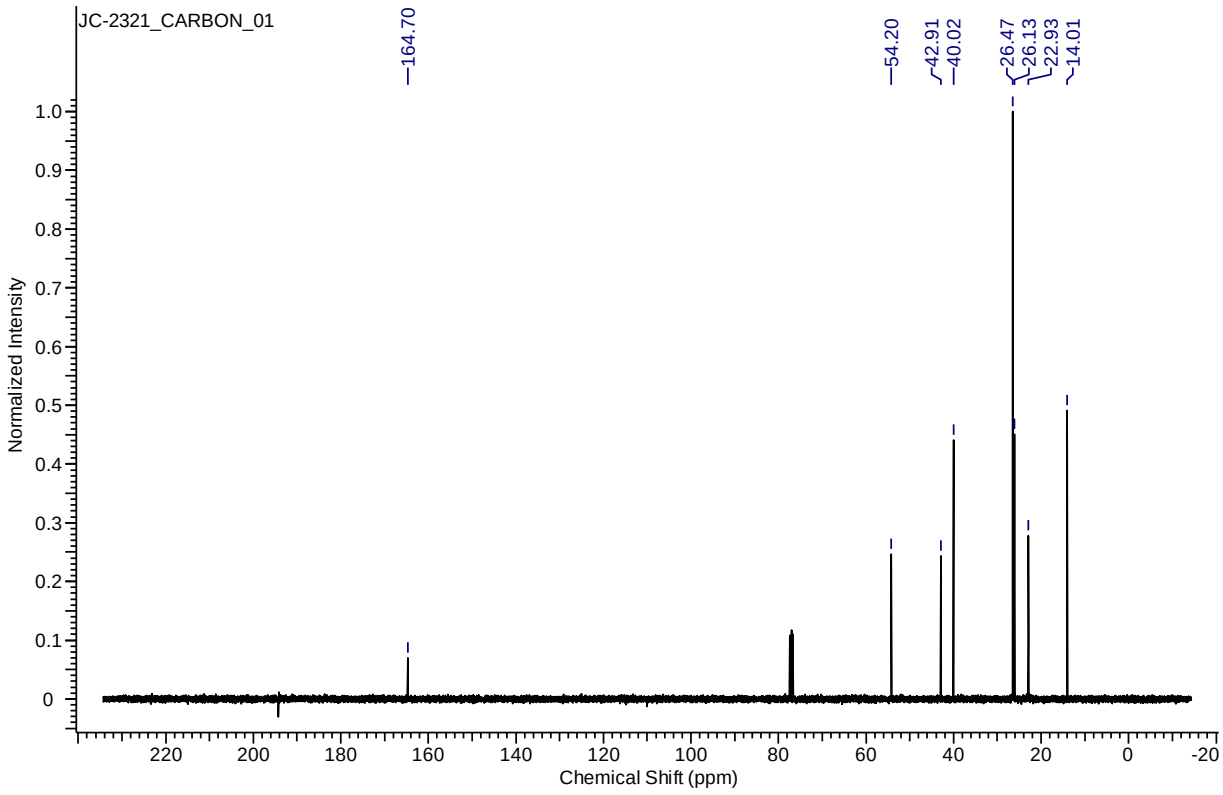
JC-2321_CARBON_01
164.70
54.20
42.91
40.02
26.47
26.13
22.93
14.01
Normalized Intensity
Chemical Shift (ppm)

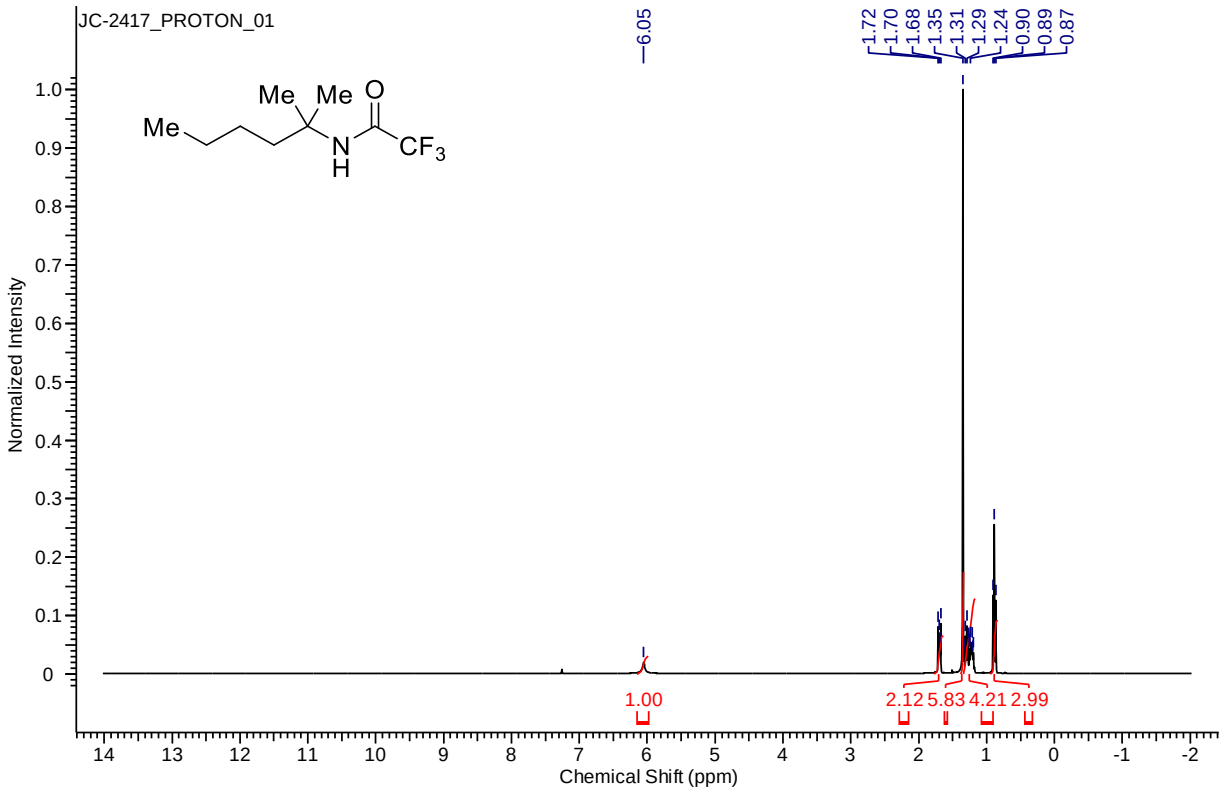
JC-2417_PROTON_01
6.05
1.72
1.70
1.68
1.35
1.31
1.29
1.24
0.90
0.89
0.87
Me
Me
Me
O
N
H
CF3
1.00
2.12
5.83
4.21
2.99
Normalized Intensity
Chemical Shift (ppm)

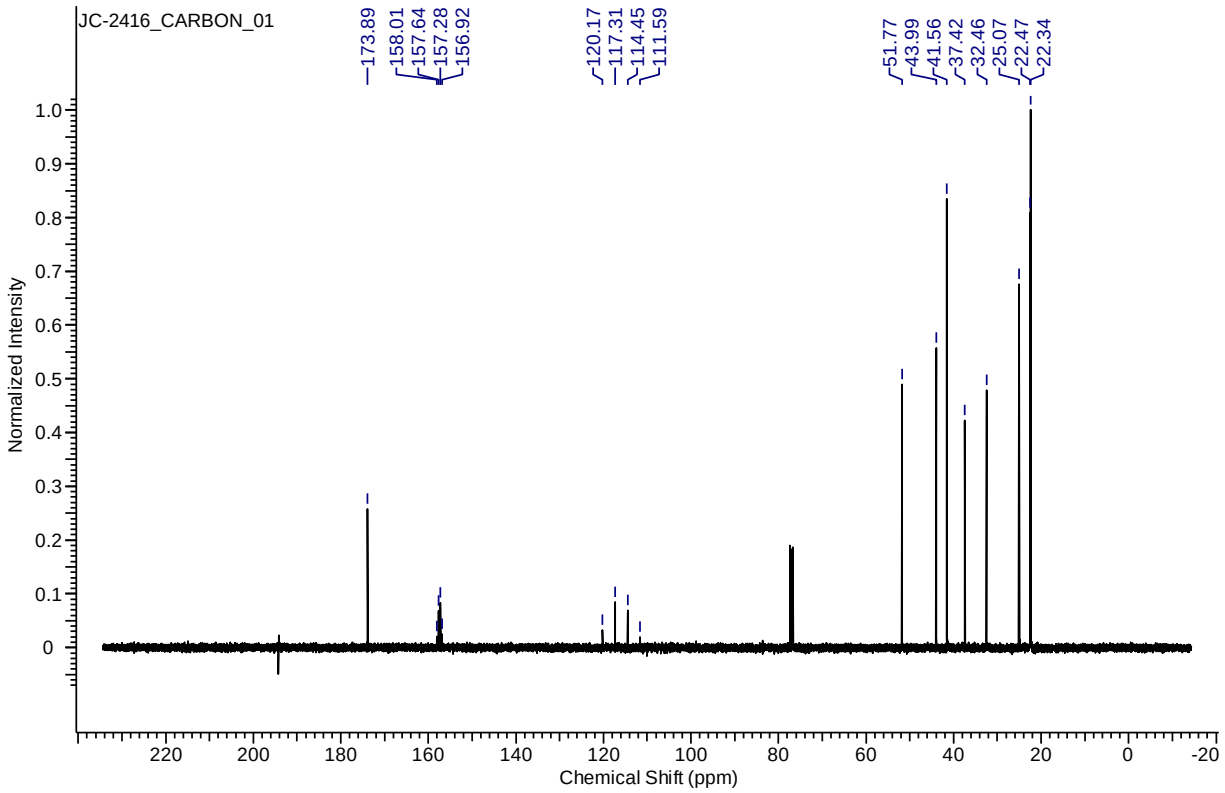
JC-2416_CARBON_01
173.89
158.01
157.64
157.28
156.92
120.17
117.31
114.45
111.59
51.77
43.99
41.56
37.42
32.46
25.07
22.47
22.34
Normalized Intensity
Chemical Shift (ppm)

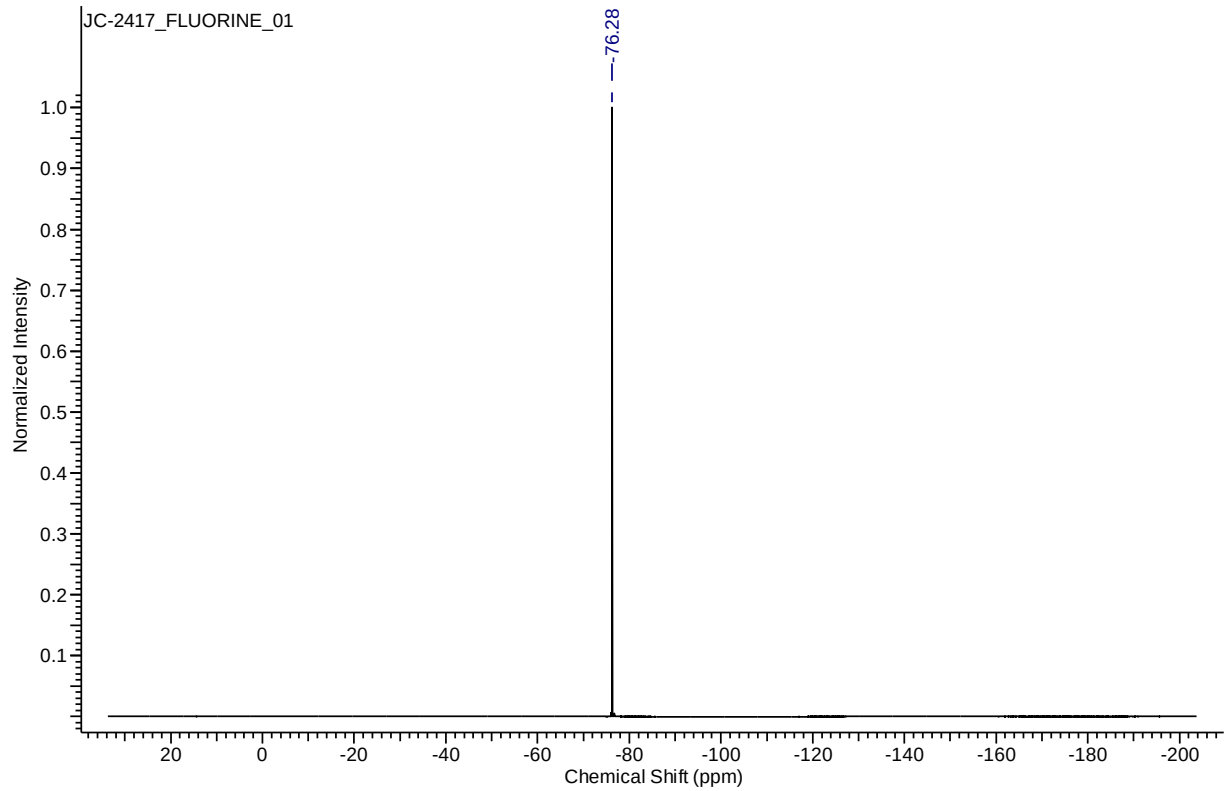
JC-2417_FLUORINE_01
-76.28
Normalized Intensity
Chemical Shift (ppm)

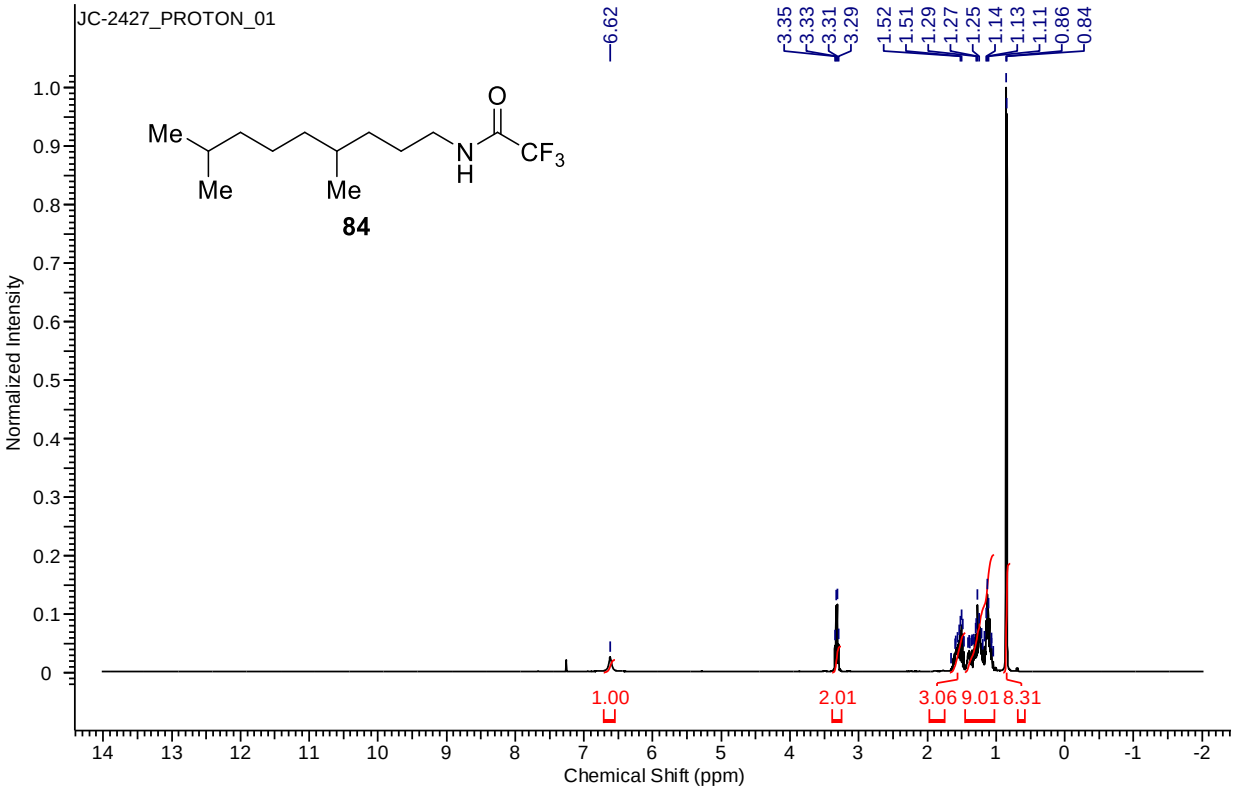
JC-2427_PROTON_01
6.62
3.35
3.33
3.31
3.29
1.52
1.51
1.29
1.27
1.25
1.14
1.13
1.11
0.86
0.84
Me
Me
Me
N
H
O
CF3
84
1.00
2.01
3.06
9.01
8.31
Normalized Intensity
Chemical Shift (ppm)

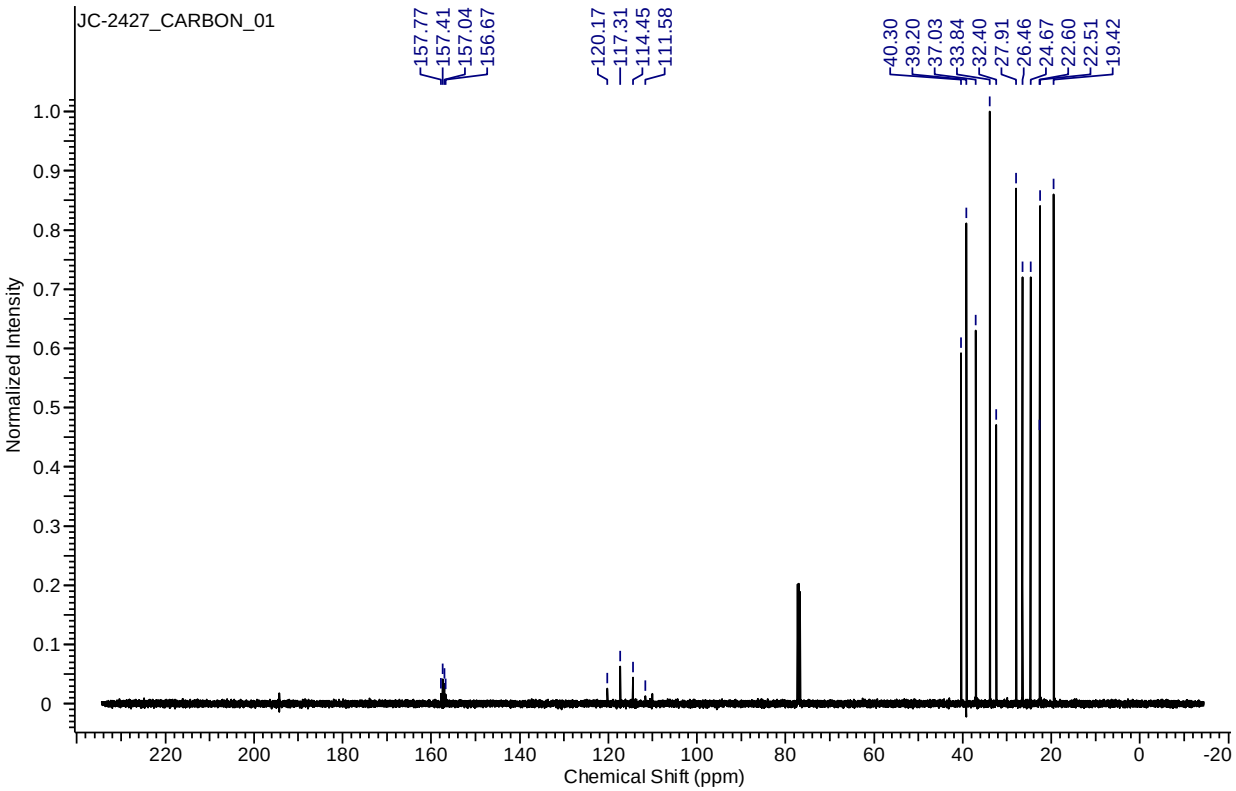
JC-2427_CARBON_01
157.77
157.41
157.04
156.67
120.17
117.31
114.45
111.58
40.30
39.20
37.03
33.84
32.40
27.91
26.46
24.67
22.60
22.51
19.42
Normalized Intensity
Chemical Shift (ppm)

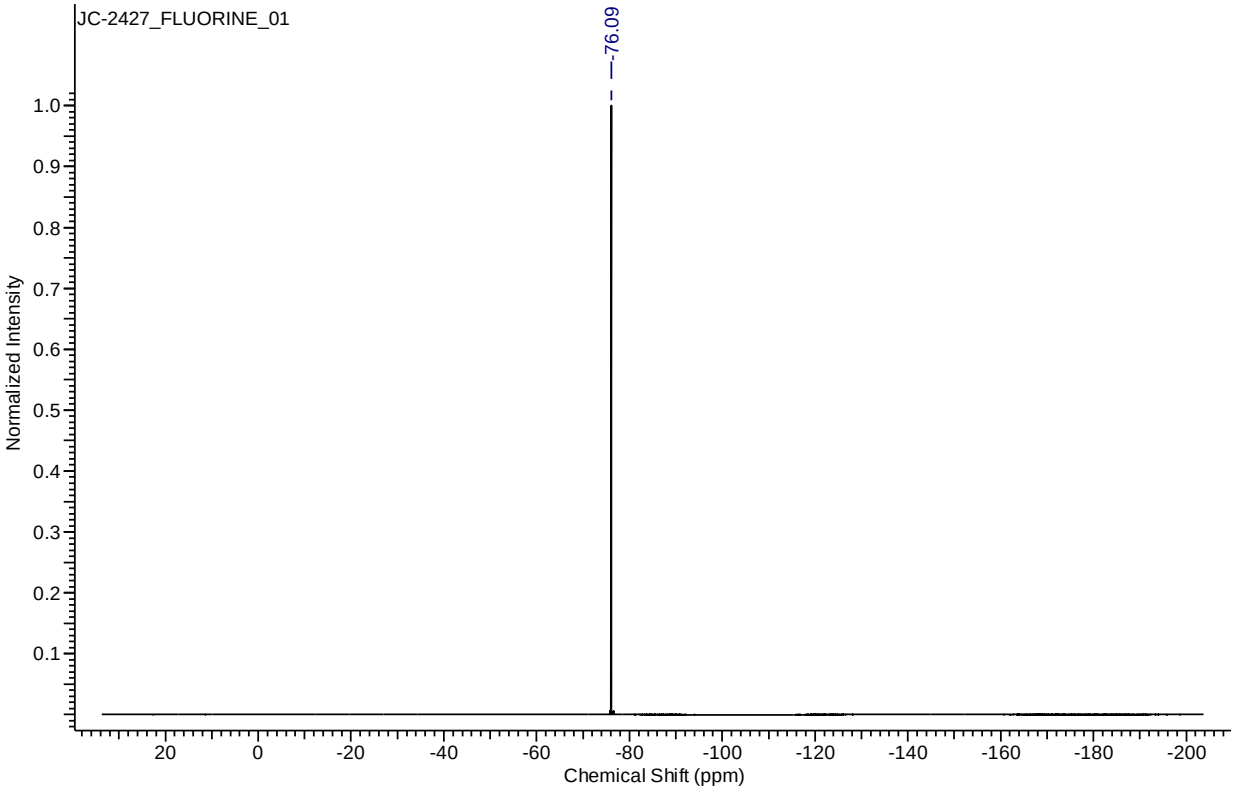
JC-2427_FLUORINE_01
-76.09
Normalized Intensity
Chemical Shift (ppm)

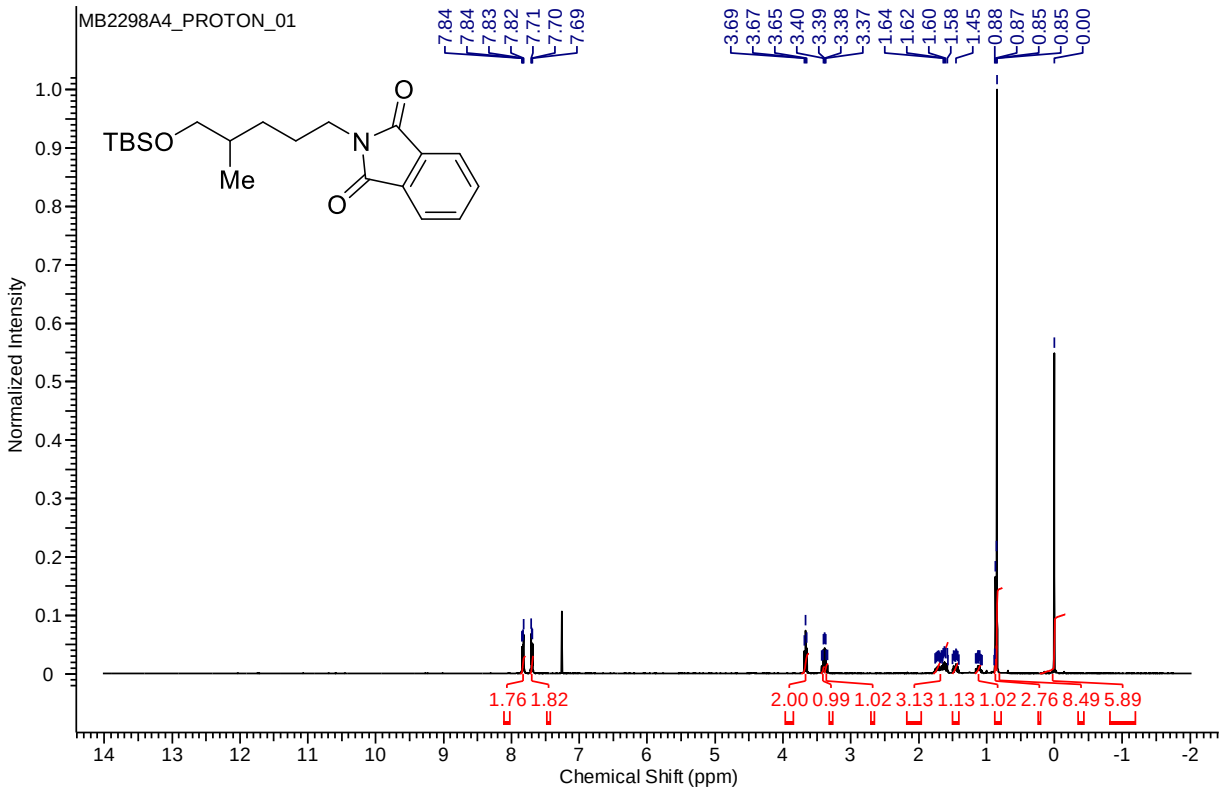
MB2298A4_PROTON_01
7.84
7.84
7.83
7.82
7.71
7.70
7.69
3.69
3.67
3.65
3.40
3.39
3.38
3.37
1.64
1.62
1.60
1.58
1.45
0.88
0.87
0.85
0.85
0.00
TBSO
Me
N
O
O
Normalized Intensity
1.76 1.82
2.00 0.99 1.02 3.13 1.13 1.02 2.76 8.49 5.89
Chemical Shift (ppm)

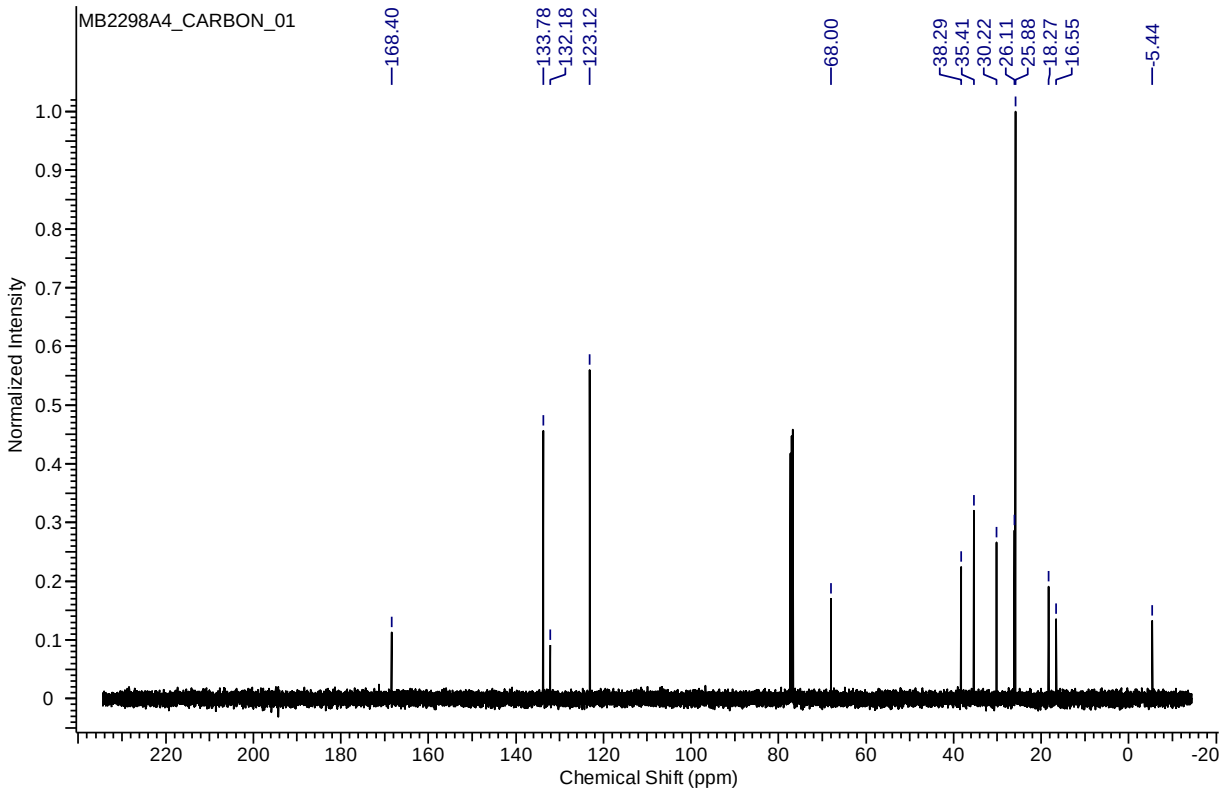
MB2298A4_CARBON_01
168.40
133.78
132.18
123.12
68.00
38.29
35.41
30.22
26.11
25.88
18.27
16.55
-5.44
Normalized Intensity
Chemical Shift (ppm)

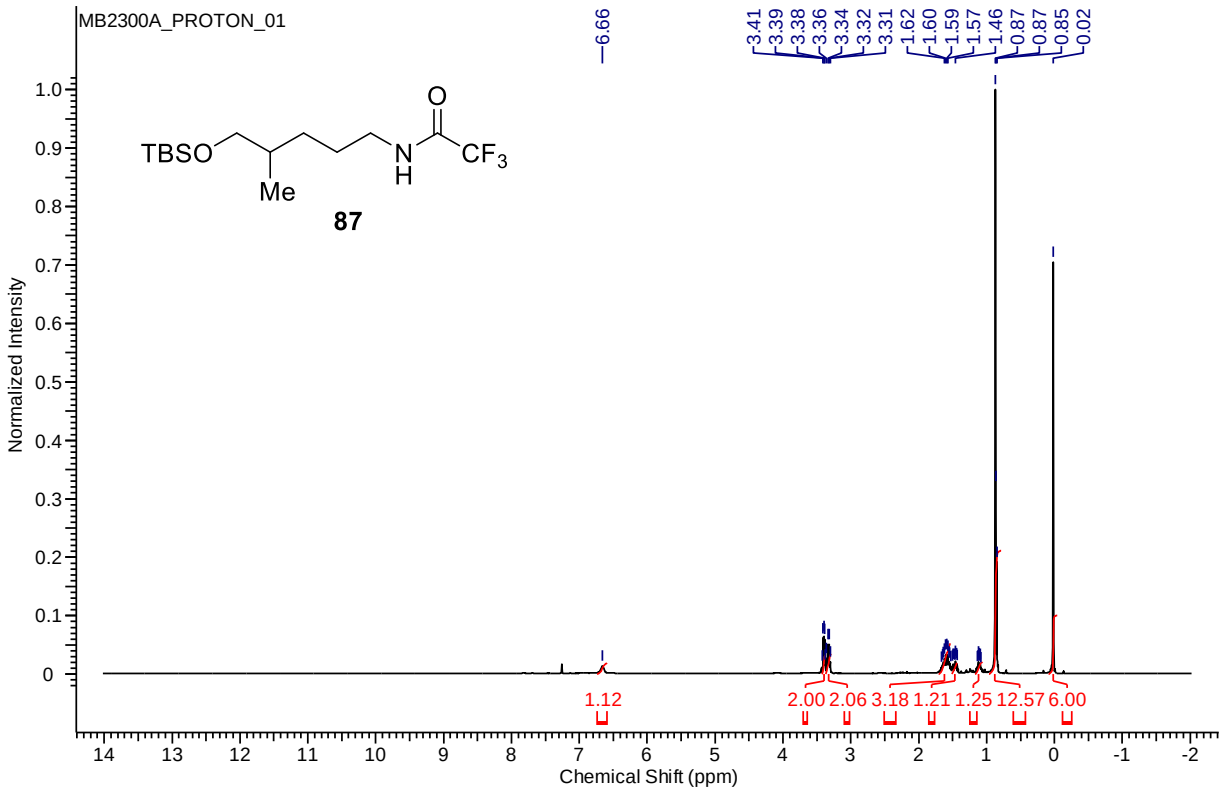
MB2300A_PROTON_01
6.66
3.41
3.39
3.38
3.36
3.34
3.32
3.31
1.62
1.60
1.59
1.57
1.46
0.87
0.87
0.85
0.02
TBSO
Me
N
H
O
CF3
87
Normalized Intensity
Chemical Shift (ppm)
1.12
2.00 2.06 3.18 1.21 1.25 12.57 6.00

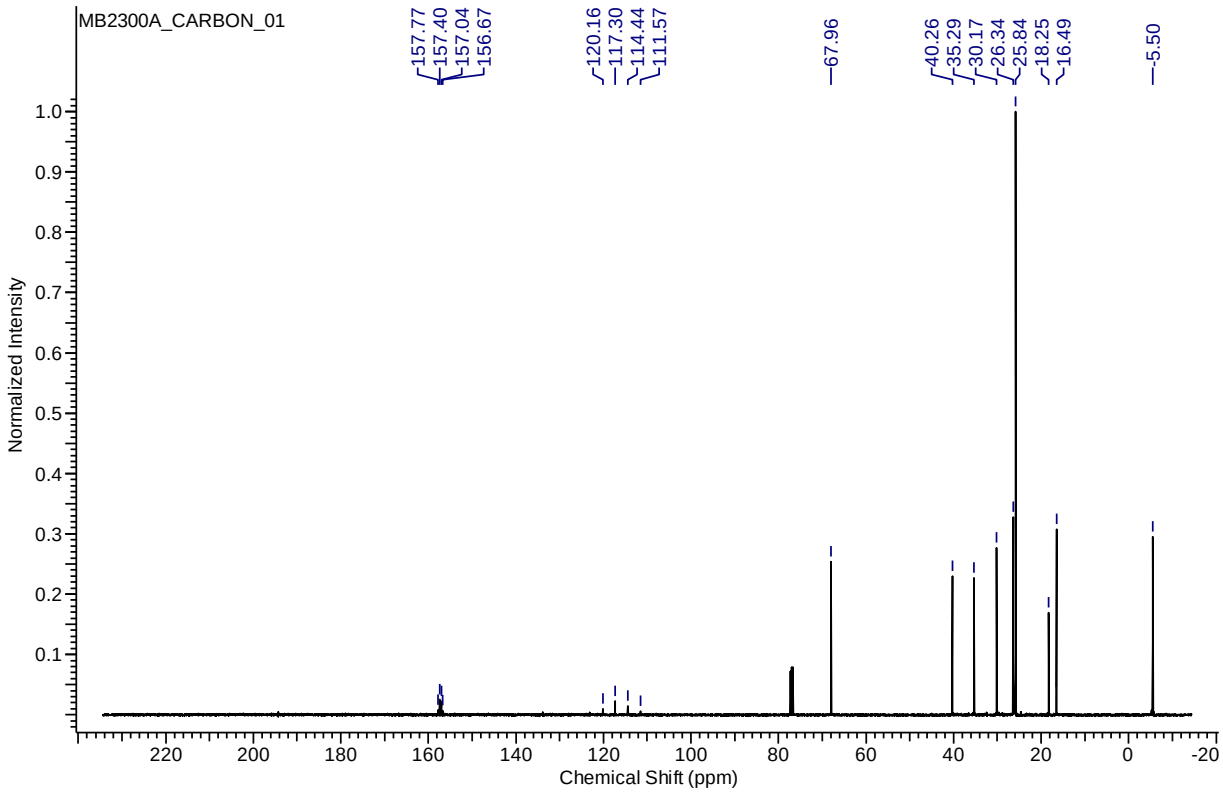
MB2300A_CARBON_01
157.77
157.40
157.04
156.67
120.16
117.30
114.44
111.57
67.96
40.26
35.29
30.17
26.34
25.84
18.25
16.49
-5.50
Normalized Intensity
Chemical Shift (ppm)

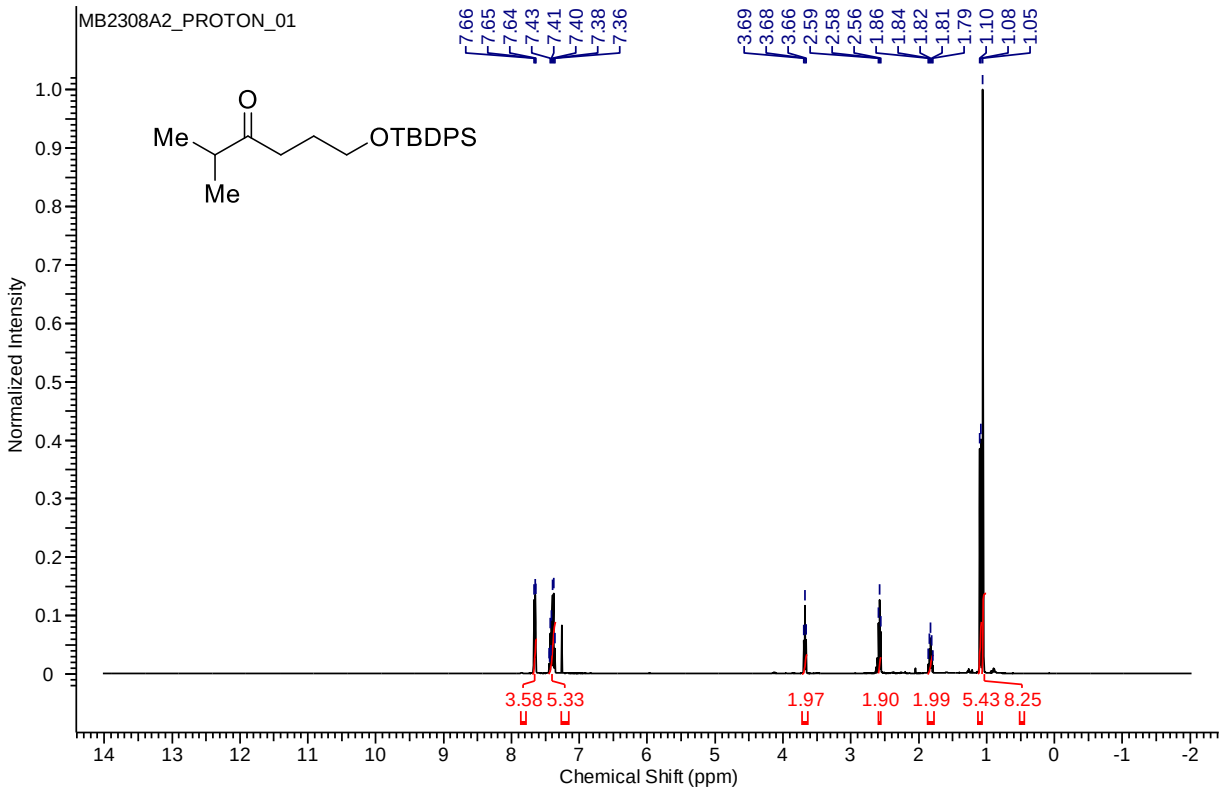
MB2308A2_PROTON_01
7.66
7.65
7.64
7.43
7.41
7.40
7.38
7.36
3.69
3.68
3.66
2.59
2.58
2.56
1.86
1.84
1.82
1.81
1.79
1.10
1.08
1.05
O
Me
OTBDPS
Me
Normalized Intensity
3.58
5.33
1.97
1.90
1.99
5.43
8.25
Chemical Shift (ppm)

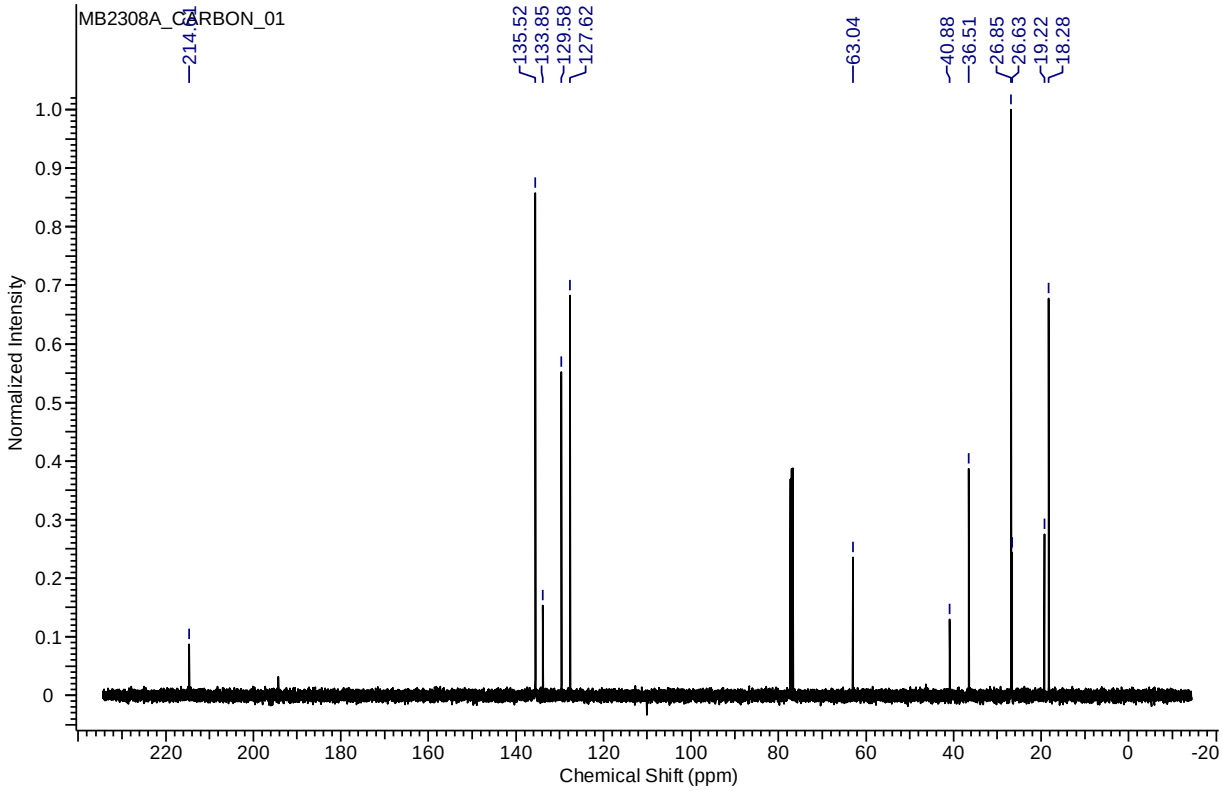
MB2308A_CARBON_01
214.21
135.52
133.85
129.58
127.62
63.04
40.88
36.51
26.85
26.63
19.22
18.28
Normalized Intensity
Chemical Shift (ppm)

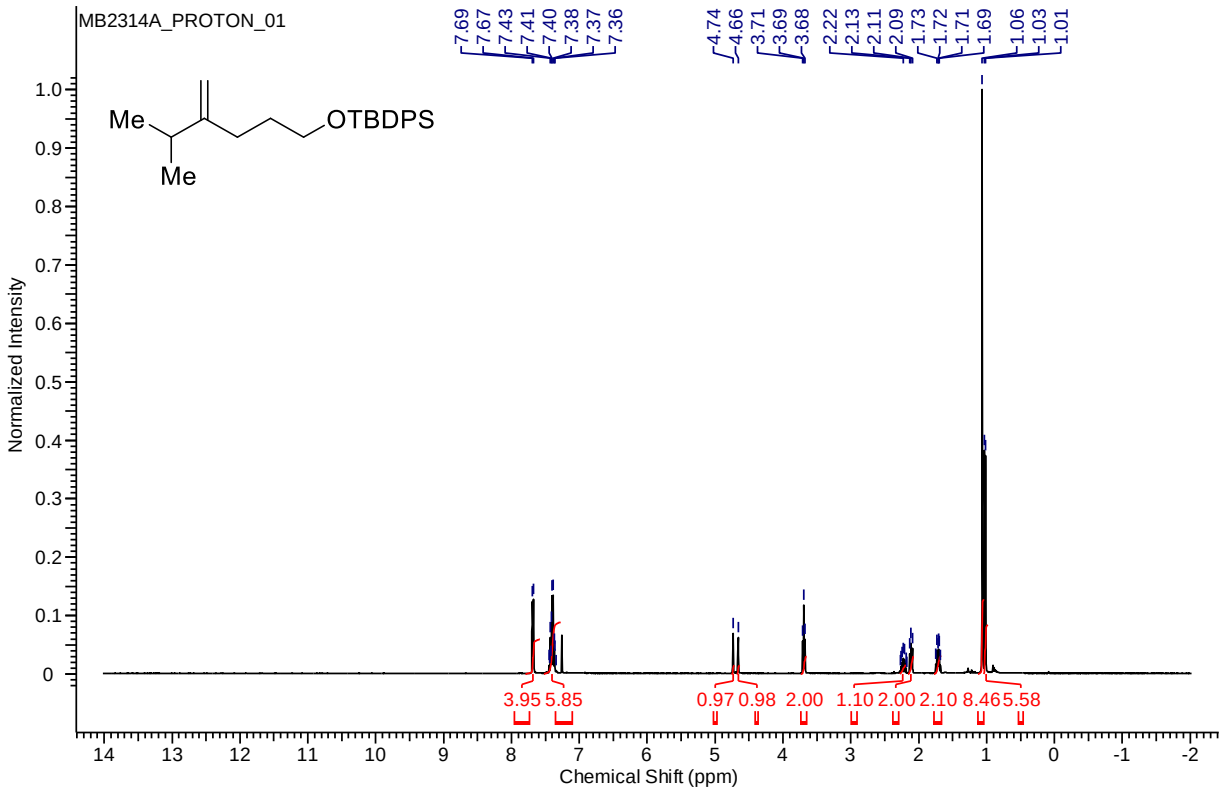
MB2314A_PROTON_01
7.69
7.67
7.43
7.41
7.40
7.38
7.37
7.36
4.74
4.66
3.71
3.69
3.68
2.22
2.13
2.11
2.09
1.73
1.72
1.71
1.69
1.06
1.03
1.01
Me
Me
OTBDPS
3.95
5.85
0.97
0.98
2.00
1.10
2.00
2.10
8.46
5.58
Normalized Intensity
Chemical Shift (ppm)

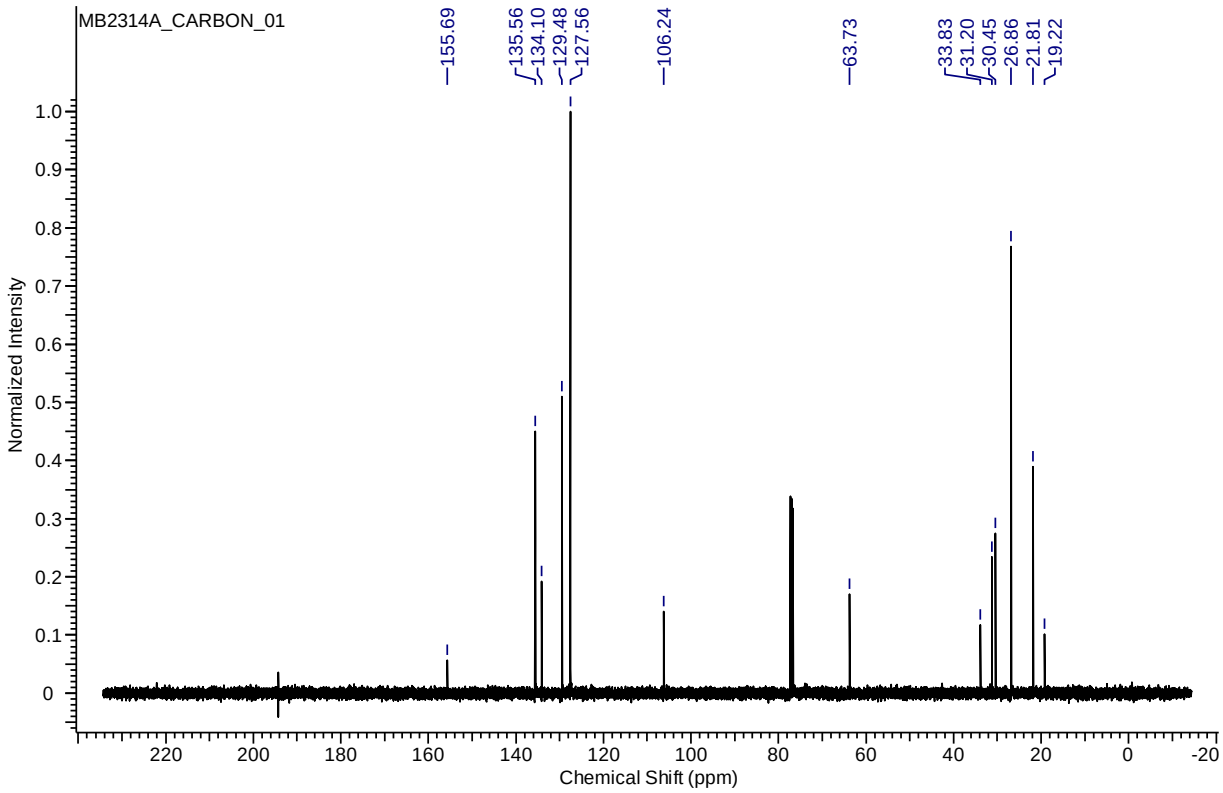
MB2314A_CARBON_01
155.69
135.56
134.10
129.48
127.56
106.24
63.73
33.83
31.20
30.45
26.86
21.81
19.22
Normalized Intensity
Chemical Shift (ppm)

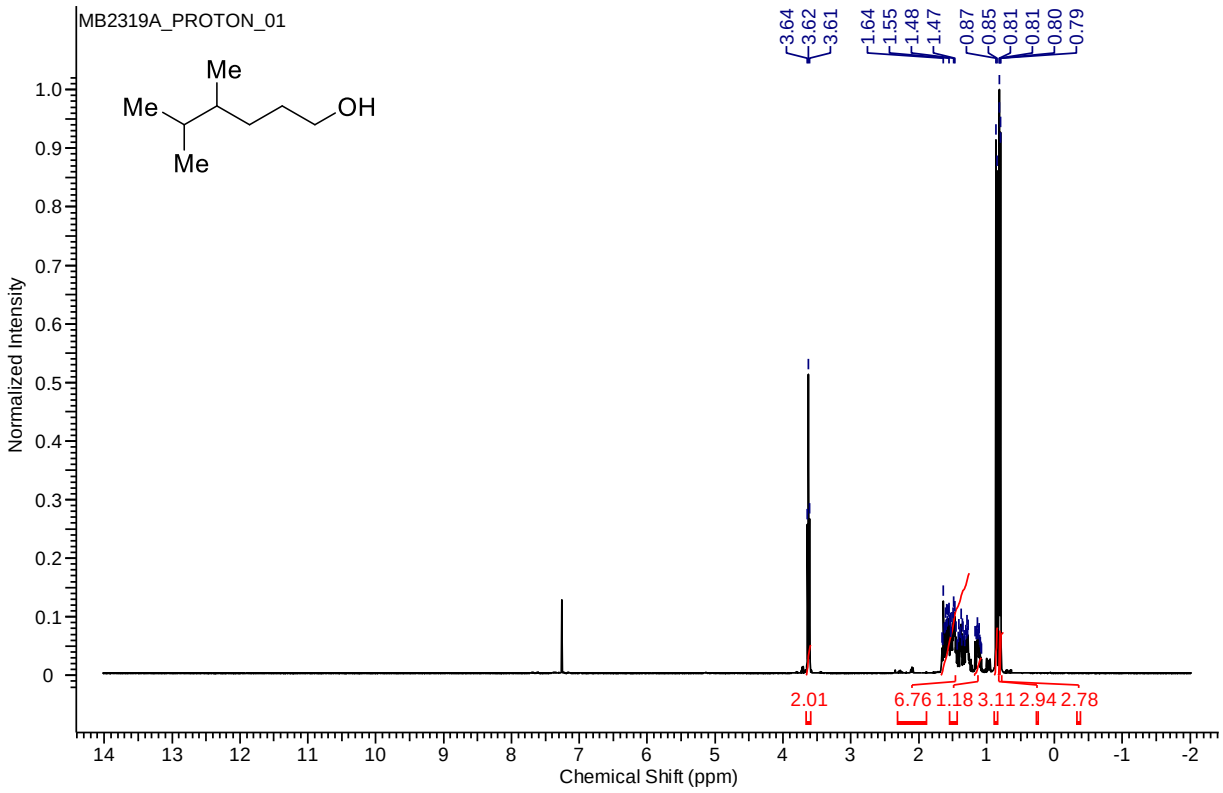
MB2319A_PROTON_01
Me
Me
Me
OH
3.64
3.62
3.61
1.64
1.55
1.48
1.47
0.87
0.85
0.81
0.81
0.80
0.79
2.01
6.76
1.18
3.11
2.94
2.78
Normalized Intensity
Chemical Shift (ppm)

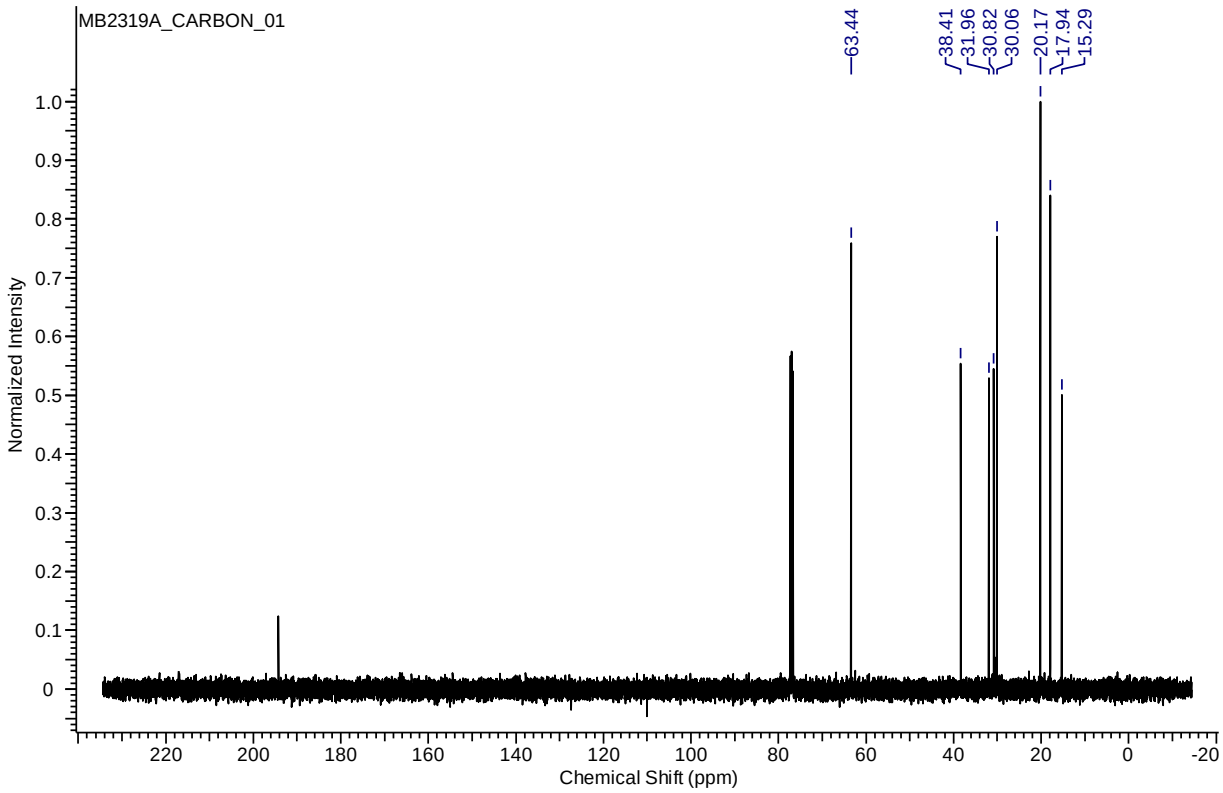
MB2319A_CARBON_01
63.44
38.41
31.96
30.82
30.06
20.17
17.94
15.29
Normalized Intensity
Chemical Shift (ppm)

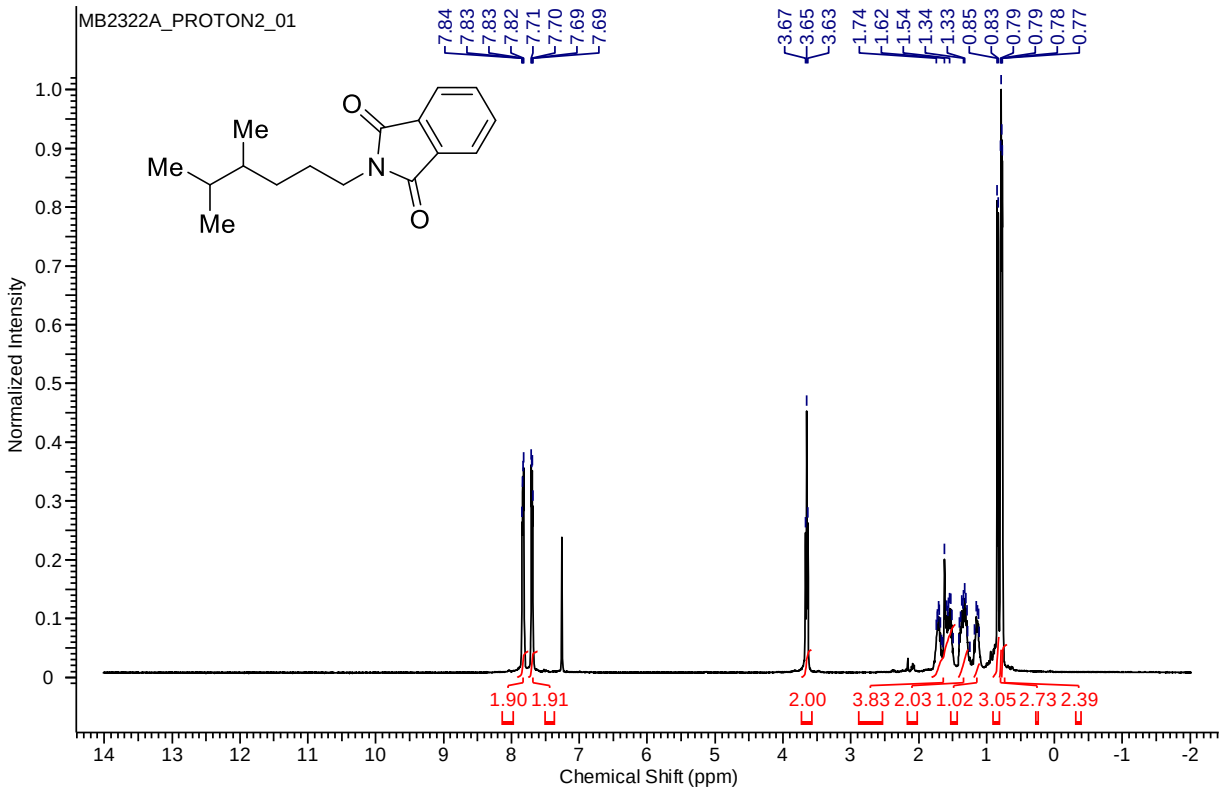
MB2322A_PROTON2_01
7.84
7.83
7.83
7.82
7.71
7.70
7.69
7.69
3.67
3.65
3.63
1.74
1.62
1.54
1.34
1.33
0.85
0.83
0.79
0.79
0.78
0.77
Me
Me
Me
N
O
O
1.90 1.91
2.00
3.83 2.03 1.02 3.05 2.73 2.39
Normalized Intensity
Chemical Shift (ppm)

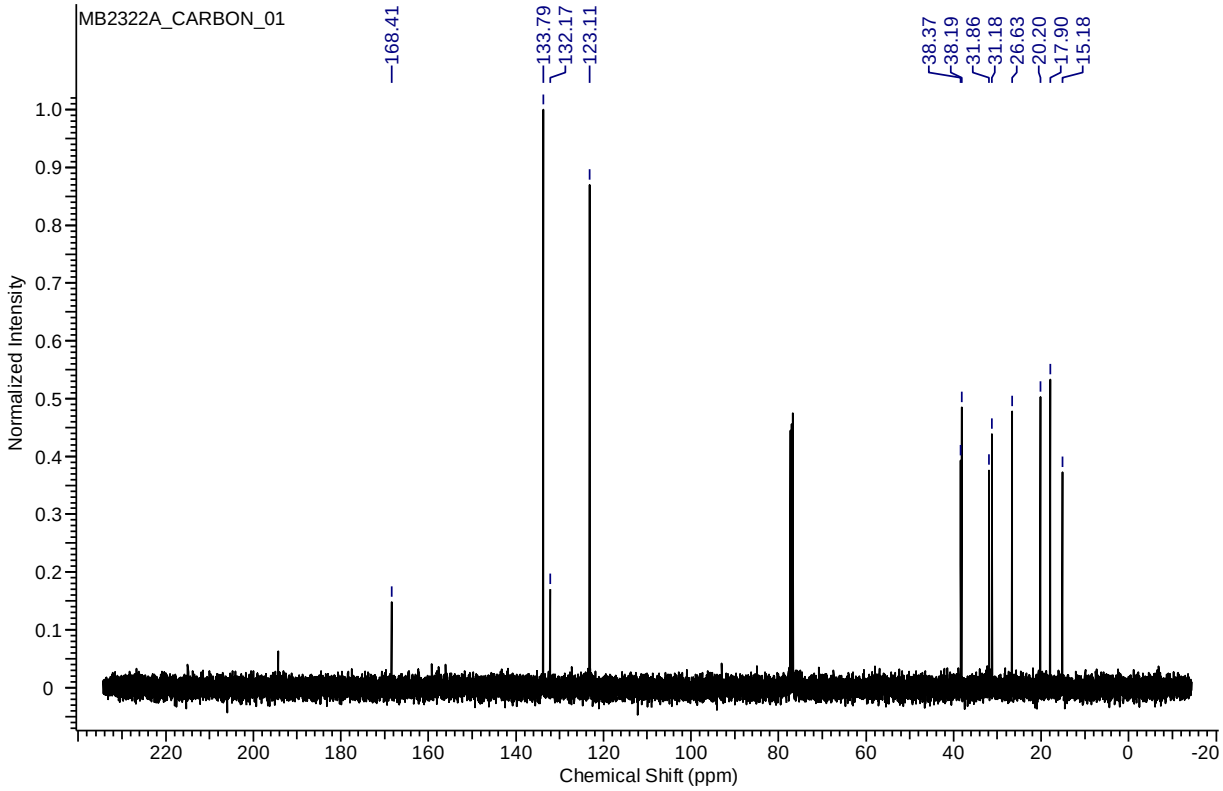
MB2322A_CARBON_01
168.41
133.79
132.17
123.11
38.37
38.19
31.86
31.18
26.63
20.20
17.90
15.18
Normalized Intensity
Chemical Shift (ppm)

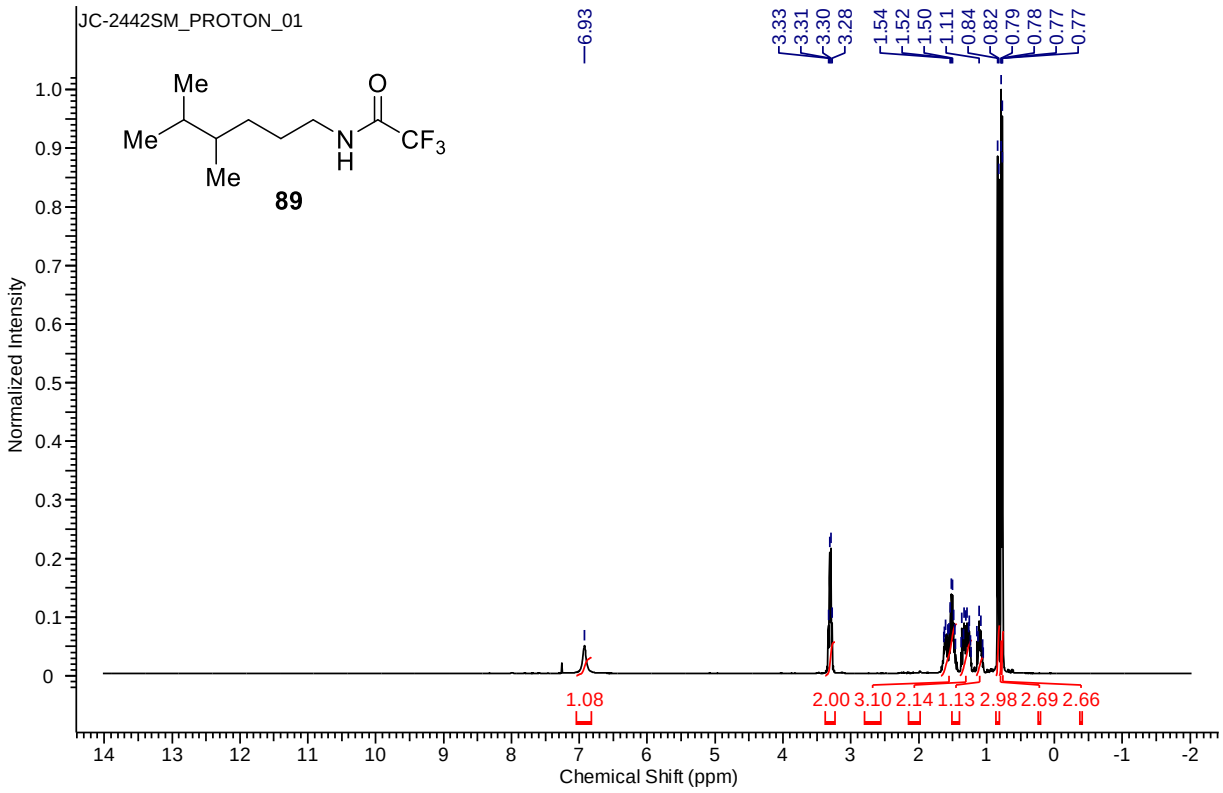
JC-2442SM_PROTON_01
Me
Me
Me
O
N
H
CF3
89
6.93
3.33
3.31
3.30
3.28
1.54
1.52
1.50
1.11
0.84
0.82
0.79
0.78
0.77
0.77
1.08
2.00 3.10 2.14 1.13 2.98 2.69 2.66
Normalized Intensity
Chemical Shift (ppm)

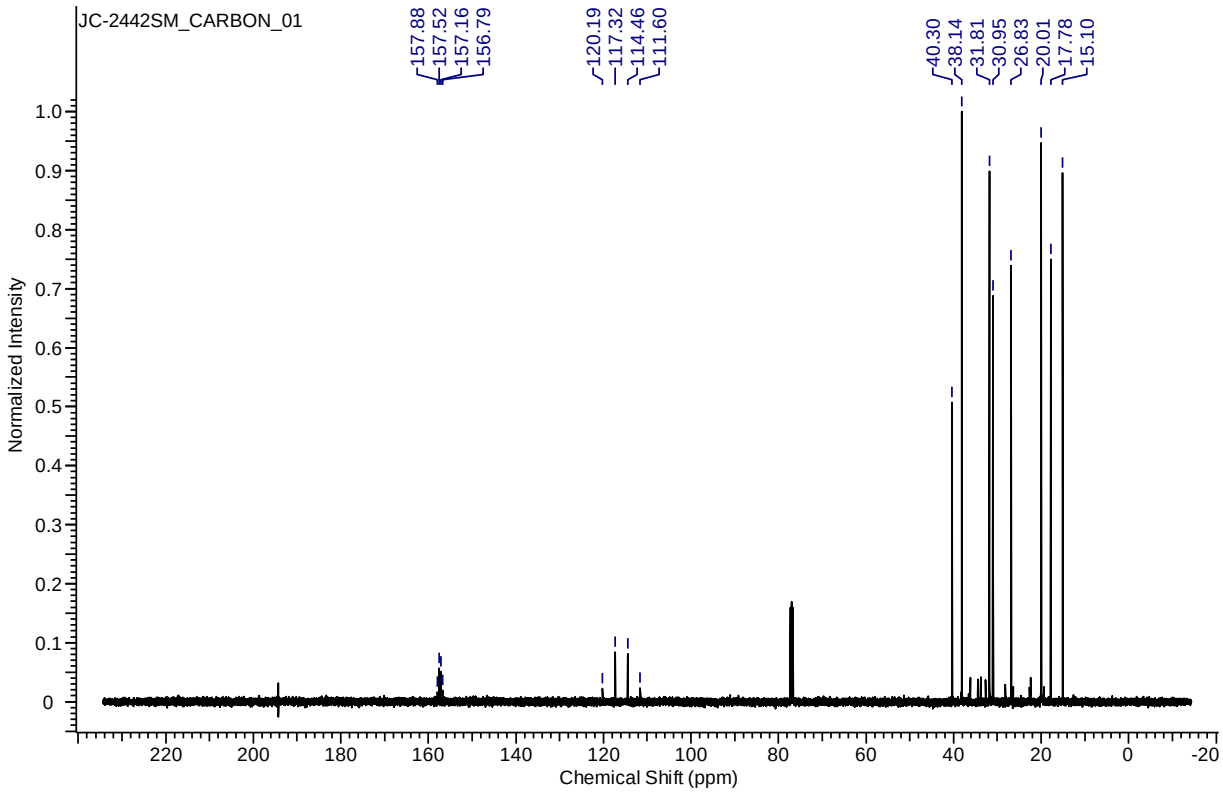
JC-2442SM_CARBON_01
157.88
157.52
157.16
156.79
120.19
117.32
114.46
111.60
40.30
38.14
31.81
30.95
26.83
20.01
17.78
15.10
Normalized Intensity
Chemical Shift (ppm)

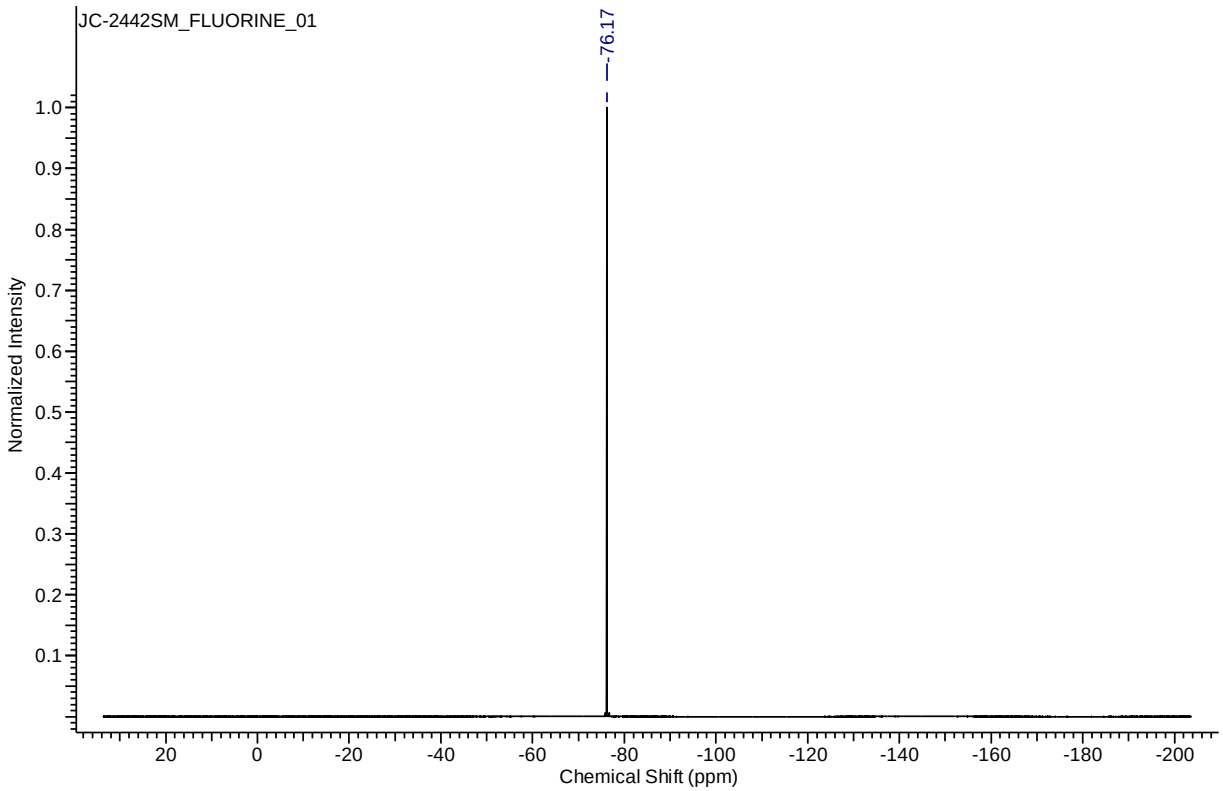
JC-2442SM_FLUORINE_01
-76.17
Normalized Intensity
Chemical Shift (ppm)

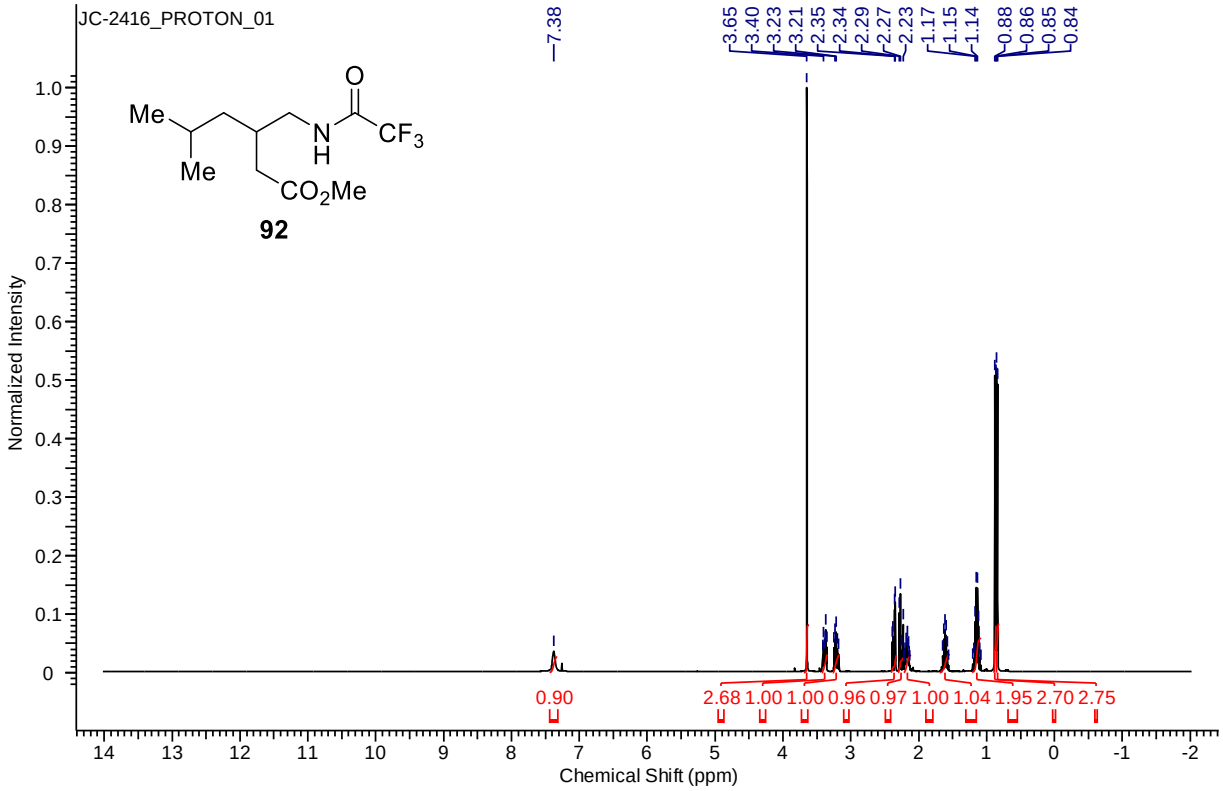
JC-2416_PROTON_01
7.38
3.65
3.40
3.23
3.21
2.35
2.34
2.29
2.27
2.23
1.17
1.15
1.14
0.88
0.86
0.85
0.84
Me
Me
N
H
O
CF3
CO2Me
92
0.90
2.68 1.00 1.00 0.96 0.97 1.00 1.04 1.95 2.70 2.75
Normalized Intensity
Chemical Shift (ppm)

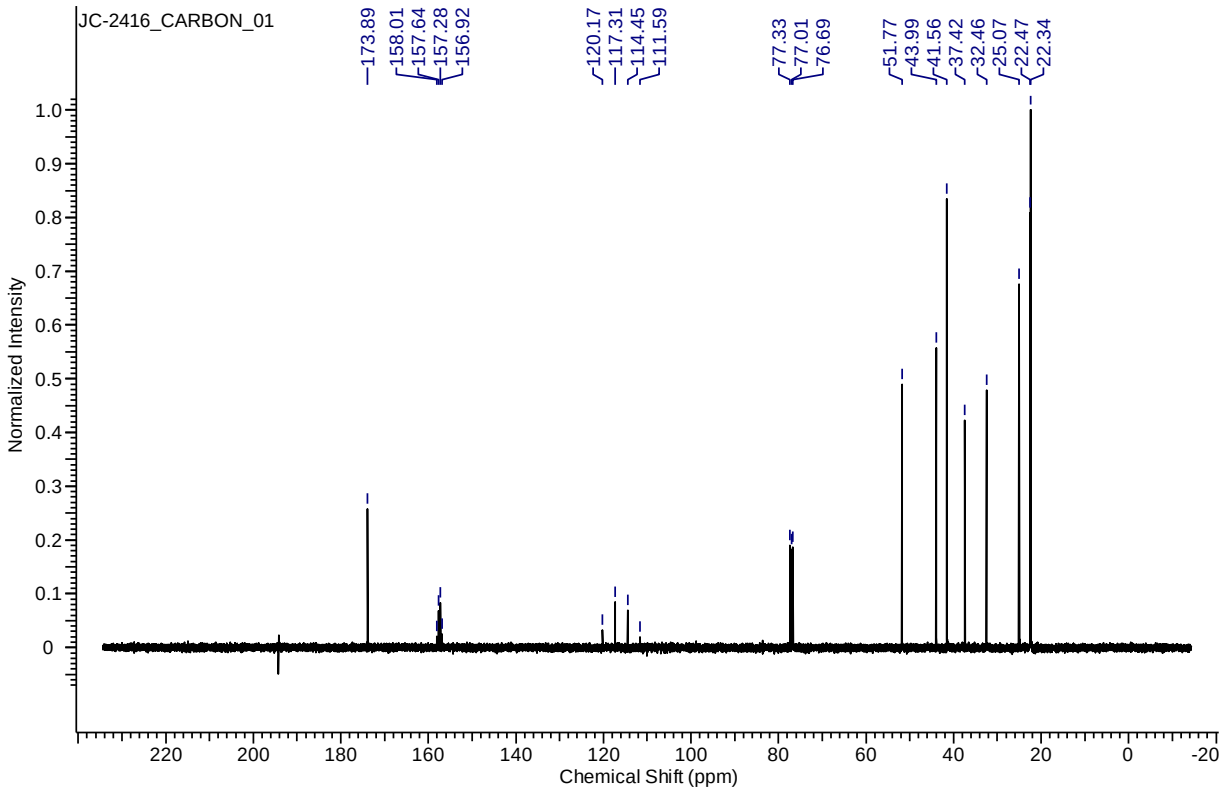
JC-2416_CARBON_01
173.89
158.01
157.64
157.28
156.92
120.17
117.31
114.45
111.59
77.33
77.01
76.69
51.77
43.99
41.56
37.42
32.46
25.07
22.47
22.34
Normalized Intensity
Chemical Shift (ppm)

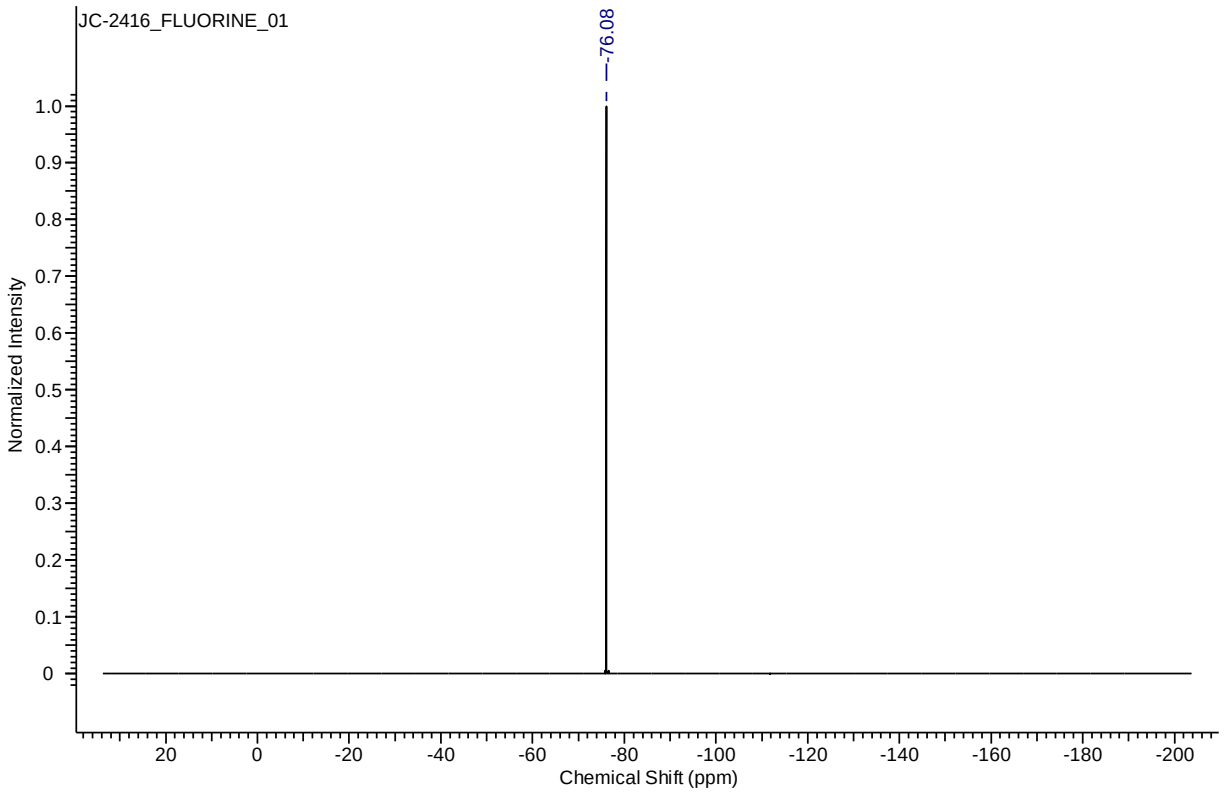
JC-2416_FLUORINE_01
-76.08
Normalized Intensity
Chemical Shift (ppm)

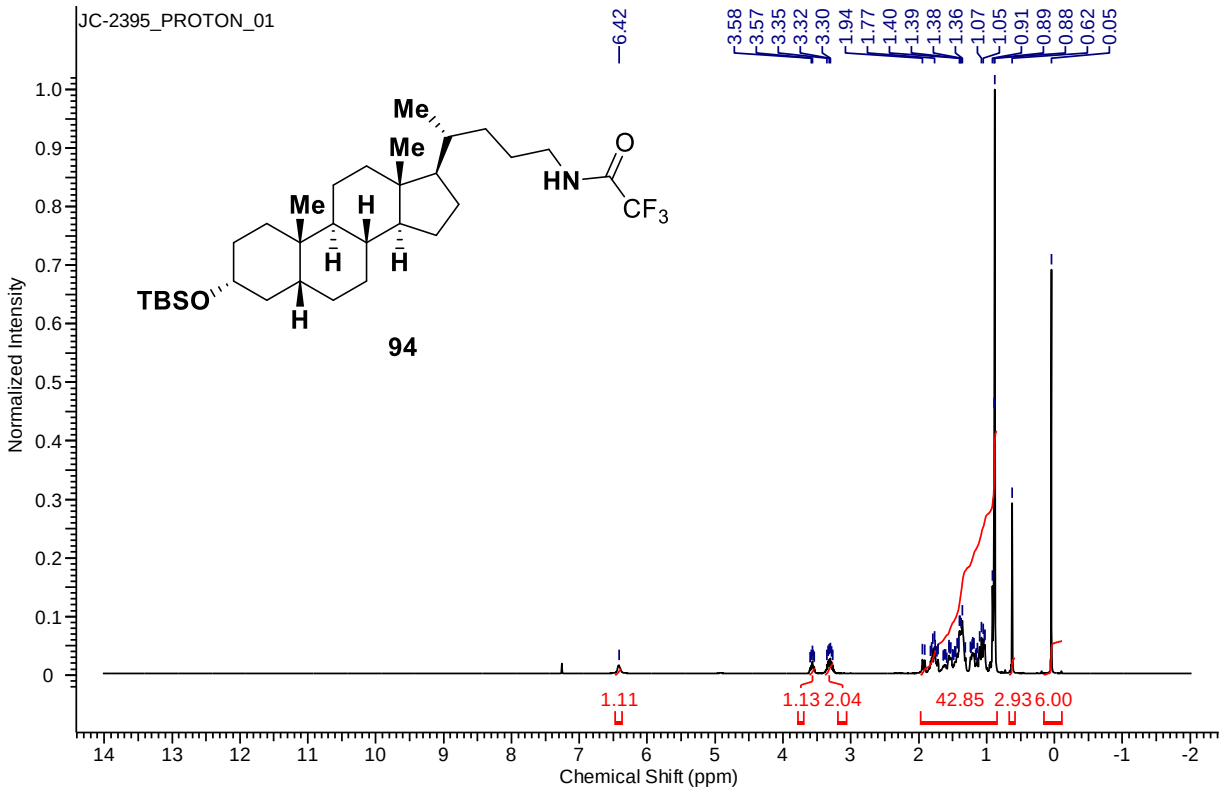
JC-2395_PROTON_01
6.42
3.58
3.57
3.35
3.32
3.30
1.94
1.77
1.40
1.39
1.38
1.36
1.07
1.05
0.91
0.89
0.88
0.62
0.05
Me
Me
Me
H
H
H
H
TBSO
HN
O
CF3
94
1.11
1.13
2.04
42.85
2.93
6.00
Normalized Intensity
Chemical Shift (ppm)

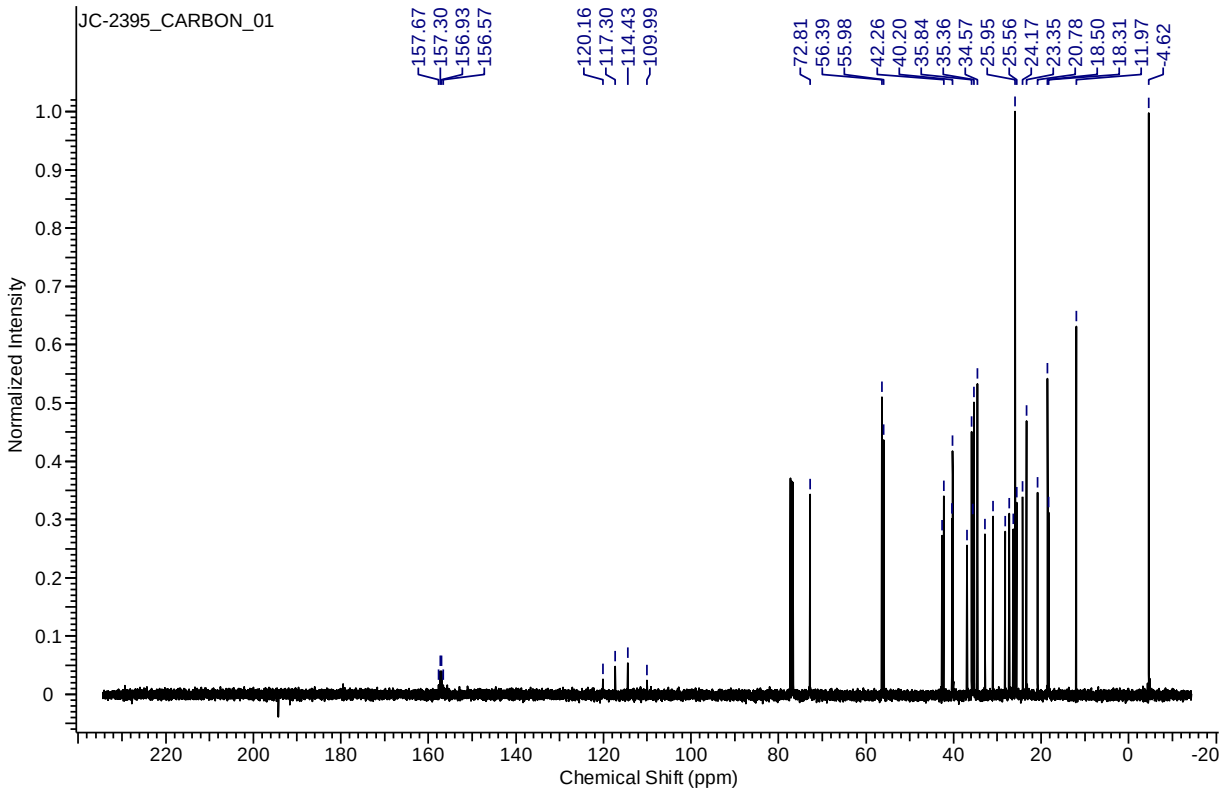
JC-2395_CARBON_01
157.67
157.30
156.93
156.57
120.16
117.30
114.43
109.99
72.81
56.39
55.98
42.26
40.20
35.84
35.36
34.57
25.95
25.56
24.17
23.35
20.78
18.50
18.31
11.97
4.62
Normalized Intensity
Chemical Shift (ppm)

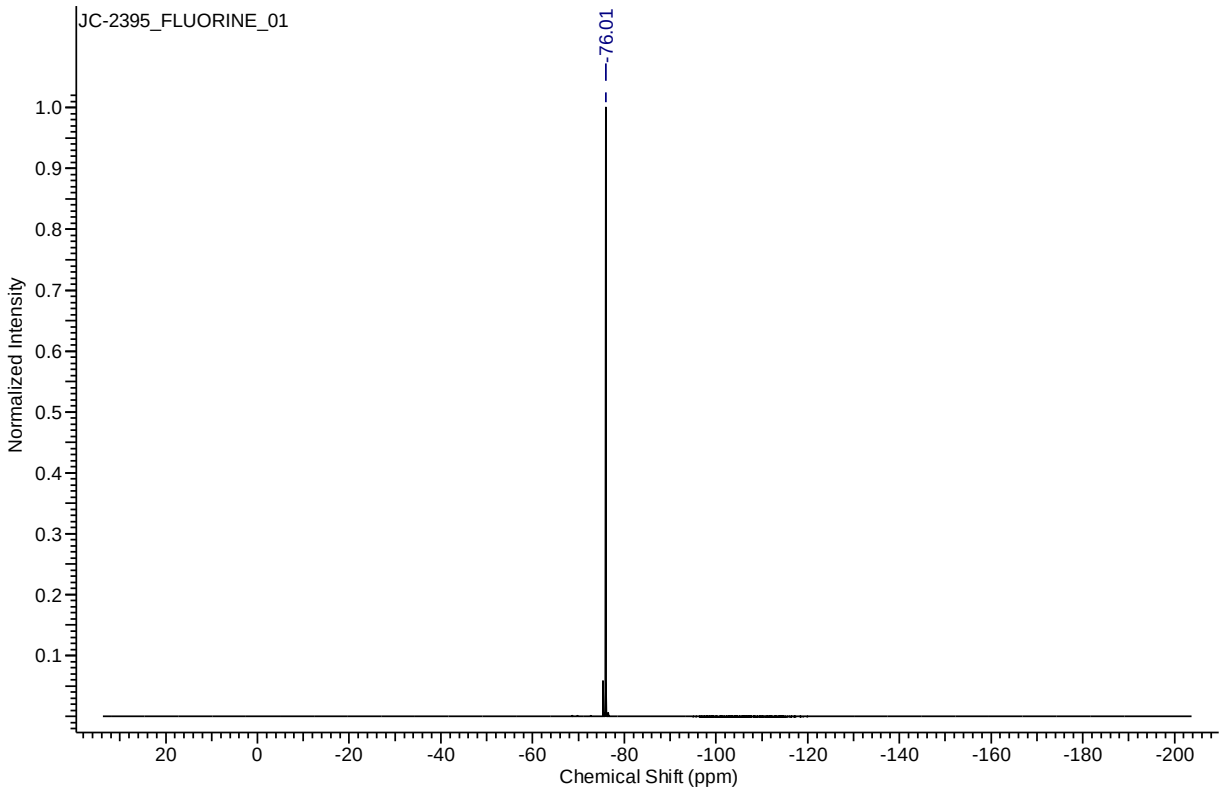
JC-2395_FLUORINE_01
-76.01
Normalized Intensity
Chemical Shift (ppm)

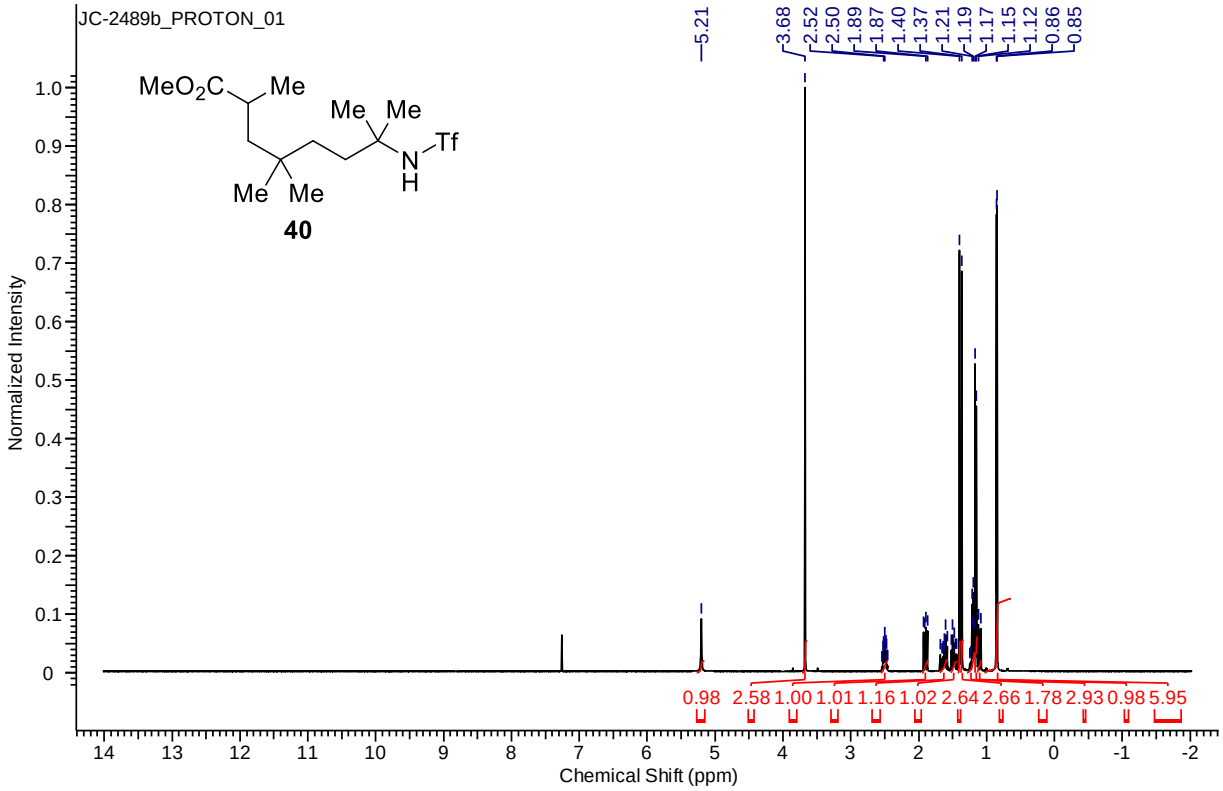
JC-2489b_PROTON_01
MeO2C
Me
Me
Me
N
Tf
H
Me
Me
40
5.21
3.68
2.52
2.50
1.89
1.87
1.40
1.37
1.21
1.19
1.17
1.15
1.12
0.86
0.85
0.98
2.58
1.00
1.01
1.16
1.02
2.64
2.66
1.78
2.93
0.98
5.95
Normalized Intensity
Chemical Shift (ppm)

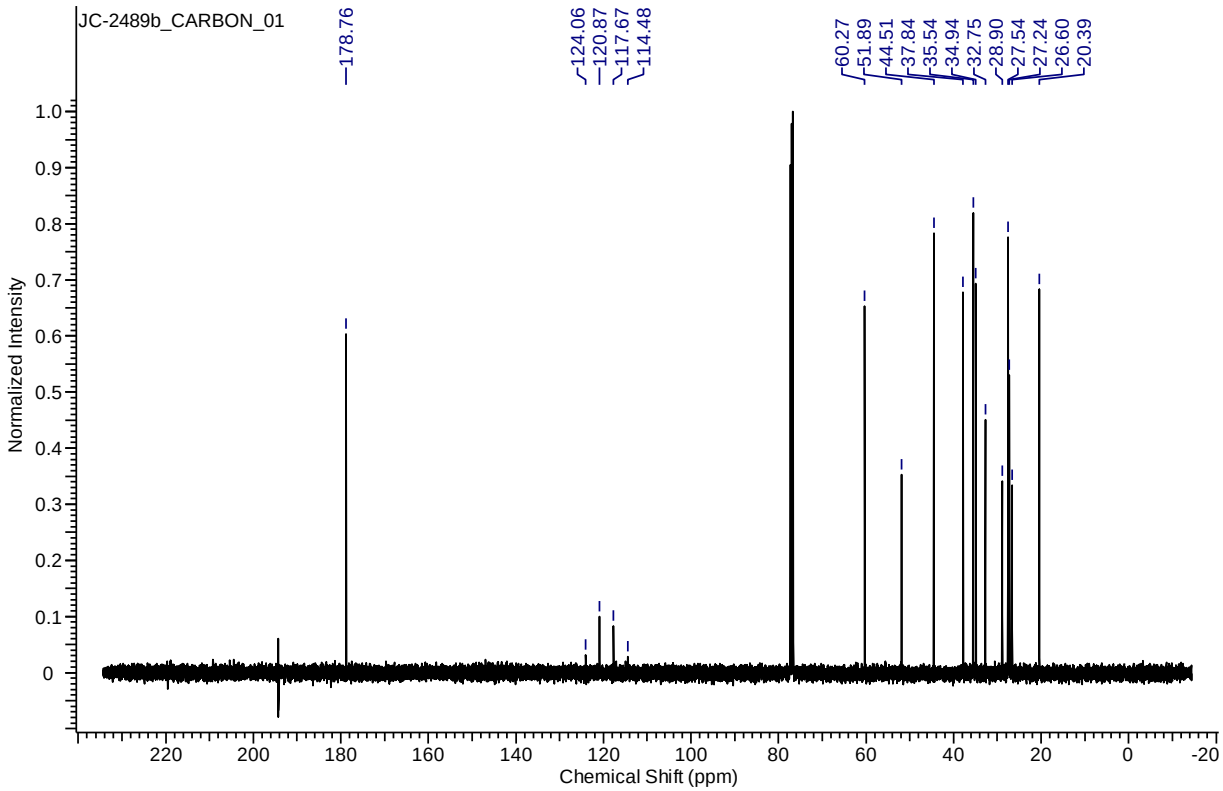
JC-2489b_CARBON_01
178.76
124.06
120.87
117.67
114.48
60.27
51.89
44.51
37.84
35.54
34.94
32.75
28.90
27.54
27.24
26.60
20.39
Normalized Intensity
Chemical Shift (ppm)

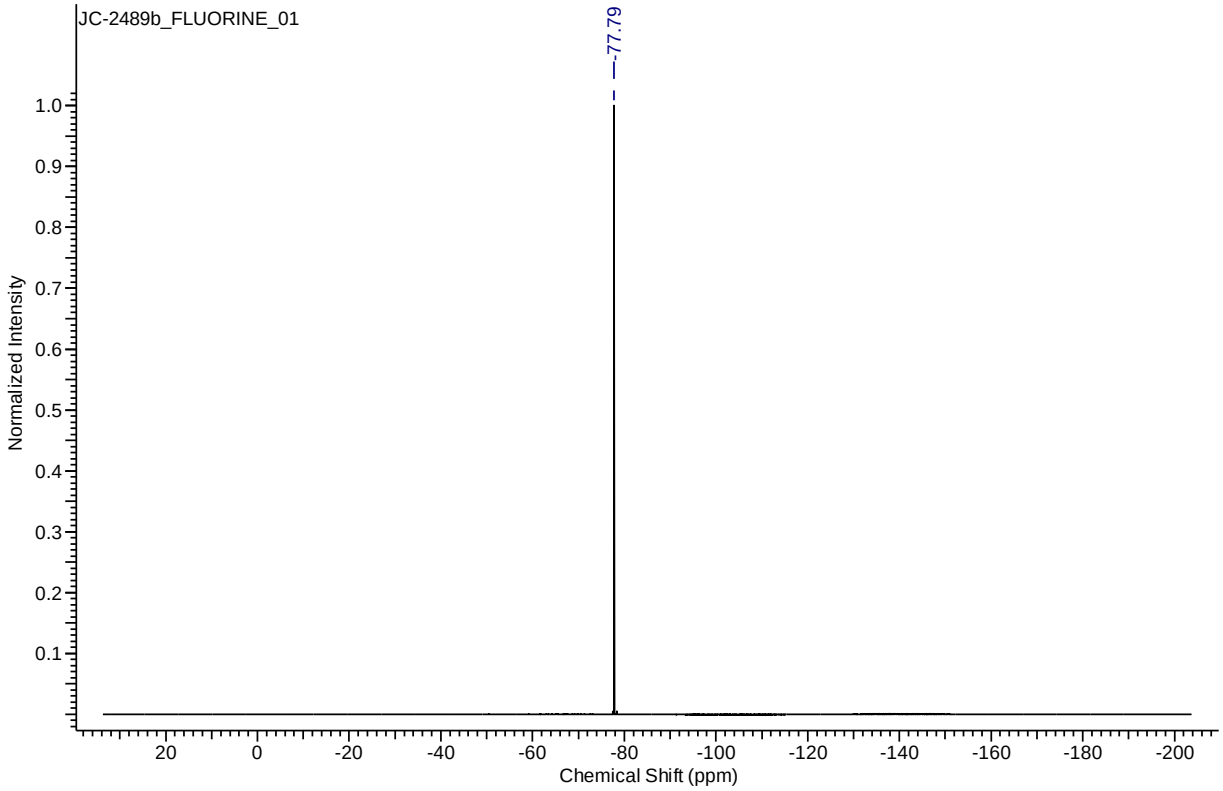
JC-2489b_FLUORINE_01
-77.79
Normalized Intensity
Chemical Shift (ppm)

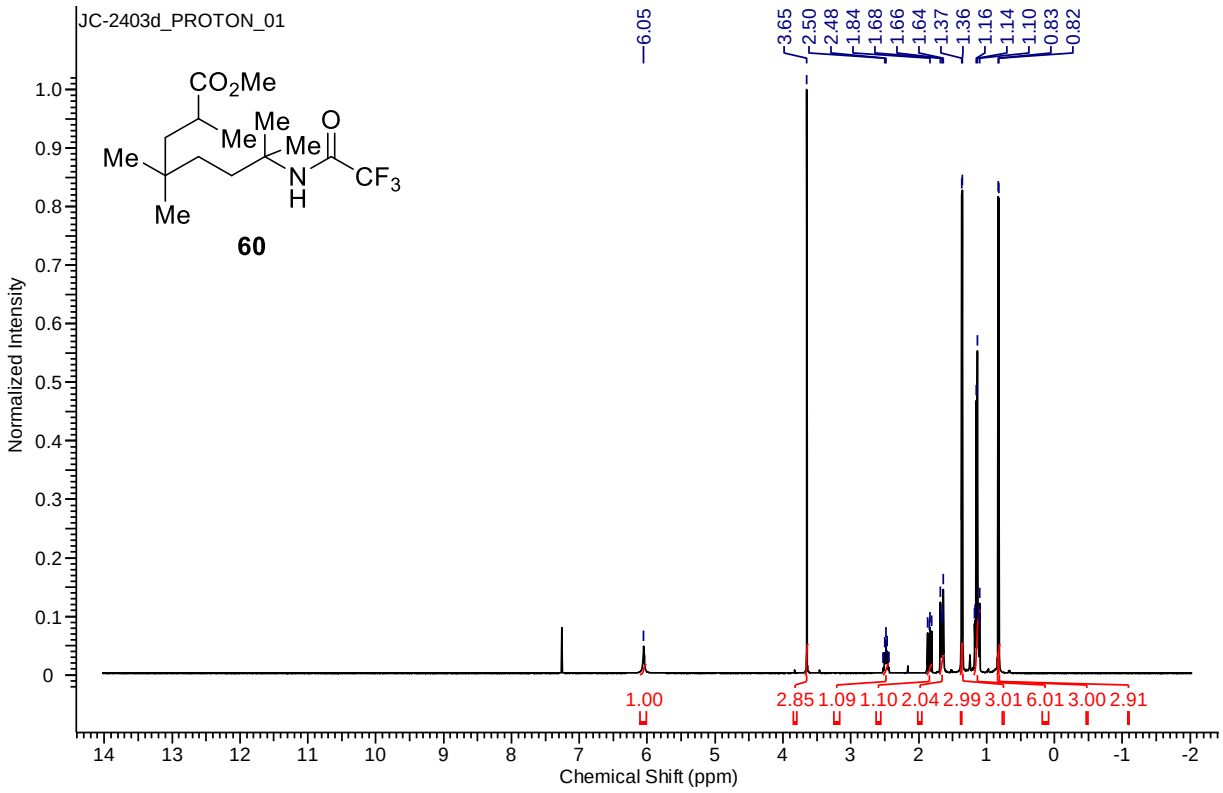
JC-2403d_PROTON_01
CO2Me
Me
Me
Me
Me
O
N
H
CF3
Me
60
6.05
3.65
2.50
2.48
1.84
1.68
1.66
1.64
1.37
1.36
1.16
1.14
1.10
0.83
0.82
1.00
2.85
1.09
1.10
2.04
2.99
3.01
6.01
3.00
2.91
Normalized Intensity
Chemical Shift (ppm)

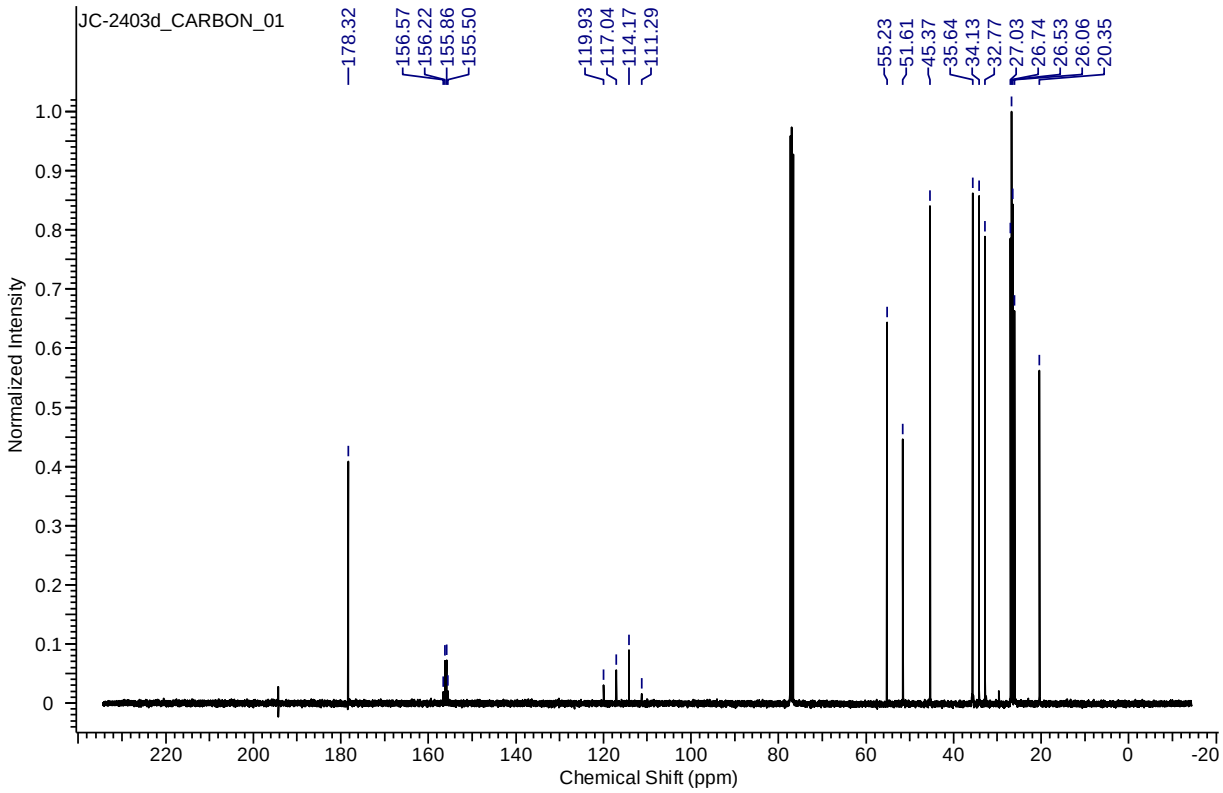
JC-2403d_CARBON_01
178.32
156.57
156.22
155.86
155.50
119.93
117.04
114.17
111.29
55.23
51.61
45.37
35.64
34.13
32.77
27.03
26.74
26.53
26.06
20.35
Normalized Intensity
Chemical Shift (ppm)

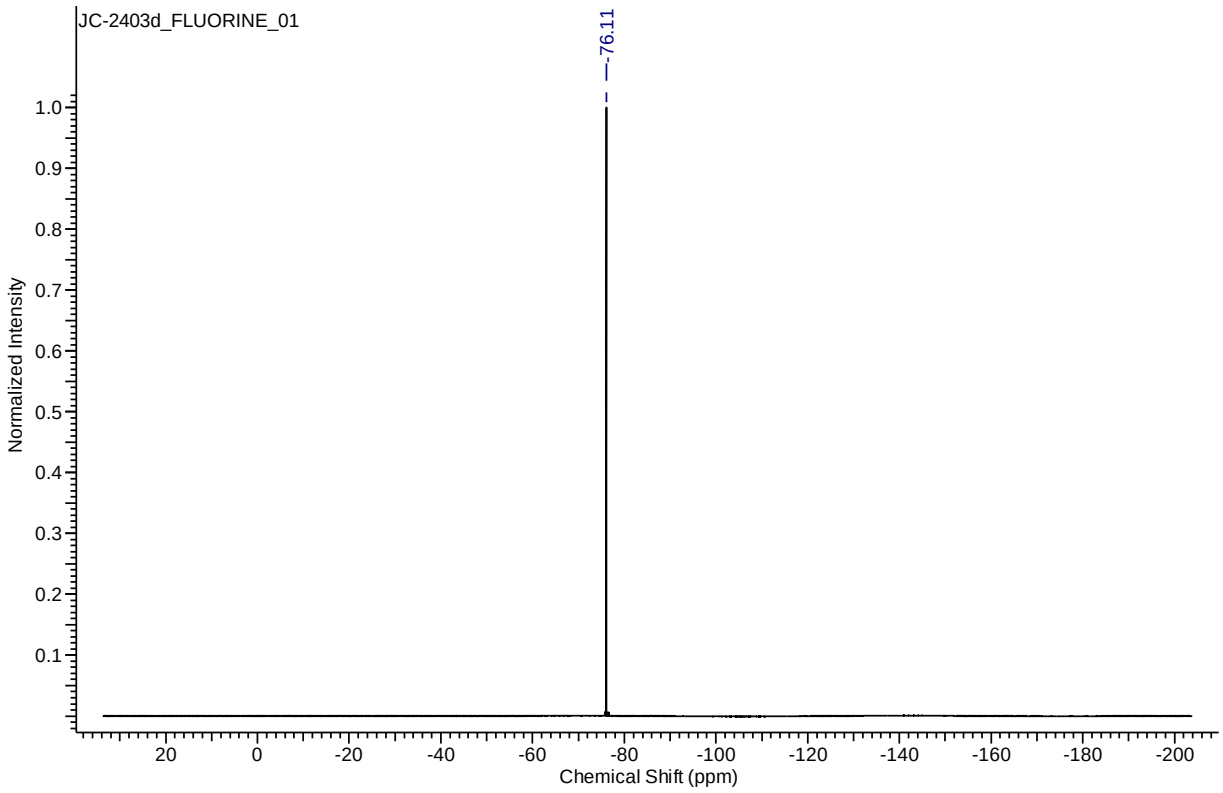
JC-2403d_FLUORINE_01
-76.11
Normalized Intensity
Chemical Shift (ppm)

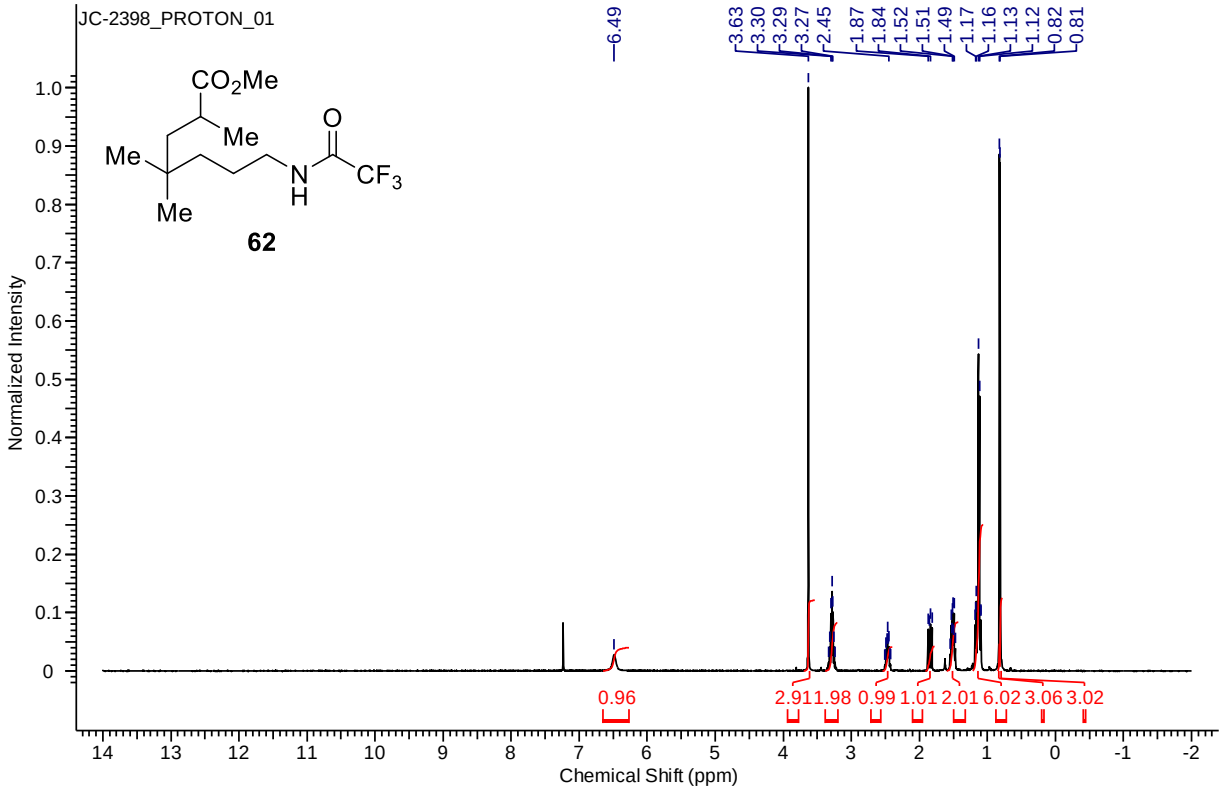
JC-2398_PROTON_01
6.49
3.63
3.30
3.29
3.27
2.45
1.87
1.84
1.52
1.51
1.49
1.17
1.16
1.13
1.12
0.82
0.81
CO2Me
Me
Me
Me
N
H
O
CF3
62
0.96
2.91
1.98
0.99
1.01
2.01
6.02
3.06
3.02
Normalized Intensity
Chemical Shift (ppm)

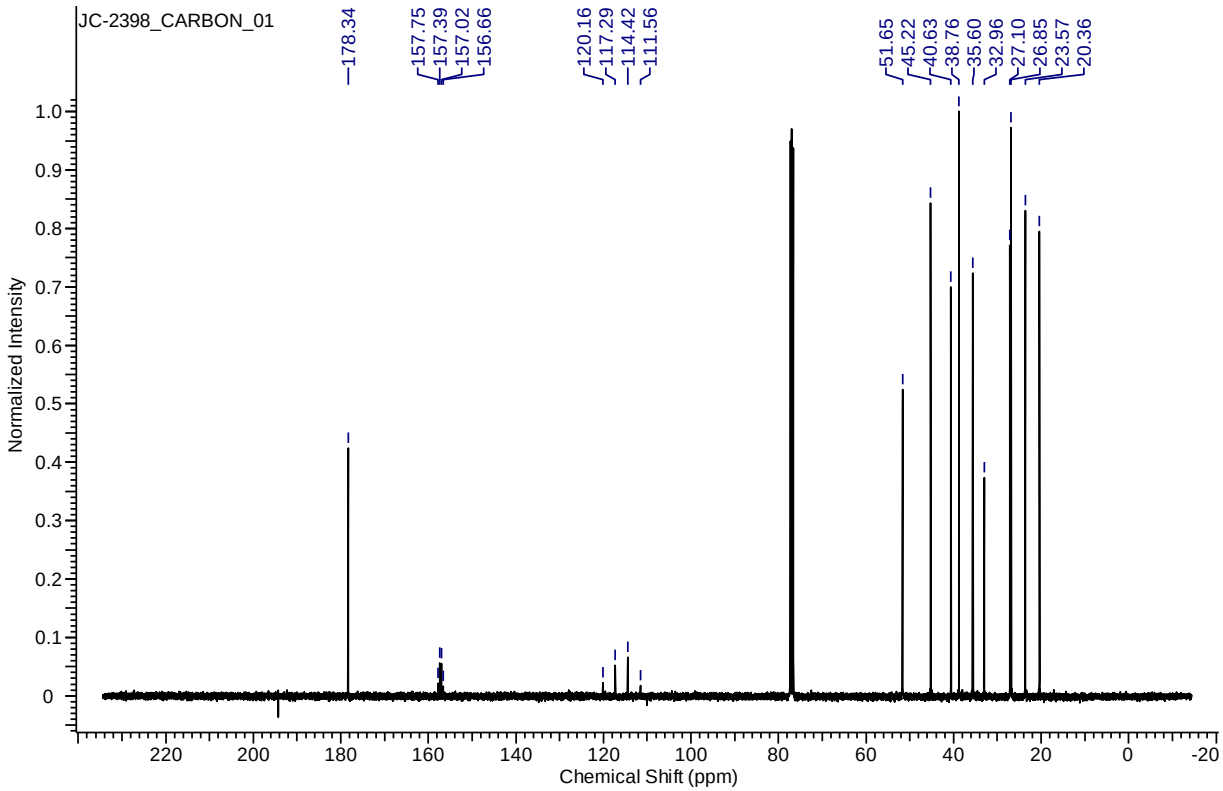
JC-2398_CARBON_01
178.34
157.75
157.39
157.02
156.66
120.16
117.29
114.42
111.56
51.65
45.22
40.63
38.76
35.60
32.96
27.10
26.85
23.57
20.36
Normalized Intensity
Chemical Shift (ppm)

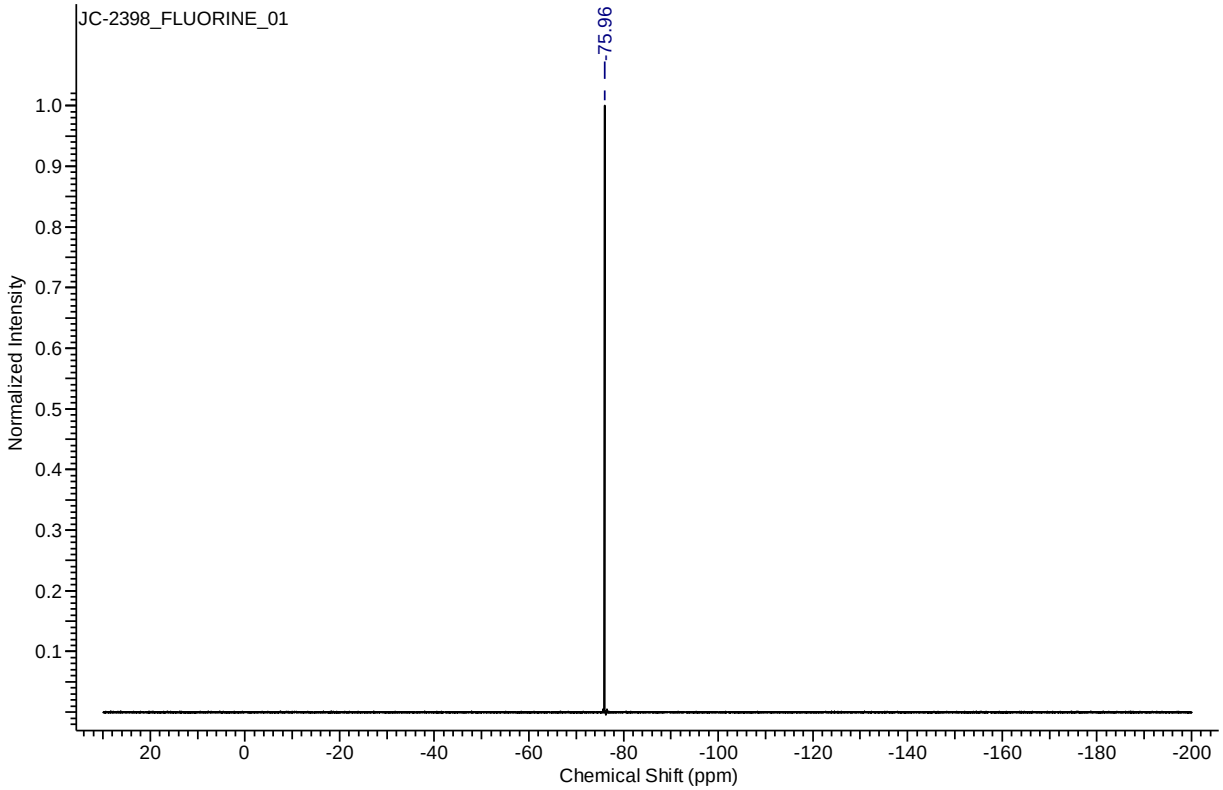
JC-2398_FLUORINE_01
-75.96
Normalized Intensity
Chemical Shift (ppm)

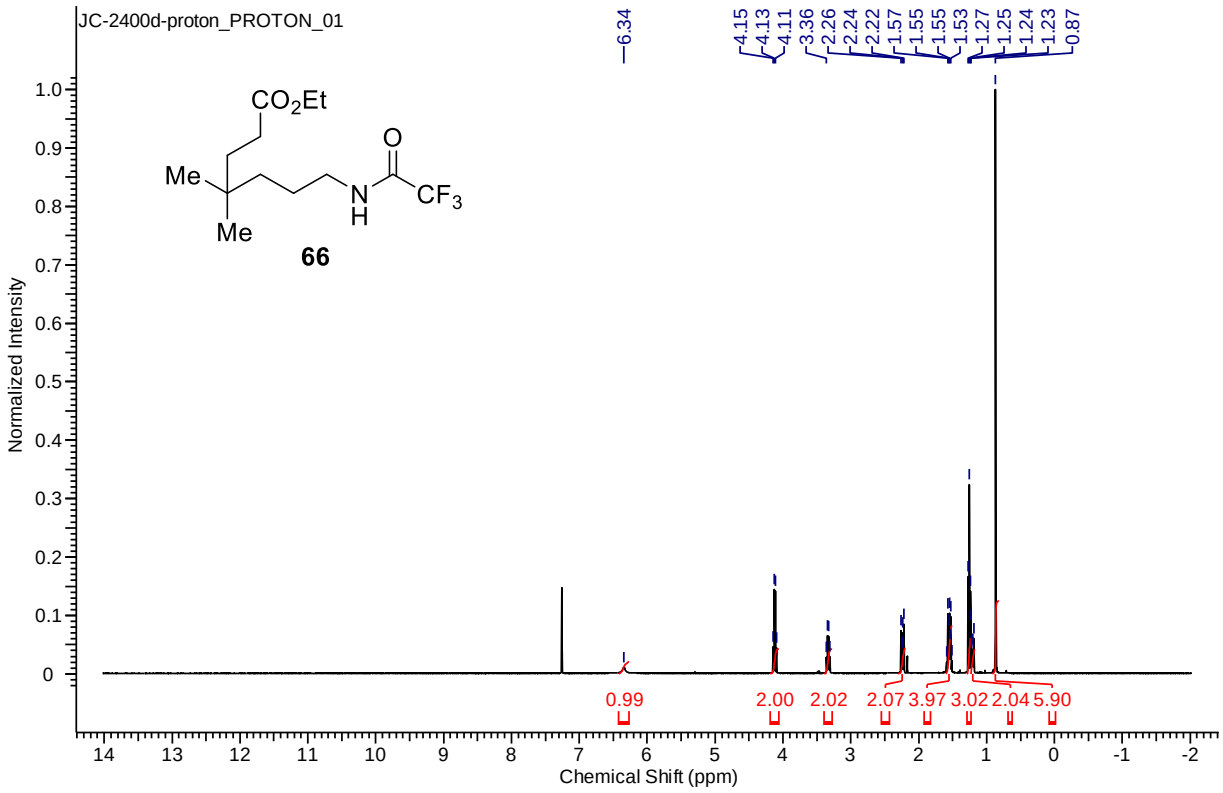
JC-2400d-proton_PROTON_01
CO2Et
Me
Me
N
H
O
CF3
66
6.34
4.15
4.13
4.11
3.36
2.26
2.24
2.22
1.57
1.55
1.55
1.53
1.27
1.25
1.24
1.23
0.87
0.99
2.00
2.02
2.07
3.97
3.02
2.04
5.90
Normalized Intensity
Chemical Shift (ppm)

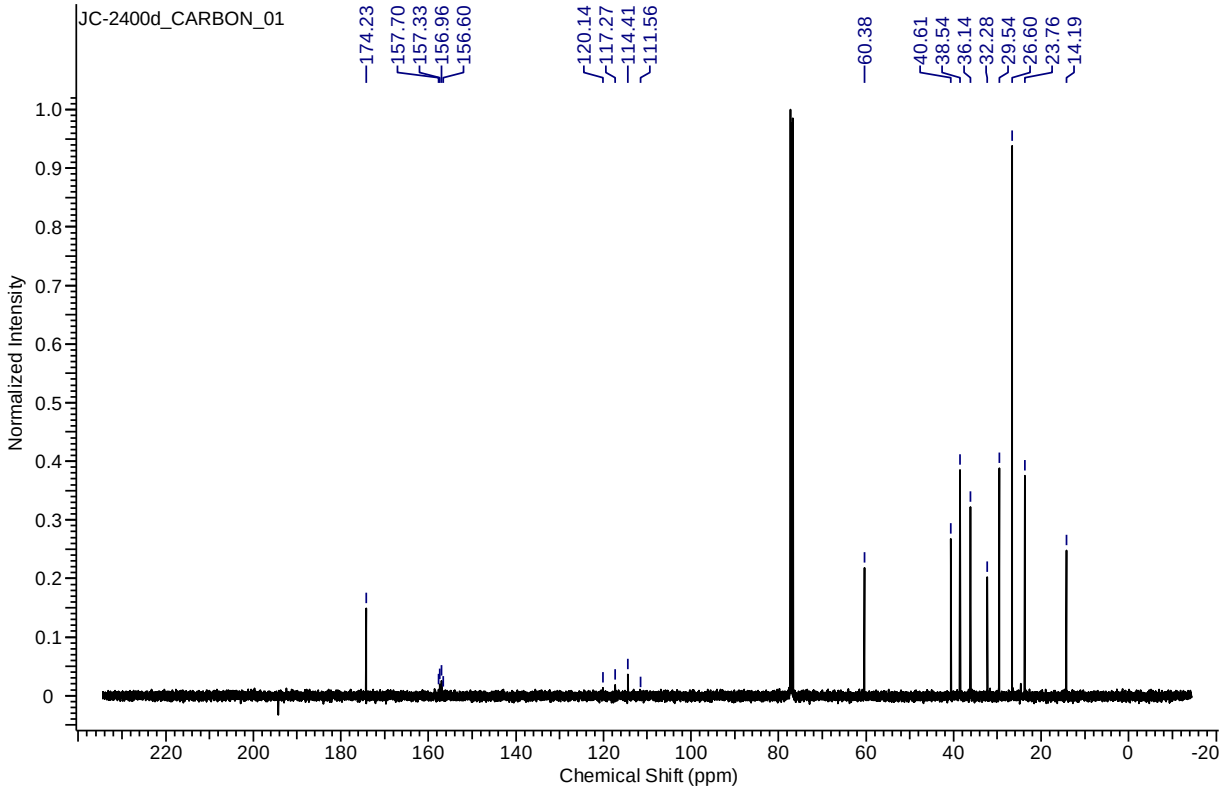
JC-2400d_CARBON_01
174.23
157.70
157.33
156.96
156.60
120.14
117.27
114.41
111.56
60.38
40.61
38.54
36.14
32.28
29.54
26.60
23.76
14.19
Normalized Intensity
Chemical Shift (ppm)

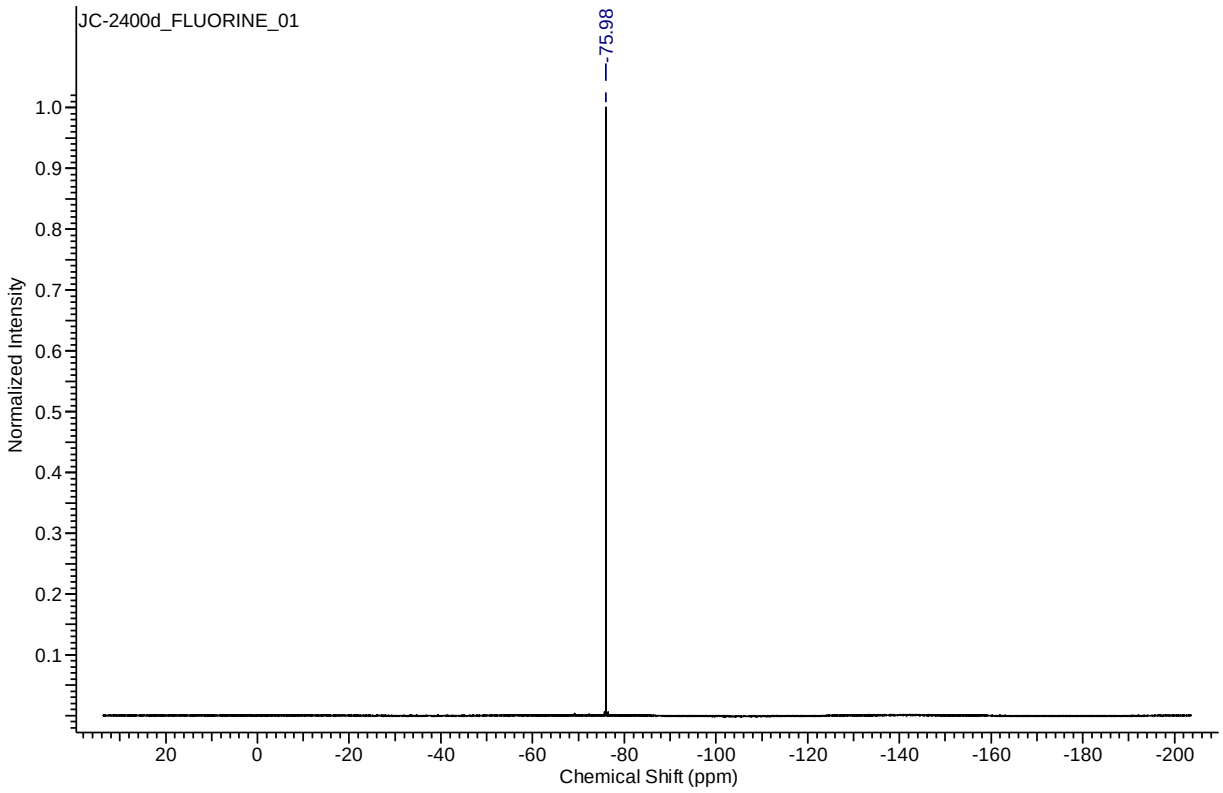
JC-2400d_FLUORINE_01
-75.98
Normalized Intensity
Chemical Shift (ppm)

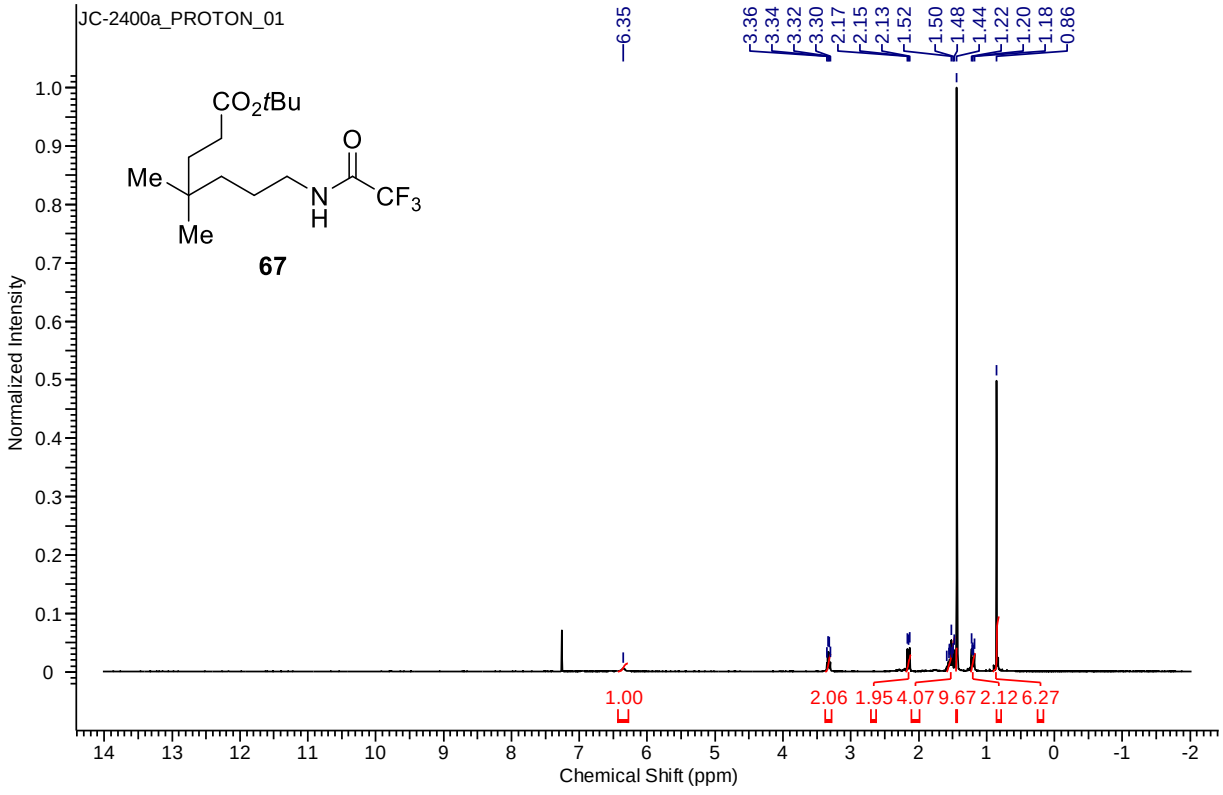
JC-2400a_PROTON_01
6.35
3.36
3.34
3.32
3.30
2.17
2.15
2.13
1.52
1.50
1.48
1.44
1.22
1.20
1.18
0.86
CO2tBu
Me
Me
N
H
O
CF3
67
1.00
2.06
1.95
4.07
9.67
2.12
6.27
Normalized Intensity
Chemical Shift (ppm)

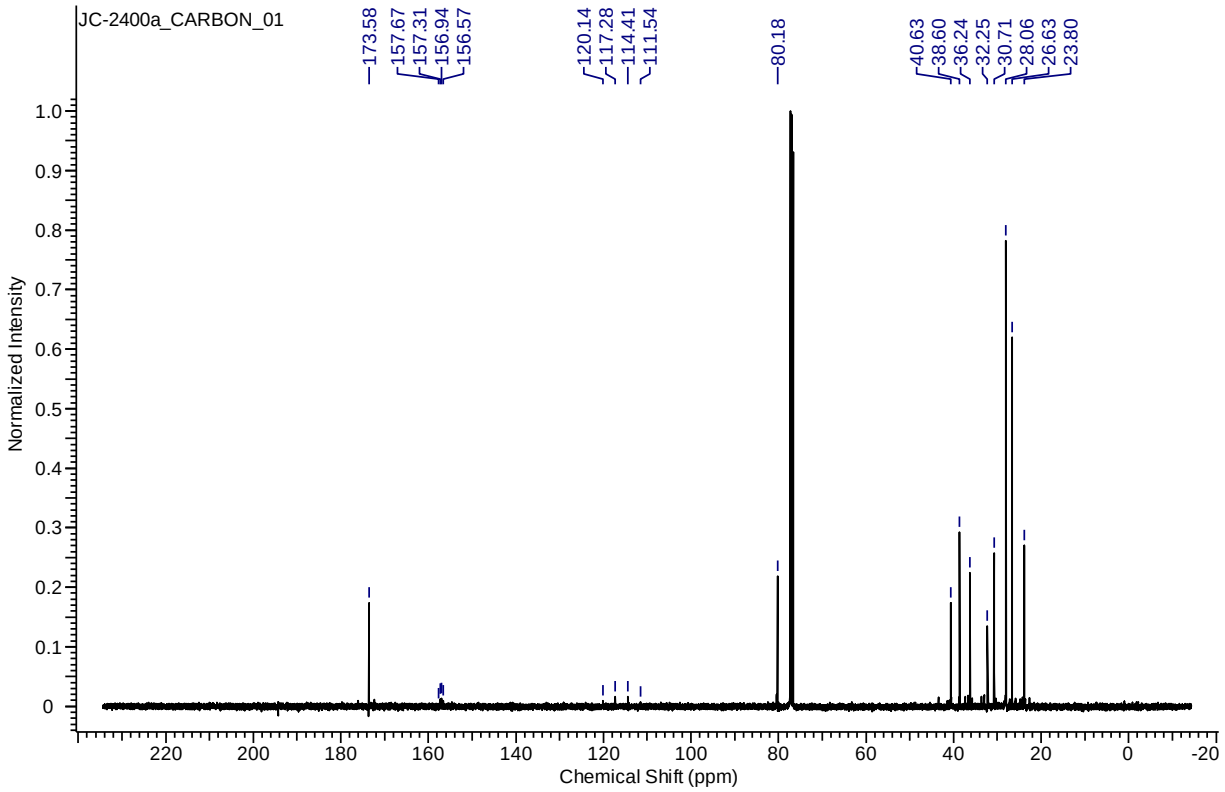
JC-2400a_CARBON_01
173.58
157.67
157.31
156.94
156.57
120.14
117.28
114.41
111.54
80.18
40.63
38.60
36.24
32.25
30.71
28.06
26.63
23.80
Normalized Intensity
Chemical Shift (ppm)

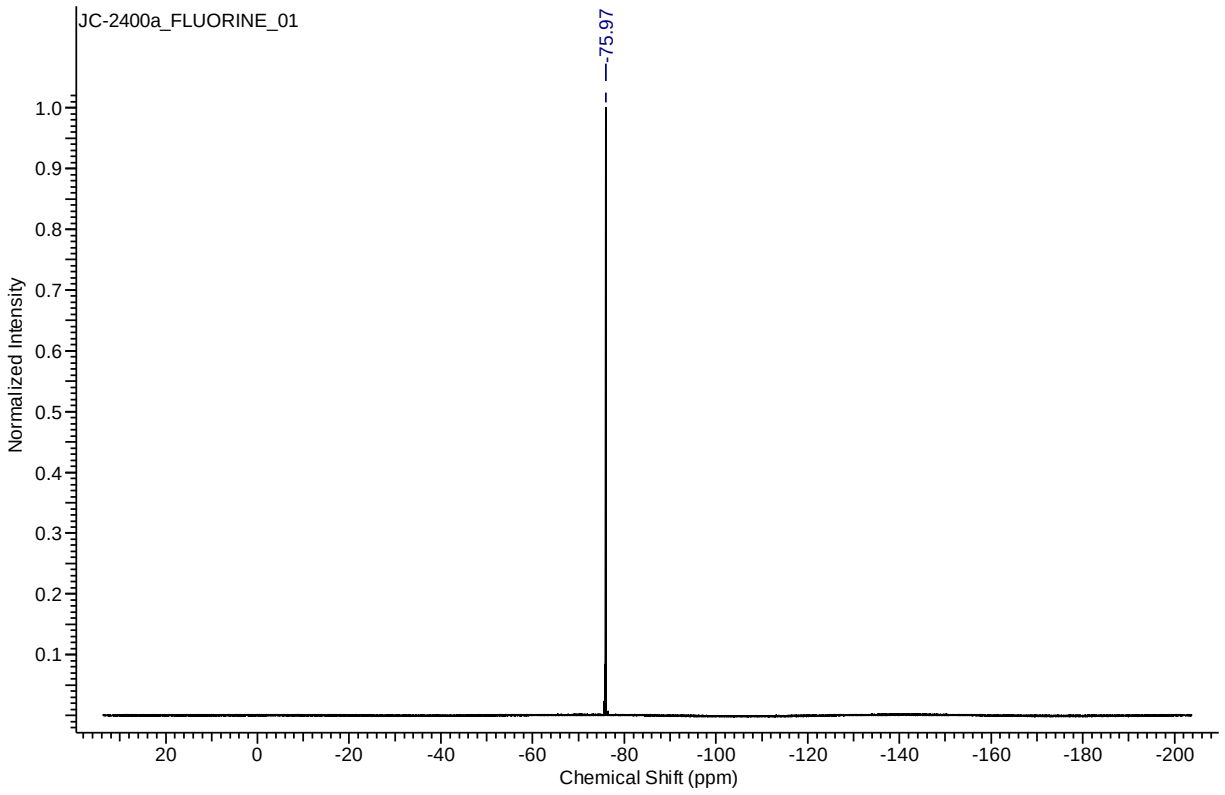
JC-2400a_FLUORINE_01
-75.97
Normalized Intensity
Chemical Shift (ppm)

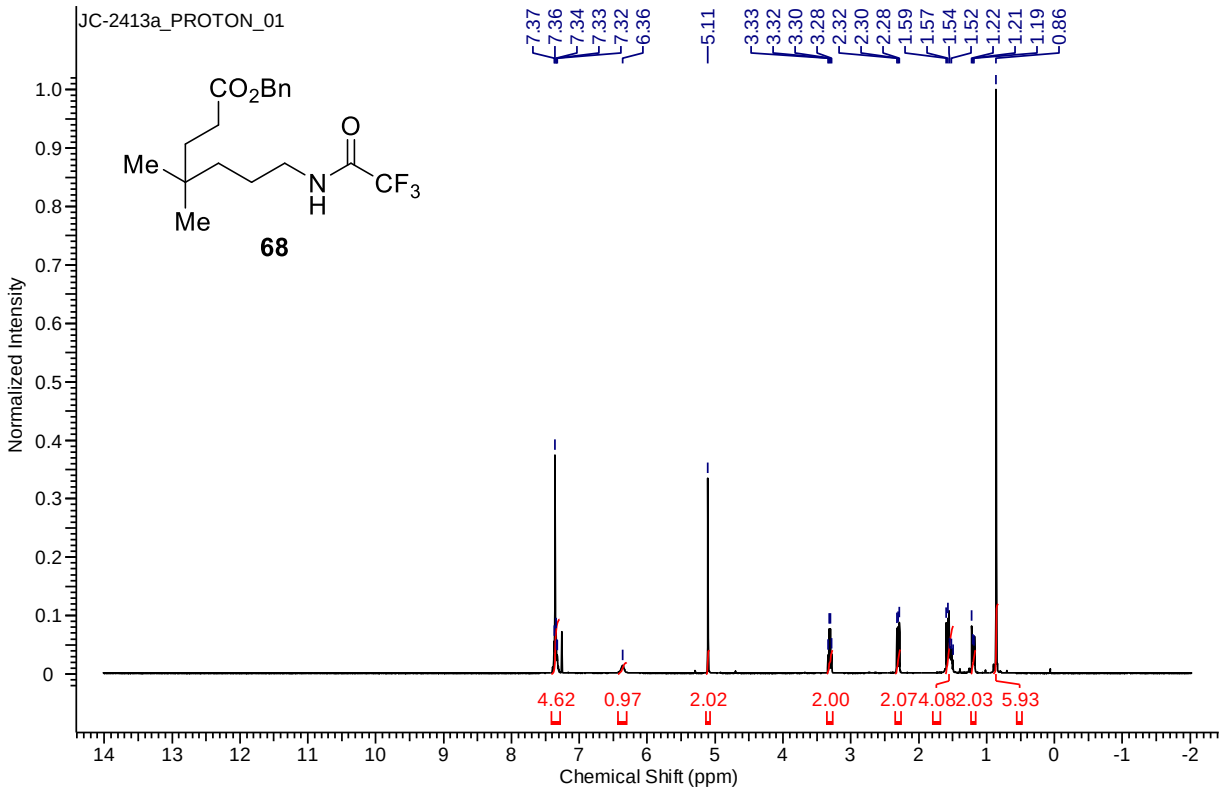
JC-2413a_PROTON_01
7.37
7.36
7.34
7.33
7.32
6.36
5.11
3.33
3.32
3.30
3.28
2.32
2.30
2.28
1.59
1.57
1.54
1.52
1.22
1.21
1.19
0.86
CO2Bn
Me
Me
N
H
O
CF3
68
Normalized Intensity
4.62
0.97
2.02
2.00
2.07
4.08
2.03
5.93
Chemical Shift (ppm)

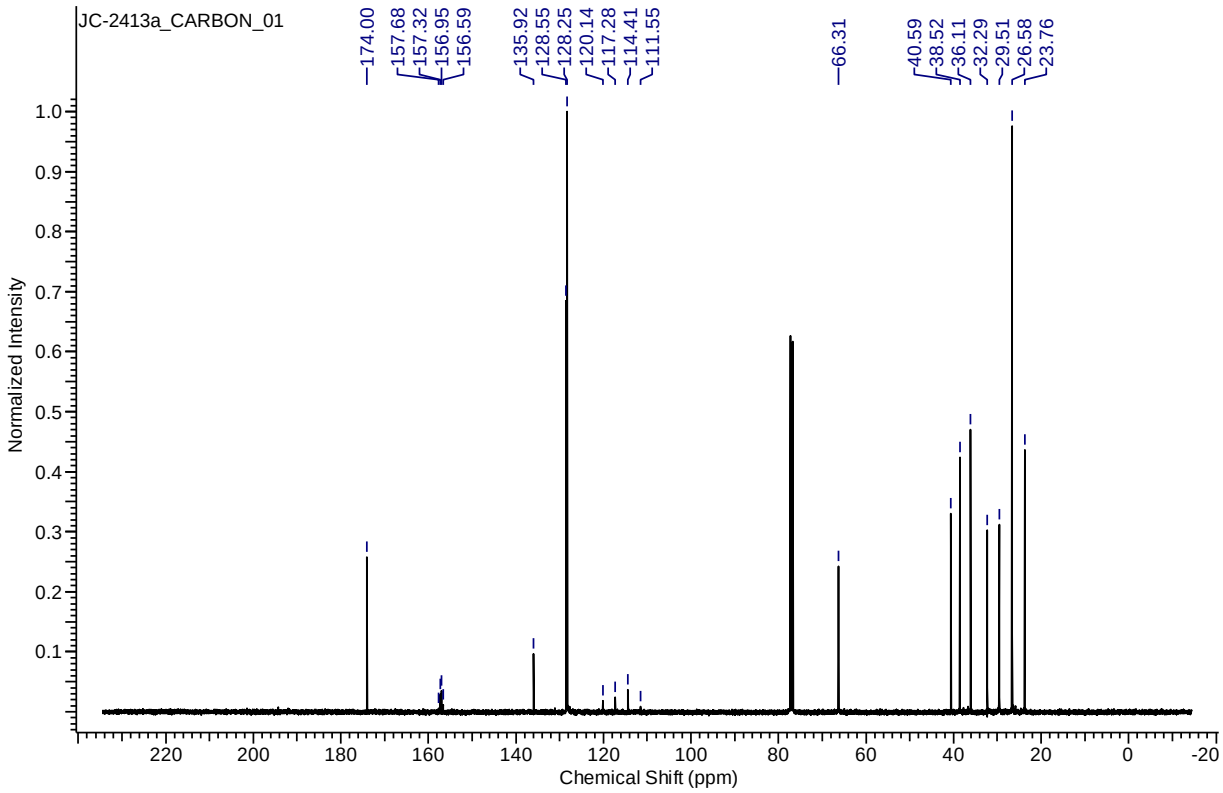
JC-2413a_CARBON_01
174.00
157.68
157.32
156.95
156.59
135.92
128.55
128.25
120.14
117.28
114.41
111.55
66.31
40.59
38.52
36.11
32.29
29.51
26.58
23.76
Normalized Intensity
Chemical Shift (ppm)

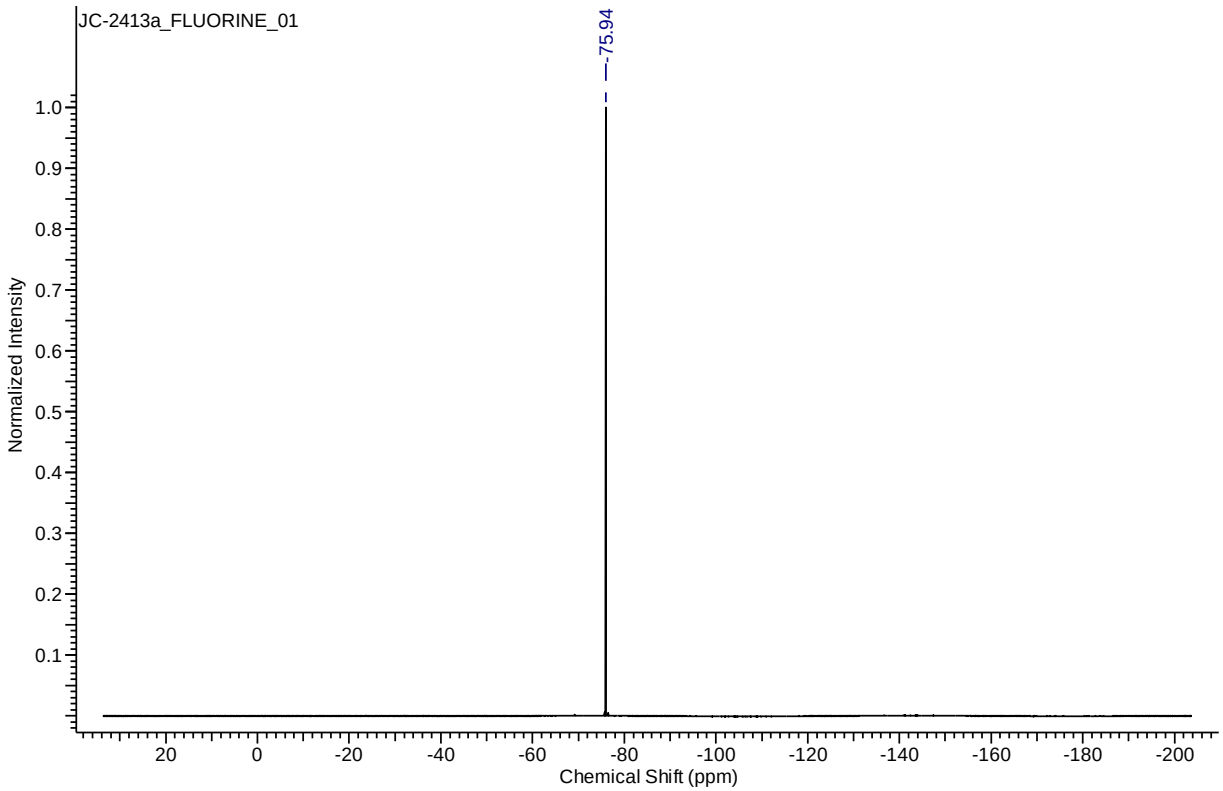
JC-2413a_FLUORINE_01
-75.94
Normalized Intensity
Chemical Shift (ppm)

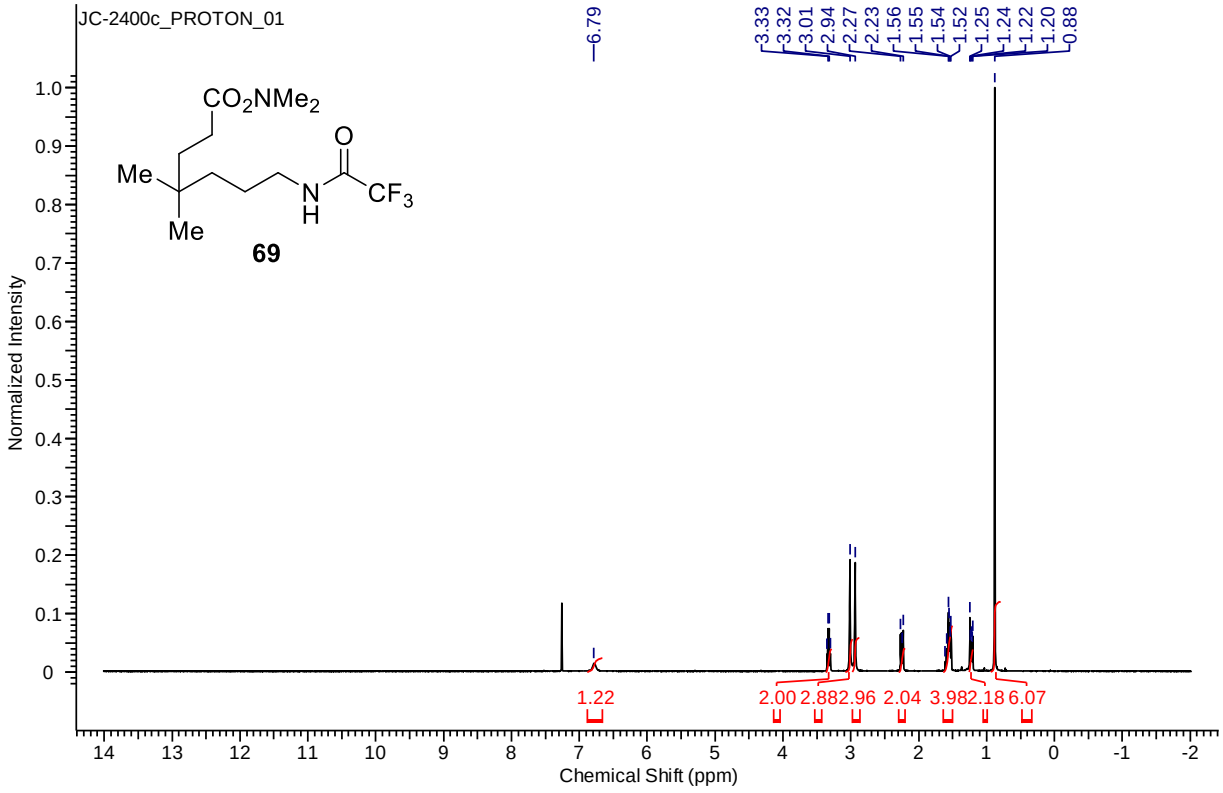
JC-2400c_PROTON_01
6.79
3.33
3.32
3.01
2.94
2.27
2.23
1.56
1.55
1.54
1.52
1.25
1.24
1.22
1.20
0.88
CO2NMe2
Me
Me
N
H
O
CF3
69
1.22
2.00
2.88
2.96
2.04
3.98
2.18
6.07
Normalized Intensity
Chemical Shift (ppm)

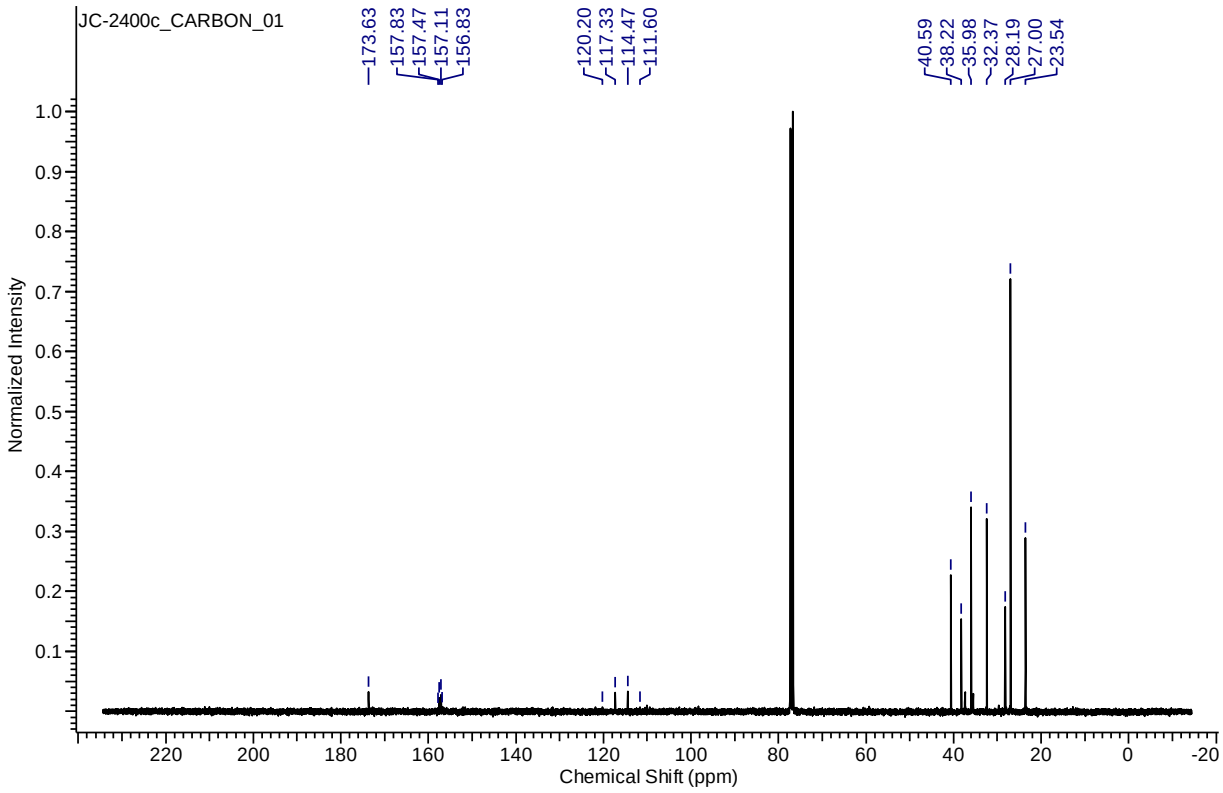
JC-2400c_CARBON_01
173.63
157.83
157.47
157.11
156.83
120.20
117.33
114.47
111.60
40.59
38.22
35.98
32.37
28.19
27.00
23.54
Normalized Intensity
Chemical Shift (ppm)

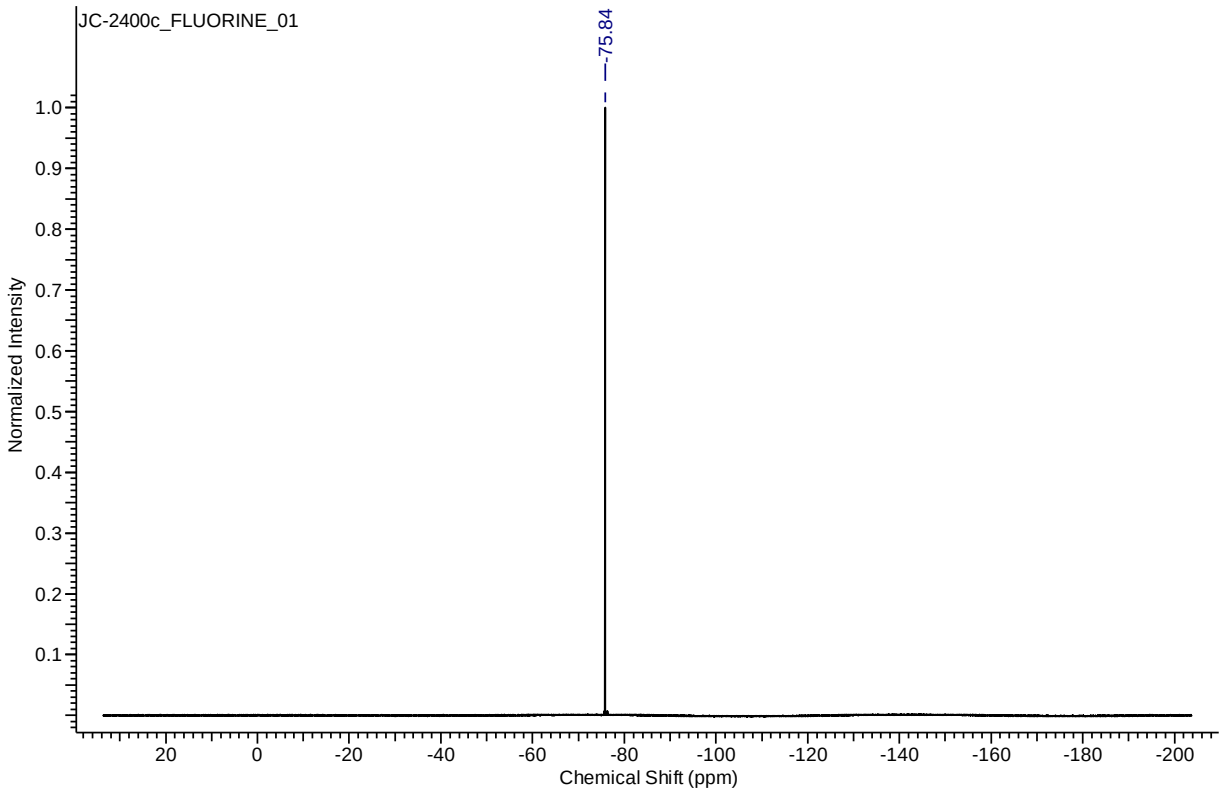
JC-2400c_FLUORINE_01
-75.84
Normalized Intensity
Chemical Shift (ppm)

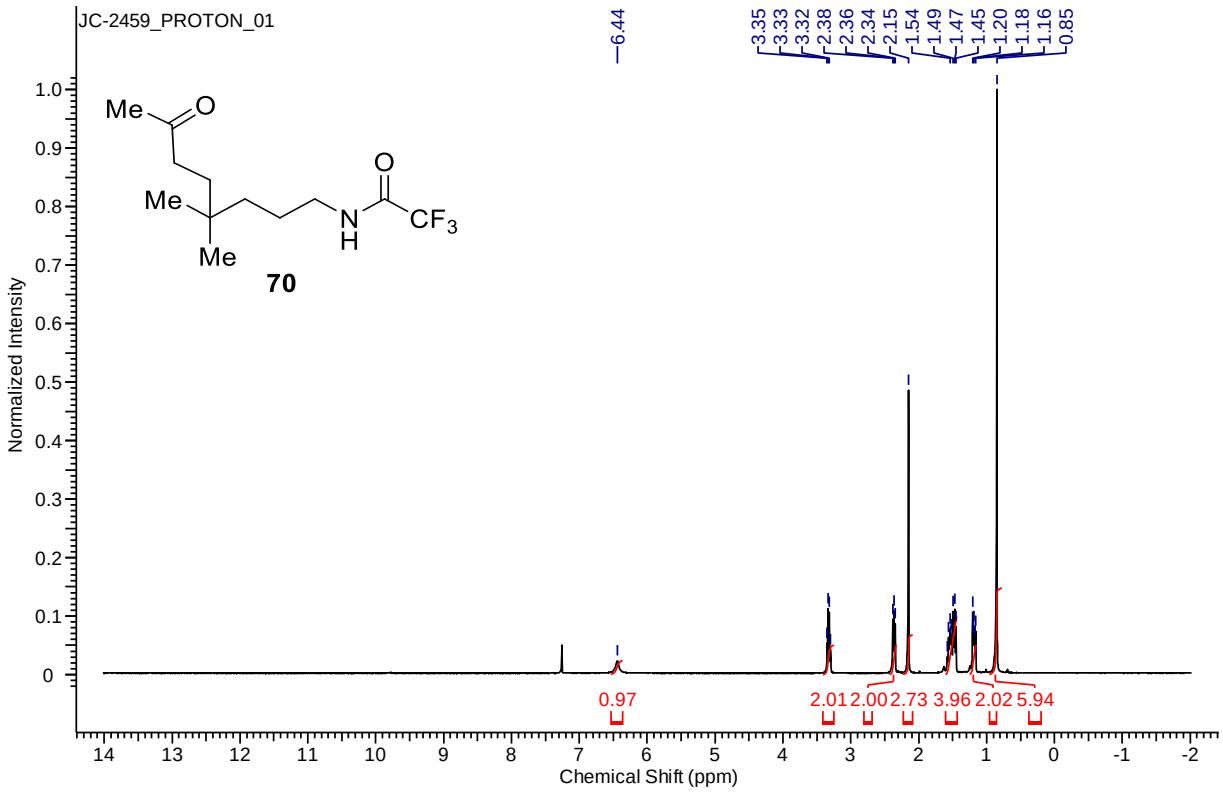
JC-2459_PROTON_01
Me
O
Me
N
H
O
CF3
Me
70
6.44
3.35
3.33
3.32
2.38
2.36
2.34
2.15
1.54
1.49
1.47
1.45
1.20
1.18
1.16
0.85
0.97
2.01
2.00
2.73
3.96
2.02
5.94
Normalized Intensity
Chemical Shift (ppm)

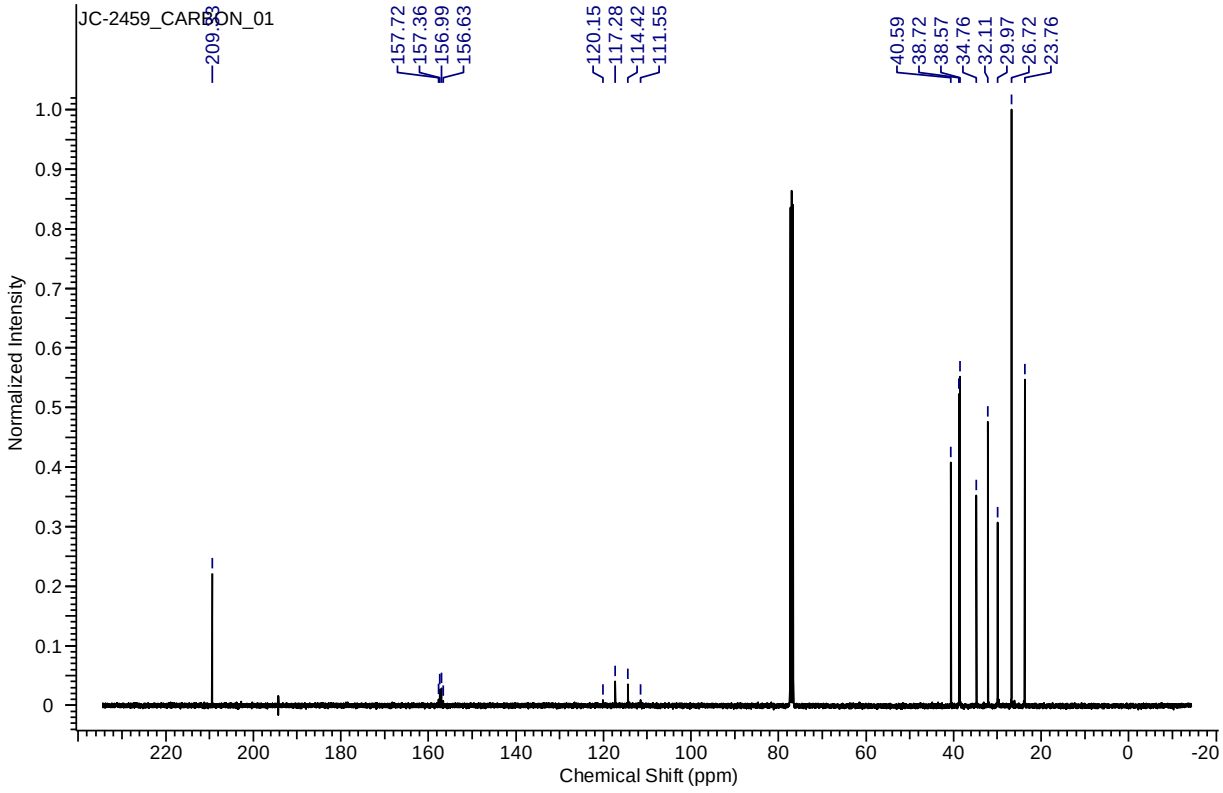
JC-2459_CARBON_01
209.83
157.72
157.36
156.99
156.63
120.15
117.28
114.42
111.55
40.59
38.72
38.57
34.76
32.11
29.97
26.72
23.76
Normalized Intensity
Chemical Shift (ppm)

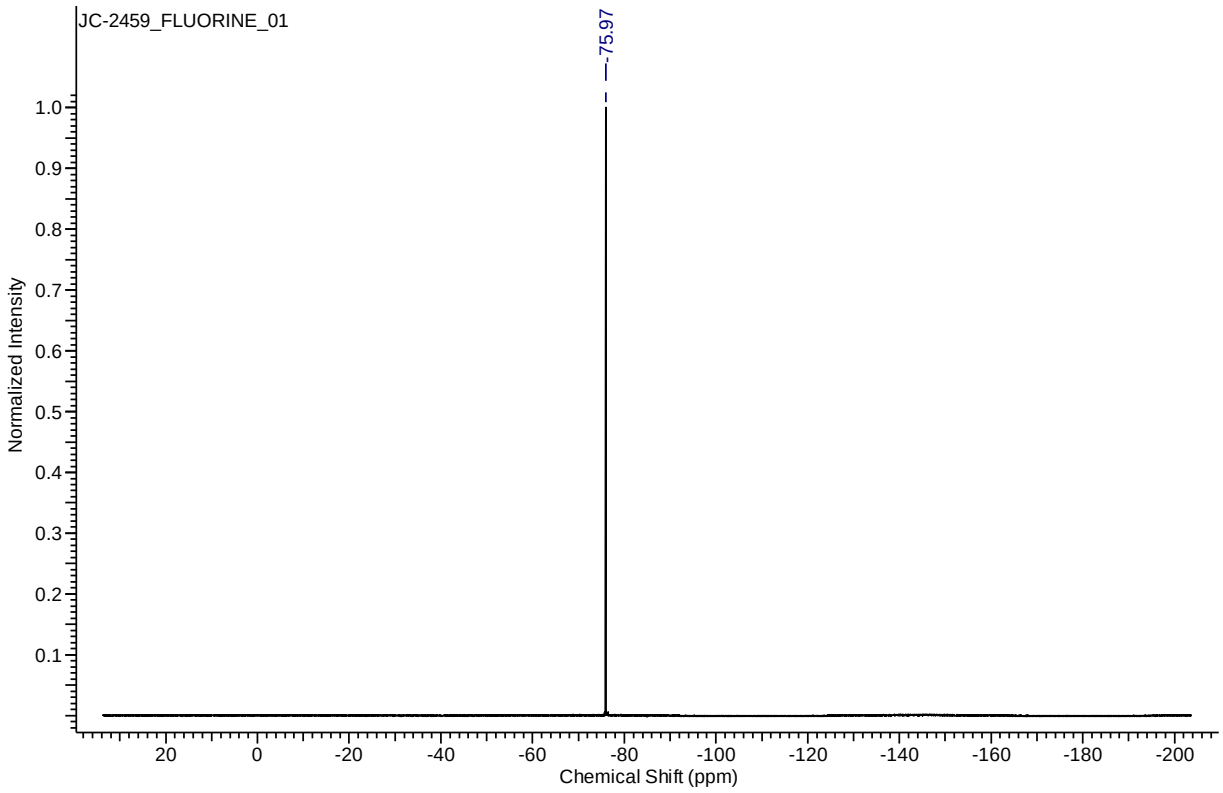
JC-2459_FLUORINE_01
-75.97
Normalized Intensity
Chemical Shift (ppm)

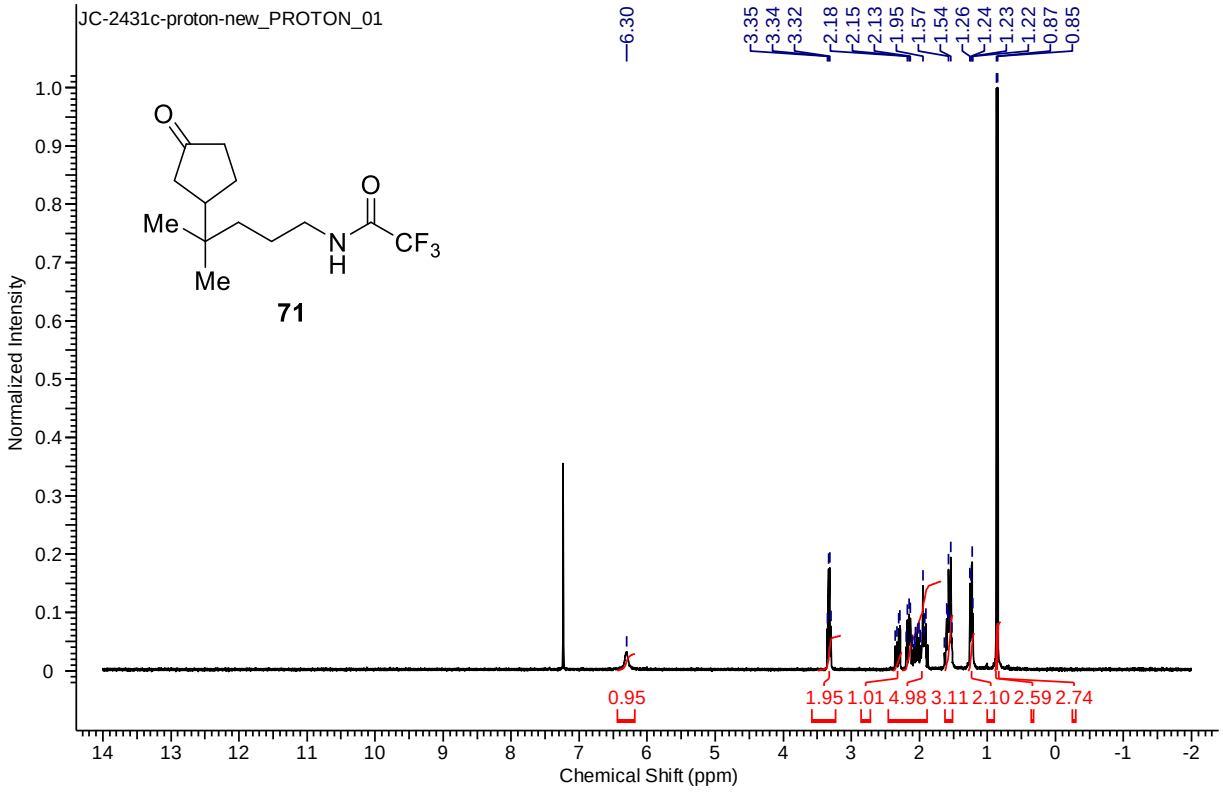
JC-2431c-proton-new_PROTON_01
6.30
3.35
3.34
3.32
2.18
2.15
2.13
1.95
1.57
1.54
1.26
1.24
1.23
1.22
0.87
0.85
Me
Me
N
H
O
O
CF3
71
0.95
1.95
1.01
4.98
3.11
2.10
2.59
2.74
Normalized Intensity
Chemical Shift (ppm)

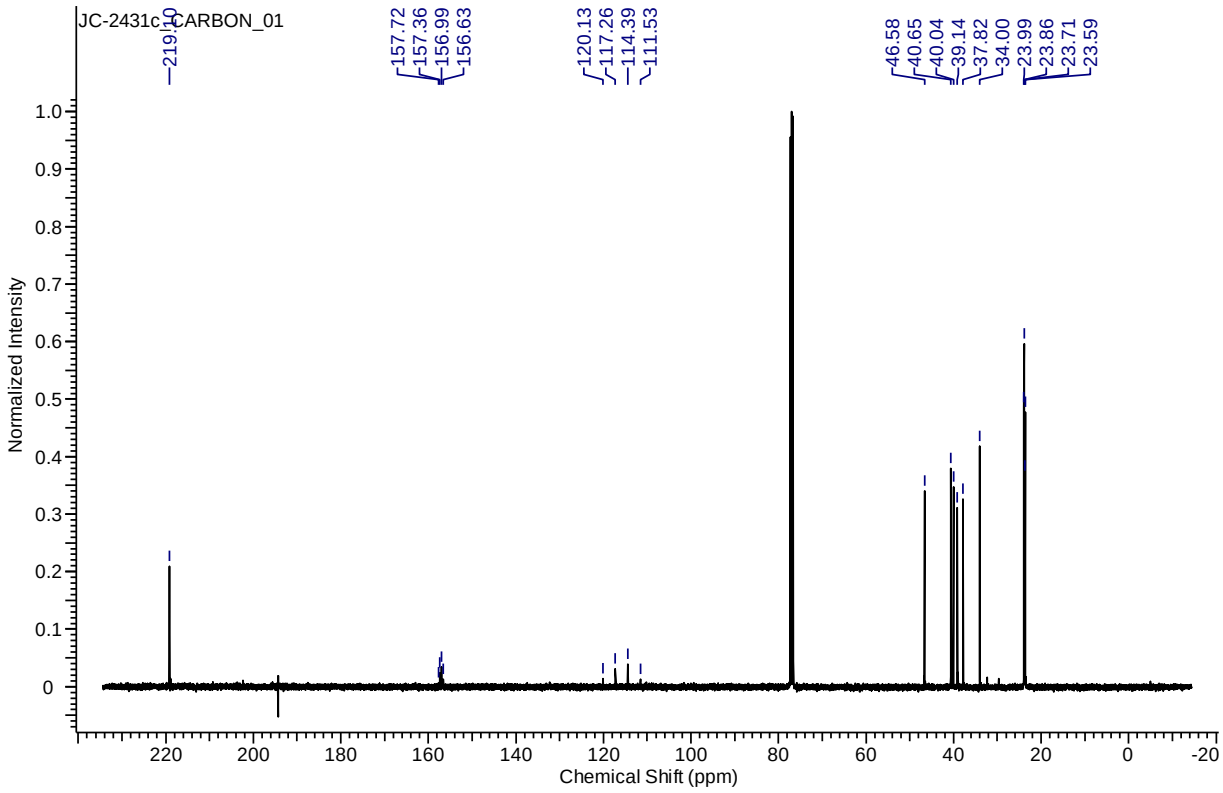
JC-2431c_CARBON_01
219.10
157.72
157.36
156.99
156.63
120.13
117.26
114.39
111.53
46.58
40.65
40.04
39.14
37.82
34.00
23.99
23.86
23.71
23.59
Normalized Intensity
Chemical Shift (ppm)

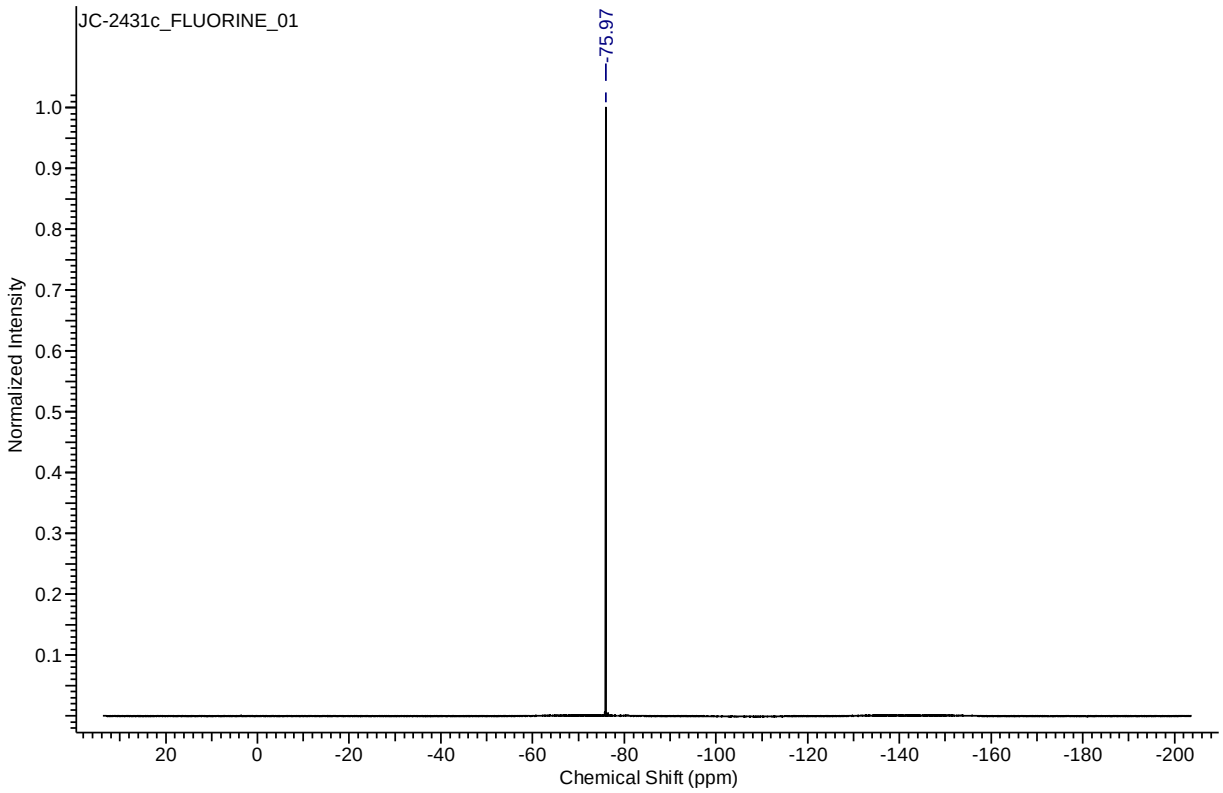
JC-2431c_FLUORINE_01
-75.97
Normalized Intensity
Chemical Shift (ppm)

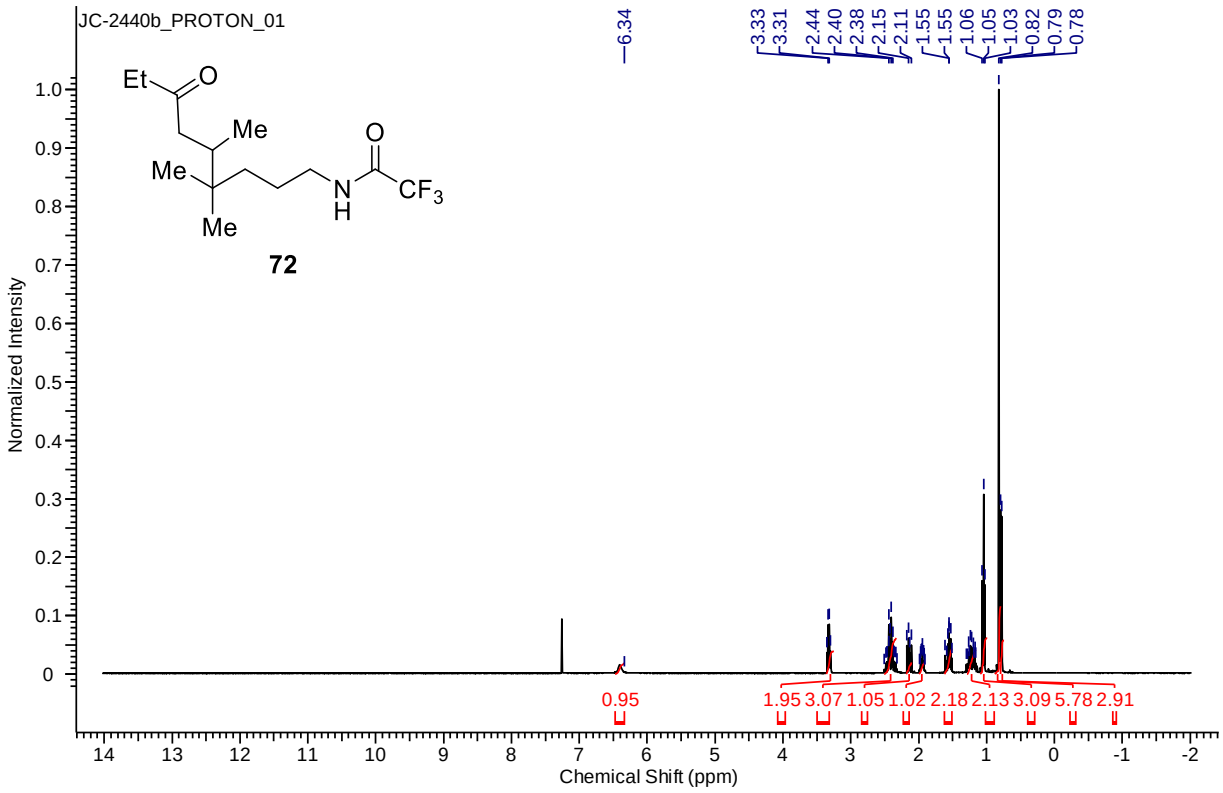
JC-2440b_PROTON_01
Et
O
Me
Me
Me
O
N
H
CF3
72
6.34
3.33
3.31
2.44
2.40
2.38
2.15
2.11
1.55
1.55
1.06
1.05
1.03
0.82
0.79
0.78
0.95
1.95 3.07 1.05 1.02 2.18 2.13 3.09 5.78 2.91
Normalized Intensity
Chemical Shift (ppm)

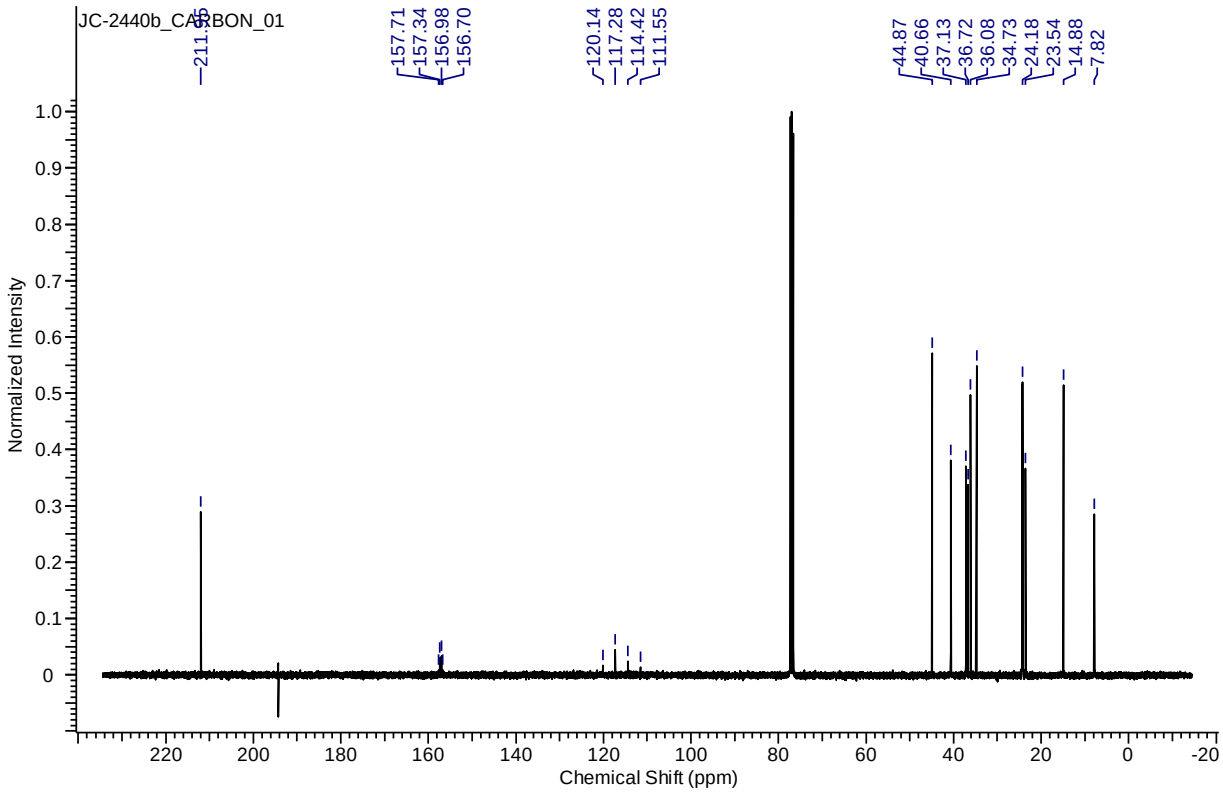
JC-2440b_CARBON_01
211.45
157.71
157.34
156.98
156.70
120.14
117.28
114.42
111.55
44.87
40.66
37.13
36.72
36.08
34.73
24.18
23.54
14.88
7.82
Normalized Intensity
Chemical Shift (ppm)

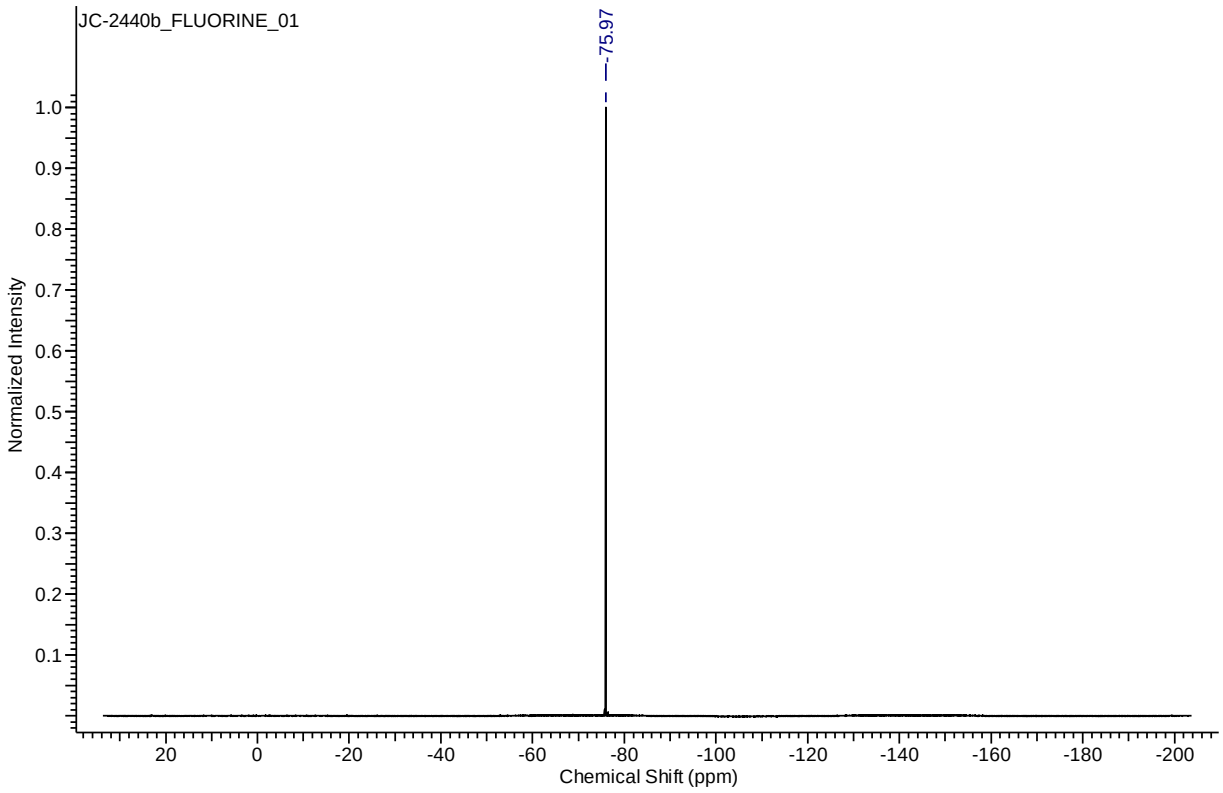
JC-2440b_FLUORINE_01
-75.97
Normalized Intensity
Chemical Shift (ppm)

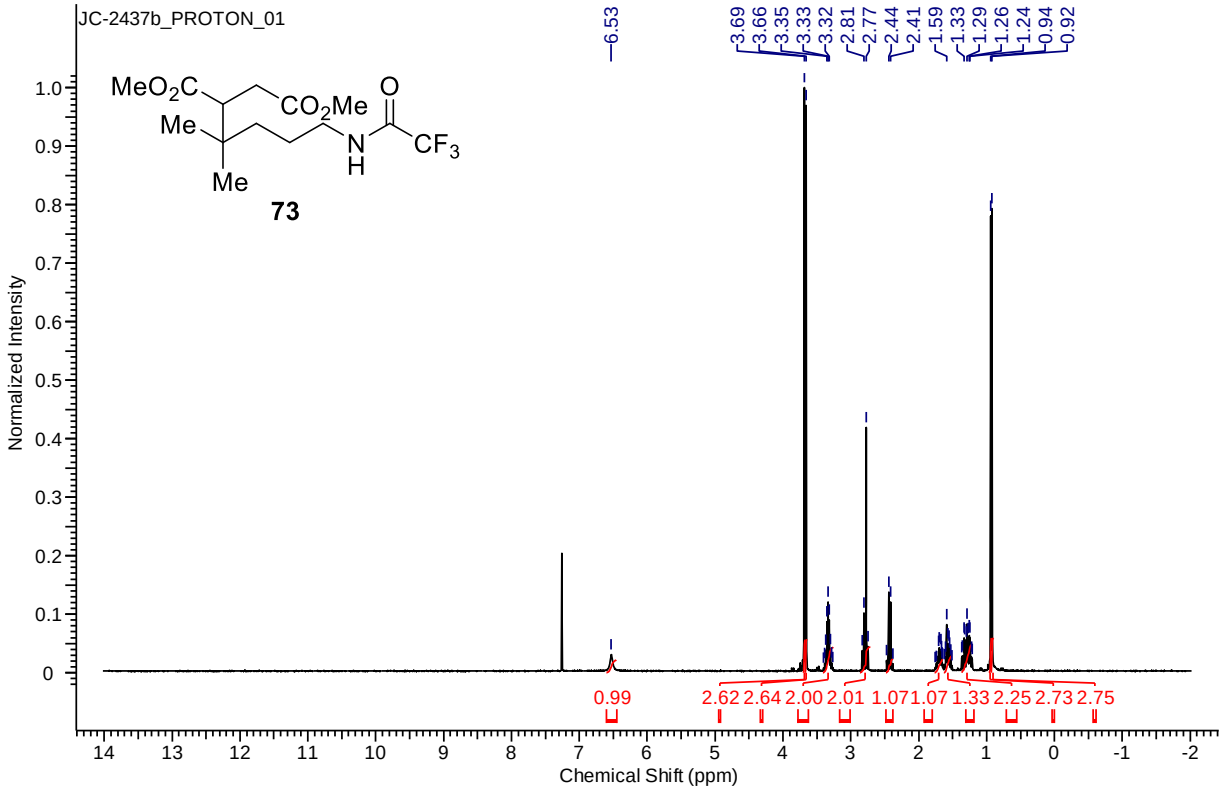
JC-2437b_PROTON_01
MeO2C
CO2Me
Me
Me
N
H
O
CF3
73
6.53
3.69
3.66
3.35
3.33
3.32
2.81
2.77
2.44
2.41
1.59
1.33
1.29
1.26
1.24
0.94
0.92
0.99
2.62
2.64
2.00
2.01
1.07
1.07
1.33
2.25
2.73
2.75
Normalized Intensity
Chemical Shift (ppm)

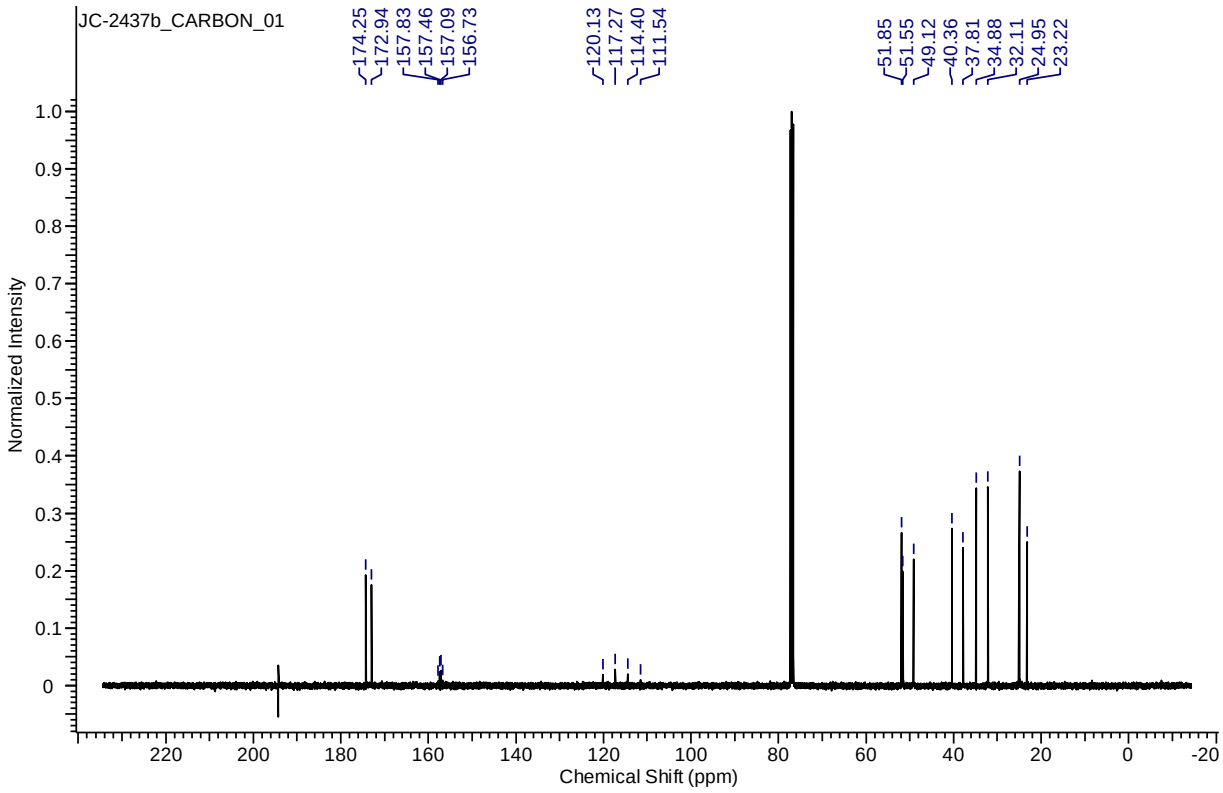
JC-2437b_CARBON_01
174.25
172.94
157.83
157.46
157.09
156.73
120.13
117.27
114.40
111.54
51.85
51.55
49.12
40.36
37.81
34.88
32.11
24.95
23.22
Normalized Intensity
Chemical Shift (ppm)

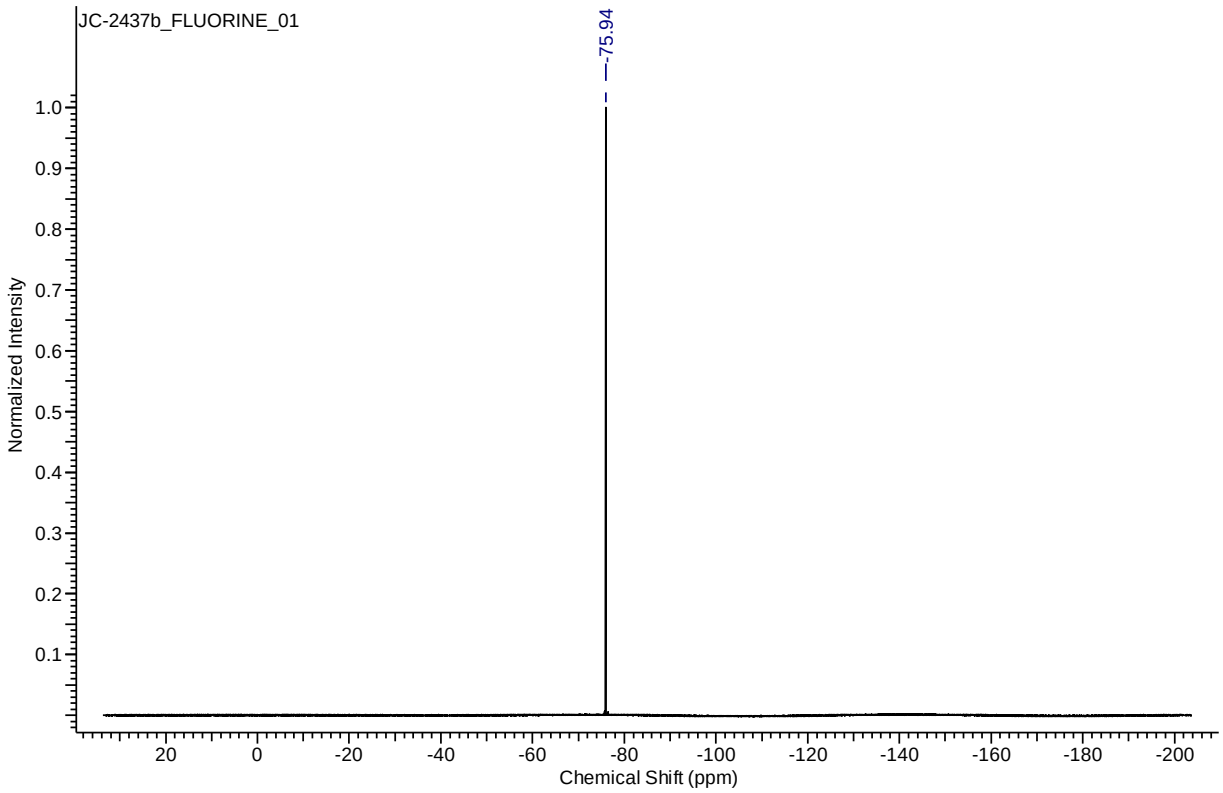
JC-2437b_FLUORINE_01
-75.94
Normalized Intensity
Chemical Shift (ppm)

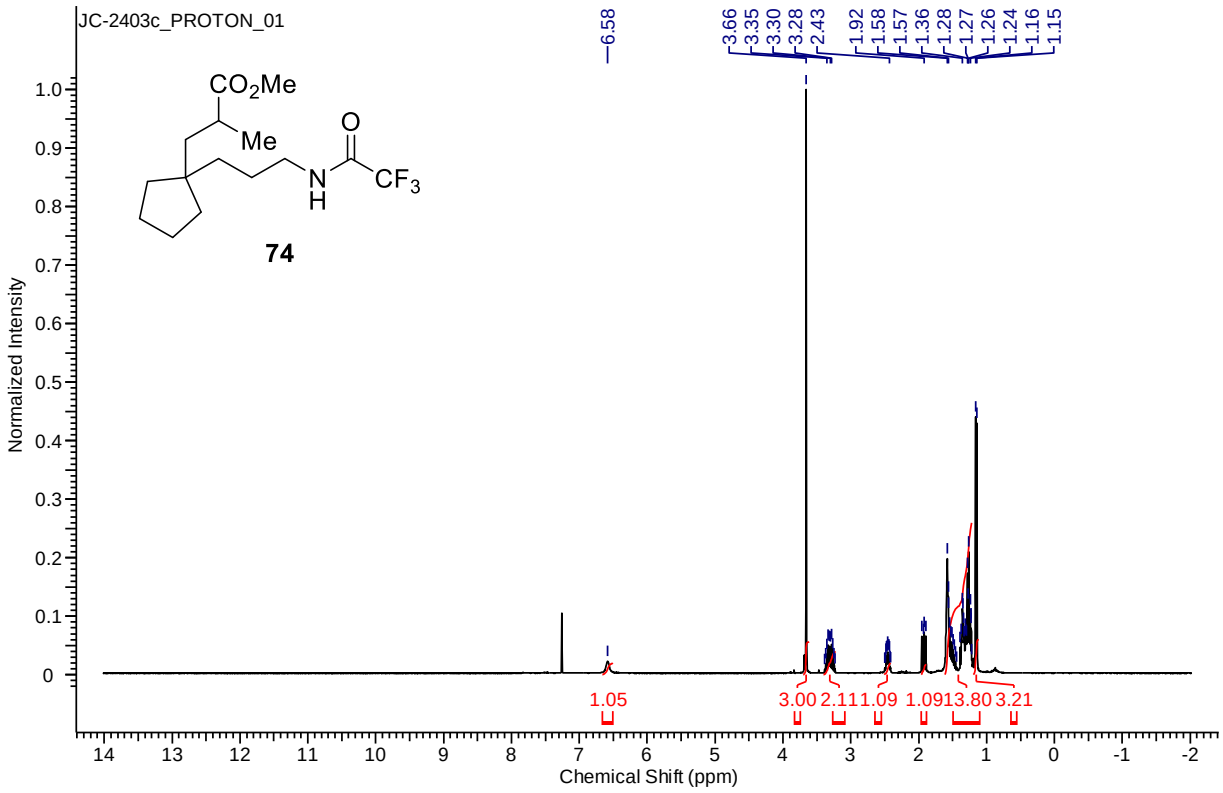
JC-2403c_PROTON_01
6.58
3.66
3.35
3.30
3.28
2.43
1.92
1.58
1.57
1.36
1.28
1.27
1.26
1.24
1.16
1.15
CO2Me
Me
O
N
H
CF3
74
Normalized Intensity
1.05
3.00
2.11
1.09
1.09
13.80
3.21
Chemical Shift (ppm)

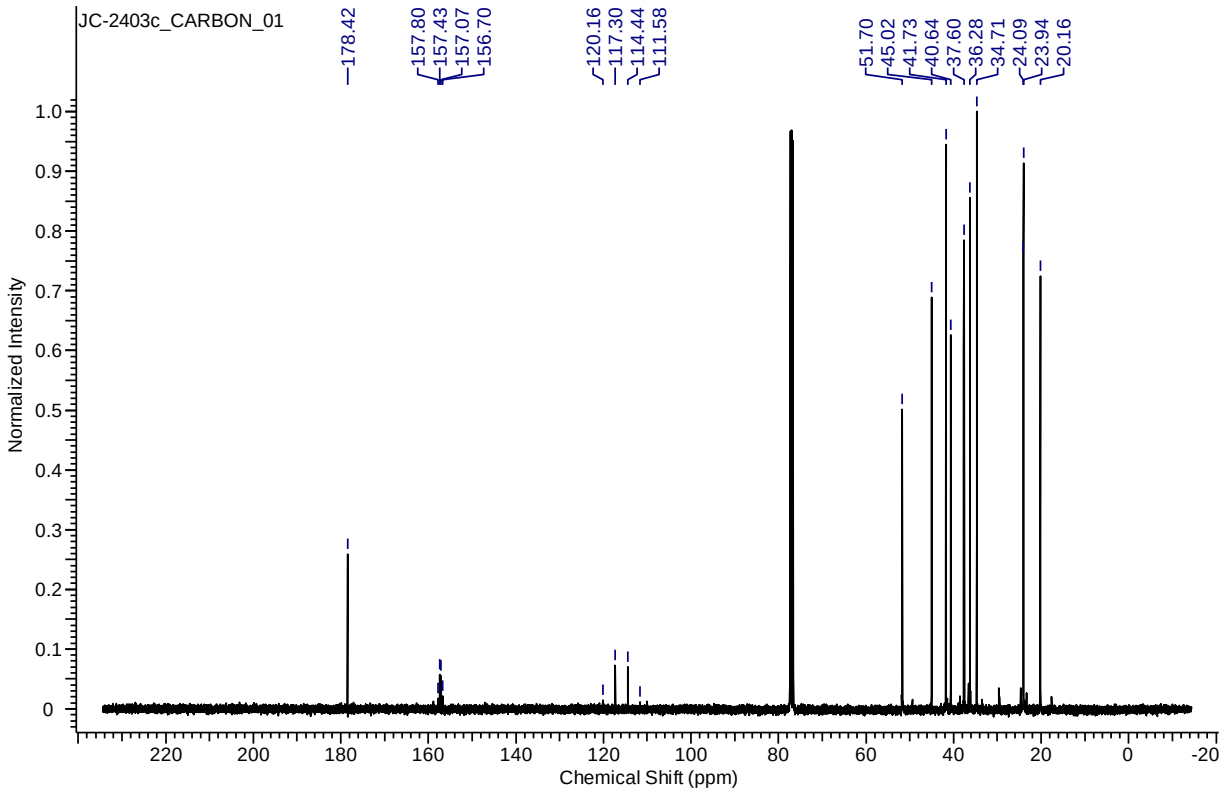
JC-2403c_CARBON_01
178.42
157.80
157.43
157.07
156.70
120.16
117.30
114.44
111.58
51.70
45.02
41.73
40.64
37.60
36.28
34.71
24.09
23.94
20.16
Normalized Intensity
Chemical Shift (ppm)

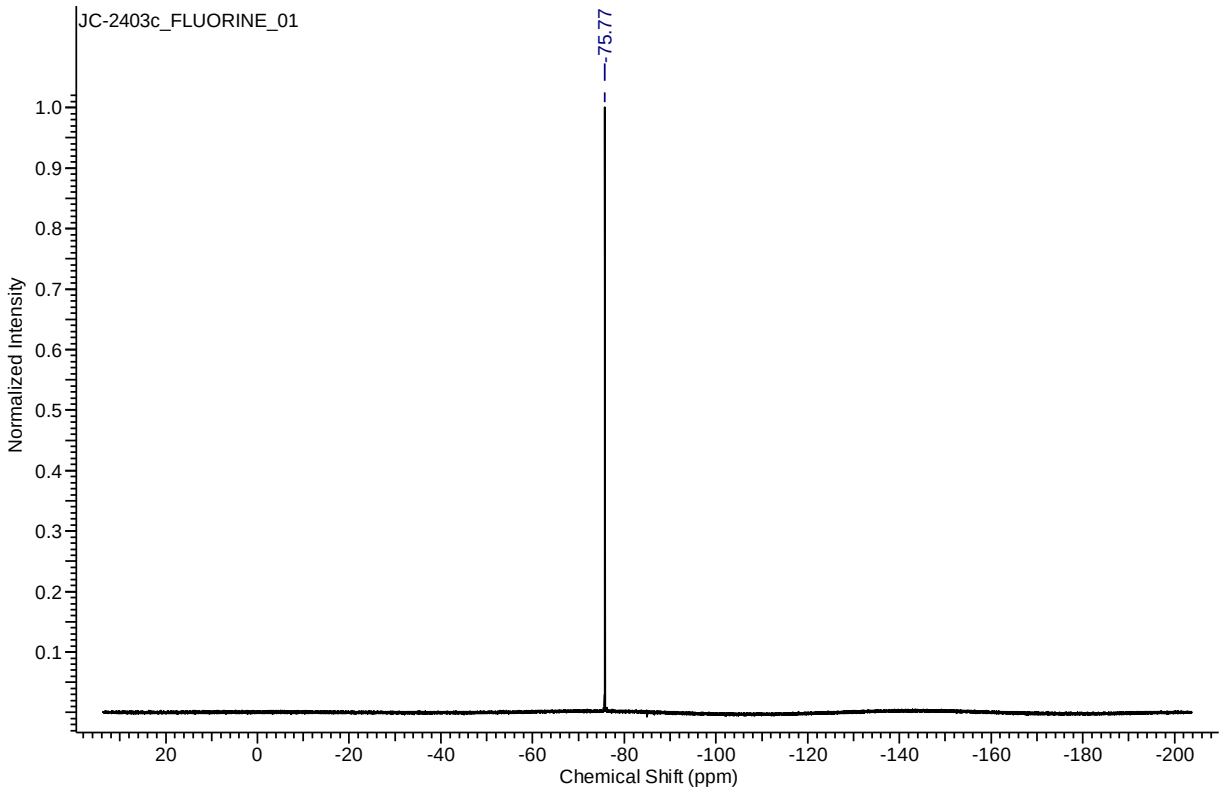
JC-2403c_FLUORINE_01
-75.77
Normalized Intensity
Chemical Shift (ppm)

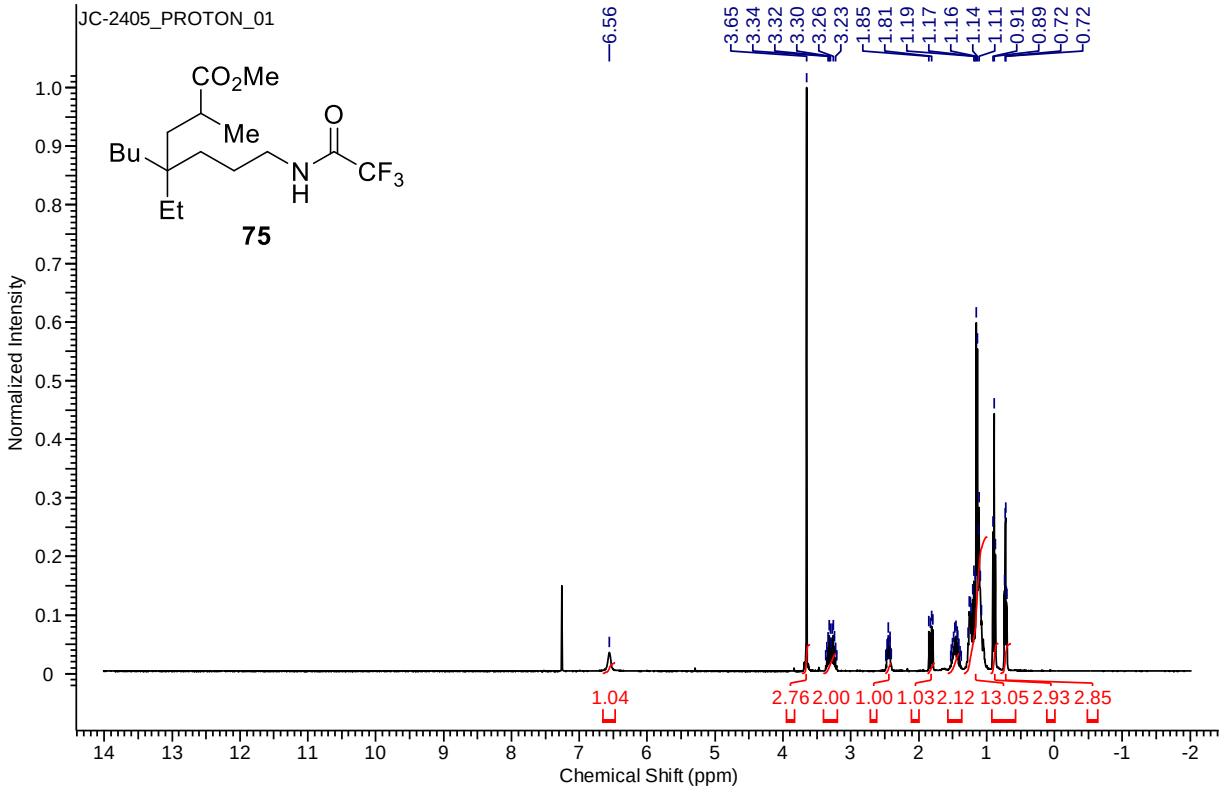
JC-2405_PROTON_01
6.56
3.65
3.34
3.32
3.30
3.26
3.23
1.85
1.81
1.19
1.17
1.16
1.14
1.11
0.91
0.89
0.72
0.72
CO2Me
Me
Bu
Et
N
H
O
CF3
75
1.04
2.76
2.00
1.00
1.03
2.12
13.05
2.93
2.85
Normalized Intensity
Chemical Shift (ppm)

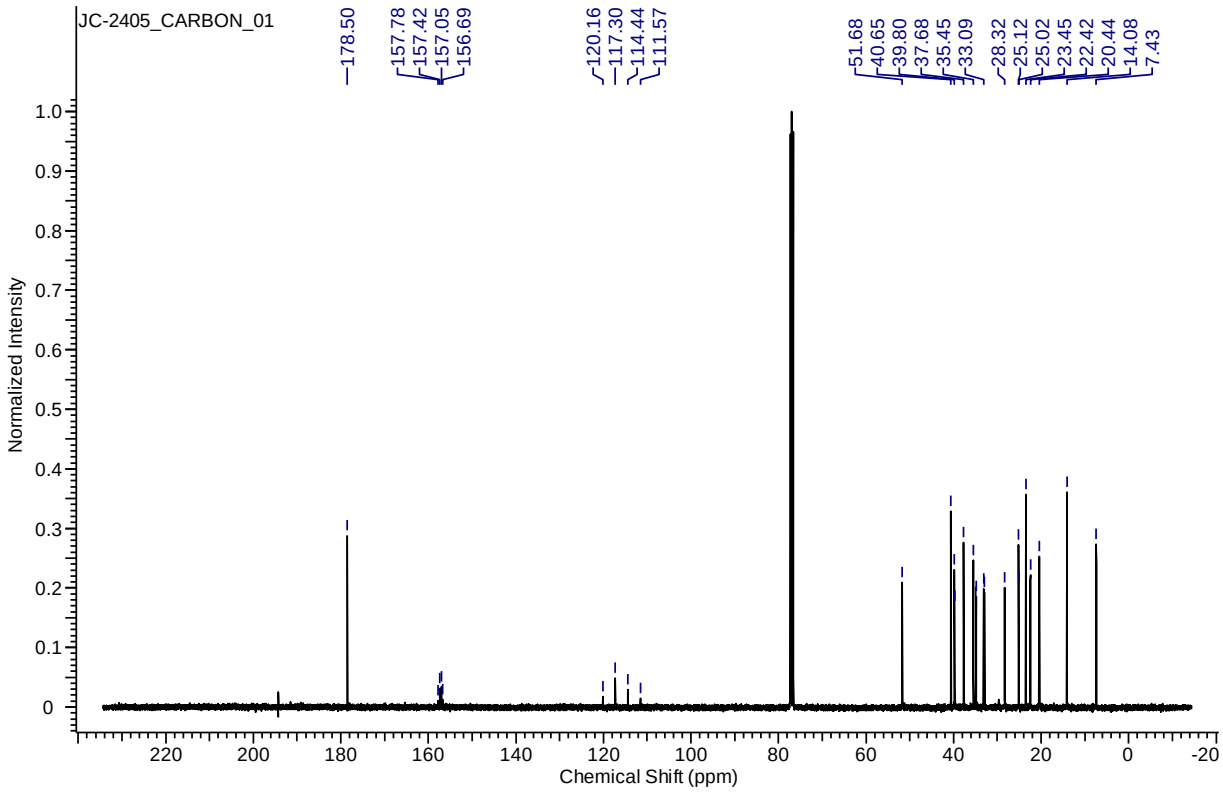
JC-2405_CARBON_01
178.50
157.78
157.42
157.05
156.69
120.16
117.30
114.44
111.57
51.68
40.65
39.80
37.68
35.45
33.09
28.32
25.12
25.02
23.45
22.42
20.44
14.08
7.43
Normalized Intensity
Chemical Shift (ppm)

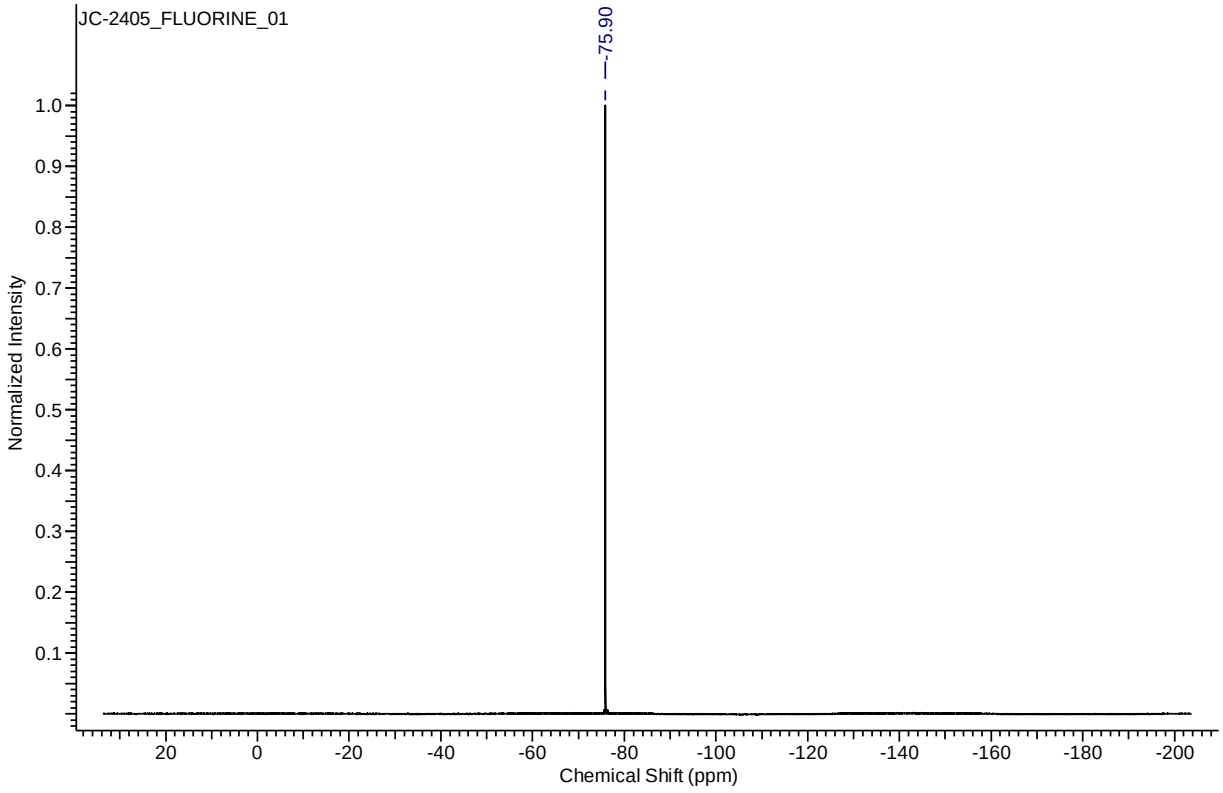
JC-2405_FLUORINE_01
-75.90
Normalized Intensity
Chemical Shift (ppm)

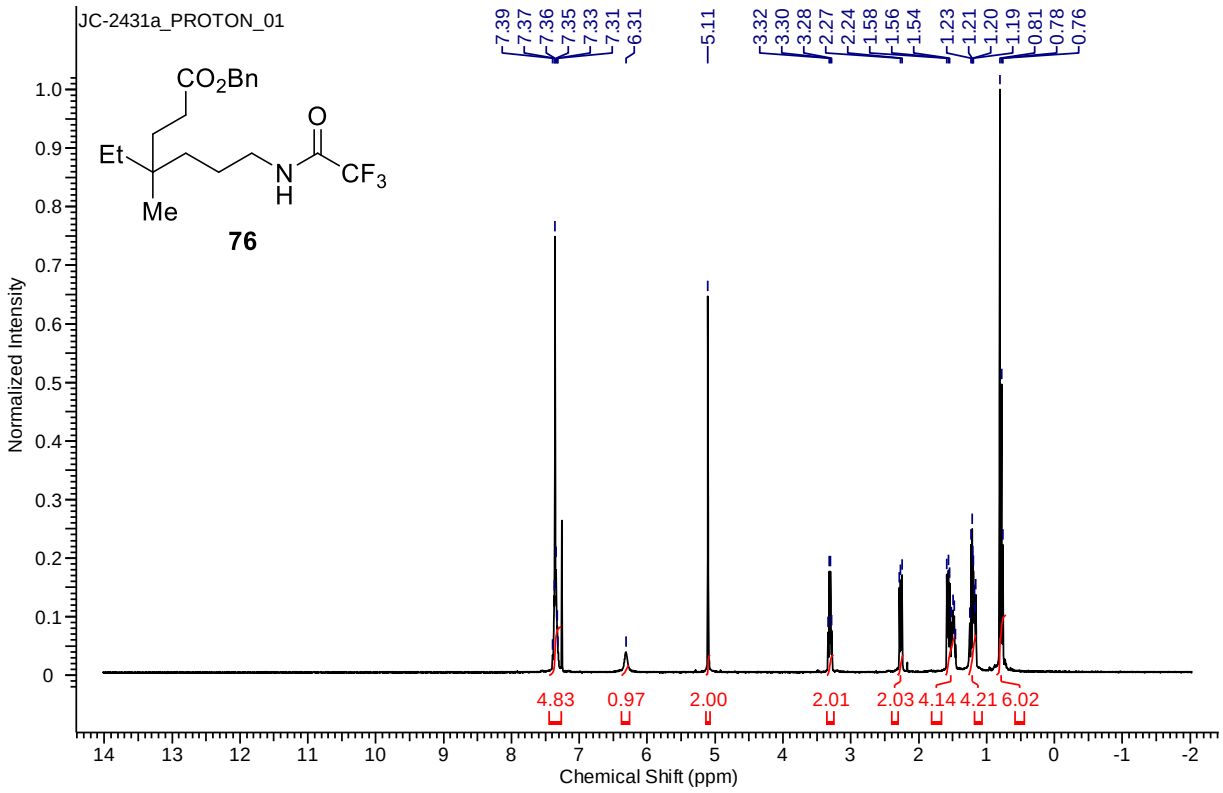
JC-2431a_PROTON_01
7.39
7.37
7.36
7.35
7.33
7.31
6.31
5.11
3.32
3.30
3.28
2.27
2.24
1.58
1.56
1.54
1.23
1.21
1.20
1.19
0.81
0.78
0.76
CO2Bn
Et
Me
N
H
O
CF3
76
Normalized Intensity
4.83
0.97
2.00
2.01
2.03
4.14
4.21
6.02
Chemical Shift (ppm)

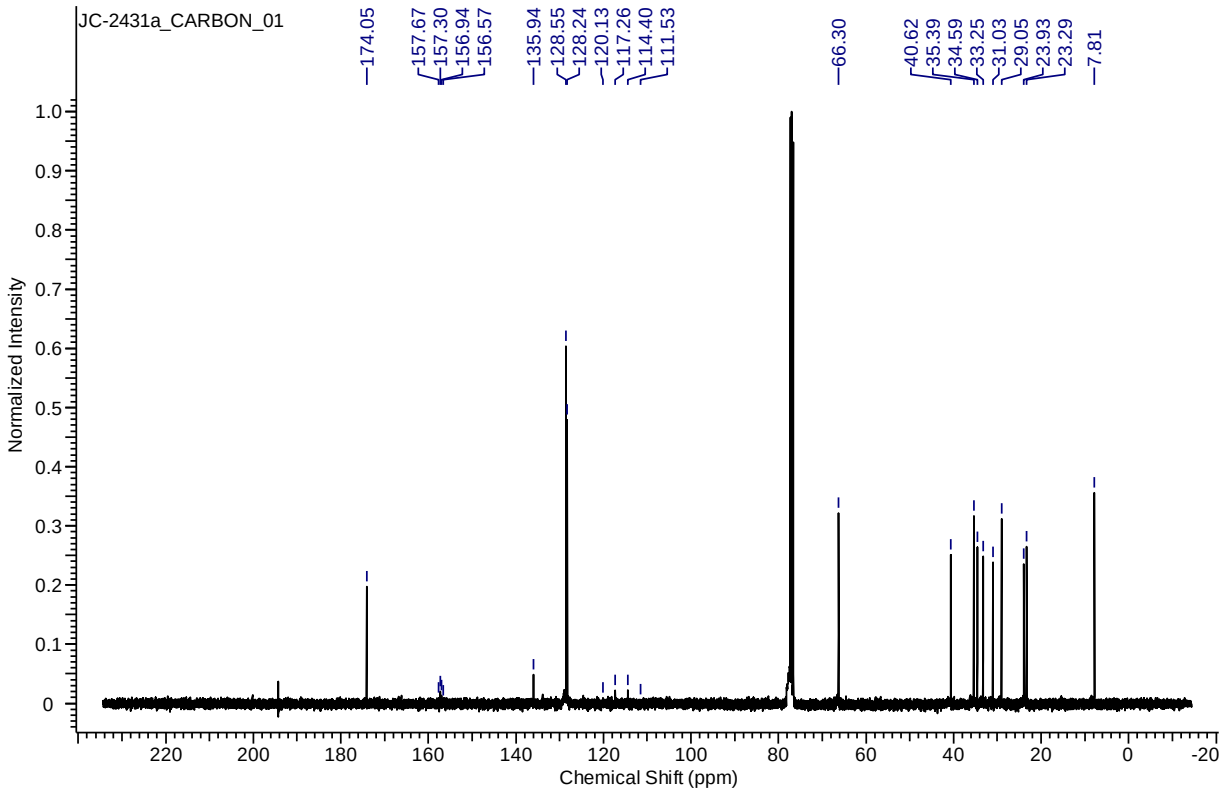
JC-2431a_CARBON_01
174.05
157.67
157.30
156.94
156.57
135.94
128.55
128.24
120.13
117.26
114.40
111.53
66.30
40.62
35.39
34.59
33.25
31.03
29.05
23.93
23.29
7.81
Normalized Intensity
Chemical Shift (ppm)

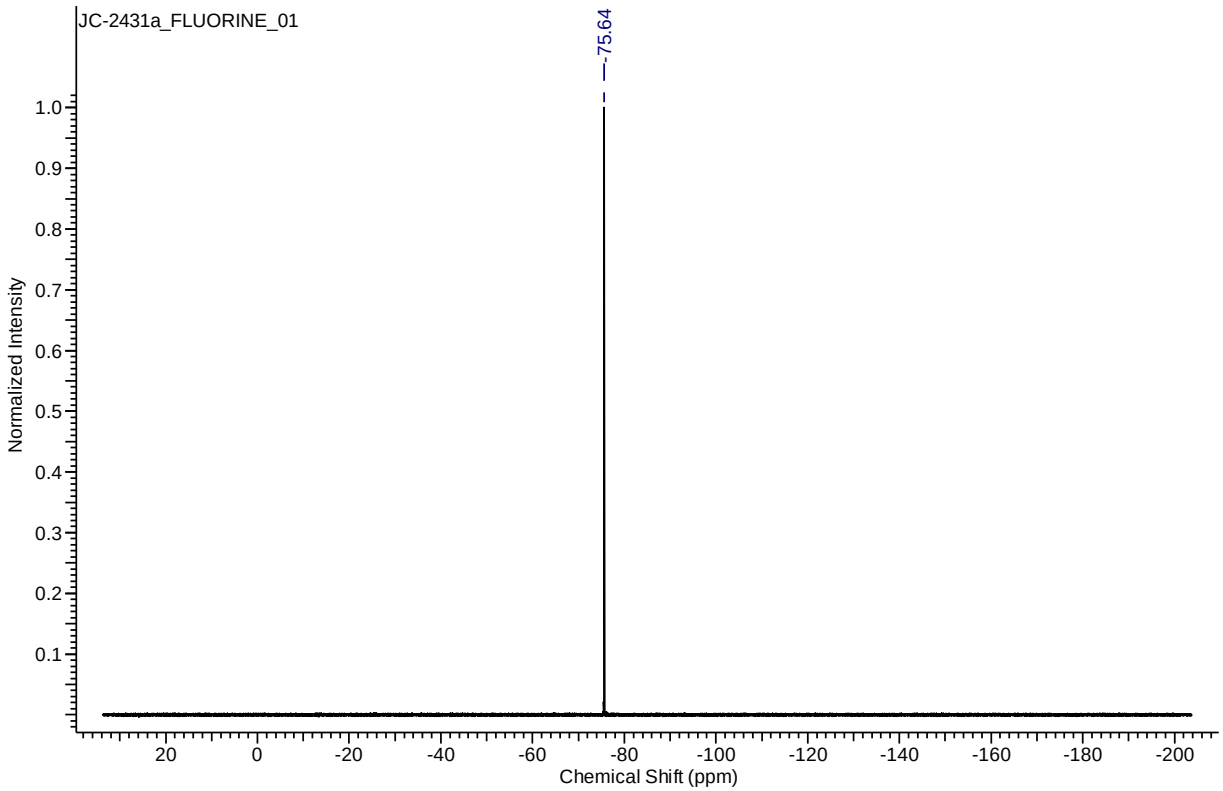
JC-2431a_FLUORINE_01
-75.64
Normalized Intensity
Chemical Shift (ppm)

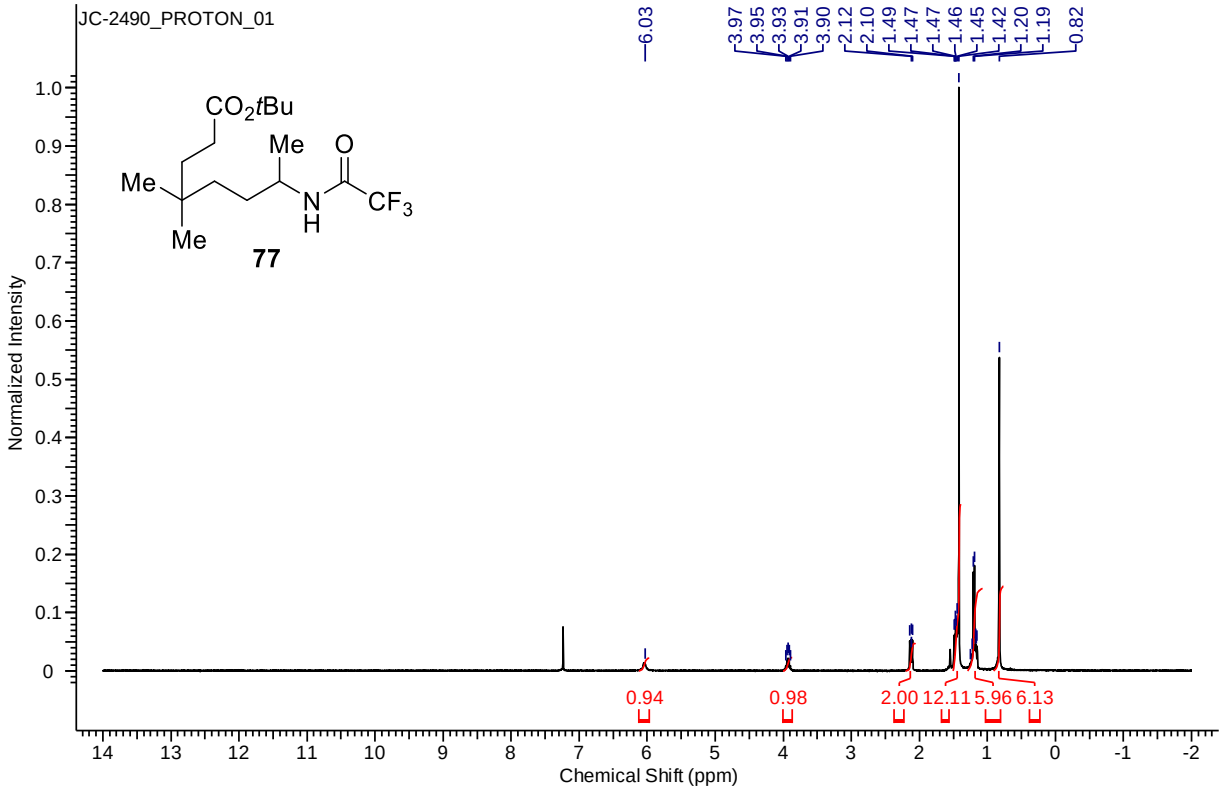
JC-2490_PROTON_01
6.03
3.97
3.95
3.93
3.91
3.90
2.12
2.10
1.49
1.47
1.47
1.46
1.45
1.42
1.20
1.19
0.82
0.94
0.98
2.00
12.11
5.96
6.13
Normalized Intensity
Chemical Shift (ppm)

CO2tBu
Me
O
Me
N
H
CF3
Me

77

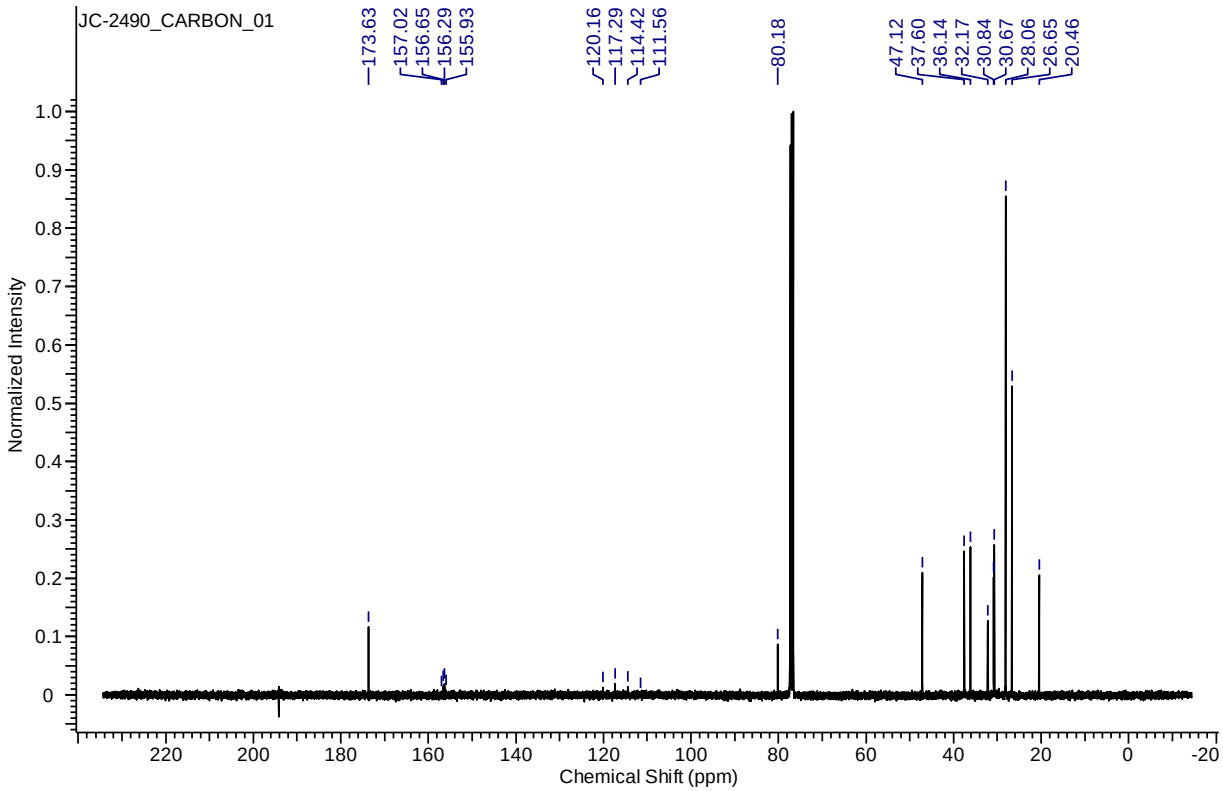
JC-2490_CARBON_01
173.63
157.02
156.65
156.29
155.93
120.16
117.29
114.42
111.56
80.18
47.12
37.60
36.14
32.17
30.84
30.67
28.06
26.65
20.46
Normalized Intensity
Chemical Shift (ppm)

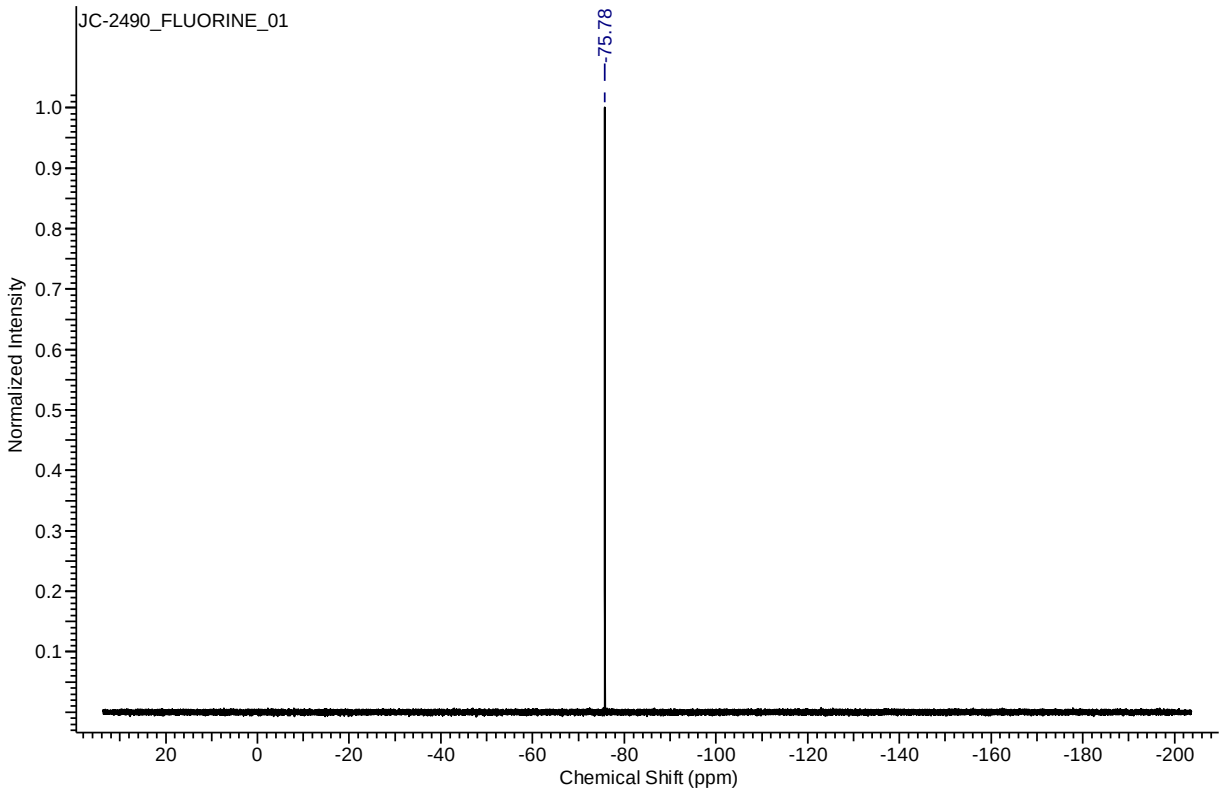
JC-2490_FLUORINE_01
-75.78
Normalized Intensity
Chemical Shift (ppm)

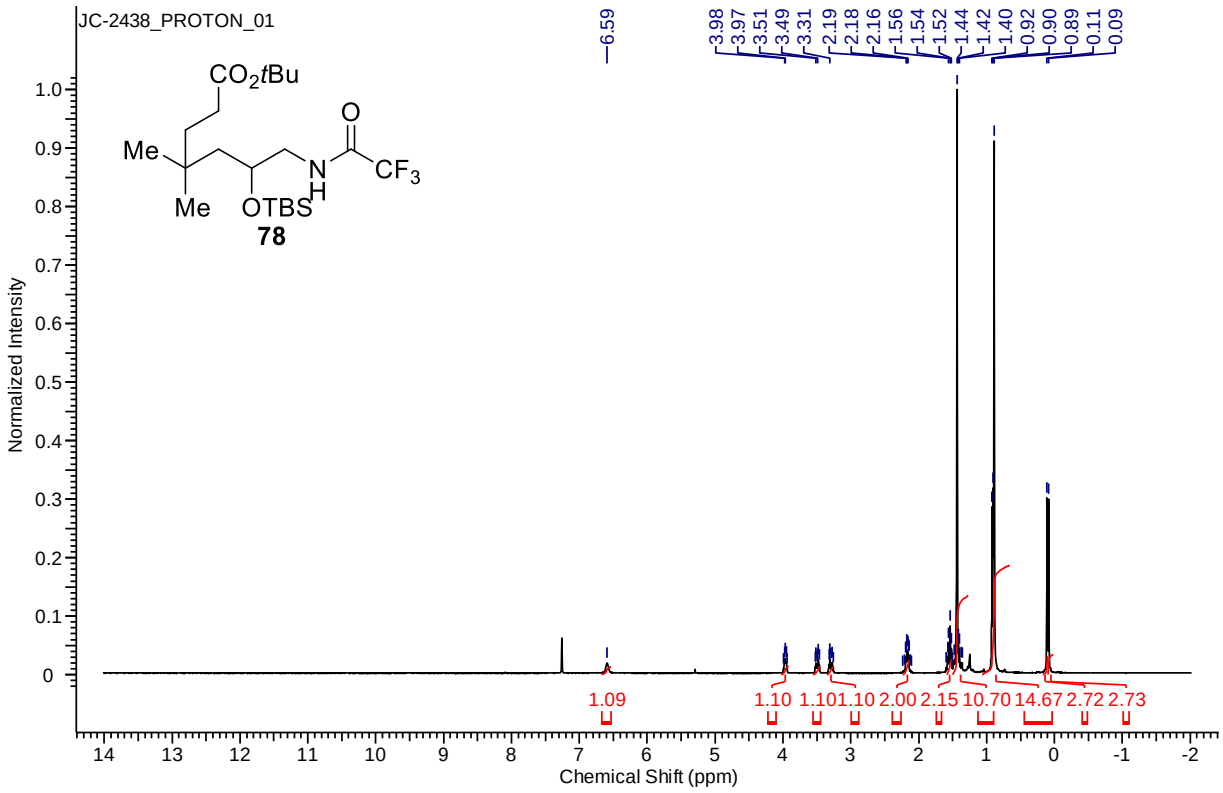
JC-2438_PROTON_01
CO2tBu
Me
Me
OTBS
N
H
O
CF3
78
Normalized Intensity
Chemical Shift (ppm)
6.59
3.98
3.97
3.51
3.49
3.31
2.19
2.18
2.16
1.56
1.54
1.52
1.44
1.42
1.40
0.92
0.90
0.89
0.11
0.09
1.09
1.10
1.10
1.10
2.00
2.15
10.70
14.67
2.72
2.73

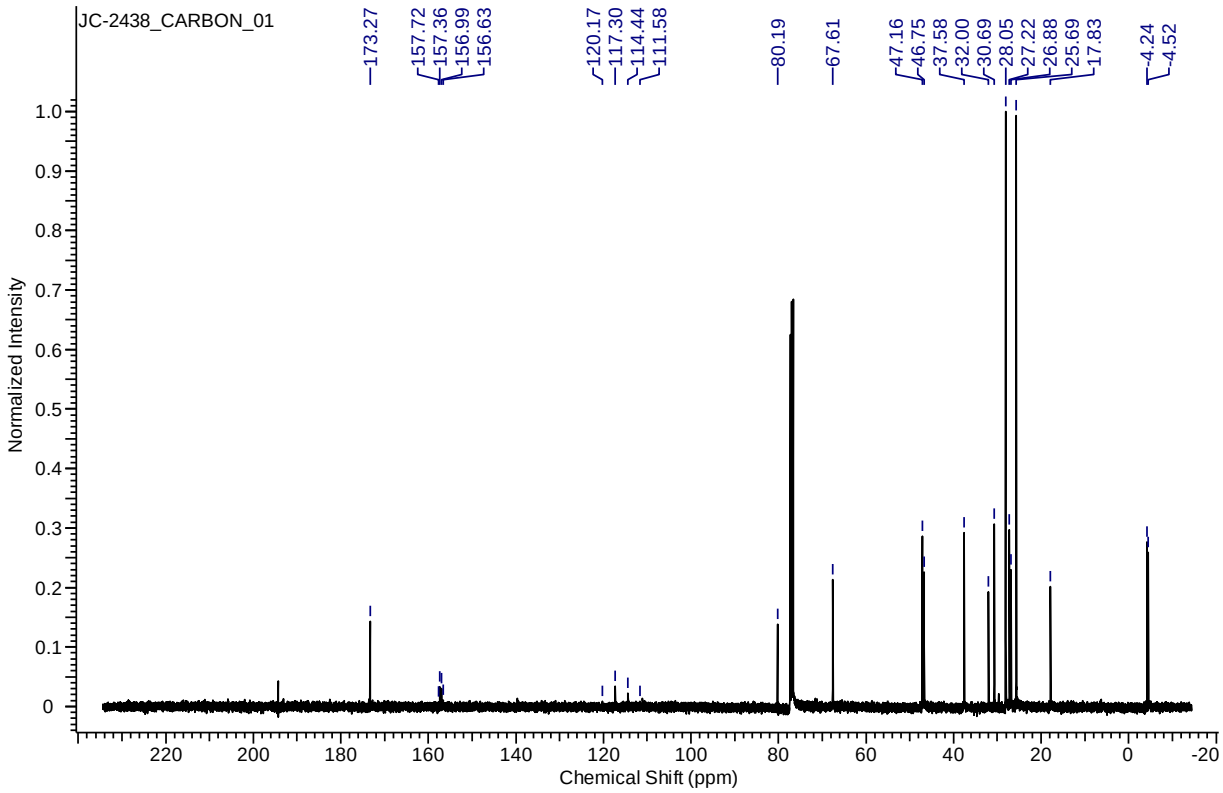
JC-2438_CARBON_01
Normalized Intensity
Chemical Shift (ppm)
173.27
157.72
157.36
156.99
156.63
120.17
117.30
114.44
111.58
80.19
67.61
47.16
46.75
37.58
32.00
30.69
28.05
27.22
26.88
25.69
17.83
-4.24
-4.52

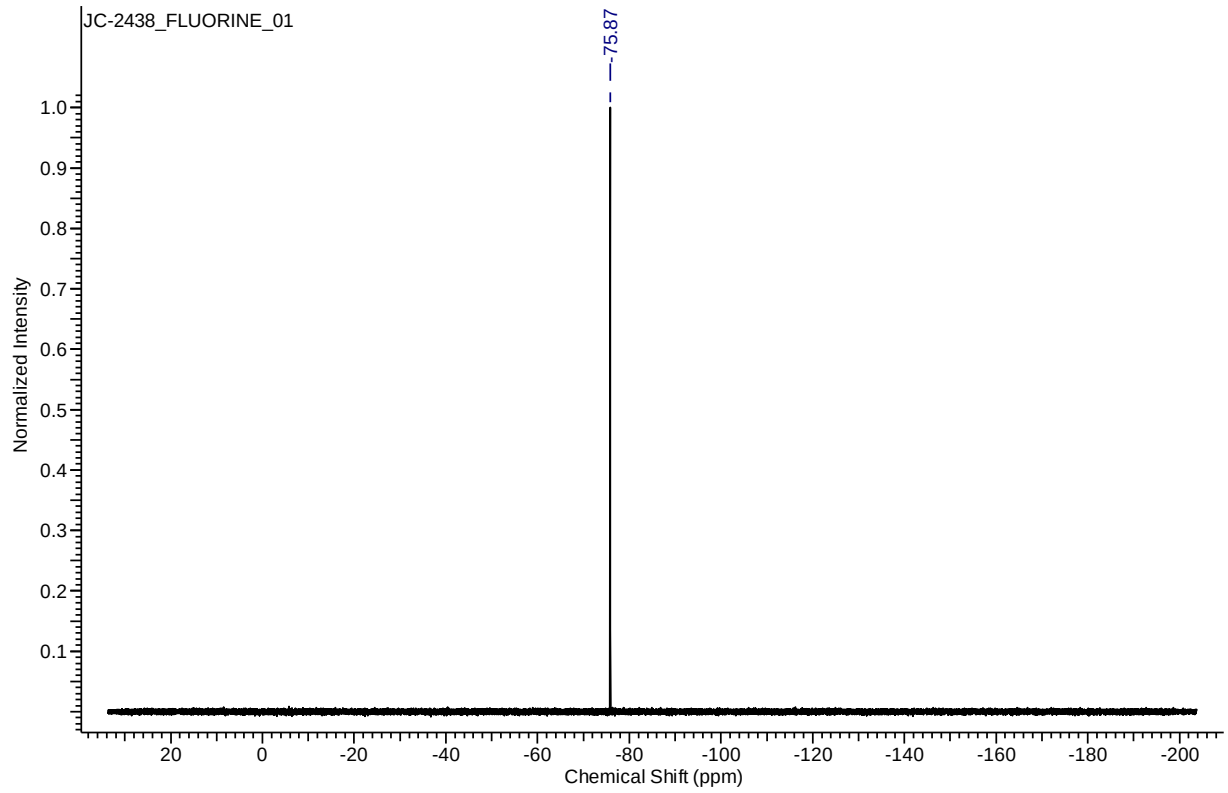
JC-2438_FLUORINE_01
-75.87
Normalized Intensity
Chemical Shift (ppm)

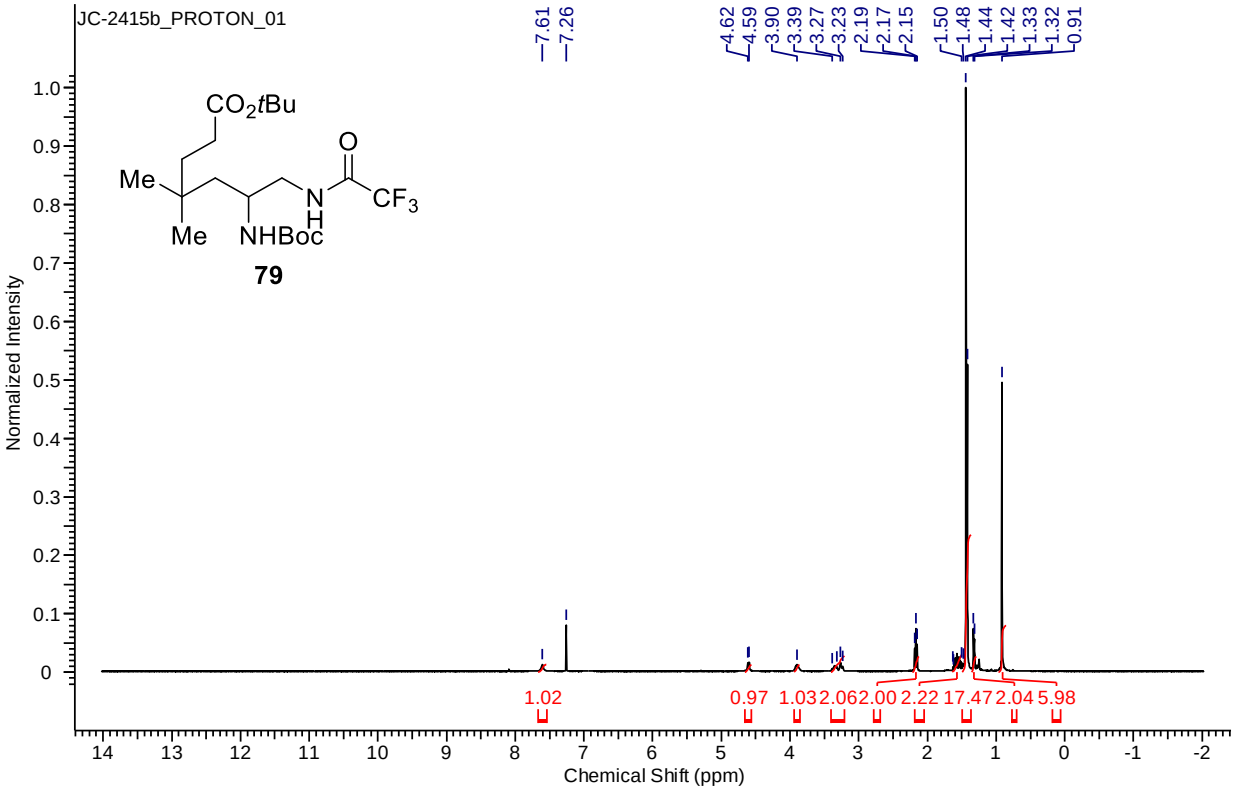
JC-2415b_PROTON_01
7.61
7.26
4.62
4.59
3.90
3.39
3.27
3.23
2.19
2.17
2.15
1.50
1.48
1.44
1.42
1.33
1.32
0.91
CO2tBu
Me
O
N
H
CF3
Me
NHBoc
79
1.02
0.97
1.03
2.06
2.00
2.22
17.47
2.04
5.98
Normalized Intensity
Chemical Shift (ppm)

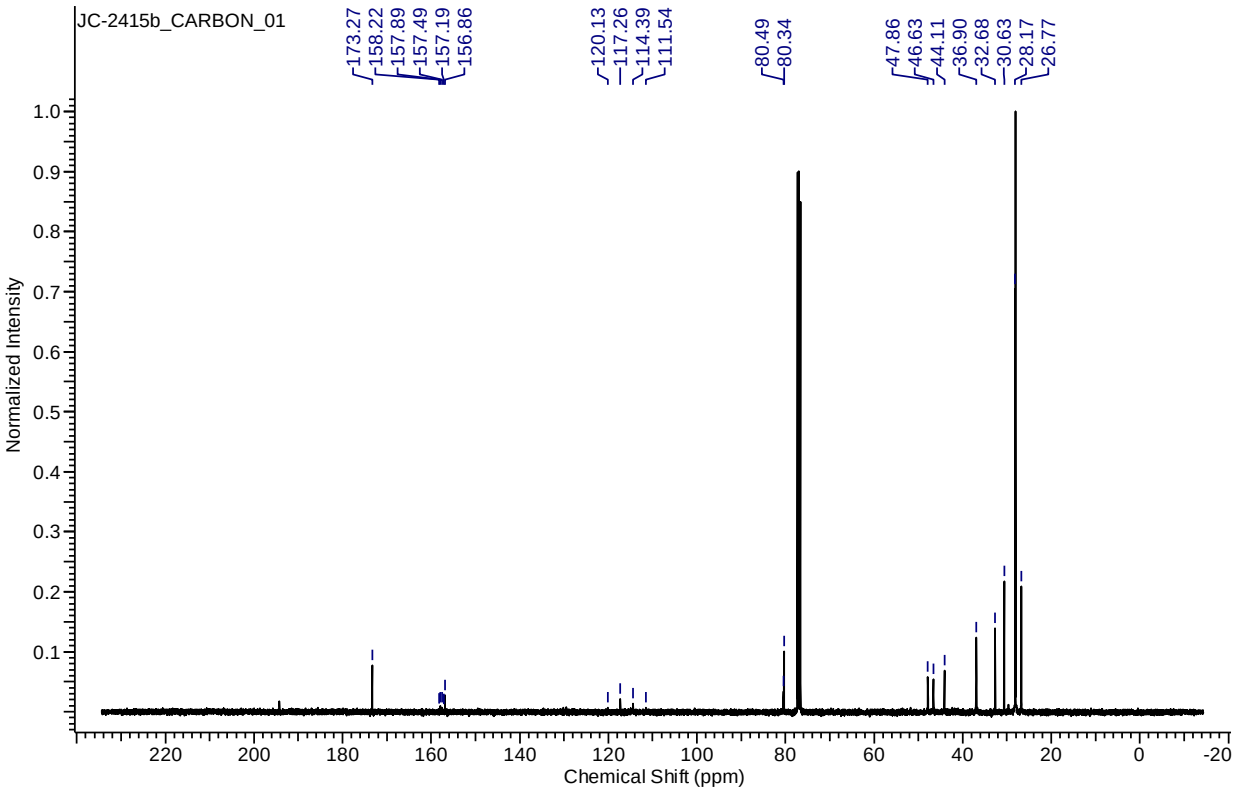
JC-2415b_CARBON_01
173.27
158.22
157.89
157.49
157.19
156.86
120.13
117.26
114.39
111.54
80.49
80.34
47.86
46.63
44.11
36.90
32.68
30.63
28.17
26.77
Normalized Intensity
Chemical Shift (ppm)

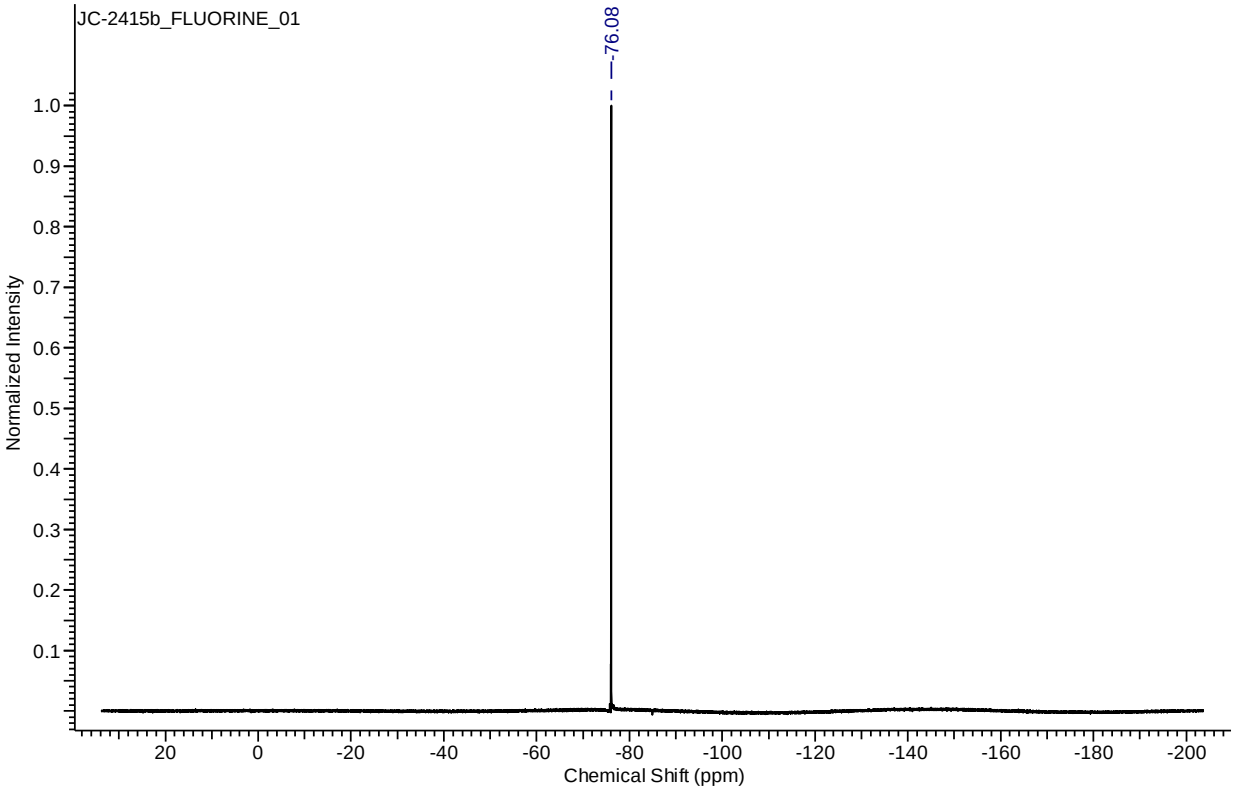
JC-2415b_FLUORINE_01
-76.08
Normalized Intensity
Chemical Shift (ppm)

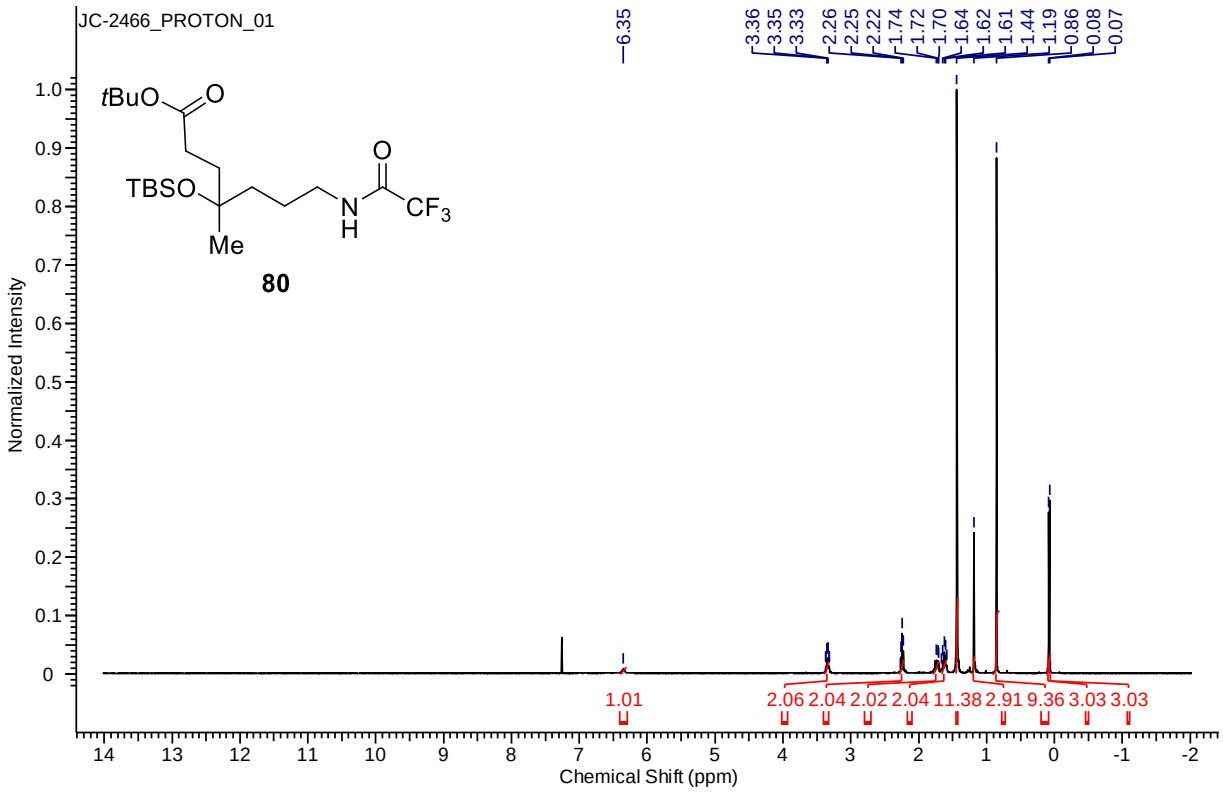
JC-2466_PROTON_01
tBuO
O
TBSO
Me
N
H
O
CF3
80
Normalized Intensity
Chemical Shift (ppm)
6.35
3.36
3.35
3.33
2.26
2.25
2.22
1.74
1.72
1.70
1.64
1.62
1.61
1.44
1.19
0.86
0.08
0.07
1.01
2.06 2.04 2.02 2.04 11.38 2.91 9.36 3.03 3.03

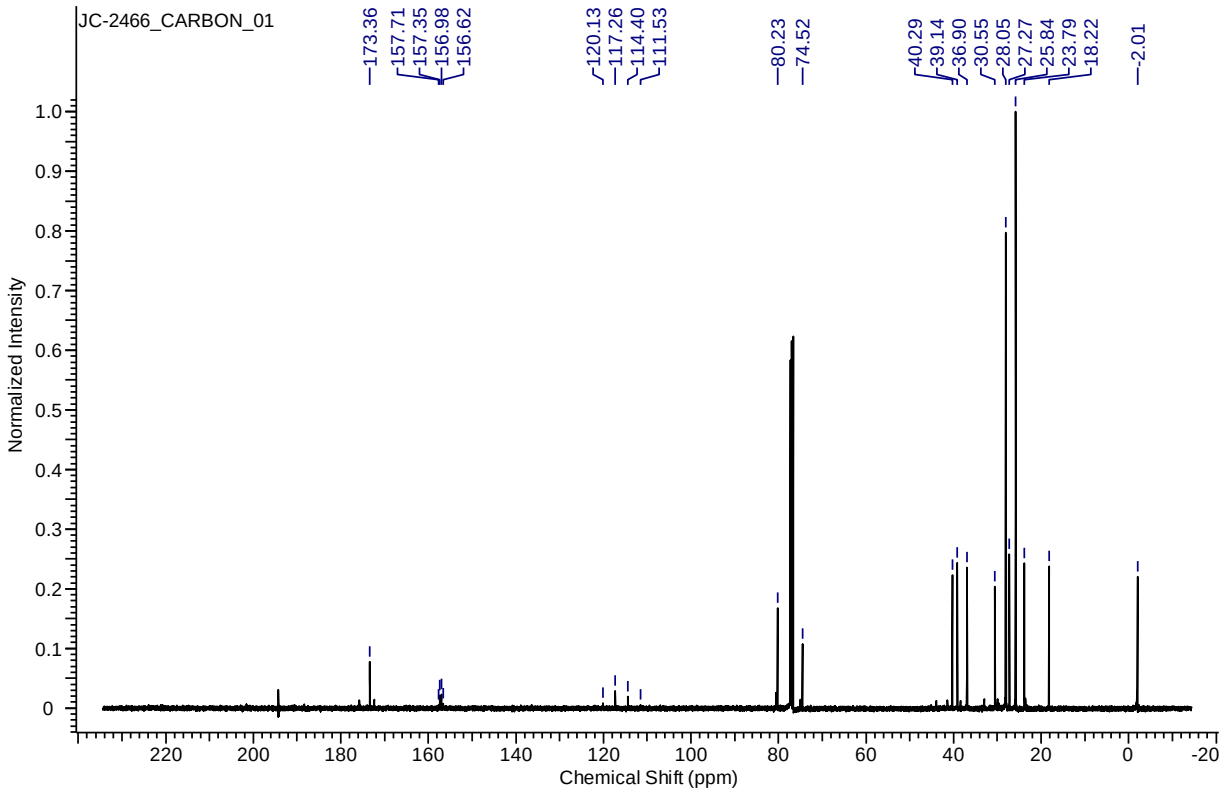
JC-2466_CARBON_01
Normalized Intensity
Chemical Shift (ppm)
173.36
157.71
157.35
156.98
156.62
120.13
117.26
114.40
111.53
80.23
74.52
40.29
39.14
36.90
30.55
28.05
27.27
25.84
23.79
18.22
2.01

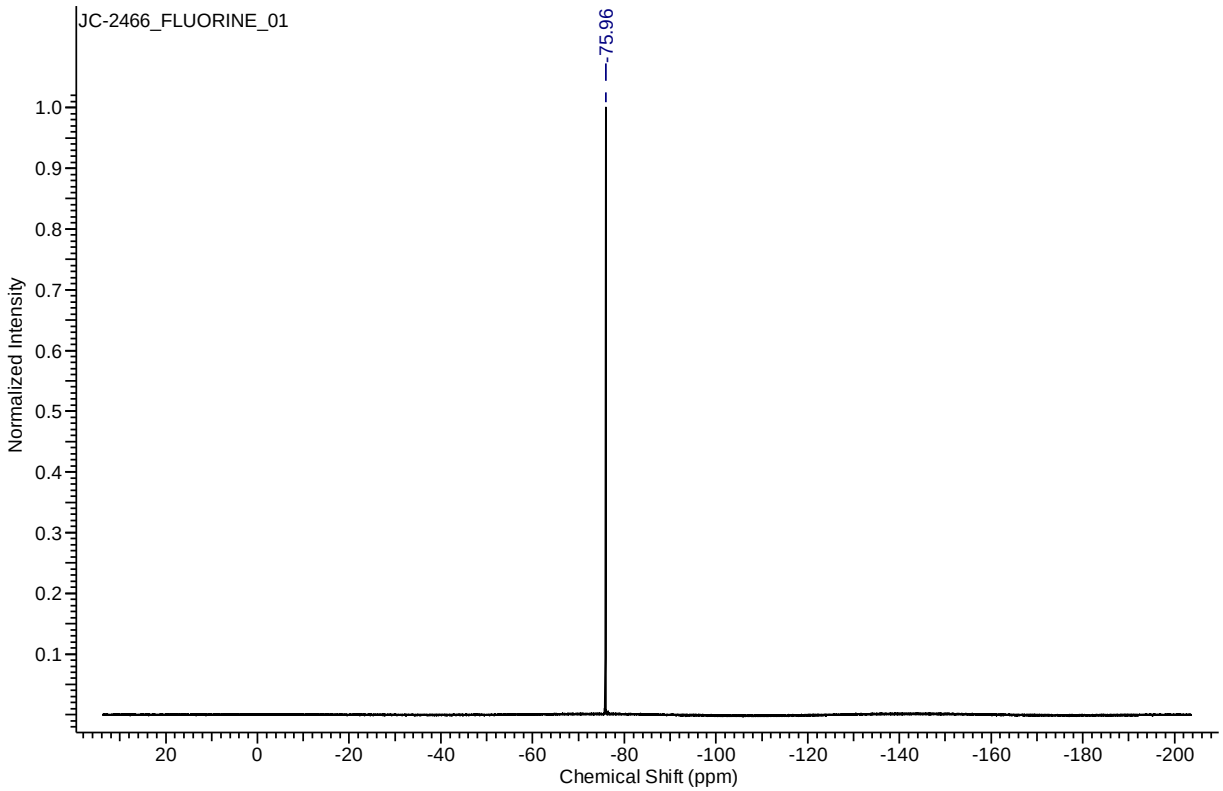
JC-2466_FLUORINE_01
-75.96
Normalized Intensity
Chemical Shift (ppm)

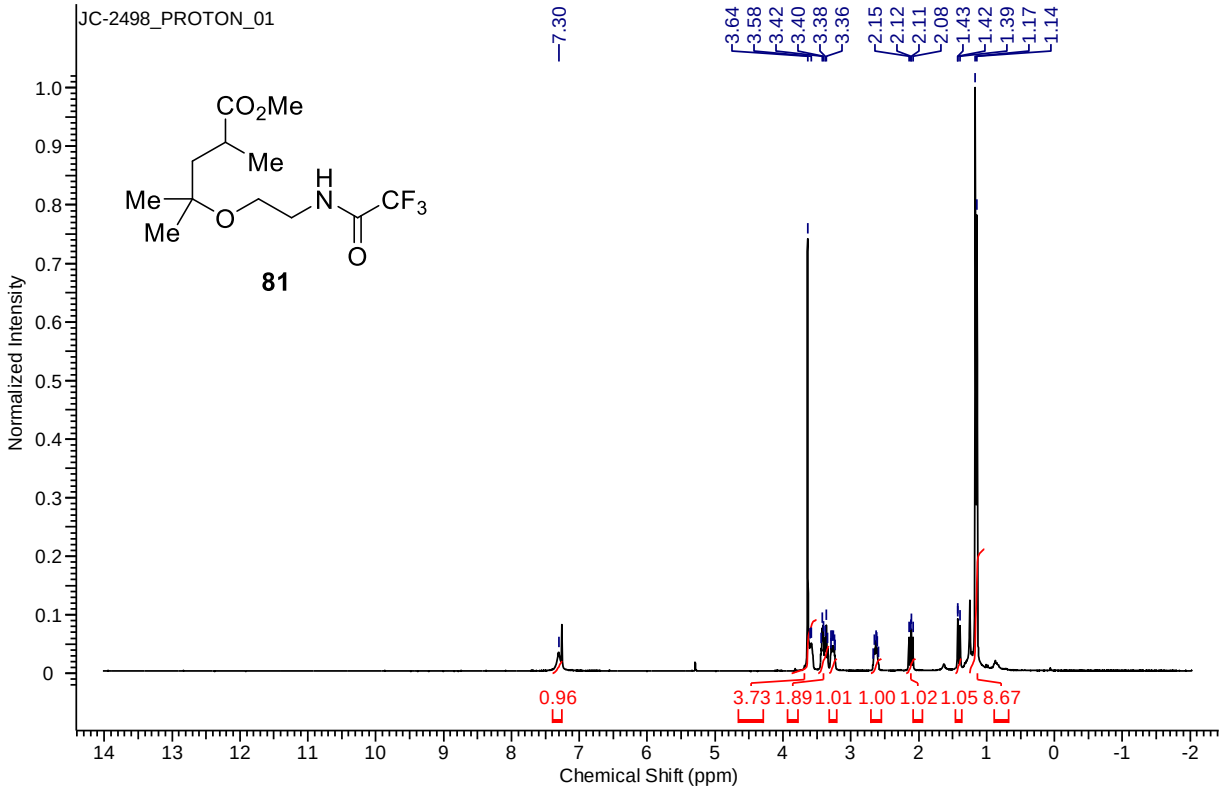
JC-2498_PROTON_01
7.30
3.64
3.58
3.42
3.40
3.38
3.36
2.15
2.12
2.11
2.08
1.43
1.42
1.39
1.17
1.14
0.96
3.73
1.89
1.01
1.00
1.02
1.05
8.67
Normalized Intensity
Chemical Shift (ppm)

CO2Me
Me
Me
Me
O
H
N
CF3
O

81

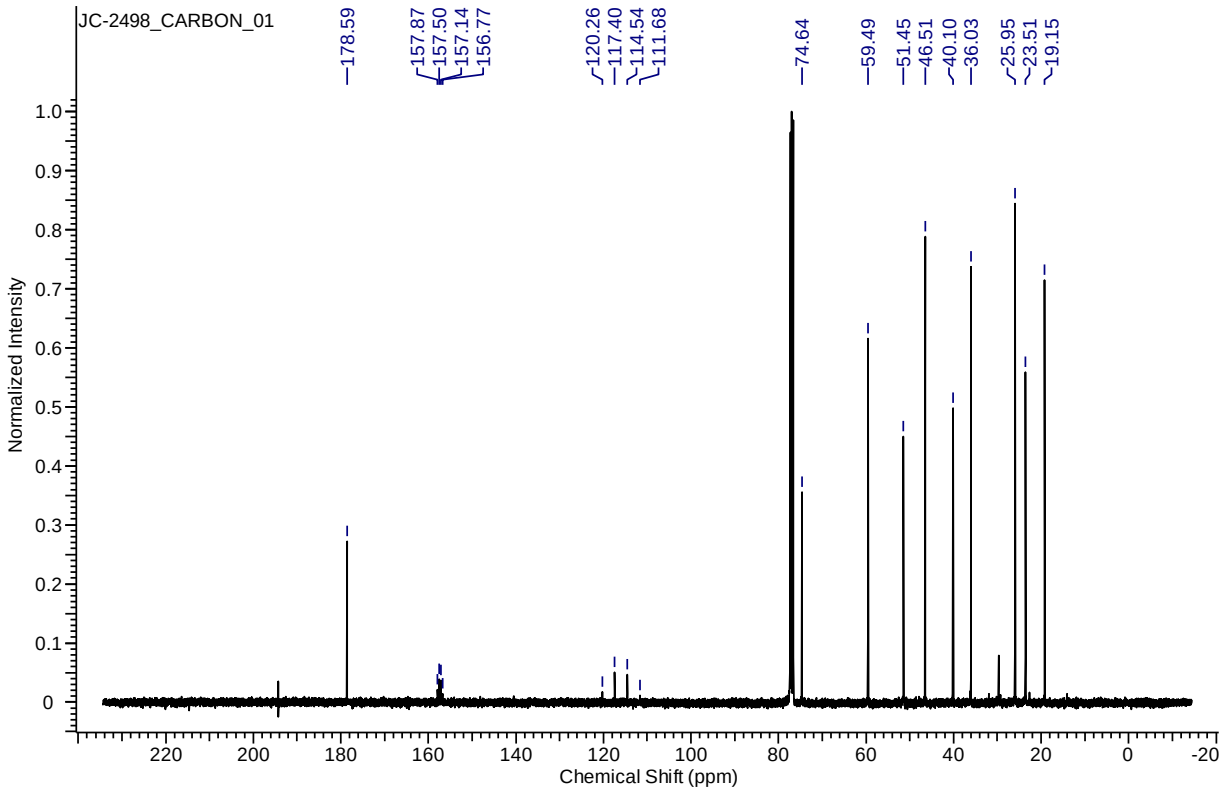
JC-2498_CARBON_01
178.59
157.87
157.50
157.14
156.77
120.26
117.40
114.54
111.68
74.64
59.49
51.45
46.51
40.10
36.03
25.95
23.51
19.15
Normalized Intensity
Chemical Shift (ppm)

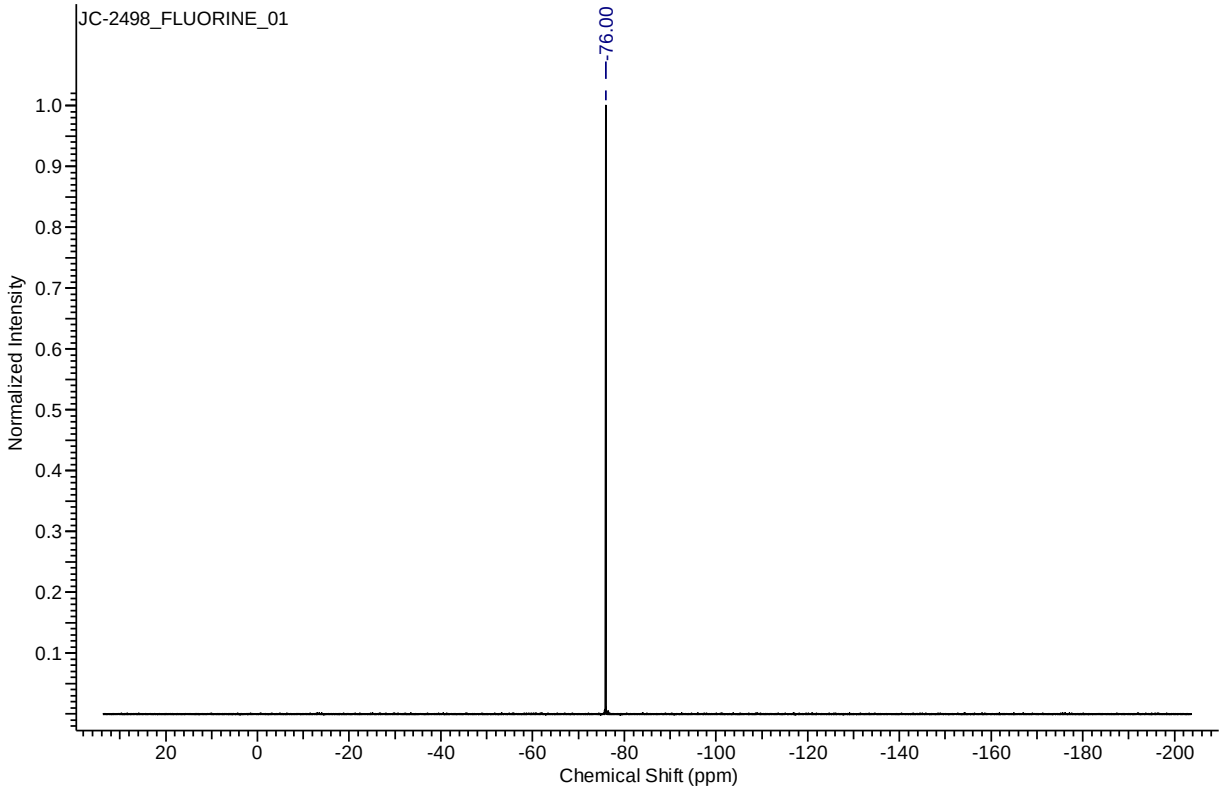
JC-2498_FLUORINE_01
-76.00
Normalized Intensity
Chemical Shift (ppm)

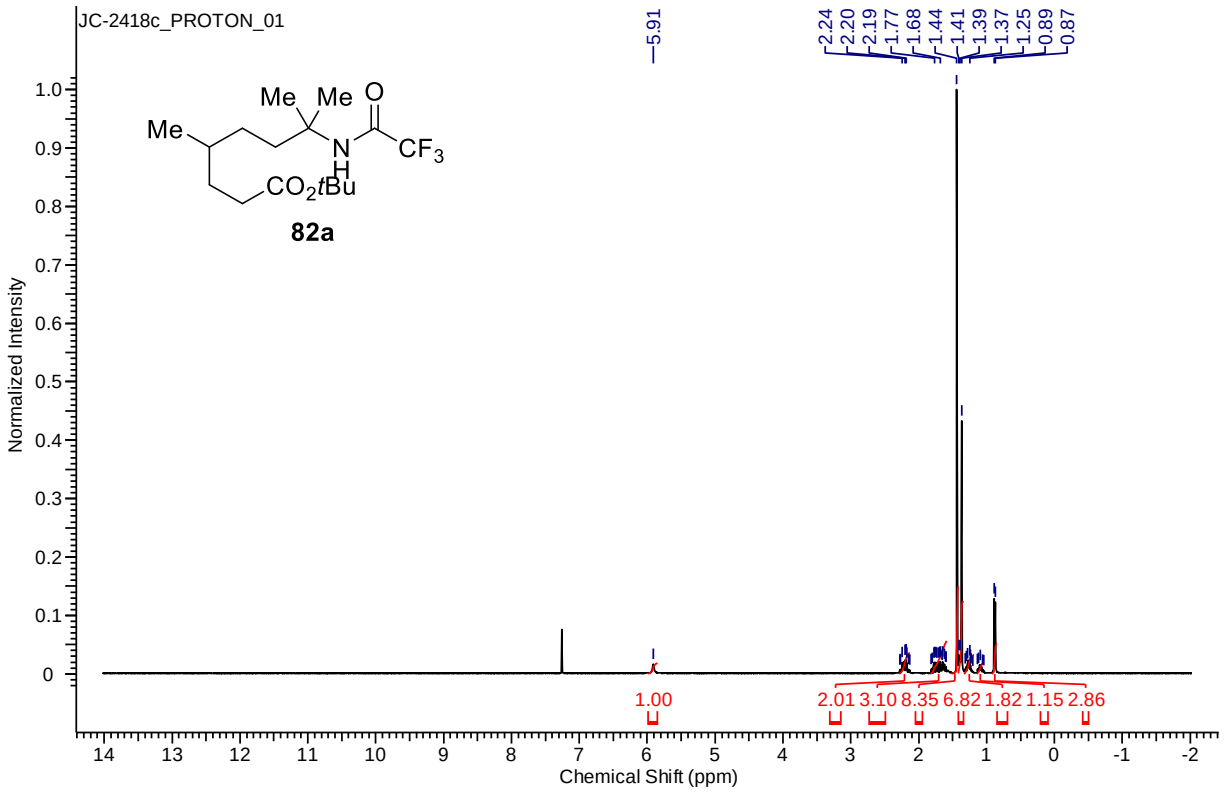
JC-2418c_PROTON_01
Me
Me
Me
O
N
H
CF3
CO2tBu
82a
5.91
2.24
2.20
2.19
1.77
1.68
1.44
1.41
1.39
1.37
1.25
0.89
0.87
1.00
2.01
3.10
8.35
6.82
1.82
1.15
2.86
Normalized Intensity
Chemical Shift (ppm)

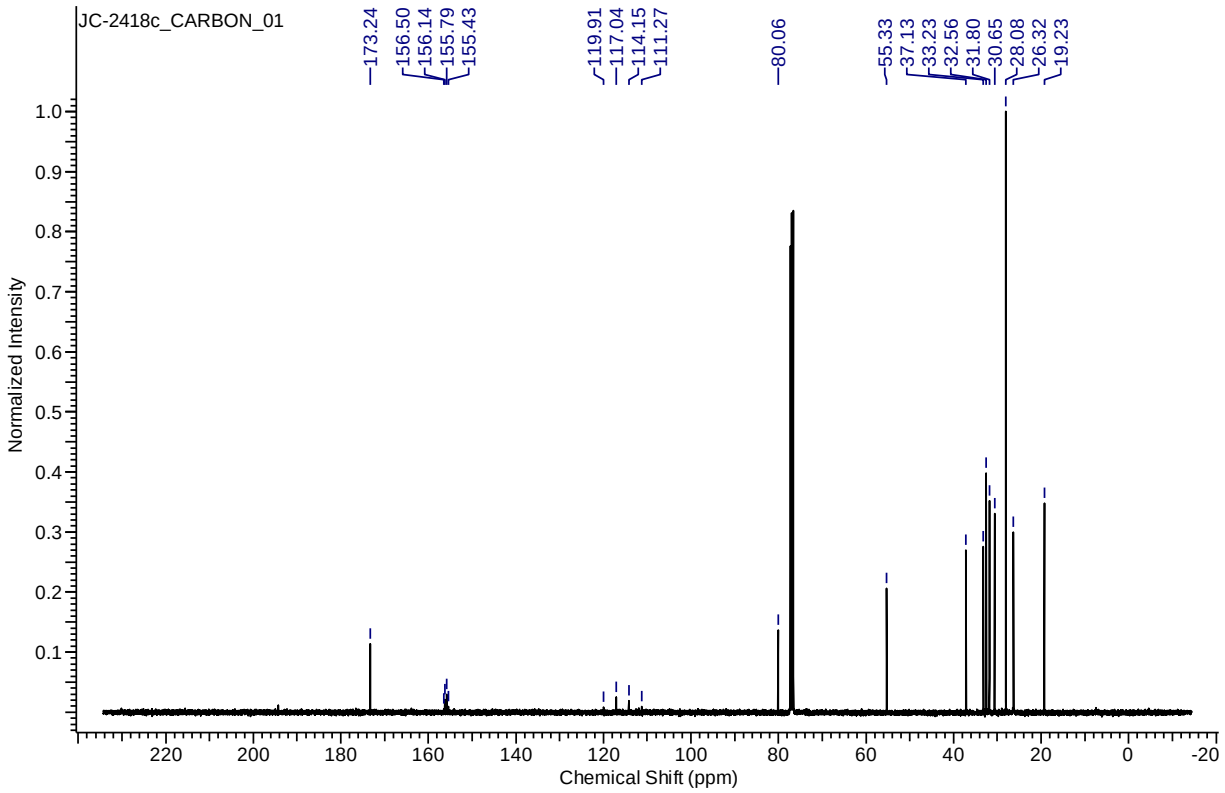
JC-2418c_CARBON_01
173.24
156.50
156.14
155.79
155.43
119.91
117.04
114.15
111.27
80.06
55.33
37.13
33.23
32.56
31.80
30.65
28.08
26.32
19.23
Normalized Intensity
Chemical Shift (ppm)

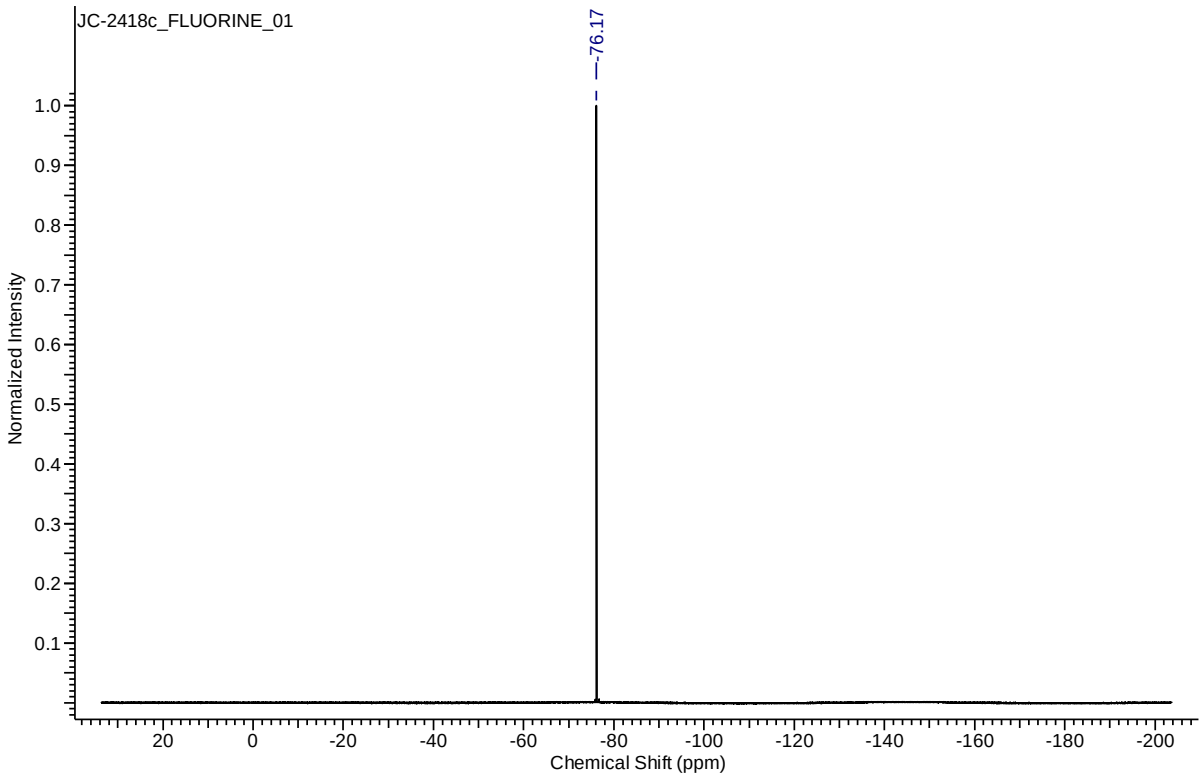
JC-2418c_FLUORINE_01
-76.17
Normalized Intensity
Chemical Shift (ppm)

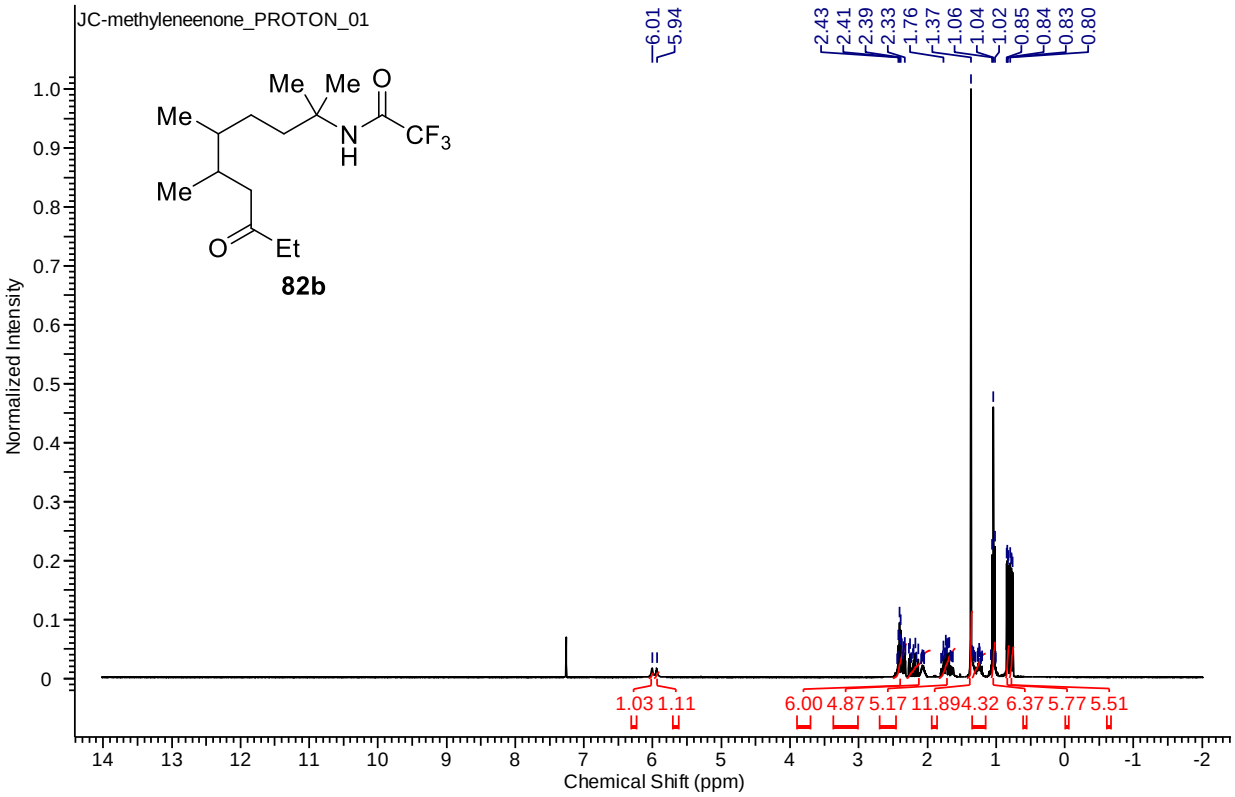
JC-methyleneenone_PROTON_01
6.01
5.94
2.43
2.41
2.39
2.33
1.76
1.37
1.06
1.04
1.02
0.85
0.84
0.83
0.80
1.03 1.11
6.00 4.87 5.17 11.89 4.32 6.37 5.77 5.51
Me
Me
Me
O
N
H
CF3
O
Et
82b
Normalized Intensity
Chemical Shift (ppm)

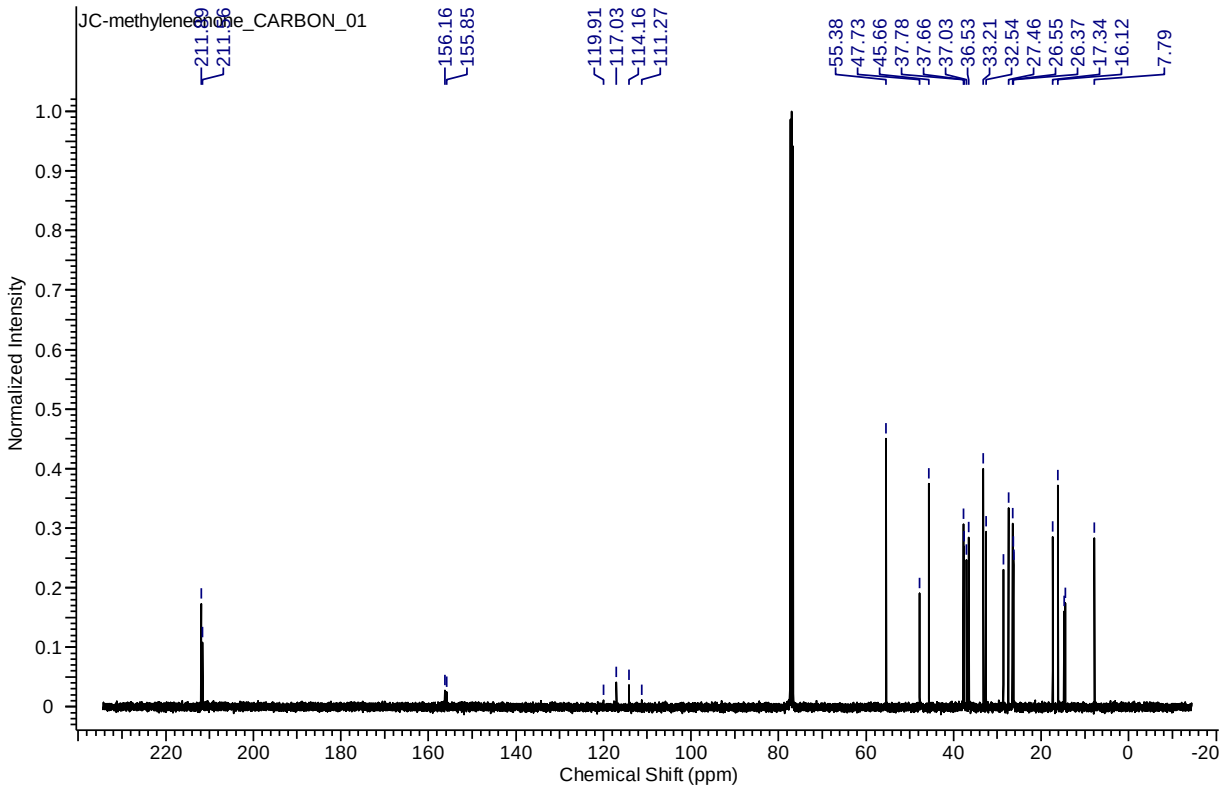
JC-methyleneenone_CARBON_01
211.89
211.66
156.16
155.85
119.91
117.03
114.16
111.27
55.38
47.73
45.66
37.78
37.66
37.03
36.53
33.21
32.54
27.46
26.55
26.37
17.34
16.12
7.79
Normalized Intensity
Chemical Shift (ppm)

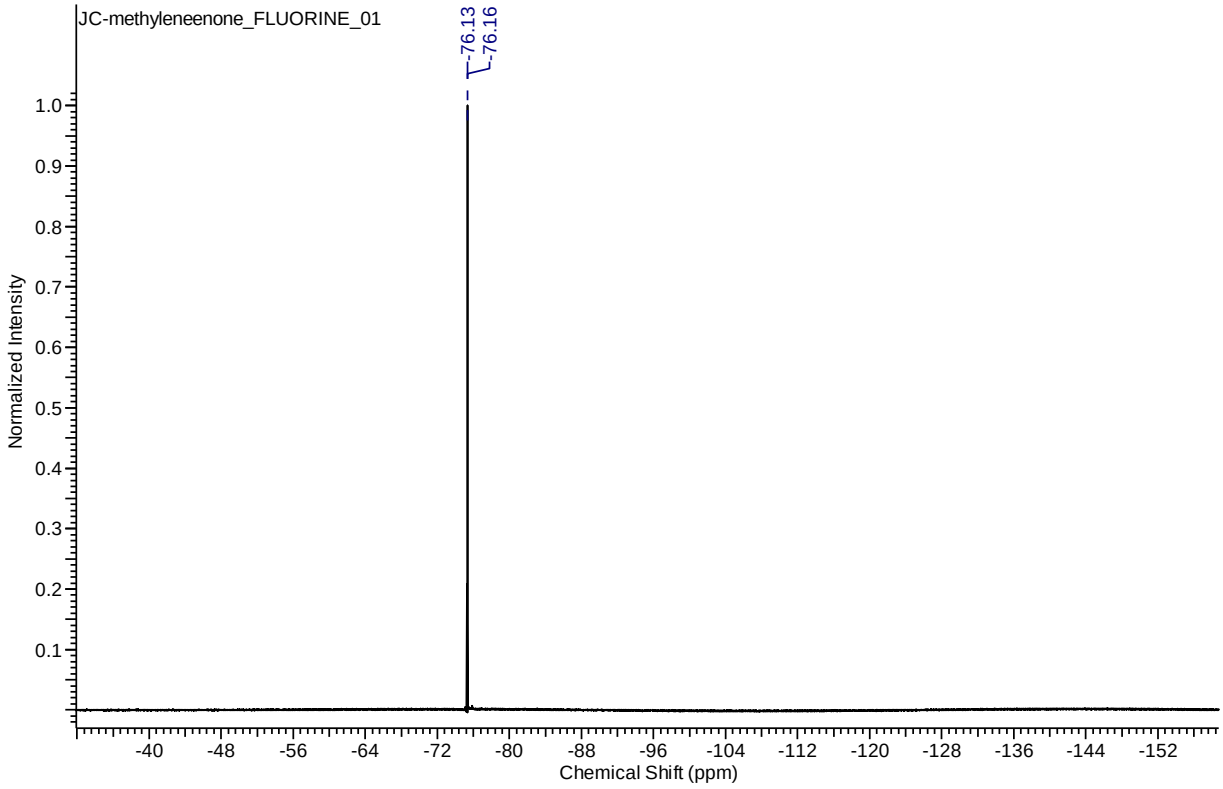
JC-methyleneenone_FLUORINE_01
-76.13
-76.16
Normalized Intensity
Chemical Shift (ppm)

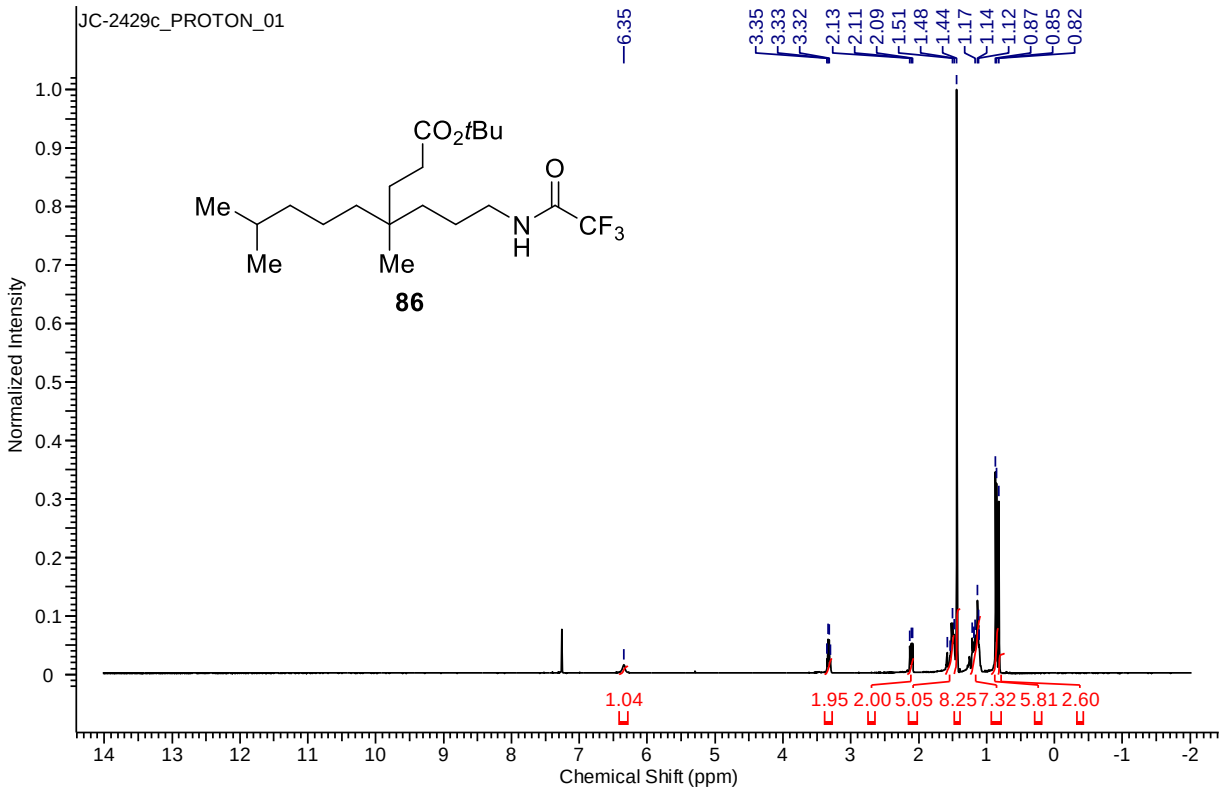
JC-2429c_PROTON_01
6.35
3.35
3.33
3.32
2.13
2.11
2.09
1.51
1.48
1.44
1.17
1.14
1.12
0.87
0.85
0.82
CO2tBu
O
Me
N
H
CF3
Me
Me
86
Normalized Intensity
1.04
1.95
2.00
5.05
8.25
7.32
5.81
2.60
Chemical Shift (ppm)

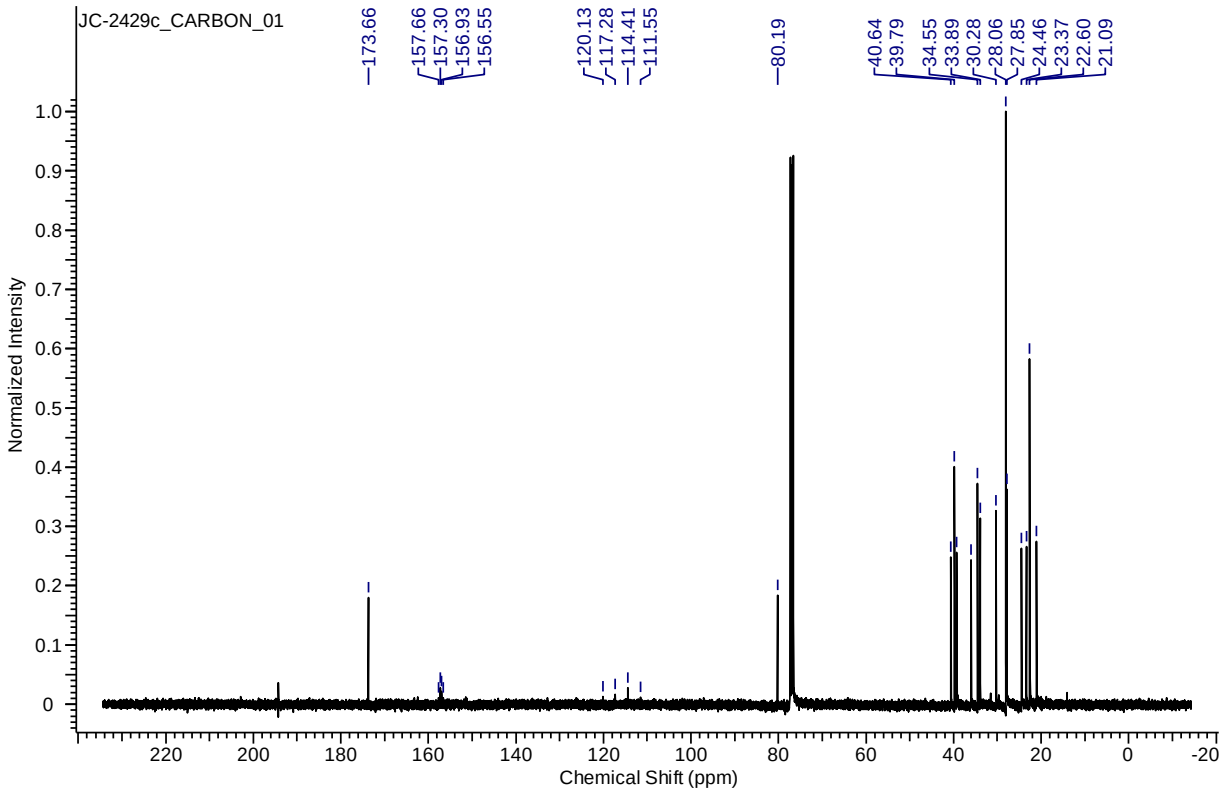
JC-2429c_CARBON_01
173.66
157.66
157.30
156.93
156.55
120.13
117.28
114.41
111.55
80.19
40.64
39.79
34.55
33.89
30.28
28.06
27.85
24.46
23.37
22.60
21.09
Normalized Intensity
Chemical Shift (ppm)

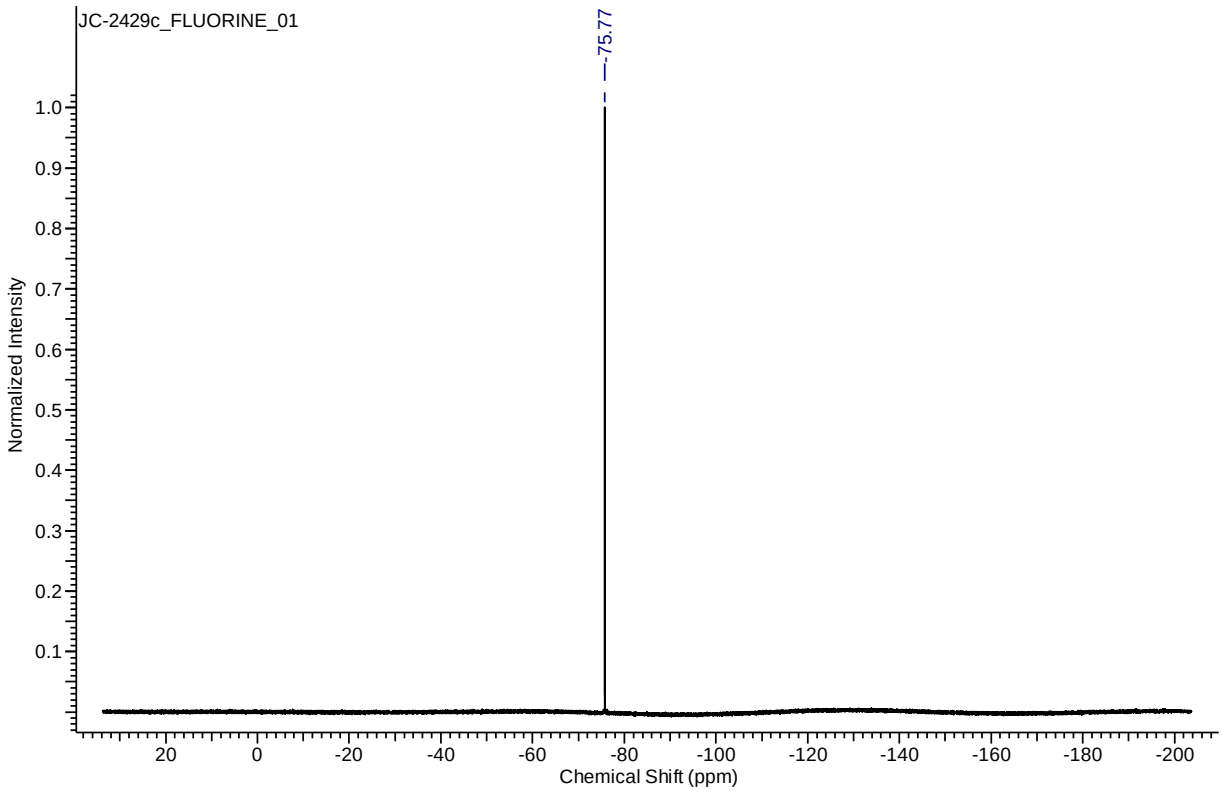
JC-2429c_FLUORINE_01
-75.77
Normalized Intensity
Chemical Shift (ppm)

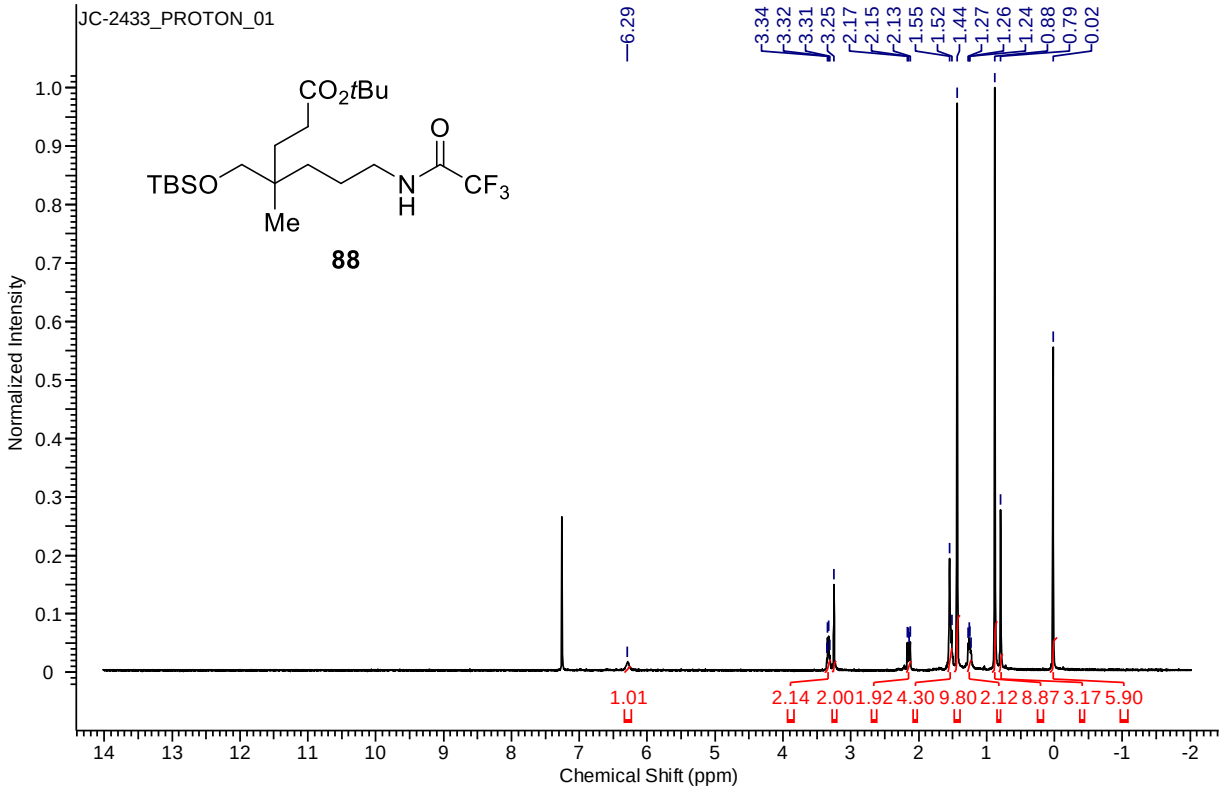
JC-2433_PROTON_01
6.29
3.34
3.32
3.31
3.25
2.17
2.15
2.13
1.55
1.52
1.44
1.27
1.26
1.24
0.88
0.79
0.02
CO2tBu
TBSO
Me
N
H
O
CF3
88
1.01
2.14
2.00
1.92
4.30
9.80
2.12
8.87
3.17
5.90
Normalized Intensity
Chemical Shift (ppm)

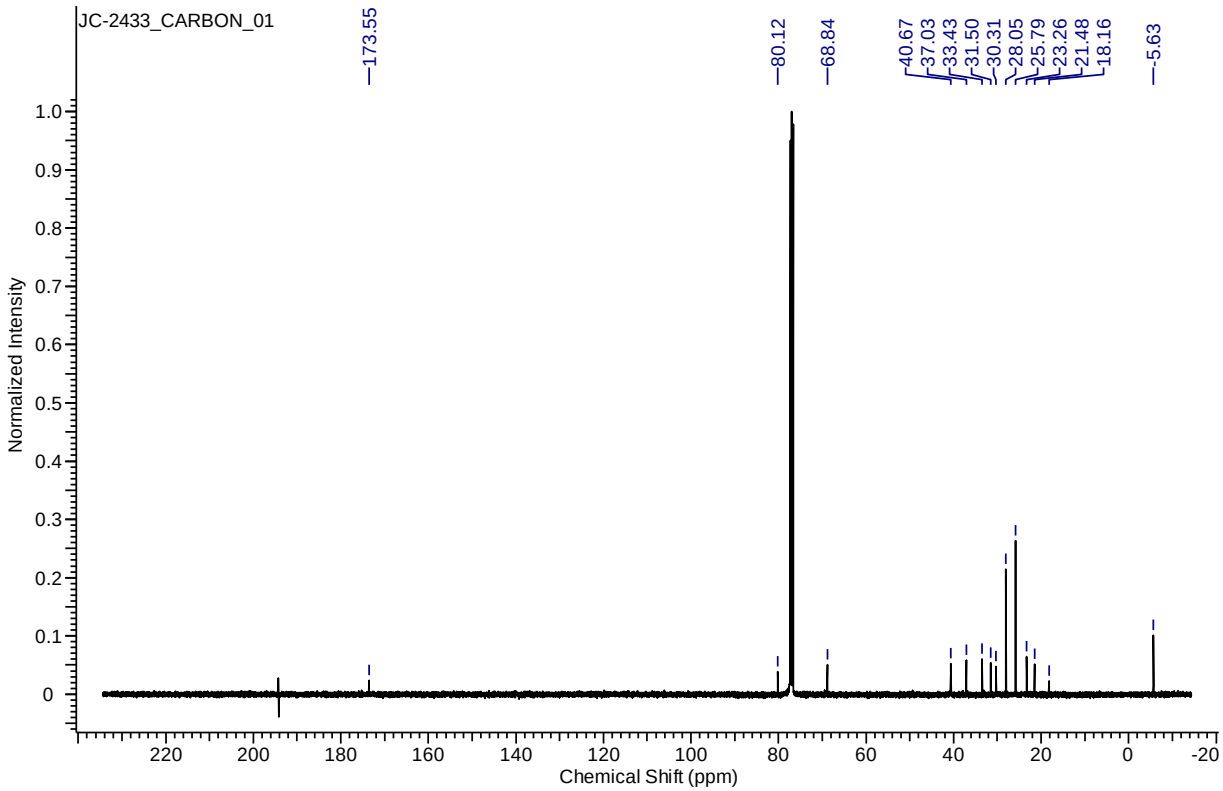
JC-2433_CARBON_01
173.55
80.12
68.84
40.67
37.03
33.43
31.50
30.31
28.05
25.79
23.26
21.48
18.16
-5.63
Normalized Intensity
Chemical Shift (ppm)

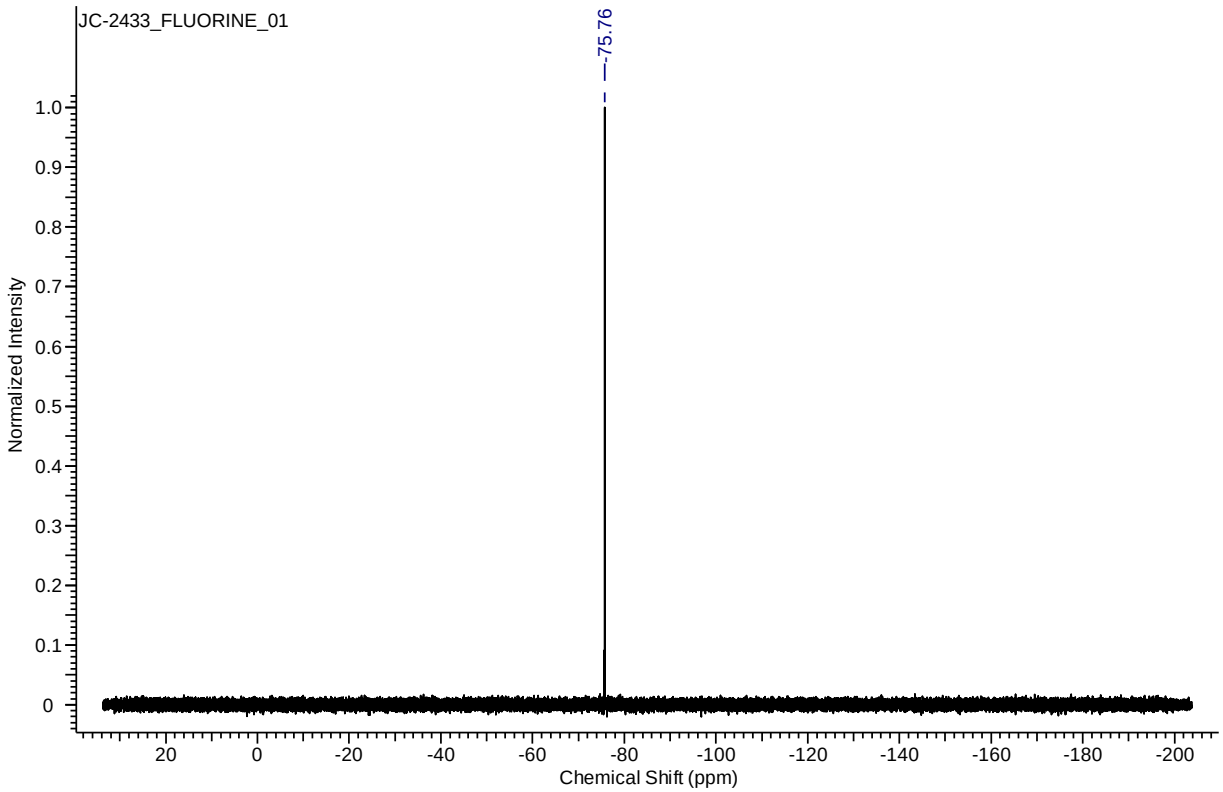
JC-2433_FLUORINE_01
-75.76
Normalized Intensity
Chemical Shift (ppm)

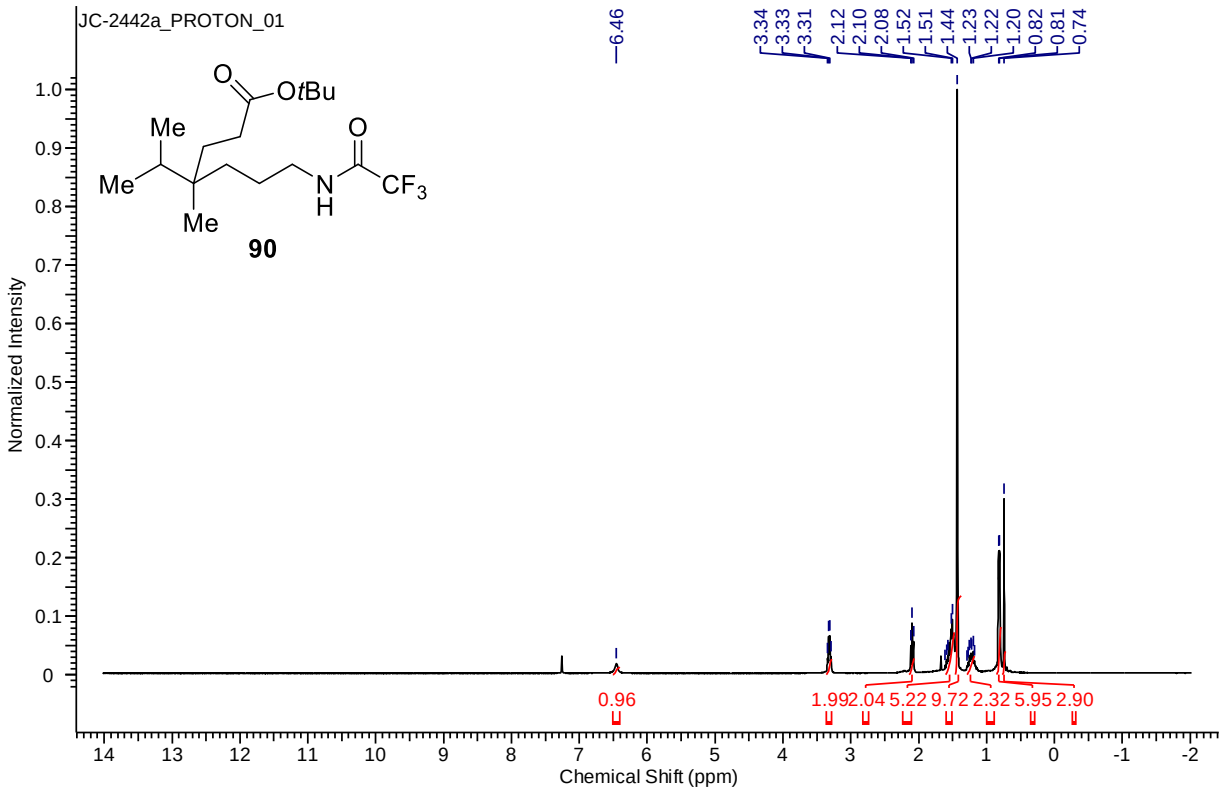
JC-2442a_PROTON_01
O
OtBu
Me
O
Me
N
H
CF3
Me
90
6.46
3.34
3.33
3.31
2.12
2.10
2.08
1.52
1.51
1.44
1.23
1.22
1.20
0.82
0.81
0.74
0.96
1.99
2.04
5.22
9.72
2.32
5.95
2.90
Normalized Intensity
Chemical Shift (ppm)

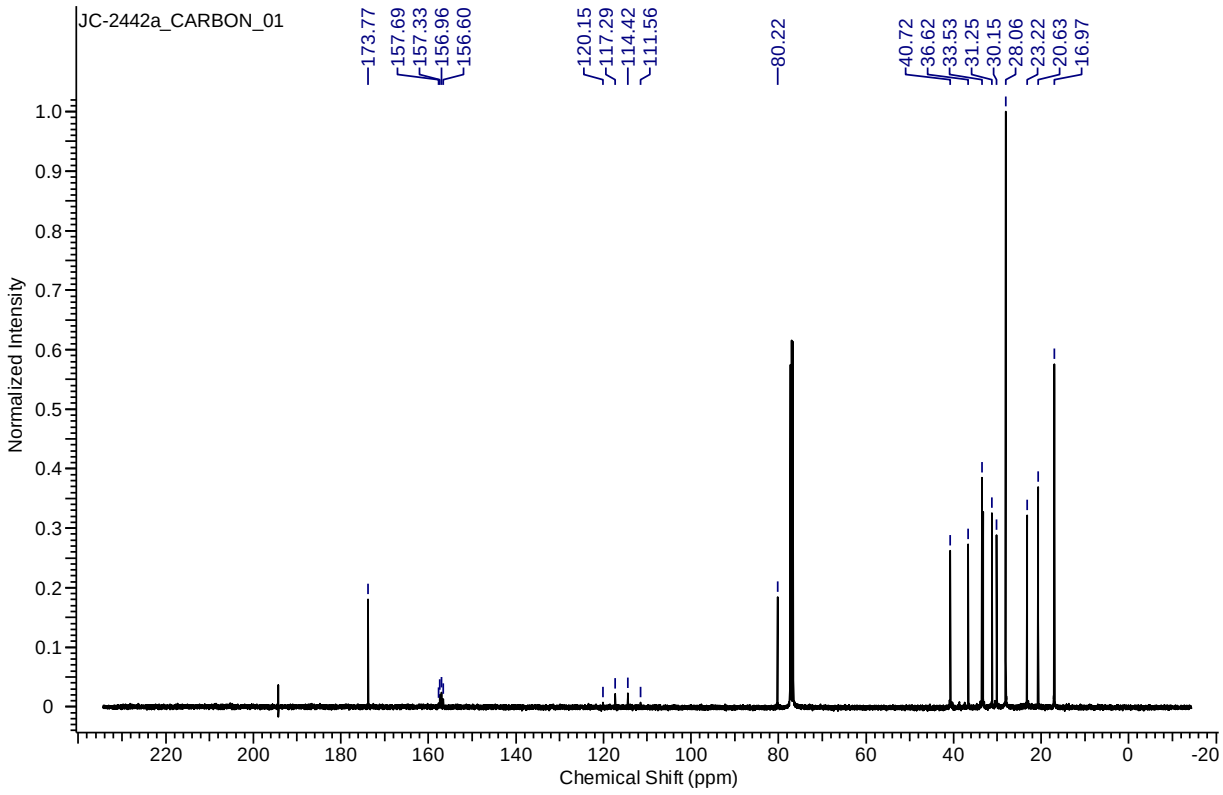
JC-2442a_CARBON_01
173.77
157.69
157.33
156.96
156.60
120.15
117.29
114.42
111.56
80.22
40.72
36.62
33.53
31.25
30.15
28.06
23.22
20.63
16.97
Normalized Intensity
Chemical Shift (ppm)

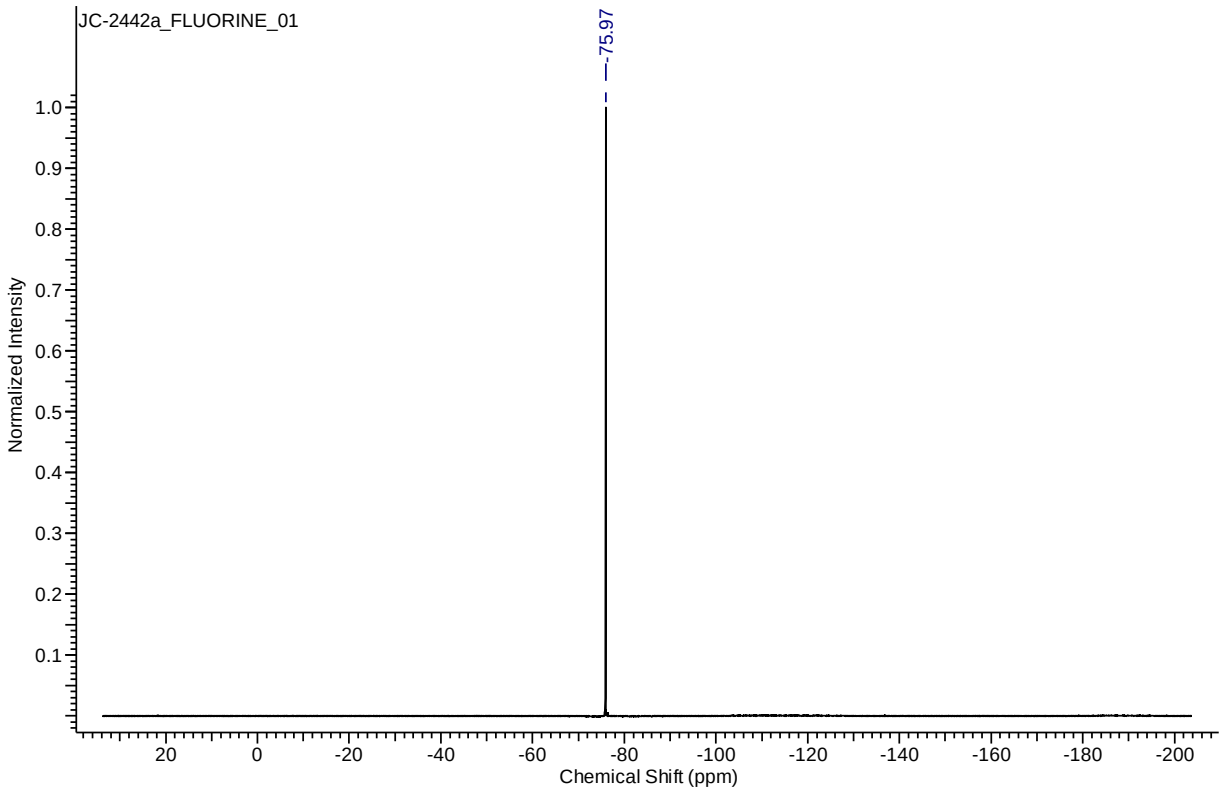
JC-2442a_FLUORINE_01
-75.97
Normalized Intensity
Chemical Shift (ppm)

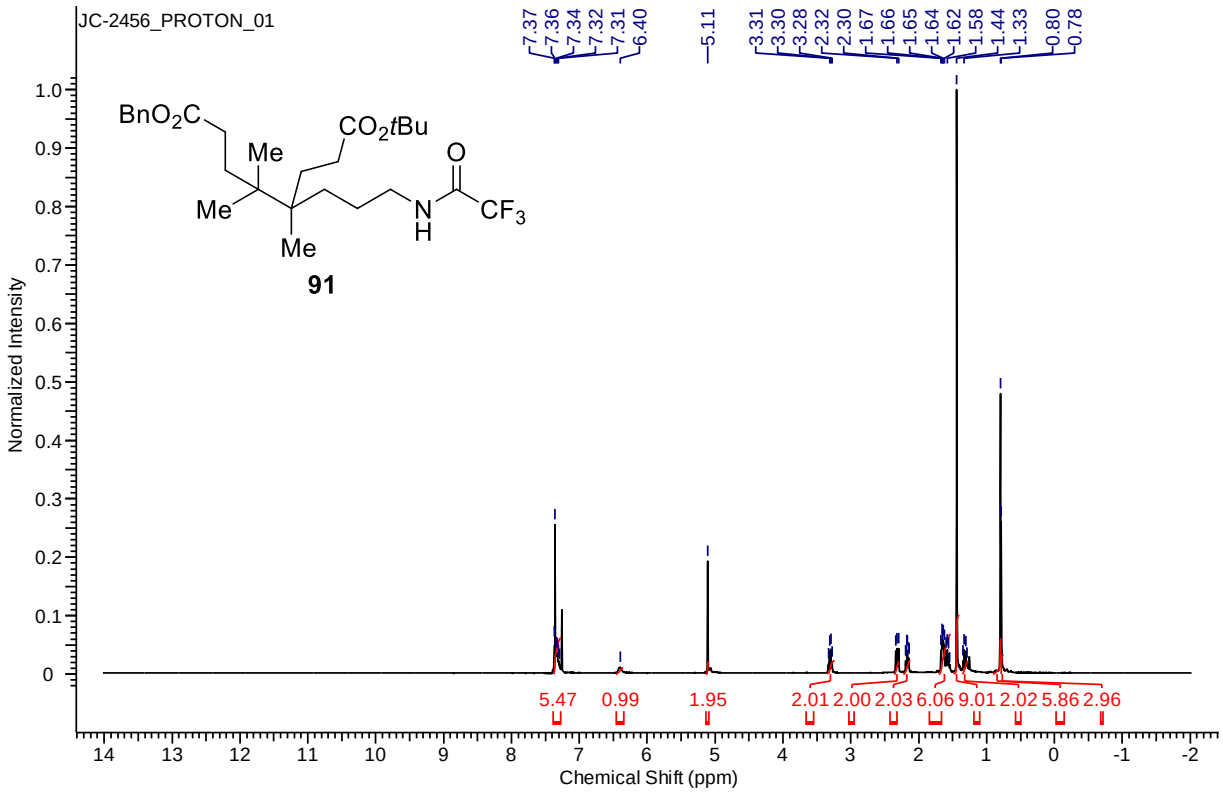
JC-2456_PROTON_01
7.37
7.36
7.34
7.32
7.31
6.40
5.11
3.31
3.30
3.28
2.32
2.30
1.67
1.66
1.65
1.64
1.62
1.58
1.44
1.33
0.80
0.78
BnO2C
CO2tBu
Me
Me
Me
O
N
H
CF3
91
5.47
0.99
1.95
2.01
2.00
2.03
6.06
9.01
2.02
5.86
2.96
Normalized Intensity
Chemical Shift (ppm)

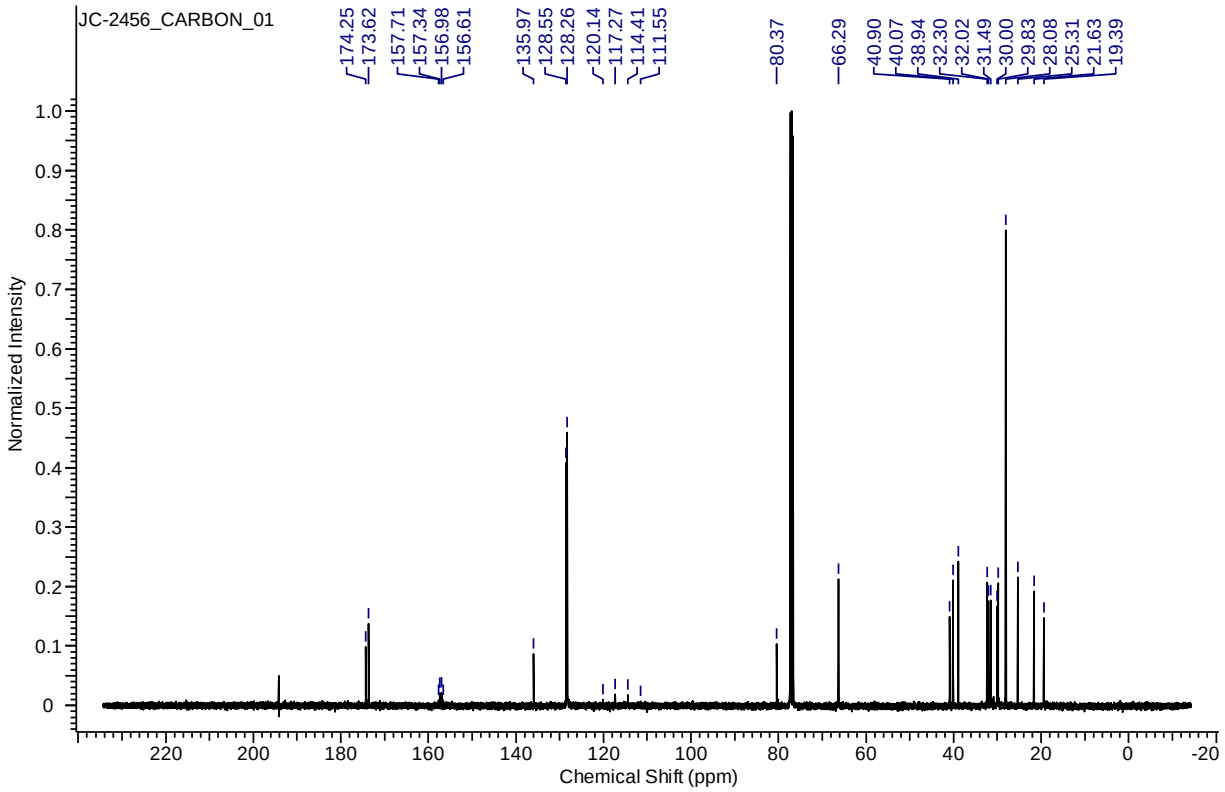
JC-2456_CARBON_01
174.25
173.62
157.71
157.34
156.98
156.61
135.97
128.55
128.26
120.14
117.27
114.41
111.55
80.37
66.29
40.90
40.07
38.94
32.30
32.02
31.49
30.00
29.83
28.08
25.31
21.63
19.39
Normalized Intensity
Chemical Shift (ppm)

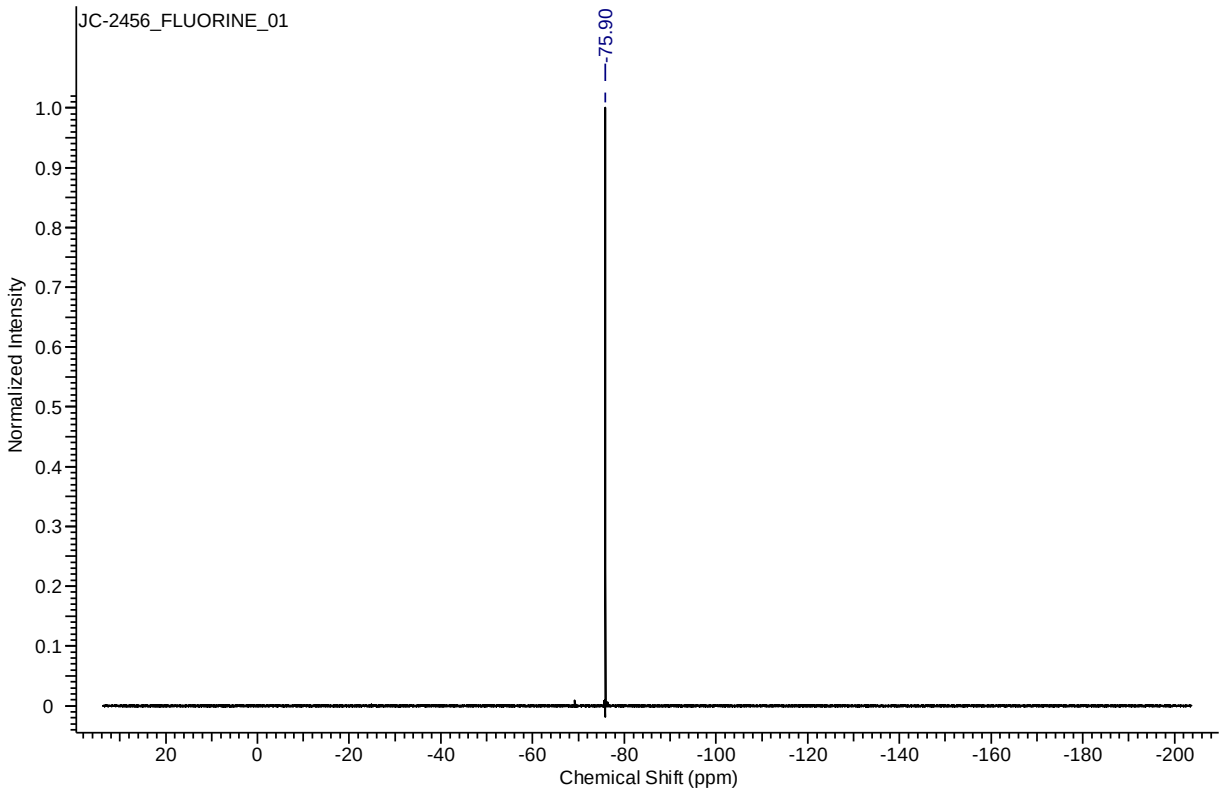
JC-2456_FLUORINE_01
-75.90
Normalized Intensity
Chemical Shift (ppm)

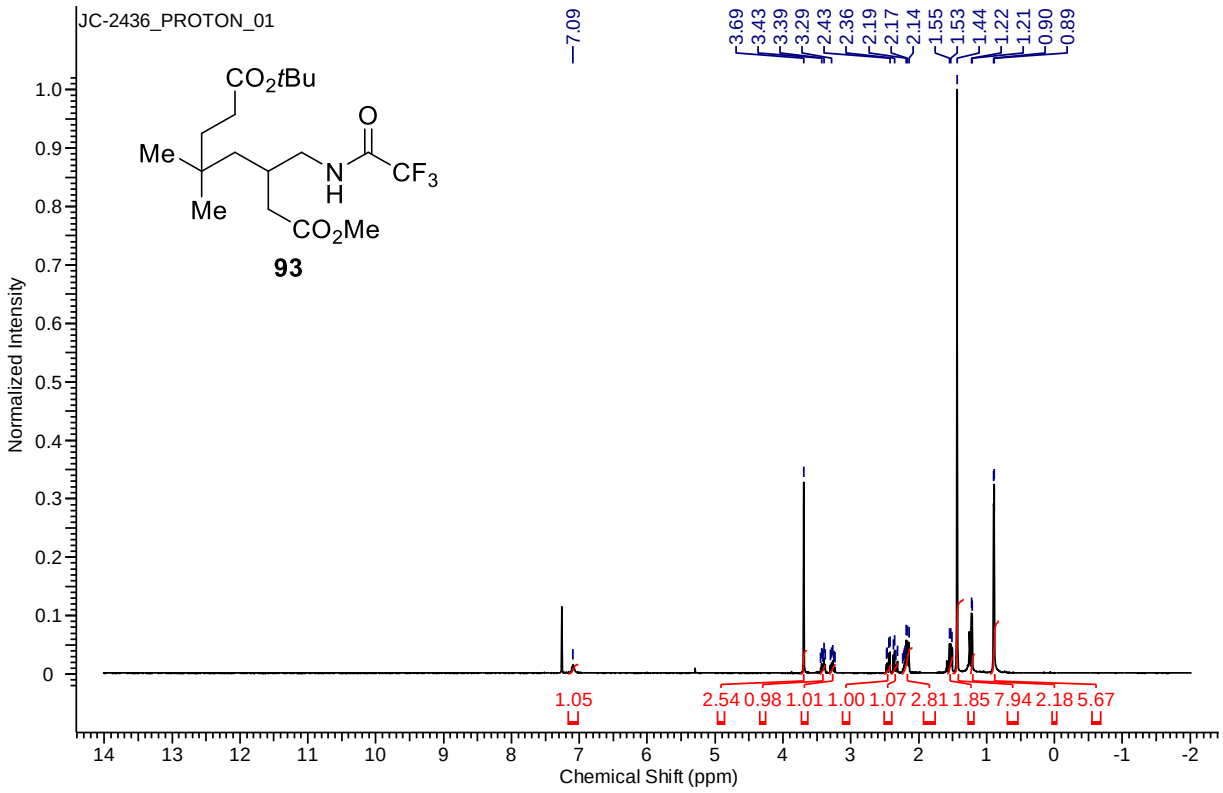
JC-2436_PROTON_01
CO2tBu
Me
Me
N
H
O
CF3
CO2Me
93
7.09
3.69
3.43
3.39
3.29
2.43
2.36
2.19
2.17
2.14
1.55
1.53
1.44
1.22
1.21
0.90
0.89
1.05
2.54 0.98 1.01 1.00 1.07 2.81 1.85 7.94 2.18 5.67
Normalized Intensity
Chemical Shift (ppm)

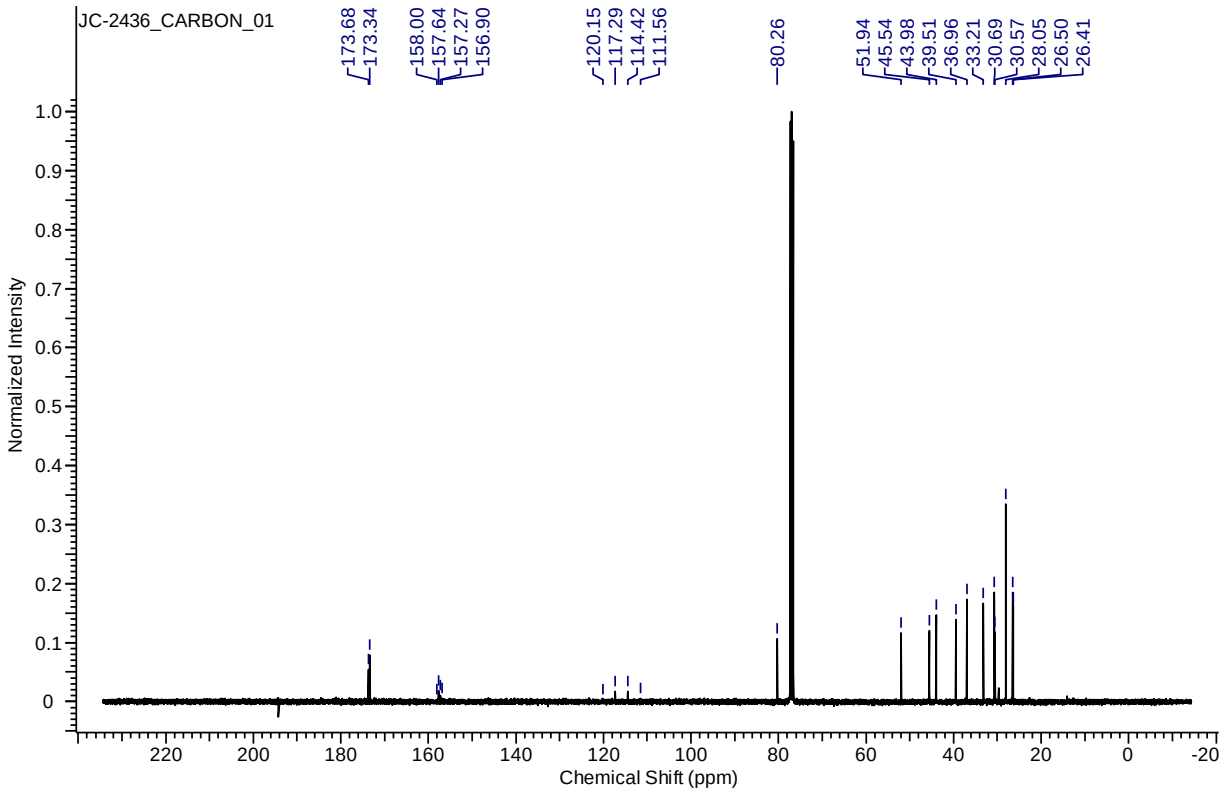
JC-2436_CARBON_01
173.68
173.34
158.00
157.64
157.27
156.90
120.15
117.29
114.42
111.56
80.26
51.94
45.54
43.98
39.51
36.96
33.21
30.69
30.57
28.05
26.50
26.41
Normalized Intensity
Chemical Shift (ppm)

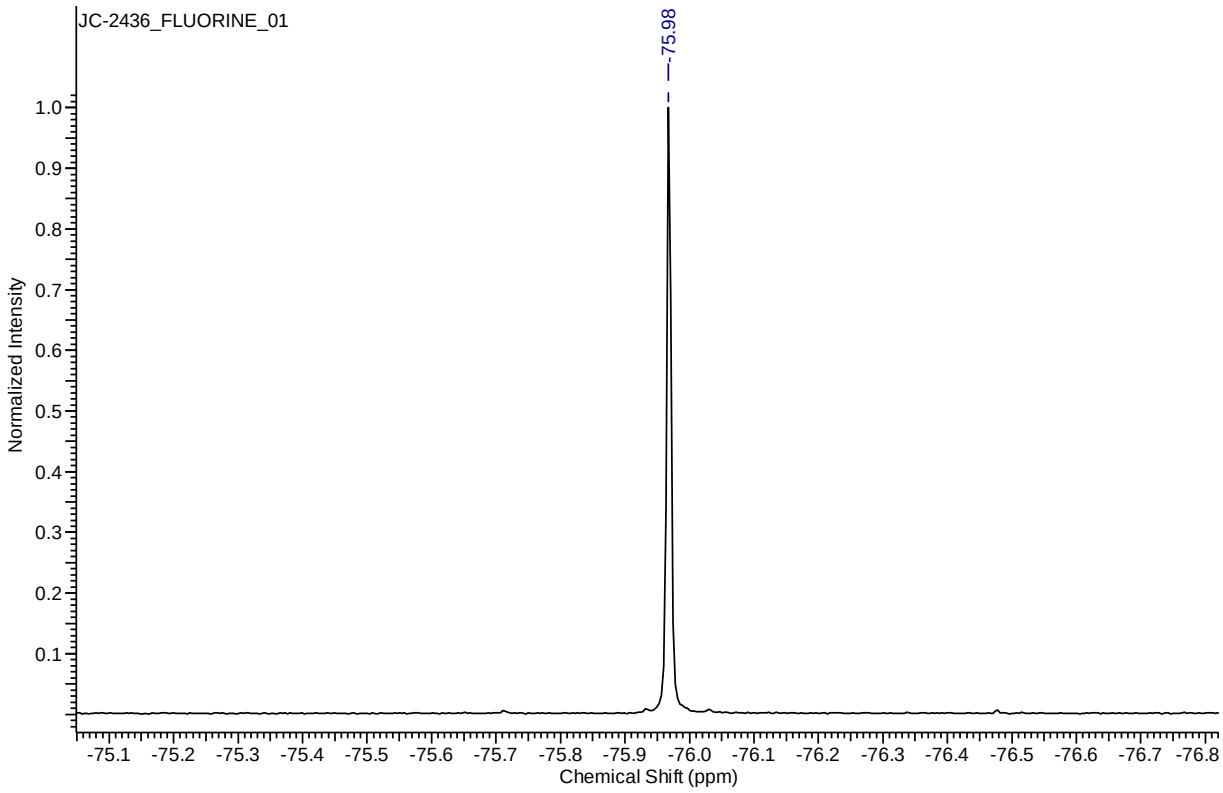
JC-2436_FLUORINE_01
-75.98
Normalized Intensity
Chemical Shift (ppm)

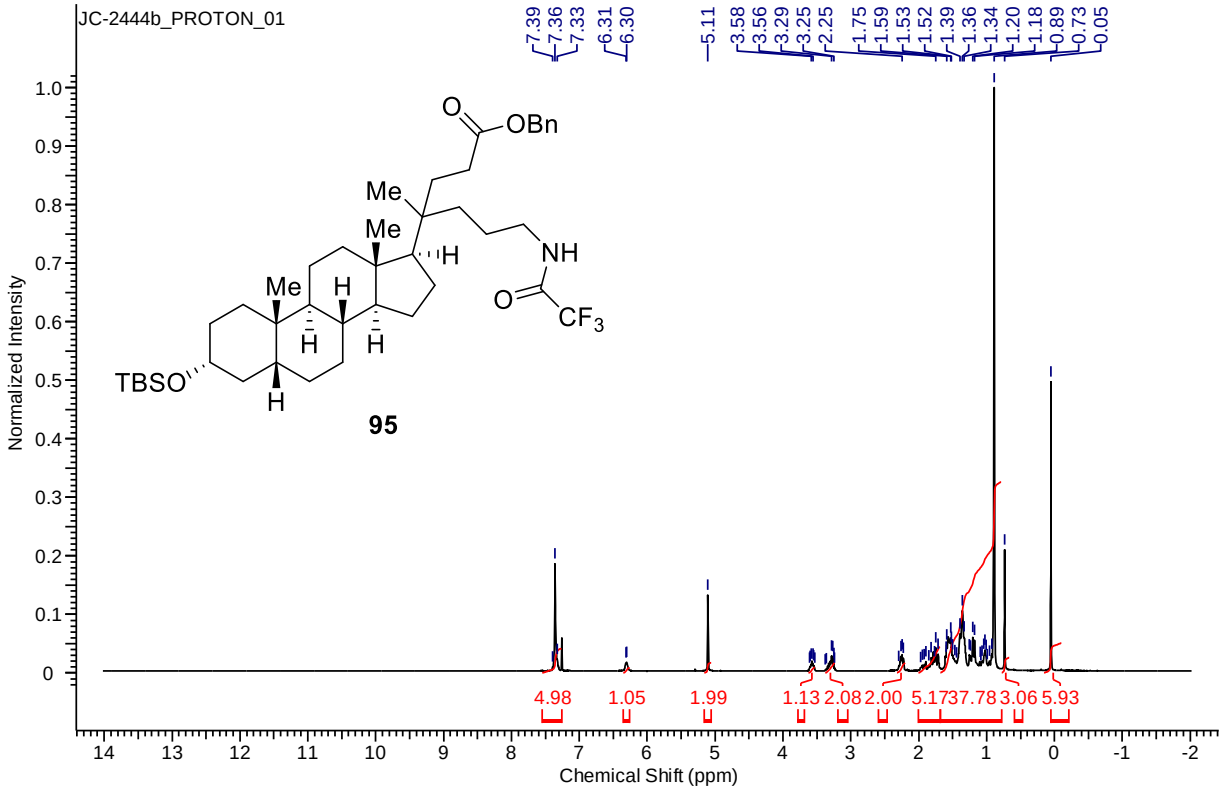
JC-2444b_PROTON_01
7.39
7.36
7.33
6.31
6.30
5.11
3.58
3.56
3.29
3.25
2.25
1.75
1.59
1.53
1.52
1.39
1.36
1.34
1.20
1.18
0.89
0.73
0.05
OBn
Me
Me
H
NH
Me
H
O
CF3
H
H
TBSO
H
95
4.98
1.05
1.99
1.13
2.08
2.00
5.17
37.78
3.06
5.93
Normalized Intensity
Chemical Shift (ppm)

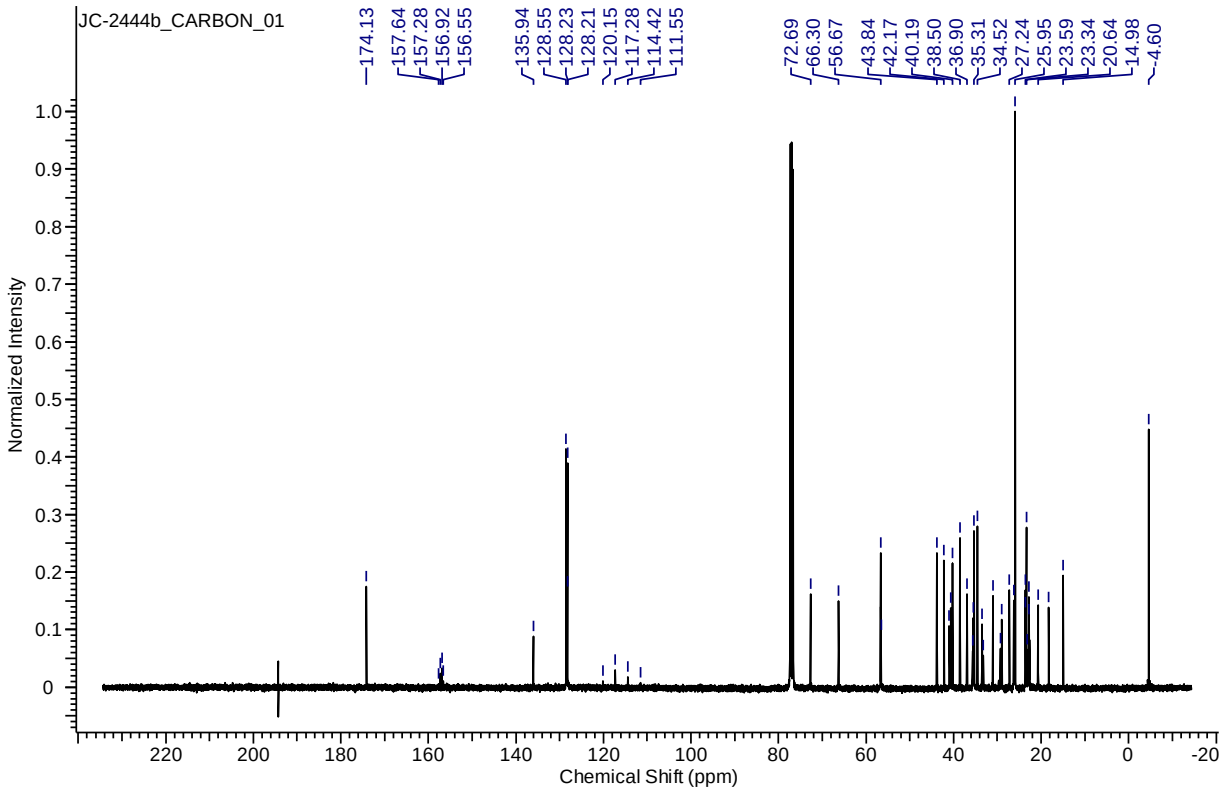
JC-2444b_CARBON_01
174.13
157.64
157.28
156.92
156.55
135.94
128.55
128.23
128.21
120.15
117.28
114.42
111.55
72.69
66.30
56.67
43.84
42.17
40.19
38.50
36.90
35.31
34.52
27.24
25.95
23.59
23.34
20.64
14.98
-4.60
Normalized Intensity
Chemical Shift (ppm)

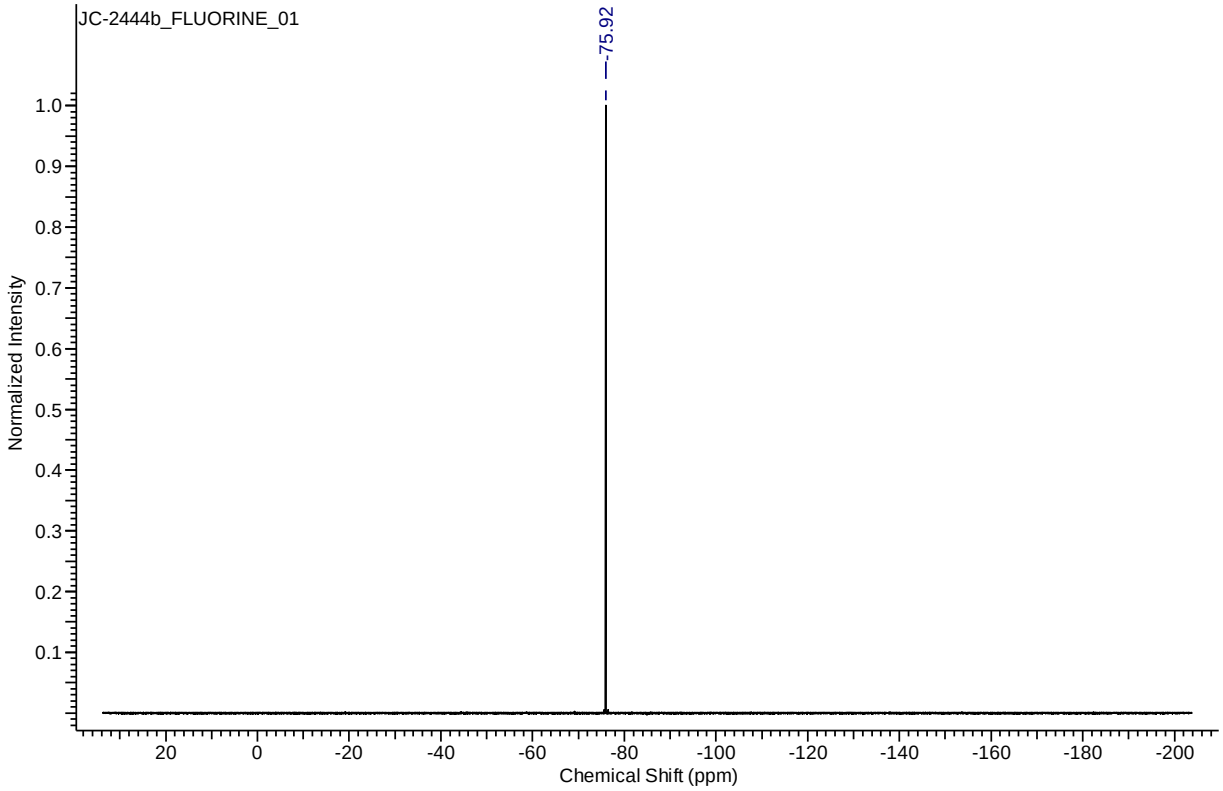
JC-2444b_FLUORINE_01
-75.92
Normalized Intensity
Chemical Shift (ppm)

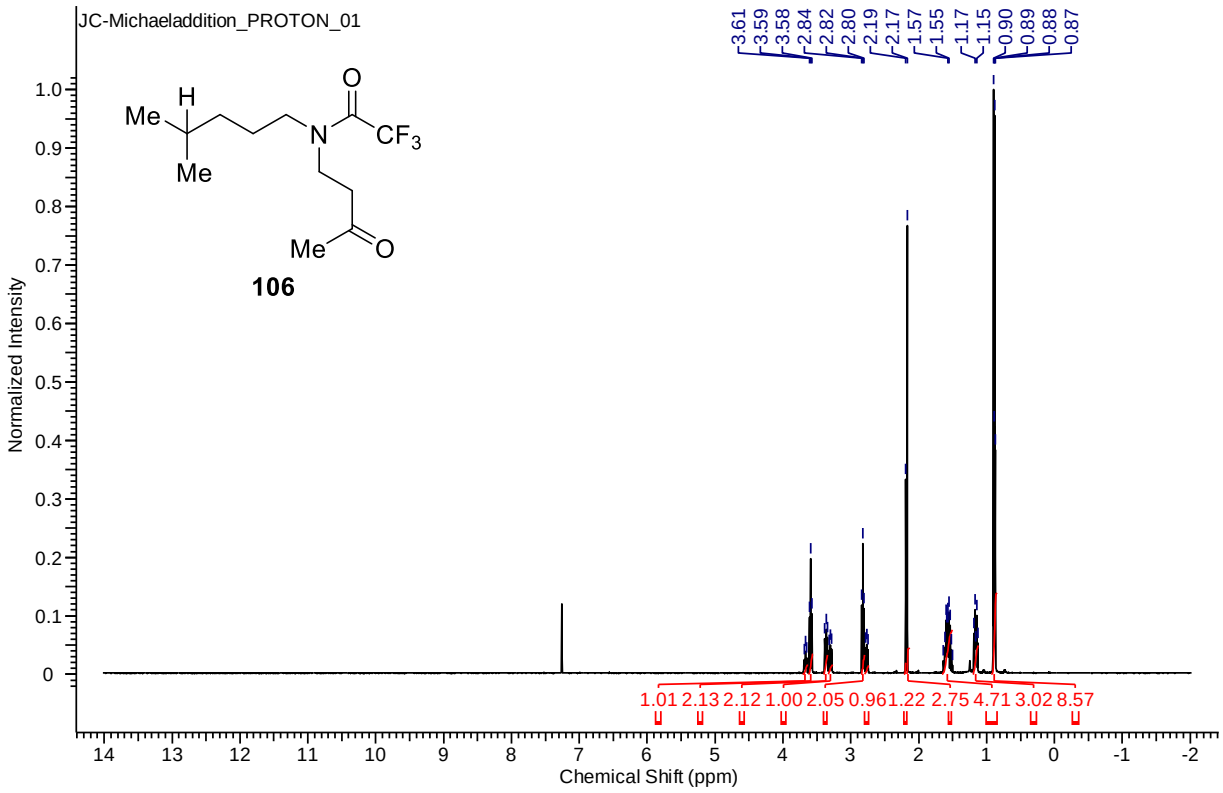
JC-Michaeladdition_PROTON_01
106
Normalized Intensity
Chemical Shift (ppm)
3.61 3.59 3.58 2.84 2.82 2.80 2.19 2.17 1.57 1.55 1.17 1.15 0.90 0.89 0.88 0.87
1.01 2.13 2.12 1.00 2.05 0.96 1.22 2.75 4.71 3.02 8.57

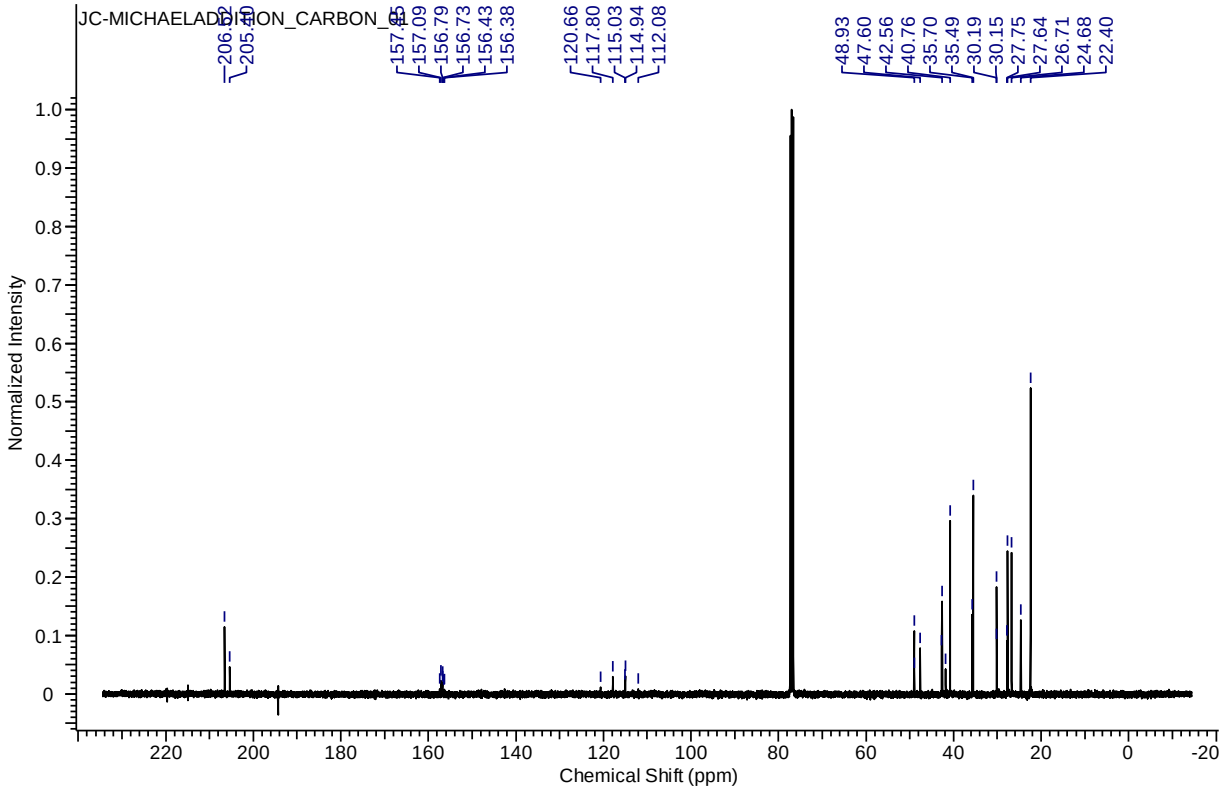
JC-MICHAELADDITION_CARBON_01
Normalized Intensity
Chemical Shift (ppm)
206.12 205.40
157.45 157.09 156.79 156.73 156.43 156.38
120.66 117.80 115.03 114.94 112.08
48.93 47.60 42.56 40.76 35.70 35.49 30.19 30.15 27.75 27.64 26.71 24.68 22.40

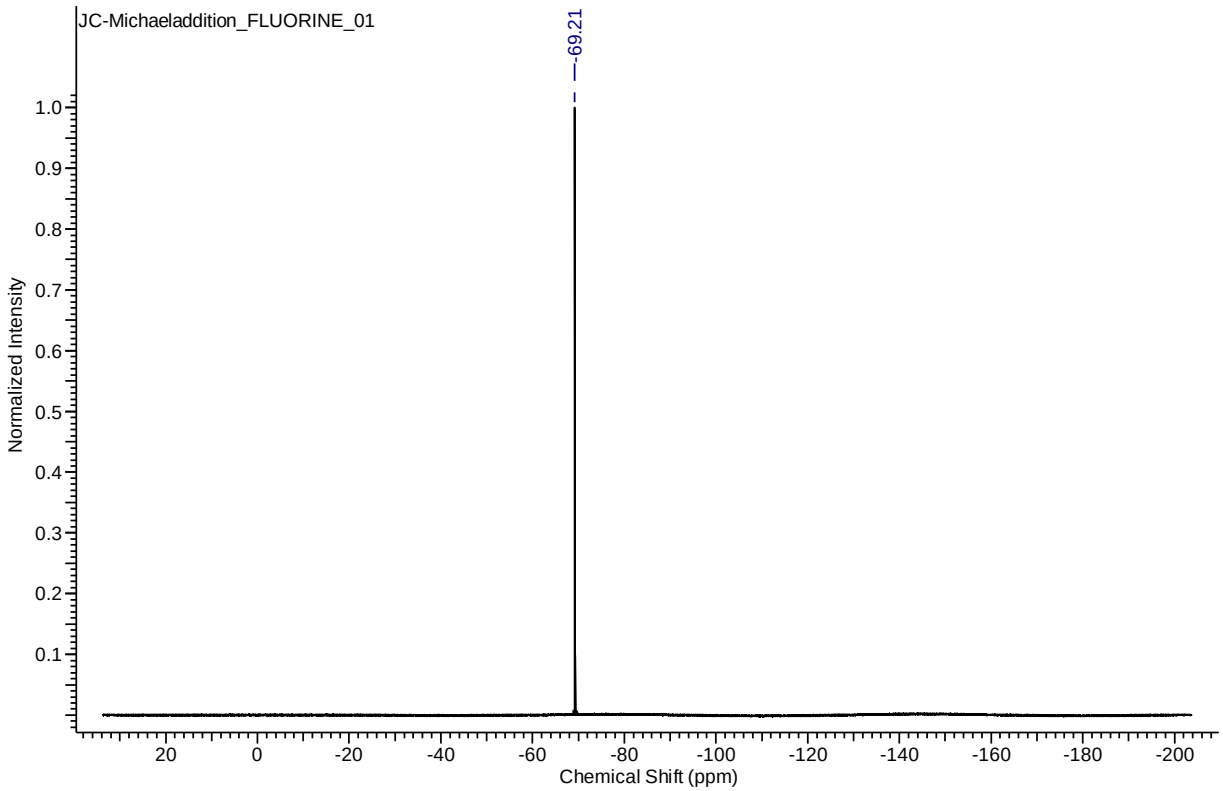
JC-Michaeladdition_FLUORINE_01
-69.21
Normalized Intensity
1.0
0.9
0.8
0.7
0.6
0.5
0.4
0.3
0.2
0.1
20
0
-20
-40
-60
-80
-100
-120
-140
-160
-180
-200
Chemical Shift (ppm)

REFERENCES

1. Ochiai, M., Miyamoto, K., Kaneaki, T., Hayashi, S., Nakanishi, W. *Science* **2011**, *332*, 448-451.

2. Menche, D.; Hassfeld, J.; Li, J.; Mayer, K.; Rudolph, S. *J. Org. Chem.* **2009**, *74*, 7220-7229.

3. Douat-Casassus, C.; Pulka, K.; Claudon, P.; Guichard, G. *Org. Lett.* **2012**, *14*, 3130–3133.

4. Yasuda, M.; Shimizu, K.; Yamasaki, S.; Baba, A. *Org. Biomol. Chem.* **2008**, *6*, 2790-2795.

5. Shchepin, R; Navarathna, D. H. M. L. P.; Dumitru, R.; Lippold, S.; Nickerson, K. W.; Dussault, P. H. *Bioorganic & Med. Chem.* **2008**, *16*, 1842-1848.

6. Chen, C.; Hecht, M. B.; Kavara, A.; Brennessel, W. W.; Mercado, B. Q.; Weix, D. J.; Holland, P. L. *J. Am. Chem. Soc*. **2015**, *137*, 13244-13247.

7. Marshall, J. A.; Yanik, M. M. *J. Org. Chem.* **2001**, *66*, 1373–1379.

8. Kholod, I.; Vallat, O.; Buciumas, A.-M.; Neier, R. *ARKIVOC* **2014**, *3*, 256-273.

9. Andruszkiewicz, R.; Silverman, R. B. *Synthesis* **1989**, 953-955.

10. Chu, X; Battle, C. H.; Zhang, N.; Aryal, G. H.; Mottamal, M.; Jayawickramarajah, J. *Bioconjugate Chem.* **2015**, *26*, 1606-1612.

11. Cismesia, M. A.; Yoon, T. P *Chem. Sci.* **2015**, *6*, 5426-5434.

12. Bordwell, F. G. *Acc. Chem. Res.* **1988**, *21*, 456-463.

13. Gomes, J. R. B.; Ribeiro da Silva, M. D. M. C.; Riberiro da Silva, M. A. V. *J. Phys. Chem. A.* **2004**, *108*, 2119-2130.

14. Blanksby, S. J.; Ellison, G. B. *Acc. Chem. Res.* **2003**, *36*, 255-263.

15. Cain, E. N.; Solly, R. K. *J. Am. Chem. Soc.* **1973**, *95*, 4791-4796.

16. Eidman, K. F.; Nichols, P. J. Trifluoroacetic acid. *E-EROS Encyclopedia of Reagents for Organic Synthesis.* Wiley, New York. (2004).

17. Francesca, D.; Frenna, V.; Ghelfi, F.; Macaluso, G.; Marullo, S.; Spinelli, D. *J. Phys. Chem. A.* **2010**, *114*, 10969-10974.

18. Stetzenbach, K. K.; Jensen, S. L.; Thompson, G. M. *Environ. Sci. Technol.* **1982***, 16*, 250-254.